REPORT

WASH MODEL CONFIGURATION, CALIBRATION, AND VALIDATION FOR THE ST. LUCIE ESTUARY WATERSHED

Prepared for
FDEP
Tallahassee, FL

December 11, 2008

URS

URS Corporation
1625 Summit Lake Drive, Ste. 200
Tallahassee, FL 32317
Project 12006946

Table of Contents

Executive Summary **ES-1**

1. Section 1 ONE Introduction **1-1**

2. Section 2 TWO Data Summary **2-1**

2.1 Basin Characterization 2-1
2.2 Model Configuration Data 2-1
2.2.1 Basin Physical Characteristics 2-1
2.2.2 Hydrologic and Hydrodynamic Characteristics 2-6
2.3 Model Forcing Data- Hydrology and Hydrodynamics 2-8
2.3.1 USGS Tide Gages 2-8
2.3.2 Flow and Stage data 2-9
2.3.3 Agricultural Irrigation Practices 2-10
2.3.4 Rainfall 2-10
2.3.5 Evapotranspiration 2-10
2.3.6 Water Budgets 2-10
2.4 Model Forcing data- Water Quality 2-11
2.4.1 Solar Radiation 2-11
2.4.2 Temperature 2-11
2.4.3 Regional Winds 2-12
2.4.4 EMC Development 2-12
2.5 Model Calibration Data 2-16
2.5.1 USGS Salinity Regime 2-16
2.5.2 SFWMD Routine Monthly Monitoring Program 2-17
2.5.3 Seasonal Variability 2-21

3. Section 3 THREE Model Development **3-1**

3.1 MODEL SELECTION 3-1
3.2 MODEL HIERARCHY 3-2
3.3 MODEL CONFIGURATION 3-3
3.4 MODEL DOMAIN AND GRID 3-3
3.5 GRID ATTRIBUTES 3-3
3.5.1 Secondary Basin 3-3
3.5.2 Soils 3-3
3.5.3 Land-use 3-4
3.5.4 Topography 3-4
3.6 HYDROLOGY 3-4
3.6.1 Canals, Rivers and Streams 3-4
3.6.2 Groundwater and Surface Water Interactions 3-5
3.6.3 Overland Flow Routing 3-6
3.6.4 Structures 3-6
3.6.5 Rainfall Configuration 3-6
3.6.6 Reservoirs 3-7

Table of Contents

3.7 BOUNDARY CONDITIONS 3-7
3.8 SIMULATION PERIODS AND TIMESTEP 3-8
3.9 MODEL INPUT DATA 3-10
3.9.1 Areal-Based Mean Concentrations 3-10
3.9.2 SOD 3-28
3.9.3 Re-aeration 3-29
3.9.4 Light Penetration 3-30

4. Section 4 FOUR Hydrologic and Hydrodynamic Calibration and Validation 4-32

4.1 Hydrologic and Hydrodynamic Calibration and Validation for the C-23, C-24 and C-44 Basin models 4-32
4.2 Hydrologic and Hydrodynamic Calibration of the SLE model 4-38

5. Section 5 FIVE Water Quality Calibration and Validation 5-1

6. Section 6 SIX Sensitivity Analysis 6-1

7. Section 7 SEVEN Lake Okeechobee Influences 7-1

8. Section 8 EIGHT Natural Conditions 8-1

9. Section 9 NINE Additional Data Needs 9-1

9.1 Unresolved Data Gaps/Needs 9-1

10. Section 10 TEN Conclusions 10-1

11. Section 11 ELEVEN References 11-1

Tables

Table ES-1 Calibration Parameters for each WaSh Model

Table 2-1 Shapefiles for the SLE Basin Physical Characteristics

Table 2-2 1999 Land-use Within the SLE System by FLUCCS Code

Table 2-3 Adjusted Land-use Within the SLE System by FLUCCS Code

Table 2-4 Operational Criteria of SLE Structures

Table 2-5 Average of the Daily-Averaged Flow and Stage Data for Structure Stations in each Upland Basin

Table 2-6 Average of the Daily-Averaged Flow and Stage Data for Structure Stations in each Basin

Table 2-7 Monthly variation of Daily Averaged wind speeds (m/s)

Table 2-8 BOD values measured in SLE April 12, 2006

Table 2-9 Measured Data Summary for Structure Stations

Table 2-10 Measured Data Summary for Estuary Stations

Table 2-11 Measured Chlorophyll Data Summary for Estuary Stations

Table 3-1 Water Routing Operations for Each Cell Type

Table 3-2 Summary of Model Calibration and Validation Periods

Table 3-3 Summary of TN Values from Four Site-Specific Data Sets

Table 3-4 Summary of TP Values from Four Site-Specific Data Sets

Table 3-5 ABMC Values for TN Used in the WaSh Model

Table 3-6 ABMC Values for TP Used in the WaSh Model

Table 3-7 Literature BOD EMC Values Based on Harvey Harper's 2003 analysis.

Table 3-8 Representative Re-aeration Coefficient Values

Table 4-1 WaSh Model Calibrated Hydrologic Parameters

Table 4-2 Calibrated Irrigation Demand Module Parameters applied to Citrus Land-use

Table 4-3 Calibrated Irrigation Supply and Application Model Parameters

Table 4-4 Calibrated Tertiary Canal Properties for each Land-use

Table 4-5 Frequency Metrics of Calibration and Validation for Flow in Upland Basins

Table 4-6 Time Series Metrics of Calibration and Validation for Flow in Upland Basins

Table 4-7 Annual Average Water Budgets for the C-23, C-24 and C-44 Basin Models

Table 4-8 Annual Average Water Budgets Basins Draining Directly into the SLE

Table 5-1 Calibration Parameters for Each WaSh Model

Table 5-2 Percentile Metrics for the Upland Basins in the SLEW

Table 5-3 Time-Series Metrics for the Upland Basins in the SLEW

Table 5-4 Percentile Metrics for the SLE Basin

Table 5-5 Time-Series Metrics for the SLE Basin

Table 5-6 Nutrient Load Calculations for each Basin in the SLEW

Table 8-1 Cross-over Map for 1967 to 1943 Land-use Data Set

Table 8-2 Land-use Crossover for each Basin with Acreage and Percentage of Land Within each 1999 FLUCS Level

Table 8-3 Comparison of Median Concentrations for Existing and Natural Condition Model Simulations

Table 8-4 Historic or "Natural Conditions" Nutrient Load Calculations for each Basin in the SLEW

Table 9-1 Data Gaps in SLE Datasets

Figures

Figure 1-1 Location of WBID's in St. Lucie Estuary

Figure 2-1 Map of Basin Boundaries, Canal Systems and Control Structures

Figure 2-2 Map of Model Basin Domains

Figure 2-3 Flow Connectivity of Basins

Figure 2-4 Map of Subbasin Boundaries

Figure 2-5a 1999 Land Use Designations

Figure 2-5b Adjusted Land Use Designations

Figure 2-6a Watershed Soil Designations

Figure 2-6b Winder Soils Designations

Figure 2-7 Topographic Digital Elevation Map (DEM)

Figure 2-8 Hydrography showing Primary Canals, Secondary and Tertiary Canals, and Natural Rivers and Streams

Figure 2-9 Bathymetric Raster Grid of SLE overlaying the Topographic DEM

Figure 2-10 Map of Data Sampling Stations

Figure 2-11 St. Lucie Estuary representative tide gage data at US1 and A1A stations

Figure 2-12 C-24 Flow Discharge

Figure 2-13 C-23 Flow Discharge

Figure 2-14 C-44 Flow Discharge

Figure 2-15 S308 Flow Discharge

Figure 2-16 NEXRAD rainfall station locations for South Florida

Figure 2-17 Evapo-transpiration data used in the model – prior to adjustments (top), fully adjusted (center), and seasonal Averages (bottom).

Figure 2-18 Solar Radiation Data Time Series and Seasonal Average Plots

Figure 2-19 Surface Water Station Time Series Plots

Figure 2-20 Wind Rose Diagram indicating dominant wind direction and speed in Lake Worth region

Figure 2-21 YSI Sondes Locations

Figure 2-22 Correlation of YSI continuous DO measurements, with grab sample and profile data from the 2005 FDEP monitoring program

Figure 2-23 BOD and SOD Sample Locations

Figure 2-24 ISCO point source monitoring stations from FDEP and The Institute for Food and Agricultural Sciences (IFAS)

Figure 2-25 IFAS ISCO Total Nitrogen Data

Figure 2-26 IFAS ISCO Total Phosphate Data

Figure 2-27 FDEP ISCO Total Nitrogen Data

Figure 2-28 Location of SFWMD SLT Stations

Figure 2-29 Example showing Land Use associated with SLT Stations

Figure 2-30 SLT Station 26 Nutrient Data

Figure 2-31 SLT Station 19 Nutrient Data

Figure 2-32 SLT Station 11 Nutrient Data

Figure 2-33 FDEP BMP Study Sample Locations

Figure 2-34 Seasonal Variations in Total Nitrogen and Total Phosphorus at a FDEP Grab Sample “Citrus” Station

Figure 2-35 Seasonal Variations in Total Nitrogen and Total Phosphorus at a FDEP Grab Sample “Pasture” Station

Figure 2-36 Location of Residuals in St. Lucie County

Figure 2-37 Nutrient loads from residuals

Figure 2-38 Circle I Ranch Site Map with Residual pile and sampling locations

Figure 2-39 Computation of the fraction of TN and TP generated from Residuals

Figure 2-40 St. Lucie Estuary representative salinity data at US1 and A1A stations

Figure 2-41 St. Lucie Estuary representative salinity data at US1 and A1A stations

Figure 2-42 St. Lucie Estuary representative salinity data at US1 and A1A stations

Figure 2-43 St. Lucie Estuary representative salinity data at US1 and A1A stations

Figure 2-44 St. Lucie Estuary representative salinity data at HR1 station

Figure 2-45 Examples of seasonal variability in C24 Basin

Figure 3-1 The System and Elements Comprising the WaSh Model

Figure 3-2 Model Configuration of tidally-influenced SLE Basin and structurally-controlled C-24, C-23 and C-44 basins

Figure 3-3 C-24 Primary Basin boundary and model grid

Figure 3-4 C-24 Secondary Basin boundaries and model grid

Figure 3-5 C-24 Hydrogroup soils classifications

Figure 3-6 C-24 Basin 1999 Adjusted land-use coverage

Figure 3-7 C-24 Basin 1999 model assigned land-use

Figure 3-8a C-24 Basin land-use, showing poor correlation between actual Land-use (top) and the model assigned land-use (bottom)

Figure 3-8b C-24 Basin land-use, showing poor correlation between actual land-use (top) and the model assigned land-use (bottom)

Figure 3-9a C-24 Basin land-use, before adjustment.

Figure 3-9b C-24 Basin land-use, after adjustment

Figure 3-10 Topography as mapped on Model Grid for C-24 basin

Figure 3-11 C-24 Hydrology showing Primary, Secondary and Tertiary canals

Figure 3-12 Model Configuration- C-24 Basin Grid Cell Designation with Primary Reach and Hydrography

Figure 3-13 C-24 Basin with Flow Paths

Figure 3-14 NEXRAD rainfall station locations in vicinity of C-24 and North Fork basins (WaSh model grids shown)

Figure 3-15 Mapping of NEXRAD stations onto WaSh model C-24 basin grid cells

Figure 3-16 Reservoir configuration in models

Figure 3-17 Measured TN and TP values for individual grab samples at each SLT Station with the mean concentration for that station

Figure 3-18 Measured TN and TP values for individual grab samples at each BMP Station with the mean concentration for that station

Figure 3-19 IFAS ISCO Total Nitrogen Data

Figure 3-20 IFAS ISCO Total Phosphate Data

Figure 3-21 FDEP ISCO Total Nitrogen Data

Figure 3-22 ABMC values for each ISCO Station

Figure 323 Median TN values for sample stations listed in Table 3-3, organized by Land Use

Figure 3-24 Median TP values for sample stations listed in Table 3-4, organized by Land Use
Figure 3-25 Template for Total Nitrogen and Total Phosphorus
Figure 3-26 ABMC Ratios for Total Nitrogen
Figure 3-27 ABMC Ratios for Total Phosphorous
Figure 3-28 Measured SOD and Model Fit to Data
Figure 3-29 Light Penetration configuration in the WaSh Model
Figure 4-1 Hydrodynamic Calibration for C-24 Basin
Figure 4-2 Hydrodynamic Calibration for C-23 Basin
Figure 4-3 Hydrodynamic Calibration for C-44 Basin
Figure 4-4 Hydrodynamic Validation for C-24 Basin
Figure 4-5 Hydrodynamic Validation for C-23 Basin
Figure 4-6 Basin Hierarchy for SLE Model salinity calibration
Figure 4-7 Salinity Calibration for the SLE Model
Figure 5-1 C24 Simulation Results during Calibration Period (1995-2000) and Validation Period (2001-2005)
Figure 5-2 HR1 Simulation Results during Calibration Period (1995-2000) and Validation period (2001-2005)
Figure 6-1 Sensitivity of D.O. to change in BOD ABMC value
Figure 6.2 Sensitivity of D.O. to change in SOD value
Figure 7-1 Basin Hierarchy for estimating Lake Okeechobee influence on the North Fork in the SLE model
Figure 7-2 Output Concentrations from SLE Model with Lake Okeechobee Influence`
Figure 8-1 Historic Land Use for SLE Model Domain Combined 1943 Davis Coverage and 1967 Davis Coverage
Figure 8-2 Historic Land Use for C-24 Basin - GIS Coverage (top-right) and Adjusted Grid Coverage (bottom-left)
Figure 8-3 C-24 basin model output for Current Land-use and Historic Conditions

Appendices

Appendix A Measured Water Quality Data for Upland Basins and Estuary Stations
Appendix B Control Structure Operational Criteria
Appendix C WaSh Model Documentation
Appendix D Calibration and Validation Plots for Upland Basins and Estuary Stations

The Florida Department of Environmental Protection (FDEP) is developing Total Maximum Daily Loads (TMDL) for nutrients and Dissolved Oxygen (D.O.) for Water Body IDs (WBIDs) in the Saint Lucie Estuary (SLE) and adjacent watersheds. The D.O. impairment for the water bodies has been attributed to nutrient impacts. In order to provide a general purpose tool for evaluating the impacts of nutrients on D.O. in the North Fork and St. Lucie Estuary (SLE) a watershed hydrologic, hydraulic and water quality model been developed. The St. Lucie Estuary Watershed (SLEW) encompasses many basins that all influence the conditions in the SLE. A comprehensive modeling approach has been developed in which all basins contributing to the SLE are included in the modeling analysis. The inclusion of adjacent basins is necessitated both by the "watershed approach" suggested by the Environmental Protection Agency (USEPA) (USEPA, 2004) and adopted by the FDEP due to the physical processes affecting the water dissolved oxygen, BOD and chlorophyll in St. Lucie Estuary. This provides an integrated approach, and provides the FDEP with a calibrated tool for evaluating existing and future contision in the SLEW and SLE.

The FDEP has contracted URS to use the WaSh model for the hydrodynamic and water quality analysis of the St. Lucie Estuary Watershed. The WaSh model is a hydrologic, hydrodynamic and water quality model originally developed for the unique hydrologic conditions in south Florida. Additionally, the WaSh model was previously configured and applied to basins draining to the SLE for previous hydrodynamic studies conducted by the South Florida Water Management District. Building on the existing hydrodynamic framework, many updates to the models were developed, such as

- Update of land-use classifications
- Site-specific, aerial-based mean concentrations were developed and implemented
- The simulation of tidal flows in the SLE was implemented
- A water quality simulation was included

The model has been configured and successfully calibrated and validated for all of the basins influencing the SLE. The flow calibration consisted of comparisons of daily flow measurements over a six year period of 1995-2000, and comparisons to monthly salinity data for a three year period of 2003-2005. The water quality module was calibrated by comparing model simulation output to measured monthly nutrient, D.O. and chlorophyll data for the same six year period. Subsequent validation was conducted for the consecutive five year period of 2001-2005.

The values obtained for key water quality parameters are show in the Table ES-1 below.

Table ES-1. Calibration Parameters for each WaSh Model.

WaSh In-Stream Parameter	Units	Definition	C23	C24	C44	SLE
MIX_VERTICAL	ft^2/sec	Vertical Mixing Coefficient	-	-	-	0.1
KE1	ft^{-1}	Extinction Coeff.	1.000	1.000	1.000	1.000
KE2	ft^{-1}	Extinction Coeff.	1.000	1.000	1.000	1.000
Frac_Daylight	-	Fraction of day that is daylight	0.500	0.500	0.500	0.500
GP	day^{-1}	Maximum Growth Rate	1.500	4.000	1.500	2.200
THETAGP	-	Temperature Coefficient	1.068	1.068	1.068	1.068
LIS	langleys/day	Light Intensity at Saturation	150.000	150.000	150.000	150.000
KMN	mg N/L	Half-Saturation Constant for Nitrogen	0.025	0.025	0.025	0.025
KMP	mg P/L	Half-Saturation Constant for Phosphorus	0.001	0.001	0.001	0.001
K1R	day^{-1}	Endogenous Respiration	0.150	0.150	0.150	0.150
THETA1R	-	Temperature Coefficient	1.045	1.045	1.045	1.045
VS4	ft/day	Phytoplankton Settling Velocity	0.000	0.000	0.000	0.000
KDP	day^{-1}	Death Rate	0.350	0.350	0.350	0.350
APC	-	Phosphorus to carbon ratio	0.025	0.025	0.025	0.025
K83	day^{-1}	Dissolved organic phosphorus mineralization at 20°C	0.140	0.110	0.130	0.110
THETA83	-	Temperature Coefficient	1.080	1.080	1.080	1.080
KMPC	mg C/L	Half saturation constant for phytoplankton limitation of phosphorus recycle	1.000	1.000	1.000	1.000
FOP	-	Fraction of dead and respired phytoplankton recycled to the organic phosphorus pool	0.500	0.500	0.500	0.500

WaSh In-Stream Parameter	Units	Definition	C23	C24	C44	SLE
VS2	ft/day	Organic phosphorus settling velocity	0.000	0.000	0.000	0.000
ANC	-	Nitrogen to carbon ratio	0.250	0.250	0.250	0.250
K71	day^{-1}	Organic Nitrogen mineralization at 20°C	0.035	0.030	0.040	0.080
THETA71	-	Temperature Coefficient	1.080	1.080	1.080	1.080
K12	day^{-1}	Nitrification Rate	0.470	0.047	0.047	0.047
THETA12	-	Temperature Coefficient	1.030	1.030	1.030	1.030
KNIT	mg O_2/L	Half Saturation rate for oxygen	2.000	2.000	2.000	2.000
K2D	day^{-1}	Denitrification rate at 20°C	0.050	0.050	0.050	0.050
THETA2D	-	Temperature Coefficient of Denitrification rate	1.045	1.045	1.045	1.045
KNO3	mg O_2/L	Michaelis constant for Denitrification	0.100	0.100	0.100	0.100
FON	-	Fraction of dead and respired phytoplankton recycled to the ammonia nitrogen pool	0.500	0.500	0.500	0.500
VS3	ft/day	Organic nitrogen settling velocity	0.000	0.000	0.000	0.000
AOC	-	Oxygen to carbon ratio	2.670	2.670	2.670	2.670
KD	day^{-1}	Deoxygenation rate @ 20°C	0.150	0.075	0.150	0.150
THETAD	-	Temperature Coefficient	1.047	1.047	1.047	1.047
KBOD	mg O_2/L	Half saturation constant for oxygen limitation	0.900	0.900	0.900	0.900
SOD	g O_2/m^2-day	Sediment Oxygen Demand	5.960	5.960	5.960	3.000
THETA2	-	SOD Temperature coefficient	1.03	1.03	1.03	1.03
VS5	ft/day	BOD settling velocity	0.000	0.000	0.000	0.000
K2	day^{-1}	Reaeration Rate	0.300	0.300	0.300	1.200

WaSh In-Stream Parameter	Units	Definition	C23	C24	C44	SLE
THETA1R	-	Endogenous Respiration Temperature coefficient	1.000	1.000	1.000	1.000
K1	day^{-1}	Endogenous Respiration	0.500	0.500	0.500	0.500

The calibrated and validated model was also applied to determine the amount of time that discharges from Lake Okeechobee would influence conditions in the North Fork of the SLE. A special version of the model was configured with tracers to determine the amount of lake discharge and ambient water occurring in the North Fork, South Fork and St. Lucie Estuary. Results indicate that lake discharges can intermittently comprise approximately 20% of the water in the North Fork.

The model was reconfigured to historic or "natural" conditions by changing the land-use designations in the model configuration to represent conditions in 1943. Both the calibrated and validated models for each basin for both existing conditions and natural conditions have been delivered to the FDEP for use in their future evaluation of SLE conditions and BMAP options.

The Florida Department of Environmental Protection is developing Total Maximum Daily Loads for Water Body IDs (WBIDs) in the Saint Lucie Estuary and adjacent watersheds. A number of WBIDs within the SLEW have been verified as impaired for Dissolved Oxygen (D.O.) due to nutrient impacts. Impacted WBIDs are identified in Figure 1-1. The FDEP has therefore contracted the development of a watershed hydrologic, hydraulic and water quality model to provide a quantitative tool for evaluating existing and future water quality conditions the SLE and SLEW.

The SLEW is composed of 9 basins that drain into the SLE: C24, C23, C44, S153, Basin 4, Basin 5, Basin 6, North Fork, and Tidal St. Lucie. The SLE is also tidally connected to the Indian River Lagoon (IRL). Discharges from three of the upland basins contributing flow the North Fork are highly managed by gated structures, and discharges from Lake Okeechobee do occasionally reach the North Fork. The processes controlling DO are difficult to quantify in estuaries, since they are time-varying on many scales and involve physical, chemical and biological interactions. The influence of nutrients loads, the sea-floor (i.e. sediment oxygen demand (SOD)), the effect of waves and vertical mixing on re-aeration, non-point source loading from multiple land-uses and hydrodynamic residence time all combine to produce large temporal and spatial variations in D.O. Long term monthly data collected in the SLE and upland basins, as well as high-frequency D.O. data sets collected in the SLE indicate vertical variations in D.O. levels and significant temporal variations on daily to seasonal time scales.

Due to these considerations, the multiple factors influencing D.O. levels in the SLE, and the numerous basins with discharges to the SLE, the FDEP has adopted a comprehensive modeling approach. Four separate models were developed to represent the entire SLE system. Three models, each representing one of the basins separated from the SLE by structures, were calibrated and validated first. These are referred to as the C24, C23 and C44 models, respectively. Their simulation flow and water quality outputs were provided as inputs to the forth model. The fourth model represents the combined North Fork (NF), Tidal St. Lucie (or South Fork) (TSL), B-4, B-5 and B-6 basins, which needed to be modeled together since their surface water systems were all directly connected to the SLE and influenced by tidal flows. This forth model, referred to as the SLE model, also includes the North Fork, South Fork and Middle Fork, with the downstream boundary located at the end of the Middle fork, just upstream of the confluence with the Indian River Lagoon. This comprehensive approach provides a set of models that can simulate conditions in the entire SLEW.

The FDEP has selected the WaSh model (URS 2003; URS 2008a,b,c) for the analysis. The WaSh model is a hydrologic, hydrodynamic and water quality model originally developed for the unique hydrologic conditions in south Florida. Also the WaSh model was previously configured and applied to basins draining to the SLE for studies conducted by the South Florida Water Management District (URS, 1999). Building on the existing hydrodynamic framework, many updates to the models were developed, such as:

- Update of land-use classifications
- Site-specific, aerial-based mean concentrations were developed and implemented
- The simulation of tidal flows in the SLE was implemented
- A water quality simulation was included

This report documents additional development of the WaSh model for the SLE and upland basins. The model development includes review of hydrologic, hydrodynamic and water quality data, model setup and configuration, calibration and validation. In addition to the model development, it was reconfigured to represent historic conditions as defined by the alteration of landuse documented in 1943 and used to access the influence of the Lake Okeechobee discharge through the C-44 canal on conditions in the North Fork.

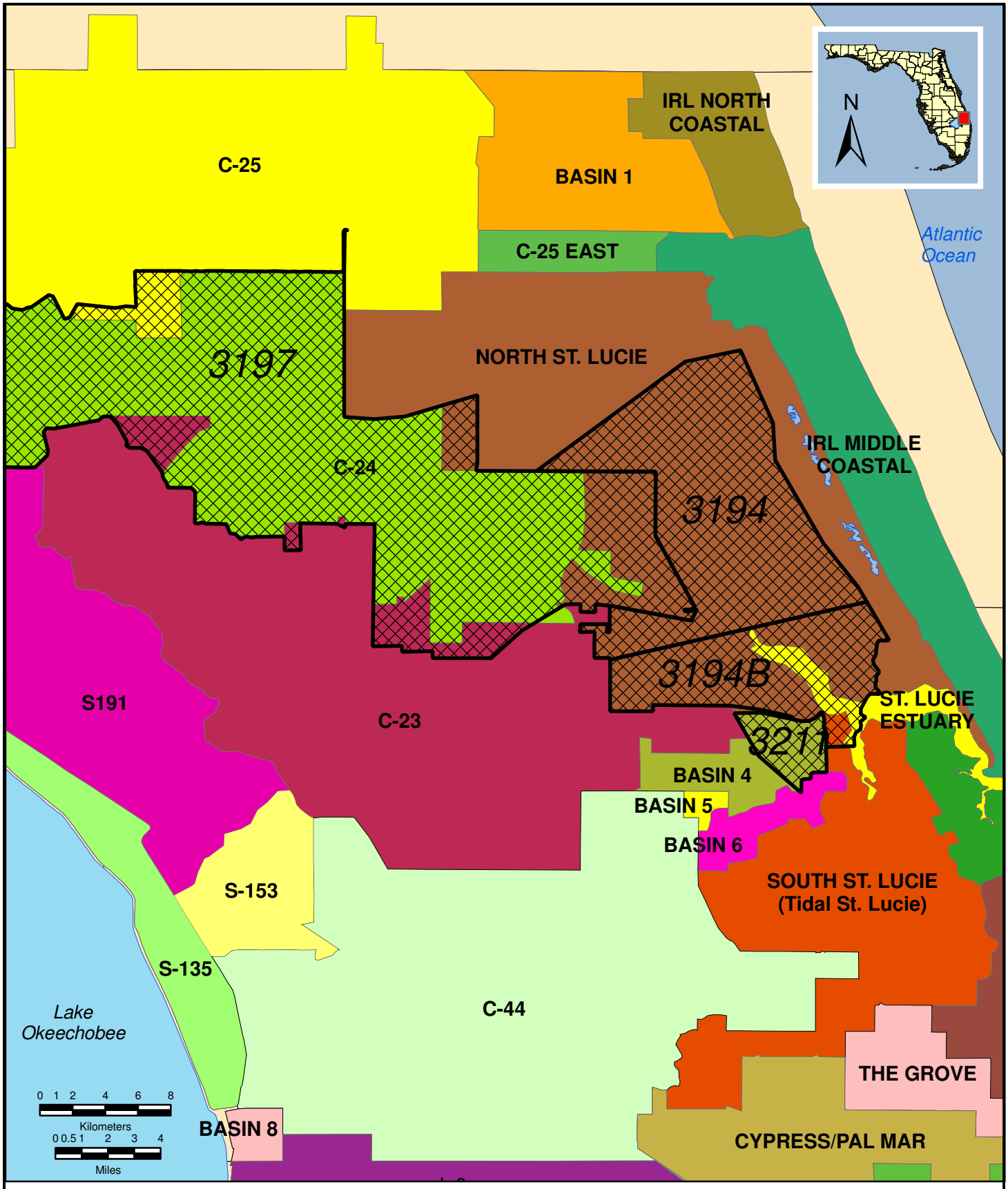

URS

Figure 1-1. Location of WBIDs in St. Lucie Estuary Watershed (GIS coverages provided by FDEP.)

2.1 BASIN CHARACTERIZATION

The St. Lucie Estuary (SLE) is located near the Martin and St. Lucie County line on the east coast of south central Florida about 30 miles from the eastern edge of Lake Okeechobee. The inner SLE is comprised of the North Fork and the South Fork of the St. Lucie River, and has a total surface area of approximately 6.4 square miles. The two forks converge to form a single middle estuary with a surface area of 4.7 square miles. The middle estuary extends east for approximately 5 miles until it meets the Indian River Lagoon, before opening to the Atlantic Ocean at the St. Lucie Inlet. Five tributaries to the estuary provide drainage for a watershed that encompasses 827 square miles (SFWMD data).

Although the SLE was once a fresh water system, the opening of the St. Lucie inlet in 1892 instigated the switch to a brackish system. In 1937 following the completion of the Okeechobee Waterway by the USACE, the SLE was connected to Lake Okeechobee via a 152-mile-long cross-state canal system, the C-44 canal. The connection of the Lake to the estuary allowed lake levels to be lowered in preparation for and during times of excess rain to prevent flooding near the lake shore.. Consequently, during periods of high discharge from the lake, the estuary water quality is degraded by a lowering of salinity, an increase in turbidity, and an increase in nutrients from the lake.

Water quality, water quantity and meteorological data in the St. Lucie Estuary have a very distinct seasonal signal. The dry, winter months are characterized by less rainfall, lower nutrient, and higher dissolved oxygen, while the wetter summer months are characterized by higher rainfall, higher nutrients, and lower dissolved oxygen.

Further degradation of the estuary has been precipitated by both the continued urbanization of the coastal regions of St. Lucie and Martin Counties and by the agricultural activities in the western regions of the watershed.

2.2 MODEL CONFIGURATION DATA

2.2.1 Basin Physical Characteristics

Watershed modeling of the SLE system is dependent on the accurate representation of the many physical parameters present within each drainage basin. A map of the SLE and its corresponding watershed (SLEW) is shown in Figure 2.1. Many literature sources include the C-25 basin in the SLEW. However, for modeling purposes in this project, C-25 basin was not included. C-25 basin has been determined to drain directly into the Indian River Lagoon (IRL), and therefore, it does not directly contribute to the SLEW.

The St. Lucie Estuary Watershed is composed of 9 basins that drain into the SLE: C24, C23, C44, S153, Basin 4, Basin 5, Basin 6, North Fork, and Tidal St. Lucie. For the modeled SLE basins, GIS shapefiles, including include basin boundaries, land-use, soil type, hydrography and topographic features, were obtained from SFWMD. Table 2.1 lists the shapefiles analyzed and the date of the file creation.

Table 2.1. Shapefiles for the SLE Basin Physical Characteristics.

Date Type	Shapefile Name	Source	Date
Basin	Hyhdbwtr.shp	SFWMD	5/6/2005
Subbasin		SFWMD	8/9/2004
1999 Land Use	Lscndclu04.zip	SFWMD	11/16/2005
Soils	Sossrunt.shp	SFWMD	4/29/2008
Canals	Hysur24k.shp	SFWMD	5/6/2005
Primary Reach	Hysurcrc.shp Hysur24k.shp	SFWMD	5/16/2005 5/6/2005
Topography	dem200ftint	SFWMD	10/7/2004
Bathymetry	Lfbthirl98	SFWMD	4/29/2008

2.2.1.1 Basin Boundaries

Three basins drain directly to the North Fork of the St. Lucie Estuary (C-24, C-23 and the North Fork (NF) Basin) (Figure 2.1). Five other basins drain to the South Fork of the St. Lucie Estuary, (C-44, B-4, B-5 and B-6 and the Tidal St. Lucie (TSL) Basin). Basin S153 drains into the C44 basin and ultimately into the TSL.

Three upland basins are separated from the North and South Fork by control structures (Structure S49 in C-24, Structure S97 in C-23 and Structure S-80 in C-44) (Figure 2.1). Canal C44 is unique in that it is also connected to Lake Okeechobee via the S308C structure. Flows can be directed either from the C-44 canal into Lake Okeechobee or from Lake Okeechobee to the C-44 Canal. All of the other basins are tidally-connected to the SLE (North Fork or South Fork). The NF basin has an upstream structure, the Gordy Road Structure, a gate which controls flows from the northern sections of the NF basin into the St. Lucie River and ultimately to the North Fork of the SLE.

The model domains and flow connectivity of the basins are shown in Figure 2.2 and 2.3 respectively. All discharges from the C-23, C-24 and C-44 basins are collected into the C-23, C-24 and C-44 canals and discharged into the SLE at the outfall structures. The remaining basins are tidally-connected to the SLE (except for a portion of the North St. Lucie basin upstream of the Gordy Road Structure) as depicted in Figure 2.1.

2.2.1.2 Subbasin Boundaries

The secondary basin boundaries add refinement to the overland flow regime or flow pathing within each primary basin. In the case of South Florida, proper identification of secondary basin systems is especially important due to the shallow grade of topography within the region. As topographic resolution can often be too coarse or too subtle in South Florida to distinguish the flow patterns, the assistance of additional secondary boundaries produces more accurate drainage

patterns. Secondary basin boundaries are defined by SFWMD and provided on their GIS website as a GIS shapefile. Secondary basin coverages are often updated as subbasin boundary delineation often changes with the construction of roads, buildings, control structures, stormwater drainage, etc. The secondary basin structure if the SLEW is presented in Figure 2.4.

2.2.1.3 Land Use

Land-use data was available from the SFWMD GIS database in polygon shapefile formats. Land use designations shapefile were available using data for 1988, 1995 and 1999. Attempts were made to correlate the three datasets and note the change of land use through time. However, due to inconsistent nomenclature and designation codes in the two earlier coverages, analysis of land use was begun with the 1999 dataset. Analysis for FLUCCS level two designations is presented in Table 2.2, which tabulates the area in acreage and percentage of basin for each land use. A map of the 1999 land use shapefile is presented in Figure 2.5a.

Table 2-2. 1999 Land-use Within the SLE System by FLUCCS Code. All values given as acres and percentages.

1999	C24		C23		C44		SLE	
FLUCCS Level 2 Land Use	Acres	Percentage	Acres	Percentage	Acres	Percentage	Acres	Percentage
110	1229	1.4	1459	1.3	1812	1.4	11141	6.5
120	2524	2.9	654	0.6	315	0.2	28938	16.8
130	295	0.3			186	0.1	5587	3.2
140	38	0.0	9	0.0	204	0.2	3892	2.3
150	55	0.1	48	0.0	77	0.1	1408	0.8
160			412	0.4			288	0.2
170	21	0.0	662	0.6	98	0.1	1914	1.1
180	666	0.8	135	0.1	210	0.2	3704	2.1
190	74	0.1	25	0.0	149	0.1	7229	4.2
210	49260	56.3	50915	45.2	38238	29.5	23092	13.4
220	17483	20.0	32188	28.6	42752	33.0	28161	16.3
230	36	0.0	105	0.1	63	0.0	974	0.6
240	81	0.1	165	0.1	647	0.5		0.0
250	38	0.0	538	0.5	620	0.5	477	0.3
260	0	0.0	217	0.2	0	0.0	155	0.1
310	168	0.2	297	0.3	1830	1.4	825	0.5
320	46	0.1	1341	1.2	3855	3.0	1841	1.1
330			42	0.0	693	0.5	1448	0.8
410	853	1.0	2106	1.9	9333	7.2	19025	11.0
420	396	0.5	559	0.5	1122	0.9	3398	2.0

1999	C24		C23		C44		SLE	
FLUCCS Level 2 Land Use	Acres	Percentage	Acres	Percentage	Acres	Percentage	Acres	Percentage
430	36	0.0	71	0.1	1030	0.8	1614	0.9
440							84	0.0
510	362	0.4	584	0.5	885	0.7	3451	2.0
520	8	0.0	94	0.1	629	0.5	937	0.5
530	791	0.9	1089	1.0	333	0.3	3041	1.8
540							106	0.1
560							8	0.0
610	3091	3.5	4322	3.8	3299	2.5	5376	3.1
620	2262	2.6	2152	1.9	2815	2.2	1963	1.1
630	368	0.4	1036	0.9	218	0.2	299	0.2
640	6488	7.4	8779	7.8	8748	6.8	6376	3.7
740	294	0.3	1109	1.0	940	0.7	965	0.6
810	511	0.6	463	0.4	611	0.5	3417	2.0
820			11	0.0	6	0.0	59	0.0
830	100	0.1	940	0.8	7802	6.0	1442	0.8
Grand Total	87573	100.0	112525	100.0	129519	100.0	172634	100.0

Significant land use changes have occurred constantly in the St. Lucie Basin. Thus, the 1999 SFWMD land use layer was updated during model development. Current land use refinement was achieved with the assistance of local and county governments, which provided recent changes in land use codes and classifications. The City of Port St. Lucie, the City of Stuart, Martin County, and St. Lucie County all provided GIS data to optimize efforts in the development of land use mapping. Each agency was provided the coverage and was requested to provide improvements and offer more current land-use updates. Agricultural land uses in the basin were updated based on information provided by Linda Crane, Florida Department of Agriculture and Consumer Services, Office of Agricultural Water Policy. This information consisted of a hand-drawn map that was digitized by FDEP staff. This was considered the most up-to-date information available regarding agricultural land uses in the St. Lucie Basin.

FDEP personnel developed land use crosswalks between FLUCCS level 2 codes and each local area land use designation. Under the supervision of FDEP, the land-use shapefiles were updated accordingly.

A summary of the adjusted land-use is provided in Table 2-3. All land-uses were analyzed based on their Level Two FLUCCS codes.

Table 2-3. Adjusted Land-use Within the SLE System by FLUCCS Code. All values given as acres and percentages.

Adjusted	C24		C23		C44		SLE	
FLUCCS Level 2 Land Use	Acres	Percentage	Acres	Percentage	Acres	Percentage	Acres	Percentage
110	1210	1.4	1788	1.6	1911	1.5	10257	6.0
120	3743	4.3	790	0.7	287	0.2	34582	20.3
130					459	0.4	5634	3.3
140			58	0.1	275	0.2	3152	1.8
150					551	0.4	1658	1.0
160	275	0.3	1570	1.4	0	0.0	447	0.3
170	13	0.0	439	0.4	184	0.1	1427	0.8
180	92	0.1	92	0.1	92	0.1	4293	2.5
190	1238	1.4	3590	3.2	92	0.1	8081	4.7
210	48541	55.4	51147	45.5	49775	38.4	24637	14.4
220	18424	21.0	33038	29.4	43414	33.5	30771	18.0
230	36	0.0	459	0.4	92	0.1	0	0.0
240	72	0.1	139	0.1	1117	0.9	656	0.4
250			304	0.3	566	0.4	368	0.2
260					0	0.0	275	0.2
310	2661	3.0	4317	3.8	1737	1.3	310	0.2
320	454	0.5	502	0.4	2330	1.8	1942	1.1
330			92	0.1	418	0.3	956	0.6
410	129	0.1	1809	1.6	4756	3.7	21144	12.4
420	281	0.3	92	0.1	392	0.3	2090	1.2
430	92	0.1	92	0.1	415	0.3	1145	0.7
440					92	0.1	46	0.0
510	11	0.0	187	0.2	30	0.0	2370	1.4
520			25	0.0	280	0.2	608	0.4
530	77	0.1	85	0.1	7200	5.5	1384	0.8
540					0	0.0	167	0.1
560							0	0.0
610	3198	3.7	2528	2.2	1917	1.5	3609	2.1
620	2366	2.7	2094	1.9	2053	1.6	1338	0.8
630	333	0.4	2293	2.0	2556	2.0	184	0.1

Adjusted	C24		C23		C44		SLE	
FLUCCS Level 2 Land Use	Acres	Percentage	Acres	Percentage	Acres	Percentage	Acres	Percentage
640	3494	4.0	2907	2.6	4781	3.7	3330	2.0
740	419	0.5	983	0.9	632	0.5	344	0.2
810	156	0.2	564	0.5	869	0.7	2178	1.3
820					0	0.0	0	0.0
830	259	0.3	544	0.5	459	0.4	1259	0.7
Grand Total	87574	100.0	112526	100.0	129732	100.0	170642	100.0

A regional plot of the adjusted land-use data is presented in Figure 2.5b.

2.2.1.4 Soils

The polygon shapefile coverage for soils was obtained from the SFWMD GIS database. The coverage designates the lithology of the SLE, which consist of predominantly fine sand with pockets of muck and loam. The polygons are also attributed with the "hydrogroup" designation, which generally defines a soil's ability to absorb, hold or repel surface water and groundwater can be determined. Soil types for the SLE are shown as an example in Figure 2.6a.

Some of the soils in the SLE basins have been classified as Winder Soils . Windsor soils have a what characteristics" that may affect the runoff concentration of nutrients. A map of the Windsor soils is show in Figure 2.6b.

2.2.1.5 Topography

Topographic elevation data was provided by SFWMD on a 50-foot grid. Point data was converted into a three-dimensional Digital Elevation Map (DEM) to represent the topographic coverage. The DEM is presented in Figure 2.7.

2.2.2 Hydrologic and Hydrodynamic Characteristics

The St. Lucie Estuary system is influenced by a variety of drainage networks, including natural streams and rivers, structurally-controlled canal systems, surface runoff, groundwater, and tidal influences. The estuary itself is comprised of the North Fork basin and the South Fork or Tidal St. Lucie basin. Both basins experience significant fluctuations in natural conditions due to tidal influences. Located adjacent to the North and South Fork basins are Basins 4, 5, & 6, which are also tidally-influenced.

2.2.2.1 Canals

Due to the shallow nature of the topography in the area, the region was historically characterized as draining via sheet flow. The entire region was covered in predominantly wetlands which drained in a thin sheet of water over the land. In efforts to control the drainage patterns of the region to better plan for urbanization and agricultural irrigation, an extensive network of canals

has been established. Current hydrologic coverage of the surface water drainage of the SLEW is shown in Figure 2.8. All of the SLE basins have either the entire basin or significant portions of the basin drained by a canal system. The canal system can be divided into three components: a tertiary canal system, a secondary canal system, and a primary canal system. The tertiary system consists of dense networks of narrow, shallow canals within the agricultural lands used to control soil water levels and provide water for local irrigation. Water levels in the tertiary system are controlled by a series of weirs operated by the local land owners. Little stage data is available regarding water levels, volumes or flows of secondary or tertiary canals. The tertiary canals are linked to a secondary system of canals, which were built to provide a connection between tertiary systems and the project canals.

The project canals reside under the jurisdiction of the U.S. Army Corps of Engineers and are operated in conjunction with the Water Management Districts. There are three major canals that drain the SLE watershed: C24, C23 and C44. A surface water connection exists between the C24 and C25 basins, via the G81 spillway gate structure. However, inter-basin transfers occur very infrequently, and therefore, this connection was not included in the model configuration of the C24 basin. Canal cross-sectional data was obtained from SFWMD for C24 and C23. These blueprints offered channel design information, channel width and channel depth specifications. C24 data was based on a hydrographic survey performed by the Wantman Group in October of 2005, which delineated both design channel criteria and existing data. Channel depths illustrated the most significant difference, due to sediment deposition on the canal bottoms and subsequent raising of the channel bed. C24 canal had widths that ranged from 80 feet in the headwaters to 200 feet at the S49 structure. Channel depths ranged from 12 feet to -15 feet elevation NGVD. C23 canal blueprints were obtained from Canal repair surveys conducted by the Engineering and Construction Department of SFWMD in May of 2005.Channel widths ranged from 120 feet in the headwaters to 200 feet at the S48 structure. Canal depths ranged from 15 feet to 3 feet in elevation NGVD. Canal design data was unavailable for C44 canal. As a substitute for design blueprints, Google Earth was employed and used to measure the channel widths along the length of the canal. Widths range from 250 feet near Lake Okeechobee to 450 feet near the S80 structure. Design criteria of the S80 structures was used as a guideline to estimate canal depth. The minimum flow criteria of 9.5 feet was used as the canal depth for C44.

Water levels and flows in each of the project canals are measured with gages mounted at each structure. The flow in these canals is predominately towards the SLE, providing drainage of the upland basins. (Figure 2.1) Flow from the S308 structure often discharged from Lake Okeechobee and routed from the lake, through C-44 canal, and into the SLE via structures located just upstream of the entrances into the St. Lucie Estuary. Table 2-2 contains the operational criteria for each control structure.

Table 2-4. Operational Criteria of SLE Structures.

Structure	Width	Gates	Bypass Stage	Wet Season	Dry Season
S49	150	2	26.5	19.5	21.0
S97	125	2	19.0	21	22.8
S80	140	7	20.56	18	18
S308	116	4	26.0	14.5	14.5

The water levels in the project canals, which are maintained by the gates, are governed by a maintenance schedule. The general principle of the schedule is to maintain water levels in the project canals at preset dry and wet season levels. Deviations from this overall objective are made to accommodate high rain periods and droughts.

The gates are operated according to guidelines which are published in the U.S. Army Corps of Engineers Water Control Plan for Lake Okeechobee and Everglades Agricultural Area, (2000). The actual operation criteria for opening and closing gates is published in the Structures Book (SFWMD, 2004). The published operational criteria are provided in Appendix A. Typically the gates open when the stage exceeds a critical level, and then remain open until the stage drops below another lower critical level. Each gate operated by SFWMD may vary in details of opening rates, the maximum allowable opening, and opening and closing criteria, and each gate at a structure may be operated differently, but in general the stage criteria are changed for the wet and dry season. The published criteria are not always adhered to, and during extreme events or in anticipation of high rainfall or drought conditions, the operation of the structures may be varied from the criteria to improve the response of the system.

2.2.2.2 Estuary Description and Bathymetry

The St. Lucie Estuary is one of the largest brackish waterbodies on the East coast of Florida. The main branch of the estuary spans from the St. Lucie inlet at the junction with the Indian River Lagoon and spreads Northwest for 3.5 miles. Just past the A1A bridge, the estuary makes a due West turn, until it hits the Roosevelt bridge at US1 2.5 miles beyond. At US1, the Estuary branches out into the North and South Fork. The estuary width spans from 1000 meters at the inlet to nearly 2000 meters at east of the Roosevelt bridge. The North Fork averages approximately 1200 meters in width for a length of 4.5 miles, while the South Fork averages 700 meters width or three miles. Channel depths of the estuary range up to 5.4 meters, but the average depth of the main channel is approximately 3 meters.

A raster grid of the SLE bathymetry is presented in Figure 2.9, overlaying the topographic DEM from Figure 2.7. The bathymetric raster was created by using bathymetric sounding data from the "Indian River Lagoon-St. Lucie Estuary Bathymetry" shapefile provided on the SFWMD GIS database and converting it to a raster grid with grid cells of 1000 feet.

2.3 MODEL FORCING DATA- HYDROLOGY AND HYDRODYNAMICS

2.3.1 USGS Tide Gages

Two tide gage stations were located within St. Lucie estuary collecting tide data for the period of 2002-2005. One station was located on the A1A bridge near the St. Lucie inlet and one was located on Hwy. US1 bridge near the branch of the North and South Fork (Figure 2.10). Data was collected by the USGS on 30-minute intervals by continuous YSI devices. Two graphs of representative data are presented in Figure 2.11.

The diurnal fluctuation of the tides averages 1.25 meters with tides varying from -1.0 feet at lowest tide to 2.75 feet at highest tide. The US1 station tide variation tends to be 0.25 higher than tides at the A1A station and lags by approximately 1 hour. The upper graph contains several spikes in the tide data graphs indicating storm events, likely associated with autumn storm

season. The bottom graph illustrates a period of lost data, when the US1 bridge instrumentation was inoperable.

2.3.2 Flow and Stage data

Water quantity flow and stage data was obtained from SFWMD's DBHydro database. For the purpose of flow, daily flow measurements for the outflow structures for the C-24, C-23 and C-44 basins is available from 1965 through present. A table summarizing flow and stage data for the 1995-2005 sampling period used for this project is presented in Table 2-3. Structure S308 gages flow either in the canal from the lake or into the lake from the canal. During the 1995-2005 period, water flowed into the lake 16% of the time, into the canal 57% of the time, and was zero 27% of the time. No flow data was available for the estuary. In Figures 2.12 through 2.15, measured flow data from each of the above structures is presented in the form of time series plots, cumulative time series plots, frequency distributions, seasonal averages, and annual averages.

Table 2-5. Average of the Daily Averaged Flow and Stage Data for Structure Stations in each Upland Basin.

Basin	Structure	Ave. Stage (ft)	Ave. Flow (cfs)
C-24	S-49	19.0	246.8
C-23	S-97	20.4	202.7
C-44	S-80	14.0	684.2
C-44	S308	13.85	-510, 1 [1]

[1] Note that flow through S30 can be directed into the canal from the lake or into the lake from the canal. Negative flow is into the lake and positive flow is into the canal. Averages are for individual flow directions. Zero flow days are excluded from averages.

The residence time of runoff in the canal systems is highly variable and is dependent on antecedent water levels in the project canals. After periods of low or no rainfall, the canal system water levels will be low, and subsequent rainfall will be stored in the system. To a certain degree, the project canals may act as elongated reservoirs. The residence times for the water in the system can be high, on the order of days to weeks. During high rainfall periods, the system can act much more like a natural stream, with continuous flow to the outfall structures. There is also a high degree of re-circulation. As water is pumped from the canals onto the fields for irrigation, it returns back to the local canals as ground water flow. The entire canal system can act both like a reservoir and as a naturally flowing river system.

Despite the intensive canal system, a number of basins in the SLEW have natural drainage routes to the SLE. The smaller basins B-4, B-5, and B-6 and the NF and TSL basins all contain smaller canal systems, but most of these canals drain into natural streams and rivers that do not have structural control.

2.3.3 Agricultural Irrigation Practices

Other unique characteristics of the watershed are the irrigation practices. Water for irrigation is drawn both from the tertiary canal systems and from the Floridan aquifer. However, the rates, amounts and timing of the irrigation are not known, nor are the relative volumes of water drawn from either the canals or from the Floridan. This is an important aspect, since water drawn from the Floridan is essentially an additional input of water into the system that will affect the average flow rates through the canal system. It is estimated that about 28.5% of the irrigation water was derived from subsurface sources. It is necessary to supplement this missing information with an estimate of 'irrigation demand' in the modeling analysis.

2.3.4 Rainfall

Rainfall data was obtained from the recently updated and corrected NEXRAD database maintained by Dr. Fuelberg at Florida State University (FSU). The database contains rainfall data for 2-mile by 2-mile cells across the southern portion of Florida. The hourly data covers the period of 1996-2004 with one gap during March of 1999. The centers of the 2-mile by 2-mile cells covering south Florida are identified in Figure 2-16.

The NEXRAD data did not cover the entire calibration and validation period and was missing data for the March, 1999 period. For these periods supplemental rainfall data was used. Rainfall data was previously developed for each basin using a Theison Polygon approach (URS, 2000) and those data were adopted when the NEXRAD data was not available.

2.3.5 Evapotranspiration

Evapotranspiration (ET) data was provided by SFWMD. Data originated in the DBHydro database for monitoring station SVWX. The ET data was reported on a daily basis for the calibration/validation period. The data had been previously reviewed for quality control by Dr. Yongshan Wan of SFWMD for the given period of 1965 through 2000. Experience-based adjustments were made to correct anomalies in the ET data. To complete the dataset for the 2001-2005 period, additional data was downloaded from DBHydro for weather station SVWX. This data was adjusted in similar manner and amended to the existing time series for input to the model. A time series plots of original (top) and corrected (center) ET data are provided in Figure 2-17, along with a seasonal average plot (bottom).

2.3.6 Water Budgets

Basin-wide water budgets can be developed from the measured data for the C-24, C-23 and C-44 basins, using the daily discharge data at the basin outfalls, measured rainfall from the NEXRAD data base and the basin areas. However, in each basin an unknown amount of irrigation water is pumped from the Floridan Aquifer, and therefore the complete budget cannot be developed. A comparison between rainfall and discharge for each basin is provided in Table 2.6. The C44 basin discharge in cfs includes contributions from Lake Okeechobee.

Table 2-6. Average of the Daily-Averaged Flow and Stage Data for Structure Stations in each Basin.

Basin	Acres	Rainfall (inches/yr)	Discharge (cfs)	Discharge (inches/yr)	External Irrigation (inches/yr)	Losses* (inches/yr)
C-24	87,6	54.6	246.8	24.7	1	30.9
C-23	112,3	50.1	202.7	15.6	1.5	36.0
C-44	115,9	53.6	684.2*	14.2	0.5	39.9
SLE	171,3	51.1	N/A	N/A	N/A	N/A

Estimates of the annual irrigation contribution, available in URS (2000) were used to complete the budget. It appears that the discharge from the C24 basin, on a per-acre basis, is significantly larger than those for the C23 and C44 basin, even when considering the uncertainty in the irrigation contributions. Currently, there is no definitive explanation for this difference in the measured data for each basin. However; undocumented inter-basin transfers of water may have occurred and could explain the differences.

2.4 MODEL FORCING DATA- WATER QUALITY

Many water quality monitoring programs have been developed throughout the years to aid in the understanding of the SLE system and to aid in the quantification of the general health of the system as a whole. Data sources investigated are listed below.

2.4.1 Solar Radiation

Solar radiation promotes algae growth through photosynthesis and by increasing water temperature. It also can affect evapotranspiration, decreasing the amount of water in the drainage systems of each the basin, which inversely increases potential algae growth by a decrease in flow, a limitation in gate operations, and a resultant increase in water temperature due to the decrease in volume.

Due to the limited availability of monitoring stations, one station was used to provide this input for all SLE models. Weather monitoring station SVWX provided the data for the entire calibration period. Station SVWX is located in Figure 2-10. A time series plot and seasonal average plot of the data are provided in Figure 2-18.

2.4.2 Temperature

Monthly surface water temperatures were collected at the structure stations S49, S80, and S97. Additional water temperature data was provided at Gordy Road structure, located on C-24 canal and HR1 station located in the SLE. Monitoring stations are located in Figure 2.1. Time Series plots of the temperature data is provided in Figure 2-19. These data were used as input into the models.

2.4.3 Regional Winds

Wind data was collected from the National Data Buoy Center's (NDBC) C-MAN station LKWF1 stationed on a pier in Lake Worth, FL. This station offered the most comprehensive wind dataset in the SLE area. The Station has archived hourly wind data from 1984 to October of 2004. Data was collected for the majority of the calibration/validation period. Wind direction, wind speed and wind gust data were available. A wind rose diagram is presented in Figure 2-20, indicating the dominant wind characteristics in the St. Lucie area. Winds are predominantly generated from the easterly direction and have higher wind speeds in the drier, winter months. Seasonally distributed, daily averaged winds are presented in Table 2-8.

Table 2-7. Monthly variation of Daily Averaged wind speeds (m/s).

Month	Maximum	Mean	Minimum
1	13.48	5.40	2.21
2	12.39	5.57	2.07
3	12.06	6.09	2.45
4	12.27	5.84	1.40
5	10.76	5.30	1.80
6	10.06	4.54	1.87
7	9.85	4.21	1.83
8	11.30	4.19	1.93
9	19.70	5.16	1.17
10	13.94	5.97	1.75
11	16.98	6.14	2.18
12	15.91	5.61	2.22

These wind data were used indirectly in the model to estimate the range of the re-aeration coefficient values.

2.4.4 EMC Development

2.4.4.1 FDEP 2005 Estuary WQ Monitoring Program

In April of 2005, FDEP began a water quality sampling program in the SLE. The program was designed to last for one year and to encompass several different analytical parameters. Three YSI-Sondes devices were placed throughout the estuary in stations identified in Figure 2-21. The devices collected continuous data at those three locations for one year, beginning in April of 2005 and concluding in March of 2006. In addition to the high-frequency data, FDEP conducted bi-weekly sampling in eight stations throughout the estuary and analyzed those samples for nutrients, chlorophyll, and several physical parameters. Sampling locations are also identified in Figure 2-21.

2.4.4.1.1 High Frequency DO Dataset

The YSI-Sondes devices collected continuous measurements on 30-minute intervals for DO, salinity, temperature, specific conductance, water depth and pH. Devices were serviced on a monthly basis, at which time data was downloaded and the devices were recalibrated. Data was then analyzed and corrected by FDEP personnel based on a system developed by FDEP, to account for inaccurate readings recorded during systematic buildup of sediments and biota on the Sondes devices. Corrected DO data was provided by FDEP for analysis. A sample of the DO measurements is presented in Figure 2-22 for both top and bottom measurements at station C.

2.4.4.1.2 Biweekly Sampling

Biweekly sampling began in March of 2005, which included the profile field measurements of DO, temperature, pH, and salinity on roughly 0.5 m depth intervals. Top and bottom interval sample were collected and sent for laboratory analysis. Analysis was conducted for each of the above parameters plus color, conductivity, turbidity, conductance and total suspended solids. Additionally, the samples were analyzed for total nitrogen, total phosphorus and the chlorophyll suite: Chlorophyll-A, Chlorophyll-B, Chlorophyll-C, Chlorophyll-A (Corrected) and Phaeophytin. An example of the grab sample data is shown in Figure 2-22 for DO, with a comparison to profile data and the continuous YSI data.

2.4.4.2 BOD

No regular BOD sampling program in has yet been initiated in the SLE. The only site-specific BOD data available for SLE was provided by FDEP following a one-day sampling event on April 12, 2006, in which 18 stations were sampled throughout the estuary. Sample stations are indicated in Figure 2-23. Table 2-7 lists the BOD measurements collected. The mean value was 2.7 mg/L, with a maximum of 4.5 mg/L and minimum of 1.4 mg/L.

Table 2-8. BOD values measured in SLE April 12, 2006.

SITE LOCATION	DATE SAMPLED	TIME	RESULT	UNITS
16A	4/12/06	12:32	1.8	mg/L
16B	4/12/06	13:15	2.7	mg/L
16C	4/12/06	12:07	4.5	mg/L
MIDWAY	4/12/06	13:43	3.4	mg/L
18A	4/12/06	14:17	3.9	mg/L
18B	4/12/06	14:03	2.4	mg/L
NT	4/12/06	13:33	1.9	mg/L
7T	4/12/06	13:11	1.8	mg/L
121	4/12/06	9:44	4.5	mg/L
BESSEY 5	4/12/06	10:12	2.9	mg/L

SITE LOCATION	DATE SAMPLED	TIME	RESULT	UNITS
R00S	4/12/06	12:50	1.6	mg/L
21B	4/12/06	10:30	4.3	mg/L
27P	4/12/06		4	mg/L
22B	4/12/06	12:12	1.6	mg/L
ST	4/12/06	10:50	1.8	mg/L
25B	4/12/06	8:58	1.8	mg/L
SFDP	4/12/06	9:30	2.1	mg/L
SFORK	4/12/06	9:58	1.4	mg/L

2.4.4.3 SOD

Literature-based, SOD data was found from the EPA. During a sampling program operated from 1977-2001, in-situ chambers measured SOD and water temperature. SOD values were reported in mean, minimum, and maximum. Bottom sediments at each sample location were analyzed in order to correlate the SOD values with specific sediments. SOD values for water bodies in Florida, Georgia and Alabama were analyzed in an effort characterize SOD values, which could correspond to similar water bodies in the SLE.

The EPA, in conjunction with FDEP also collected site-specific values at four stations in the SLE, in March and again in June of 2005. Sample locations are identified in Figure 2-23.

2.4.4.4 IFAS ISCO

The Institute for Food and Agricultural Sciences (IFAS) ISCO dataset was collected from an EMC study conducted by University of Florida periodically from 2001 to 2004. Each station was separated and analyzed based one of two land uses: urban (residential or recreational) or agricultural. The station locations and their associated land-uses are shown in Figure 2-24. Total Nitrogen data at the North and South Pasture stations are shown in Figure 2-25. The intra-event data is compressed on the time scale in these plots due to the long deployment period. However, it is evident that there is large variability within each event and within the means for each event. Data for Total Phosphorus are shown in Figure 2-26 for the Butterfield and Elkham stations. The range of values within each event indicates a large degree of variability, and the means are not as consistent for these stations.

2.4.4.5 FDEP ISCO

Seven sample locations were established by FDEP and data was collected during rainfall events over three months in the Fall of 2005. Sample locations represented four different land-use designations: golf course, residential, agriculture-citrus, and agriculture-pastures. Station locations are shown in Figure 2-24. Time series plots are provided in Figure 2-27 for Total

Nitrogen for two events at the Floresta stations and for three events occurring at the Gator Trace station. The data within a single event indicates some variability, although the mean values for each event are less variable.

2.4.4.6 Urban Runoff Study (SLT stations)

A study conducted by SFWMD is the most comprehensive dataset used in ABMC development. For forty-five stations located throughout the SLEW (Figure 2-28), grab sample data were collected approximately every two weeks spanning Fall of 2001 through the end of 2005 and analyzed for nutrients. The SLT stations were not originally associated with a land-use, and therefore, the association needed to be established. Land-use designations were developed by plotting the location of each SLT station over a GIS coverage of land-use, along with a sub-basin boundary designations. An example of this plot for SLT-15 is shown in Figure 2-29. Primary land-use was established based on the positioning of the station location. Secondary land-uses were established based on land-uses identified "upstream" of the station. If the station appeared to be affected by multiple land-uses, then it was discarded from the set for the purposes of establishing the runoff concentration inputs for the WaSh model. The land-use designations were reviewed and verified by Boyd Gunsalus of the SFWMD, who has first-hand knowledge with the sample locations. Example data for three SLT stations, representing wetlands, forest and residential land-uses is shown in Figures 2-30 through 2.32. The data are plotted to show seasonal trends with the monthly means indicated. It is clear that there is large variability within the data for both TN and TP at all sites, and a persistent seasonal trend in the mean values. The variability appears to be higher for phosphorus and the variability appears to increase during the wet season. The data indicate that the mean TP and TN increase during the wet season, by as much as a factor of 4.0 for TP and by a factor of 1.5 for Nitrogen.

2.4.4.7 FDEP BMP Study

The FDEP collected event data at stations distributed throughout the SLE basins from1998 through 2000. The stations were selected to represent different land-uses, some with implemented BMPs. The location of these stations is shown in Figure 2-33. Data was collected immediately after (or during) a rainfall event when flow was occurring at the monitoring station. Example TP and TN data for two stations, one station representing citrus and one for improved pastures, are shown in Figures 2-34 and 2-35. The data are shown as monthly mean values with confidence intervals on the means. The data are also shown as wet season and dry season means with confidence intervals on the means. The results indicate that the TN and TP concentrations are typically larger in during the wet season than during the dry season.

2.4.4.8 Grassy Waters Preserve Sampling Project

The Grassy Waters Preserve consists of nearly 13, 000 acres of wetlands located in Northern Palm Beach County. Water from the preserve is used as a potable water supply to local metropolitan areas. Although once considered the northern-most boundary of the Everglades, the wetlands are now bisected by project canals. However, the water quality is still considered pristine.

In January of 2004, FDEP initiated the first water quality monitoring program in the Grassy Waters Preserve. Samples were collected roughly every 4-6 weeks and analyzed for physical

parameters, DO, and nutrients. In the absence of adequate water quality data in the SLT dataset for the establishment of ABMC for wetlands, the Grassy Waters dataset was analyzed. Average values for TN and TP are 0.83 and 0.027 mg/L, respectively.

2.4.4.9 Residuals

Residuals comprise the solid components of sewage waste water. After waste water enters a treatment facility, the liquids and solids are separated. The liquids proceed through the treatment facility and are ultimately reintroduced into the water supply. Solids are dried and often sold to local land owners for use as fertilizer. Residuals are typically delivered to a site and deposited in large piles until they can be distributed as fertilizer. Figure 2-36 shows the distribution of the only registered residuals permits in the SLE region and Figure 2- 37 presents the water quality data from those sites. These residual piles are seen by many as significant point source discharges for nutrients. In fact, Martin County no longer permits the use of residuals as fertilizers. Runoff from residual piles has been measured with extremely high nutrient levels. However, as the areal extent of the residual piles are spatially insignificant, the volume of runoff actually in contact with the residuals is small and therefore the impact to the hydrologic system is relatively insignificant on the whole.

However, the effects of residuals on nutrient loads in runoff are much more significant when the residuals are spread out in thin layers, as when distributed as fertilizer. The lateral distribution allows for elevated nutrient levels to be introduced to a greater volume of runoff, thereby providing a much greater impact to the overall hydrologic system.

The most comprehensive water quality data for residuals was collected from Circle I Ranch. Figure 2.38 shows the location of the residual pile at the site and the water quality sampling locations. The footprint of the pile is quite small, limiting the amount of rainfall that will actually come in contact with the nutrients. Analysis in Figure 2.39 demonstrates the minimal impact on total nutrient load in the estuary. As the residual piles do not have a significant affect on the nutrient loading to the SLE, they were not considered in the modeling analysis.

2.5 MODEL CALIBRATION DATA

2.5.1 USGS Salinity Regime

Salinity as also monitored at the US1 and A1A locations (Figure 2-10). A representative sample of the salinity data is presented in Figures 2. 40 – 2-43. The plots show salinity data for each of the bridge stations during two different time periods. The general temporal trend shows an increase in salinity through the fall and into the dry, winter season (Fig. 2.11) and a general decrease in the salinity during the wetter, summer months (Fig. 2.12). Diurnal fluctuation of salinity can vary from as little as 5 parts per thousand (ppt) daily up to 20 ppt. Comparisons of surface and bottom measurements of salinity indicate that the estuary stratification varies in response to episodic freshwater discharges on daily or monthly time scales.

In Figures 2-42 and 2-43, salinity data has been separated into upper and lower zones to compare the salinity variations between the two monitoring stations. The A1A station, located closer to the inlet and therefore more strongly influenced by tidal variations than fresh water discharge, has a higher salinity than the US1 station and also a larger diurnal variation. Figure 2-42

indicates, for both stations, a general increase in salinity throughout the dry season in the fall of 2003, while Figure 2-43 indicates the general decrease in salinity in the wetter summer months of 2004.

Additional monthly salinity data is available for HR1 station, located within the North Fork. Although the data is not high-frequency data, the period of record for the salinity data set covers a longer period. HR1 salinity data is presented in Figure 2-44.

2.5.2 SFWMD Routine Monthly Monitoring Program

Water quality characteristics for each can be documented for monitoring stations adjacent to each of the control structures and at several monitoring stations within the estuary. Monitoring stations include C24S49, C23S48, C44S80, HR1, SE01, S308, SE03, SE06, SE08, and SE09. Station locations are identified in Figure 2-10. Sampling intervals averaged every two weeks. Water quality data was analyzed for the following data: Ammonia, Nitrate, Organic Nitrogen, Total Nitrogen, Orthophosphate, Total Phosphate, Dissolved Oxygen, Chlorophyll-A (Corrected), Total Suspended Solids, Color, and Turbidity. Time series data ranges from January 1995 through December 2005. A summary of water quality data is presented in Table 2-4, where data is analyzed by Minimum, 25^{th} percentile, 50^{th} percentile or median, 75^{th} percentile, maximum and mean.

Table 2-9. Measured Data Summary for Structure Stations.

C23	NH4	NO3	Norg	TN	OPO4	TPO4	D.O.	TURB	COLOR	T.SUS.SD
Maximum	0.52	0.74	2.30	2.55	0.88	0.96	11.18	25.1	305.0	71.0
75 Percentile	0.14	0.20	1.29	1.57	0.34	0.43	6.80	4.8	176.5	4.0
50 Percentile	0.04	0.09	1.04	1.28	0.20	0.28	5.31	3.3	97.0	-1.0
25 Percentile	0.01	0.04	0.82	0.96	0.10	0.17	4.25	2.6	62.0	-3.0
Minimum	0.00	-0.02	0.47	0.55	0.02	0.07	0.45	1.1	12.0	-3.0
Mean	0.09	0.14	1.07	1.29	0.24	0.30	5.55	4.4	122.0	2.3

C24	NH4	NO3	Norg	TN	OPO4	TPO4	D.O.	TURB	COLOR	T.SUS.SD
Maximum	0.39	0.61	10.45	10.50	0.80	1.02	10.70	17.0	400.0	47.0
75 Percentile	0.11	0.10	1.37	1.63	0.24	0.31	6.34	3.6	187.5	4.0
50 Percentile	0.05	0.05	1.18	1.32	0.17	0.23	4.83	2.5	107.0	1.6
25 Percentile	0.01	0.02	0.94	1.07	0.10	0.14	2.72	1.9	62.5	-3.0
Minimum	0.00	0.00	0.00	0.00	0.01	0.03	0.29	1.0	35.0	-3.0
Mean	0.08	0.08	1.29	1.45	0.18	0.25	4.70	3.0	134.0	1.6

C44	NH4	NO3	Norg	TN	OPO4	TPO4	D.O.	TURB	COLOR	T.SUS.SD
Maximum	0.44	0.63	2.53	2.80	0.23	0.28	10.34	17.8	265.0	39.0
75 Percentile	0.10	0.32	1.12	1.46	0.15	0.19	7.31	4.5	146.0	4.0
50 Percentile	0.02	0.19	0.99	1.31	0.08	0.13	6.33	3.4	95.0	-3.0
25 Percentile	0.01	0.08	0.88	1.20	0.06	0.09	5.25	2.4	64.5	-3.0
Minimum	0.00	0.00	0.00	0.03	0.03	0.06	2.13	1.1	12.0	-3.0
Mean	0.06	0.21	1.03	1.33	0.10	0.14	6.18	4.0	111.1	1.1

S308	NH4	NO3	Norg	TN	OPO4	TPO4	D.O.	TURB	COLOR	T.SUS.SD
Maximum	0.32	0.71	4.44	4.89	0.58	0.91	12.58	255.0	220.0	541.0
75 Percentile	0.06	0.36	1.66	2.01	0.07	0.23	7.99	51.7	66.5	46.0
50 Percentile	0.03	0.22	1.37	1.69	0.05	0.16	6.88	27.4	43.0	23.6
25 Percentile	0.01	0.09	1.21	1.43	0.04	0.12	5.09	14.9	32.5	13.6
Minimum	-0.02	-0.24	0.62	0.92	0.00	0.08	0.33	2.3	10.0	1.2
Mean	0.06	0.24	1.53	1.82	0.08	0.19	6.59	39.3	56.0	43.1

Measured data for the HR1 and the SE Stations are presented in Table 2-5. The DO measurements for most estuary stations were collected at discreet depth intervals. For analysis purposes, upper and lower zones were identified for each stations based on the depth of samples available and the number of sample per depth. For most stations, the upper zone was represented with the 0.5 or 1.0 meter data and the lower zone with the 2.5 or 3.0 meter data.

Table 2-10. Measured Data Summary for Estuary Stations.

HR1	NH4	NO3	Norg	TN	OPO4	TPO4	DO- Upper	DO- Lower	TURB	COLOR	T.SUS.SD
Maximum	0.58	0.67	2.31	2.34	0.88	1.04	12.27	10.66	19.5	272.0	65.0
75 Percentile	0.10	0.08	1.19	1.33	0.21	0.26	8.09	6.76	4.9	98.0	10.0
50 Percentile	0.03	0.02	0.95	1.10	0.15	0.20	7.25	5.51	3.6	48.0	6.0
25 Percentile	0.00	0.00	0.79	0.86	0.09	0.15	6.31	3.83	2.7	30.8	4.0
Minimum	0.00	-0.01	0.00	0.02	0.03	0.07	3.77	0.13	0.2	14.0	-4.0
Mean	0.07	0.06	0.99	1.12	0.17	0.22	7.29	5.34	4.6	71.5	7.3

SE01	NH4	NO3	Norg	TN	OPO4	TPO4	DO- Upper	DO- Lower	TURB	COLOR	T.SUS.SD
Maximum	0.45	0.61	2.33	2.84	0.32	0.57	9.82	8.70	110.0	180.0	116.0
75 Percentile	0.13	0.10	0.92	1.08	0.11	0.14	7.04	6.44	6.9	44.0	17.0
50 Percentile	0.06	0.02	0.74	0.86	0.06	0.08	6.33	5.96	5.4	20.0	11.0
25 Percentile	0.01	0.01	0.41	0.51	0.03	0.06	5.73	5.51	4.3	11.0	7.4
Minimum	-0.02	-0.06	-0.77	-0.51	0.00	0.01	2.58	2.47	-0.1	-1.0	-3.0
Mean	0.08	0.07	0.67	0.81	0.08	0.12	6.45	5.96	7.4	37.8	14.1

SE02	NH4	NO3	Norg	TN	OPO4	TPO4	DO- Upper	DO- Lower	TURB	COLOR	T.SUS.SD
Maximum	0.44	0.63	2.05	2.64	0.53	0.63	9.84	9.80	104.0	191.0	123.0
75 Percentile	0.12	0.13	1.04	1.26	0.13	0.18	7.14	6.24	9.0	63.0	15.0
50 Percentile	0.05	0.03	0.86	1.01	0.09	0.12	6.43	5.55	5.1	31.0	10.0
25 Percentile	0.01	0.01	0.63	0.74	0.05	0.09	5.76	4.95	3.7	18.0	6.4
Minimum	-0.02	-0.02	-0.64	-0.51	0.02	0.05	3.13	2.28	1.5	5.0	-4.0
Mean	0.08	0.08	0.82	0.97	0.11	0.16	6.42	5.56	8.4	51.2	13.4

SE03	NH4	NO3	Norg	TN	OPO4	TPO4	DO- Upper	DO- Lower	TURB	COLOR	T.SUS.SD
Maximum	0.83	0.70	2.05	2.69	0.42	0.58	9.52	9.25	139.0	210.0	120.0
75 Percentile	0.13	0.13	1.13	1.40	0.18	0.22	7.56	6.91	10.2	72.0	16.0
50 Percentile	0.06	0.04	0.92	1.09	0.12	0.17	6.74	5.93	6.1	38.5	10.8
25 Percentile	0.02	0.01	0.74	0.85	0.08	0.13	5.77	4.92	4.2	25.3	7.0
Minimum	0.00	-0.01	0.00	0.01	0.04	0.07	3.43	3.08	1.7	9.0	-4.0
Mean	0.09	0.09	0.94	1.13	0.14	0.19	6.71	5.88	10.8	59.5	14.4

SE06	NH4	NO3	Norg	TN	OPO4	TPO4	DO- Upper	DO- Lower	TURB	COLOR	T.SUS.SD
Maximum	0.54	1.10	1.72	2.60	0.59	0.74	10.00	8.93	17.8	180.0	35.0
75 Percentile	0.11	0.11	1.10	1.33	0.24	0.32	6.35	5.57	5.8	93.0	8.0
50 Percentile	0.06	0.04	0.93	1.07	0.19	0.25	5.29	4.35	4.5	56.0	6.0
25 Percentile	0.02	0.02	0.79	0.87	0.13	0.18	4.17	3.48	3.4	42.0	5.0
Minimum	0.00	-0.01	0.16	0.31	0.06	0.09	1.14	1.13	1.2	24.0	-4.0
Mean	0.08	0.08	0.95	1.12	0.20	0.27	5.31	4.52	4.8	70.4	6.4

SE08	NH4	NO3	Norg	TN	OPO4	TPO4	DO- Upper	DO- Lower	TURB	COLOR	T.SUS.SD
Maximum	0.37	0.64	2.72	3.03	0.30	0.54	9.69	x	82.2	234.0	117.0
75 Percentile	0.10	0.21	1.33	1.59	0.16	0.24	8.02	x	14.0	77.0	20.8
50 Percentile	0.05	0.09	1.04	1.29	0.11	0.19	7.31	x	8.3	45.5	12.0
25 Percentile	0.02	0.02	0.86	1.01	0.07	0.15	6.12	x	5.2	33.0	9.0
Minimum	0.00	0.00	0.00	0.01	0.03	0.08	3.34	x	0.8	-1.0	-3.0
Mean	0.07	0.14	1.09	1.31	0.12	0.21	7.11	x	13.0	62.7	17.4

SE09	NH4	NO3	Norg	TN	OPO4	TPO4	DO- Upper	DO- Lower	TURB	COLOR	T.SUS.SD
Maximum	2.08	0.65	4.92	7.09	0.29	0.36	9.93	9.87	127.0	293.0	110.0
75 Percentile	0.06	0.15	1.17	1.36	0.13	0.19	7.87	7.32	11.4	93.8	12.2
50 Percentile	0.03	0.08	0.99	1.13	0.09	0.16	6.57	6.09	6.0	53.0	8.0
25 Percentile	0.00	0.02	0.83	0.95	0.07	0.13	5.12	4.68	3.8	38.0	5.0
Minimum	0.00	-0.01	0.01	0.20	0.02	0.07	1.66	1.05	1.5	25.0	-4.0
Mean	0.06	0.12	1.05	1.24	0.10	0.17	6.40	5.93	12.3	76.2	11.0

Measured data for each station is presented graphically in Appendix A for stations C24S49, C23S48, C44S80, S308, HR1, SE03, SE06, SE08 and SE09. The data is presented in the form of time series plots, frequency distributions, and seasonal averages. The most significant characterization is evident in the seasonal variation plots. A distinct seasonal trend can be seen for a number of parameters. There is a clear indication of an increase during the summer months of ammonia, orthophosphate, total phosphate, and color, and a decrease during the summer months in dissolved oxygen.

Chlorophyll data was available for most SE stations and HR1 station through the SFWMD routine monthly sampling program. Analytical data is provided on 0.5 meter depth increments for Chlorophyll-A, Chlorophyll-B, Chlorophyll-C, Chlorophyll-A(Corrected) and Pheophytin. In addition to the regular sampling plan, additional chlorophyll data was collected at additional stations located throughout the estuary, as part of the 2005 FDEP sampling plan. Sampling locations are identified in Figure 2.10. Tabular chlorophyll data for the estuary stations is presented in Table 2-6.

Table 2-11. Measured Chlorophyll Data Summary for Estuary Stations.

HR1	CHLOR A	CHLOR B	PHAEO	CHLA2	CHLOR C
Maximum	68.20	2.80	17.00	58.60	6.40
75 Percentile	17.05	-1.00	4.10	14.00	2.05
50 Percentile	11.00	-1.00	2.00	9.55	1.00
25 Percentile	5.95	-1.00	1.00	5.25	-1.00
Minimum	1.30	-1.00	-1.00	1.20	-1.00
Mean	13.81	-0.75	2.78	11.56	0.84
SE01	**CHLOR A**	**CHLOR B**	**PHAEO**	**CHLA2**	**CHLOR C**
Maximum	62.60	1.70	16.90	55.00	6.50
75 Percentile	9.00	-1.00	2.60	7.60	0.50
50 Percentile	6.05	-1.00	1.00	5.05	-1.00
25 Percentile	4.00	-1.00	-1.00	3.30	-1.00
Minimum	-1.00	-1.00	-1.00	-1.00	-1.00
Mean	8.40	-0.88	1.28	7.07	-0.16
SE02	**CHLOR A**	**CHLOR B**	**PHAEO**	**CHLA2**	**CHLOR C**
Maximum	71.70	8.00	16.10	63.30	12.00
75 Percentile	11.55	-1.00	3.00	9.40	1.00
50 Percentile	6.80	-1.00	1.50	6.00	-1.00
25 Percentile	4.85	-1.00	-1.00	3.85	-1.00
Minimum	-1.00	-1.00	-1.00	-1.00	-1.00
Mean	9.79	-0.77	1.62	8.25	-0.03
SE03	**CHLOR A**	**CHLOR B**	**PHAEO**	**CHLA2**	**CHLOR C**
Maximum	53.50	3.10	14.00	48.70	9.80
75 Percentile	14.85	-1.00	4.00	12.60	1.40
50 Percentile	9.80	-1.00	2.00	7.00	-1.00
25 Percentile	6.00	-1.00	1.00	4.70	-1.00
Minimum	-1.00	-1.00	-1.00	-1.00	-1.00

Mean	11.73	-0.80	2.44	9.69	0.28
SE06	**CHLOR A**	**CHLOR B**	**PHAEO**	**CHLA2**	**CHLOR C**
Maximum	62.00	4.20	27.00	51.00	7.40
75 Percentile	22.53	-1.00	6.35	17.83	2.48
50 Percentile	12.45	-1.00	3.45	9.20	1.00
25 Percentile	7.00	-1.00	1.70	5.28	-1.00
Minimum	1.30	-1.00	-1.00	1.20	-1.00
Mean	15.70	-0.67	4.32	12.53	0.91
SE08	**CHLOR A**	**CHLOR B**	**PHAEO**	**CHLA2**	**CHLOR C**
Maximum	47.20	2.70	24.30	42.20	11.10
75 Percentile	18.10	-1.00	5.58	13.75	1.70
50 Percentile	12.00	-1.00	3.20	9.00	-1.00
25 Percentile	7.50	-1.00	1.90	5.93	-1.00
Minimum	1.80	-1.00	-1.00	1.10	-1.00
Mean	13.95	-0.53	4.05	11.01	0.68
SE09	**CHLOR A**	**CHLOR B**	**PHAEO**	**CHLA2**	**CHLOR C**
Maximum	52.40	15.40	23.50	47.60	14.00
75 Percentile	23.35	-1.00	6.00	18.95	1.85
50 Percentile	11.40	-1.00	3.55	9.30	-1.00
25 Percentile	5.55	-1.00	1.10	4.00	-1.00
Minimum	1.70	-1.00	-1.00	-1.00	-1.00
Mean	15.42	-0.05	3.73	12.57	0.68

No chlorophyll data is available for canal stations in the upland basins.

2.5.3 Seasonal Variability

Water quality, water quantity and meteorological data in the St. Lucie Estuary have a very distinct seasonal signal. The dry, winter months are characterized by less rainfall, lower nutrient, and higher dissolved oxygen, while the wetter summer months are characterized by higher rainfall, higher nutrients, and lower dissolved oxygen. Figure 2-45 illustrates several parameters and their seasonal signal. Calibration was designed to address matching both levels and seasonal fluctuations of the measured data.

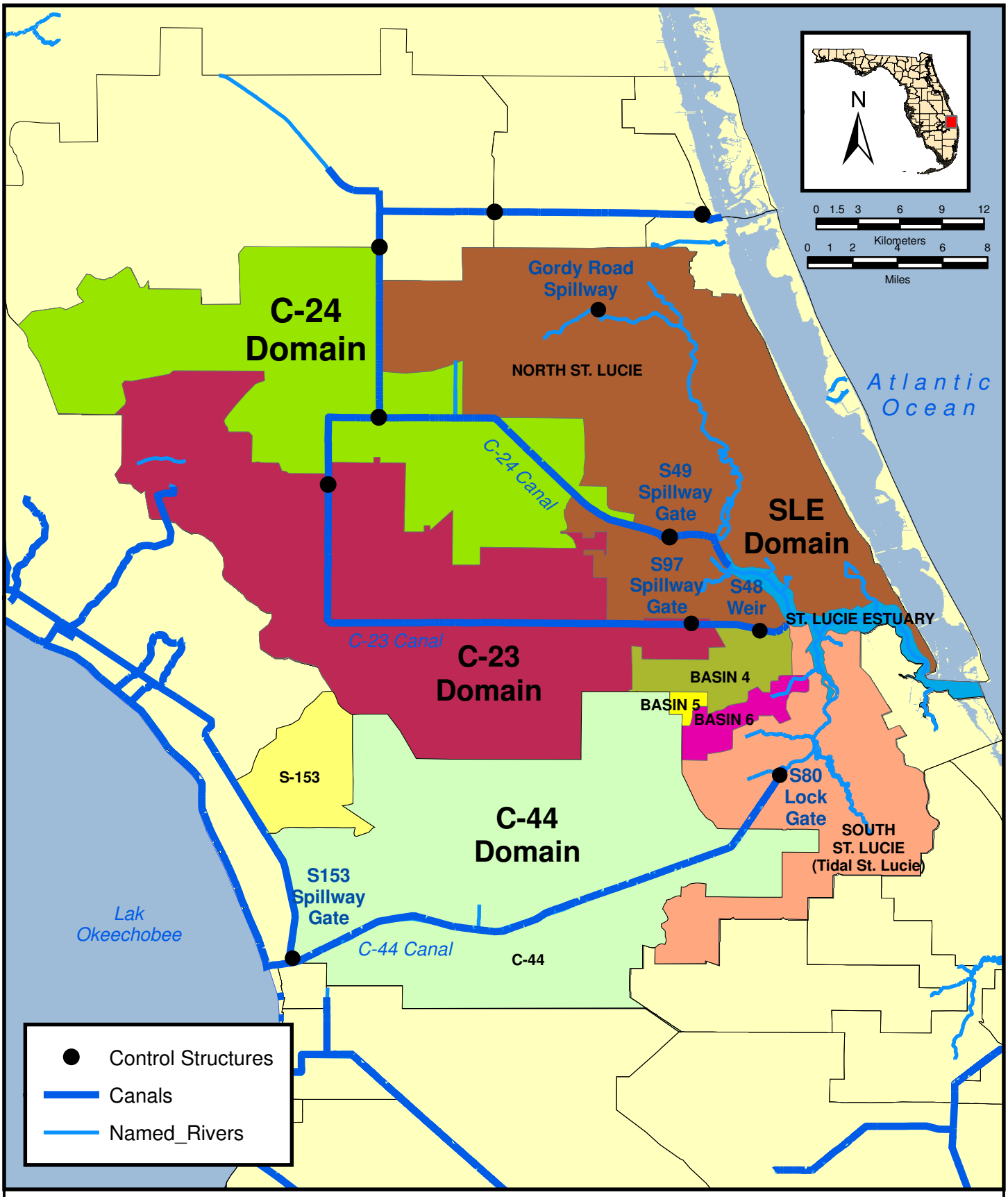

URS

Figure 2-1. Map of Basin Boundaries, Canal System and Control Structures (GIS coverages provided by SFWMD.)

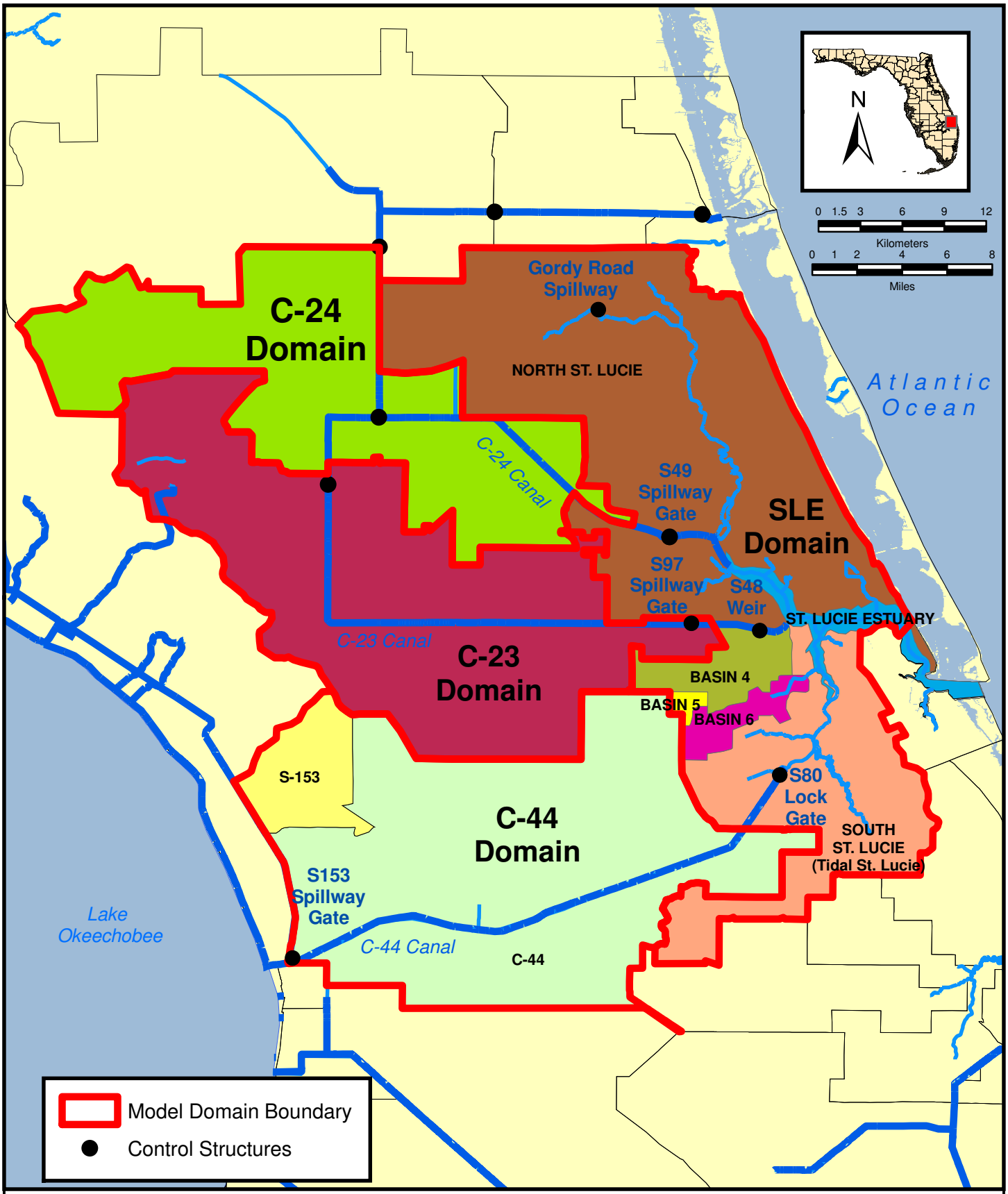

URS

Figure 2-2. Map of Model Basin Domains.
(GIS coverages provided by SFWMD.)

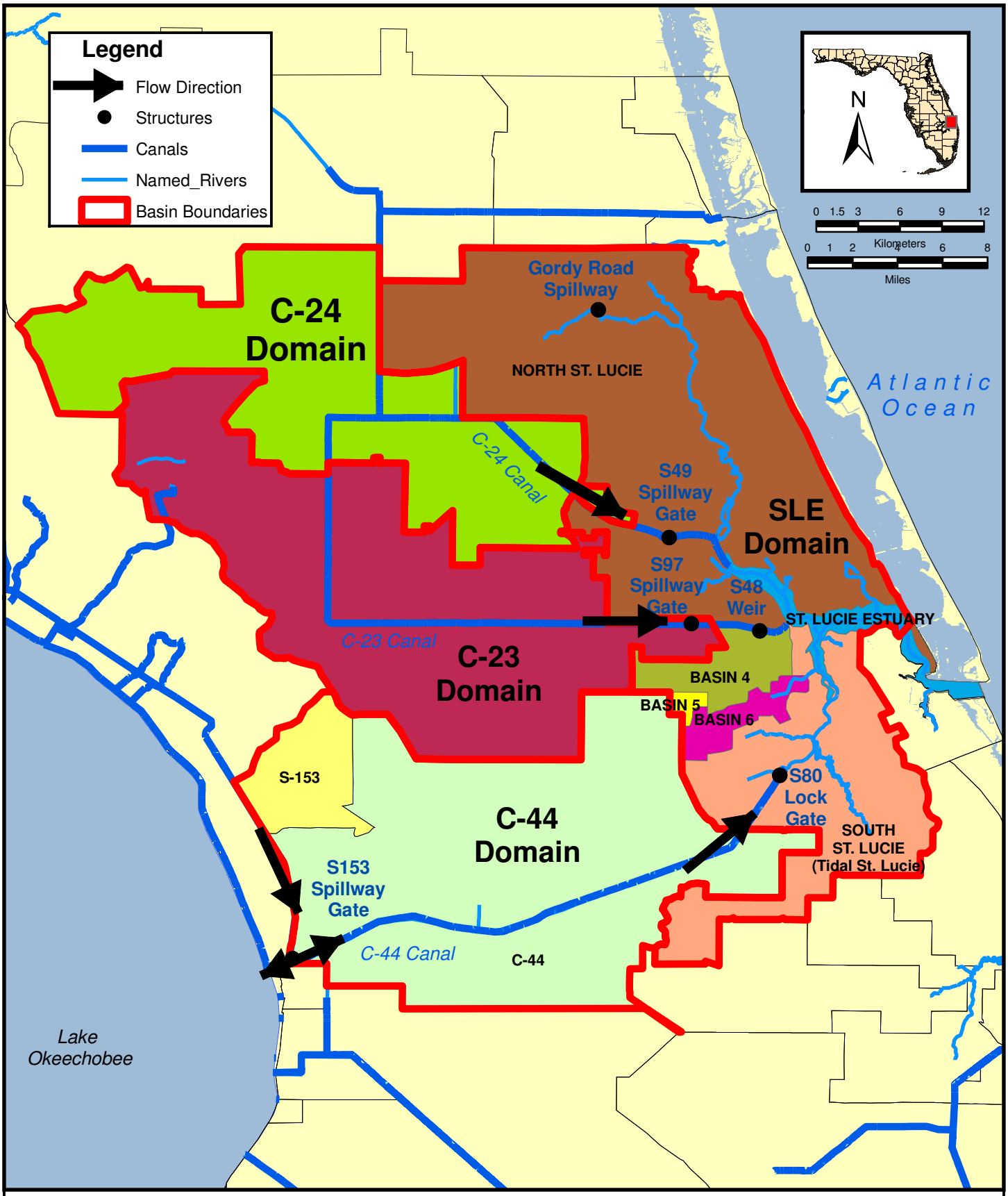

URS

Figure 2-3. Flow connectivity of Basins.
(GIS coverages provided by SFWMD)

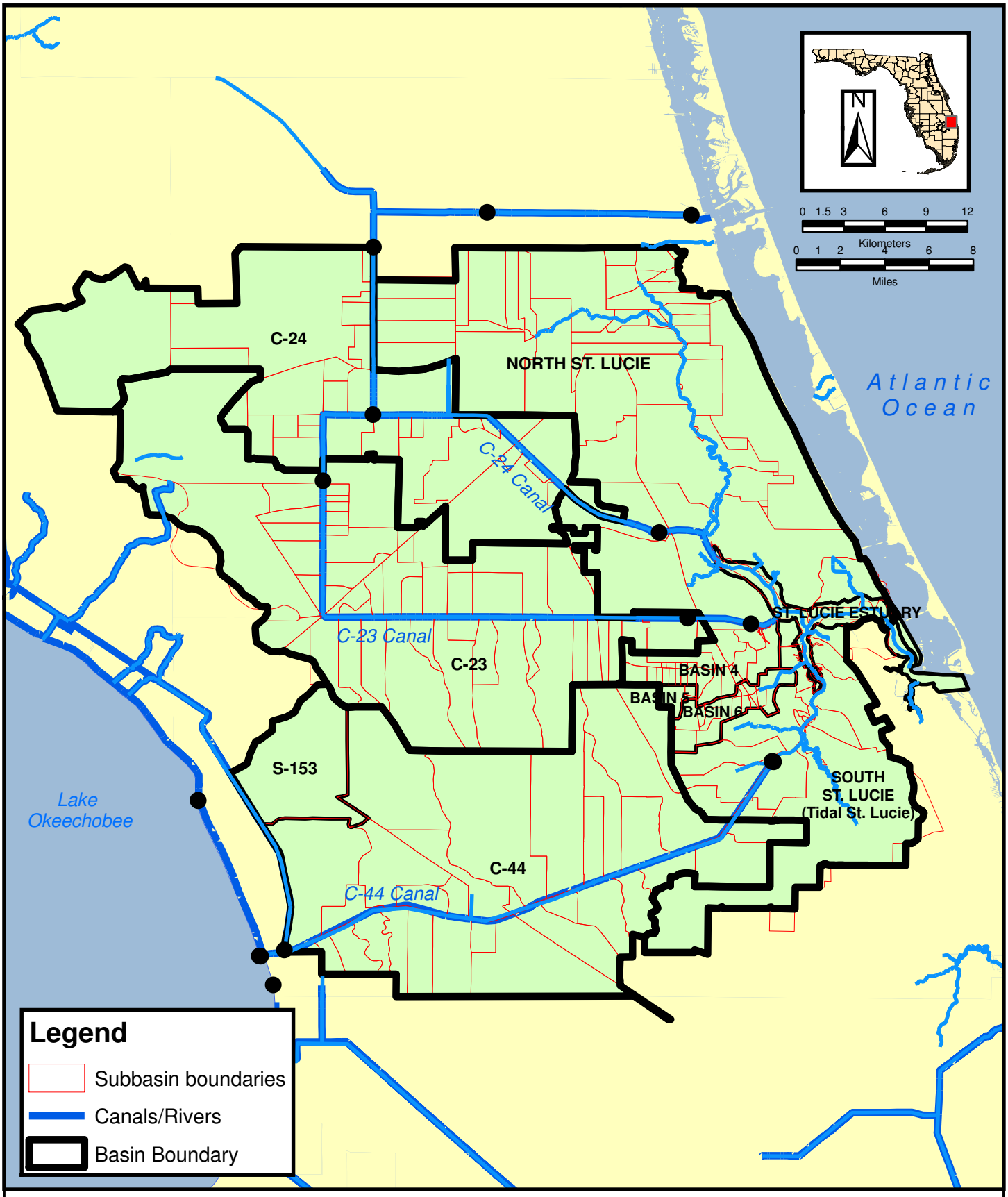

URS

Figure 2-4. Map of Subbasin Boundaries (Coverage provided by SFWMD)

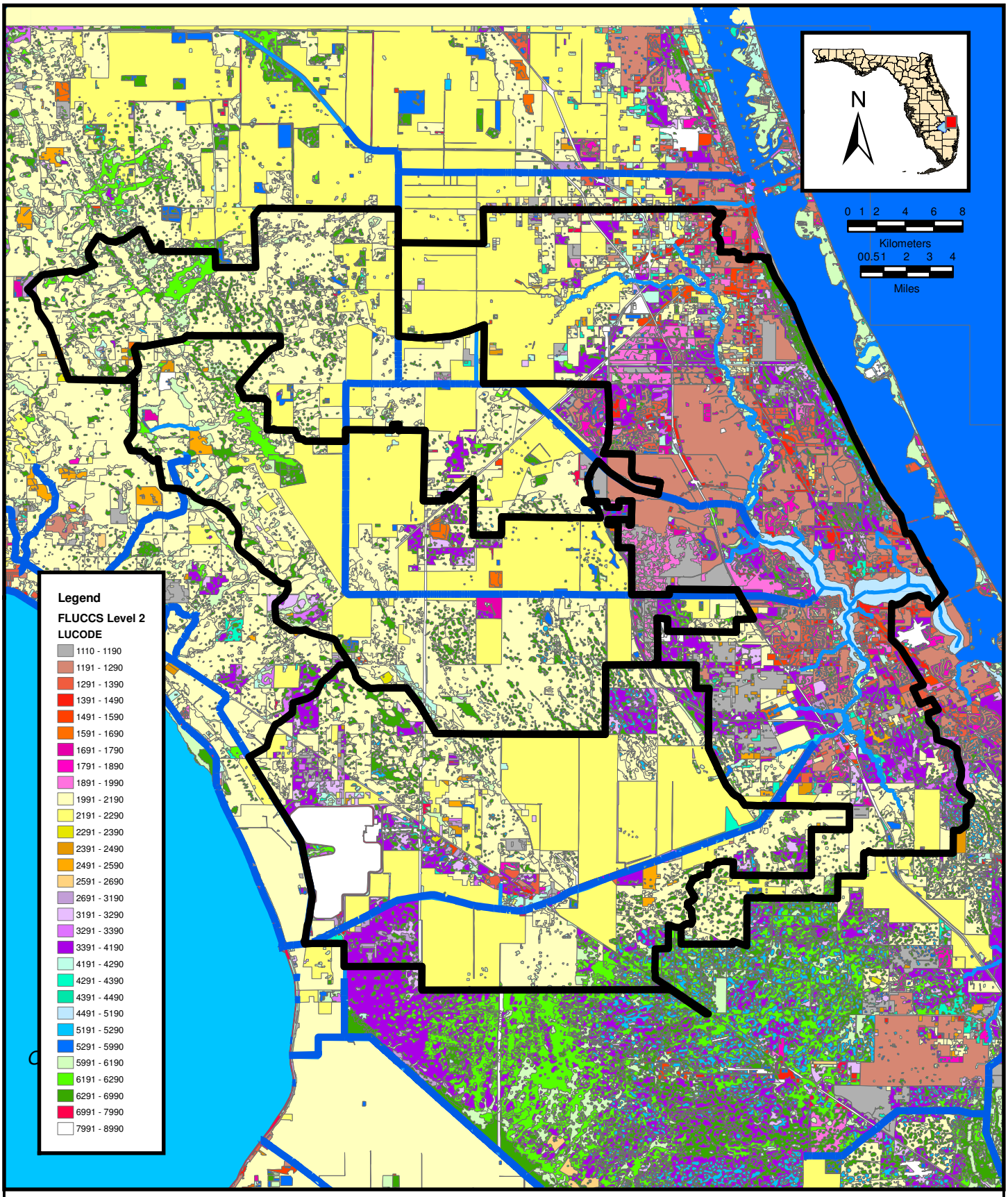

URS

Figure 2-5a. 1999 Land Use Designations.
(Information provided by SFWMD)

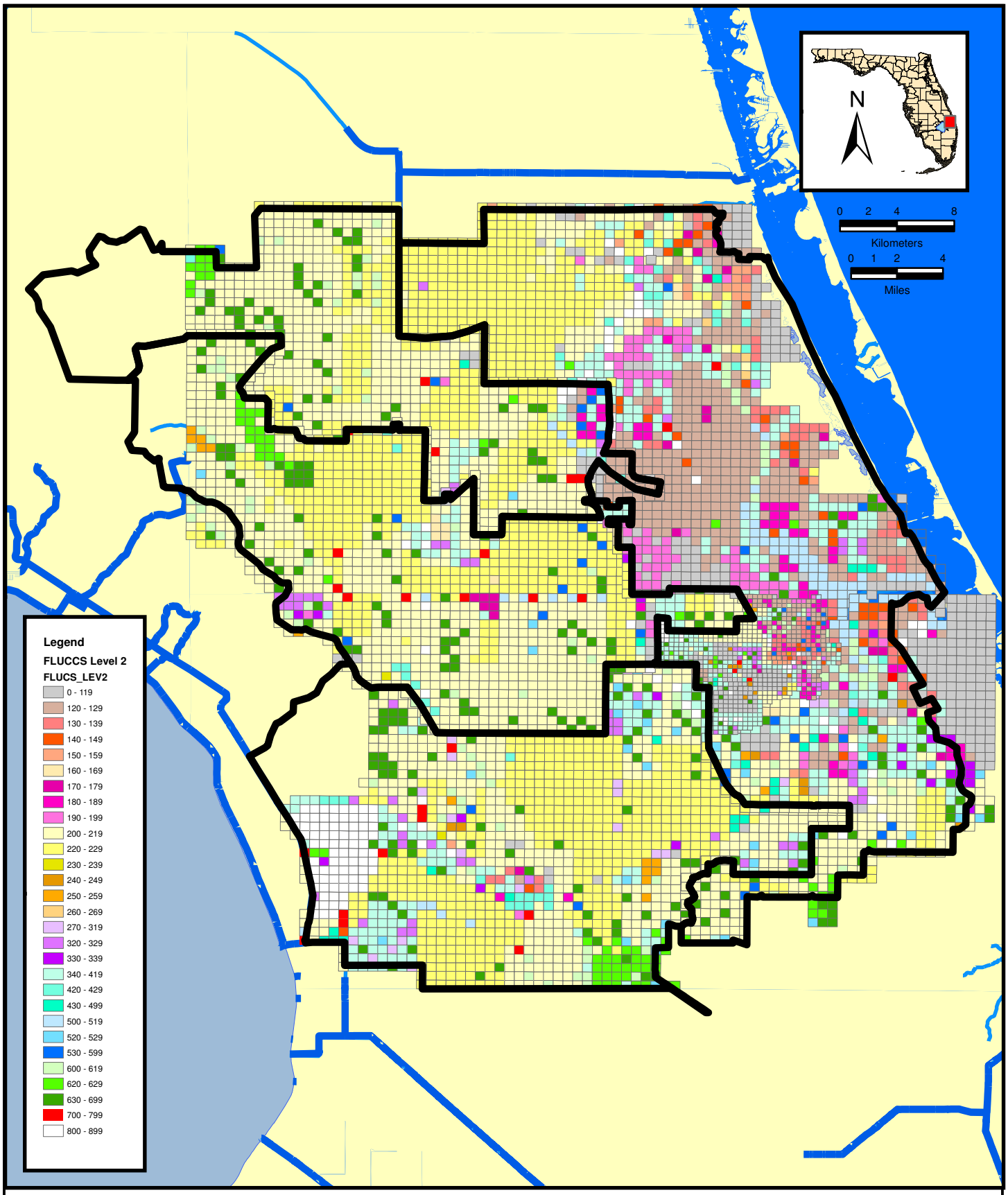

URS

Figure 2-5b. Adjusted Land Use Designations. (Information provided by FDEP)

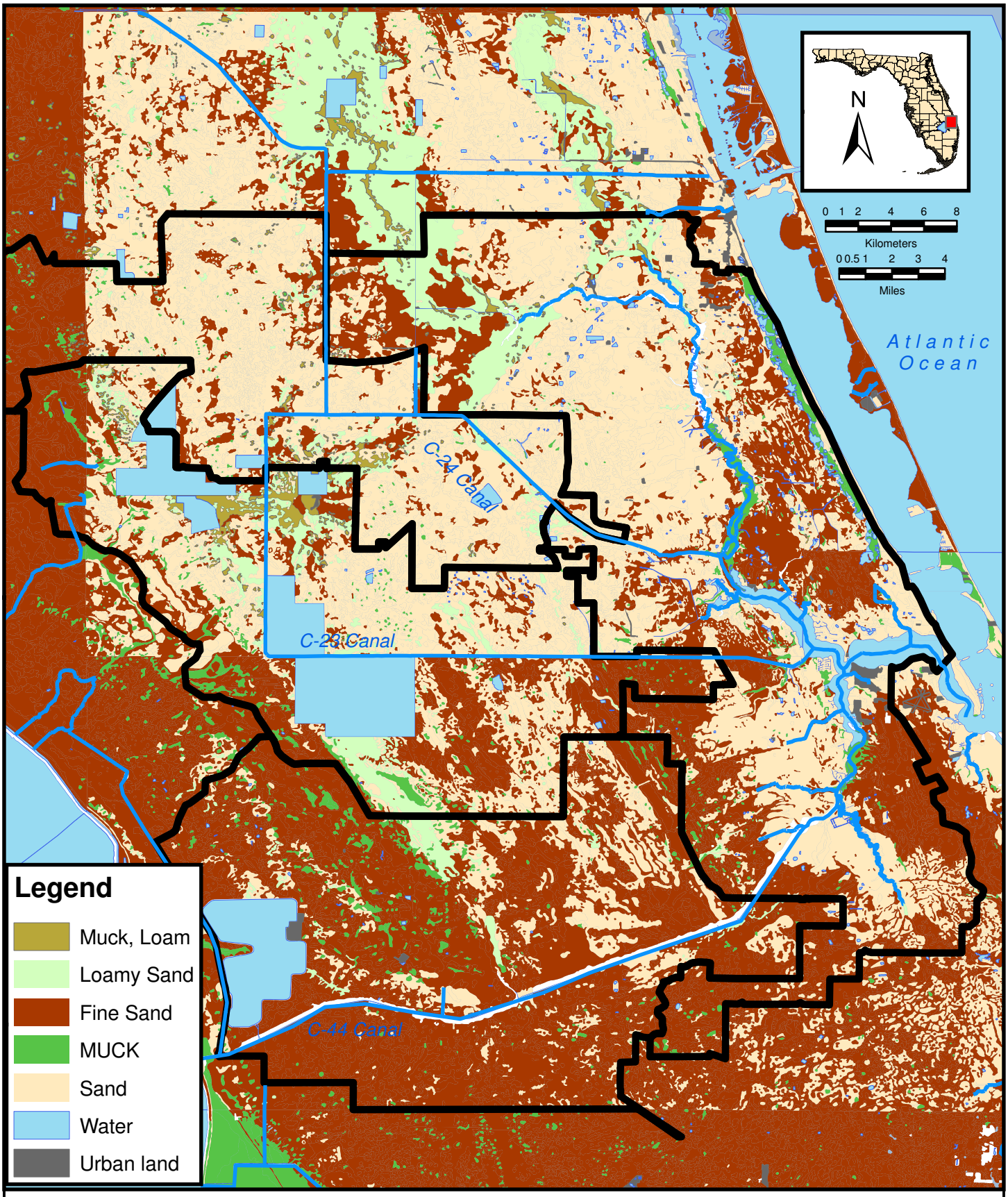

URS

Figure 2-6a. Watershed Soil Designations. (Coverage provided by SFWMD; data provided by USDA Soils Conservation Service.)

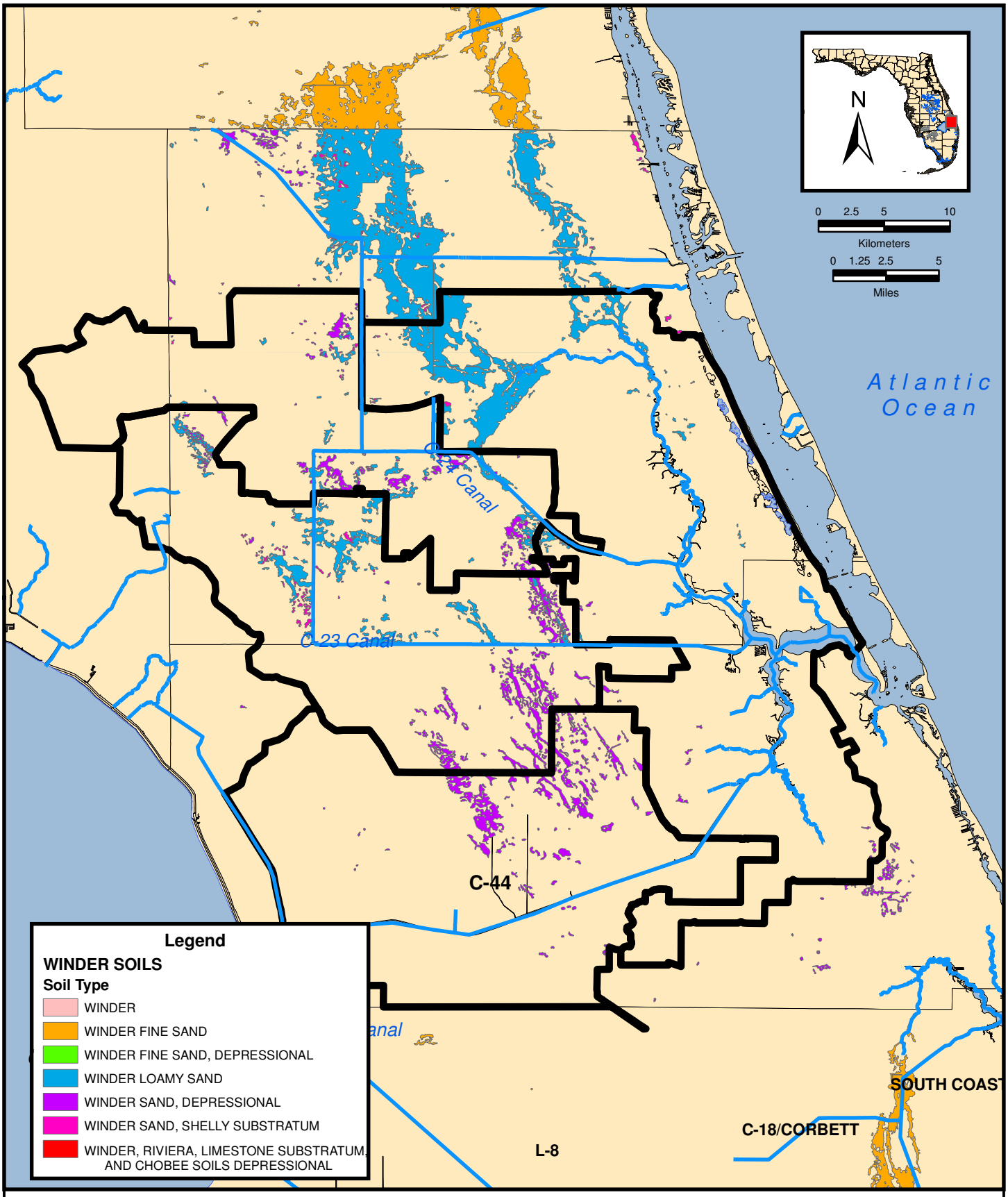

Figure 2-6b. Winder Soils Designations.
(Coverage provided by SFWMD; data provided by USDA Soils Conservation Service.)

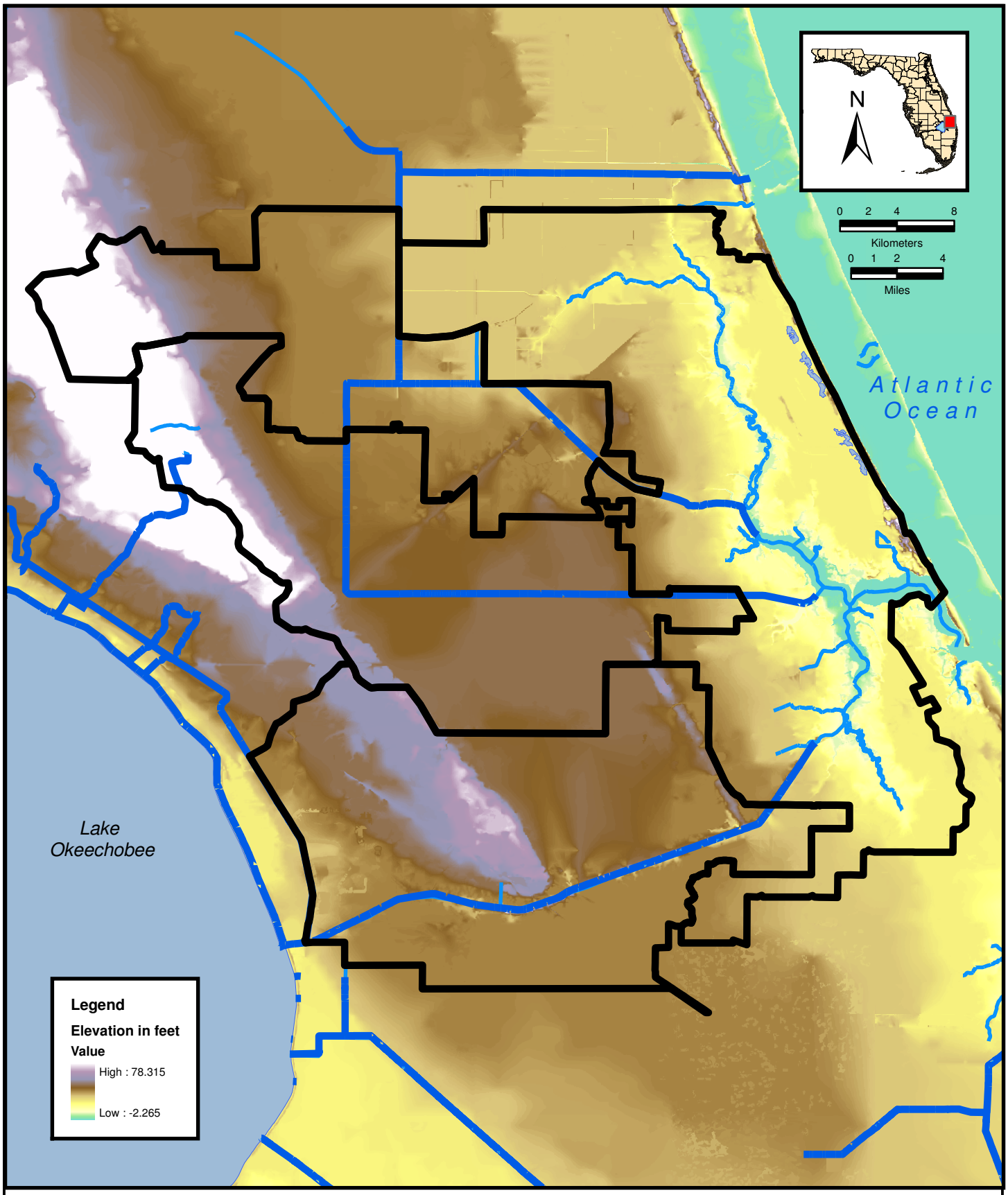

URS

Figure 2-7. Topographic Digital Elevation Map (DEM)
(Elevation data provided by SFWMD)

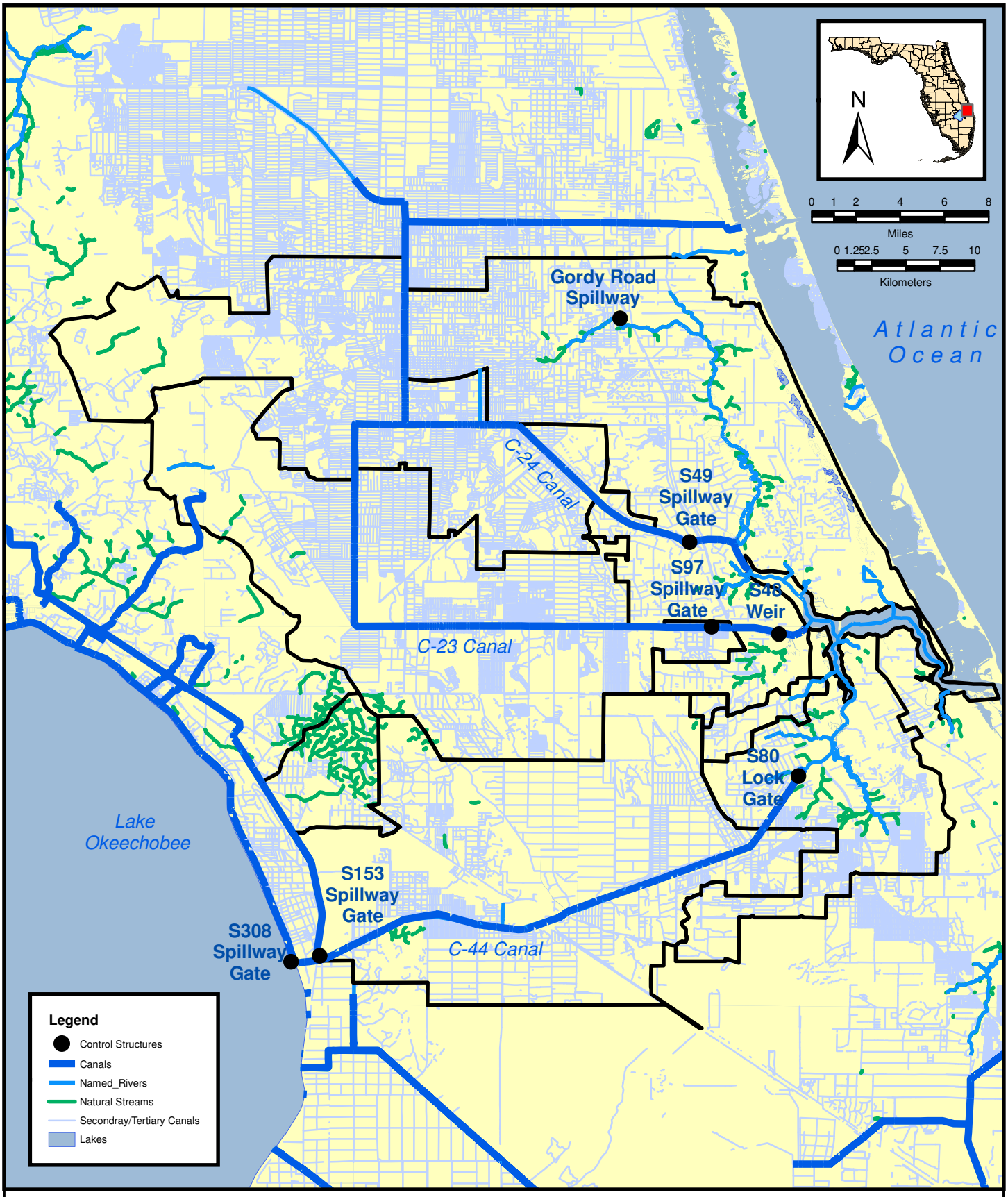

URS

Figure 2-8. Hydrography showing Primary Canals, Secondary and Tertiary Canals, and Natural Rivers and Streams. (Coverage provided by SFWMD)

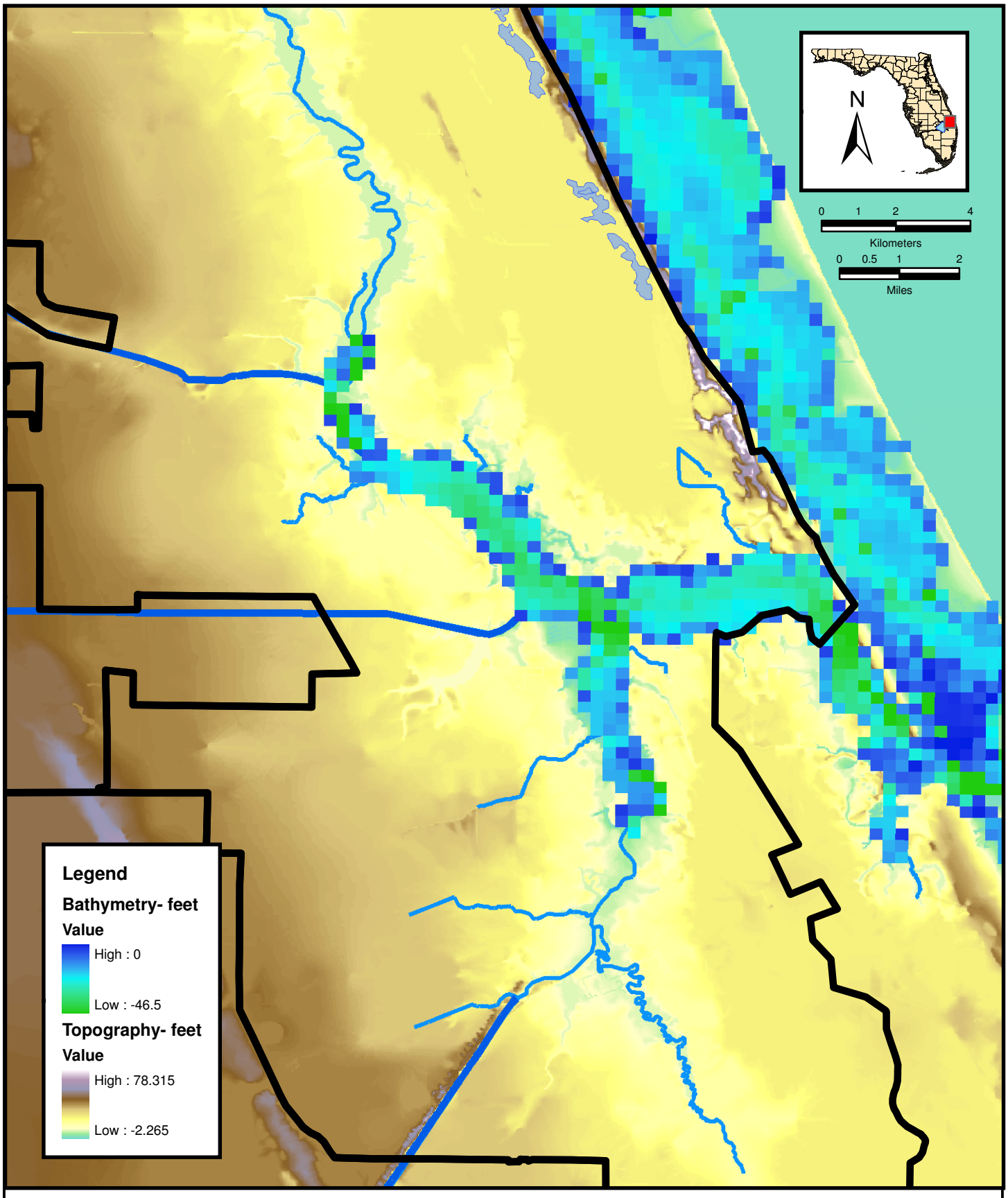

URS

Figure 2-9. Bathymetric Raster Grid of SLE overlaying the Topographic DEM (Topographic and Bathymetric data provided by SFWMD)

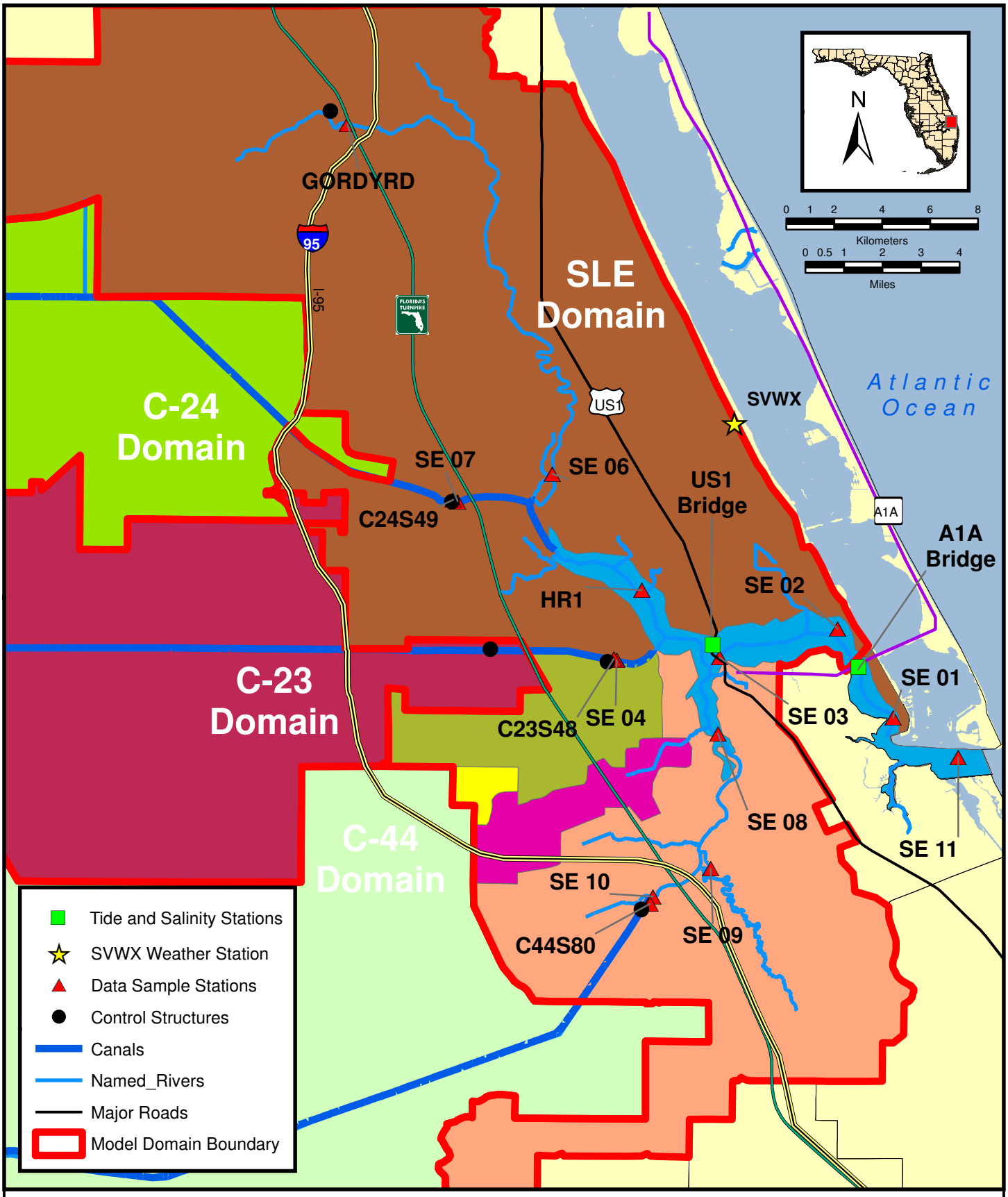

URS

Figure 2-10. Map of Data Sampling Stations.
(GIS coverages provided by SFWMD.)

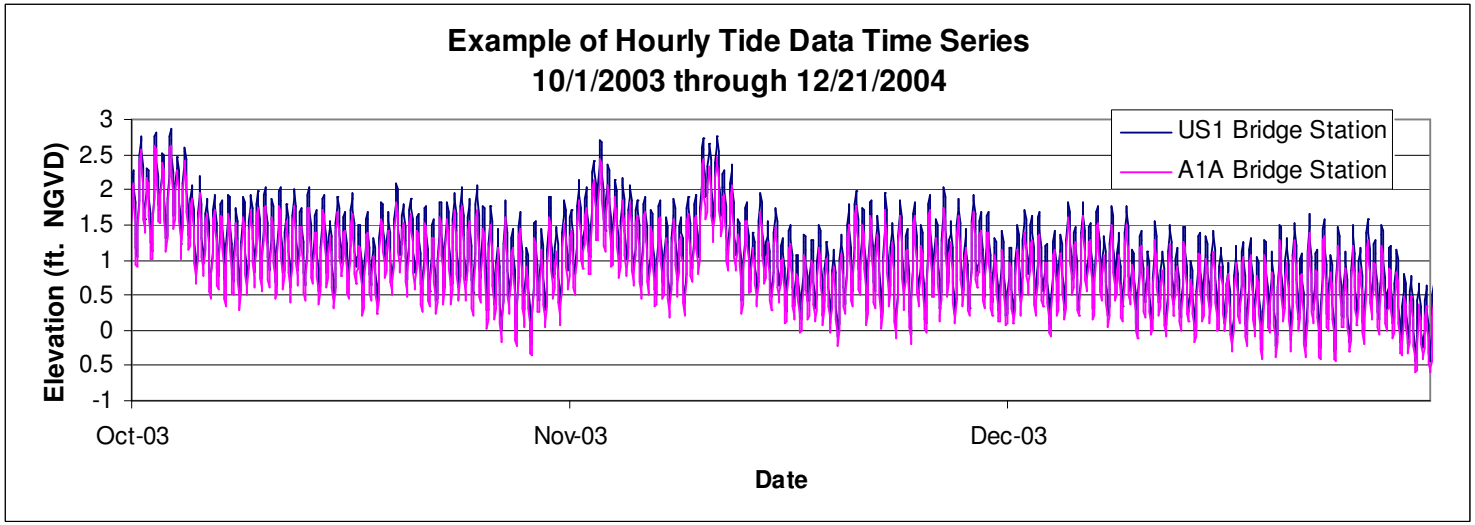

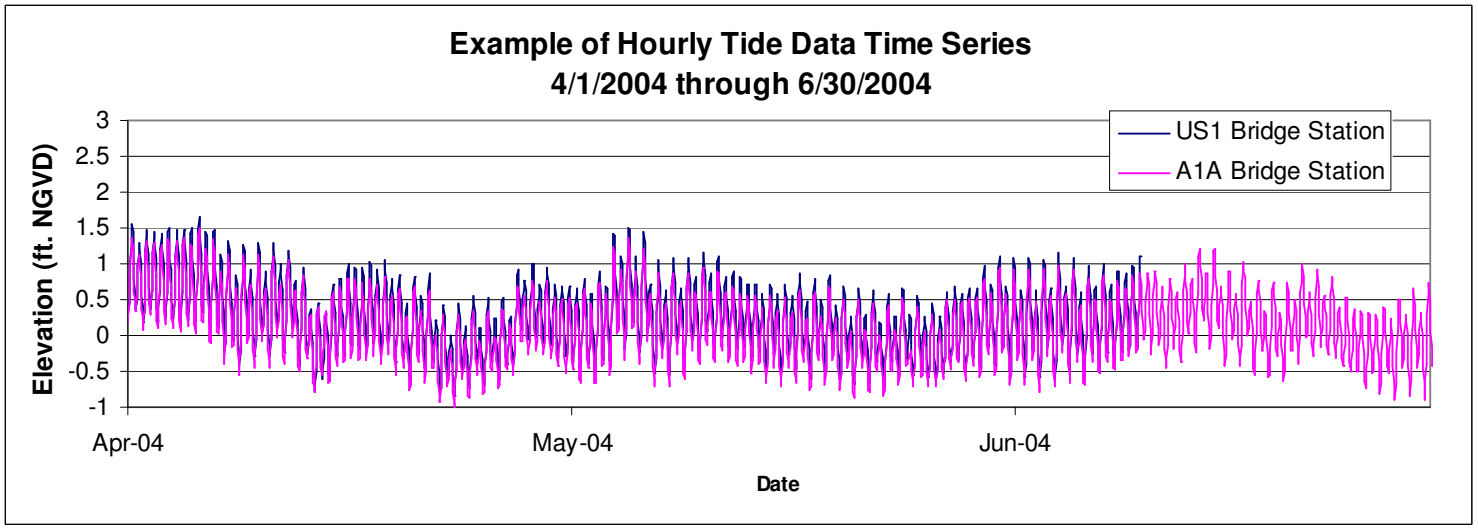

URS

Figure 2-11. St. Lucie Estuary representative tide gage data at US1 and A1A stations. (Data provided by USGS)

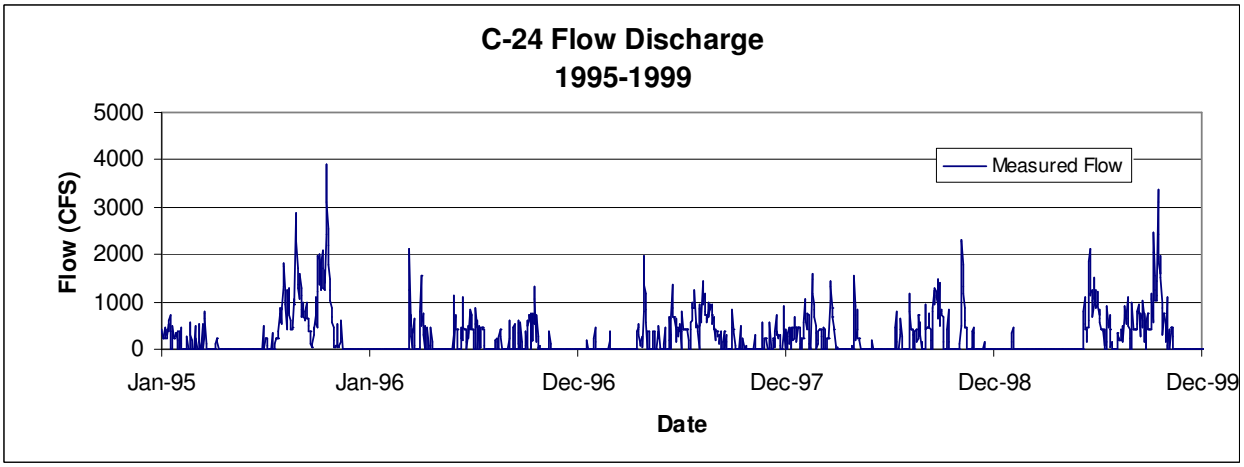

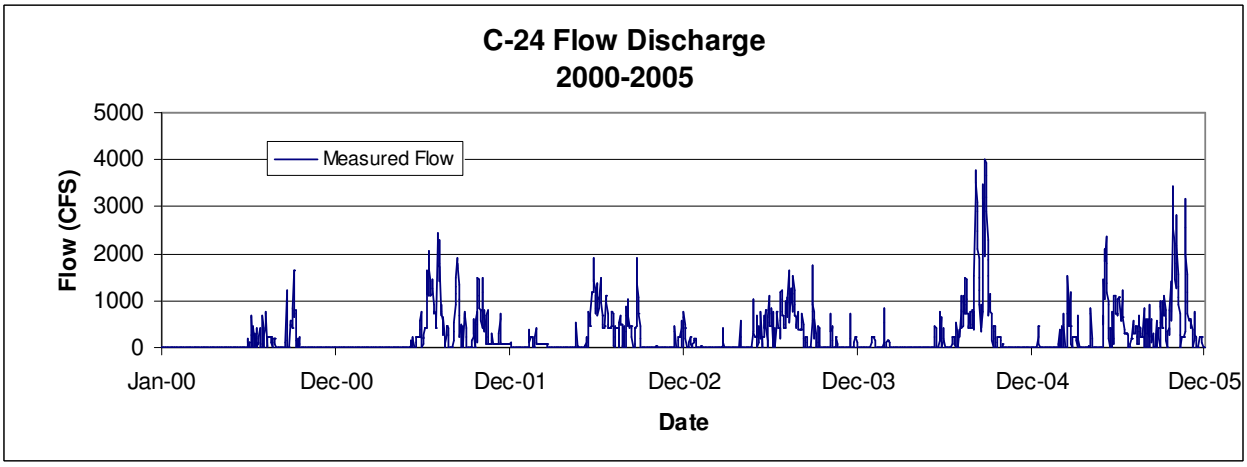

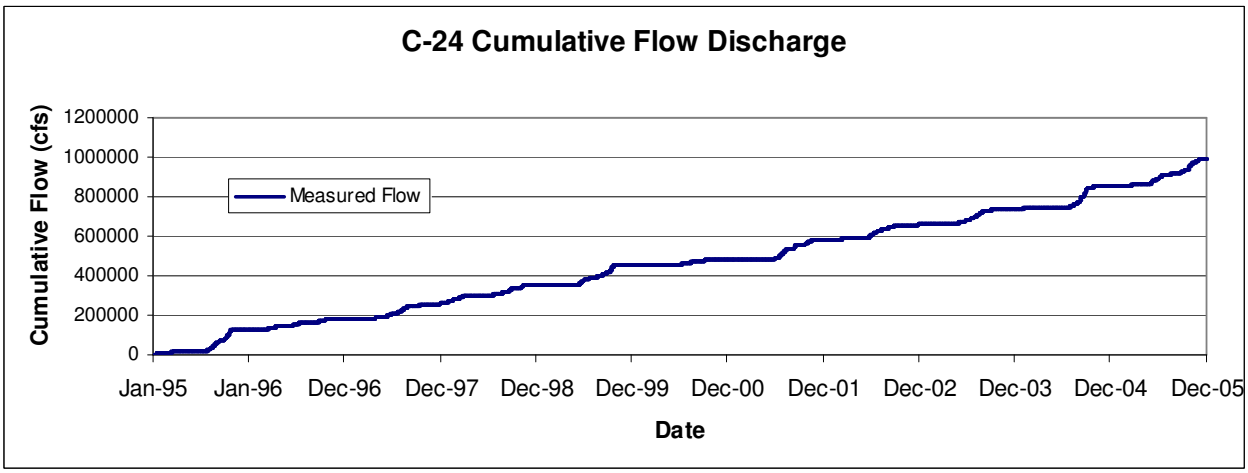

URS

Figure 2-12. C-24 Flow Discharge.

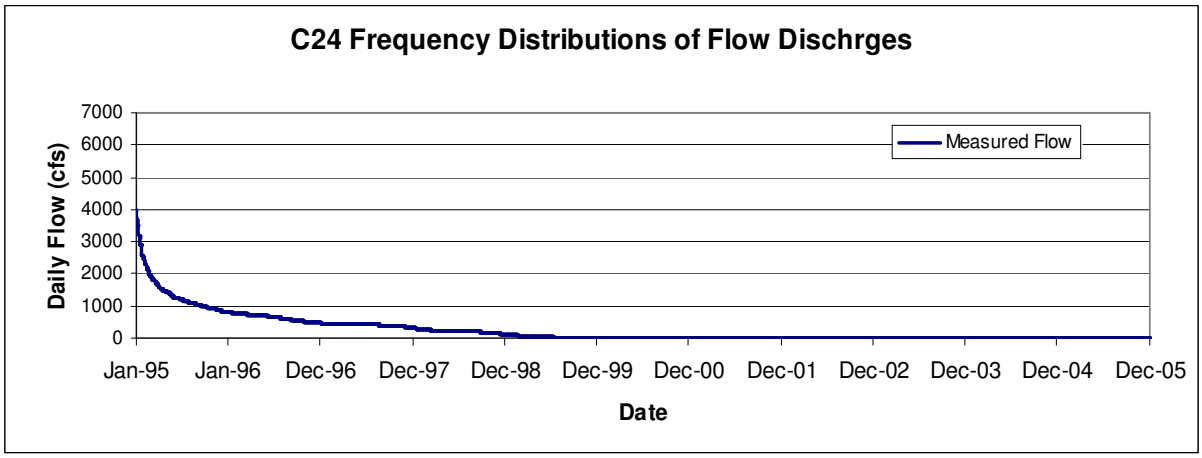

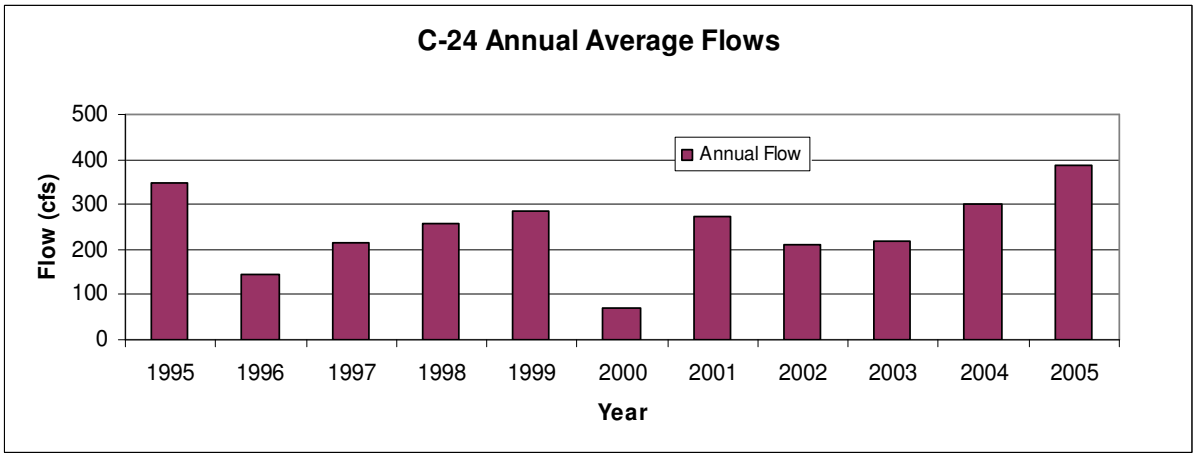

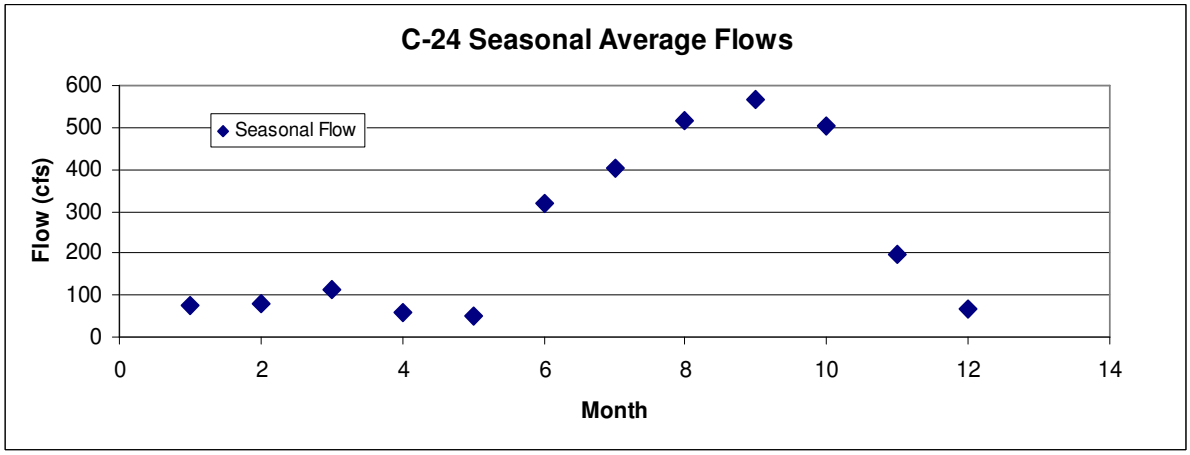

URS

Figure 2-12. C-24 Flow Discharge (cont'd.).

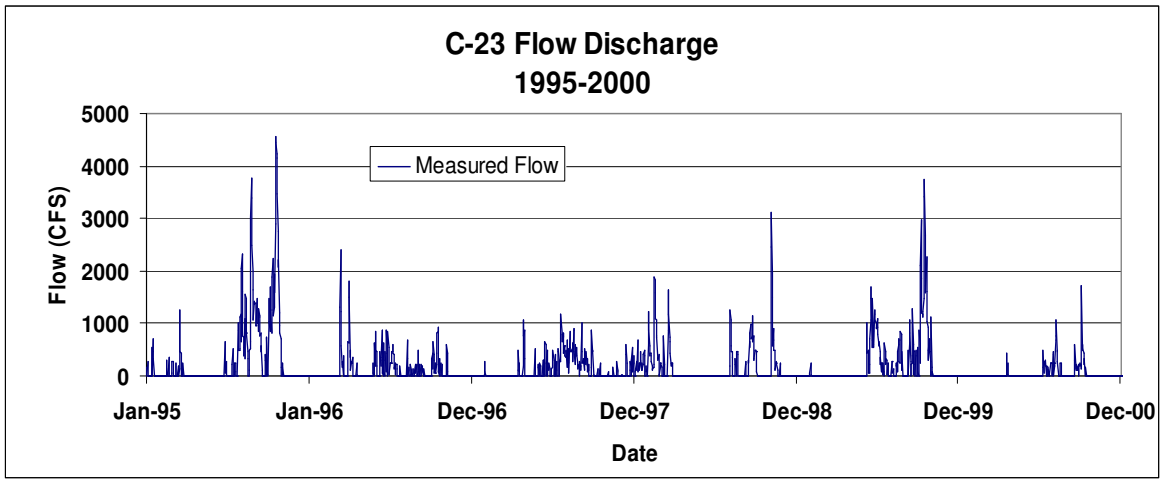

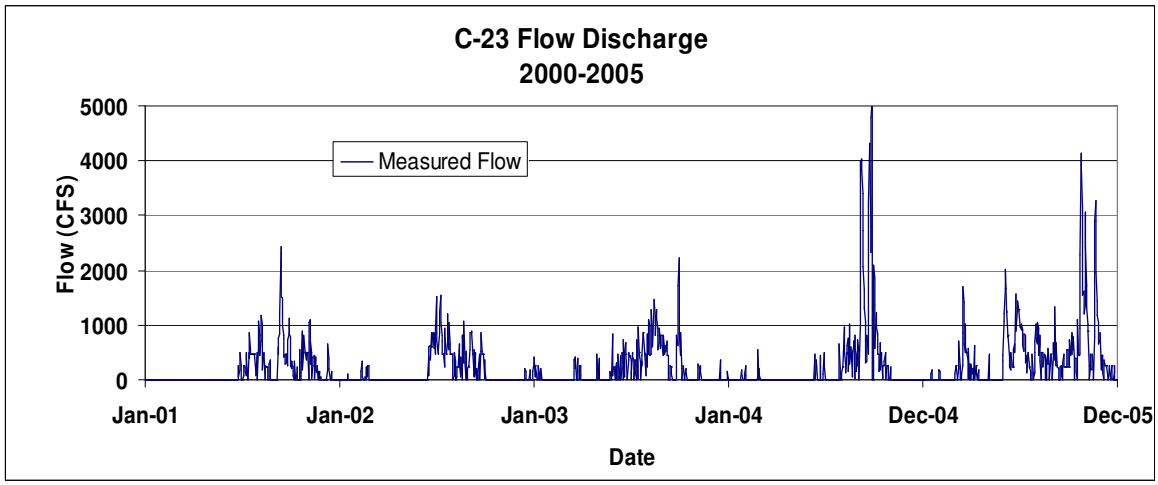

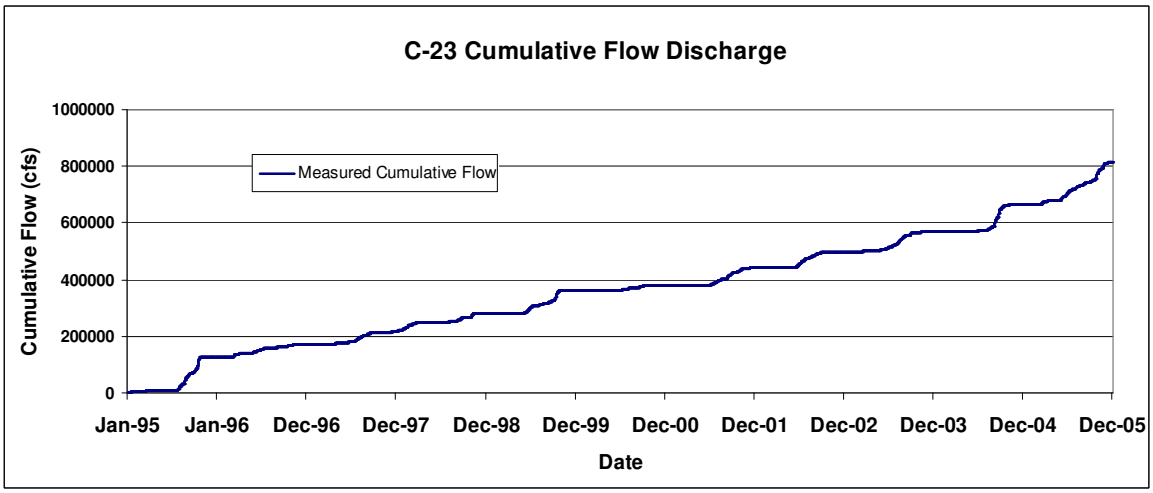

URS

Figure 2-13. C-23 Flow Discharge.

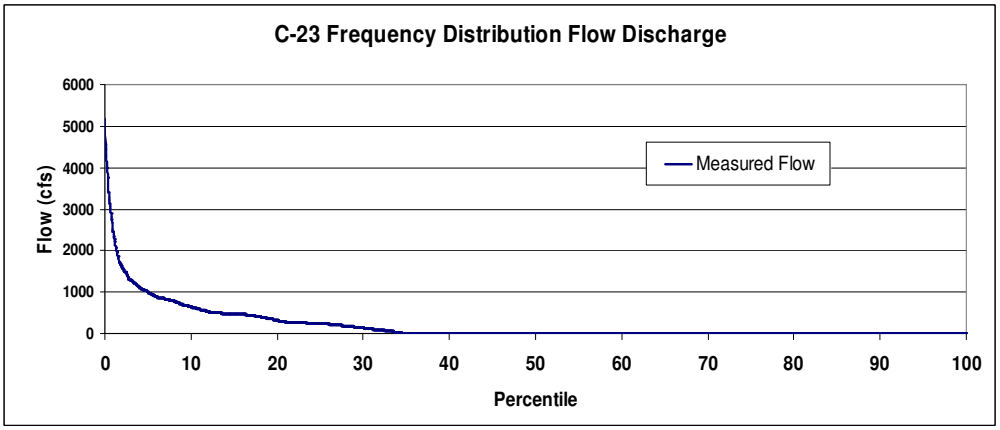

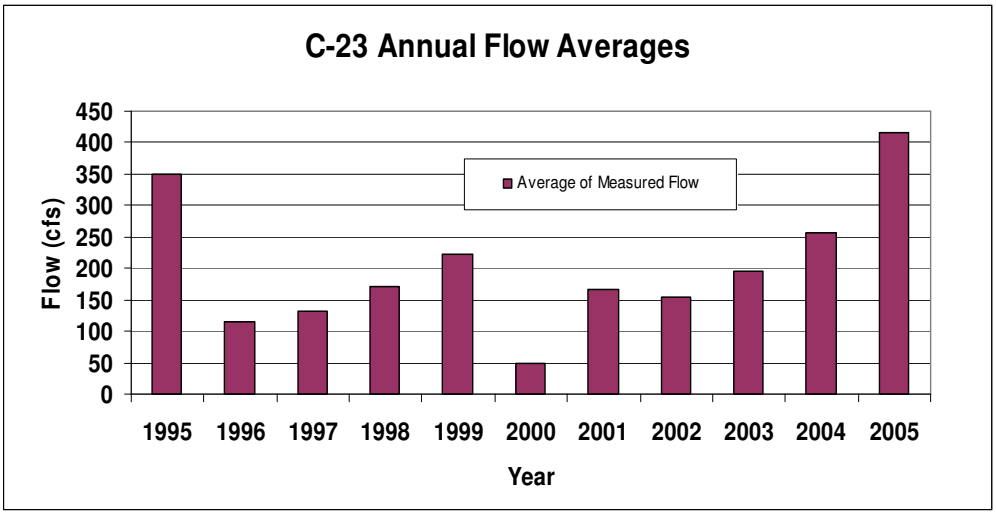

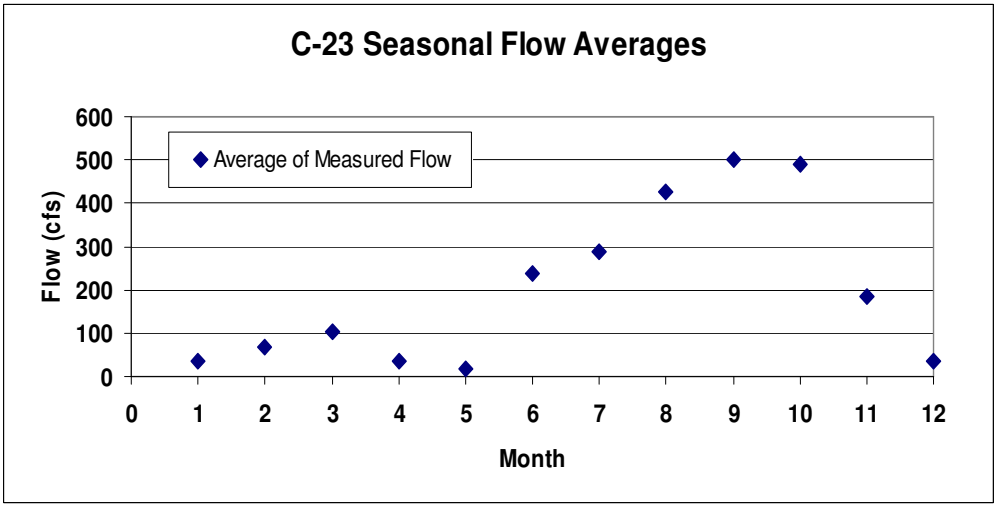

URS

Figure 2-13. C-23 Flow Discharge (cont'd.).

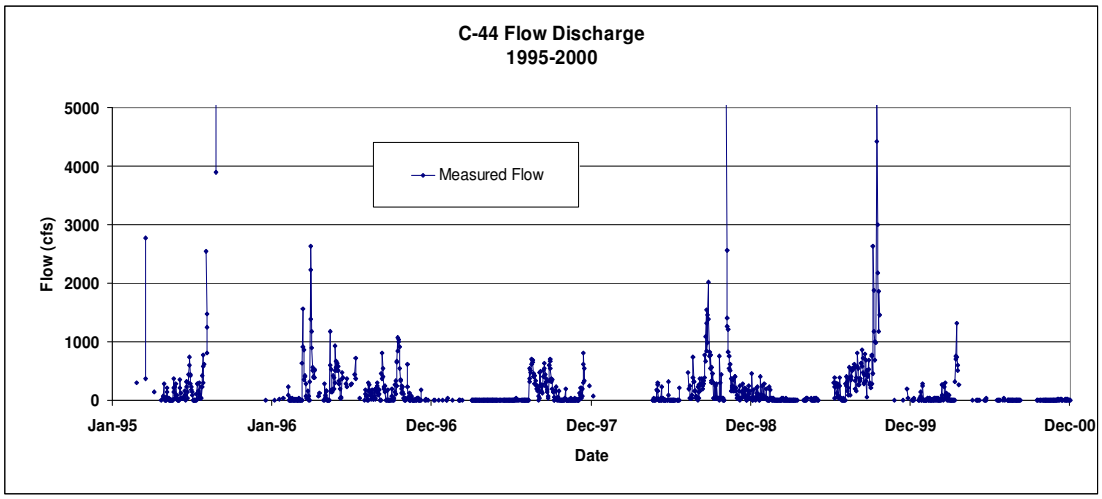

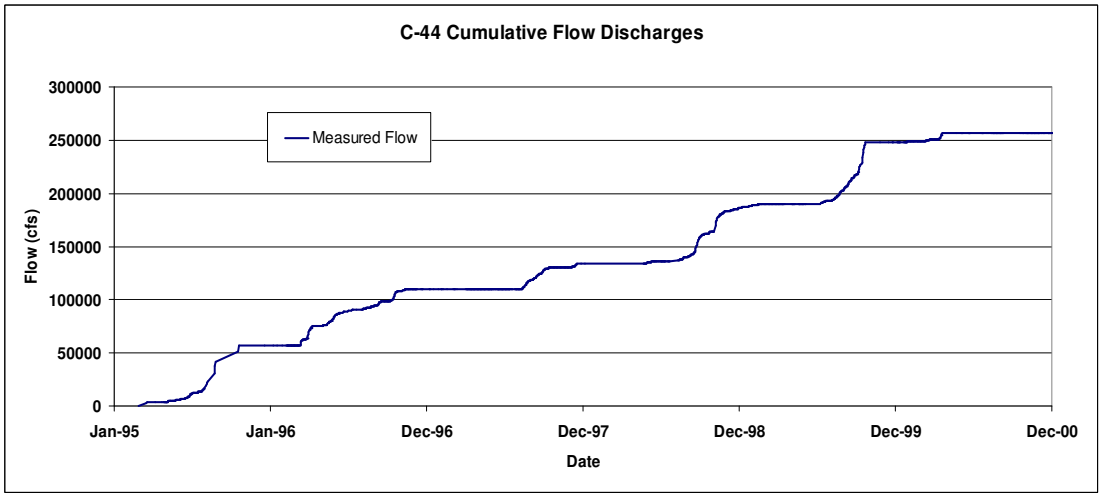

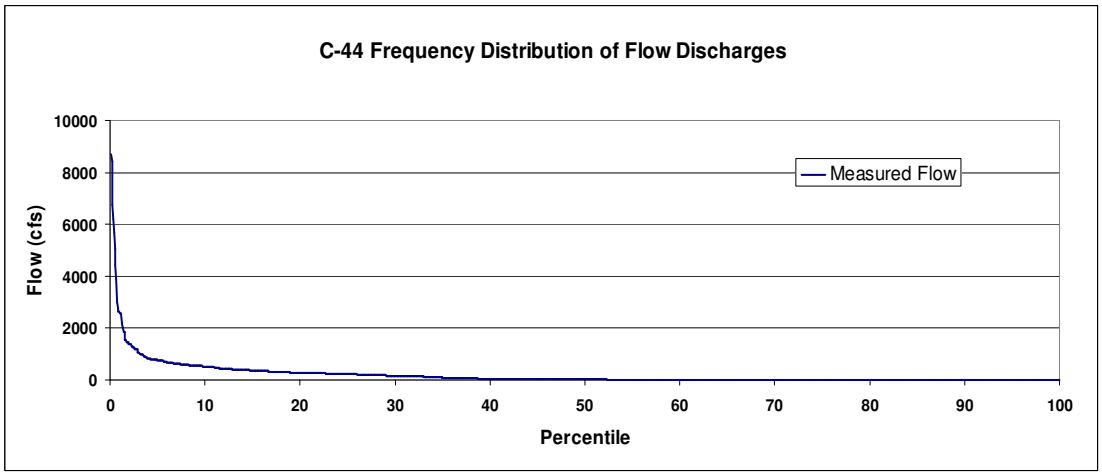

URS

Figure 2-14. C-44 Flow Discharge.

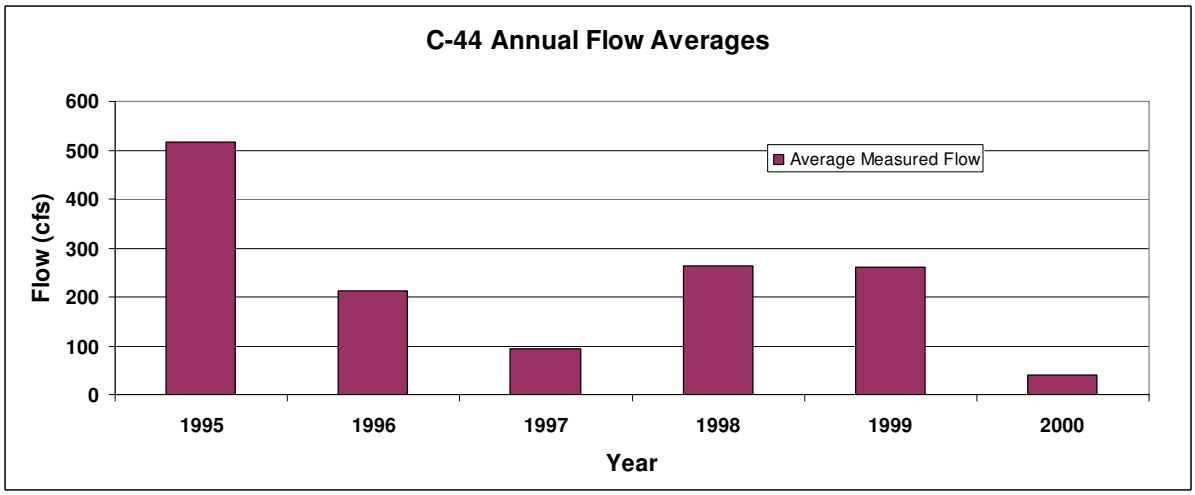

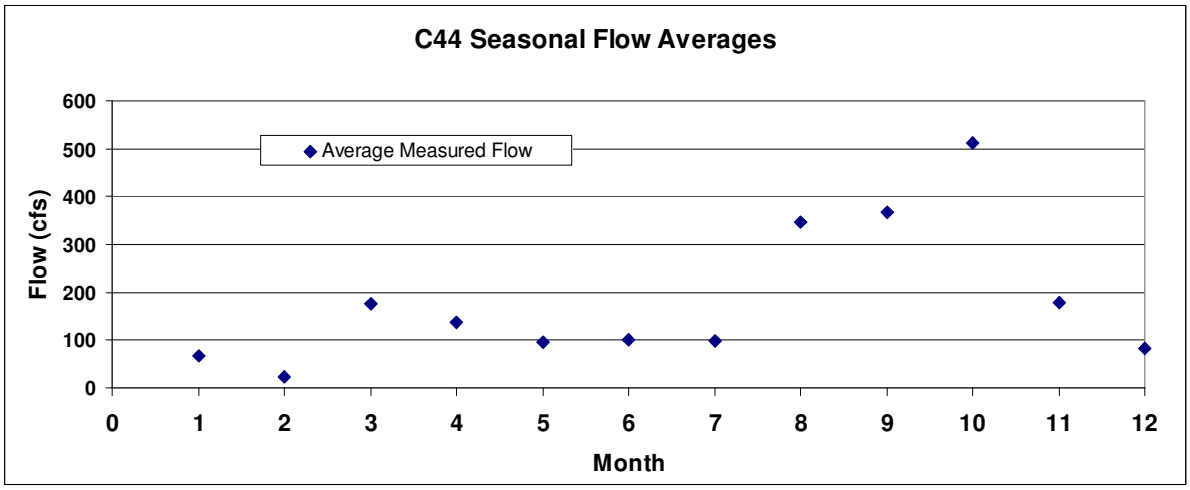

URS

Figure 2-14. C-44 Flow Discharge (cont'd.).

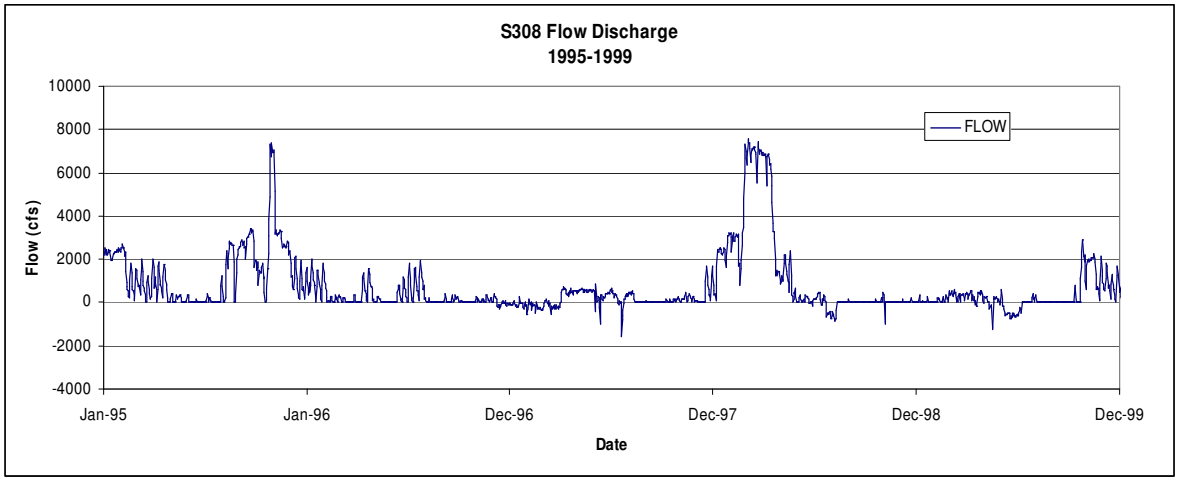

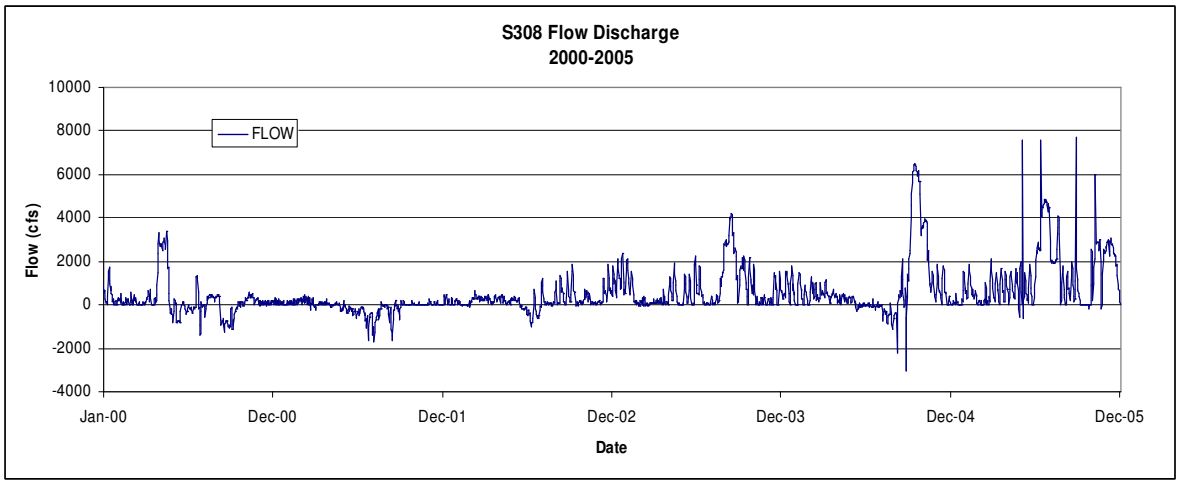

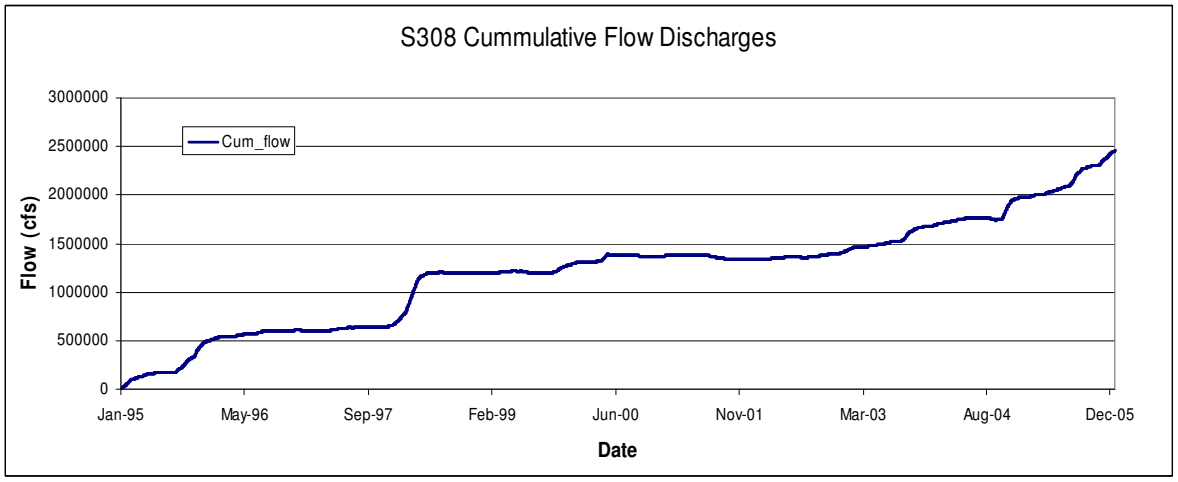

URS

Figure 2-15. S308 Flow Discharge.

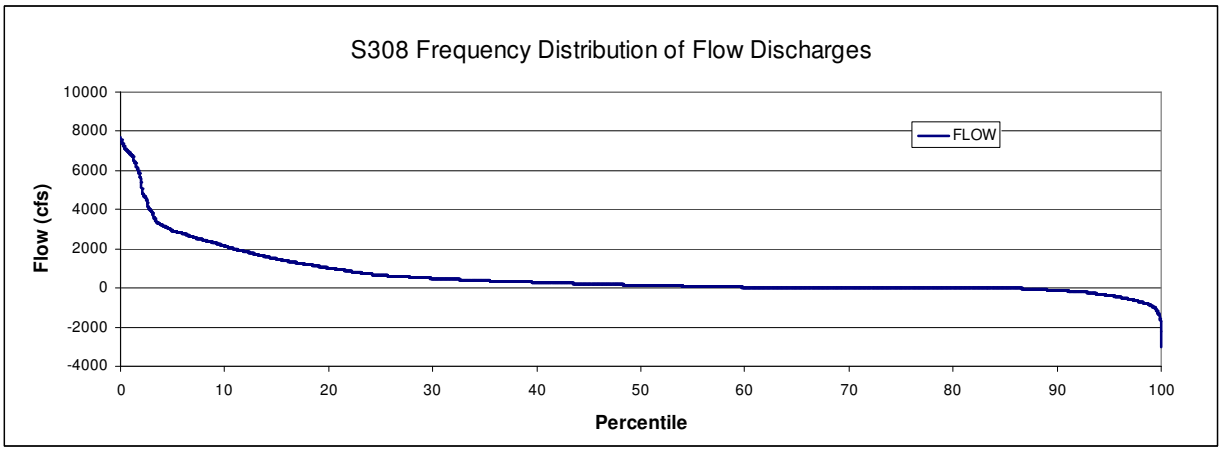

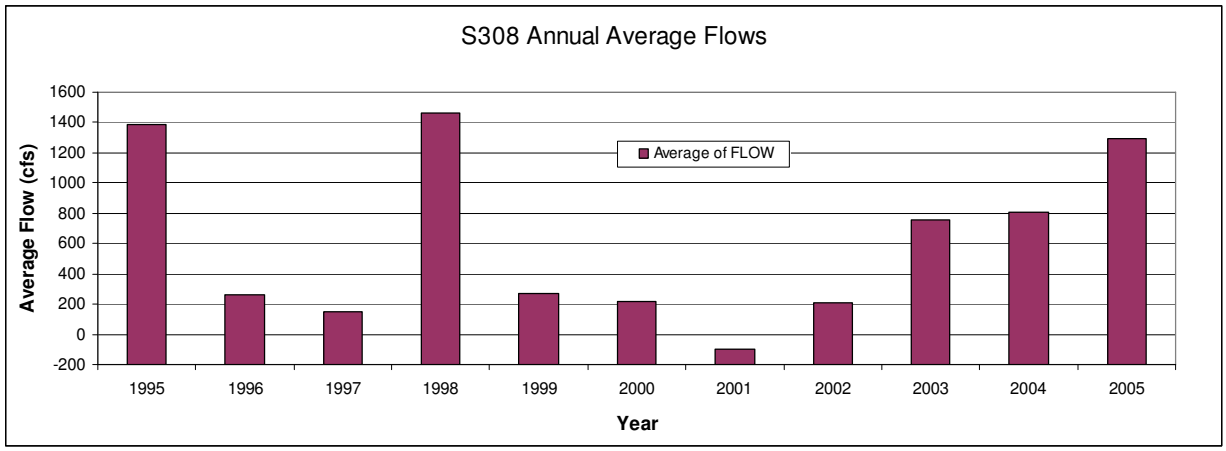

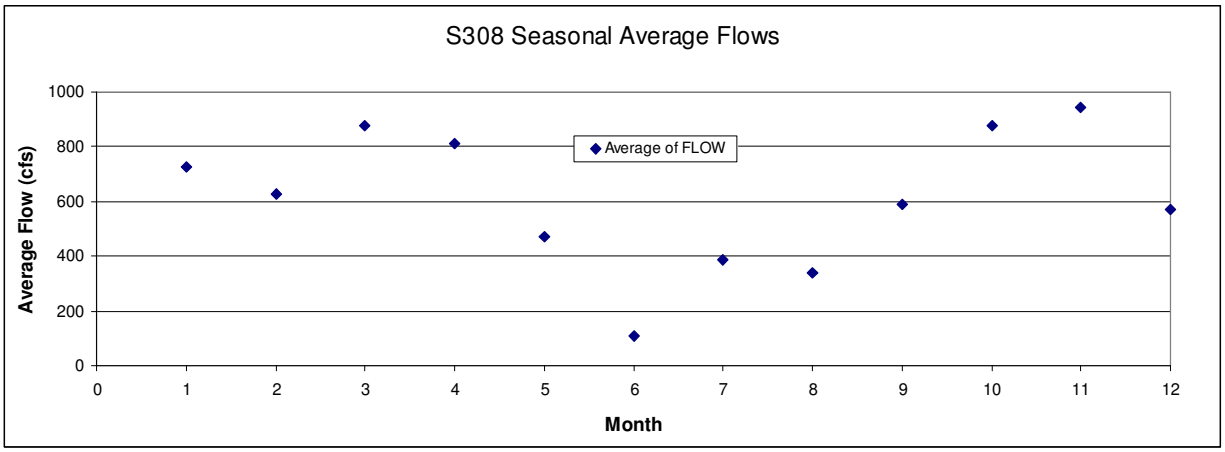

Figure 2-15. S308 Flow Discharge (cont'd.).

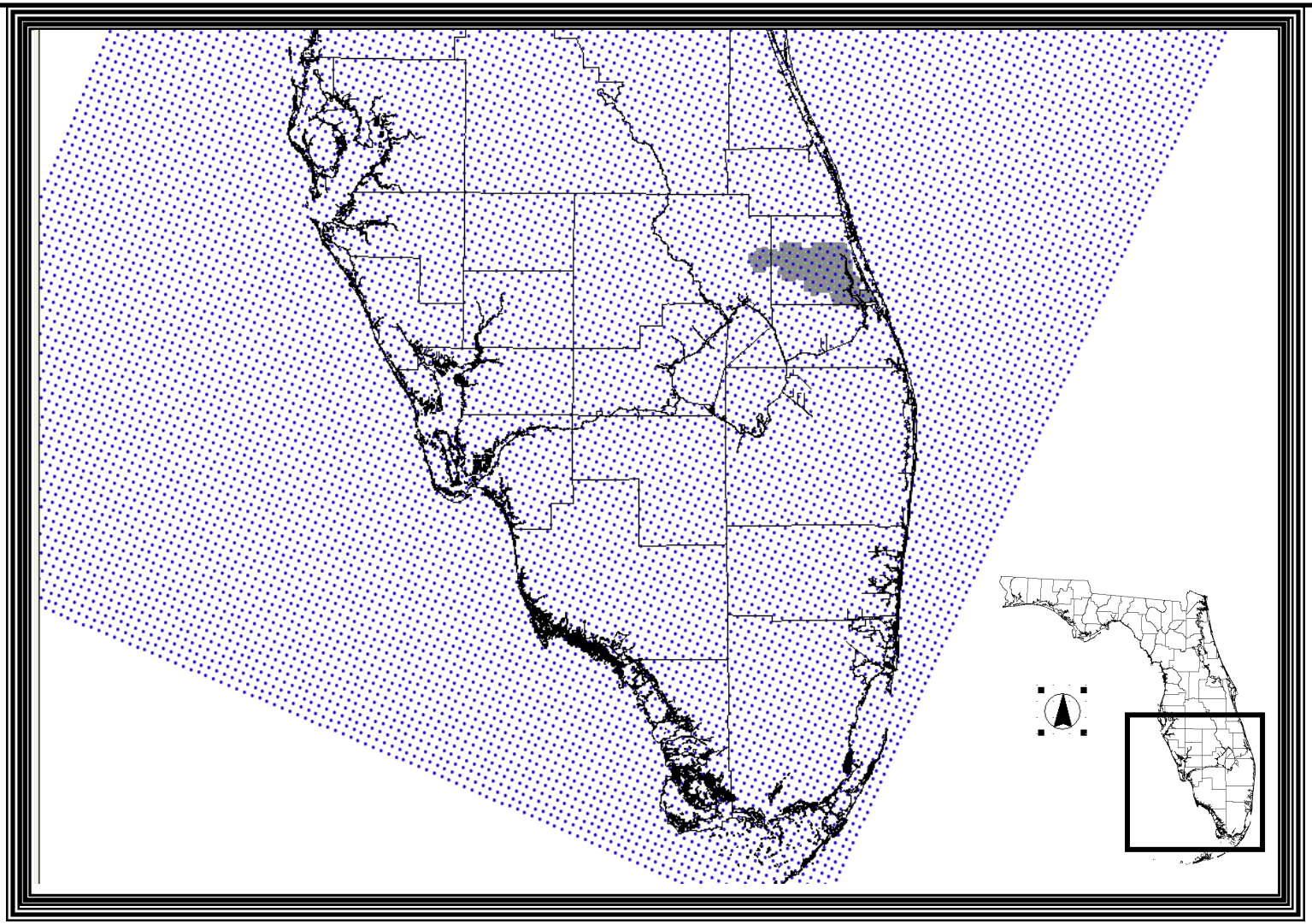

Figure 2-16. NEXRAD rainfall station locations for South Florida. (NexRad data provided by SFWMD)

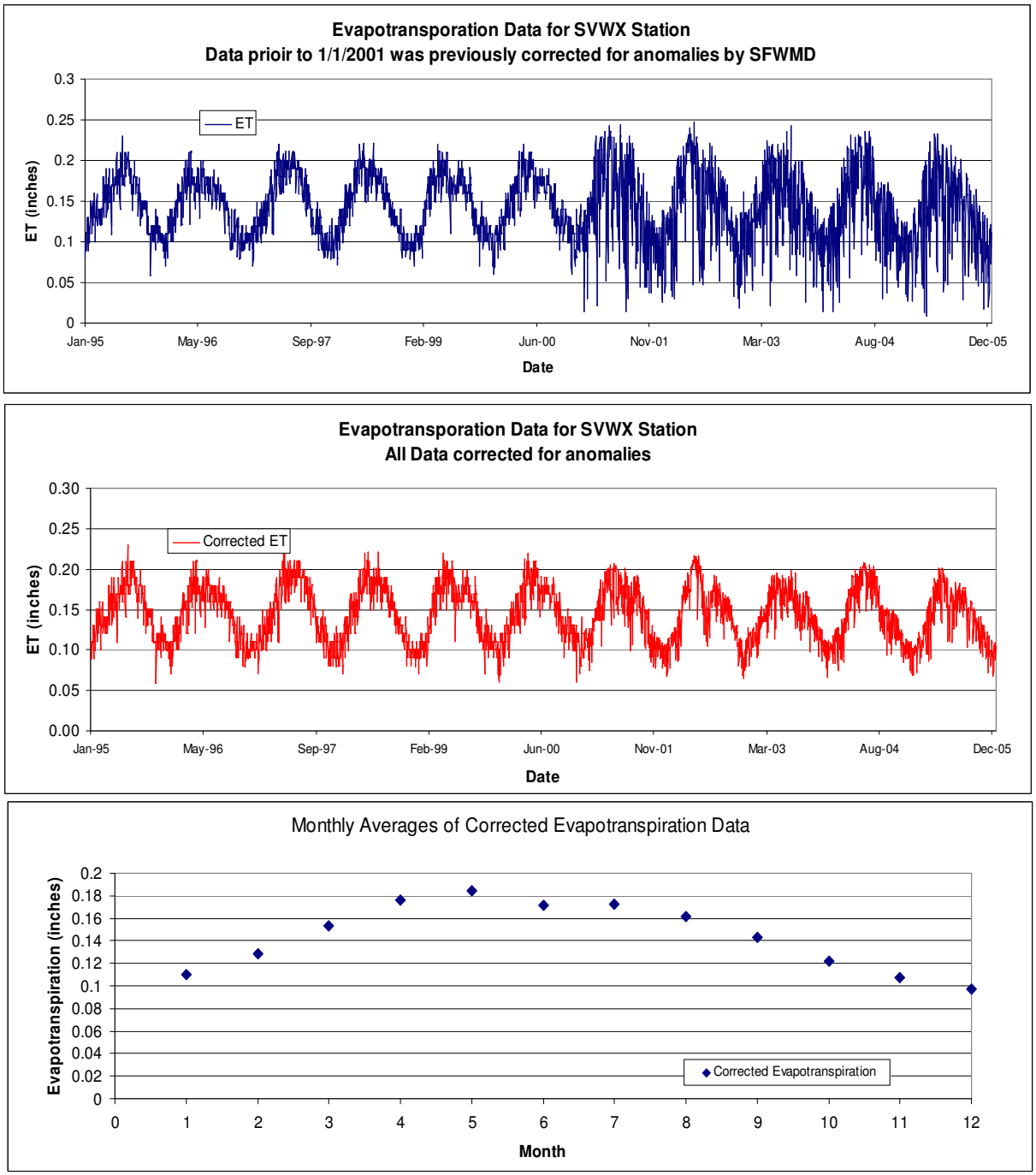

Figure 2-17. Evapo-transpiration data used in the model - prior to adjustments (top), fully adjusted (center), and seasonal Averages (bottom).

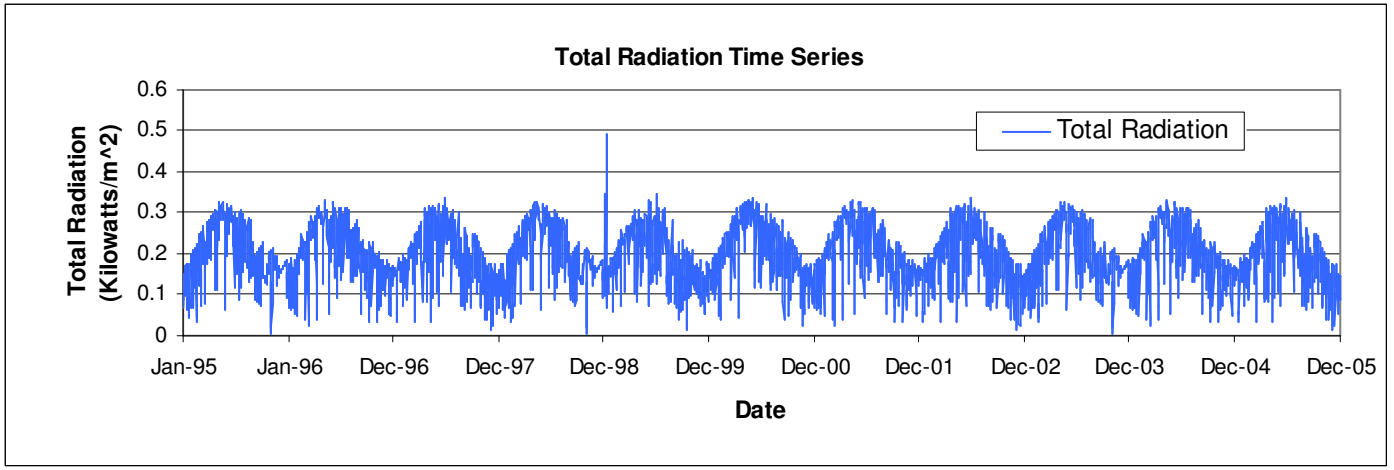

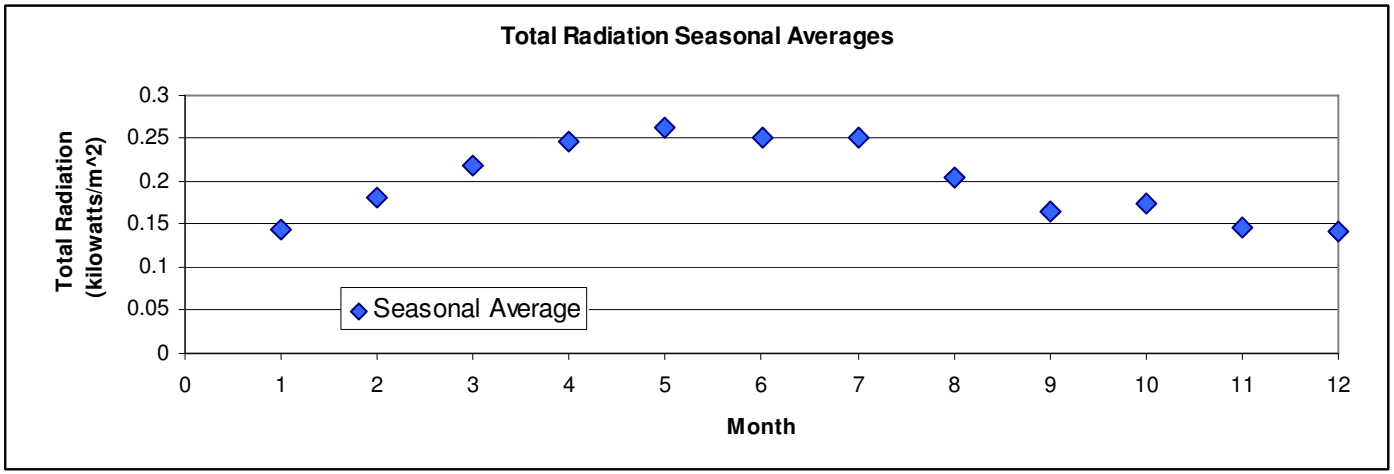

URS

Figure 2-18. Solar Radiation Data Time Series and Seasonal Average Plots. (Data provided by SFWMD DBHydro)

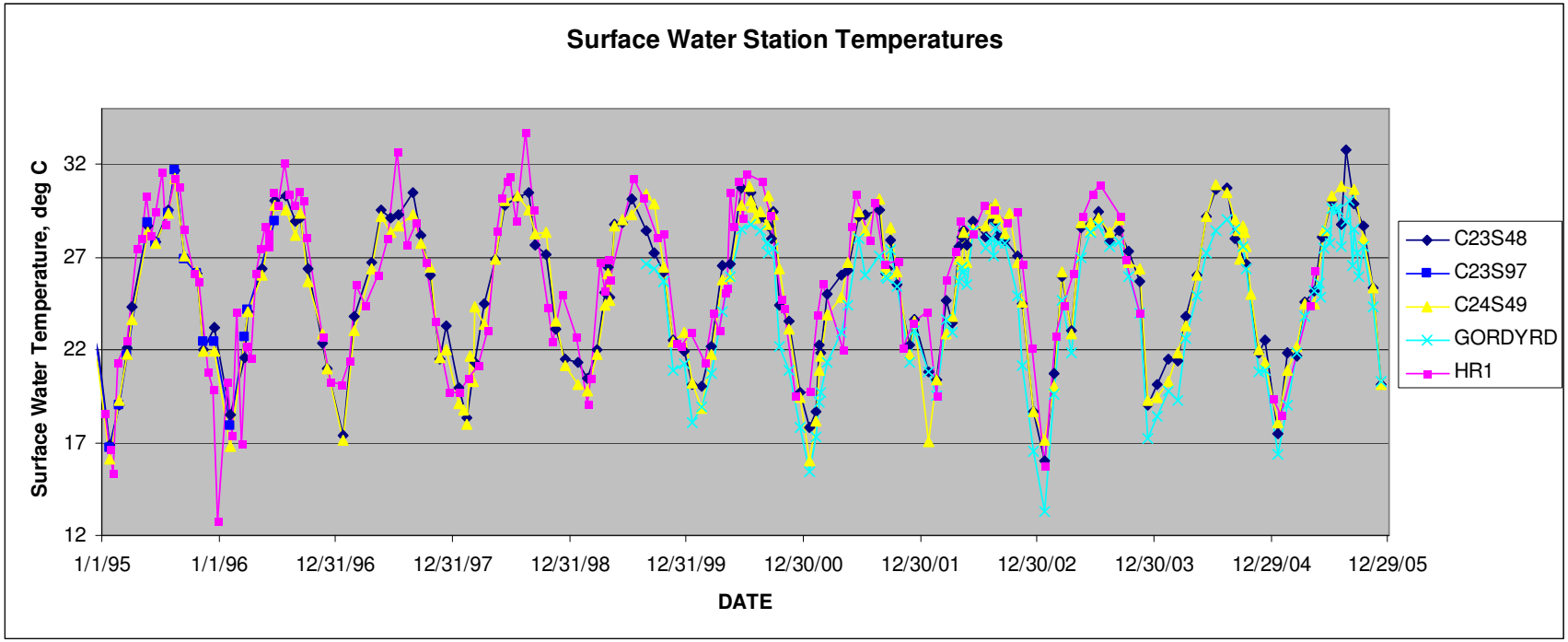

URS

Figure 2-19. Surface Water Station Time Series Plots.
(Data provided by SFWMD DBHydro)

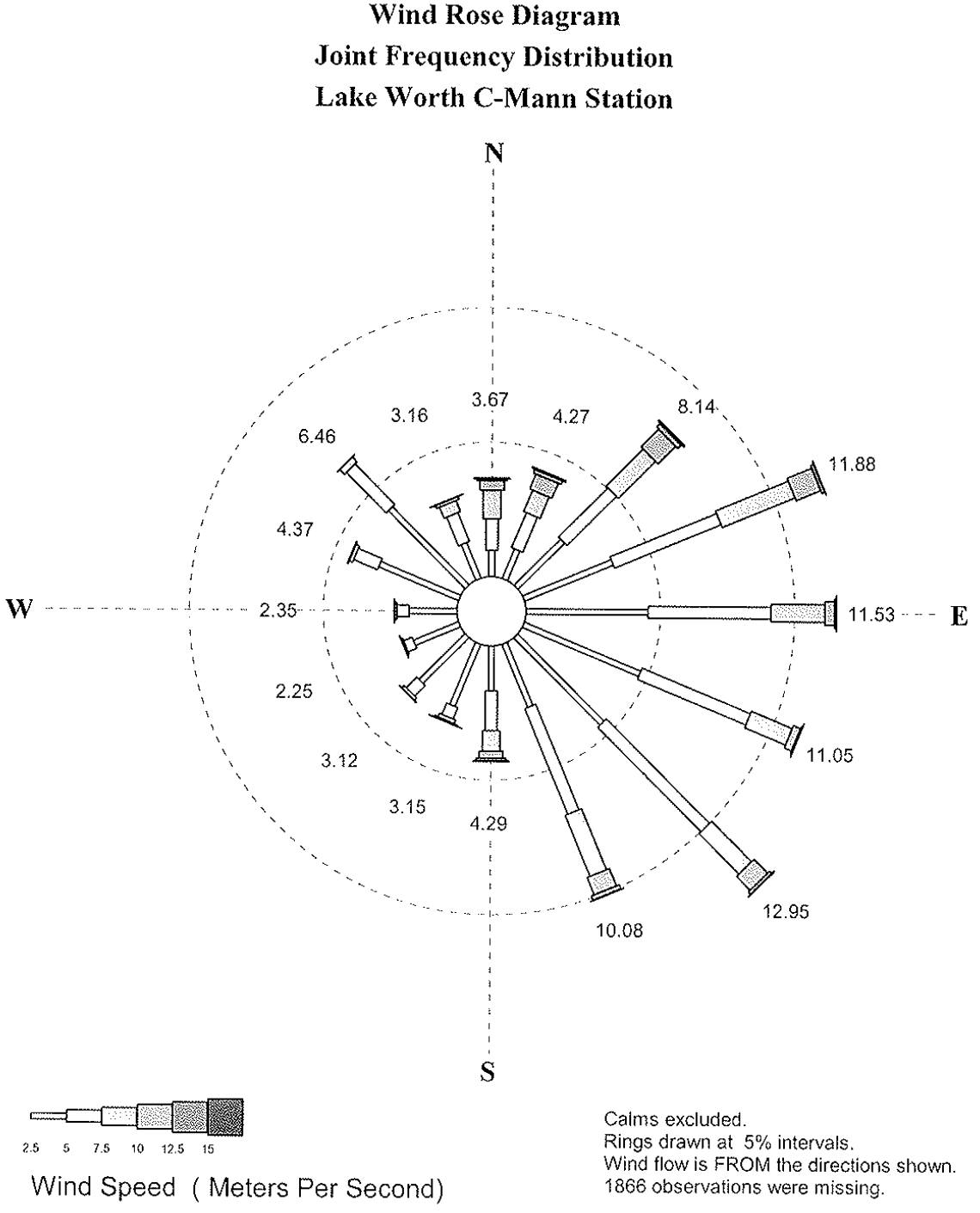

Figure 2-20. Wind Rose Diagram indicating dominant wind direction and speed in Lake Worth region. (Data provided by NOAA's NDBC.)

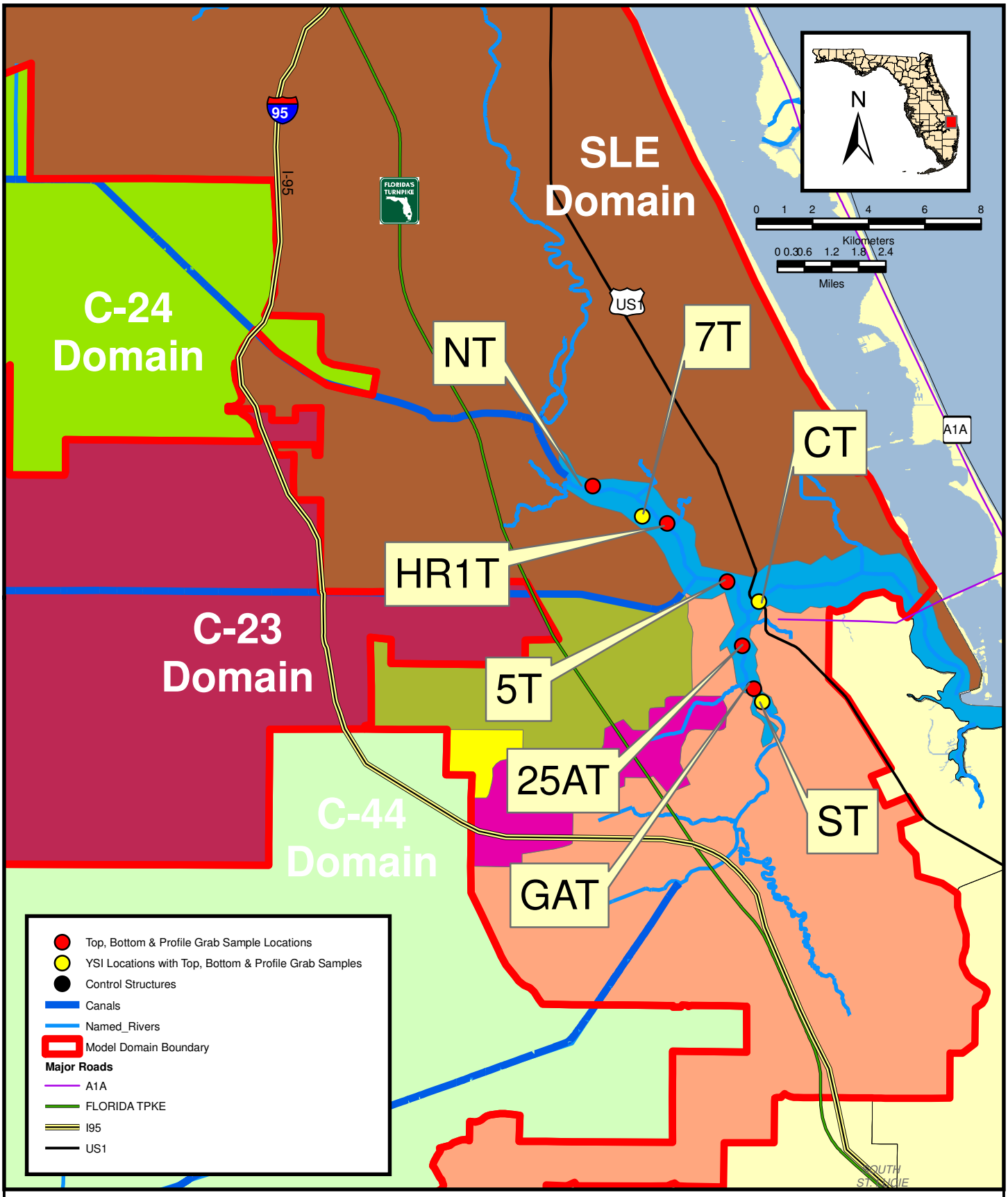

URS

Figure 2-21. YSI Sondes Locations (Locations provided by FDEP.)

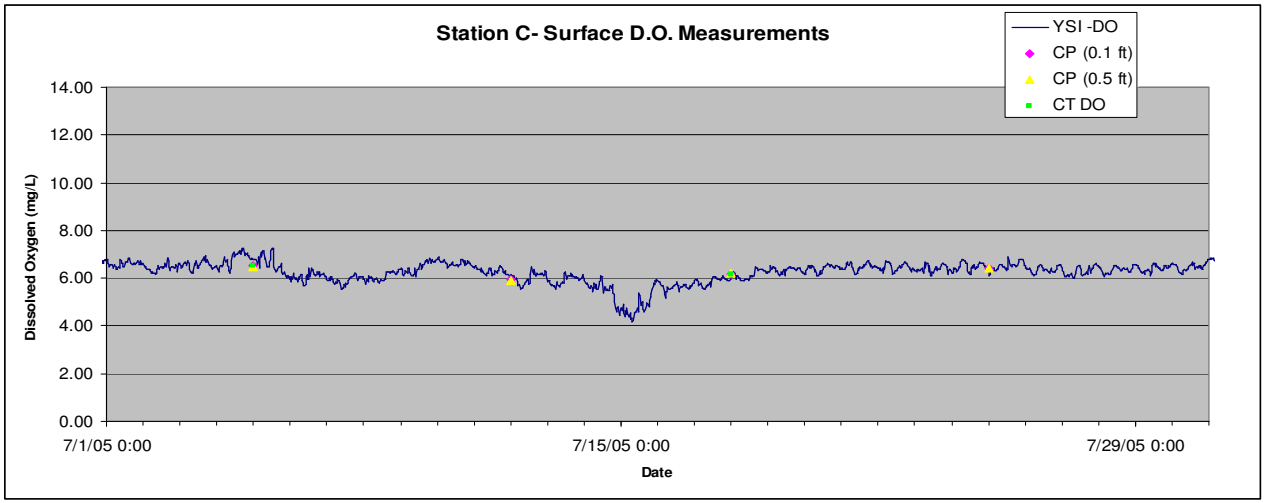

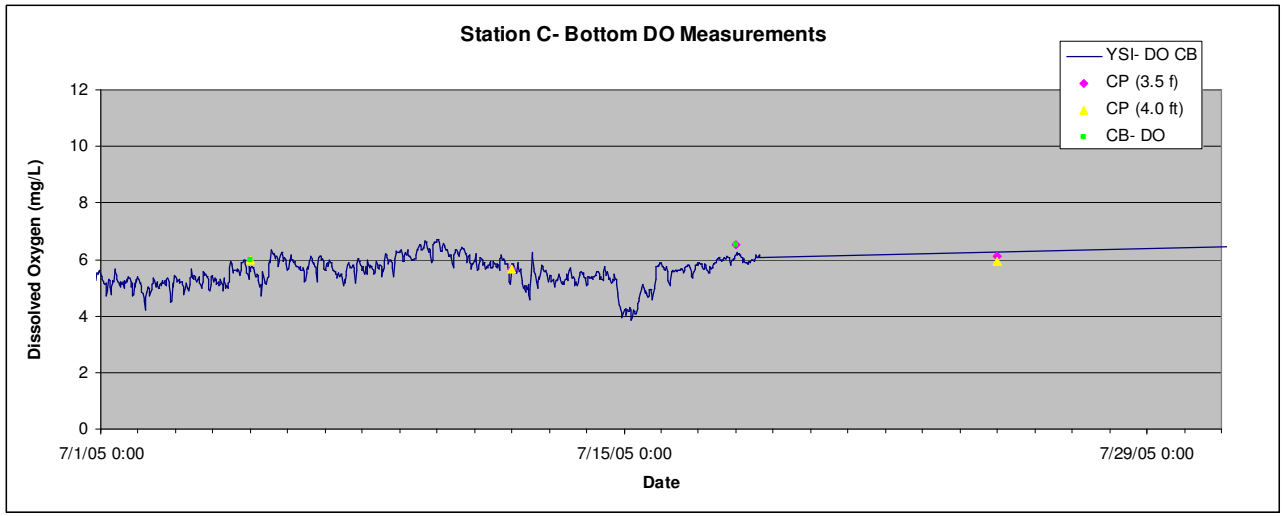

URS

Figure 2-22. Correlation of YSI continuous DO measurements, with grab sample and profile data from the 2005 FDEP monitoring program. (Data provided by FDEP)

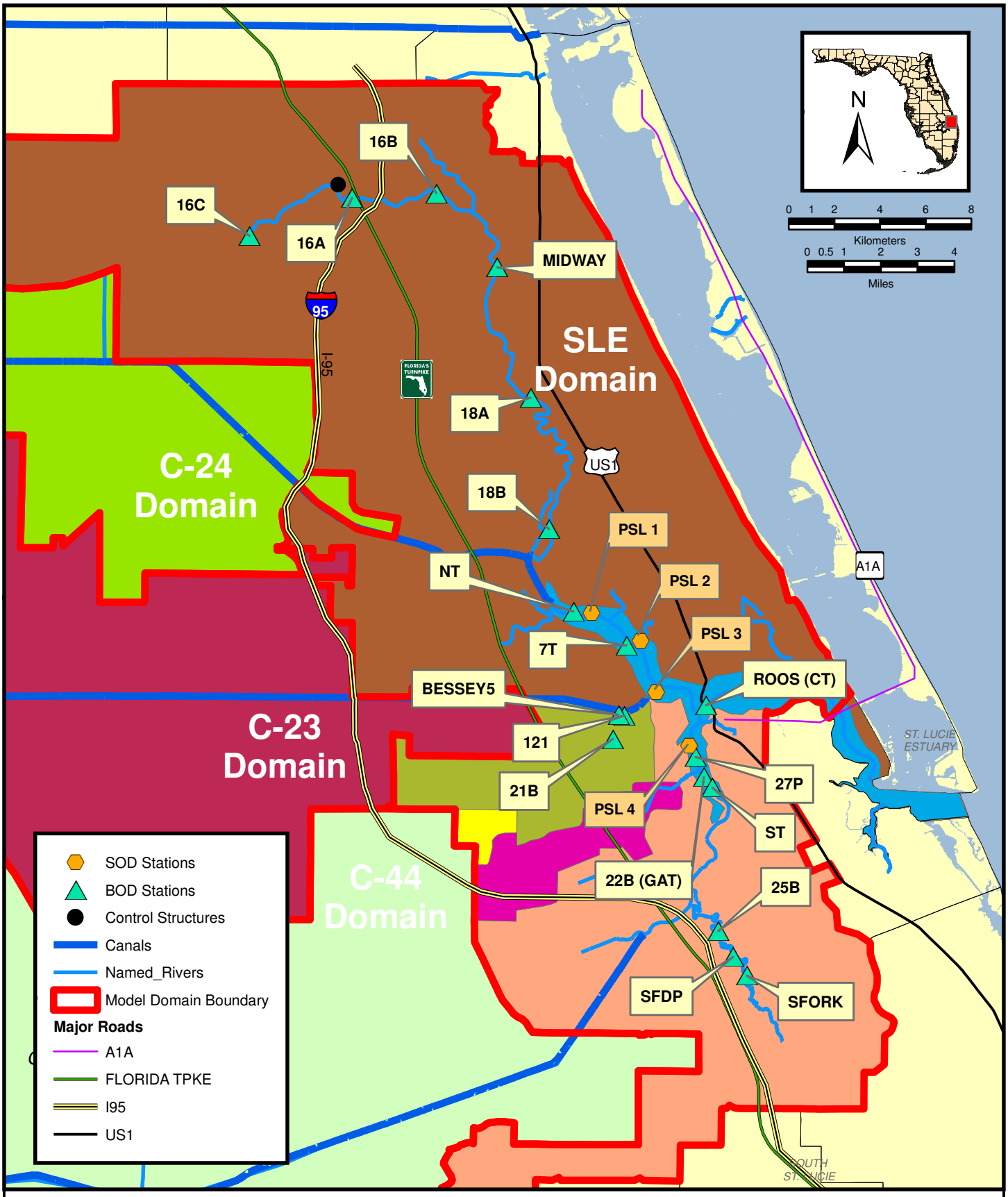

URS

Figure 2-23. BOD and SOD Sample Locations (Locations provided by FDEP.)

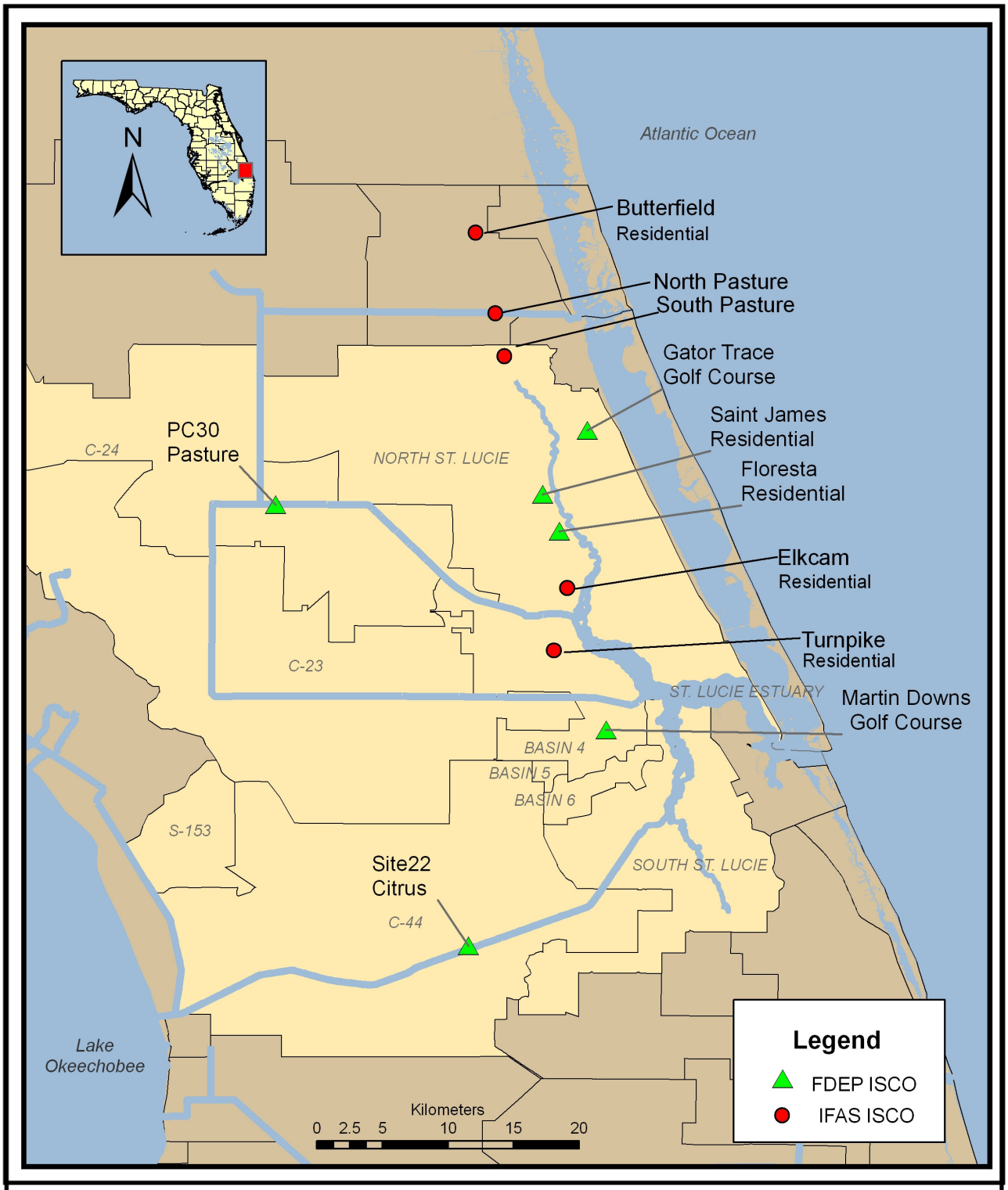

URS

Figure 2-24. ISCO point source monitoring stations from FDEP and The Institute for Food and Agricultural Sciences (IFAS).

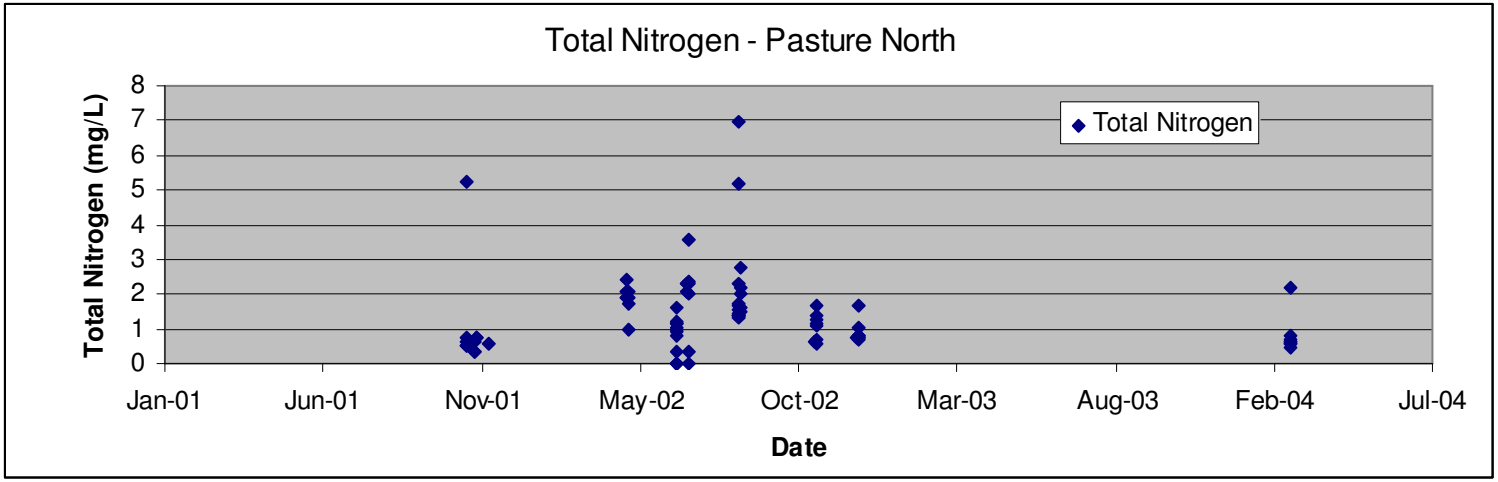

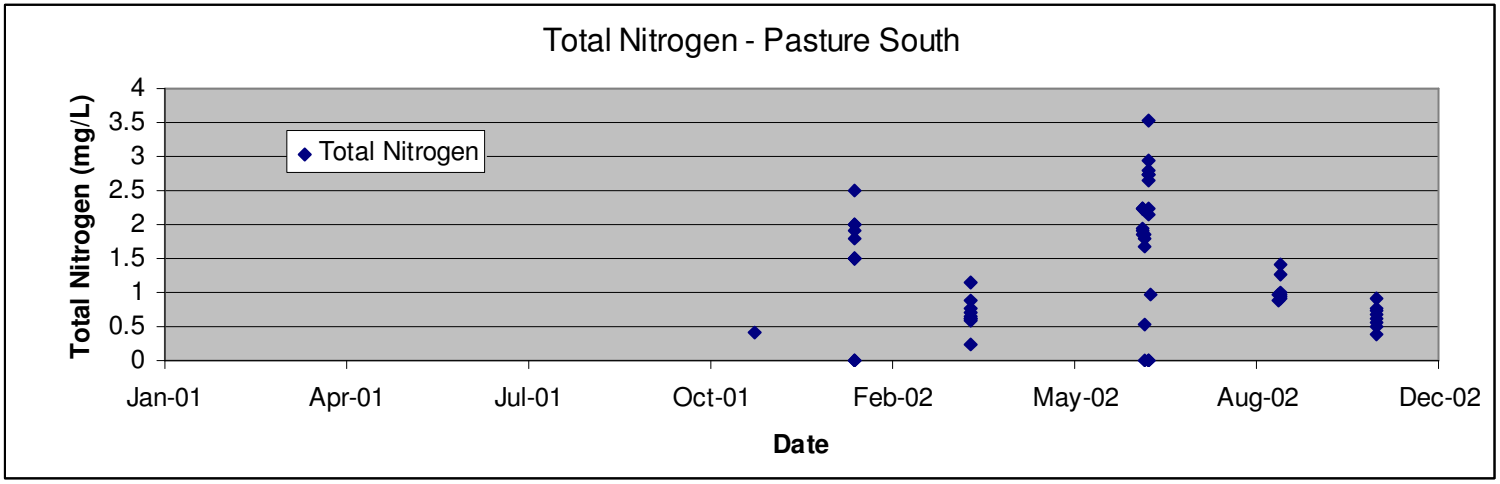

URS

Figure 2-25. IFAS ISCO Total Nitrogen Data.

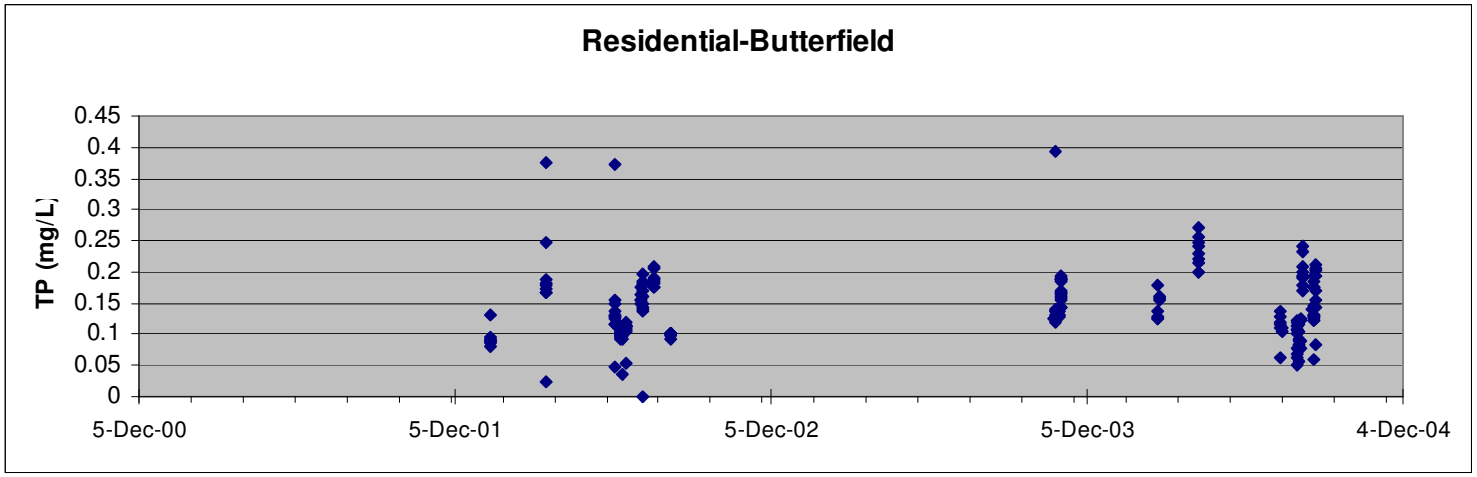

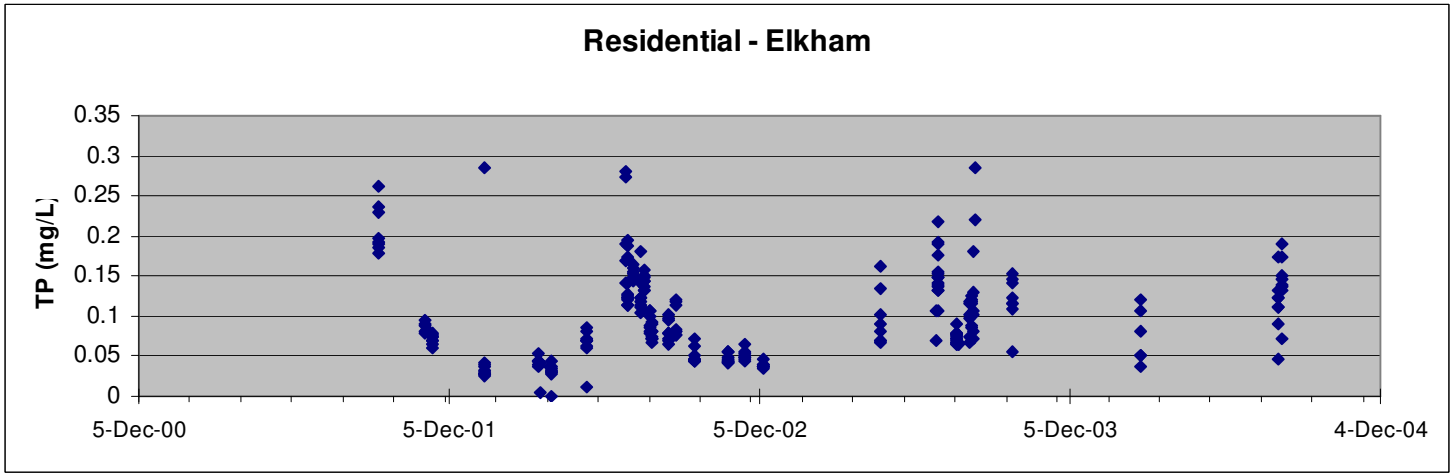

URS

Figure 2-26. IFAS ISCO Total Phosphate Data.

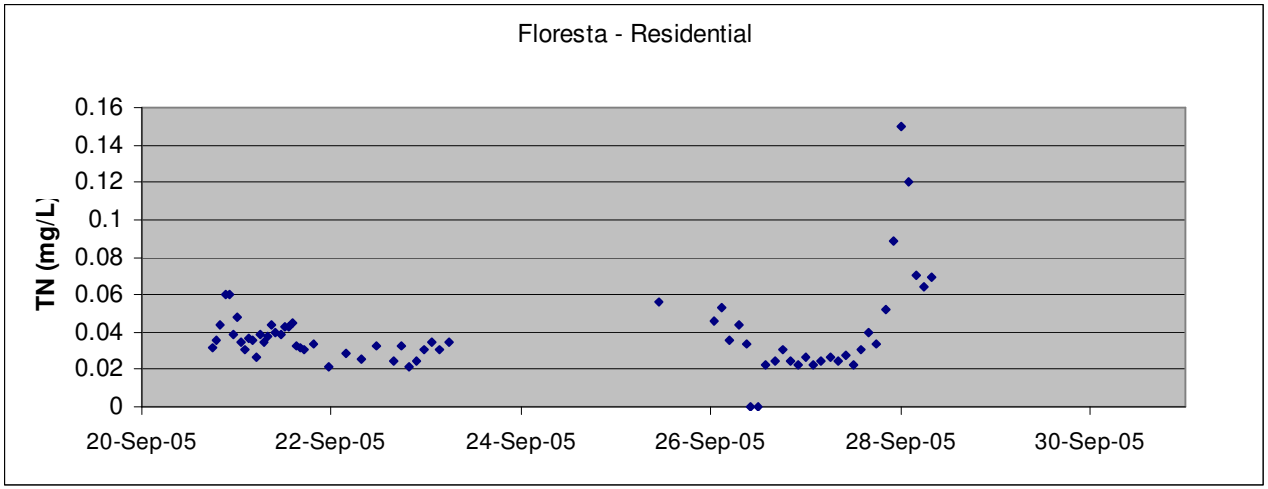

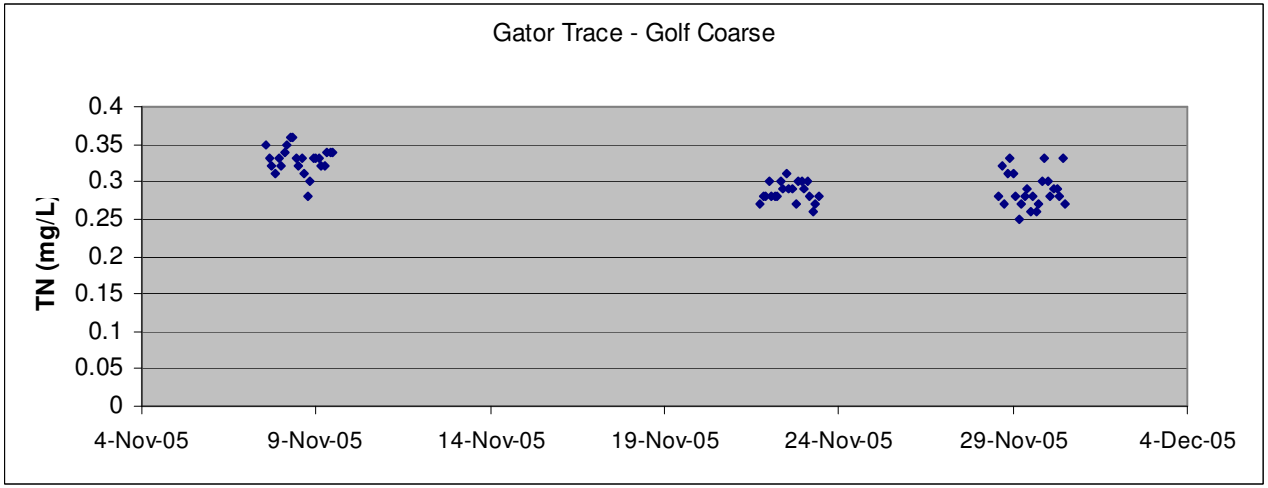

URS

Figure 2-27. FDEP ISCO Total Nitrogen Data.

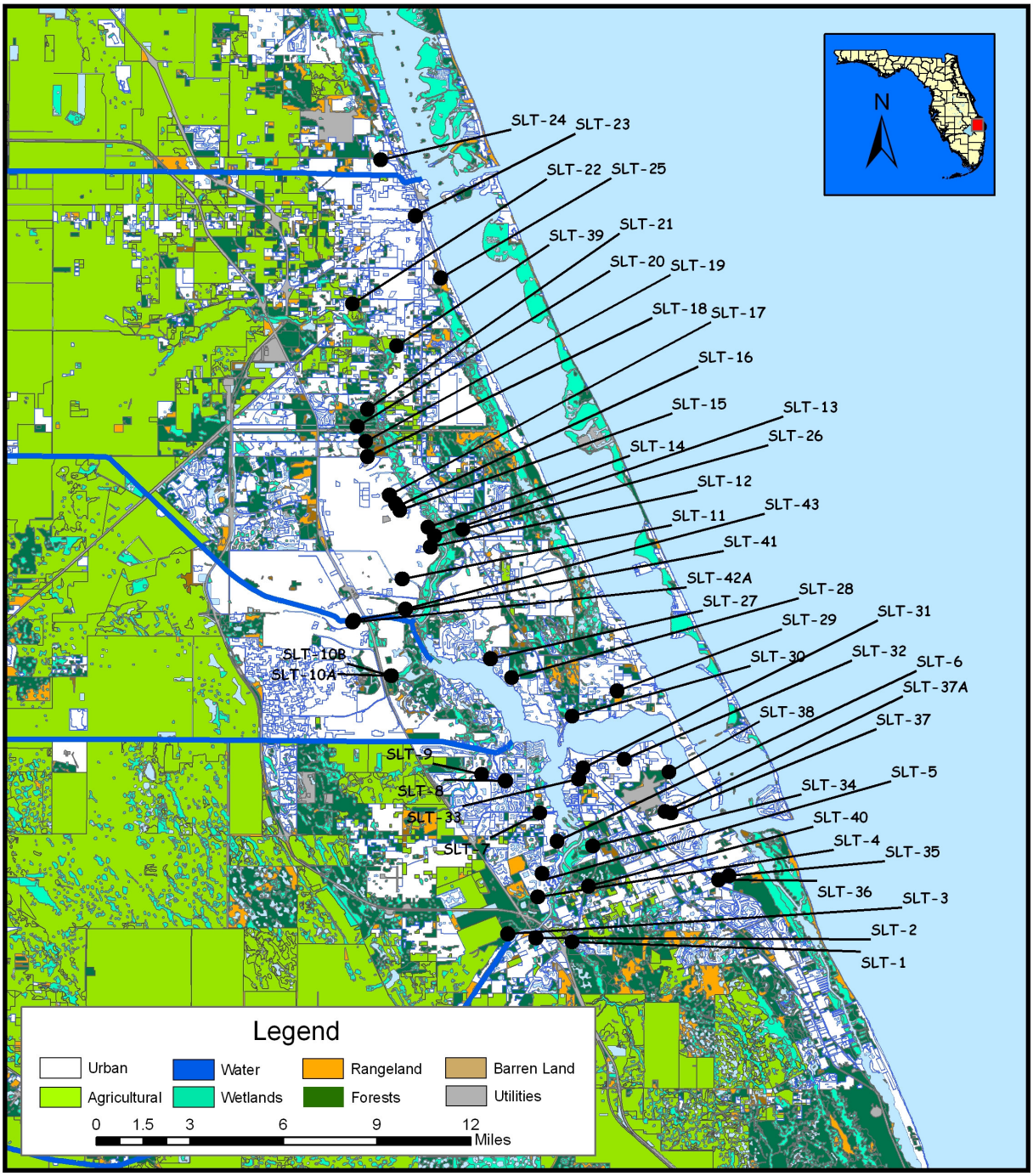

URS

Figure 2-28. Location of SFWMD SLT Stations. (Locations and Land Use data provided by SFWMD)

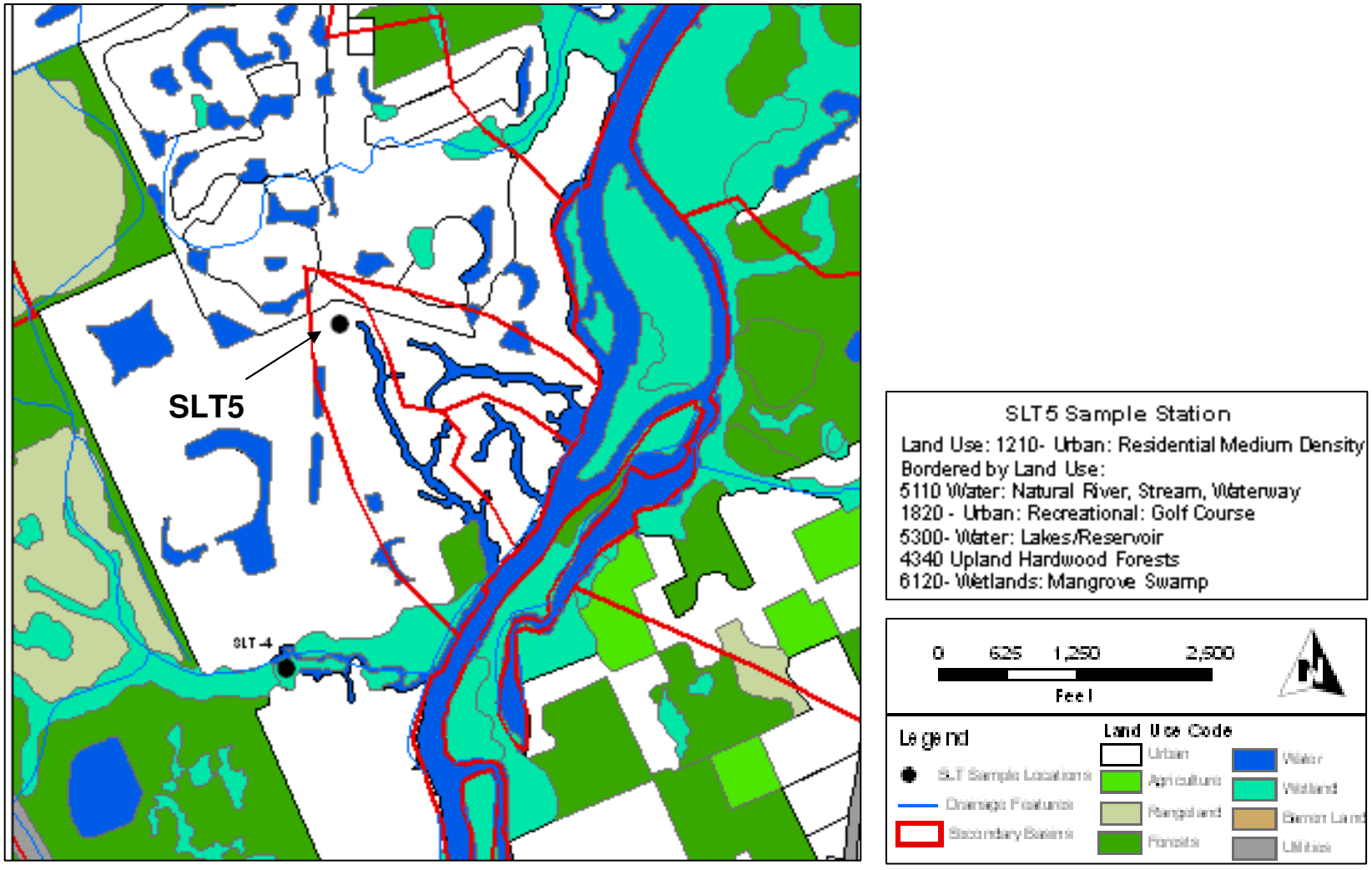

URS

Figure 2-29. Example showing Land Use associated with SLT Stations.

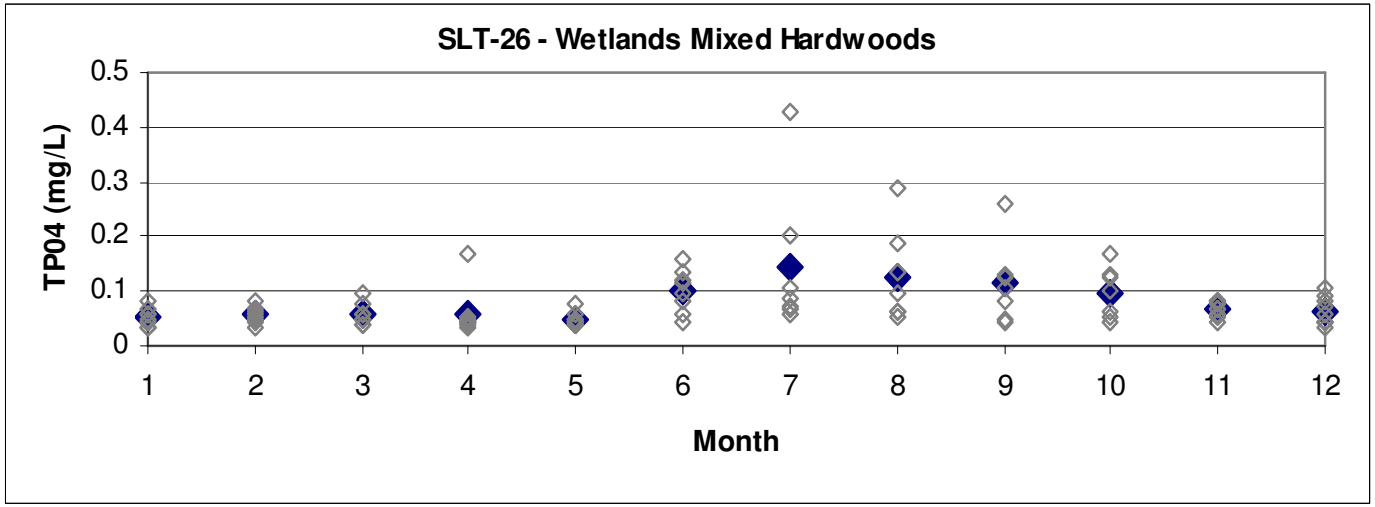

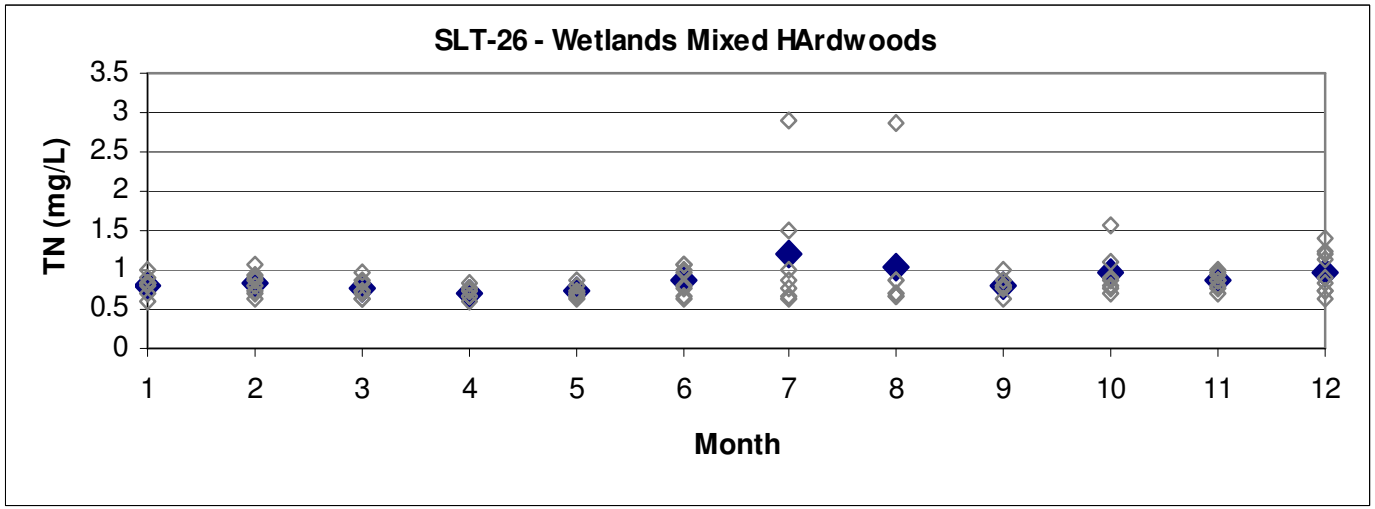

URS

Figure 2-30. SLT Station 26 Nutrient Data.

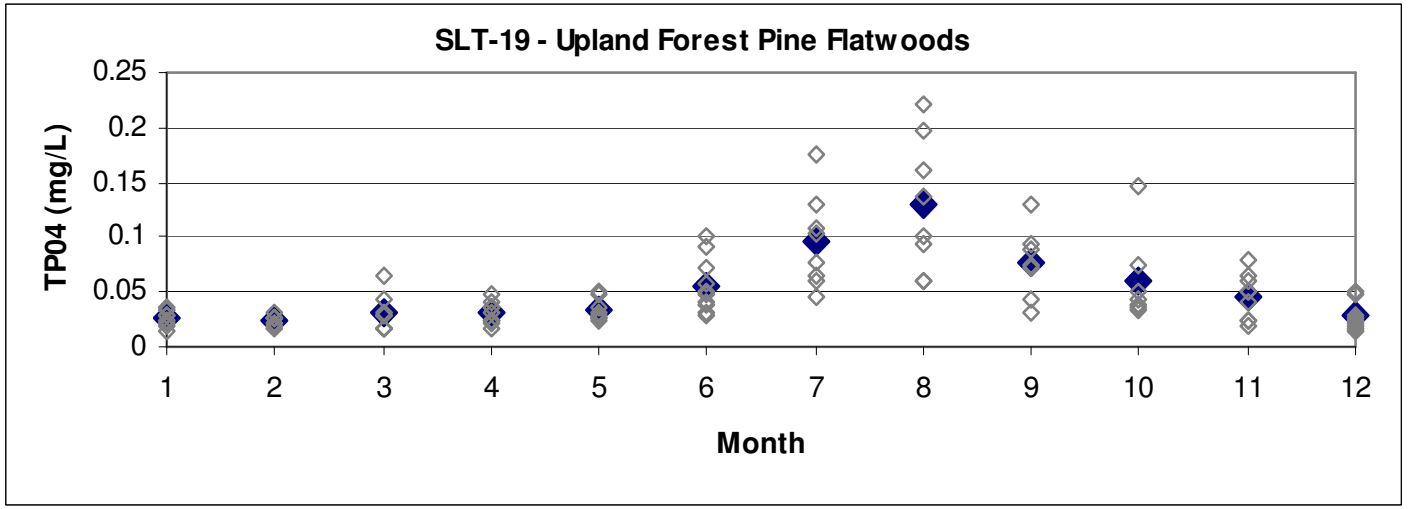

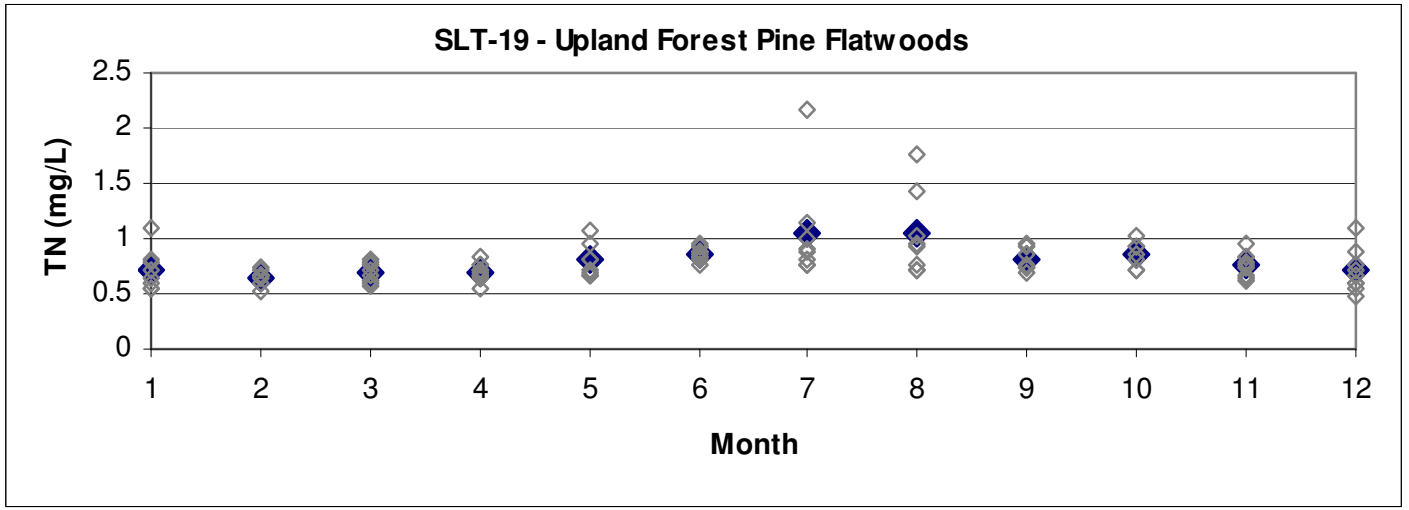

URS

Figure 2-31. SLT Station 19 Nutrient Data.

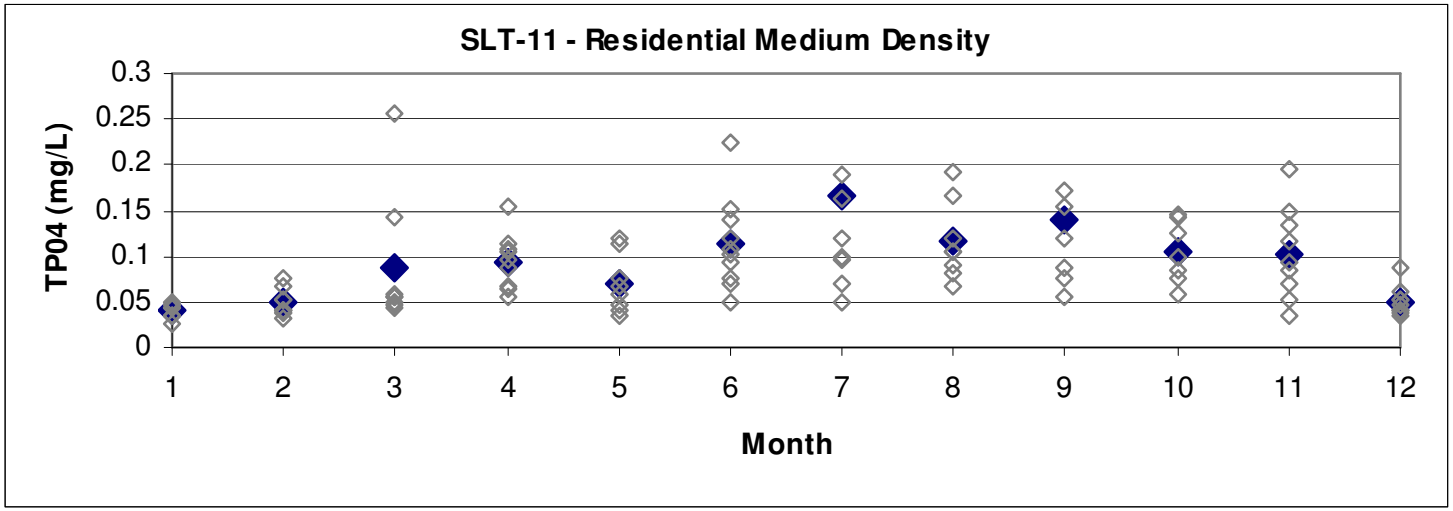

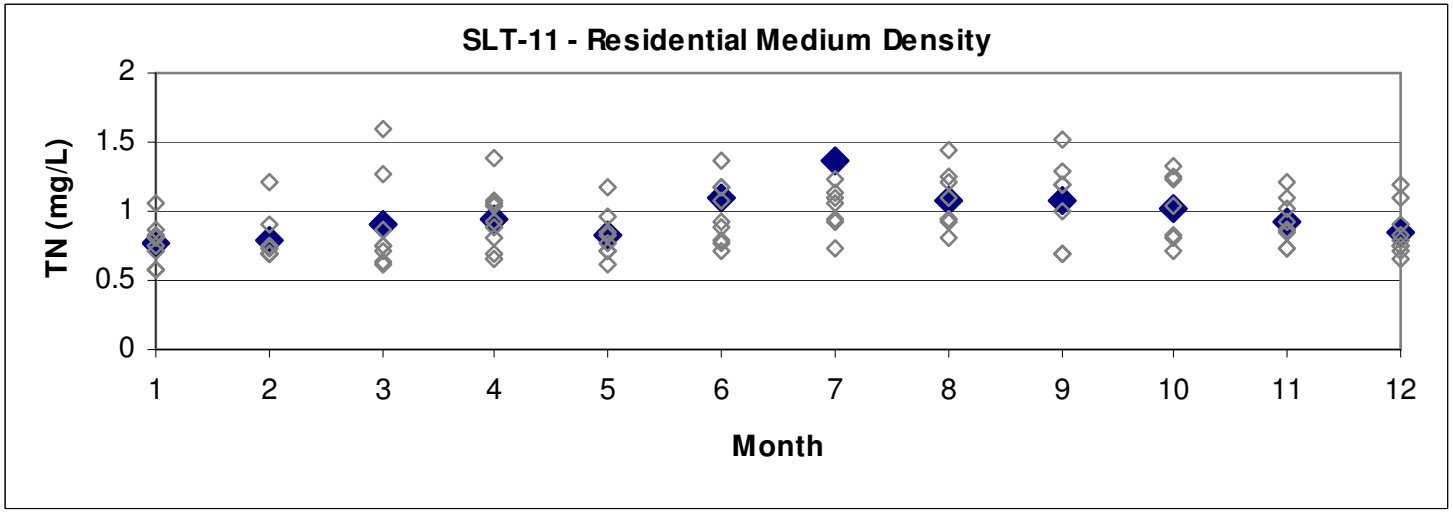

URS

Figure 2-32. SLT Station 11 Nutrient Data.

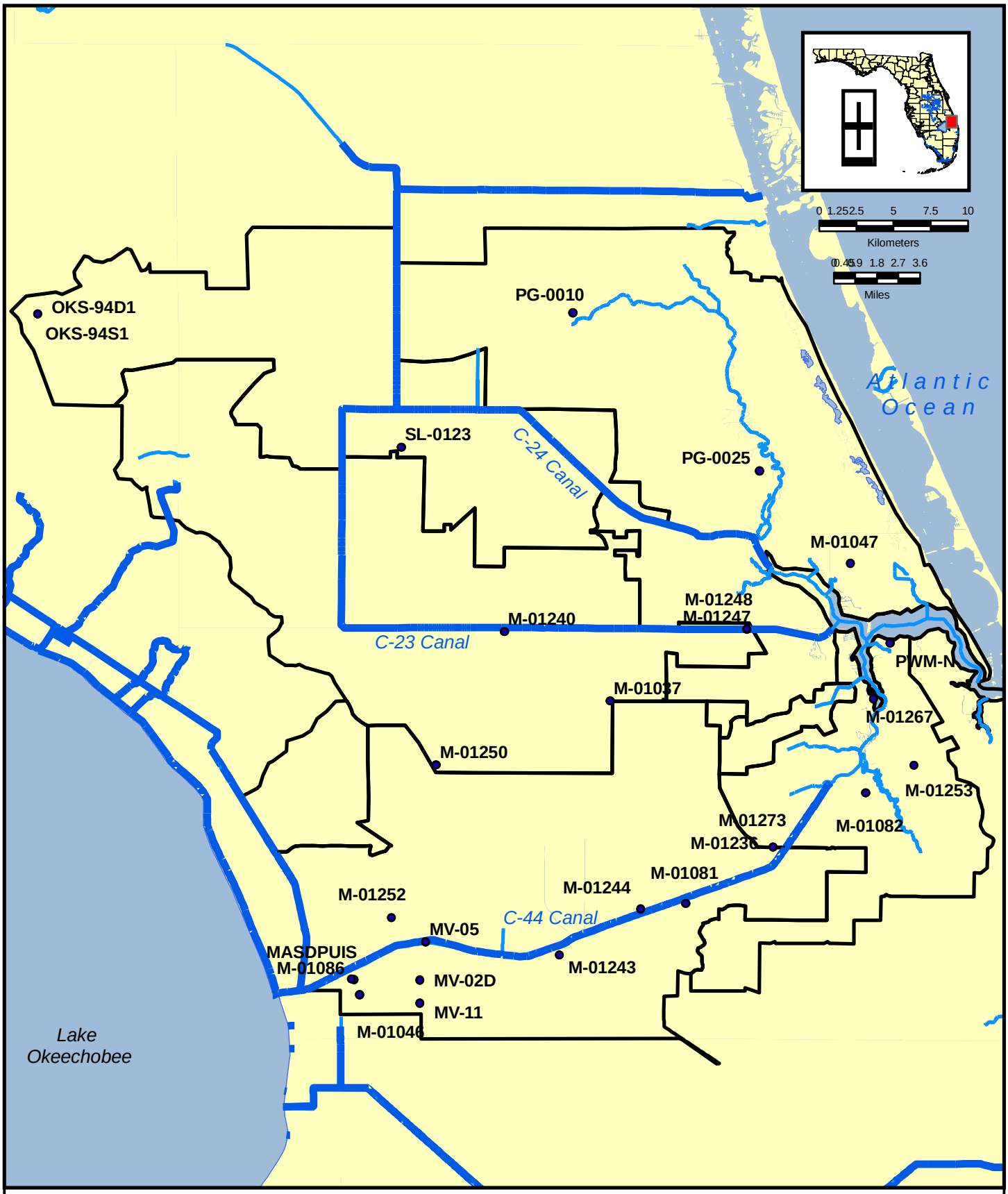

Figure 2.33. FDEP BMP Study Sample Locations.

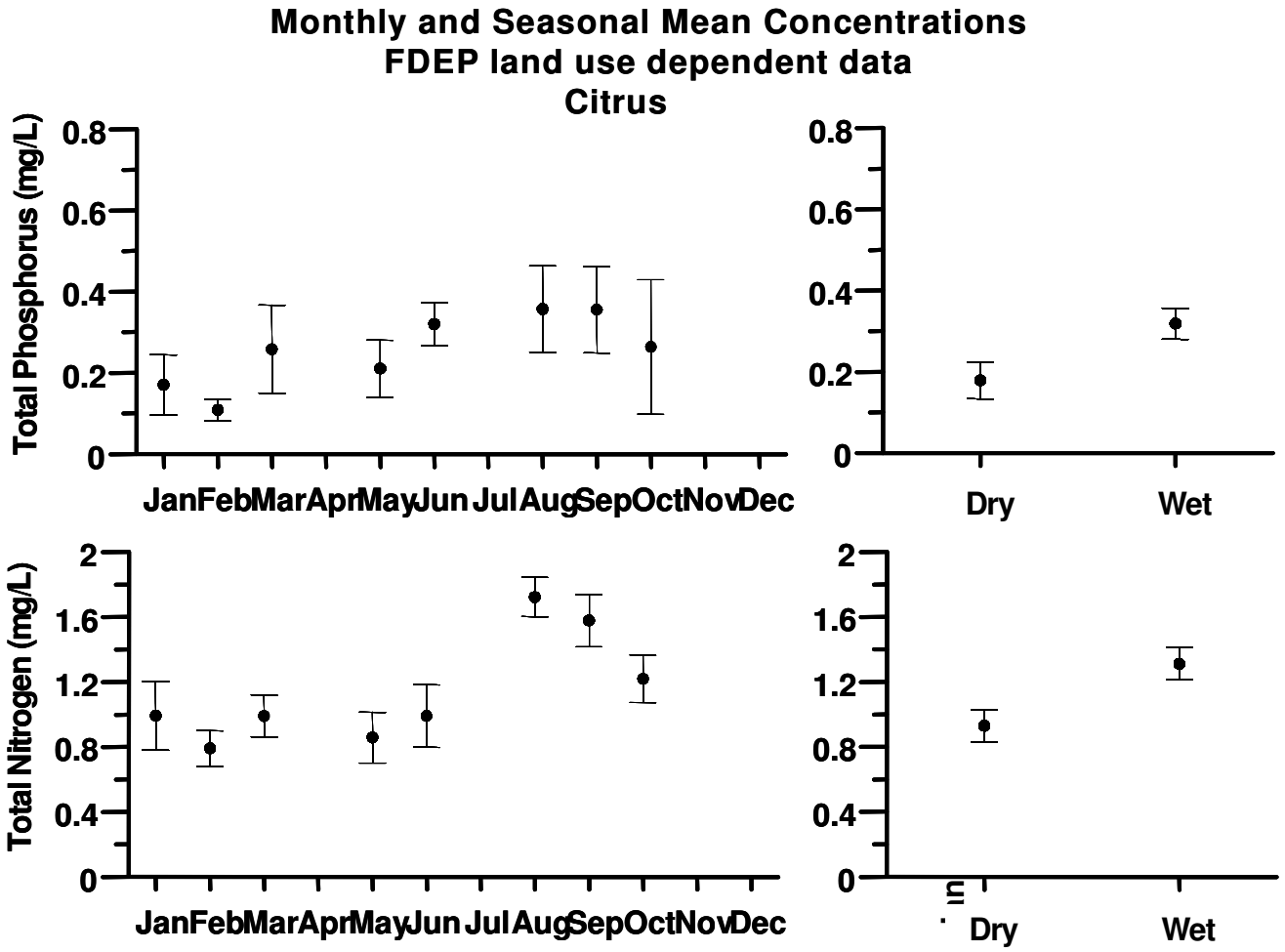

URS

Figure 2-34. Seasonal Variations in Total Nitrogen and Total Phosphorus at a FDEP Grab Sample "Citrus" Station.

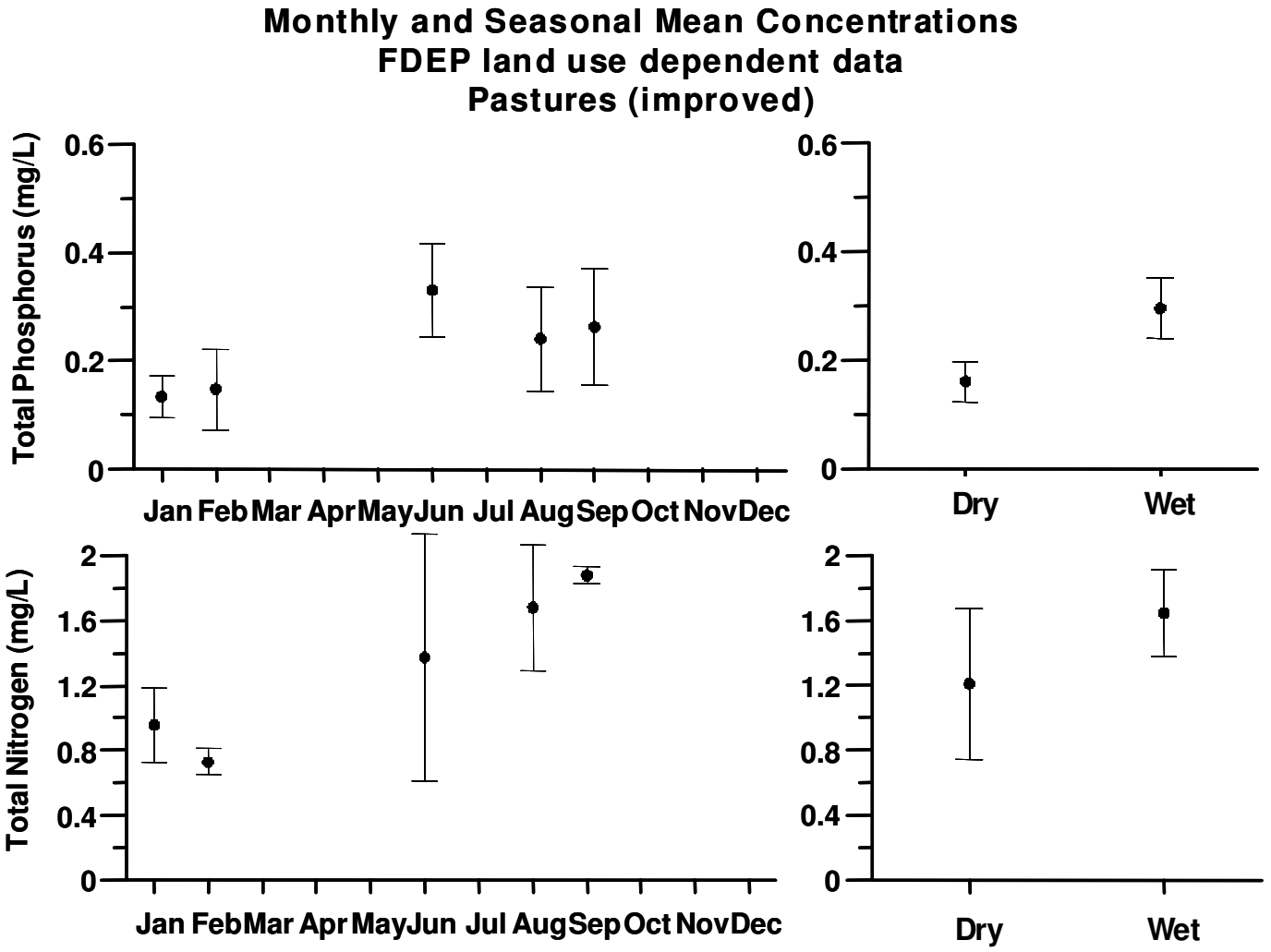

URS

Figure 2-35. Seasonal Variations in Total Nitrogen and Total Phosphorus at a FDEP Grab Sample "Pasture" Station.

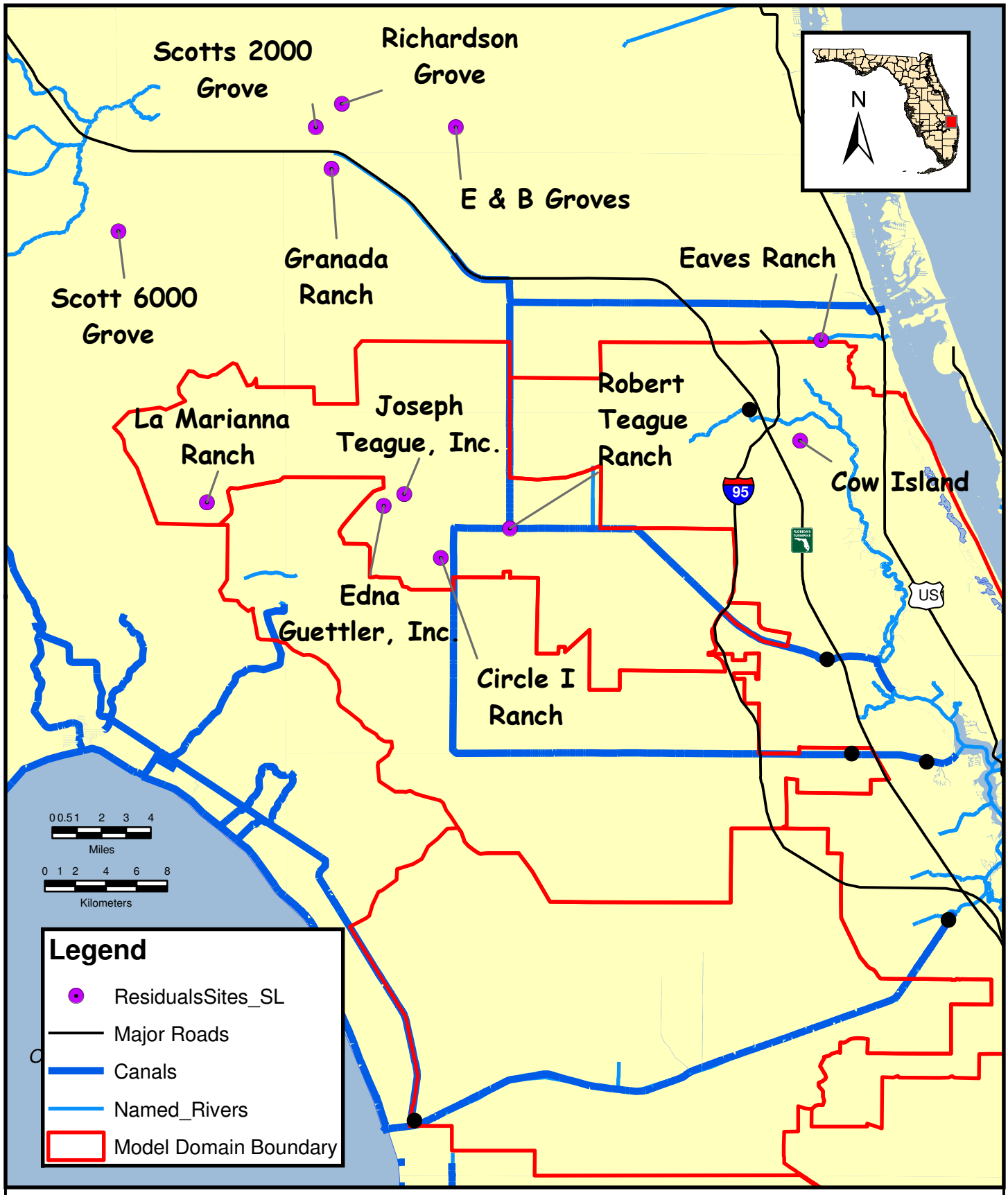

URS

Figure 2-36. Location of Residuals in St. Lucie County. (GIS coverages provided by FDEP.)

Facility	County	2001-TN	2001-TP	2002-TN	2002-TP	2003-TN	2003-P	2004-TN	2004-TP
Allapatah	Martin	633.779	198.77	506.74	159.14	0	0	0	0
BluefieldGrove	StLucie	0	0	0	0	0	0	359.407	172.471
BluefieldRanch	StLucie	0	0	7.587	2.503	29.324	11.124	16.648	15.898
CircleI	StLucie	0.497	0.303	22.463	84.217	82.076	99.183	160.846	134.205
CircleO	StLucie	0	0	17.178	18.996	0	0	0	0
Eaves	StLucie	0	0	46.212	15.987	43.436	16.682	0	0
Evans	StLucie	0	0	0	0	0	0	82.093	99.092
FloridaMaid	StLucie	0	0	0	0	89.915	37.679	77.877	28.875
Granada	StLucie	82.992	26.489	82.474	27.054	125.564	47.905	137.181	149.248
Guettler	StLucie	5.802	0.001	57.743	18.548	84.157	31.037	2.223	0.027
JosephTeague	StLucie	0	0	116.91	36.37	72.891	27.164	6.302	6.897
Modine	StLucie	0.019	0.007	16.53	24.486	60.817	18.115	66.214	1.246
RobertTeague	StLucie	0	0	73.611	23.56	107.729	40.768	41.476	38.351
TripleE	Martin	144.941	53.496	18.229	6.155	0	0	0	0

* All values reported in Tons/Year

URS

Figure 2-37. Nutrient loads from residuals.

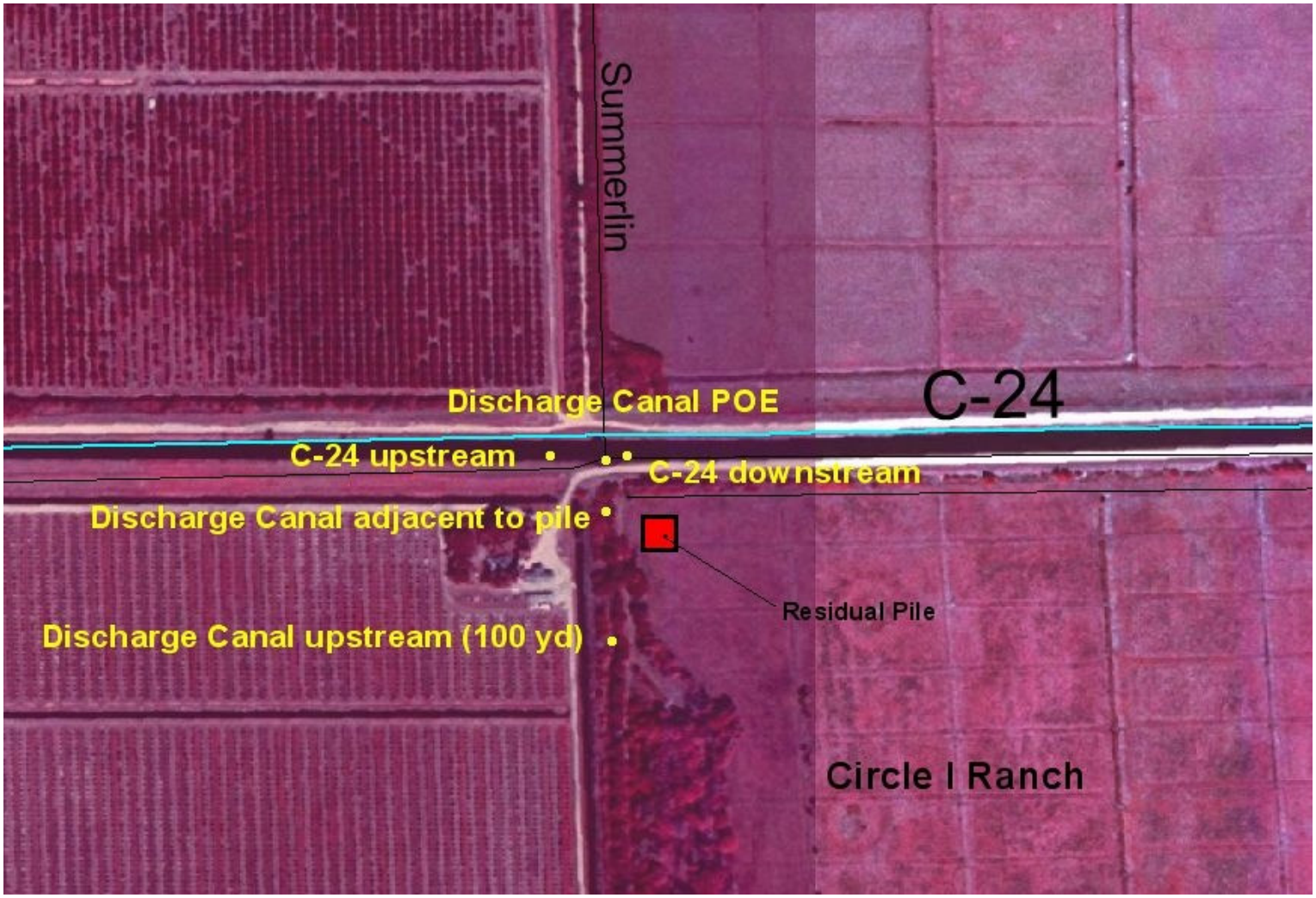

URS

Figure 2-38. Circle I Ranch Site Map with Residual pile and sampling locations.

Facility	County	Dry Tons Applied	2004 Total Nitrogen	2004 Total Phosphate		Fraction TN	Fraction TP
BluefieldGrove	StLucie	8,447.62	359.407	172.471		0.043	0.020
BluefieldRanch	StLucie	1,010.73	16.648	15.898		0.016	0.016
CircleI	StLucie	3,650.48	160.846	134.205		**0.044**	**0.037**
Evans	StLucie	6,293.82	82.093	99.092		0.013	0.016
FloridaMaid	StLucie	1,134.67	77.877	28.875		0.069	0.025
Granada	StLucie	9,165.73	137.181	149.248		0.015	0.016
Guettler	StLucie	41.91	2.223	0.027		0.053	0.001
JosephTeague	StLucie	369.41	6.302	6.897		0.017	0.019
Modine	StLucie	1,252.81	66.214	1.246		0.053	0.001
RobertTeague	StLucie	2,614.06	41.476	38.351		0.016	0.015
		33,981.25	total tons				
		1,132,708.20	ft^3 assuming 60 lbs/ft^3				
		283,177.05	ft^2 assuming 4 ft depth				
		6.50	acres				
		Relative Basin Load	Relative Residual Load	Residual Load as % of Basin Load			
		100,000.00	52	0.052			

Circle I Ranch

Log #	Location	TKN (mg/L)	TP (mg/L)
17072	Blank	0.11	0.003
17073	C-24 upstream	1.17	0.231
17074	C-24 downstream	0.86	0.231
17075	Discharge Canal POE	1.03	1.754
17076	Discharge Canal at pile	0.94	1.725
17077	Discharge Canal 100yds upstream	0.93	1.661
17078	Discharge from Field 11	1.17	1.785

URS

Figure 2-39. Computation of the fraction of TN and TP generated from Residuals.

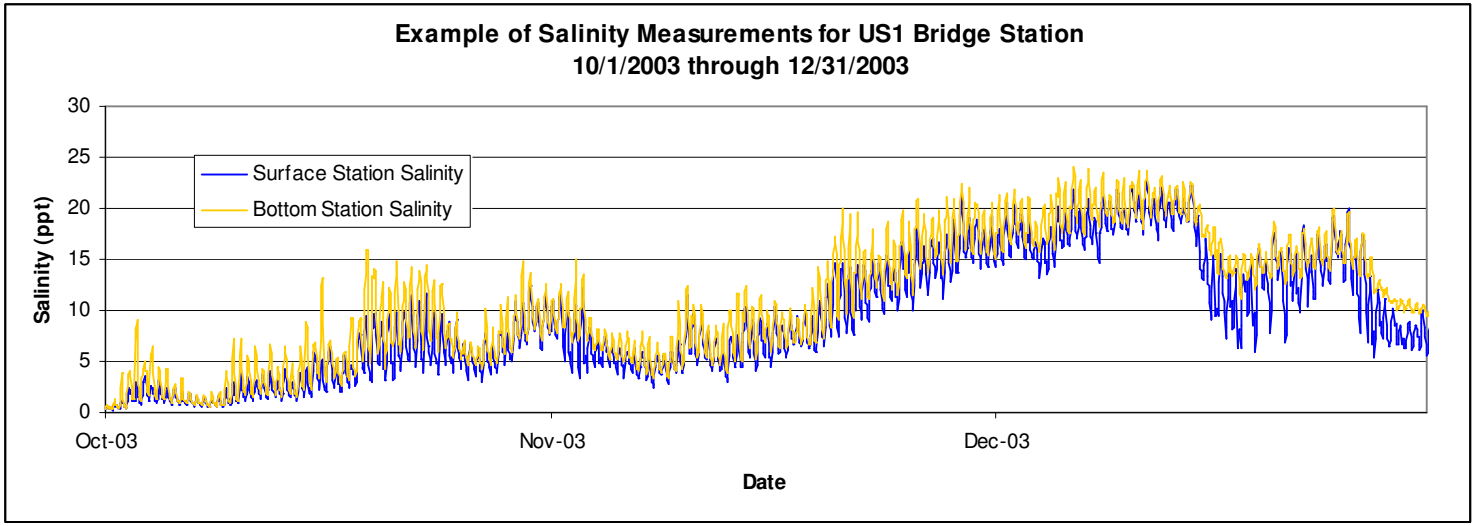

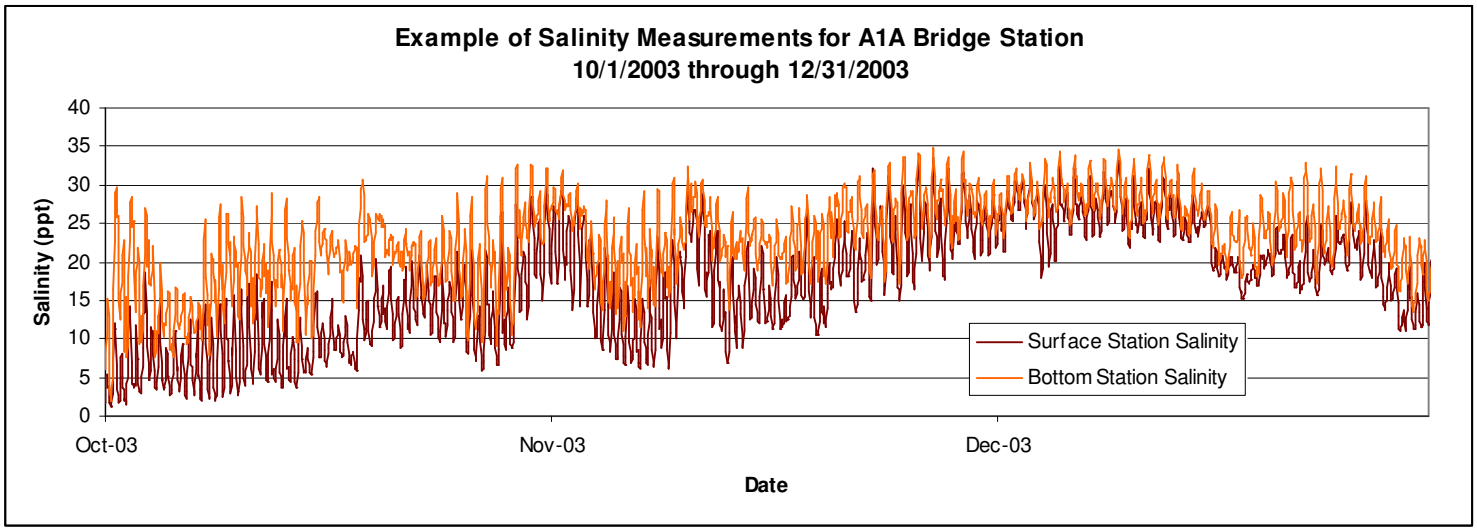

URS

Figure 2-40. St. Lucie Estuary representative salinity data at US1 and A1A stations.

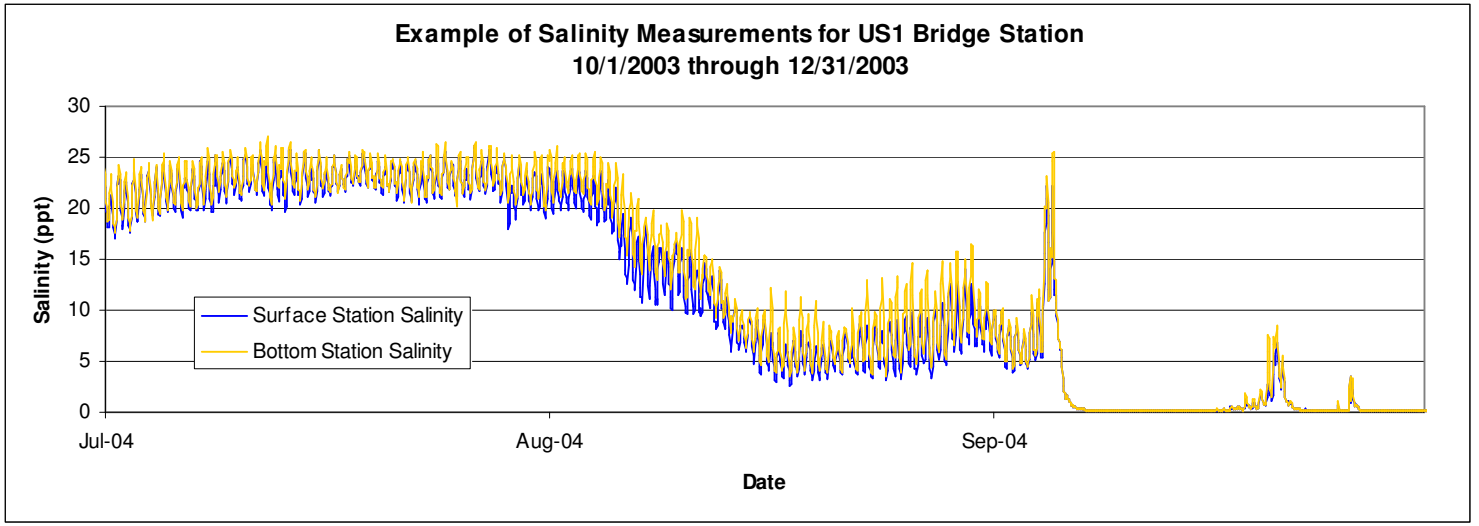

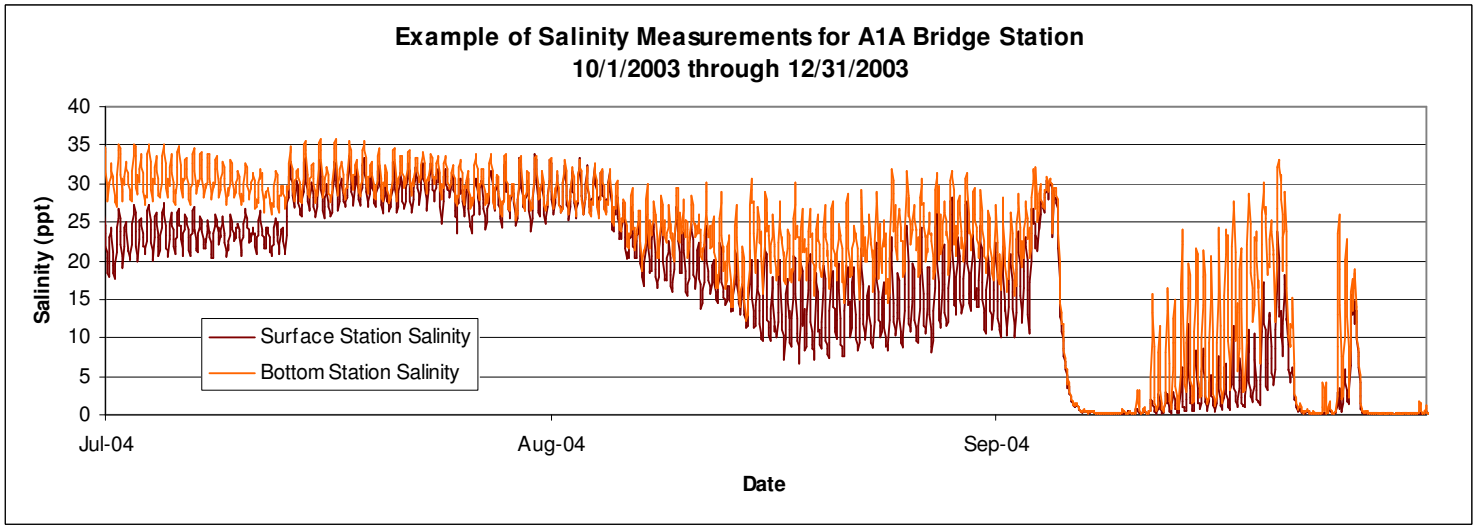

URS

Figure 2-41. St. Lucie Estuary representative salinity data at US1 and A1A stations.

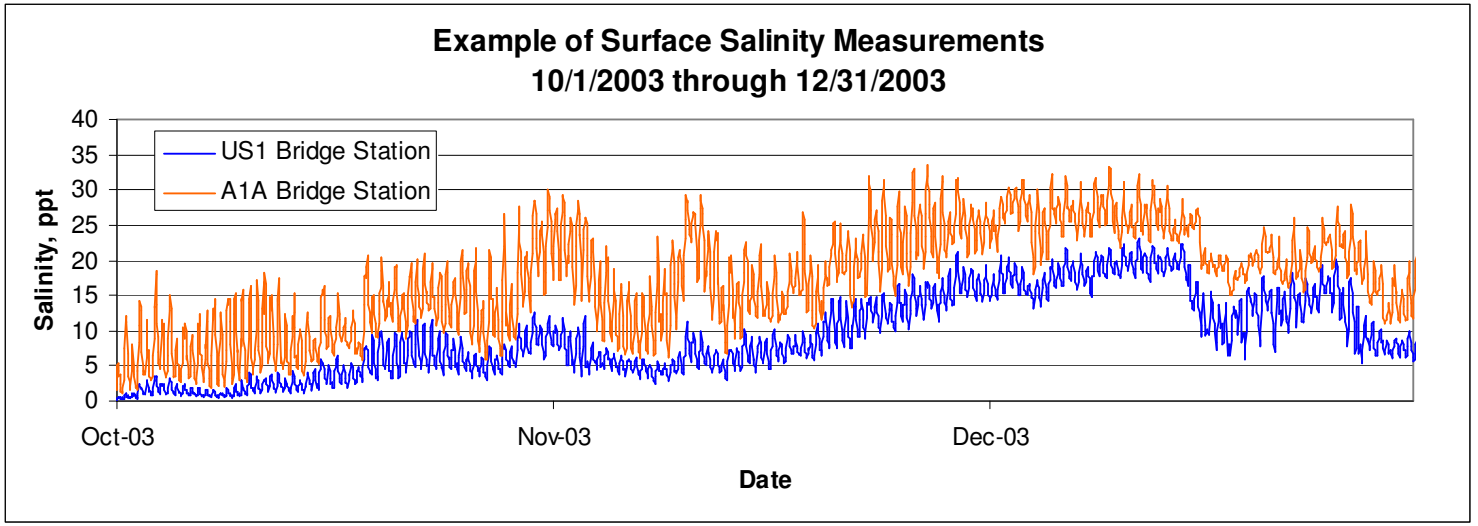

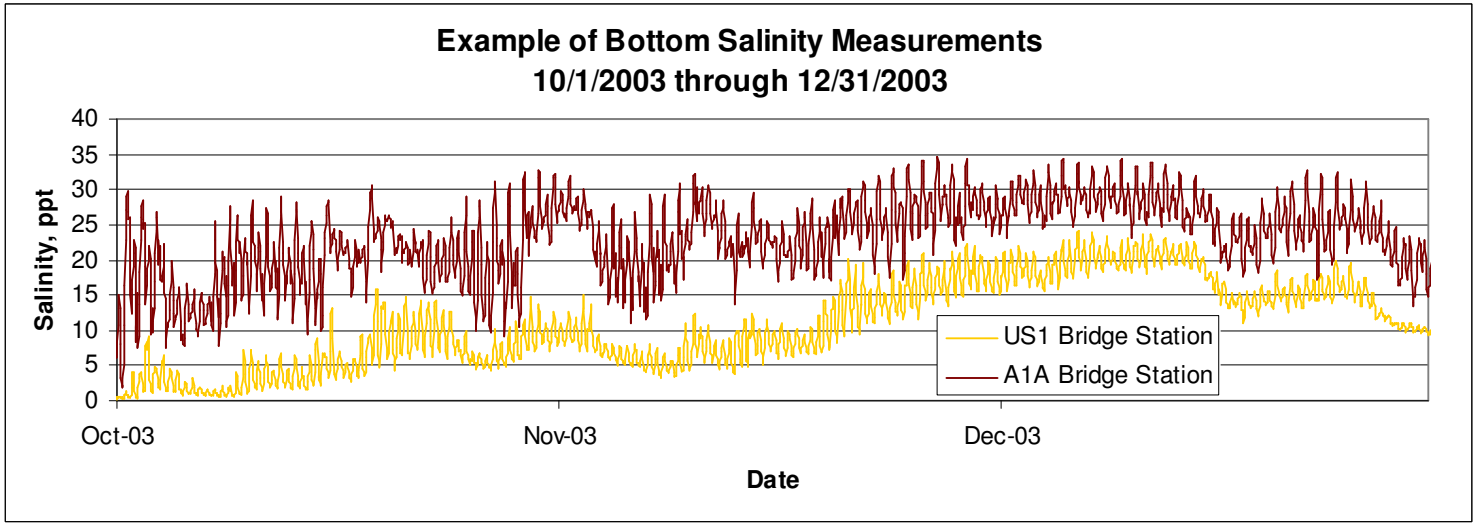

URS

Figure 2-42. St. Lucie Estuary representative salinity data at US1 and A1A stations.

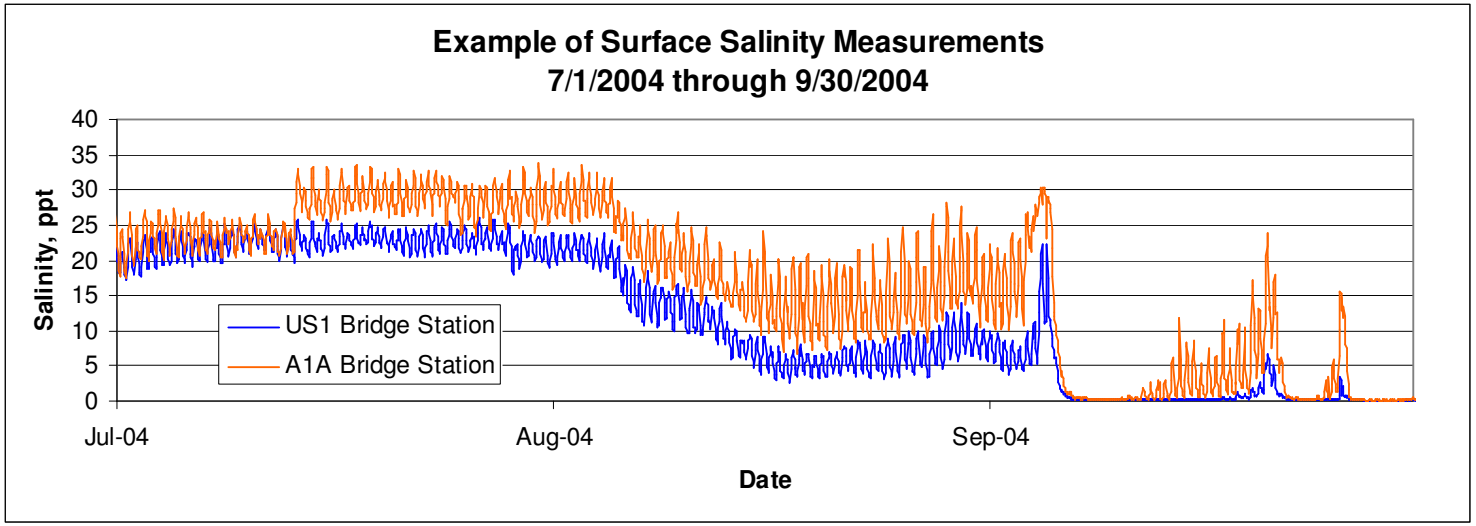

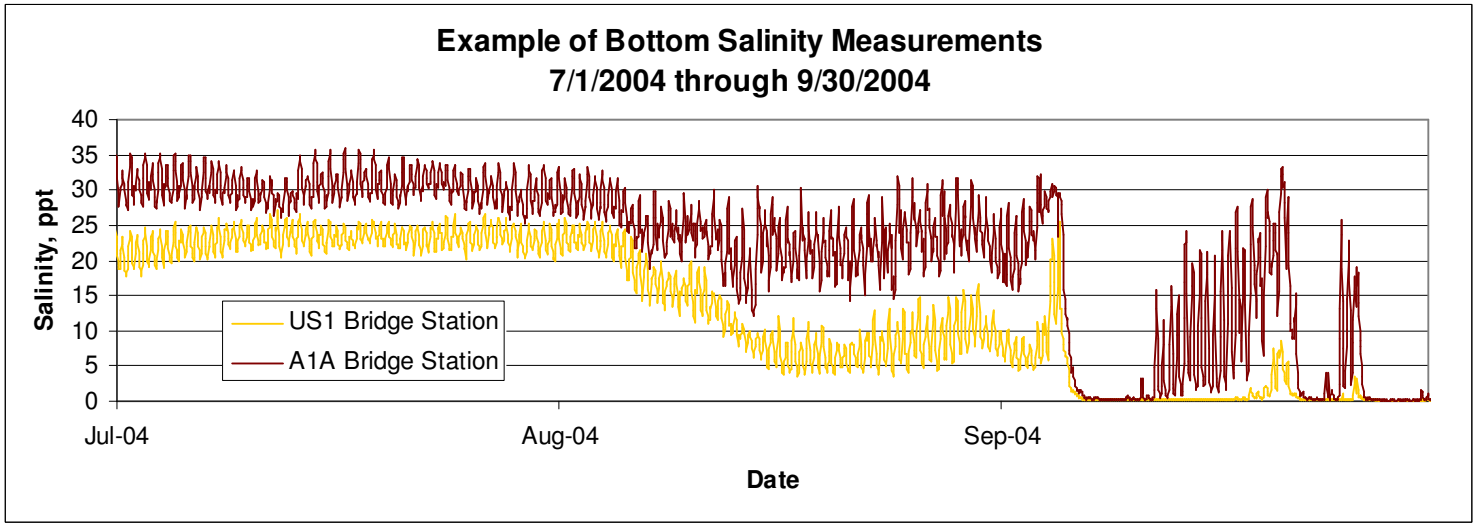

URS

Figure 2-43. St. Lucie Estuary representative salinity data at US1 and A1A stations.

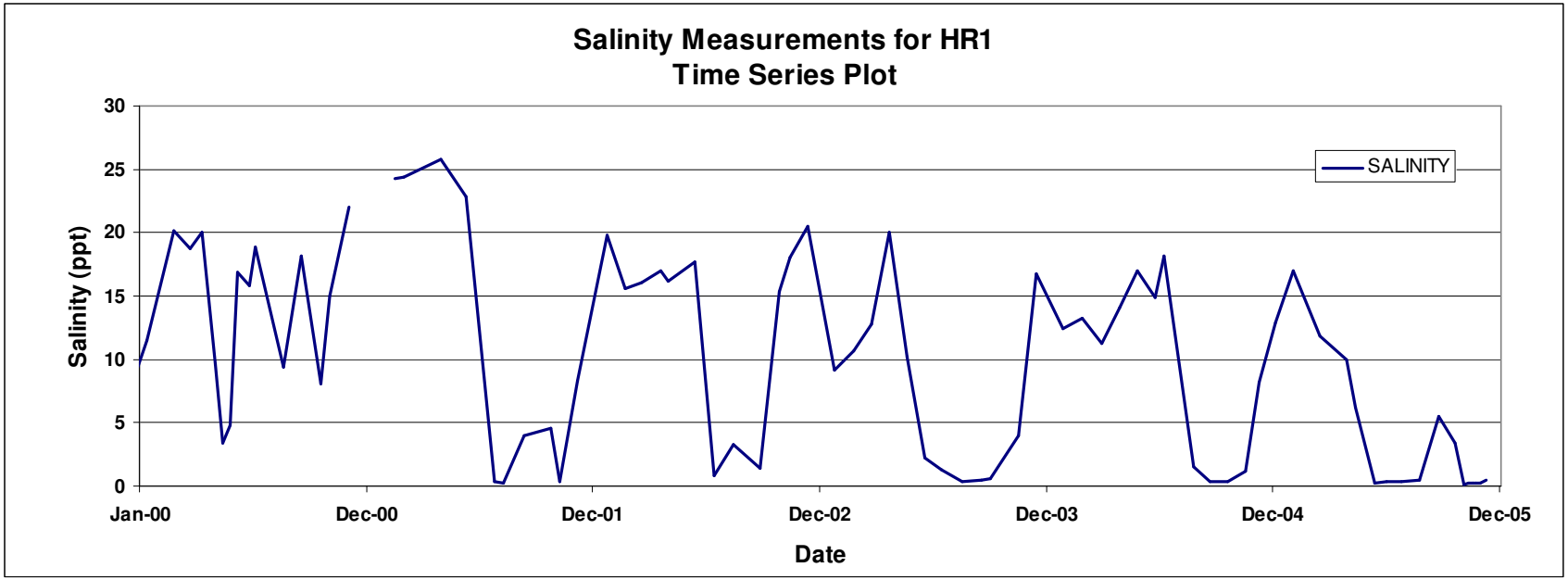

URS

Figure 2-44. St. Lucie Estuary representative salinity data at HR1 station.

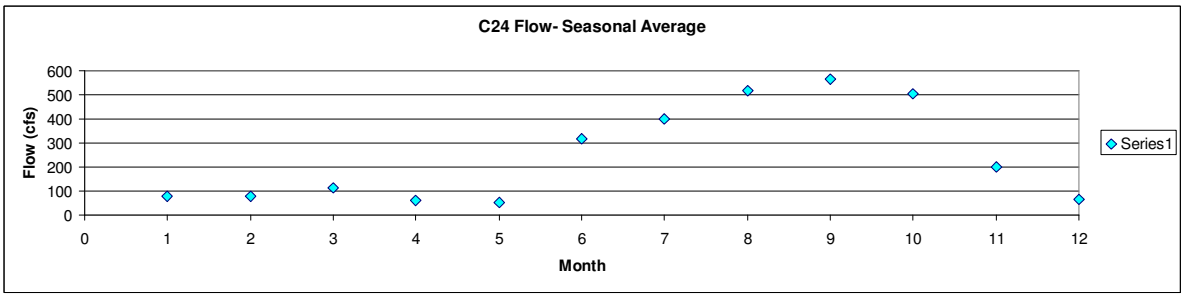

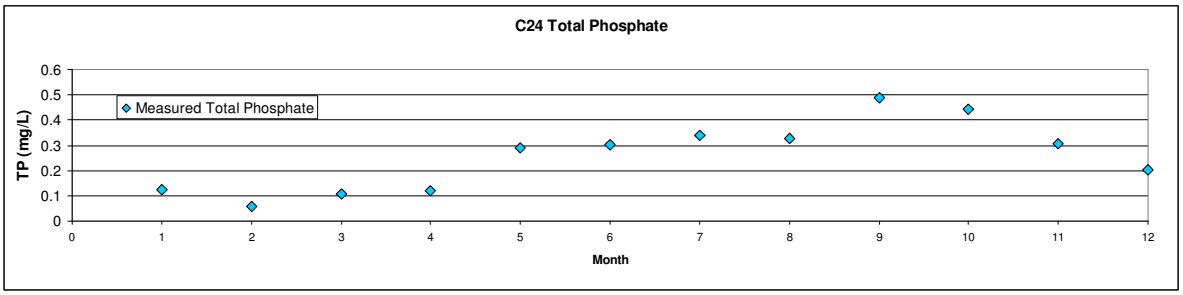

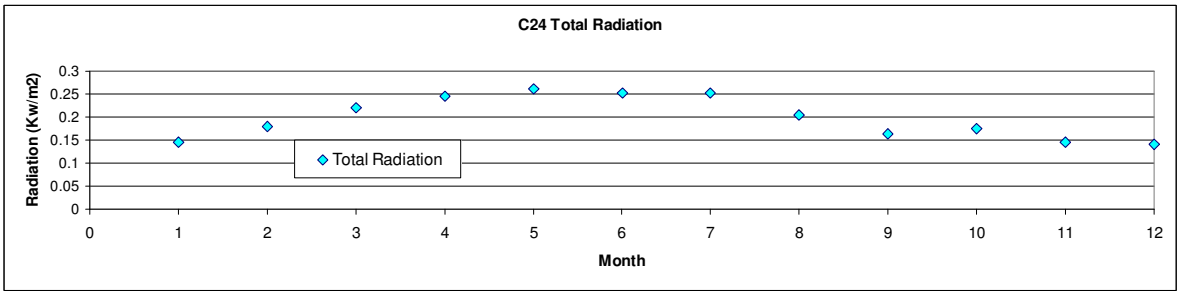

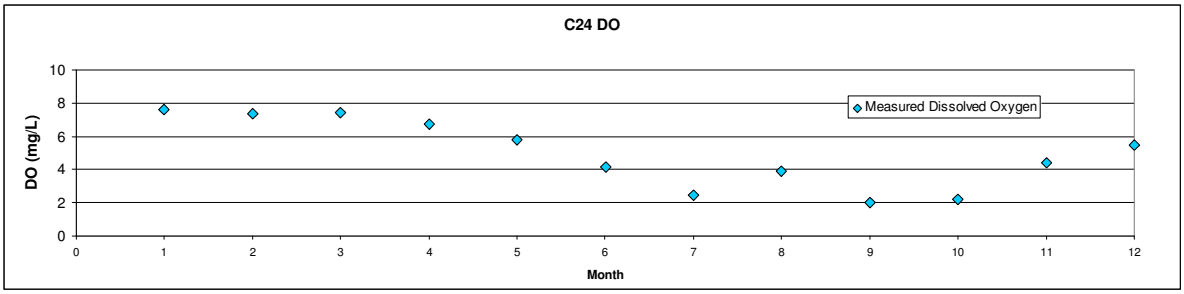

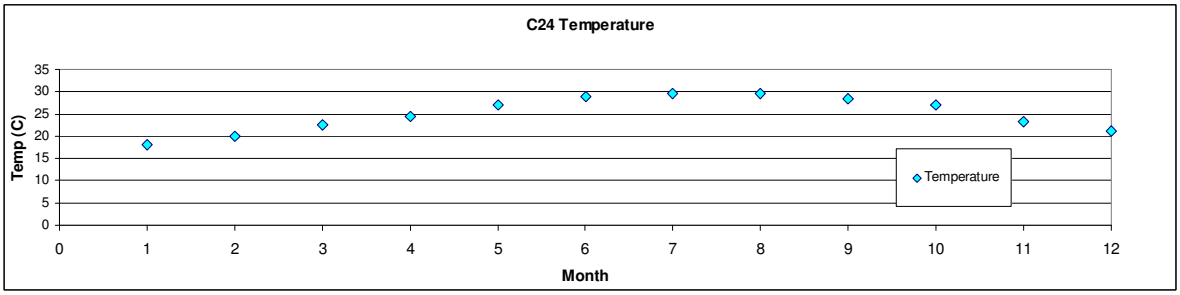

URS

Figure 2-45. Examples of Seasonal Variability in C24 Basin.

3.1 MODEL SELECTION

A comprehensive review of conditions in the watershed and the development of model selection criteria have been completed previously (URS, 1999). The selection criteria were developed for modeling analysis that could provide rigorous calibration to the available data, requiring daily simulation of flow and nutrients with highly variable residence times and controlling processes. The FDEP has similar modeling requirements, with the addition of resolving diurnal fluctuations of D.O. The analysis yielded a set of model selection criteria which are summarized below:

1. The model should represent multiple land-uses, soil types and associated water quality loads
2. The hydrodynamic simulation should represent:
    - The hydrological cycle (runoff, infiltration, evapo-transpiration)
    - Stream and Canal Flow with control structures
    - Two layer flow in the estuary
    - Irrigation demand and supply
    - Groundwater simulation
    - Coupling between groundwater and surface water
3. The water quality simulation should represent
    - Spatial distribution of runoff nutrient loads including association with land-use
    - D.O. balance including nutrient cycling and phytoplankton growth and decay
    - Groundwater loads
4. The simulation should be time dependent with a minimum of daily outputs for most quantities. Hourly outputs are needed to provide simulation of daily diurnal fluctuations in D.O. levels. This requirement is needed because the Florida State criteria for D.O. involve minimum levels at any time, as opposed to daily averages.

The WaSh model has been selected for this analysis for two primary reasons. First, it meets the model criteria established above. Secondly, it has already been applied in previous studies in the SLEW (URS, 2001). Since the WaSh model fulfilled the two criteria listed above, no other models were considered for this analysis.

The WaSh model is a coupled watershed water quality model (WaSh) originally developed with funding from the South Florida Water Management District (SFWMD) for simulating conditions in the St. Lucie Estuary (SLE) basins. WaSh is a time-dependent, coupled hydrologic and hydraulic simulation model. It includes representation of basic processes such as infiltration, runoff, evapotranspiration, percolation, groundwater flow, surface water flow, point sources and losses, and water quality fate and transport. It also includes many special features specifically required to simulate conditions in the SLE basins, such as irrigation demand and supply, high water table conditions, fully coupled groundwater and surface interactions, reservoirs and Stormwater Treatment Areas (STAs), and flow structures. The water quality module simulates the DO and algae dynamics and can be configured to represent the upper and lower layers in

estuarine segments of the model. The interaction of different modules of the WaSh model is illustrated in Figure 3.1.

The fundamental time step for the model is one day, and output from the model is provided in daily increments. However, certain model algorithms operate at shorter time steps (30 minutes to one hour), which are required to provide accurate representations of physical processes and provide numerical stability. General model outputs are daily time series of flows, stages, water quality loads and concentrations at points along the surface water flow system. Simulation results at the basin outfall can be provided at one-half hour intervals, for the purpose of viewing diurnal fluctuations in the dissolved oxygen levels due to phytoplankton production and respiration.

3.2 MODEL HIERARCHY

A strategy for configuring, forcing, calibrating and validating the WaSh model for the SLE system was developed based on the hydrodynamic characteristics of each basin and the available flow and water quality data. The modeling hierarchy is depicted in Figure 3.2. Four separate WaSh models were developed to represent the entire SLE system. Three models, each representing one of the basins separated from the SLE by structures, were calibrated and validated first. These are referred to as the C24, C23 and C44 models, respectively. The C44 model includes the S153 basin flows. The fourth model represents the combined NF, TSL, B-4, B-5 and B-6 basins, which needed to be modeled together since their surface water systems were all directly connected to the SLE and influenced by tidal flows. This forth model, referred to as the SLE model, also includes the North Fork, South Fork and Middle Fork, with the downstream boundary located at the end of the Middle fork, just upstream of the confluence with the Indian River Lagoon.

The hydrology and hydrodynamic components of the C-24, C-23 and C-44 basin models were calibrated and validated using daily flow data collected at their outflow structures (S49, S48, and S80). For the SLE model, no flow data was available. However, salinity data was available at Station HR1, sufficient for completing a model calibration. In order to calibrate the flows for the SLE model, the discharges from the calibrated C-24, C-23 and C-44 basins models were used as inflow conditions at their discharge points within the SLE basin model. Prior to using the C-44 discharges, the calibrated C-44 model was rerun with measured daily Lake Okeechobee discharges included as input at the western end of the C-44 canal. This model simulation produced C-44 discharges that include both the calibrated C-44 basin drainage and the measured contributions from Lake Okeechobee.

The approach for the water quality calibration and validation are identical to those for flow. The C-24, C-23 and C-44 basin models were calibrated first to data collected at their outfall stations (S49, S48, and S80). Then, their discharges are used in the SLE model calibration. There is sufficient data at stations within the SLE for calibration and validation (SE01, SE02, SE06, SE03, SE08, and SE09). Prior to using the C-44 discharges in the SLE model calibration and validation, the calibrated C-44 model was rerun with measured daily Lake Okeechobee loads included as input at the western end of the C-44 canal.

3.3 MODEL CONFIGURATION

The spatial distribution of physical characteristics in the WaSh model is represented on a uniform Cartesian grid. The spatial distribution of land-use, soil type, topography, canals, rivers and streams and control structures are required to configure each of the four basin models. The spatial distribution was obtained in the form of GIS shapefiles, the contents of which were mapped onto each model grid. For this application, the WaSh model uses an ArcView 3.2 Graphical User Interface (GUI). Models were constructed using six input data shapefiles, including primary basins, secondary basins, soil type, hydrology, land-use, and topography. For each of the models, a cell size was chosen that would maximize the resolution of basin drainage features without sacrificing model efficiency and run time.

3.4 MODEL DOMAIN AND GRID

The grid extent for each basin model was selected to cover the entire basin. The basin boundary shapefile was used to define the extent and a Cartesian grid was constructed that covered the entire basin. Grid cells that were located outside the basin boundary were set as inactive. Cells that intersected the boundary were clipped to the basin boundary so that the total area of the basin was preserved in the model grid. For each of the structurally controlled basins C-24, C-23, and C-44, a grid cell length of 2000 ft was used, creating grid cells which covered an area of 4,000,000 sq. ft each. For the St. Lucie Estuary model, due to the inclusion of the smaller basins 4,5, & 6, a grid cell length of 1500 ft was used, creating grid cell areas of 2,2250,000. Primary basin boundary coverage was acquired from SFWMD GIS database. C-24 primary basin boundary and model grid is presented as an example in Figure 3.3.

3.5 GRID ATTRIBUTES

After defining the model grid and extents, each grid cell was assigned physical attributes controlling the hydrodynamics of the basin. This GIS shapefile mapping was achieved by using attributes from secondary basin, land-use, soils, topography, and hydrology coverages.

3.5.1 Secondary Basin

The secondary basin boundary coverage is a polygon feature, which adds a more control to the overland flow regime or flow path within each primary basin. During model generation, the secondary basins help to constrain the cell-to-cell surface flow paths based on documented drainage patterns. As topographic resolution can often be too course or too subtle in South Florida for the model to distinguish, the assistance of additional secondary boundaries produces more accurate drainage patterns. C-24 secondary basins are presented as an example in Figure 3.4.

3.5.2 Soils

Soil types are used in model generation, as they guide the selection of model parameters that affect the run-off and/or infiltration for each grid cell. The polygon feature of soils coverage includes a hydrogroup attribute, which defines a grid cell the ability to absorb, hold or repel surface and groundwater based on the dominant soil type. Soil type for C-24 basin is shown as an

example in Figure 3.5. Note the areas which are not shaded in the model domain. These indicate areas for which no data is available. For these areas, the soils data was extrapolated from the closest region with data.

3.5.3 Land-use

Each grid cell was attributed with a land-use designation, as the land-use attribute is a key parameter controlling the selection of model parameters that affect hydrology, irrigation practices and water quality runoff concentrations. The 1999 land-use coverage was used for attributing the grid, as it provided the most complete and accurate dataset available for current land-uses. The land-use coverages were subject to quality assurance reviews by state, county and local agencies. An example of C-24 basin land-use is presented in Figure 3.6.

Upon model generation, the WaSh model assigns to each grid cell the most dominant land-use within that cell (Figure 3.7). When dominant land-uses are assessed basin-wide, the smaller land-use polygon features can often be overlooked by the model and, therefore, under-represented in each model basin. This typically happens, for instance, when wetlands in a basin consist of small patches distributed throughout a forested area or pasture land. The small patches never dominate the cell area and are therefore overlooked, resulting in an under-representation of the wetlands land-use in the model configuration. Thus, the percentage of each category of grid-generated land-use varies from the actual land-use coverage for the basin (Figures 3.8a & 3.8b). One method to eliminate this artifact of the grid discretization is to use smaller grid cells. However, this approach will require many more cells to represent the basin, and will lead to unreasonable simulation times. An alternate approach is to manually alter the land-use in individual cells so that the grid-based land-use designation preserves an accurate representation of current land-use within each basin.

For land-use analysis, spatial distribution of each FLUCS Level 3 codes was calculated for the updated 1999 dataset and for the attributed model grid. Land-use of individual grid cells were then changed until the proper percentage of each land-use category was represented within the grid. Manual reassignment of land-use was performed in a manner that would closely resemble the actual land-use patterns of the updated 1999 land-use coverage.

3.5.4 Topography

A three-dimensional DEM/TIN topography coverage was created in ArcView using a point shapefile with elevation data. Using the TIN, the model assigned the average elevation within each cell to the cell. The TIN coverage, as mapped onto C-24 basin model grid is shown in Figure 3.10.

3.6 HYDROLOGY

3.6.1 Canals, Rivers and Streams

Hydrology coverage is a polyline feature including both natural and man-made drainage features. This coverage includes rivers, streams, and primary, secondary and tertiary canals. The coverage was updated to differentiate the tertiary canals and the primary canals, rivers and streams that are explicitly represented in the reach network. An example of C-24 basin hydrology overlaying the

C-24 basin model grid is shown in Figure 3.11. The tertiary canal coverage was mapped onto the grid cells with the attribute of total length of canals. The canal widths and bottom elevations were obtained from default values based on the cell land-use type attribute. The default values were obtained in a previous calibration effort (URS, 2001) and used here as initial estimates of the canal properties. The remaining coverage for primary canals, rivers and streams was used to develop the reach network. Using the arcs that were designated as primary reaches, rivers or streams, the arcs were digitized to create the reach network. In order to accurately represent the flow characteristics within each reach, the canal or river dimensions must be entered in the model. Optimally, canal blueprints were used to calculate canal dimensions. When they were unavailable, aerial photos and structure depth data was used. Each primary reach segment was then assigned a width and depth appropriate for that segment.

The WaSh model has the option to simulate the canal (or river) systems as a single layer or as two layers. The two-layer option was developed to improve the representation of deeper channels or in stratified systems in which vertical mixing is inhibited and distinct upper and lower layers develop. The single layer option was used for the C-23, C-24 and C-44 basin models, since there was no depth dependent data to warrant a multiple layer model. However, there is depth-dependent salinity and water quality data available for the SLE and therefore in the SLE model the two-layer option was used.

3.6.2 Groundwater and Surface Water Interactions

The WaSh model requires additional cell attributes to represent the connection between reach segments, cells, cells with tertiary canals, and connections with the groundwater table. The connections are identified in the WaSh model by a cell attribute that controls the physical interactions that are applied to each cell. The available cell attributes and their influence on the hydrology and hydrodynamic simulations are described in Table 3-1. The WaSh GUI provides a tool for mapping the cell-type attribute onto each cell. This tool was applied to each of the 4 models. The results of the digitizing of the reach network and the cell-type mapping are shown in Figure 3.12 for the C-24 basin model.

Table 3-1. Water Routing Operations for Each Cell Type.

Cell-Type	Flow Routing Operations
Free	Infiltration is directed to cell groundwater Surface water is directed to a nearby cell's canals, reach or reservoir*
Canal	Infiltration is directed to cell groundwater Surface water is directed to cell canals Groundwater and canal surface water allowed to exchange
Free-Reach	Infiltration is directed to cell groundwater Surface water is directed to the cell's reach or nearby cell's canals Groundwater and reach surface water allowed to exchange
Canal-Reach	Infiltration is directed to cell groundwater Surface water is directed to cell canals Groundwater and be exchanged with canal surface water and with reach surface water Canal and reach surface water can be exchanged
Free-Reservoir	Infiltration is directed to cell groundwater Surface water is directed to the cell's reservoir or nearby cell's canals ** Groundwater and reservoir surface water allowed to exchange
Canal-	Infiltration is directed to cell groundwater Surface water is directed to cell canals

Cell-Type	Flow Routing Operations
Reservoir	Groundwater can be exchanged with canal surface water and with reservoir surface water
* a nearby canal cell or reach is determined by the flow network which is discussed in the next section ** the surface water does not necessarily have to drain to the coincident reach in a free-reach cell, for instance, in the case that a dike separates the reach from surface water runoff.	

3.6.3 Overland Flow Routing

The WaSh model also represents the details of the overland runoff. Overland flow is designated by a cell-to-cell connections which guide the direction that runoff is routed. The flow continues from cell-to-cell until it reaches a surface water body, either cells with tertiary canals, a segment of the reach network or a reservoir. The WaSh GUI provides a tool that estimates the overland flow paths based on topographic gradients. Drainage of surf ace water will be routed from each cell to another, down-gradient cell.

Due to the flat terrain characteristics of South Florida and the intense canal network, the model can overlook hydrologic features, resulting in the generation of improper flow paths. At this point, flow paths must be manually redirected. With the secondary basin boundaries and hydrology coverage as guidelines, flow directions were manually realigned using a WaSh model GUI tool, to provide an accurate representation of the actual overland drainage patterns. An example of the overland flow drainage developed for the C-24 basin model is shown in Figure 3.13.

3.6.4 Structures

Four structures were explicitly represented in the basin models. These structures have a profound effect on the daily discharges and their proper representation is critical to a successful calibration. The structures are the gates at the outfalls of the C-24, C-23 and C-44 canals (S-49, S-48 and S-80) and the Gordy Road Structure. These structures were explicitly represented in the models and the published operational criteria were used to configure the gate model parameters. However, the actual gates are not always operated according to the published criteria and adjustments are made manually to their operation in anticipation of large rainfall events and projected draughts. These types for gate operations cannot be modeled accurately and therefore their effect must be considered in the interpretation of the calibration and validation results. Also, the WaSh model representation of gated structure operations does not include all operational controls, and therefore it is necessary to adjust the WaSh model implementation of the structures during the flow calibration to best represent their role in controlling discharges. The details of the adjustments are discussed in Section 4.0.

3.6.5 Rainfall Configuration

The NexRad cell coverage presented in Figure 2.16 was used to spatially vary the rainfall time series data used in the model. Figure 3.14 shows the cell centers for the rainfall database and the footprint of the C-24 and North Fork basins within the St. Lucie Watershed.

The ESRI GIS software was used to find the nearest NEXRAD cell for each of the WaSh model cells. Each model grid cell was attributed with appropriate NexRad rainfall station index ID through a spatial join. Figure 3.15 shows a color-coded mapping of the WaSh model cells

indicating which NEXRAD cell rainfall data is used for each cell in C-24 basin model. There are 45 NEXRAD stations used in the C-24 basin model. This mapping was applied to all four models and the results were used to create the rainfall input file for each of the basin models.

3.6.6 Reservoirs

The Florida Power and Light reservoir in the C-44 basin comprises 5772 acres and due to this relatively large size, it is explicitly represented in the model configuration. The extent of the reservoir and its representation in the C-44 basin model are shown in Figure 3-16. The dark grey cells have been set as inactive since they are totally overlain by the reservoir. The light grey cells are only partially covered, and their cell areas have been adjusted to account for the covered portions.

The reservoir provides cooling water for the FPL operations. It is operated such that the water elevation in the reservoir is maintained at a prescribed level. When the reservoir water elevation is high, water is discharges to Lake Okeechobee and when the water level is low, water is pumped from the Lake. Thus the interaction with the C-44 basin is minor, and the reservoir collects a small amount of runoff from surrounding land.

In order to represent these conditions, the reservoir was configured so that water is discharged form the reservoir when the water elevation exceeded 4.0 ft elevation and the groundwater exchange coefficient was set to zero. During the model simulation, the occasional runoff generated from the neighboring areas (i.e. light grey cells) during runoff events would accumulate in the reservoir. When the reservoir water elevation exceeded the critical elevation of 4.0 feet, water was discharged from the system.

3.7 BOUNDARY CONDITIONS

The boundary conditions are only required for the SLE model and are needed to specify conditions at the downstream tidally-influenced boundary in the reach network. Tidal amplitude data is required to specify the stage at the downstream boundary. When the model simulation predicts flow into the estuary from beyond the downstream boundary, salinity and water quality parameter values are needed to set the concentrations for the inflows. The other three basin models have control structures at the basin outlets and there is no downstream influence on the flows or water quality in those basin models.

Hourly tide amplitude data was available for the period of 2002 – 2005 at the A1A bridge station. The period of record for the tidal forcing data is shorter than the 11-year period desired for model calibration and validation of the SLE model flow. However, the water quality calibration is based on comparisons to monthly data, and is less likely to be highly dependent on the daily forcing. Therefore, it is possible to create an 11-year period of record for calibration and validation by repeating the 4-year data. This approach will provide reasonable estimates of the tidal forcing at the boundary, but will not always be synchronized with the true tidal phase. Also, the synthesized data set will not be representative of non-tidal water fluctuations and related flows due to storm surges or other influences. These limitations need to be considered in the interpretation of the model water quality calibration results, and are an inherent limitation due to limited forcing data.

Hourly salinity data was available at the US1 bridge station, which is adjacent to the model downstream boundary, and was used as forcing data for the model. This data set is limited to the same shorter time period as the tidal amplitude data (2002-2005). The water quality calibration does not require salinity data, and therefore, the water quality calibration and validation is not restricted by the period of record for the flow forcing data.

Water quality data was available at two stations in the vicinity of the SLE model downstream boundary, SE01 and SE02. These data sets consist of monthly grab sample data for selected parameters covering the 11-year calibration and validation period. The measured data from the SE01 and SE02 were interpolated between sampling dates to create a daily concentration record. The data sets from both stations were then averaged and the resulting time series was used as the downstream boundary conditions for the SLE model water quality simulations.

3.8 SIMULATION PERIODS AND TIMESTEP

For the purpose of flow, daily flow measurements for the outflow structures for the C-24, C-23 and C-44 basins is available from 1965 through present. For water quality calibration of these basin models and the SLE model, monthly grab sample data is available from 1979 to present. However, the entire period of record was not used for the flow nor the water quality calibration and validation for two primary reasons. First, land-uses have changed in the basins over the 40 year period, and secondly there is a general consensus that the data used for developing the TMDL should represent the same time period as the data that was used for establishing the impairment. For these reasons, the 11 year period was selected for the combined calibration and validation of the 4 models, with the calibration being completed for the 1995-1999 period, and the validation for the 2000-2005 period.

There was insufficient data to develop initial conditions for the model, and therefore, the WaSh model was implemented with a 'spin-up' period consisting of 1993-1994. The 'spin-up' period reduces the impact of 'assumed' initial conditions on the model simulations. In a previous study (2004, URS) the typical spin-up period was found to be about one year. Two years were applied in this study to be conservative, since the forcing data was generally available.

There are two notable exceptions to the calibration and validation approach described above. First, there is no flow data for a calibration of flows in the SLE model and salinity data was used. There is long term monthly salinity data at the HR1 station location in the North Fork that provides a basis for calibration for the 11 year period 1995-2005. However, hourly salinity data at the downstream end of the model, which is needed to force the model, was only available for the five year period 2001-2005. Applying a two-year spin-up period for the model applications, the flow calibration for the SLE model was limited to the 3 year period, 2004-2005 and no validation period was available. Although the calibration for the hydrologic calibration of the SLE basin is shorter, due to the limited availability of the measured data, the land-use depended parameter values obtained from the calibration and validation of the C23, C24 and C44 basins should be directly applicable to the SLE basin, and therefore diminish limitations due to data availability.

The second modification to the calibration and validation plan affected the C44 basin model validation. In a previous modeling analysis of the C44 basin (HDR, 2004) the SFWMD modified the measured data at the S-80 structure to exclude the influence of Lake Okeechobee regulatory releases. This modified data set was available from the WaSh Model C-44 Recalibration effort

performed by the SFWMD and URS. The measured flows for S-80 and S-308 were used to develop a time series from January 1, 1982 through December 31, 2000 that represented the runoff from the basin, excluding any effects of both regulatory and irrigation releases from Lake Okeechobee. The procedure applied by the SFWMD to remove the regulatory release flows was as follows: When flow from S-308 was from the Lake to C-44, the flow records were ignored (due to regulatory release influence). The number of ignored records represents 33% of the time period from 1982 to 1995. When the flows at S-308 were from S-308 to the Lake, the S-80 and S-308 flows were combined and recorded. This procedure was used solely for the calibration of the C44 basin model. For the calibration of the SLE model, the calibrated and validated C44 model included as inputs, the measured Lake discharges so that the outputs from the C44 model used in the SLE model included the Lake flows and loads.

The modified data set provided measured flow data representing C44 basin discharges for the 1995-1999 calibration period. URS has attempted to extend the SFWMD procedure to provide the same type of data for the 2000-2005 period for validation. However, the procedure caused approximately 70% of the daily flows to be removed from the record, yielding a data set with large gaps and therefore insufficient for application in the modeling analysis. Therefore, no flow or water quality validation was conducted for the C-44 basin. The calibration and validation periods are summarized in Table 3-2.

Table 3-2. Summary of Model Calibration and Validation Periods.

Basin	Analysis	Calibration	Validation	Data Stations
C-24	Flow	1995-2000	2001-2005	S-49
	Water Quality	1995-2000	2001-2005	S-49
C-23	Flow	1995-2000	2001-2005	S-48
	Water Quality	1995-2000	2001-2005	S-48
C-44	Flow	1995-2000	-	S-80
	Water Quality	1995-2000	-	S-80
SLE	Flow	2003-2005	-	
	Water Quality	1995-2000	2001-2005	HR1, SE01, SE02, SE06, SE03, SE08, SE09

The fundamental time step for the model is one day, and output from the model is provided in daily increments. However, certain model algorithms operate at shorter time steps (30 minutes to one hour), which are required to provide accurate representations of physical processes and provide numerical stability. General model outputs are daily time series of flows, stages, water quality loads and concentrations at points along the surface water flow system. Simulation results at the basin outfall can be provided at one-half hour intervals, for the purpose of viewing diurnal fluctuations in the dissolved oxygen levels due to phytoplankton production and respiration.

3.9 MODEL INPUT DATA

In addition to the configuration data, the Wash model requires specification of the runoff concentrations for nutrients and BOD, the re-aeration parameter, light penetration and various rate coefficients. There is site-specific data available to guide the selection of the runoff concentration, the SOD, the re-aeration coefficients and light penetration. The development of parameter values for these model inputs are discussed below. The remaining model inputs for the rate coefficients used as model calibration parameters are discussed in Section 5.0.

3.9.1 Areal-Based Mean Concentrations

The WaSh model requires input representing runoff concentrations for nutrients (ammonia, nitrate, organic nitrogen, phosphate and organic phosphorus), carbonaceous biological oxygen demand, (CBOD), phytoplankton mass and D.O. for the water quality simulation. These data are needed to characterize the spatial distribution of runoff loadings in the basins. Ideally, sufficient event mean concentrations (EMC) data would be available to determine the spatial distribution of the loadings, as well as seasonal or higher frequency temporal variations. There is little true EMC data available for the area and available data is not representative of all areas. The term 'tur' is used ere to indicate a flow weighted average concentration for an indivicula runoff event. Howver, a number of data sources have been identified for use in developing approximations to the EMC values needed for the WaSh model input. There are data sets representing site-specific data, regional data sets, as well as data summaries available in the literature

The five following sources of data were found useful for the development of the land-use and soil type dependent values:

1) IFAS ISCO
2) FDEP ISCO
3) Urban Runoff Study (SLT stations)
4) FDEP BMP Study
5) Synoptic BOD data

In addition to these data sets, data from the Grassy Waters Preserve site, which represents a large wetlands area, and data from the Harvey Harper publications, which document EMC values in various geographic/environmental regions across the state, were used to supplement the site-specific data sets. The general strategy for developing approximate EMC values for the WaSh model is to develop them from the site-specific data, and then use the regional or literature values to fill in missing data or replace values from the site-specific data that are suspect, either due to outliers or insufficient number of samples.

In the development of the runoff concentrations used for the WaSh model, the term EMC has been replaced with the term "area based mean concentrations" (ABMCs) for different land-uses and soil types and then use that data set to assign the loading concentrations in the WaSh model gird cells. The term ABMC is used here to indicate that the values are measured (or derived from the measured data) and not representative of true EMC values. Whereas true EMC values are based on flow weighted concentrations averages over a single rainfall event, the values developed herein are rather comprised of numerous samples at a site and are only approximations of true EMC values.

The general approach for developing the AMBCs was to

1) collect data from measurement stations within the basins
2) obtain the average values for each parameter at that station
3) associate the value with a land-use
4) group the station by land-use and sue the median value for each group as the ABMC

Measured grab sample data from the Urban Runoff and the FDEP BMP Studies are presented in Figures 3-17 and 3-18 respectively, with the mean concentrations for each station. The two IFAS ISCO and FDEP ISCO data sets contain numerous measurements during a single rainfall event. The individual TN and TP measurements for various events are shown for several stations in Figures 3-19 through 3-21. There appears to be a high degree of variation in the individual measurements within a single event as well as between events. In order to be consistent with the Urban Runoff Study and the FDEP BMP study, which consists of single grab samples, the values for each runoff event in the ISCO-based data sets (Figure 3-22) were averaged to obtain the single sample value for each event.

A summary of the data available for each station in the four data sets is shown in Table 3-3 for TN and in Table 3-4 for TP. For each station, the associated land use and the average, median, standard deviation and number of samples is shown.

Table 3-3. Summary of TN Values from Four Site-Specific Data Sets.

Station	Land Use	Source	Average (mg/L)	Median (mg/L)	Max (mg/L)	Min (mg/L)	StDev (mg/L)	# of Samples
19	Agriculture-Field crops - sugarcane	FDEP-Grab	1.73	1.55	2.77	1.05	0.80	4
4	Agriculture-Improved Pasture	FDEP-Grab	1.22	1.29	1.93	0.67	0.50	5
11	Agriculture-Improved Pasture	FDEP-Grab	1.45	1.33	2.54	0.61	0.88	4
24	Agriculture-Improved Pasture	FDEP-Grab	1.55	1.19	3.11	0.68	1.01	5
32	Agriculture-Improved Pasture	FDEP-Grab	1.83	1.74	2.93	0.93	0.83	4
SLT-24	Agriculture-Improved Pasture	SFWMD-Grab	1.05	0.98	3.18	0.01	0.45	97
61	Agriculture-Pastures	FDEP-Grab	0.90	0.90	1.29	0.51	0.55	2
63	Agriculture-Pastures	FDEP-Grab	1.45	1.36	2.64	0.72	0.73	5
84	Agriculture-Pastures	FDEP-Grab	1.12	1.05	1.66	0.72	0.45	4
Pasture-North	Agriculture-Pastures	IFAS-ISCO	1.13	0.96	2.27	0.42	0.62	10
Pasture-South	Agriculture-Pastures	IFAS-ISCO	1.28	1.05	2.53	0.40	0.79	7
PC30	Agriculture-Pastures	FDEP-ISCO	0.98	0.97	1.26	0.73	0.22	4
38	Agriculture-Row crops	FDEP-Grab	1.56	1.45	2.28	1.07	0.52	4
53	Agriculture-Row crops	FDEP-Grab	1.47	1.24	3.18	0.70	0.91	6
SLT-3	Agriculture-Row crops	SFWMD-Grab	1.37	1.17	6.66	0.08	1.06	46
87	Agriculture-Unimproved Pasture	FDEP-Grab	0.69	0.68	1.00	0.39	0.22	6
48	Agriculture-Nurseries and Vineyards-	FDEP-Grab	2.72	2.35	4.47	1.35	1.59	3
91	Agriculture-Nurseries and Vineyards-	FDEP-Grab	1.26	1.26	1.62	0.91	0.50	2
72	Agriculture-Nurseries-Sod Farms	FDEP-Grab	0.83	0.77	1.36	0.53	0.29	7
89	Agriculture-Specialty Farms-Dairies	FDEP-Grab	32.52	24.57	80.47	3.55	30.91	5

Station	Land Use	Source	Average (mg/L)	Median (mg/L)	Max (mg/L)	Min (mg/L)	StDev (mg/L)	# of Samples
18	Agriculture-Specialty Farms-Horse Farms	FDEP-Grab	1.26	1.26	1.26	1.26	0.00	1
2	Agriculture-Tree Crops-Citrus	FDEP-Grab	0.58	0.58	0.58	0.58	0.00	1
20	Agriculture-Tree Crops-Citrus	FDEP-Grab	0.82	0.68	1.51	0.51	0.34	7
22	Agriculture-Tree Crops-Citrus	FDEP-Grab	0.92	0.97	1.39	0.52	0.33	7
43	Agriculture-Tree Crops-Citrus	FDEP-Grab	1.27	1.18	2.33	0.42	0.74	6
59	Agriculture-Tree Crops-Citrus	FDEP-Grab	1.35	1.36	1.91	0.75	0.50	4
60	Agriculture-Tree Crops-Citrus	FDEP-Grab	1.94	1.94	2.43	1.45	0.69	2
66	Agriculture-Tree Crops-Citrus	FDEP-Grab	0.78	0.60	1.37	0.55	0.35	5
68	Agriculture-Tree Crops-Citrus	FDEP-Grab	0.96	0.85	1.44	0.59	0.43	3
76	Agriculture-Tree Crops-Citrus	FDEP-Grab	1.26	1.27	1.80	0.73	0.54	3
81	Agriculture-Tree Crops-Citrus	FDEP-Grab	1.74	1.66	2.59	1.10	0.54	5
82	Agriculture-Tree Crops-Citrus	FDEP-Grab	0.80	0.80	0.80	0.80	0.00	1
86	Agriculture-Tree Crops-Citrus	FDEP-Grab	0.86	0.82	1.41	0.57	0.29	7
2B	Agriculture-Tree Crops-Citrus	FDEP-Grab	1.33	1.61	1.81	0.58	0.66	3
60X	Agriculture-Tree Crops-Citrus	FDEP-Grab	1.27	1.27	1.27	1.27	0.00	1
68B	Agriculture-Tree Crops-Citrus	FDEP-Grab	1.45	1.88	1.89	0.57	0.76	3
A	Agriculture-Tree Crops-Citrus	FDEP-Grab	1.09	0.88	2.24	0.43	0.72	5
O	Agriculture-Tree Crops-Citrus	FDEP-Grab	1.36	1.37	1.79	0.88	0.38	6
P	Agriculture-Tree Crops-Citrus	FDEP-Grab	1.21	1.30	1.45	0.78	0.25	8
Site22	Agriculture-Tree Crops-Citrus	FDEP-ISCO	0.97	0.97	0.97	0.97	0.00	1
X	Agriculture-Tree Crops-Citrus	FDEP-Grab	2.32	2.28	3.06	1.62	0.72	3
SLT-1	Forest--	SFWMD-Grab	0.94	0.90	1.42	0.01	0.22	38
SLT-10A	Forest--	SFWMD-Grab	0.90	0.89	1.31	0.59	0.17	47

Station	Land Use	Source	Average (mg/L)	Median (mg/L)	Max (mg/L)	Min (mg/L)	StDev (mg/L)	# of Samples
SLT-10B	Forest--	SFWMD-Grab	0.82	0.81	1.28	0.01	0.21	44
SLT-26	Forest--	SFWMD-Grab	0.87	0.80	2.90	0.60	0.35	95
SLT-4	Forest--	SFWMD-Grab	0.95	0.88	3.93	0.01	0.55	36
E	Urban--	FDEP-Grab	0.74	0.49	1.84	0.30	0.53	8
J	Urban--	FDEP-Grab	1.44	1.34	3.64	0.44	1.08	7
SLT-23	Urban--	SFWMD-Grab	0.85	0.80	1.89	0.54	0.26	94
V	Urban--	FDEP-Grab	0.92	0.84	1.69	0.33	0.47	7
77	Urban-Commercial-	FDEP-Grab	0.39	0.37	0.56	0.22	0.12	6
SLT-25	Urban-Commercial-	SFWMD-Grab	1.06	1.08	1.32	0.77	0.13	15
SLT-31	Urban-Commercial-	SFWMD-Grab	0.78	0.69	2.07	0.37	0.33	85
SLT-39	Urban-Commercial-	SFWMD-Grab	1.11	0.96	8.65	0.11	1.02	66
SLT-33	Urban-Commercial-Cemeteries	SFWMD-Grab	0.86	0.84	1.28	0.44	0.17	34
55	Urban-Industrial-	FDEP-Grab	0.77	0.77	1.03	0.60	0.17	5
39	Urban-Recreational-Golf Course	FDEP-Grab	2.16	2.17	2.88	1.40	0.73	4
41	Urban-Recreational-Golf Course	FDEP-Grab	2.61	2.61	2.61	2.61	0.00	1
58	Urban-Recreational-Golf Course	FDEP-Grab	1.14	1.16	1.83	0.42	0.63	4
79	Urban-Recreational-Golf Course	FDEP-Grab	1.17	1.04	2.29	0.61	0.68	5
Gator Trace	Urban-Recreational-Golf Course	FDEP-ISCO	1.78	1.77	1.90	1.67	0.12	3
Golf-North	Urban-Recreational-Golf Course	IFAS-ISCO	1.30	1.39	1.89	0.02	0.50	18
Golf-South	Urban-Recreational-Golf Course	IFAS-ISCO	2.91	3.07	3.47	1.84	0.57	6
Martin Downs	Urban-Recreational-Golf Course	FDEP-ISCO	0.86	0.86	0.86	0.86	0.00	1
R	Urban-Recreational-Golf Course	FDEP-Grab	1.62	1.56	2.04	1.28	0.28	5
SLT-19	Urban-Recreational-Golf Course	SFWMD-Grab	0.80	0.76	2.16	0.48	0.23	100

Station	Land Use	Source	Average (mg/L)	Median (mg/L)	Max (mg/L)	Min (mg/L)	StDev (mg/L)	# of Samples
SLT-20	Urban-Recreational-Golf Course	SFWMD-Grab	0.74	0.67	1.53	0.48	0.26	29
SLT-21	Urban-Recreational-Golf Course	SFWMD-Grab	0.83	0.80	3.12	0.33	0.30	97
15	Urban-Residential-	FDEP-Grab	0.86	0.79	1.19	0.64	0.19	8
35	Urban-Residential-	FDEP-Grab	0.93	1.00	1.81	0.27	0.61	5
42	Urban-Residential-	FDEP-Grab	0.92	0.83	2.01	0.41	0.58	6
47	Urban-Residential-	FDEP-Grab	1.14	1.14	1.41	0.88	0.26	3
55	Urban-Residential-	FDEP-Grab	0.77	0.77	1.03	0.60	0.17	5
BARTOWC	Urban-Residential-	FDEP-Grab	1.56	1.41	2.54	0.88	0.70	4
Butterfield	Urban-Residential-	IFAS-ISCO	1.54	1.64	2.28	0.30	0.47	24
Elkham	Urban-Residential-	IFAS-ISCO	1.22	1.14	2.21	0.62	0.42	30
Floresta	Urban-Residential-	FDEP-ISCO	0.72	0.72	0.77	0.67	0.07	2
HOWARDC	Urban-Residential-	FDEP-Grab	1.76	1.85	2.31	1.02	0.55	4
I	Urban-Residential-	FDEP-Grab	0.69	0.73	1.01	0.35	0.24	8
Monterrey	Urban-Residential-	IFAS-ISCO	1.44	1.44	1.46	1.41	0.04	2
PSL ONE	Urban-Residential-	FDEP-Grab	1.00	1.00	1.00	1.00	0.00	1
PSL TRE	Urban-Residential-	FDEP-Grab	1.26	1.26	1.26	1.26	0.00	1
PSL TWO	Urban-Residential-	FDEP-Grab	1.67	1.67	1.67	1.67	0.00	1
PSL100-FTNOF	Urban-Residential-	FDEP-Grab	1.41	1.41	1.41	1.41	0.00	1
PSLNF-@PLATT	Urban-Residential-	FDEP-Grab	1.26	1.26	1.26	1.26	0.00	1
PSLNF-SLRCAN	Urban-Residential-	FDEP-Grab	1.49	1.49	1.49	1.49	0.00	1
PSLWCANA	Urban-Residential-	FDEP-Grab	1.49	1.49	1.49	1.49	0.00	1

Station	Land Use	Source	Average (mg/L)	Median (mg/L)	Max (mg/L)	Min (mg/L)	StDev (mg/L)	# of Samples
LSO								
SCOTTC	Urban-Residential-	FDEP-Grab	1.35	1.16	2.10	1.10	0.43	5
St James	Urban-Residential-	FDEP-ISCO	0.74	0.74	0.74	0.74	0.00	1
Turnpike	Urban-Residential-	IFAS-ISCO	1.68	1.74	2.60	1.01	0.59	6
SLT-8	Urban-Residential High Density-	SFWMD-Grab	0.95	0.93	1.50	0.64	0.19	43
SLT-36	Urban-Residential Low Density-	SFWMD-Grab	1.75	1.59	4.56	0.74	0.75	82
SLT-11	Urban-Residential Medium Density-	SFWMD-Grab	0.97	0.88	3.77	0.57	0.38	100
SLT-12	Urban-Residential Medium Density-	SFWMD-Grab	1.27	0.97	3.58	0.55	0.77	29
SLT-13	Urban-Residential Medium Density-	SFWMD-Grab	1.38	1.14	5.64	0.66	0.97	28
SLT-14	Urban-Residential Medium Density-	SFWMD-Grab	1.23	1.19	1.99	0.56	0.41	30
SLT-15	Urban-Residential Medium Density-	SFWMD-Grab	0.98	0.95	2.50	0.29	0.46	38
SLT-16	Urban-Residential Medium Density-	SFWMD-Grab	0.81	0.73	2.13	0.41	0.34	24
SLT-17	Urban-Residential Medium Density-	SFWMD-Grab	0.81	0.78	1.75	0.06	0.27	86
SLT-18	Urban-Residential Medium Density-	SFWMD-Grab	0.72	0.65	1.41	0.50	0.24	29
SLT-2	Urban-Residential Medium Density-	SFWMD-Grab	0.95	0.90	1.88	0.13	0.40	37
SLT-22	Urban-Residential Medium Density-	SFWMD-Grab	0.91	0.87	2.38	0.01	0.38	93
SLT-27	Urban-Residential Medium Density-	SFWMD-Grab	0.94	0.93	1.41	0.58	0.21	35
SLT-29	Urban-Residential Medium Density-	SFWMD-Grab	0.95	0.82	5.40	0.55	0.55	91
SLT-32	Urban-Residential Medium Density-	SFWMD-Grab	1.13	1.13	1.13	1.13	0.00	1
SLT-34	Urban-Residential Medium Density-	SFWMD-Grab	1.20	0.98	5.77	0.63	0.79	87
SLT-35	Urban-Residential Medium Density-	SFWMD-Grab	1.05	1.03	1.55	0.64	0.21	44
SLT-37	Urban-Residential Medium Density-	SFWMD-Grab	1.08	1.08	1.78	0.50	0.33	25
SLT-37A	Urban-Residential Medium Density-	SFWMD-Grab	1.13	0.96	2.27	0.55	0.45	71

Station	Land Use	Source	Average (mg/L)	Median (mg/L)	Max (mg/L)	Min (mg/L)	StDev (mg/L)	# of Samples
SLT-38	Urban-Residential Medium Density-	SFWMD-Grab	0.90	0.84	3.06	0.52	0.34	66
SLT-40	Urban-Residential Medium Density-	SFWMD-Grab	1.05	1.05	2.05	0.02	0.35	54
SLT-41	Urban-Residential Medium Density-	SFWMD-Grab	1.04	0.99	2.39	0.01	0.35	69
SLT-42A	Urban-Residential Medium Density-	SFWMD-Grab	0.67	0.68	1.10	0.01	0.23	15
SLT-43	Urban-Residential Medium Density-	SFWMD-Grab	1.07	0.85	2.25	0.02	0.61	16
SLT-5	Urban-Residential Medium Density-	SFWMD-Grab	1.10	1.01	2.50	0.68	0.34	30
SLT-6	Urban-Residential Medium Density-	SFWMD-Grab	1.81	1.77	5.43	0.01	0.79	44
SLT-7	Urban-Residential Medium Density-	SFWMD-Grab	1.05	0.96	1.98	0.07	0.31	77
SLT-9	Urban-Residential Medium Density-	SFWMD-Grab	0.95	0.94	1.52	0.03	0.26	72
46	Wetlands--	FDEP-Grab	0.94	0.94	0.94	0.94	0.00	1
85	Wetlands--	FDEP-Grab	1.06	1.02	1.41	0.78	0.27	4
OVERROAD	Wetlands--	FDEP-Grab	0.98	0.85	1.51	0.71	0.36	4
SLT-28	Wetlands-Mangrove swamps	SFWMD-Grab	0.80	0.75	1.26	0.52	0.20	33
SLT-30	Wetlands-Mangrove swamps	SFWMD-Grab	0.87	0.90	1.48	0.50	0.24	32

Table 3-4. Summary of TP Values from Four Site-Specific Data Sets.

Station	Land Use	Source	Average (mg/L)	Median (mg/L)	max (mg/L)	min (mg/L)	StDev (mg/L)	# of Samples
19	Agriculture- Sugarcane	FDEP-Grab	0.151	0.149	0.220	0.087	0.058	4
4	Agriculture-Improved Pasture	FDEP-Grab	0.239	0.228	0.377	0.091	0.105	7
11	Agriculture-Improved Pasture	FDEP-Grab	0.281	0.279	0.615	0.084	0.211	5
24	Agriculture-Improved Pasture	FDEP-Grab	0.516	0.404	1.107	0.189	0.384	5
32	Agriculture-Improved Pasture	FDEP-Grab	0.130	0.103	0.263	0.051	0.092	4

Station	Land Use	Source	Average (mg/L)	Median (mg/L)	max (mg/L)	min (mg/L)	StDev (mg/L)	# of Samples
SLT-24	Agriculture-Improved Pasture	SFWMD-Grab	0.241	0.195	0.802	0.043	0.167	96
X2	Agriculture-Improved Pasture	FDEP-Grab	0.308	0.308	0.357	0.258	0.070	2
61	Agriculture-Pastures	FDEP-Grab	0.133	0.133	0.234	0.031	0.144	2
63	Agriculture-Pastures	FDEP-Grab	0.437	0.400	0.864	0.064	0.265	6
84	Agriculture-Pastures	FDEP-Grab	0.297	0.221	0.748	0.144	0.232	6
Pasture-North	Agriculture-Pastures	IFAS-ISCO	0.174	0.088	0.625	0.005	0.199	11
Pasture-South	Agriculture-Pastures	IFAS-ISCO	0.170	0.082	0.425	0.003	0.175	8
PC30	Agriculture-Pastures	FDEP-ISCO	2.150	2.142	2.543	1.775	0.408	4
38	Agriculture-Row crops	FDEP-Grab	1.055	0.892	1.920	0.501	0.533	5
53	Agriculture-Row crops	FDEP-Grab	0.236	0.199	0.404	0.103	0.126	8
SLT-3	Agriculture-Row crops	SFWMD-Grab	0.263	0.198	1.207	0.097	0.205	45
87	Agriculture-Unimproved Pasture	FDEP-Grab	0.015	0.014	0.029	0.003	0.009	8
48	Agriculture-Nurseries and Vineyards	FDEP-Grab	1.093	0.902	1.933	0.635	0.574	4
91	Agriculture-Nurseries and Vineyards	FDEP-Grab	0.409	0.409	0.629	0.189	0.311	2
72	Agriculture-Sod Farms	FDEP-Grab	0.227	0.201	0.316	0.142	0.067	9
89	Agriculture-Dairies	FDEP-Grab	8.515	6.306	15.695	2.671	5.277	7
18	Agriculture--Horse Farms	FDEP-Grab	0.727	0.727	1.301	0.152	0.812	2
2	Agriculture-Tree Crops-Citrus	FDEP-Grab	0.161	0.161	0.161	0.161	0.000	1
20	Agriculture-Tree Crops-Citrus	FDEP-Grab	0.128	0.076	0.550	0.043	0.160	9
22	Agriculture-Tree Crops-Citrus	FDEP-Grab	0.149	0.095	0.467	0.047	0.132	9
43	Agriculture-Tree Crops-Citrus	FDEP-Grab	0.367	0.322	0.736	0.138	0.198	8
59	Agriculture-Tree Crops-Citrus	FDEP-Grab	0.047	0.045	0.078	0.021	0.020	6
60	Agriculture-Tree Crops-Citrus	FDEP-Grab	1.054	0.979	1.272	0.912	0.191	3

Station	Land Use	Source	Average (mg/L)	Median (mg/L)	max (mg/L)	min (mg/L)	StDev (mg/L)	# of Samples
66	Agriculture-Tree Crops-Citrus	FDEP-Grab	0.115	0.112	0.170	0.079	0.033	7
68	Agriculture-Tree Crops-Citrus	FDEP-Grab	0.331	0.330	0.453	0.210	0.099	4
76	Agriculture-Tree Crops-Citrus	FDEP-Grab	0.213	0.117	0.563	0.055	0.237	4
81	Agriculture-Tree Crops-Citrus	FDEP-Grab	0.525	0.416	1.441	0.106	0.505	7
82	Agriculture-Tree Crops-Citrus	FDEP-Grab	0.161	0.161	0.161	0.161	0.000	1
86	Agriculture-Tree Crops-Citrus	FDEP-Grab	0.105	0.097	0.140	0.066	0.027	9
2B	Agriculture-Tree Crops-Citrus	FDEP-Grab	0.538	0.430	1.038	0.075	0.396	5
60X	Agriculture-Tree Crops-Citrus	FDEP-Grab	0.768	0.727	0.885	0.693	0.102	3
68B	Agriculture-Tree Crops-Citrus	FDEP-Grab	0.430	0.507	0.570	0.135	0.200	4
A	Agriculture-Tree Crops-Citrus	FDEP-Grab	0.384	0.389	0.558	0.096	0.166	7
FPFC15	Agriculture-Tree Crops-Citrus	FDEP-Grab	0.110	0.110	0.110	0.110	0.000	1
FPFC16	Agriculture-Tree Crops-Citrus	FDEP-Grab	0.073	0.073	0.073	0.073	0.000	1
FPFC20	Agriculture-Tree Crops-Citrus	FDEP-Grab	0.699	0.699	0.699	0.699	0.000	1
FPFC21	Agriculture-Tree Crops-Citrus	FDEP-Grab	0.256	0.256	0.256	0.256	0.000	1
FPFC22	Agriculture-Tree Crops-Citrus	FDEP-Grab	0.217	0.217	0.217	0.217	0.000	1
FPFC25	Agriculture-Tree Crops-Citrus	FDEP-Grab	1.010	1.010	1.010	1.010	0.000	1
FPFC26	Agriculture-Tree Crops-Citrus	FDEP-Grab	0.846	0.846	0.846	0.846	0.000	1
O	Agriculture-Tree Crops-Citrus	FDEP-Grab	0.210	0.167	0.424	0.099	0.116	8
P	Agriculture-Tree Crops-Citrus	FDEP-Grab	0.143	0.119	0.393	0.046	0.099	10
Site22	Agriculture-Tree Crops-Citrus	FDEP-ISCO	0.048	0.048	0.048	0.048	0.000	1
X	Agriculture-Tree Crops-Citrus	FDEP-Grab	0.522	0.469	0.744	0.293	0.184	5
SLT-1	Forest--	SFWMD-Grab	0.108	0.099	0.217	0.055	0.036	37
SLT-10A	Forest--	SFWMD-Grab	0.103	0.097	0.180	0.051	0.037	47

Station	Land Use	Source	Average (mg/L)	Median (mg/L)	max (mg/L)	min (mg/L)	StDev (mg/L)	# of Samples
SLT-10B	Forest--	SFWMD-Grab	0.093	0.075	0.321	0.041	0.054	43
SLT-26	Forest--	SFWMD-Grab	0.080	0.061	0.426	0.032	0.059	94
SLT-4	Forest--	SFWMD-Grab	0.121	0.114	0.514	0.071	0.072	35
E	Urban--	FDEP-Grab	0.299	0.250	0.767	0.120	0.194	10
J	Urban--	FDEP-Grab	0.390	0.337	0.661	0.101	0.202	9
SLT-23	Urban--	SFWMD-Grab	0.166	0.156	0.433	0.058	0.069	94
V	Urban--	FDEP-Grab	0.394	0.412	0.625	0.154	0.150	9
77	Urban-Commercial-	FDEP-Grab	0.019	0.020	0.023	0.014	0.003	8
SLT-25	Urban-Commercial-	SFWMD-Grab	0.051	0.044	0.108	0.025	0.027	15
SLT-31	Urban-Commercial-	SFWMD-Grab	0.092	0.074	0.238	0.015	0.046	84
SLT-39	Urban-Commercial-	SFWMD-Grab	0.260	0.207	1.460	0.135	0.202	65
SLT-33	Urban-Commercial-Cemeteries	SFWMD-Grab	0.153	0.157	0.261	0.079	0.045	25
55	Urban-Industrial-	FDEP-Grab	0.113	0.097	0.221	0.052	0.058	8
39	Urban-Recreational-Golf Course	FDEP-Grab	0.246	0.224	0.376	0.178	0.072	6
41	Urban-Recreational-Golf Course	FDEP-Grab	0.706	0.706	0.706	0.706	0.000	1
58	Urban-Recreational-Golf Course	FDEP-Grab	0.081	0.088	0.099	0.049	0.022	4
79	Urban-Recreational-Golf Course	FDEP-Grab	0.234	0.223	0.421	0.091	0.119	5
58B	Urban-Recreational-Golf Course	FDEP-Grab	0.142	0.142	0.142	0.142	0.000	1
Gator Trace	Urban-Recreational-Golf Course	FDEP-ISCO	0.301	0.289	0.329	0.286	0.024	3
Golf-North	Urban-Recreational-Golf Course	IFAS-ISCO	0.083	0.068	0.189	0.041	0.043	18
Golf-South	Urban-Recreational-Golf Course	IFAS-ISCO	0.218	0.220	0.297	0.135	0.064	6
Martin Downs	Urban-Recreational-Golf Course	FDEP-ISCO	0.104	0.104	0.104	0.104	0.000	1
R	Urban-Recreational-Golf Course	FDEP-Grab	0.168	0.179	0.225	0.075	0.056	5

Station	Land Use	Source	Average (mg/L)	Median (mg/L)	max (mg/L)	min (mg/L)	StDev (mg/L)	# of Samples
R2	Urban-Recreational-Golf Course	FDEP-Grab	0.188	0.188	0.188	0.188	0.000	1
SLT-19	Urban-Recreational-Golf Course	SFWMD-Grab	0.052	0.037	0.221	0.015	0.041	99
SLT-20	Urban-Recreational-Golf Course	SFWMD-Grab	0.041	0.026	0.221	0.013	0.047	29
SLT-21	Urban-Recreational-Golf Course	SFWMD-Grab	0.042	0.037	0.291	0.009	0.032	96
15	Urban-Residential-	FDEP-Grab	0.092	0.095	0.151	0.032	0.037	12
35	Urban-Residential-	FDEP-Grab	0.100	0.105	0.186	0.028	0.063	8
42	Urban-Residential-	FDEP-Grab	0.065	0.043	0.242	0.019	0.073	8
47	Urban-Residential-	FDEP-Grab	0.041	0.039	0.064	0.021	0.022	3
55	Urban-Residential-	FDEP-Grab	0.113	0.097	0.221	0.052	0.058	8
BARTOWA	Urban-Residential-	FDEP-Grab	0.030	0.030	0.030	0.030	0.000	1
BARTOWC	Urban-Residential-	FDEP-Grab	0.509	0.396	0.774	0.303	0.216	5
Butterfield	Urban-Residential-	IFAS-ISCO	0.138	0.146	0.235	0.008	0.049	24
C105	Urban-Residential-	FDEP-Grab	0.039	0.039	0.049	0.029	0.014	2
C106	Urban-Residential-	FDEP-Grab	0.034	0.034	0.047	0.021	0.018	2
C107	Urban-Residential-	FDEP-Grab	0.061	0.061	0.101	0.021	0.057	2
C108	Urban-Residential-	FDEP-Grab	0.036	0.036	0.045	0.027	0.013	2
Elkham	Urban-Residential-	IFAS-ISCO	0.100	0.091	0.209	0.034	0.045	32
EPSLA	Urban-Residential-	FDEP-Grab	0.014	0.014	0.014	0.014	0.000	1
EPSLC	Urban-Residential-	FDEP-Grab	0.022	0.022	0.022	0.022	0.000	1
ESSEX	Urban-Residential-	FDEP-Grab	0.140	0.140	0.213	0.066	0.104	2
Floresta	Urban-Residential-	FDEP-ISCO	0.039	0.039	0.043	0.036	0.005	2
FPFC23	Urban-Residential-	FDEP-Grab	0.143	0.143	0.143	0.143	0.000	1
GRATEDIT	Urban-Residential-	FDEP-Grab	0.158	0.158	0.158	0.158	0.000	1

Station	Land Use	Source	Average (mg/L)	Median (mg/L)	max (mg/L)	min (mg/L)	StDev (mg/L)	# of Samples
HARBORVI	Urban-Residential-	FDEP-Grab	0.129	0.129	0.171	0.086	0.060	2
HOGPEN	Urban-Residential-	FDEP-Grab	0.119	0.119	0.176	0.061	0.081	2
HOWARDC	Urban-Residential-	FDEP-Grab	0.573	0.534	1.097	0.243	0.329	5
I	Urban-Residential-	FDEP-Grab	0.137	0.098	0.311	0.009	0.097	10
Monterrey	Urban-Residential-	IFAS-ISCO	0.137	0.137	0.150	0.123	0.019	2
NARANJAN	Urban-Residential-	FDEP-Grab	0.062	0.062	0.097	0.026	0.050	2
NARANJAS	Urban-Residential-	FDEP-Grab	0.068	0.068	0.083	0.052	0.022	2
PSL ONE	Urban-Residential-	FDEP-Grab	0.074	0.074	0.074	0.074	0.000	1
PSL TRE	Urban-Residential-	FDEP-Grab	0.236	0.236	0.236	0.236	0.000	1
PSL TWO	Urban-Residential-	FDEP-Grab	0.332	0.332	0.332	0.332	0.000	1
PSL100FTNOF	Urban-Residential-	FDEP-Grab	0.329	0.329	0.329	0.329	0.000	1
PSLNF@PLATT	Urban-Residential-	FDEP-Grab	0.286	0.286	0.286	0.286	0.000	1
PSLNFSLRCAN	Urban-Residential-	FDEP-Grab	0.361	0.361	0.361	0.361	0.000	1
PSLWCANALSO	Urban-Residential-	FDEP-Grab	0.351	0.351	0.351	0.351	0.000	1
RIVERPAR	Urban-Residential-	FDEP-Grab	0.028	0.028	0.029	0.027	0.001	2
SAGAMORE	Urban-Residential-	FDEP-Grab	0.127	0.127	0.165	0.089	0.054	2
SCOTTA	Urban-Residential-	FDEP-Grab	0.019	0.019	0.019	0.019	0.000	1
SCOTTC	Urban-Residential-	FDEP-Grab	0.498	0.310	1.197	0.138	0.441	5
St James	Urban-Residential-	FDEP-ISCO	0.027	0.027	0.027	0.027	0.000	1
Turnpike	Urban-Residential-	IFAS-ISCO	0.078	0.069	0.145	0.003	0.047	7

Station	Land Use	Source	Average (mg/L)	Median (mg/L)	max (mg/L)	min (mg/L)	StDev (mg/L)	# of Samples
SLT-8	Urban-Residential High Density	SFWMD-Grab	0.116	0.102	0.230	0.038	0.053	34
SLT-36	Urban-Residential Low Density	SFWMD-Grab	0.240	0.229	0.488	0.070	0.077	82
SLT-11	Urban-Residential Medium Density	SFWMD-Grab	0.094	0.077	0.533	0.026	0.069	99
SLT-12	Urban-Residential Medium Density	SFWMD-Grab	0.082	0.065	0.262	0.013	0.062	28
SLT-13	Urban-Residential Medium Density	SFWMD-Grab	0.169	0.126	0.664	0.062	0.119	28
SLT-14	Urban-Residential Medium Density	SFWMD-Grab	0.151	0.141	0.431	0.006	0.102	30
SLT-15	Urban-Residential Medium Density	SFWMD-Grab	0.192	0.170	0.841	0.034	0.151	38
SLT-16	Urban-Residential Medium Density	SFWMD-Grab	0.113	0.109	0.292	0.031	0.061	24
SLT-17	Urban-Residential Medium Density	SFWMD-Grab	0.129	0.097	0.577	0.036	0.098	85
SLT-18	Urban-Residential Medium Density	SFWMD-Grab	0.038	0.023	0.117	0.014	0.031	29
SLT-2	Urban-Residential Medium Density	SFWMD-Grab	0.349	0.328	0.769	0.127	0.150	36
SLT-22	Urban-Residential Medium Density	SFWMD-Grab	0.233	0.208	0.589	0.085	0.124	92
SLT-27	Urban-Residential Medium Density	SFWMD-Grab	0.154	0.150	0.231	0.084	0.044	32
SLT-29	Urban-Residential Medium Density	SFWMD-Grab	0.037	0.027	0.316	0.005	0.038	89
SLT-32	Urban-Residential Medium Density	SFWMD-Grab	0.147	0.147	0.147	0.147	0.000	1
SLT-34	Urban-Residential Medium Density	SFWMD-Grab	0.149	0.105	0.766	0.022	0.149	87
SLT-35	Urban-Residential Medium Density	SFWMD-Grab	0.122	0.112	0.305	0.068	0.042	44
SLT-37	Urban-Residential Medium Density	SFWMD-Grab	0.102	0.096	0.208	0.057	0.040	10
SLT-37A	Urban-Residential Medium Density	SFWMD-Grab	0.027	0.023	0.095	0.012	0.015	68
SLT-38	Urban-Residential Medium Density	SFWMD-Grab	0.119	0.090	0.606	0.040	0.093	59
SLT-40	Urban-Residential Medium Density	SFWMD-Grab	0.111	0.088	0.526	0.029	0.084	53
SLT-41	Urban-Residential Medium Density	SFWMD-Grab	0.132	0.113	0.526	0.045	0.089	68
SLT-42A	Urban-Residential Medium Density	SFWMD-Grab	0.099	0.103	0.138	0.071	0.022	14

Station	Land Use	Source	Average (mg/L)	Median (mg/L)	max (mg/L)	min (mg/L)	StDev (mg/L)	# of Samples
SLT-43	Urban-Residential Medium Density	SFWMD-Grab	0.223	0.139	0.486	0.088	0.145	15
SLT-5	Urban-Residential Medium Density	SFWMD-Grab	0.205	0.192	0.387	0.090	0.072	30
SLT-6	Urban-Residential Medium Density	SFWMD-Grab	0.313	0.244	1.122	0.103	0.188	42
SLT-7	Urban-Residential Medium Density	SFWMD-Grab	0.196	0.177	0.477	0.096	0.074	75
SLT-9	Urban-Residential Medium Density	SFWMD-Grab	0.187	0.190	0.312	0.075	0.056	62
46	Wetlands--	FDEP-Grab	0.009	0.009	0.014	0.003	0.008	2
85	Wetlands--	FDEP-Grab	0.034	0.016	0.096	0.009	0.036	5
OVERROAD	Wetlands--	FDEP-Grab	0.007	0.006	0.014	0.001	0.006	4
SLT-28	Wetlands--Mangrove swamps	SFWMD-Grab	0.150	0.144	0.257	0.063	0.056	24
SLT-30	Wetlands-Mangrove swamps	SFWMD-Grab	0.159	0.158	0.327	0.087	0.058	21

A corresponding plot of the median values for each station, organized by land use, is shown in Figures 3-23 and 3-24. The plots indicate that there is a large range of ABMC values for the stations within most land use categories.

An attempt was made to include the soil type, as well as land use, in the development of the ABMC values, with the hope that it would explain some of the variation in TP and TN for stations with the same land-use. The stations were differentiated by soil type and then reviewed to see if station with the same land-use but a different soil classification has significantly different TP and TN values. Analysis concentrated on the Winder Soils classification identified in Figure 2-6b. Unfortunately, no correlations were found and consequently, the soil type classification was not used in the development of the ABMC values.

The station data in Figures 3-23 through 3-24 were grouped by land-use and the median concentrations for TP and TN were calculated from all station medians within each land use group. The preliminary TP and TN ABMC values for each land-use applied in the WaSh model as runoff concentrations are shown in Tables 3-5 and 3-6. Both the median and average values are shown. The median values were adopted as the ABMC values.

Table 3-5. ABMC Values for TN Used in the WaSh Model.

Land Use Category	Median	Average	# of Stations
Agriculture-Field crops - sugarcane	1.55	1.55	1
Agriculture-Improved Pasture	1.29	1.31	5
Agriculture-Pastures	1.01	1.05	6
Agriculture-Row crops	1.24	1.29	3
Agriculture-Unimproved Pasture	0.68	0.68	1
Agriculture-Nurseries and Vineyards-	1.81	1.81	2
Agriculture-Sod Farms	0.77	0.77	1
Agriculture-Dairies	24.57	24.57	1
Agriculture-Horse Farms	1.26	1.26	1
Agriculture-Tree Crops-Citrus	1.22	1.21	20
Forest--	0.88	0.86	5
Urban--	0.82	0.87	4
Urban-Commercial-	0.83	0.78	4
Urban-Commercial-Cemeteries	0.84	0.84	1
Urban-Industrial-	0.77	0.77	1
Urban-Recreational-Golf Course	1.27	1.49	12
Urban-Residential-	1.21	1.21	22
Urban-Residential High Density-	0.93	0.93	1

Land Use Category	Median	Average	# of Stations
Urban-Residential Low Density-	1.59	1.59	1
Urban-Residential Medium Density-	0.95	0.96	26
Wetlands--	0.94	0.94	3
Wetlands-Mangrove swamps	0.82	0.82	2

Table 3-6. ABMC Values for TP Used in the WaSh Model.

Land Use Category	Median	Average	# of Stations
Agriculture-Field crops - sugarcane	0.149	0.149	1
Agriculture-Improved Pasture	0.254	0.253	6
Agriculture-Pastures	0.177	0.511	6
Agriculture-Row crops	0.199	0.430	3
Agriculture-Unimproved Pasture	0.014	0.014	1
Agriculture-Nurseries and Vineyards-	0.656	0.656	2
Agriculture-Sod Farms	0.201	0.201	1
Agriculture-Dairies	6.306	6.306	1
Agriculture-Horse Farms	0.727	0.727	1
Agriculture-Tree Crops-Citrus	0.217	0.332	27
Forest--	0.097	0.089	5
Urban--	0.294	0.289	4
Urban-Commercial-	0.059	0.086	4
Urban-Commercial-Cemeteries	0.157	0.157	1
Urban-Industrial-	0.097	0.097	1
Urban-Recreational-Golf Course	0.161	0.181	14
Urban-Residential-	0.097	0.139	39
Urban-Residential High Density-	0.102	0.102	1
Urban-Residential Low Density-	0.229	0.229	1
Urban-Residential Medium Density-	0.113	0.128	26
Wetlands--	0.009	0.010	3
Wetlands-Mangrove swamps	0.151	0.151	2

In discussions with the FDEP and SFWMD, it was determined that there was potentially better wetlands runoff concentration values for use in the modeling analysis. These values

are based on samples from the Grassy Waters Preserve, which is a 20-square mile wetlands preserve in Palm Beach County. The preserve is considered pristine. There were three general wetlands values available in the SLT and FDEP BMP data sets and two corresponding to Mangrove Forests land use designation. The median values for the general wetlands category and the mangrove forest category were 0.009 mg/L and 0.151 mg/L for TP and 0.94 and 0.82 mg/L for TN. The later TP value was considered high for natural wetlands and might have been influenced by surrounding lands. Since the Grassy Waters area is relatively large, the values obtained from samples there (0.17 mg/L median value for TP and 1.03 mg/L median value for TN) are likely more representative of natural wetlands conditions. In the modeling analysis, the SLT and FDEP BMP wetlands values were used for modeling existing conditions. However, for modeling the natural conditions (see section 8.0), the Grassy Waters values were used.

The SLT station data and the FDEP BMP study data indicated some seasonal trends in the ABMCs for TP and TN. The WaSh model allows for seasonally-varying input for these parameters, and therefore the ABMCs were expanded into monthly values. This was accomplished by establishing a monthly template that was applied to the ABMC for each land-use. The monthly template was established by aggregating the data for each land-use from the SLT stations data and the FDEP BMP Study data into monthly bins and then taking the average for each month. These monthly averages were then normalized so that they averaged 1.0. The normalized templates, shown in Figure 3-25, were then applied to the ABMC values in Figures 3-23 and 3-24 to develop the Monthly ABMCs (MABMC) for each land-use. These values were then applied in the WaSh model.

The ABMC data developed as input for the WaSh model is based on total nutrient levels, i.e. TN and TP. The water quality simulations require runoff concentrations for the nutrient species: ammonia, nitrate, organic nitrogen, phosphate and organic phosphorus. In order to provide these data, ratios were developed between individual species and TN and TP using the data from the SLT and FDEP BMP data sets. The ratios were used to establish the runoff concentrations for each species. Example plots of the ratios and their seasonal variation are provided in Figure 3-26 for TN and 3-27 for TP. These data were used as initial inputs into the model.

There is very little BOD data available for use in setting the WaSh ABMC values. The one synoptic survey conducted in April of 2005 produced 20 values with an average value of 3.8 mg/L. For BOD inputs, the data compiled by Harper (2003) was used to set the ABMC values. Note that the WaSh model actually requires CBOD ultimate values, and the data are BOD_5. Since no site-specific conversion data is available, the EPA recommended value of 2.47 was used to convert from BOD_5 to CBOD (USEPA, 1997). The BOD values from Harper (2003) used to set the ABMC values are listed in table 3-7. For all other land use categories, the average value of 3.8 mg/L was used.

Table 3-7. Literature BOD EMC Values Based On Harvey Harper's 2003 Analysis.

		Typical Runoff Concentrations (mg/L)		
		TN	TP	BOD
	Low-Density Residential1	1.64	0.191	4.3
	Single Family	2.18	0.3335	7.4
	Multi-Family	2.42	0.49	11
	Low-Intensity Commercial	1.12	0.18	7.4
	High-Intensity Commercial	2.83	0.43	17.2
	Industrial	1.79	0.31	9.6
Urban	Highway	2.23	0.27	6.7
	Pasture	2.48	0.476	5.1
	Citrus	2.24	0.183	2.55
	Row Crops	2.88	0.638	,-
Agriculture	General Agriculture	2.32	0.344	3.8
Forests	Undeveloped Rangeland/ Forest	1.09	0.046	1.23
	Wetland	1.01	0.09	2.63
	Open Water/Lake	1.6	0.067	1.6

1 Average of single-family and recreational/open space loading rates.

In the WaSh model, the DO in the runoff concentrations is set to saturation, which varied with the local instantaneous temperature. The phytoplankton mass concentration was set to a small value, often referred to as a seed value, equal to 0.01 mg/L. The model results were not sensitive to the phytoplankton mass concentration seed value.

The ABMC values, templates, species ratios and global values are intended to provide the best possible representation of runoff concentrations throughout each basin. It is clear from the data that was used to develop the inputs that there is significant variability within each station and between stations with similar land-uses. It is important to recognize that the application of the ABMCs using land-use is an approximation to true conditions, both spatially and temporally. Therefore, the actual input values used in the WaSh model were interpreted as initial estimates and minor 'global' adjustments to these values were allowed during the calibration process. The term 'global' is used here to emphasize that the entire ABMC database was scaled up or down uniformly, so that the relative contribution from each land use as represented in the database was retained. The details of the adjustments are discussed in the section on water quality calibration (Section 5.0).

3.9.2 SOD

A review of the site-specific data collected by the EPA in the SLE in 2005 was conducted to determine suitable data for setting the SOD values in the model. Two of the stations have sufficient SOD data, Station 1 and Station 4. However, Station 1 data exhibited erratic values within a large range of measurements collected on the same day. The large variability rendered the dataset suspect, and Station 1 data was excluded. Therefore, the data from Station 4 was used for guiding the selection of the SOD value. The three measurements in March and July at Station 4 are shown in Figure 3-28, with an average value of 1.8 mg/L.

The WaSh model uses a temperature-dependent representation of the SOD in each reach segment. It is defined by the equation:

$$SOD = SOD_0 (T - 20)^a$$

where SOD_0 is the baseline value and 'a' is a coefficient that increases the SOD as the temperature T increases above 20 degrees C. Using the measured data as guidance, as well as some minor adjustments during the calibration process, the values of SOD_0 of 1.8 mg/L and a=1.03 were adopted. A typical seasonal variation of the SOD used in the model is shown in Figure 3-25. Note that the typical water temperatures range from 20 degrees C in the winter to 30 degrees C in the summer, thus, larger SOD values occur in the summer. To create the curve in Figure 3-26, an average seasonal temperature profile, based on 10 years of daily water temperature data, was employed.

This SOD seasonal distribution was used in the SLE as well as the upland basin models (C23, C24 and C44), even though the SOD values were derived from measurements only in the SLE. The canals in the upland basins are expected to have a higher sand content than the SLE sediment, which tend to contain higher fine fractions. The literature–based SOD survey conducted by the EPA indicates that sandier sediments in canals similar to those in the upland basins might have higher SOD values than the finer sediments found in the SLE. These conclusions contradict expectations, and after discussions with FDEP and SFWMD representatives, it was decided to use the SLE-derived SOD values for the upland basin canals until better data was available.

3.9.3 Re-aeration

The flux of dissolved oxygen into the water column due to re-aeration in represented in the WaSh model with the equation:

$$F = A\,(C_{DO} - C_{DOsat})$$

Where F is the flux of D.O. in mg/hour-m^2, C_{DO} is the concentration of D.O. in the water column (mg/L) and C_{DOsat} is the saturated level for D.O. in mg/L and is dependent on the instantaneous water temperature. The rate coefficient A represents the effects of wind and flow on the re-aeration processes.

The formula by Chapra (1997) was used to provide an estimate of the re-aeration coefficient for input to the WaSh model. Chapra's formula includes both the wind and flow effects and is:

$$A = \frac{0.728\,Ws^{0.5} - 0.317\,Ws + 0.0372\,Ws^2}{H} + \frac{3.93\sqrt{C_s}}{H^{1.5}}$$

Where W_s is the wind speed in m/s, C_s is the flow velocity in m/s and H is the water depth in m.

A review of the wind data presented in section 2 indicates that the mean wind speeds each month range from 4.2 to 6.1 m/s. Flow speeds and water depths will vary for each basin. For instance the water depth in the C-24 canal is typically 5 meters, with an annual average flow of about 250 cfs. Assuming a width of about 40 meters, the cross-sectional area is about 200 m^2 and the average flow speed is about 0.35 m/s. Similar representative values can be derived for the SLE as well. Assuming a 1200 meter width, for instance at the HR1 station and a 3 meter water depth, the cross-sectional area is about 3600 m^2. Basin

discharges affecting the north fork include C-23, C-24, and the North Fork basin which add about 500 cfs. The tidal flow assuming a 0.5 meter tidal prism and 2 km^2 area upstream of the HR1 station is about 50 cfs assuming a 12 hour tidal period. The basin discharges are likely confined to the upper layer, so only half of the water depth is used in the velocity calculations associated with the discharge. The full depth is used for the tidal flows. Thus the average velocity is on the order of 30 cm/s.

Re-aeration coefficients using the Chapra formula with the representative wind speed, current speed and water depths are shown in Table 3-5. The values derived for the C24 basin are used in the C-23 and C44 basins.

Table 3-8. Representative Re-aeration Coefficient Values.

Location	Depth (m)	Wind Speed (m/s)	Flow Speed (m/s)	A
C-24	5.0	5.0	0.35	0.39
HR1	1.5	5.0	0.30	1.8

3.9.4 Light Penetration

The WaSh model calculates the algae growth rate according to the function:

$$G_p = k_c X_{RT} X_{RI} X_{RN}$$

where G_p is the specific growth rate and each X term represents a change in the growth rate due to non-optimal conditions.

X_{RN} = effect of suboptimal nutrient concentration ($0 \le X_{RT} \le 1$)

X_{RI} = effect of suboptimal light intensity ($0 \le X_{RI} \le 1$)

X_{RT} = effect of suboptimal temperature ($0 \le X_{RT} \le 1$).

The standard formulas for the nutrient dependence and temperature dependence used in the WASP model are used in the WaSh model (see WaSh model documentation in Appendix C). However, a site-specific formulation for the extinction coefficient Ke in the equation for the effect of light transmission X_{RI} has been developed. This approach was adopted because sufficient data was available to develop a formulation specifically for the site.

The instantaneous depth-averaged light factor, X_{RI}, is:

$$X_{RI} = \frac{e}{K_e D} f \left[exp\left\{ \frac{-I_a}{I_S} exp\left(-K_e D\right) \right\} - exp\left(\frac{-I_a}{I_S} \right) \right]$$

where f is the fraction of day that is daylight, I_{ais} is the average incident light intensity during daylight hours just below the surface, I_s is the saturating light intensity of phytoplankton and K_e = the light extinction coefficient, and D is the water depth.

The extinction coefficient is typically on the order of the secchi depth and represents the depth at which light penetration ceases. The extinction coefficient Ke is defined as:

$$Ke = Ke_B + Ke_{Chl}$$

where Ke_B is the background extinction coefficient which represents the effect of color, turbidity and other types of suspended material that diffracts light. Ke_{Chl} represents the affect of algae mass and is separated from the background value so that the self-limiting affects on growth can be simulated. As the algae mass increases the light attenuation is increased, and the algae growth rate is reduced due to the reduction in light penetration.

Measured secchi depths and chlorophyll-a data in the SLE were used to derive a site-specific formulation for the Ke for the modeling analysis. Figure 3-29a shows the seasonal average secchi depths for the HR1 station. In Figure 3-29b, the seasonally averaged chlorophyll-a concentrations are shown. There appears to be some correlation between the algal mass and the sechhi depths. Ideally, the effects of the algae could be separated from those of other turbidity sources. However, there is insufficient data to independently establish the contribution of algae to the light attenuation. Therefore an approximate representation of the algae mass on light penetration ahs been established. The equation adopted is:

$$Ke = \frac{(1 + C_{Chla})}{4}$$

where C_{Chla} is the carbon mass of the algae in mg/L. The algae carbon mass typically averages about 0.25 to 1.0 mg/L, which yields values of Ke of about 0.3 to 0.5. A plot of the adopted extinction coefficient function has been compared to a value based on the secchi depth in Figure 3-29c. The generally good agreement between the two quantities indicates that the extinction depth model is sufficient, since the secchi depth typically is on the same order of magnitude as the extinction coefficient. The algae carbon mass was derived by assuming a ratio of carbon-to-chlorophyll-a ratio of 30 and using the seasonal average values of the measured Chlorophyll-a.

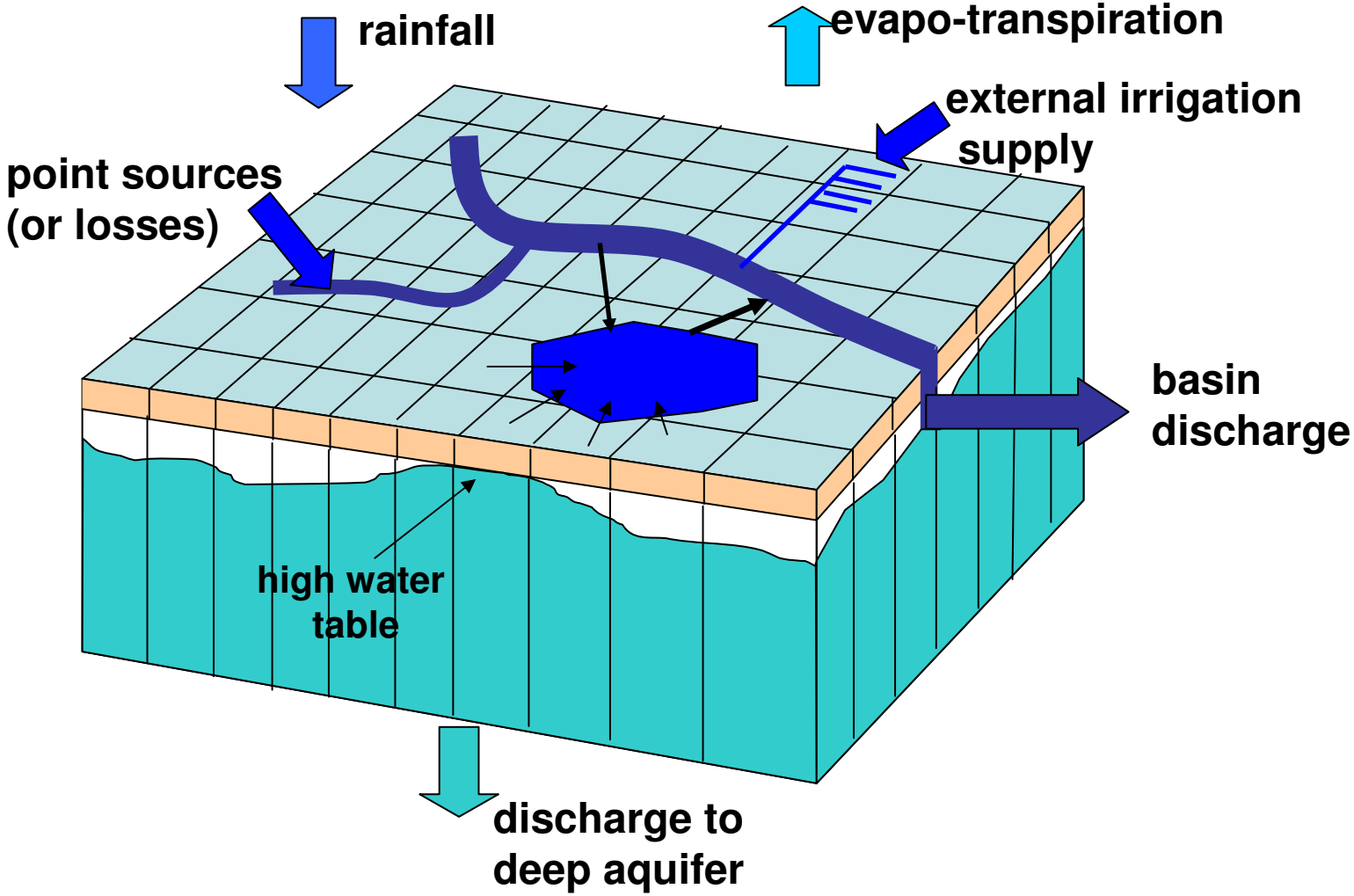

URS

Figure 3-1. The System and Elements Comprising the WaSh Model.

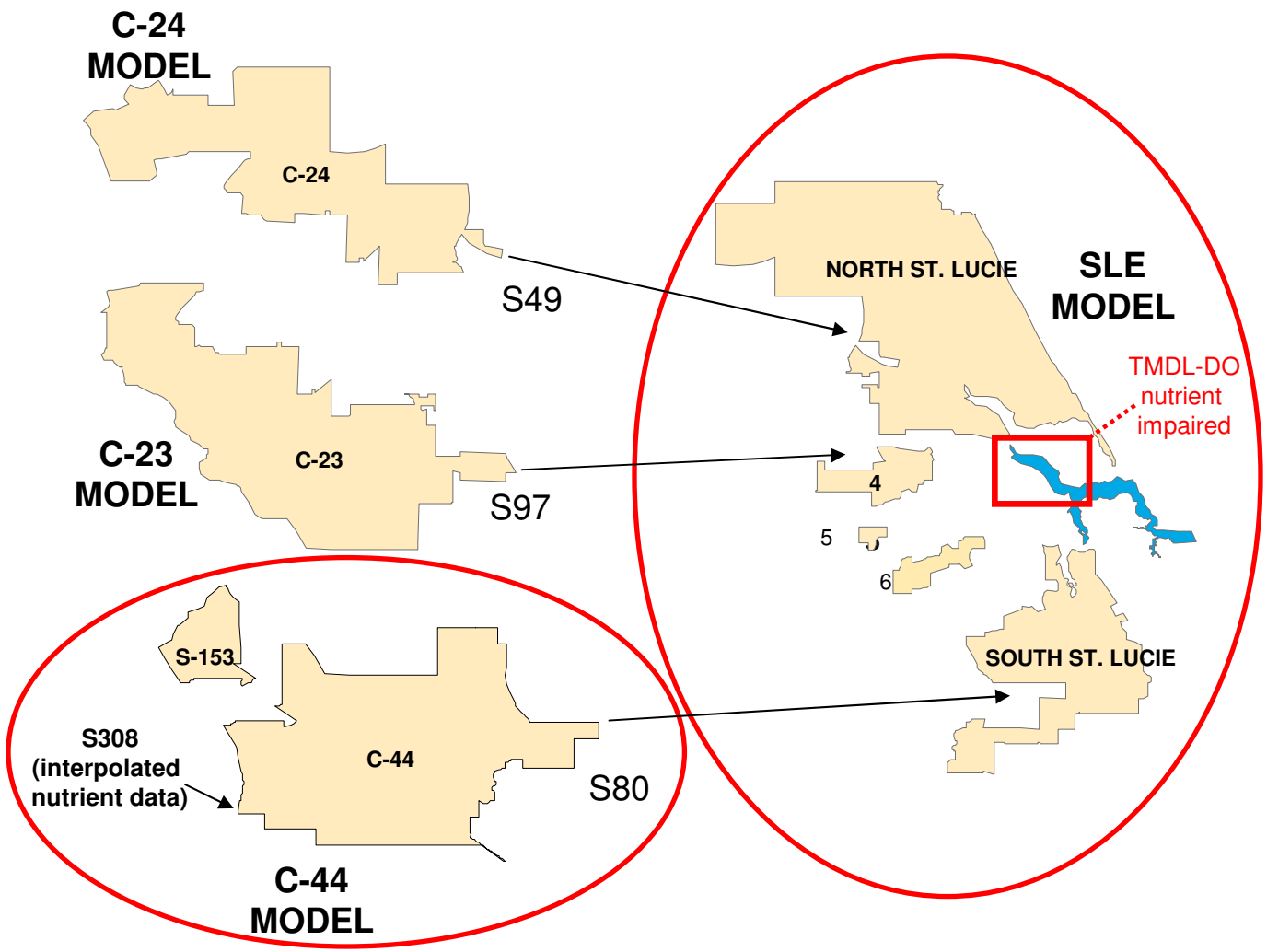

URS

Figure 3-2. Model Configuration of tidally-influenced SLE Basin and structurally-controlled C-24, C-23 and C-44 basins.

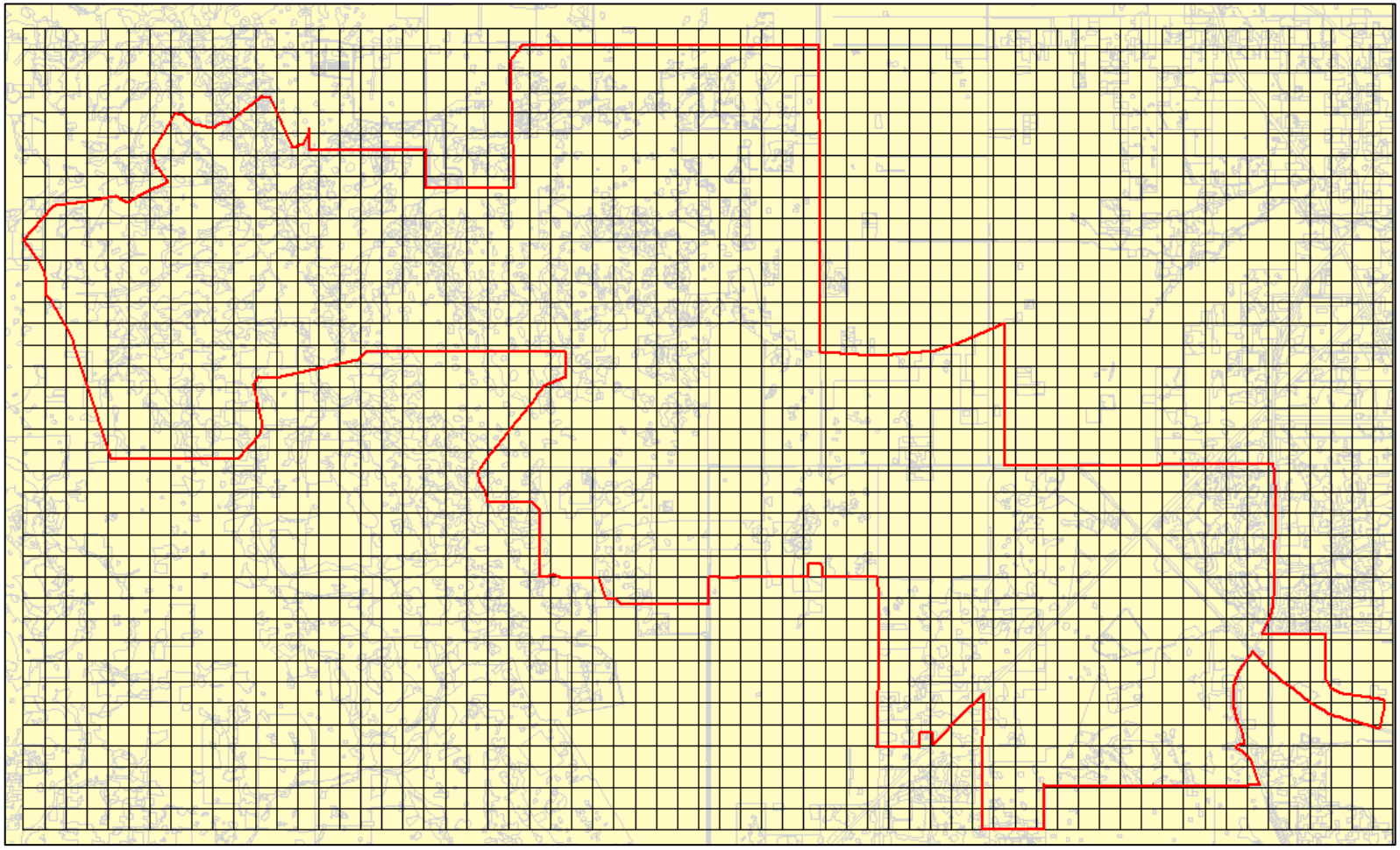

URS

Figure 3-3. C-24 Primary Basin boundary and model grid.

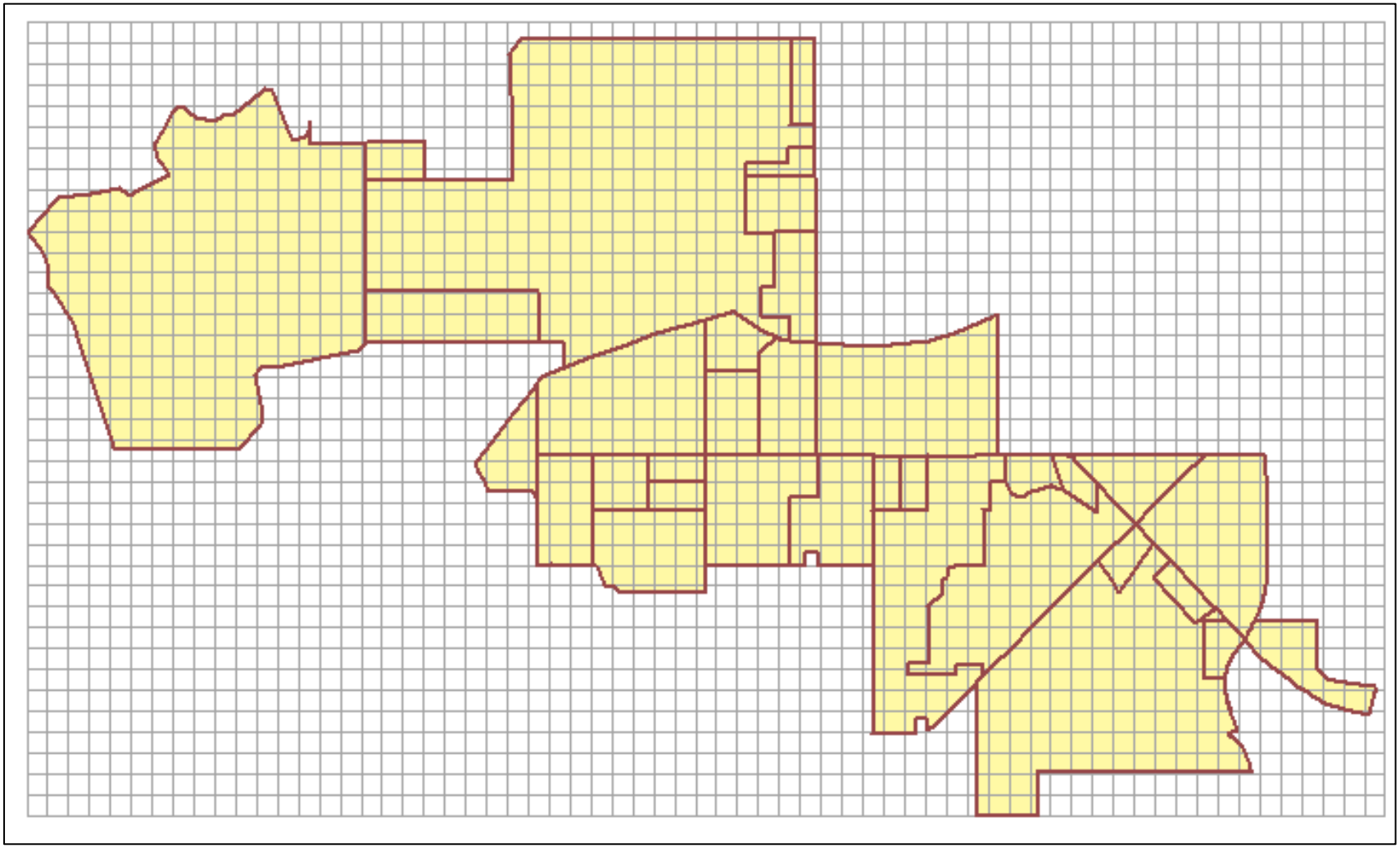

URS

Figure 3-4. C-24 Secondary Basin boundaries and model grid.

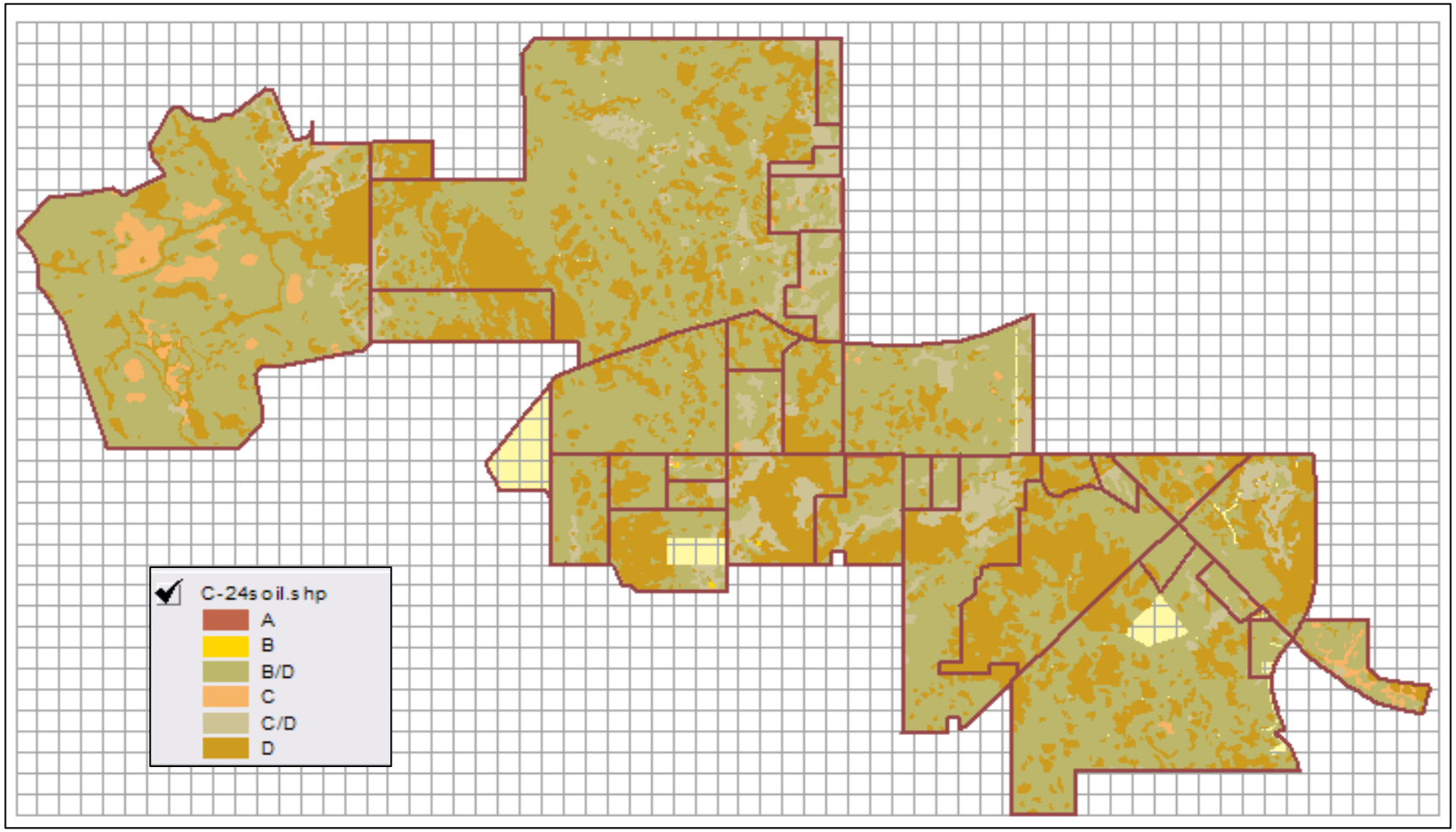

URS

Figure 3-5. C-24 Hydrogroup soils classifications.

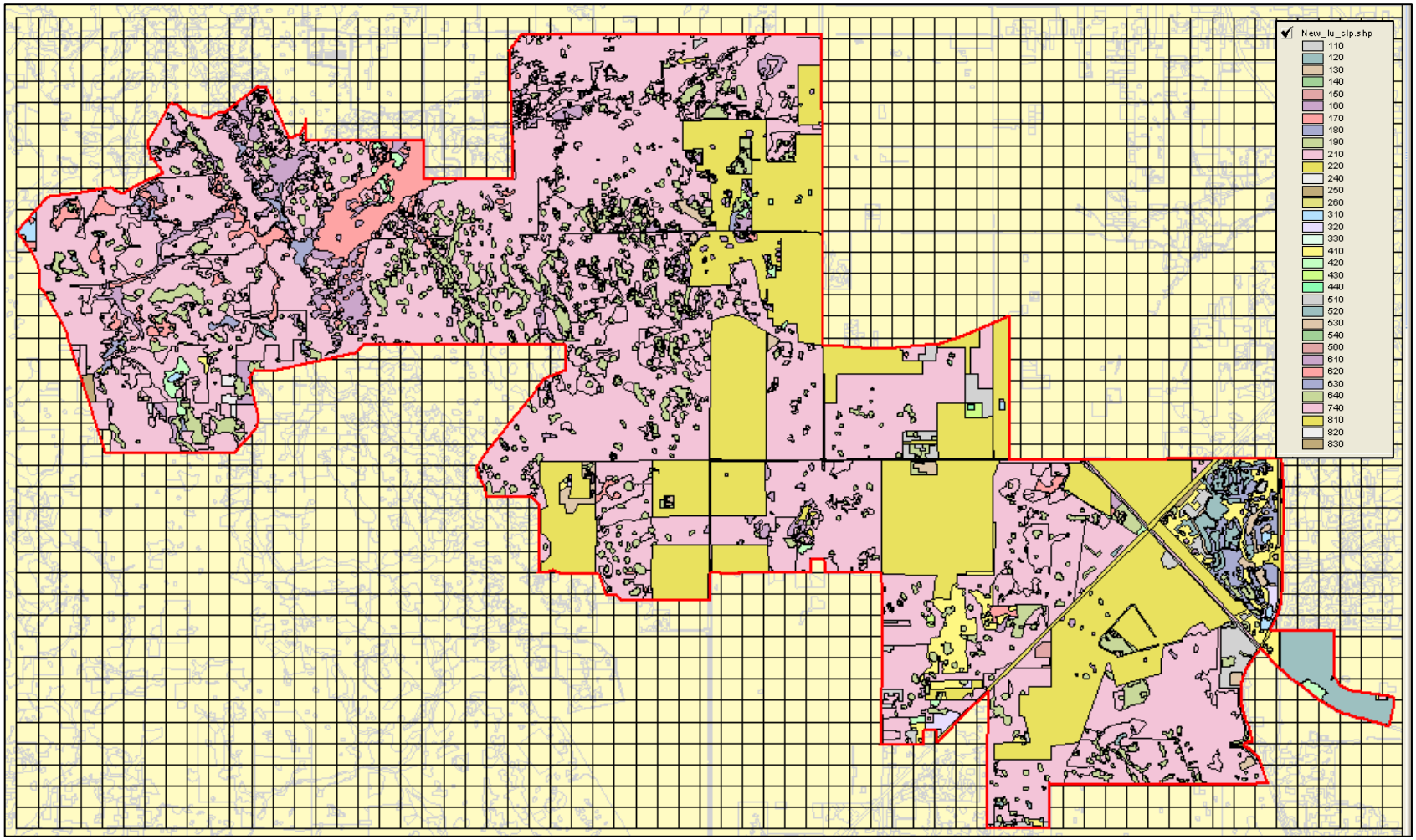

URS

Figure 3-6. C-24 Basin 1999 Adjusted land-use coverage.

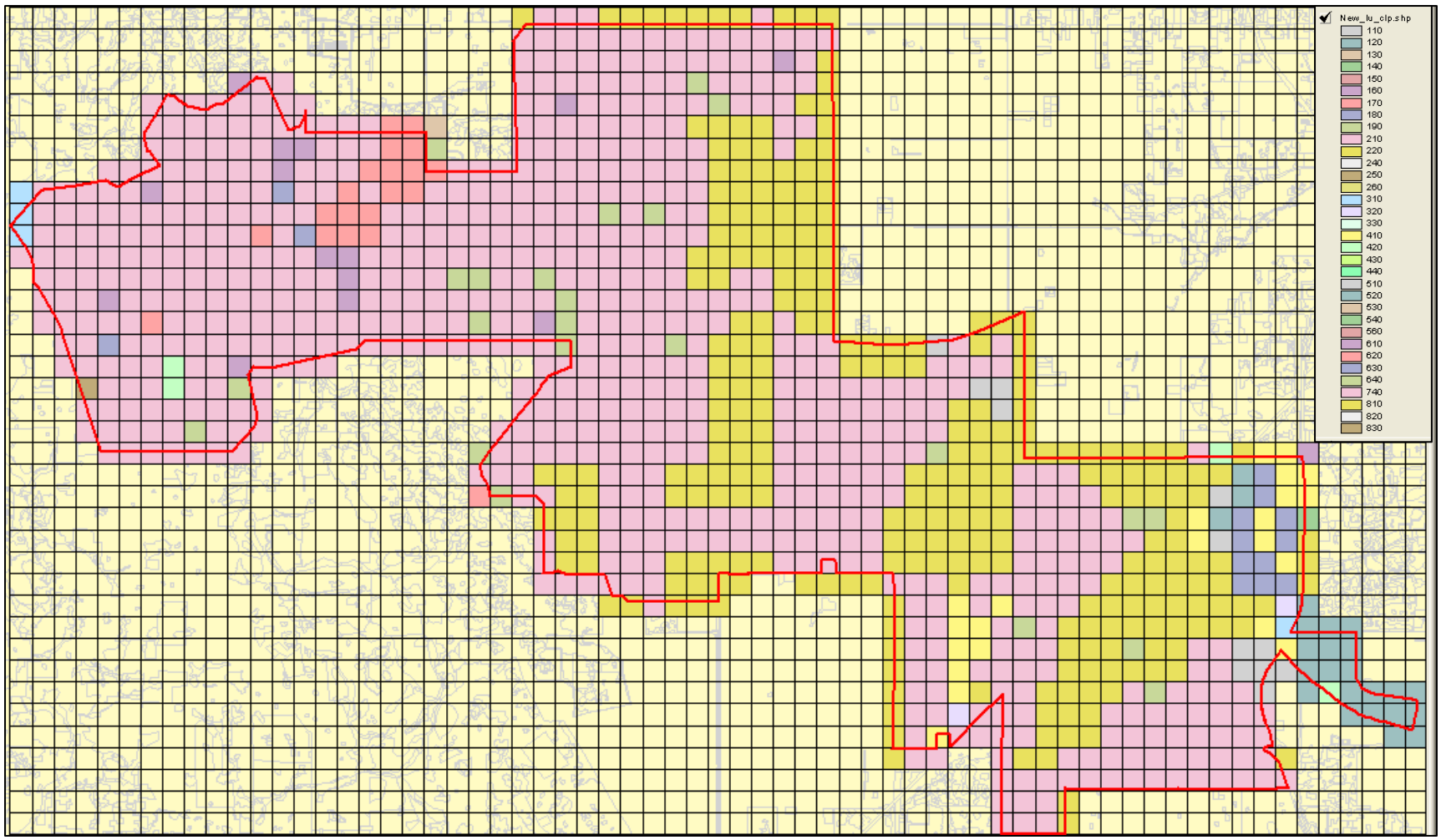

URS

Figure 3-7. C-24 Basin 1999 model assigned land-use.

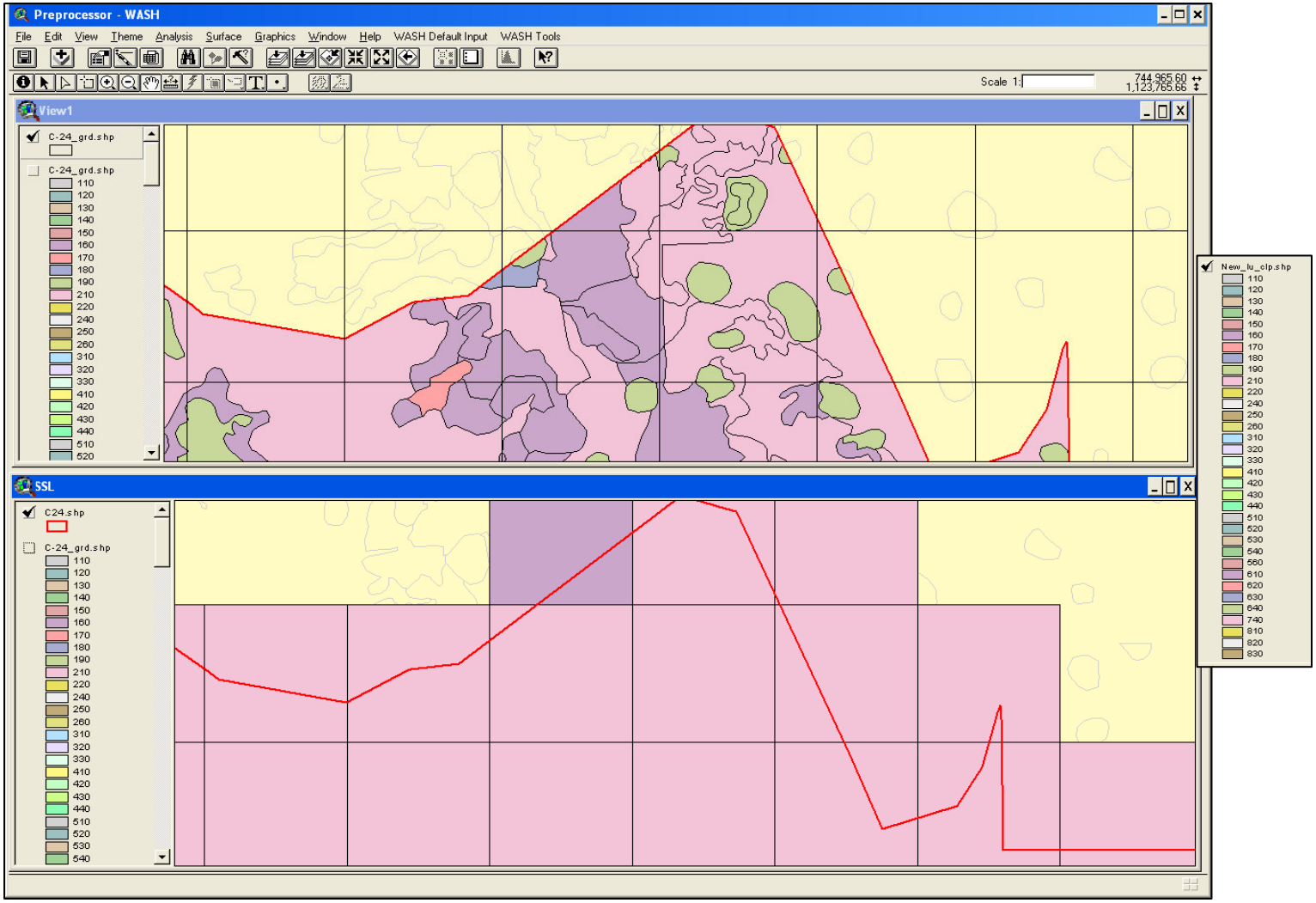

URS

Figure 3-8a. C-24 Basin land-use, showing poor correlation between actual Land-use (top) and the model assigned land-use (bottom).

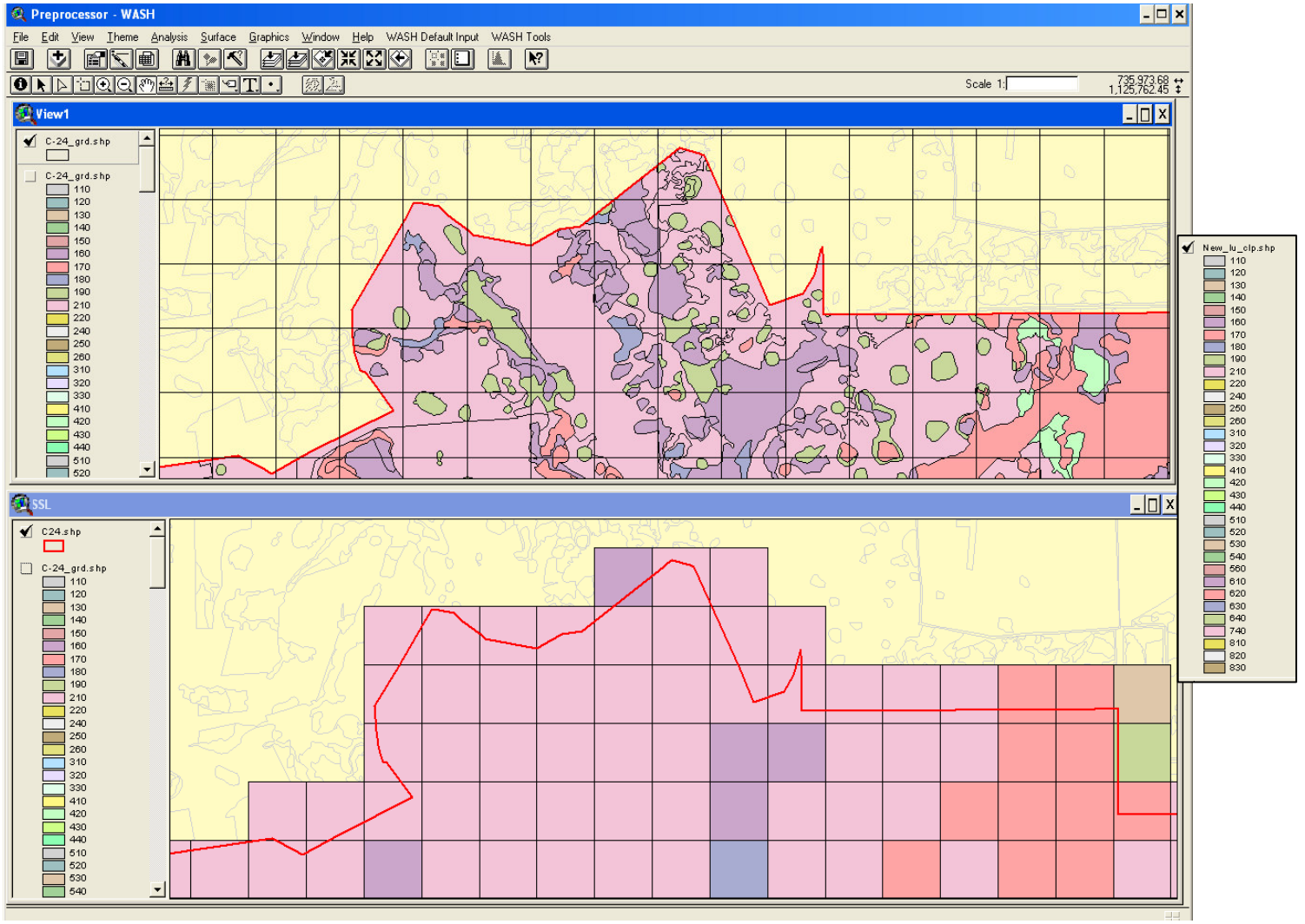

Figure 3-8b. C-24 Basin land-use, showing poor correlation between actual land-use (top) and the model assigned land-use (bottom).

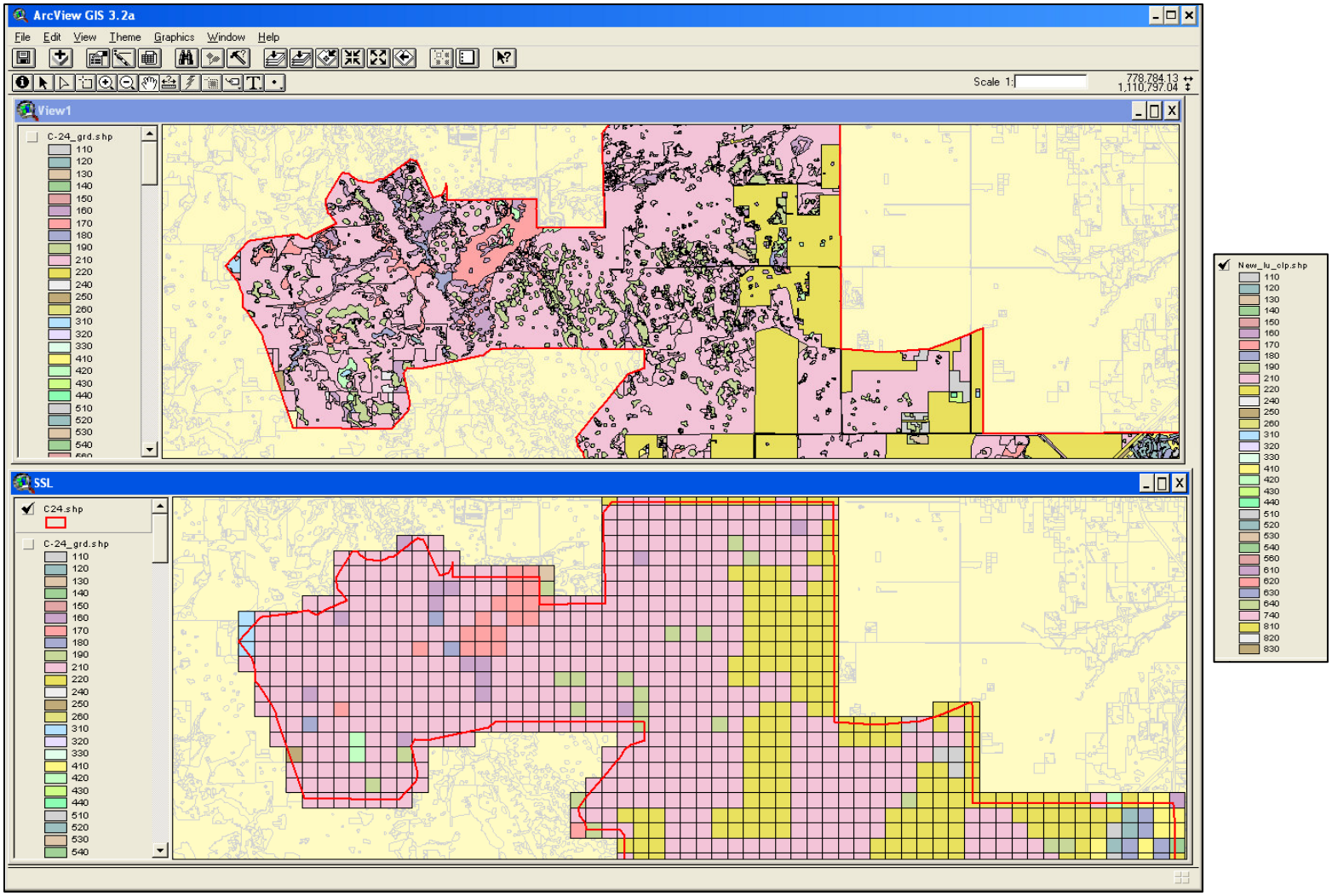

URS

Figure 3-9a. C-24 Basin land-use, before adjustment.

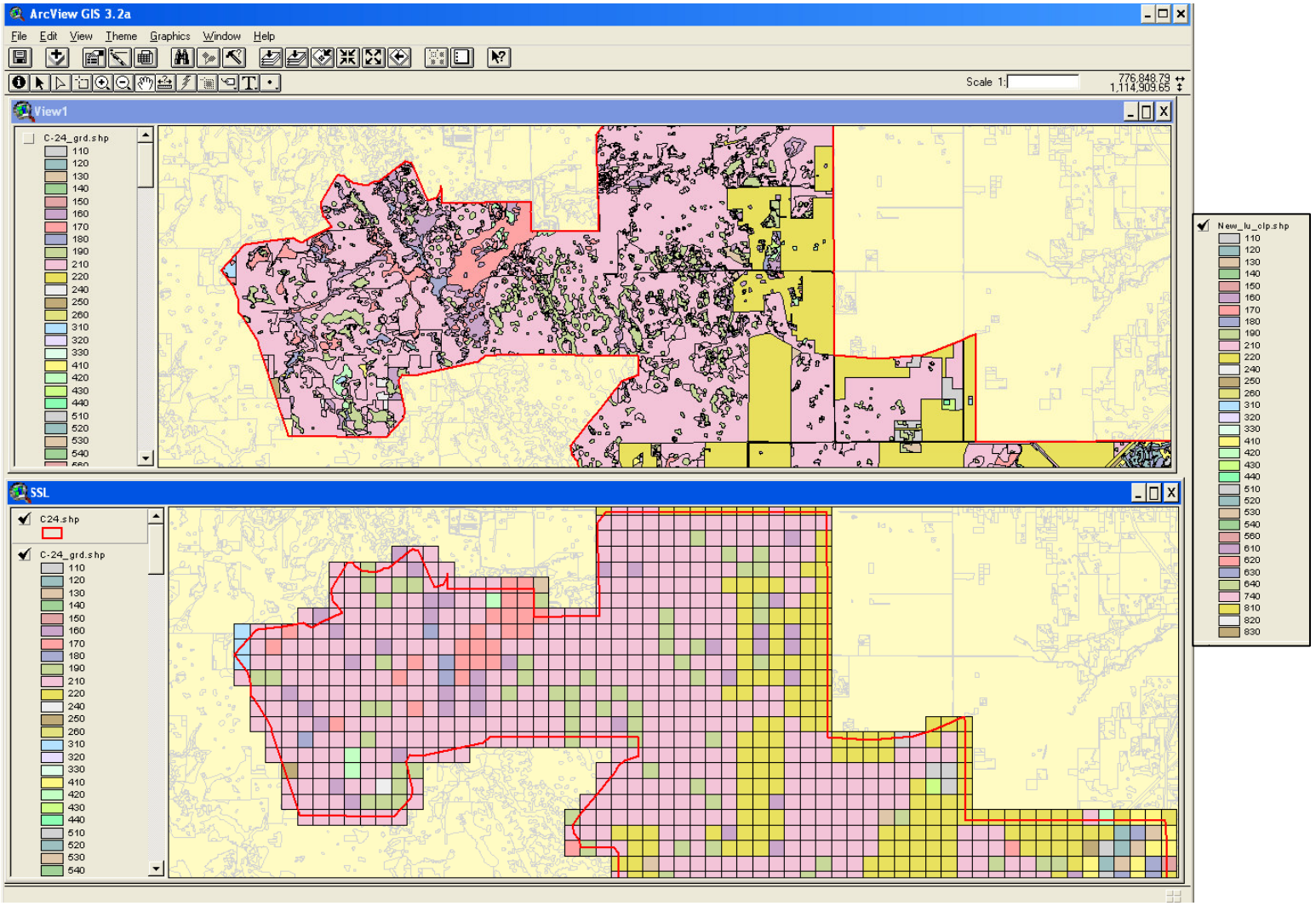

URS

Figure 3-9b. C-24 Basin land-use, after adjustment.

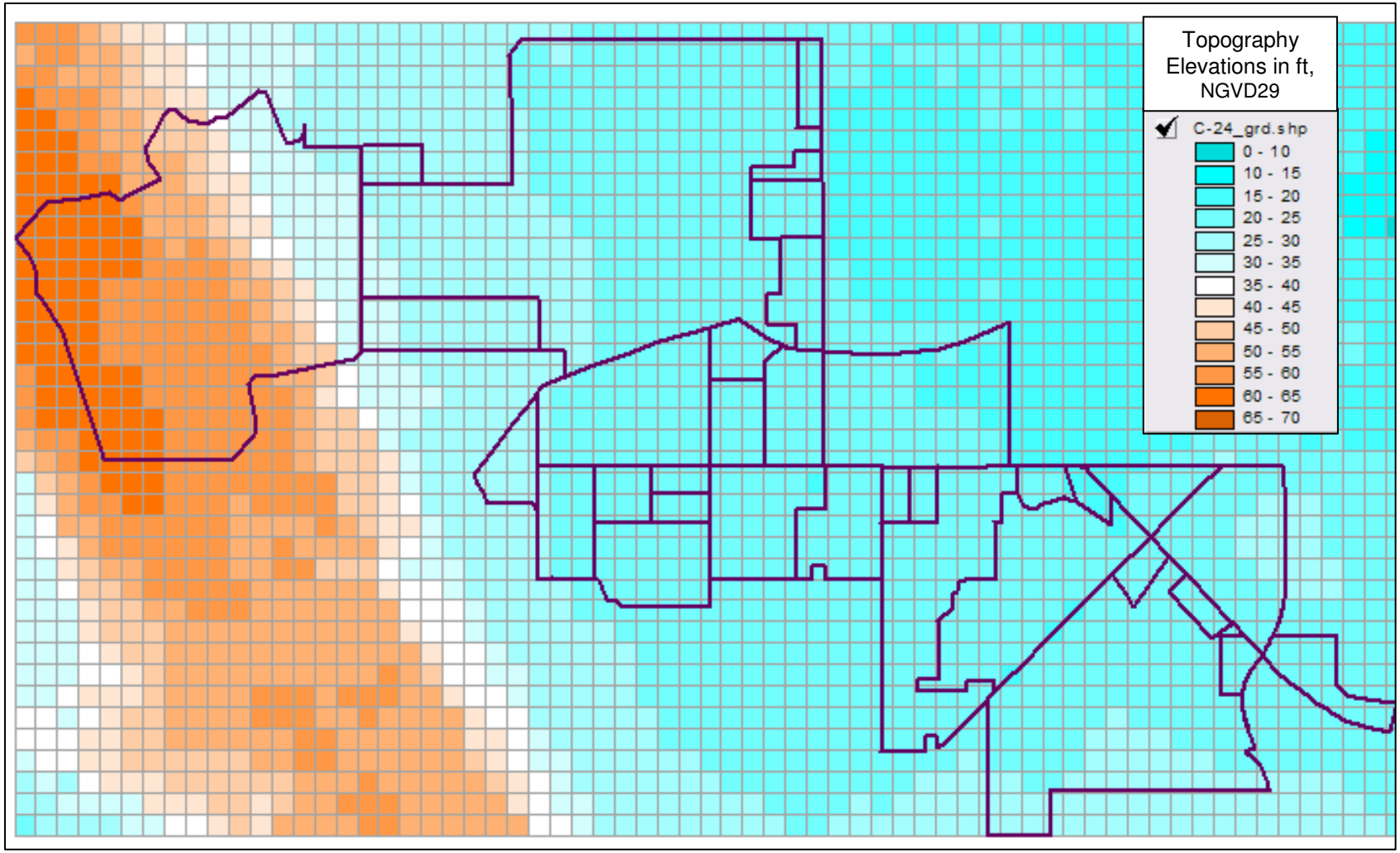

URS

Figure 3-10. Topography as mapped on Model Grid for C-24 basin.

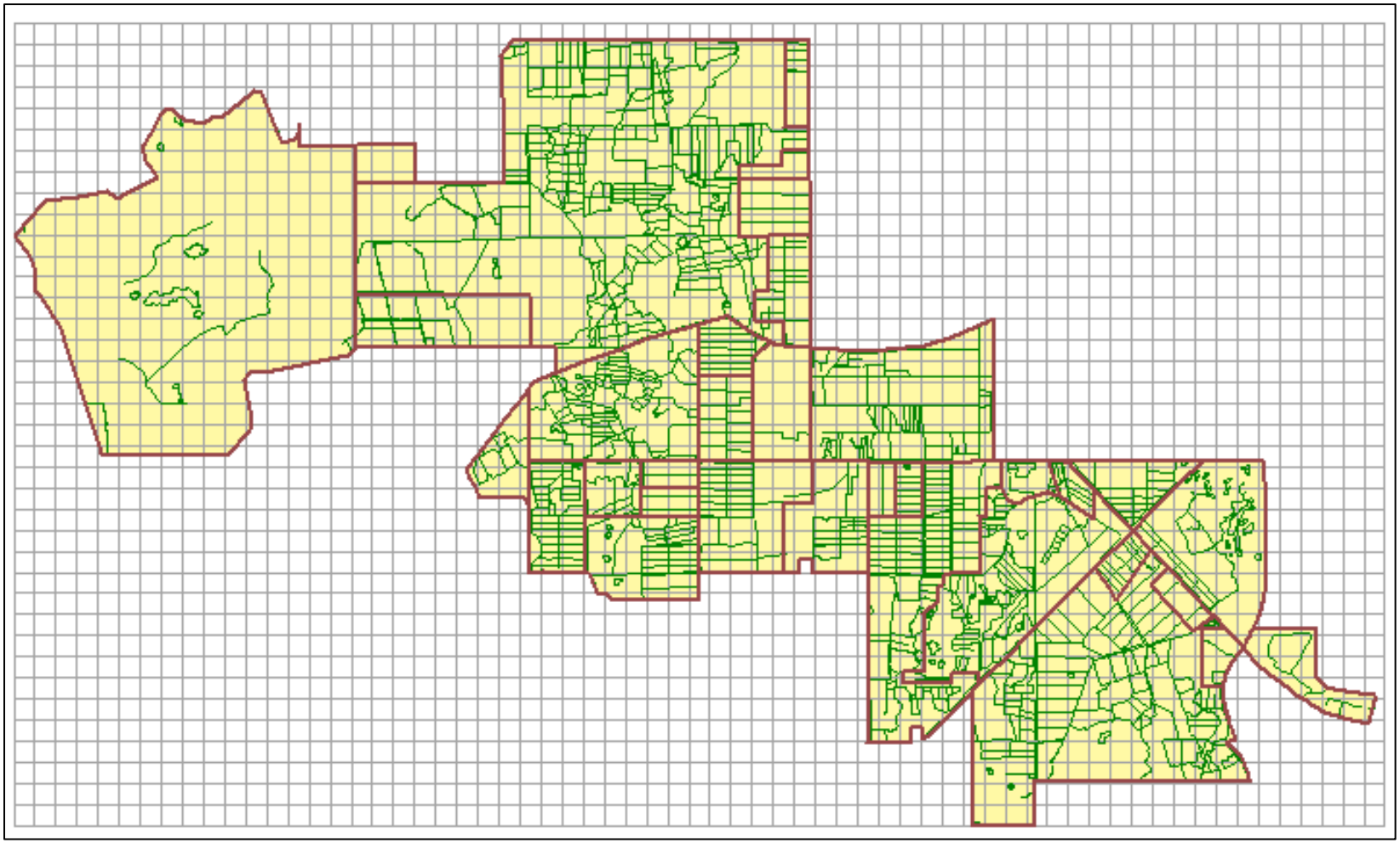

URS

Figure 3-11. C-24 Hydrology showing Primary, Secondary and Tertiary canals.

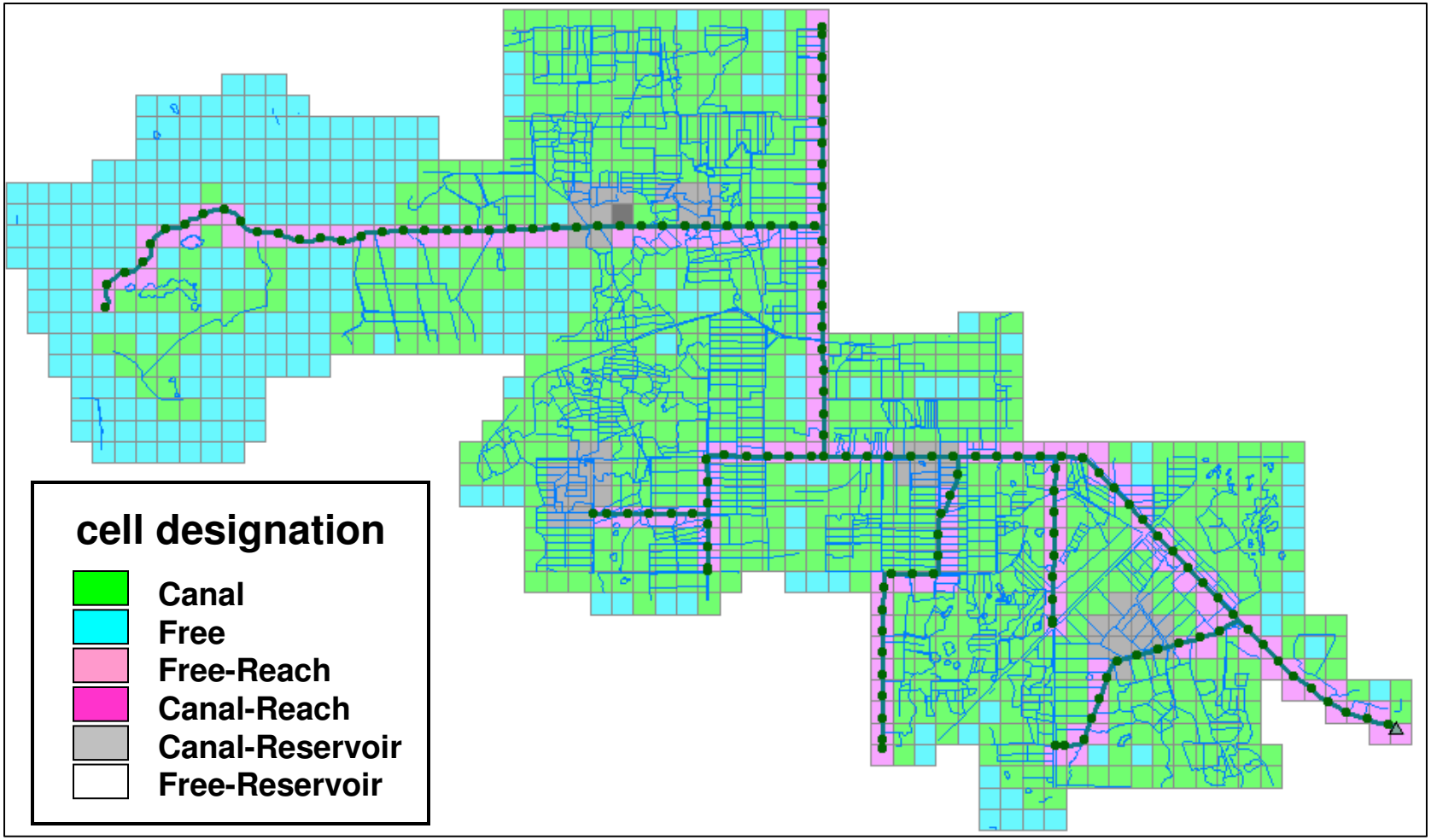

URS

Figure 3-12. Model Configuration- C-24 Basin Grid Cell Designation with Primary Reach and Hydrography.

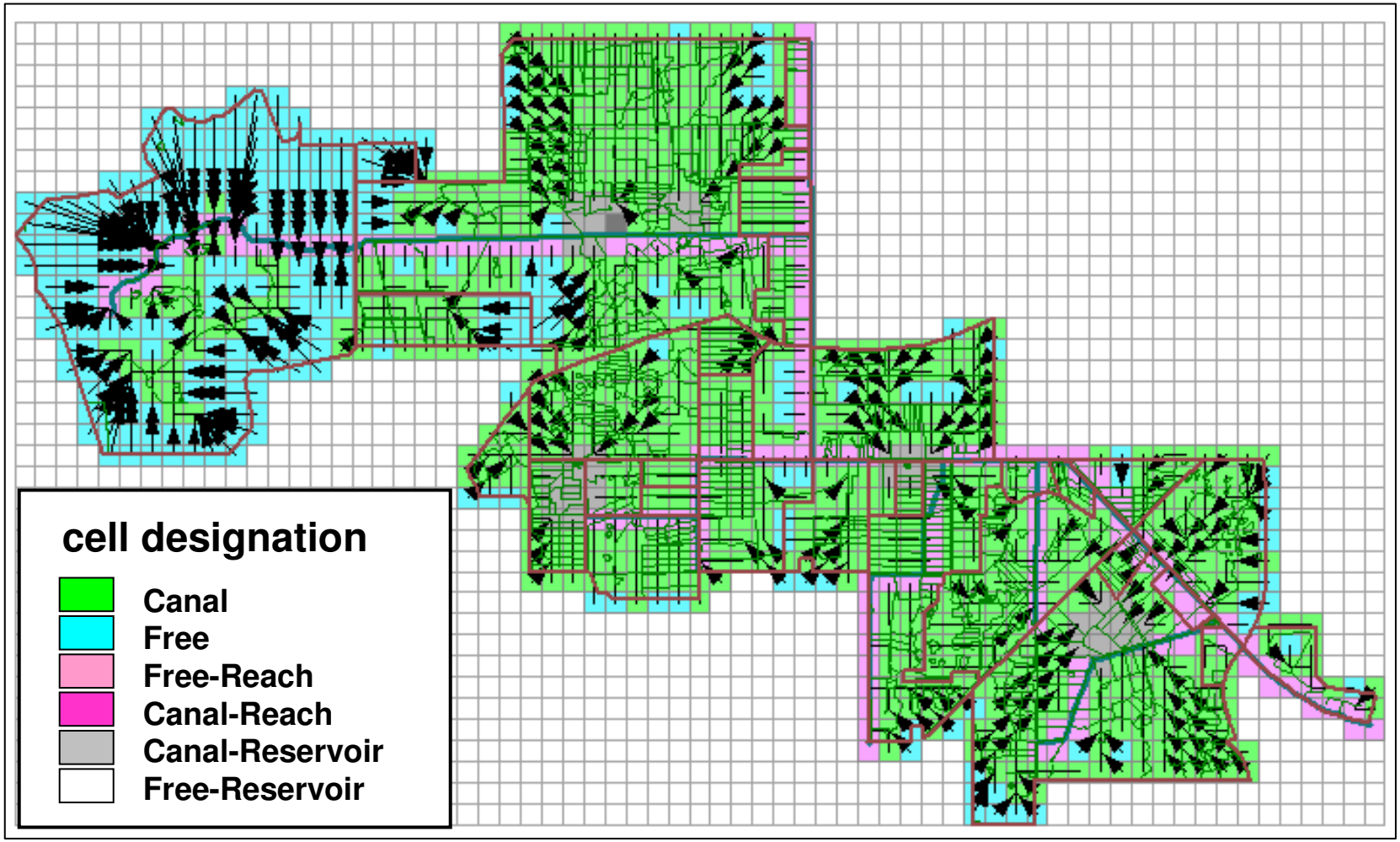

URS

Figure 3-13. C-24 Basin with Flow Paths.

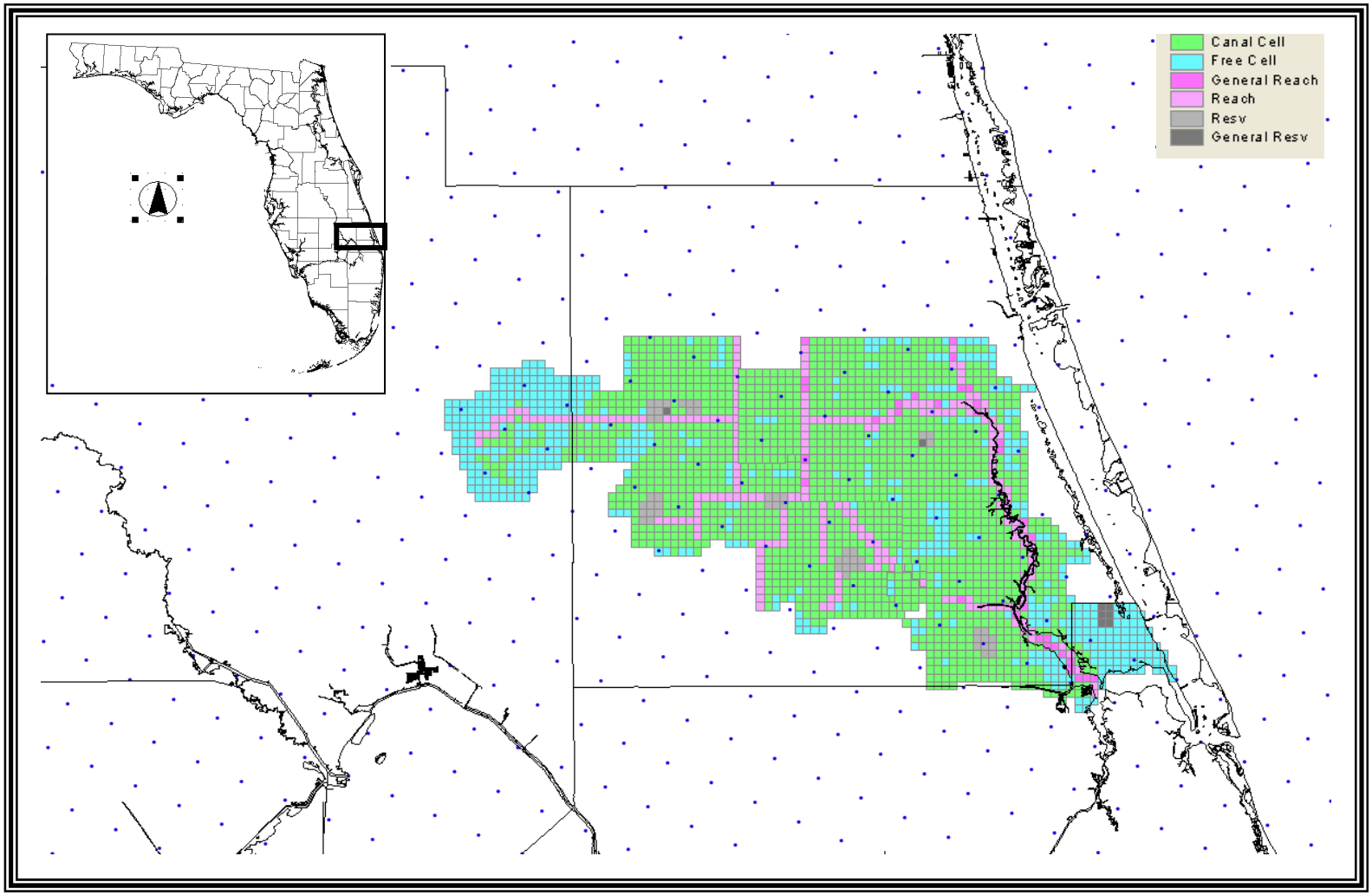

URS

Figure 3-14. NEXRAD Rainfall Station Locations in Vicinity of C-24 and North Fork Basins (WaSh Model Grids shown).

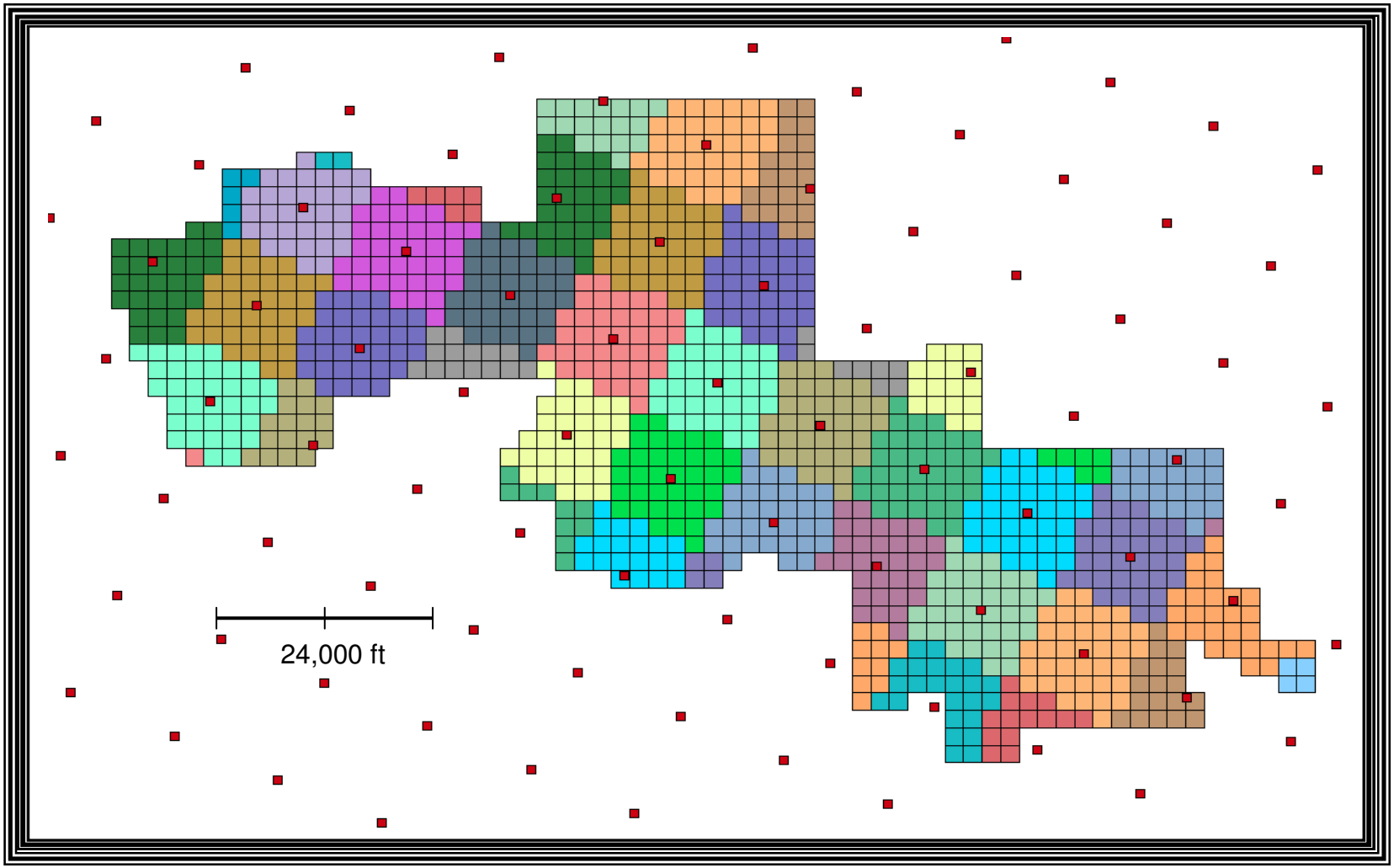

URS

Figure 3-15. Mapping of NEXRAD stations onto WaSh model C-24 basin grid cells.

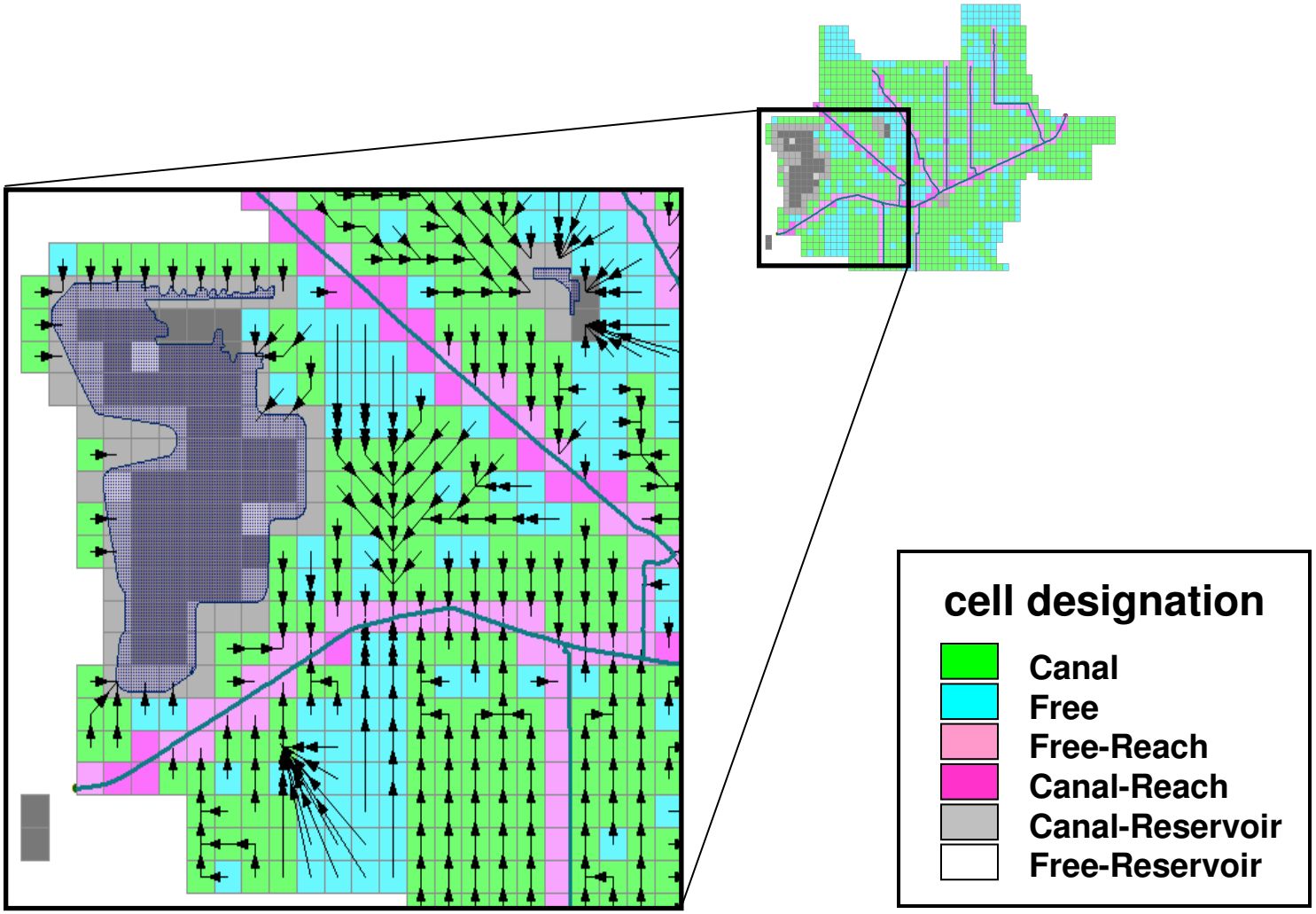

URS

Fig 3-16. Reservoir configuration in C-44 model.

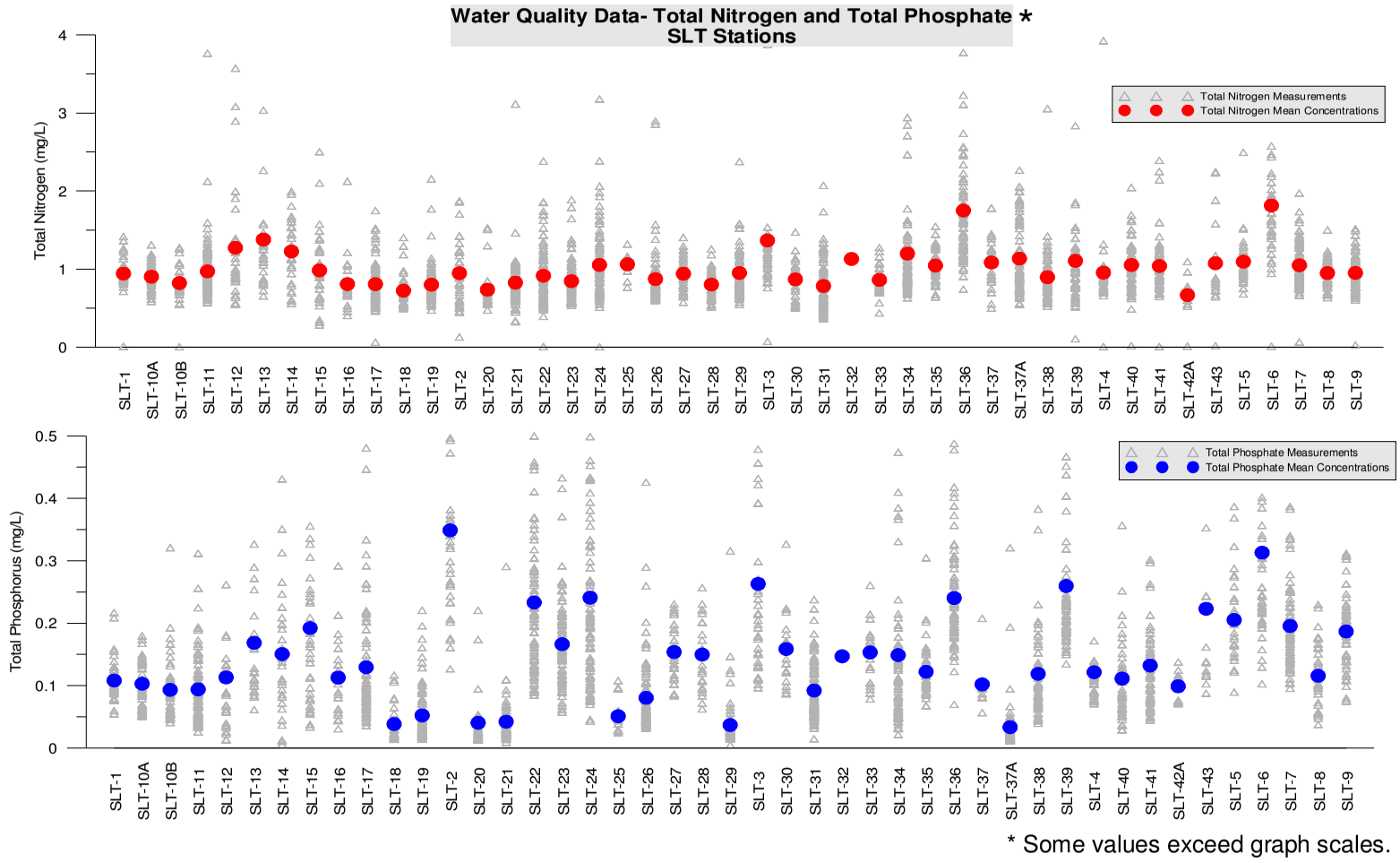

* Some values exceed graph scales.

URS

Figure 3-17. Measured TN and TP values for individual grab samples at each SLT Station with the mean concentration for that station.

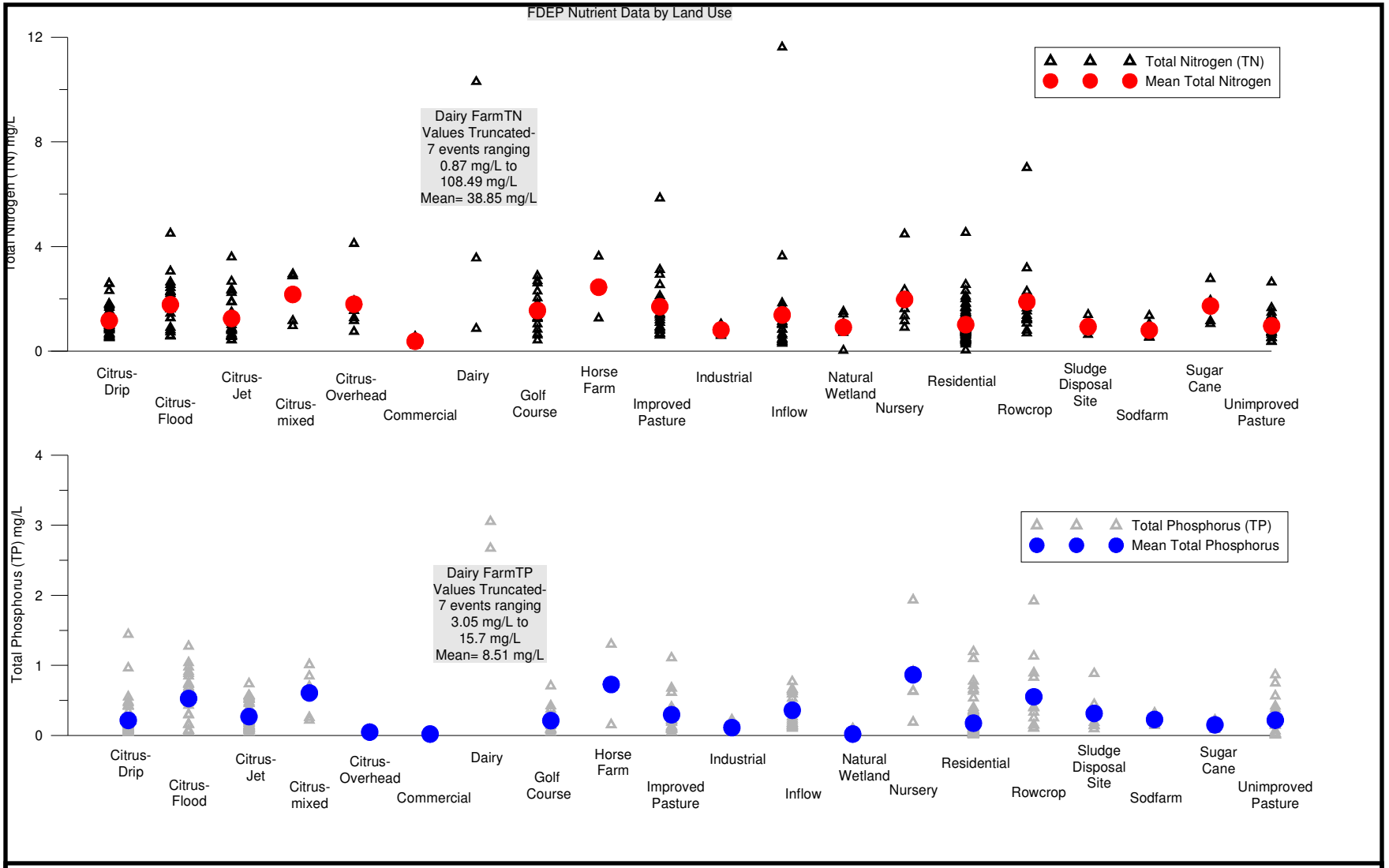

Figure 3-18. Measured TN and TP values for individual grab samples at each BMP Station with the mean concentration for that station.

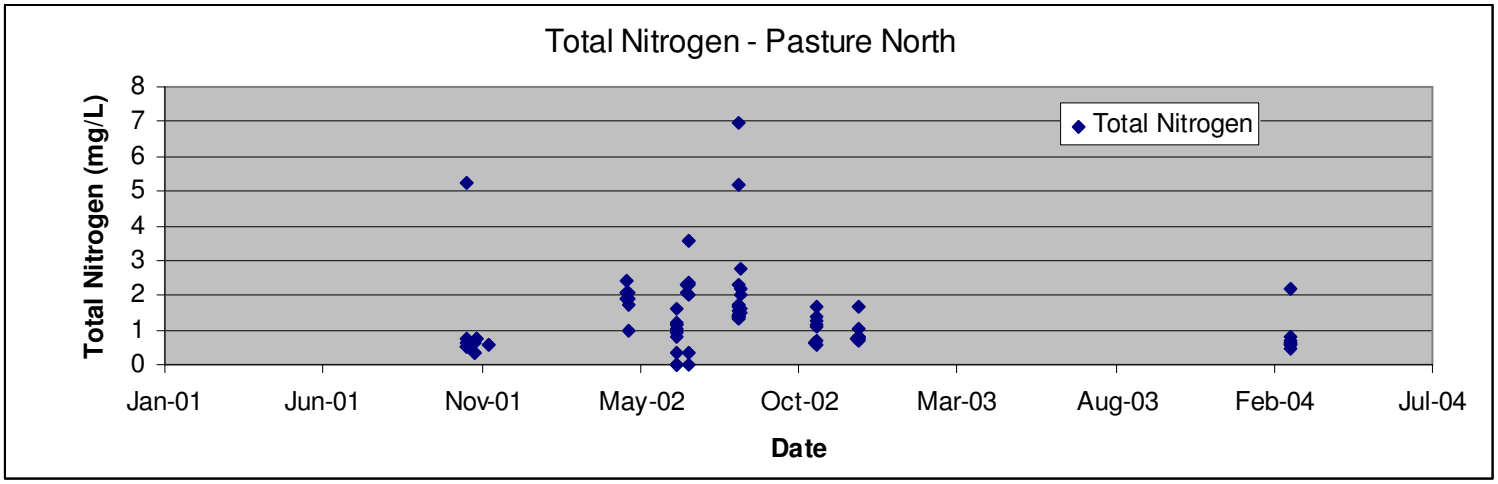

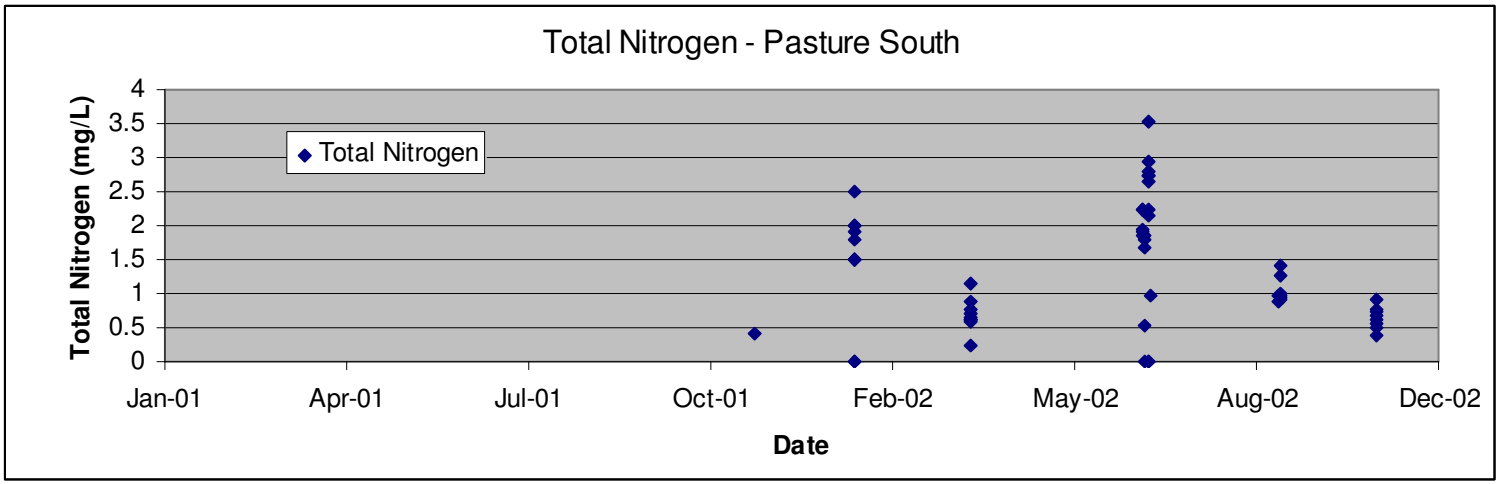

URS

Figure 3-19. IFAS ISCO Total Nitrogen Data.

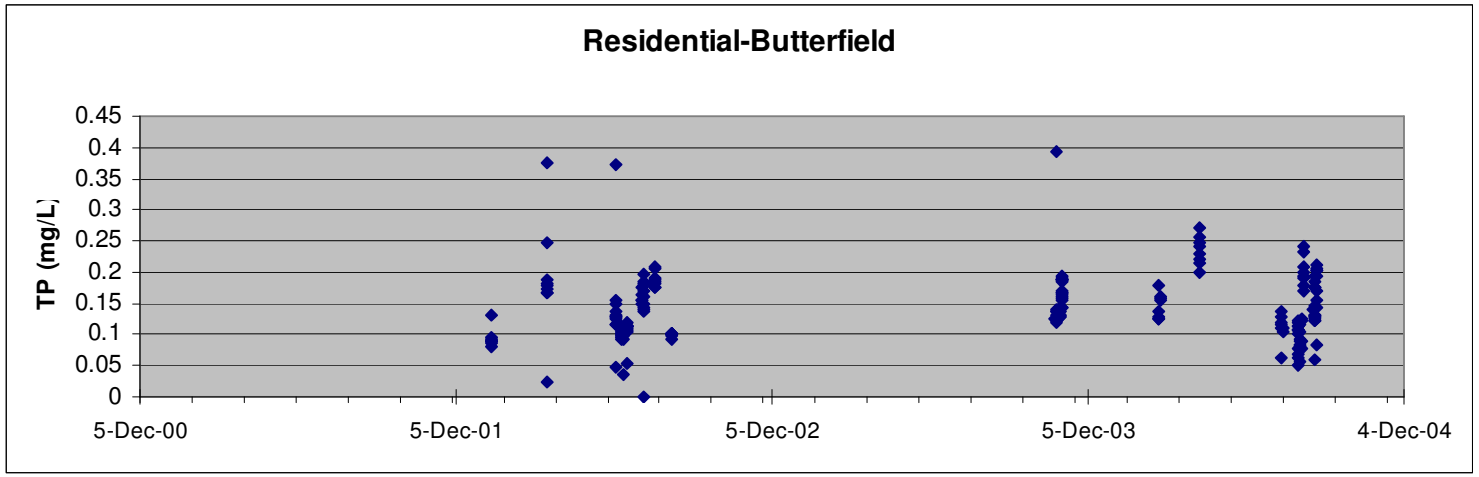

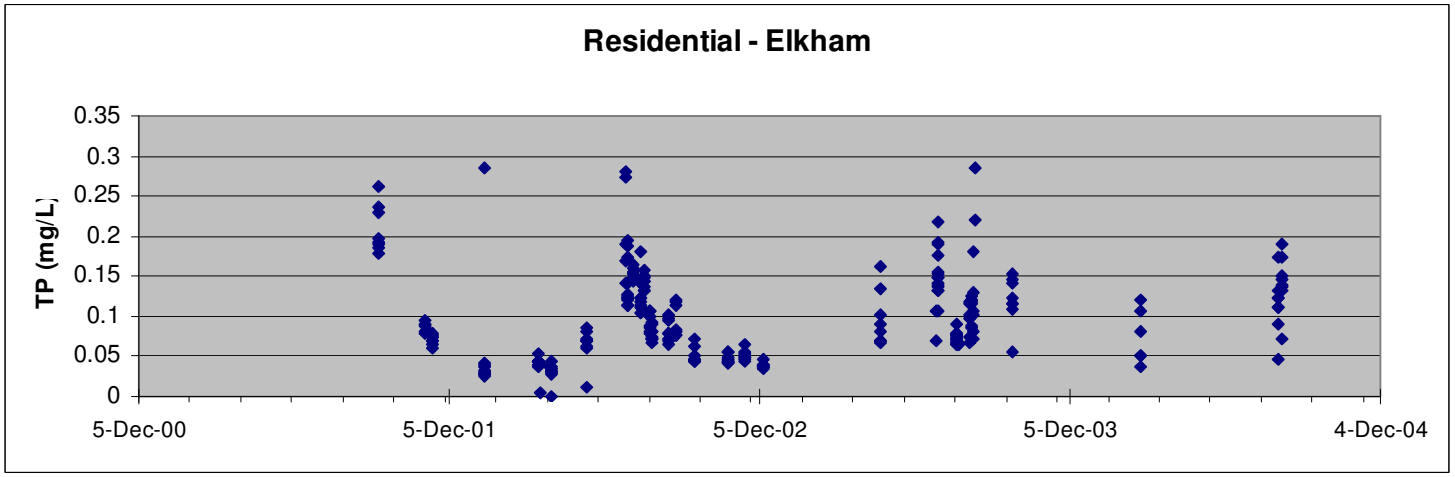

URS

Figure 3-20. IFAS ISCO Total Phosphate Data.

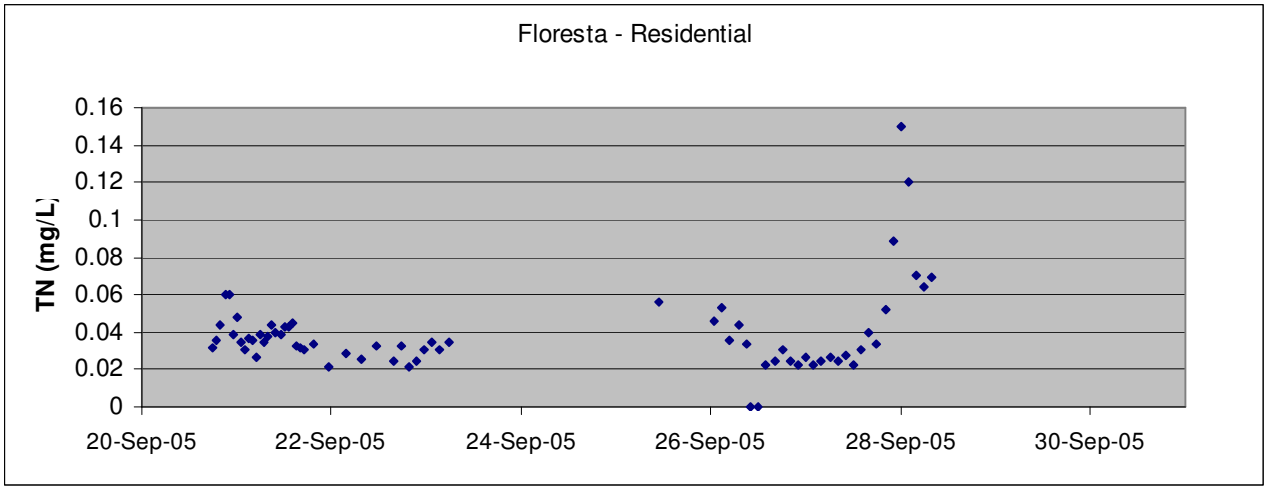

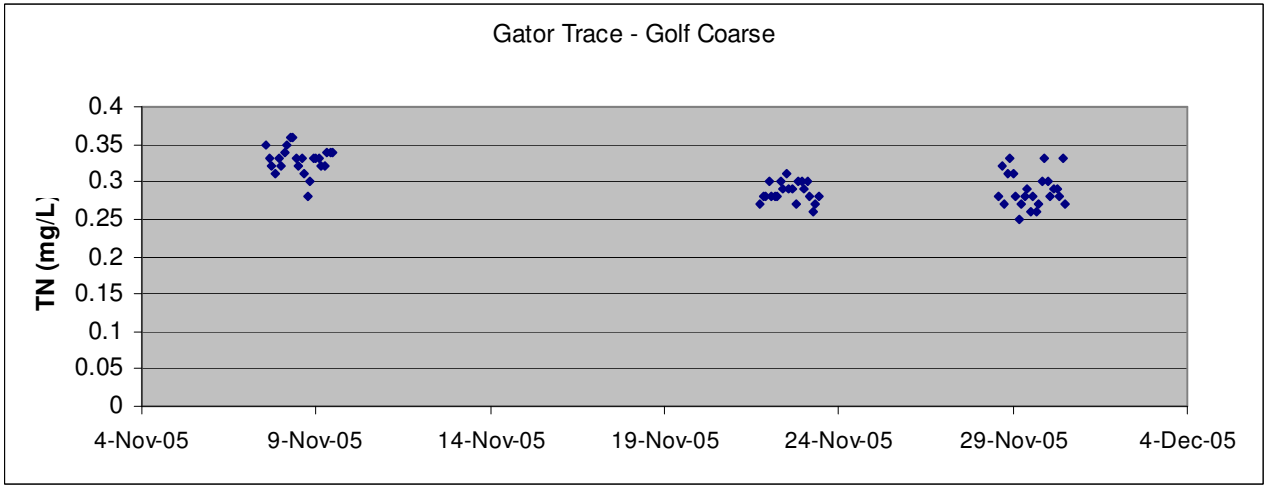

URS

Figure 3-21. FDEP ISCO Total Nitrogen Data.

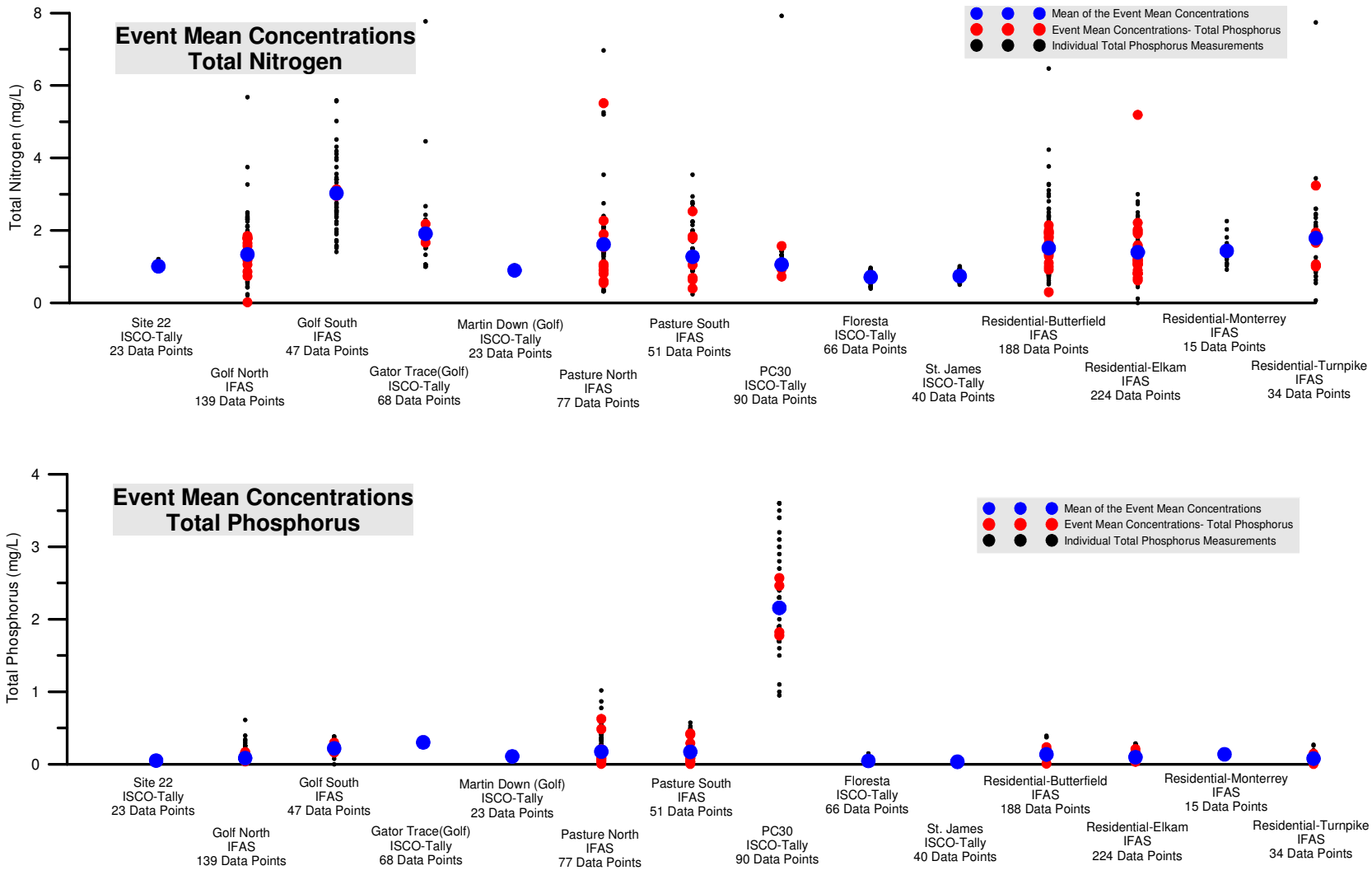

URS

Figure 3-22. ABMC values for each ISCO Station.

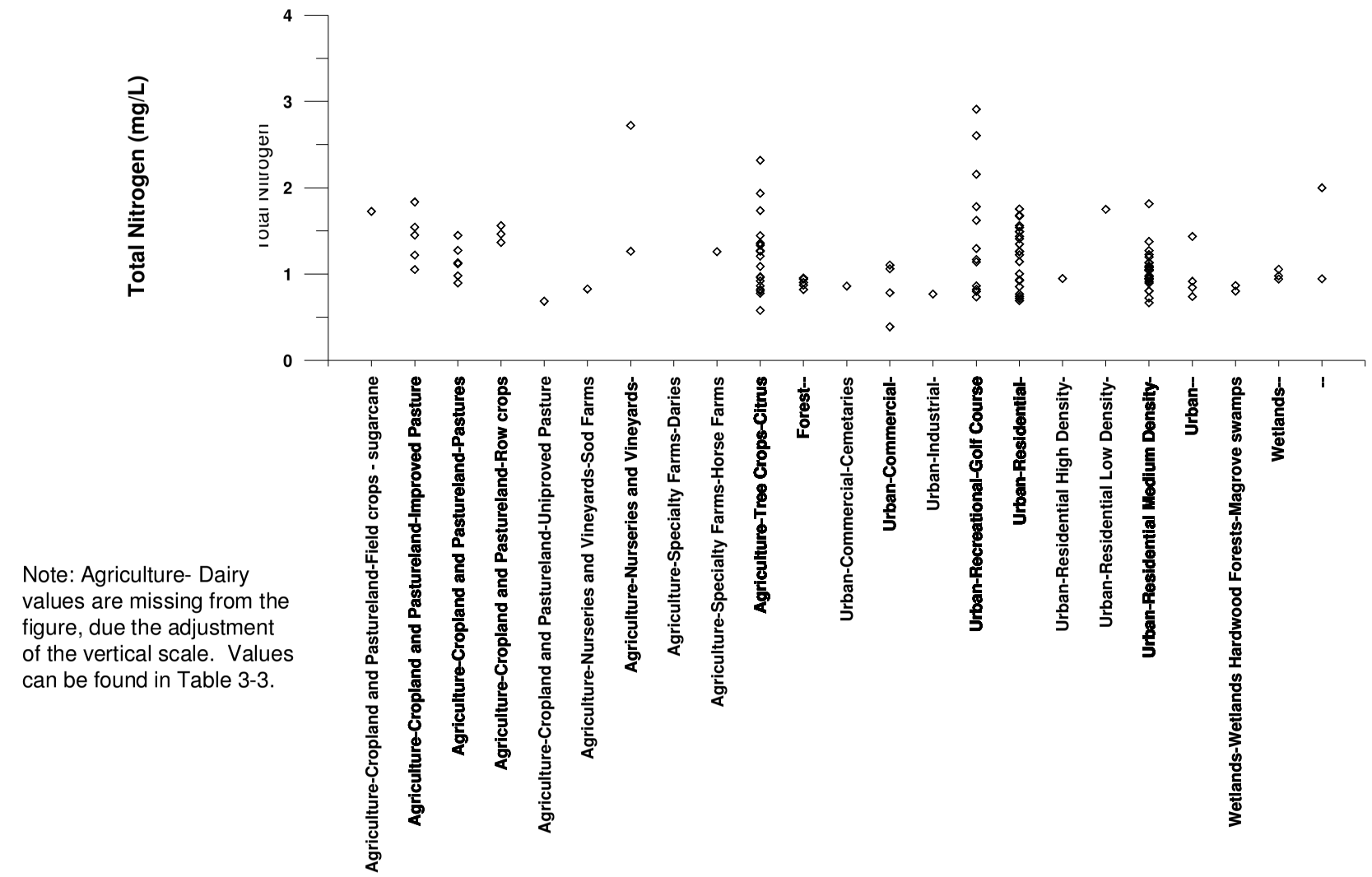

Note: Agriculture- Dairy values are missing from the figure, due the adjustment of the vertical scale. Values can be found in Table 3-3.

URS

Figure 3-23. Median TN values for sample stations listed in Table 3-3, organized by Land Use.

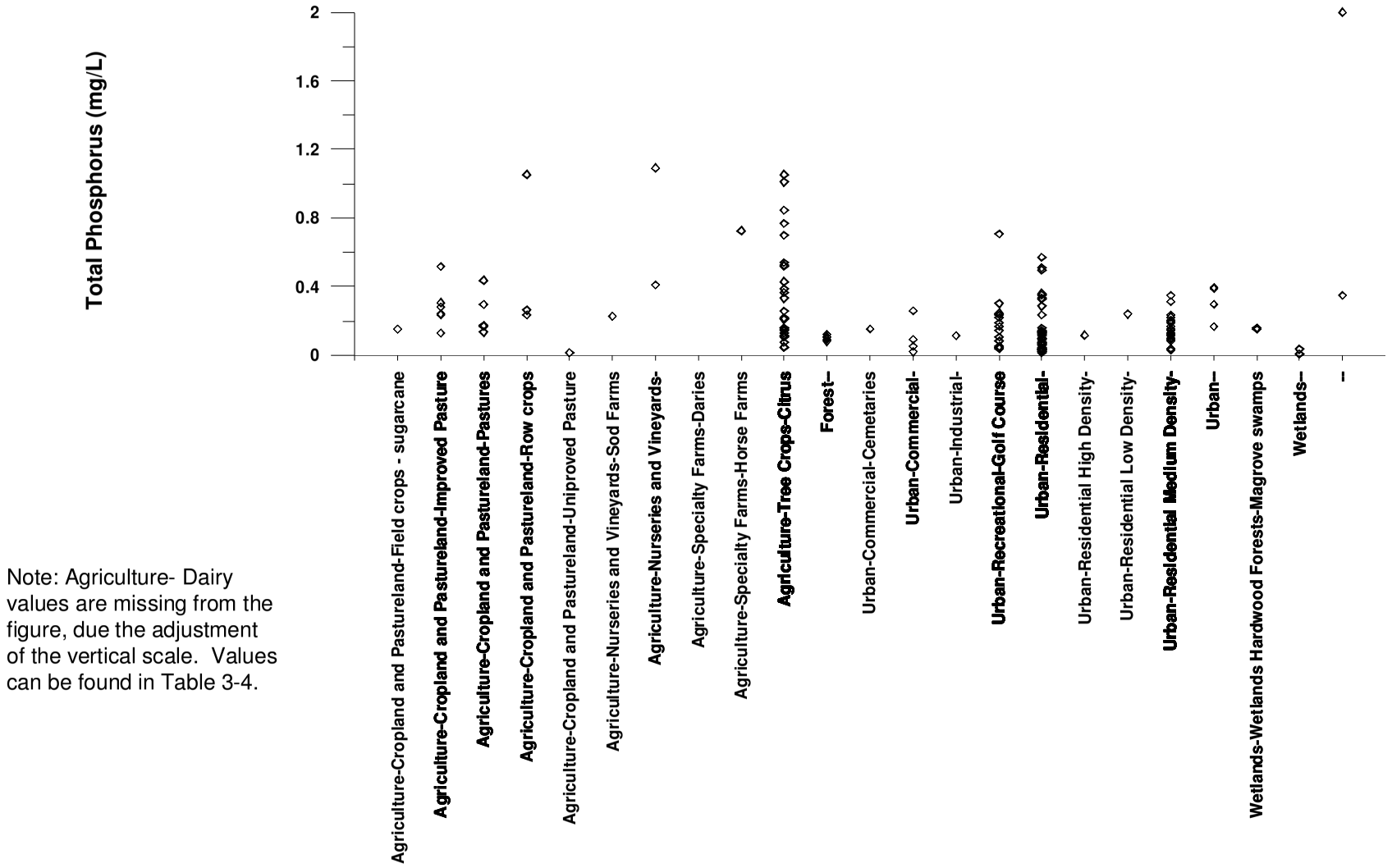

Note: Agriculture- Dairy values are missing from the figure, due the adjustment of the vertical scale. Values can be found in Table 3-4.

URS

Figure 3-24. Median TP values for sample stations listed in Table 3-4, organized by Land Use.

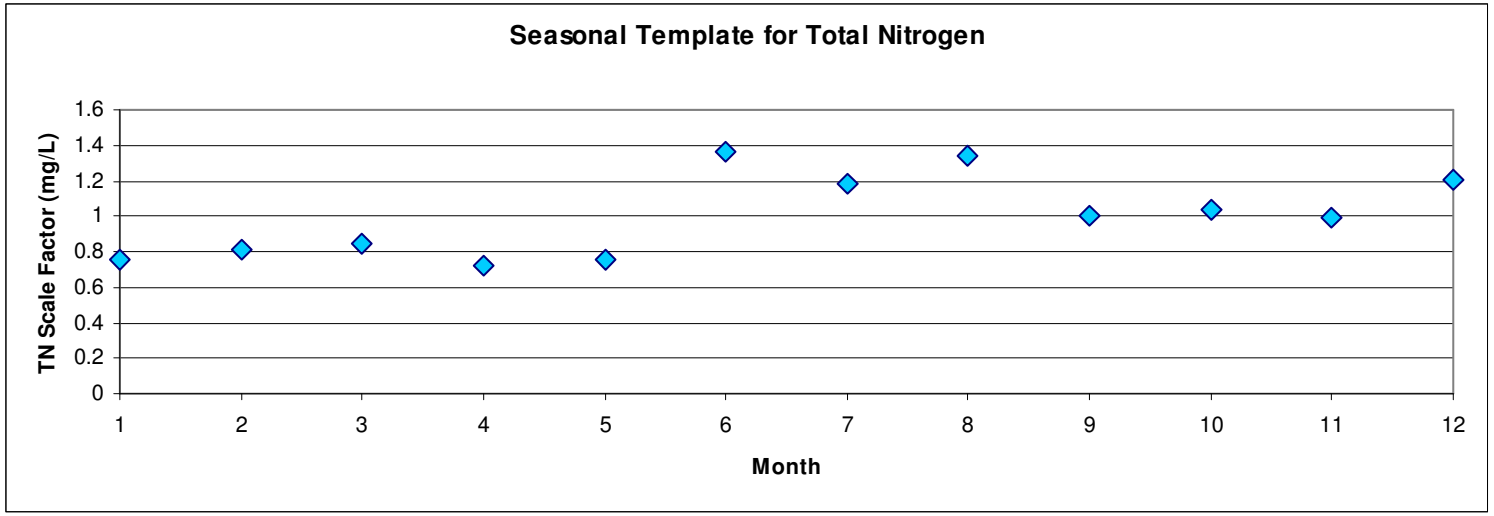

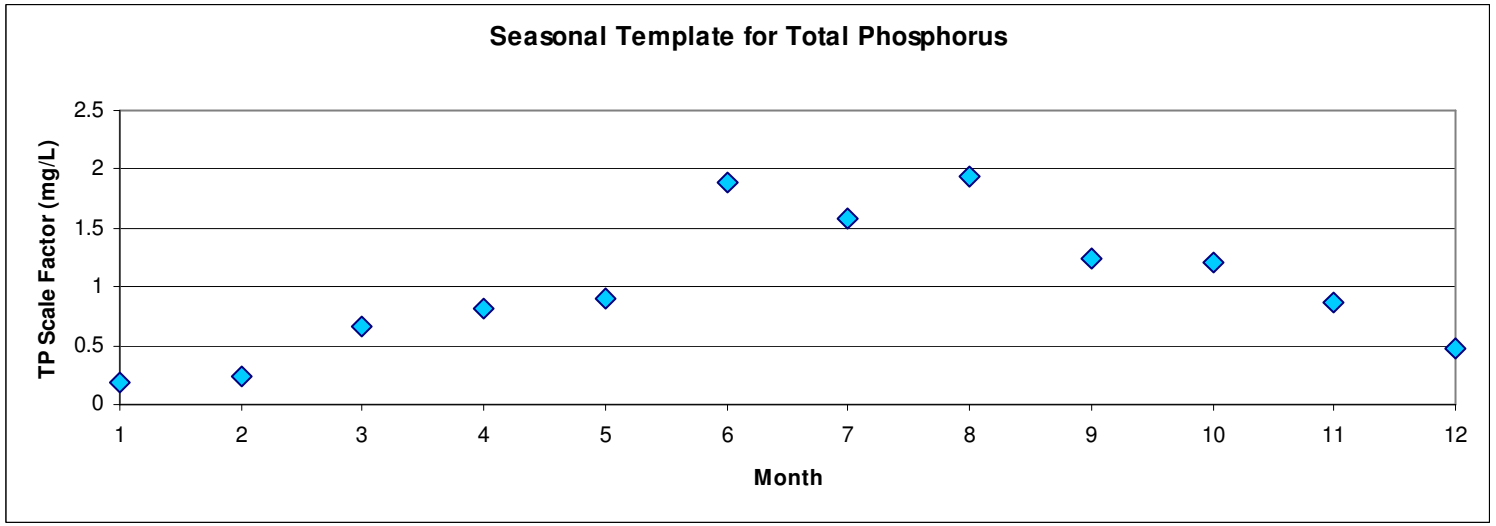

URS

Figure 3-25. Template for Total Nitrogen and Total Phosphorus.

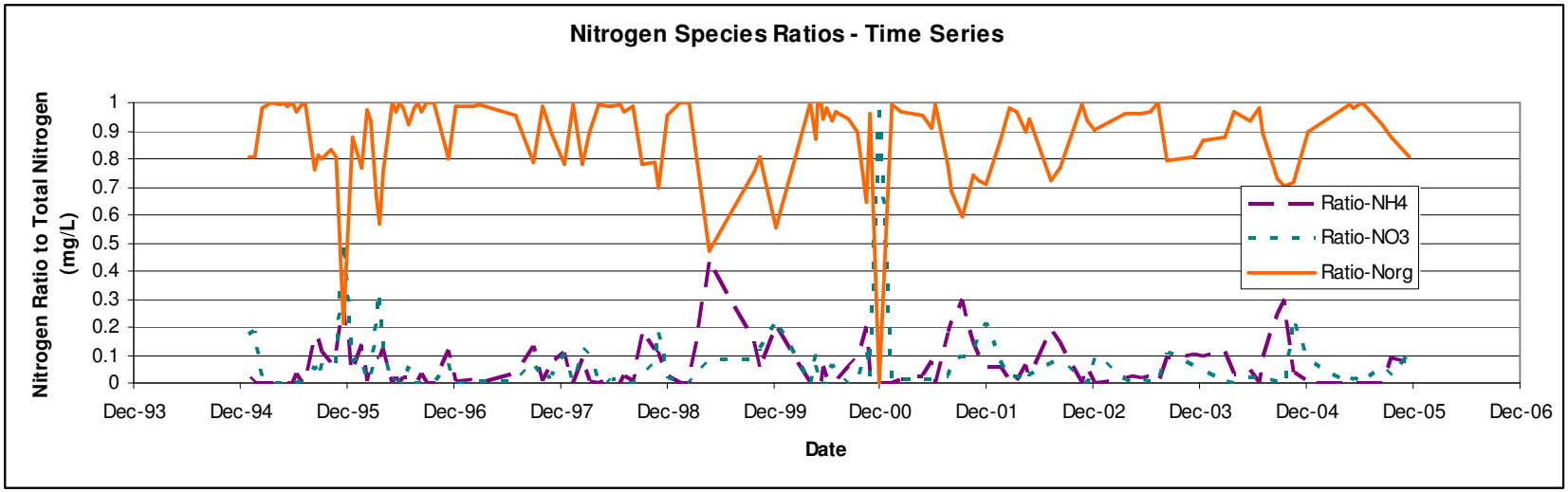

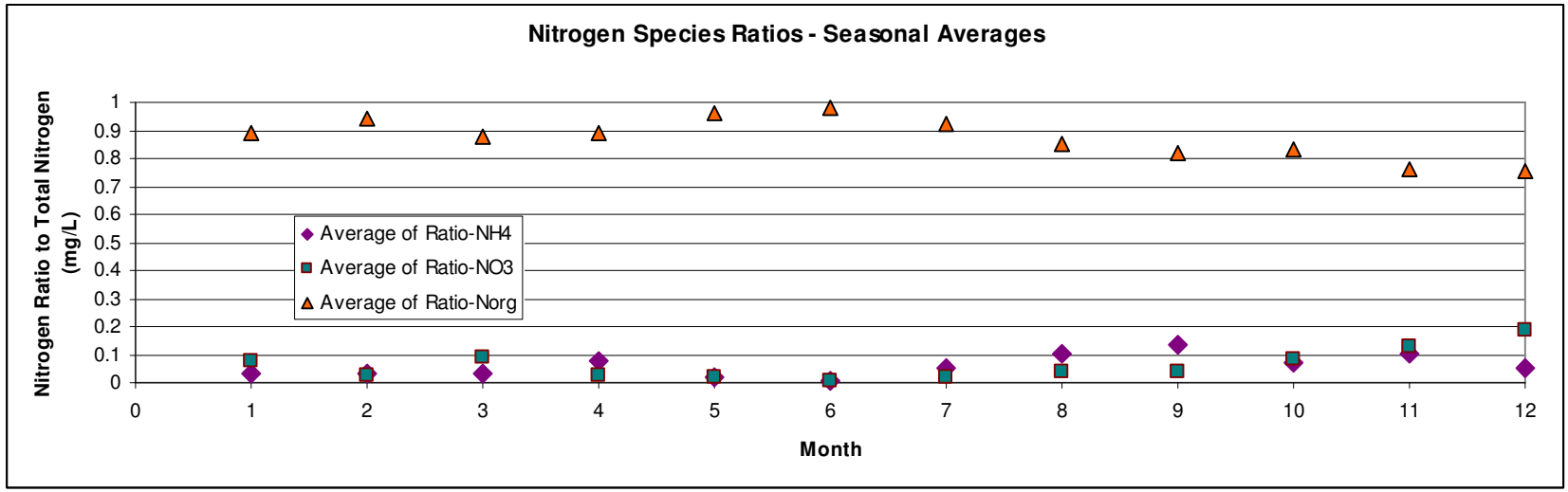

URS

Figure 3-26. ABMC Ratios for Total Nitrogen.

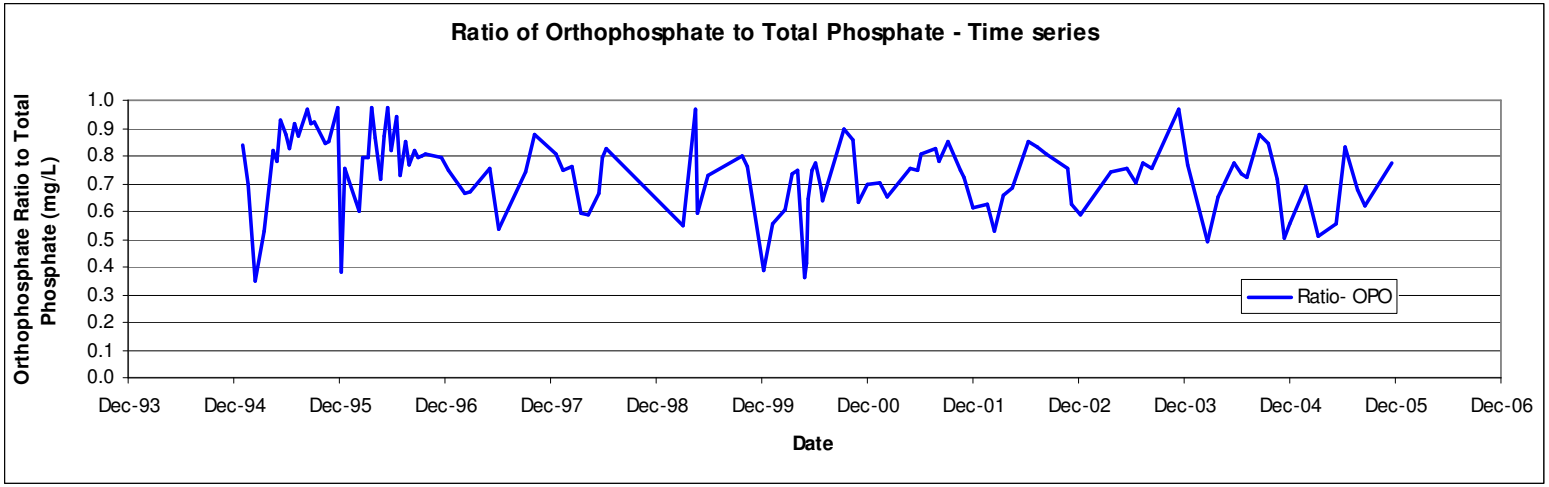

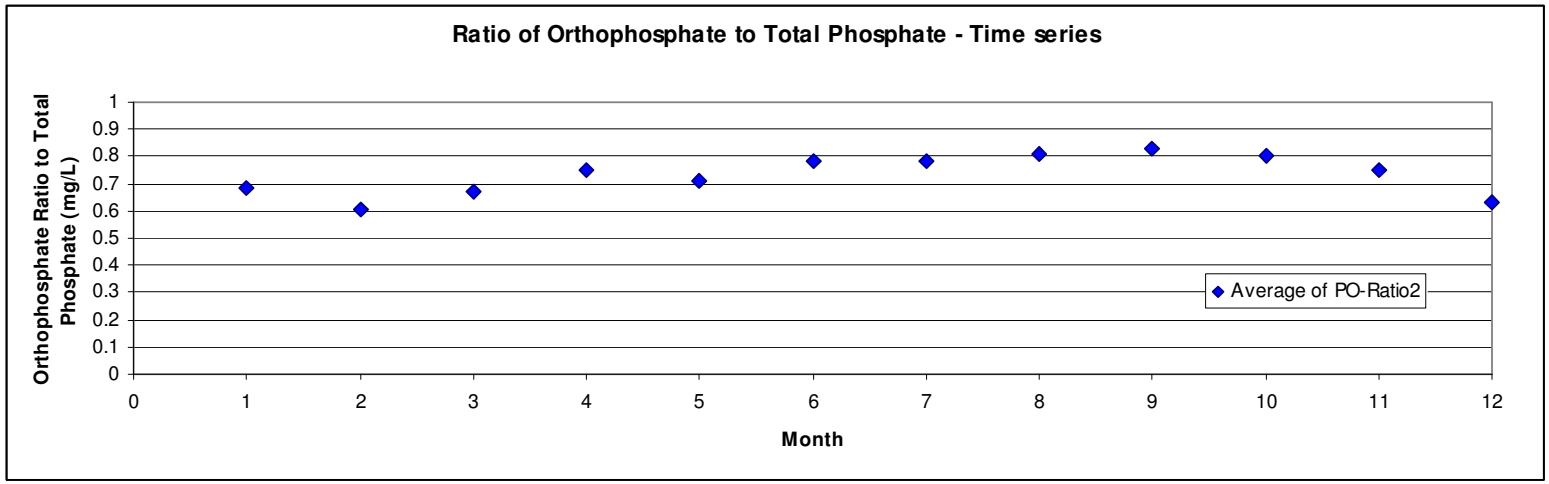

URS

Figure 3-27. ABMC Ratios for Total Phosphorus.

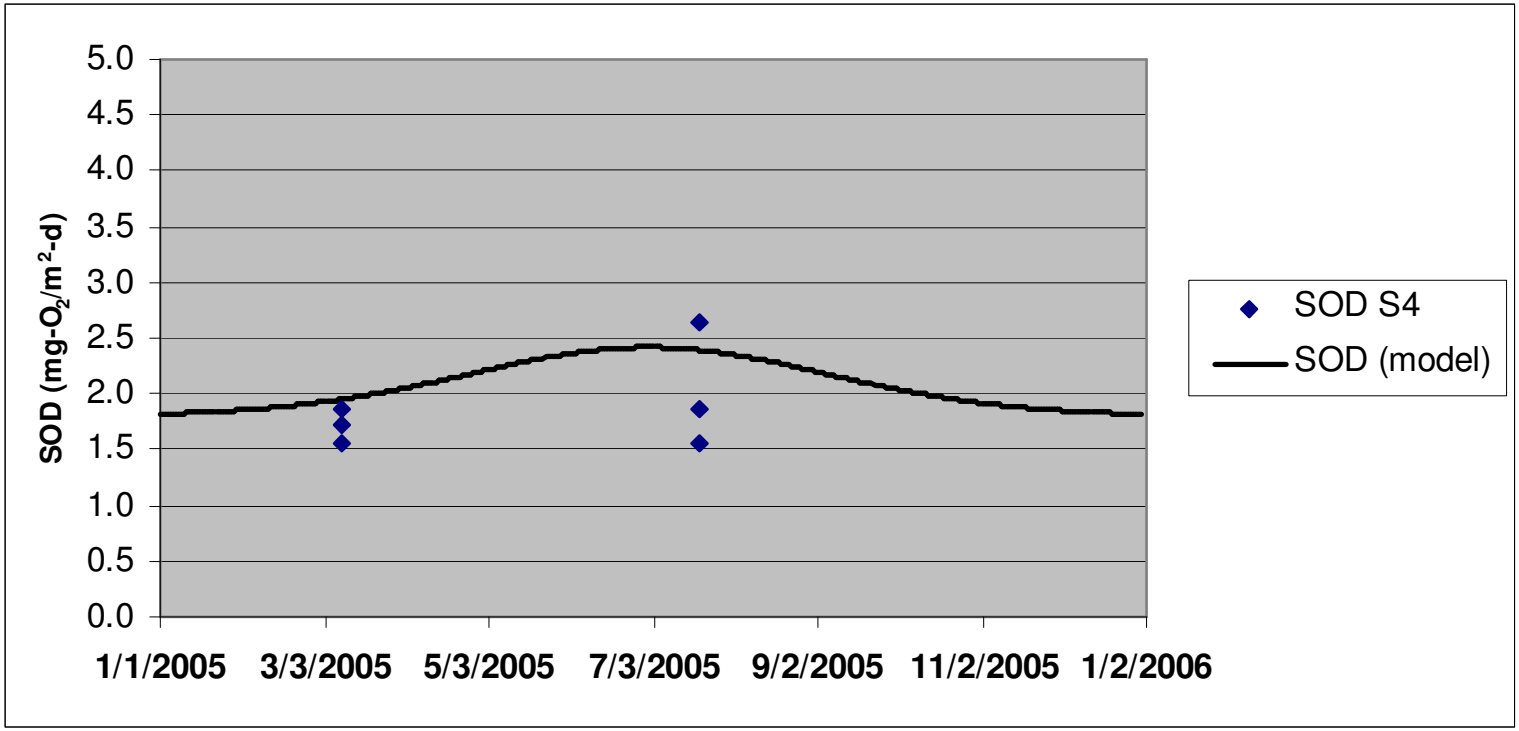

URS

Figure 3-28. Measured SOD and Model Fit to Data.

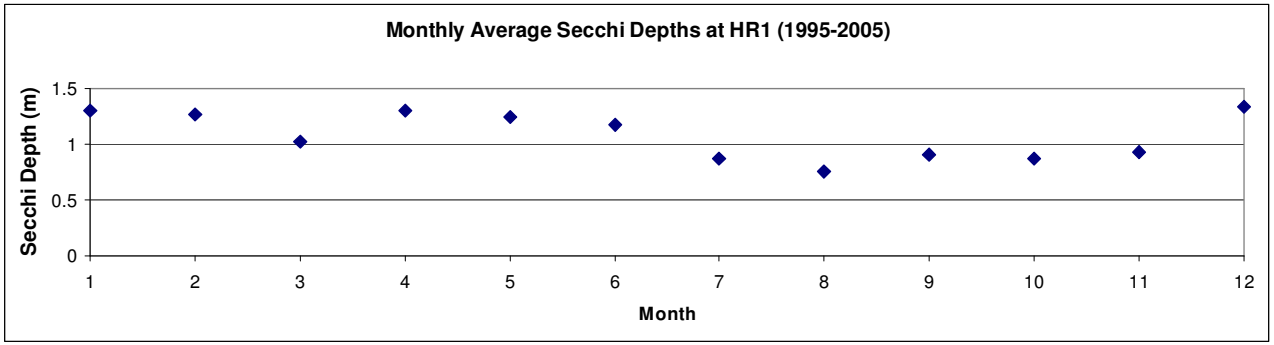

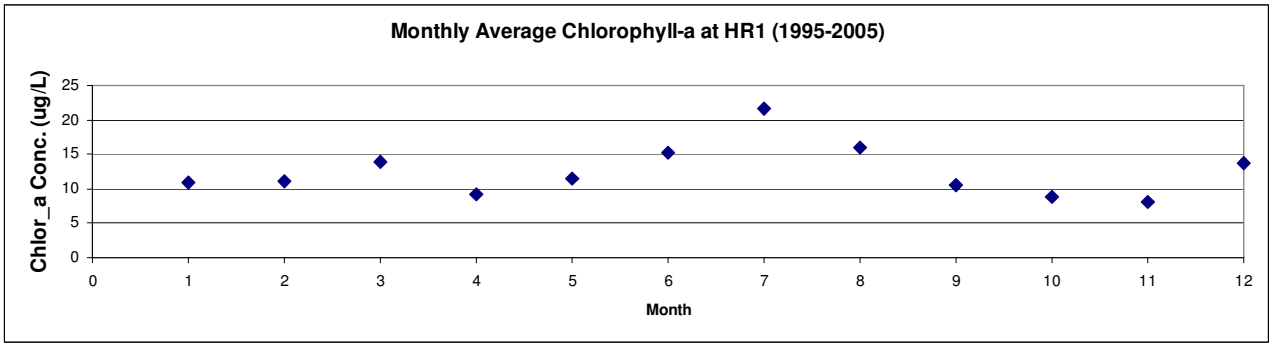

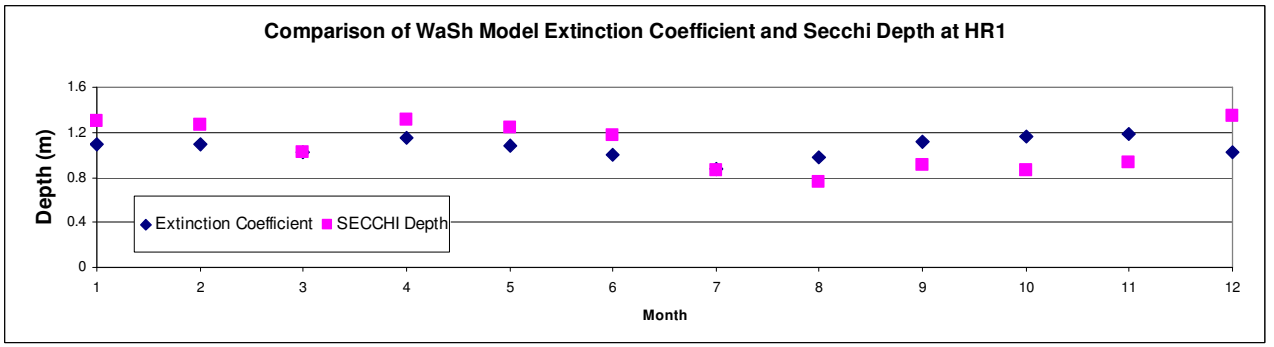

URS

Figure 3-29. Light Penetration configuration in the WaSh Model.

The calibration plan described in Section 3.0 consists of a 6-year calibration for the C-24, C-23 and C-44 basins to daily flow data and subsequent 5-year validation for the C-24 and C-23 basins. The calibration for the SLE consists of a 3-year calibration to monthly salinity data at the HR1 structure. The general approach for the calibration is to use a consistent set of model parameters for all four models, adjusting individual values for a basin only when the characteristics of a basin warranted the adjustment.

There are numerous sets of model parameters that need to be set for the model operation. The parameters are grouped into four categories:

- Hydrology parameters for infiltration, runoff and evapotranspiration
- Groundwater parameters for hydraulic conductivity and conductance
- Canal parameters for friction, pump rates and control structure operations
- Irrigation practices

In a previous model application to the SLE watershed, a system of model parameters were previously obtained via calibration (URS, 2001). Subsequent review of the calibration indicated that the predicted flows tended to over predict the period for which base flow occurred. During seasons with low rainfall, the model predicted continuous seepage into the primary canals and subsequent discharge through the structures. The measured data indicated that the seepage ceases sooner than the model predicted. Additional modeling analysis and calibration ensued to determine the causes for these anomalies (URS, 2003). The analysis indicated three potential causes for the over-prediction of the base flow conditions:

- Over-prediction of percolation
- Application of entire irrigation demand in a single day
- Use of weirs to represent gated structures

The current calibration effort was focused on improving the representation of base flow. The model parameters used in the initial calibration were adopted as initial values for calibration of the three structurally controlled basin models. Then, each of the three basins was calibrated and validated. When completed, the calibrated model parameters were applied to the SLE model and the calibration of the SLE model to the salinity data was completed.

4.1 HYDROLOGIC AND HYDRODYNAMIC CALIBRATION AND VALIDATION FOR THE C-23, C-24 AND C-44 BASIN MODELS

The model primary calibration for the C-23, C-24 and C-44 basins is based on a comparison of the simulated and measured flows at the basin outflow structures. The comparisons were made on time series, flow frequency curves and seasonal and annual variations. Quantitative metrics were applied to make comparisons between the calibration and validation, to ensure that the simulation of the validation period was within the same accuracy as the calibration period. A secondary calibration parameter was the amount of irrigation demand produced in the citrus land-use areas. There is no measured data to estimate the amount of irrigation demand, however, based on the results of previous modeling, and discussions with Dr. Y. Wan of the SFWMD, a target annual demand of 15 inches was adopted

The initial calibration focused on improving the representation of base flow and consisted of: decreasing the soil infiltration capacity so that the amount of water percolating to groundwater was reduced and the water discharging as interflow was increased.

- Modifying the irrigation module to allow for partial application of the predicted demand each day
- Replacing the weirs with gated structures and their operational criteria.

The primary parameters that were adjusted included the infiltration capacity, the interflow fraction and recession constant, the global ET parameter, the fraction of daily irrigation demand that is supplied and the gate operation criteria. The first three parameters control the amount of base flow and both direct and indirect surface runoff. They also help to reduce the period over which base flow continues to drain from the basins. Prior to the adjustment to the irrigation module, the application of the entire demand in one day would sometimes overwhelm the infiltration capacity of the soils creating unrealistic surface runoff during the dry season. The adjustment reduced the application rate and eliminated the spurious runoff events. The gate criteria affected the characteristics of the daily discharges from the outfall structures and also eliminated that artificial seepage flows over the weir crest that occurred when the outfall structures were represented with weirs. Finally, the global evapotranspiration parameter scales the daily potential evapotranspiration and affects the total annual discharge from each basin. This parameter was adjusted slightly during the calibration process because the adjustments made to each of the other parameters would alter the total discharge.

The calibration process consisted of iteratively adjusting the key model parameters in a succession of model simulations until good agreement between the measured and simulated flows was obtained. The process was applied simultaneously to all three structured basins (C-23, C-24 and C-44) so that the same model parameters are used in each basin model.

The landuse-dependent final model parameters are listed in Tables 4-1 through 4-4. The parameters were either set for each land use or for each basin, depending on their implementation. For instance, whereas the hydrology parameters are related to land-use, the irrigation practices vary from basin to basin and therefore the parameter values vary for each basin model. A detailed description of the function of each model parameter can be found in the WaSh model documentation (URS, 2005).

Table 4-1. WaSh Model Calibrated Hydrologic Parameters.

Parameter	Tree Crops	Pastureland and Others	Wetlands (short)*	Wetlands (long)*
CEPSC (in)	0.02	0.02	0.02	0.02
UZSN (in)	0.3	0.35	0.35	0.35
NSUR ($ft^{1/6}$)	0.4	0.4	0.4	0.4
INTFW (in)	0.0	0.0	0.0	0.0
LZETP	0.35	0.35	0.65	0.65
LZSN (in)	4.0	4.0	4.0	4.0
INFILT (in/hr)	0.12	0.12	0.02	0.02
LSUR (ft)	300.0	300.0	300.0	300.0

Parameter	Tree Crops	Pastureland and Others	Wetlands (short)*	Wetlands (long)*
BASETP	0.0	0.0	0.0	0.0
AGWETP	0.10	0.35	0.65	0.65

**short and long refer to the length of time the wetlands has standing water (short: < 6 months, long: > 6 months)*

Table 4-2. Calibrated Irrigation Demand Module Parameters applied to Citrus Land-use

Parameter	C-23	C-24	C-44
FLD_CAP (in/in)	0.25	0.25	0.25
WLT_PNT (in/in)	0.05	0.05	0.05
MIN_CAP (%)	60	60	60
Macro_Pore (in/in)	0.20	0.20	0.20
Micro_Pore (in/in)	0.05	0.05	0.05
ROOT_DPTH (in)	24.0	24.0	24.0
EFFICIENCY (%)	60	60	60
AZRI (%)	90	90	90

Table 4-3. Calibrated Irrigation Supply and Application Model Parameters

Parameter	C_23	C_24	C_44
Canal Source	70 %	70 %	70 %
Shallow Aquifer Source	0	0	0
External Source	30%	30%	30%
Spray Application	50%	50%	50%
Upper Moisture Zone Application	50%	50%	50%
Lower Moisture Zone Application	0%	0%	0%

Table 4-4. Calibrated Tertiary Canal Properties for each Land-use

Land-use	Depth (ft)	Width (ft)	Critical Water Depth for Pumping (ft)	Pumping Rate (inches/day)	Conductance (ft/day)
Tree Crops	10	6	3	0.55	0.05
Pasture	8	4	2	0.45	0.05

Land-use	Depth (ft)	Width (ft)	Critical Water Depth for Pumping (ft)	Pumping Rate (inches/day)	Conductance (ft/day)
Wetlands	4	2	1	0.15	0.05
Urban	15	6	3	0.57	0.05
All Others	4	2	1	0.40	0.05

The final global evapotranspiration parameters for each basin are 0.65 for the C-24 basin model, 0.85 for the C-23 basins model and 0.89 for the C-44 basin model. The value for the C-24 basin is significantly lower for the C-24 basin because the average annual discharge for that basin, which is based solely on measured data, is significantly higher than the discharge for the C-23 and C-44 basins. An attempt to understand the higher discharges in the C-24 basin as differences in annual rainfall, irrigation practices, inter-basin transfers and other basin management practices was made, but no explanation could be ascertained. Therefore, the difference in discharge was accepted as indeterminate at this time and realized in the C-24 basin model by using a different global evapotranspiration parameter.

The results of the final flow calibration are shown in Figures 4.1 through 4.3. The time series data indicate a reasonable simulation of daily flow patterns with flows from isolated rainfall events as well as continuous flows developing during the wet seasons when rainfall events occur more often.

The flow distribution curves indicate that the distribution of daily flow is well represented, especially the relatively large number of days with zero flow. The shape of the distribution in the region where the daily flow distribution goes to zero is sensitive to the gate operation criteria. The annual variations and the seasonal patterns in total discharges are also well represented. The comparisons for the C-44 basin simulation were not as good as those for the C24 and C23 basins and are likely due to the influence of the Lake on the measured data.

The results of the model validation are shown in Figures 4.4 and 4.5 for the C-23 and C-24 basin models. In general they have similar characteristics to the calibration results. As the purpose of the model validation is to show that the calibration is robust and applicable to other conditions, a quantitative assessment of the calibration and validation were made. For the time series data, the root-mean-square (RMS) error and the Pearson Correlation Coefficient were calculated from the time series data. Also, the 25^{th}, 50^{th}, 75^{th} and mean flows are compared for each basin. The results of the quantitative assessment are summarized in Table 4-5 and 4-6 for the C-2, C-24and C-44 basin models for the calibration and validation periods.

The percentiles and means for the C-23 and C-24 basin compared well. Most notably, for the 50^{th} and 25^{th} percentile flows, the simulated results matched the large number of zero-flow days indicated in the measured data. The error in the 75^{th} percentile and mean flow values for the calibration period ranged from 1 to 13 % and for the validation period, they ranged from 1 to 20 %. The largest error in the mean value was for the C-44 basin and is 27%. Again, this result is likely due to the influence of the Lake on the measured data.

The RMS errors for the flow time series were in the range of 300 to 400 cfs. These values are above the mean flows for each basin. However, as most of the flows are near zero for a large percentage of the time, a better scale for evaluating the RMS error is the range of daily flows. A review of the flow frequency diagrams in Figures 4-1, 4-2 and 4-3, the range of the daily flows for the 40 or 50% time when the flow is non-zero, is about 2000 cfs. Thus, using 2000 cfs and the full range, the RMS errors for each basin are about 15% of the full range.

The Pearson Correlation Coefficients range between 0.67 and 0.73 for the C-23 and C-24 basins, indicating a moderately strong correlation. These values are likely indicative of the model representing the strong wet/dry seasonal patterns in the flow data.

Generally, the errors between the measured and simulated results for the validation were similar to those obtained for the calibration period, indicating that the model calibration is robust and reliable.

Table 4-5. Frequency Metrics of Calibration and Validation for Flow in Upland Basins.

	C24				C23				C44			
	Calibration		Validation		Calibration		Validation		Calibration		Validation	
Metric	Measured	Simulated	Measured	Simulated	Measured	Simulated	Measured	Simulated	Measured	Simulated	Measured	Simulated
75 Percentile	381.01	342.73	417.49	383.38	147.9	128.0	299.7	238..5	230.00	218.8	-	-
50 Percentile	0.00	0.00	0.14	171.10	0.0	2.2	0.0	2.6	35.00	0.00	-	-
25 Percentile	0.00	0.00	0.00	0.00	0.0	0.8	0.0	0.7	0.00	0.00	-	-
Mean	220.29	234.34	278.76	275.63	173.7	172.1	237.6	205.3	202.81	164.10	-	-

Table 4-6. Time Series Metrics of Calibration and Validation for Flow in Upland Basins.

	C-23		C-24		C-44	
Metric	**Calibration**	**Validation**	**Calibration**	**Validation**	**Calibration**	**Validation**
RMS	307.37	297.88	323.53	319.51	456.58	-
PCC	0.73	0.68	0.67	0.67	0.38	-

The water budgets for each calibrated and validated basin are summarized in Table 4-7. These budgets are based the combined calibration and validation simulation periods

Table 4-7. Annual Average Water Budgets for the C-23, C-24 and C-44 Basin Models.

Basin	Rainfall (inches)	Evapo-transpiration (inches)	Irrigation Demand (inches)	External Irrigation Supply (inches)	Surface Discharge (inches)	Groundwater Discharge (inches)
C-23	50.1	35.1	4.6	1.5	13.4	4.92
C-24	54.6	29.4	2.6	0.73	21.7	5.0
C-44	53.6	40.0	5.1	2.2	14.9	2.2

The irrigation demand values reported in the table are based on the entire basin acreage, and have values lower than the targeted value of 15 inches. The 15 inch target applies to only the irrigated portion of the basin.

4.2 HYDROLOGIC AND HYDRODYNAMIC CALIBRATION OF THE SLE MODEL

The SLE model was calibrated using salinity data because no flow data was available in the estuary or in rivers and canals in the upland portions of the basins. The period for the calibration is 2002-2005, with a spin-up period for 2001. The calibration period was chosen based on the availability of the salinity data used as boundary conditions at the downstream end of the SLE model.

The SLE model was configured using the conservative tracer option to represent salinity transport. The approach for calibration is shown in Figure 4.6. At the western ends of the SLE model, the calibrated C-23 and C-24 basin models daily output flows were used as point source inputs to the SLE model at their discharge points. The associated salinity values were set to zero for the input flows, representing the freshwater discharges in the C-24 and C-23 basins. The C-44 basins model was executed with the Lake Okeechobee discharges through the S308 structure were included, with zero salinity assigned for the tracer value to represent zero salinity. The output from the C-44 model was then used as input to the SLE model, again with zero salinity for the tracer value. The SLE model was configured with runoff concentrations of zero, to represent the freshwater discharges from the basin. In this configuration, the SLE model simulated the salinity transport in the estuary, subject to tidal flows, freshwater discharges from the C-23, C-24 , and C-44 (including Lake Okeechobee) , and freshwater discharges from the land included in the SLE model.

The SLE model was calibrated by adjusting the lateral mixing in the estuary portion of the model. Consecutive model runs were made, and the mixing coefficient adjusted, until a reasonable agreement with the measured salinity data at the HR1 was obtained. The final calibration is shown in Figure 4.7. The results were obtained using a mixing coefficient of 200 ft^2/s in the estuary. This value is well within the range of typical dispersion values in estuaries (Fischer, et al., 1979).

The water budget for each basin draining directly into the SLE based on the calibrated model simulation is shown in Table 4-8.

Table 4-8. Annual Average Water Budgets Basins Draining Directly into the SLE.

Basin	Rainfall (inches)	Evapo-transpiration (inches)	Irrigation Demand (inches)	External Irrigation Supply (inches)	Surface Discharge (inches)	Groundwater Discharge (inches)
North Fork	51.1	31.57	2.42	0.68	16.31	5.6
South Fork	51.1	31.04	7.08	1.42	19.75	7.33
Bessey (B4/5)	51.1	29.25	0	0	16.93	4.93
Danforth (B-6)	51.1	29.51	0.53	0.18	17.21	4.92

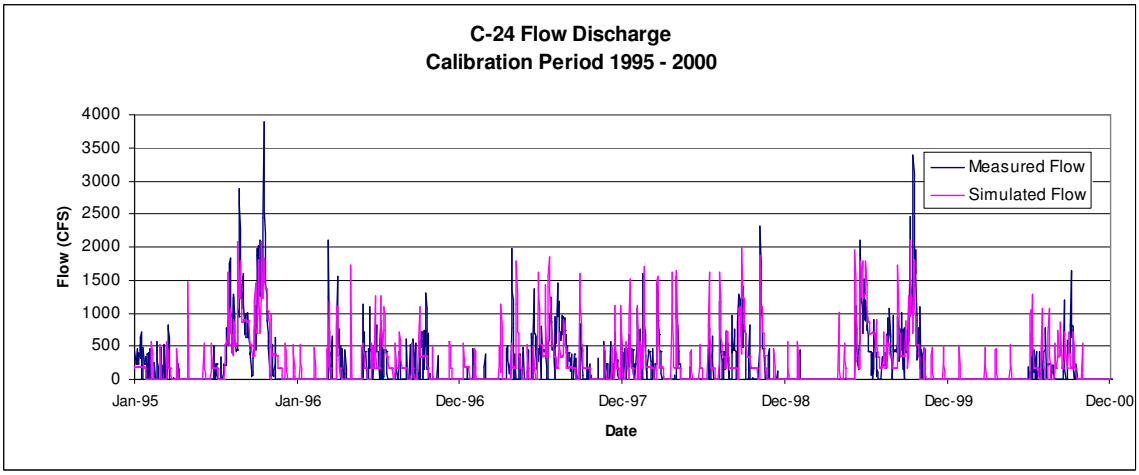

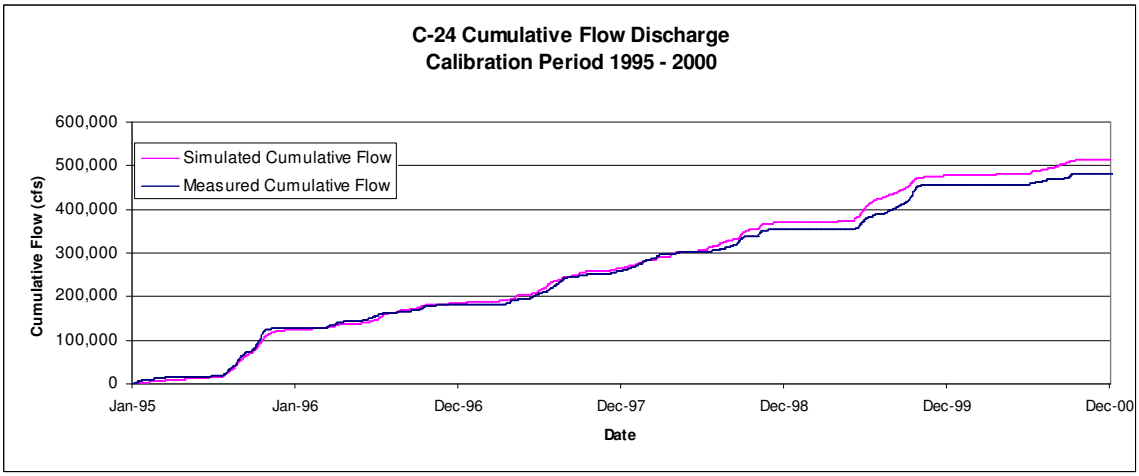

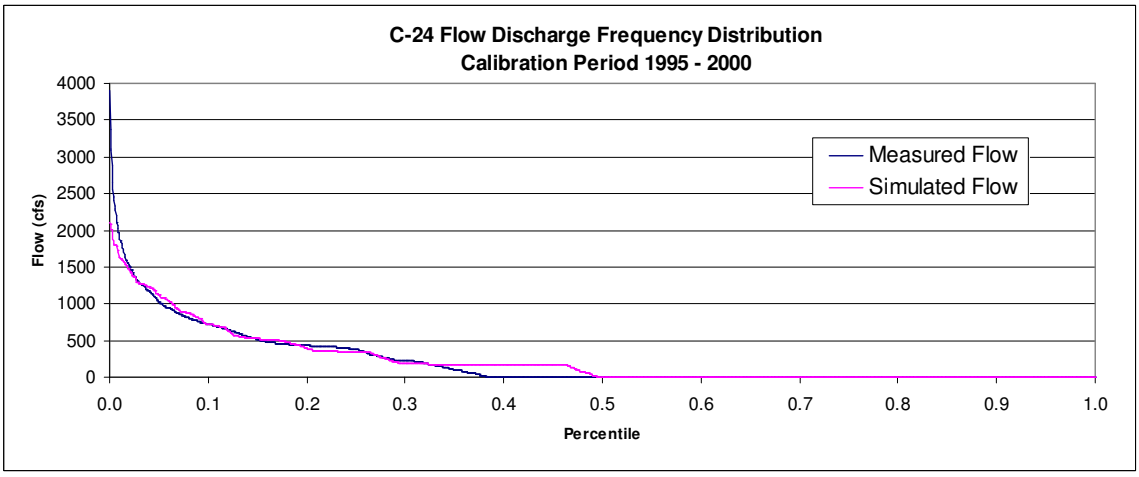

URS

Figure 4-1. Hydrodynamic Calibration for C-24 Basin.

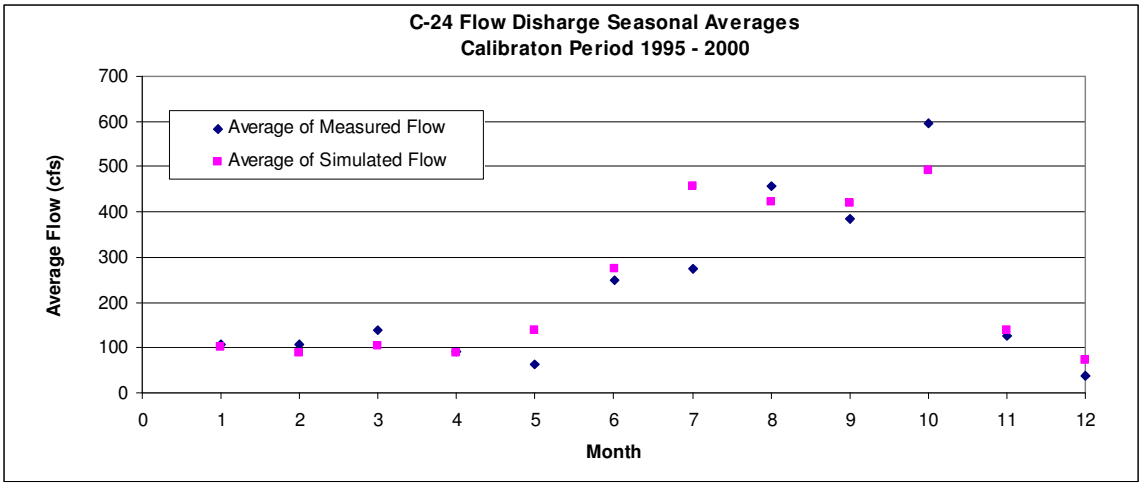

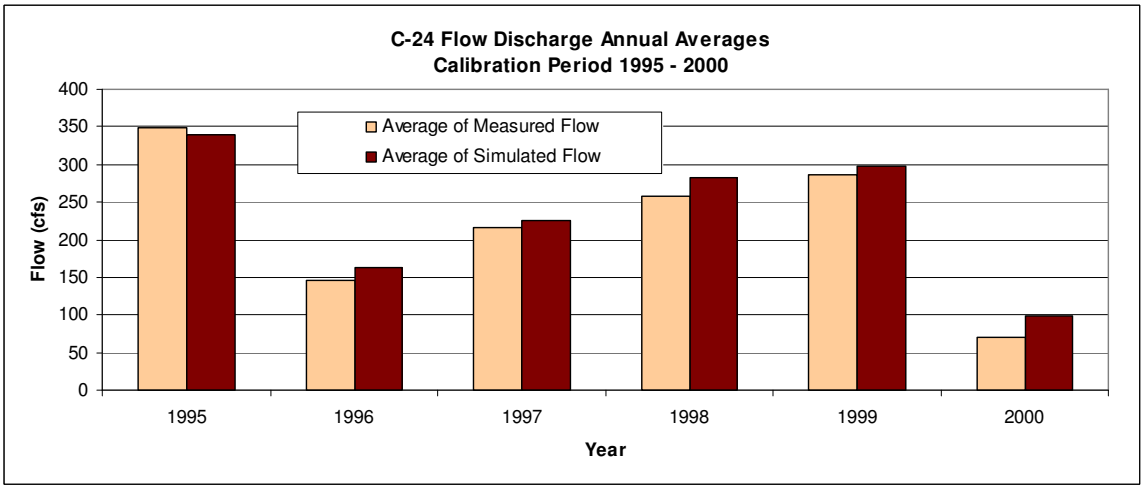

Figure 4-1. Hydrodynamic Calibration for C-24 Basin (cont'd).

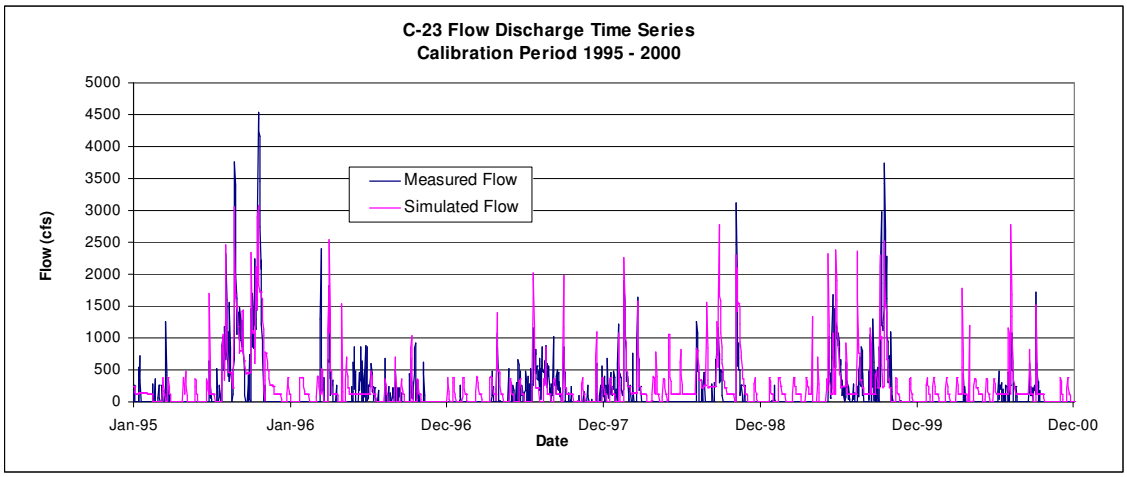

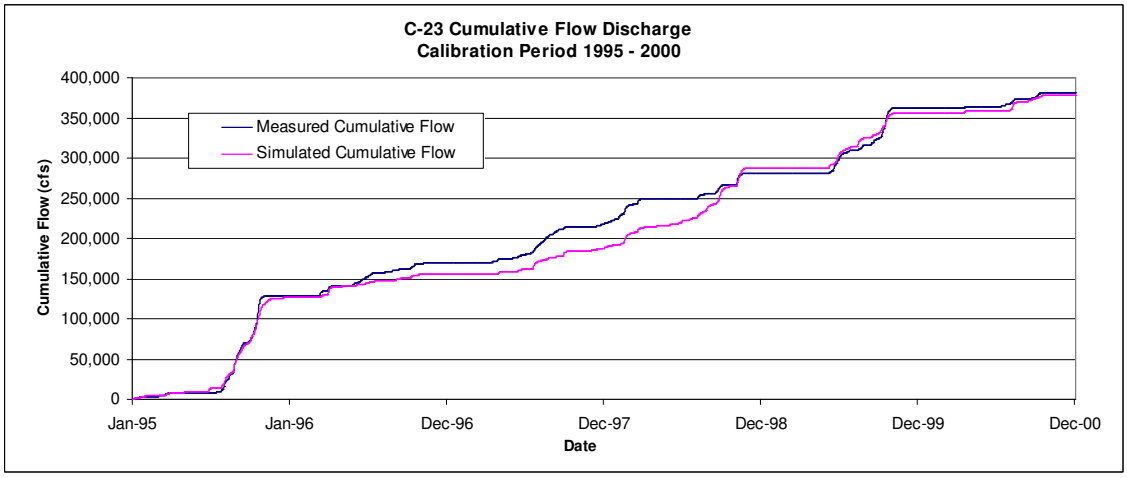

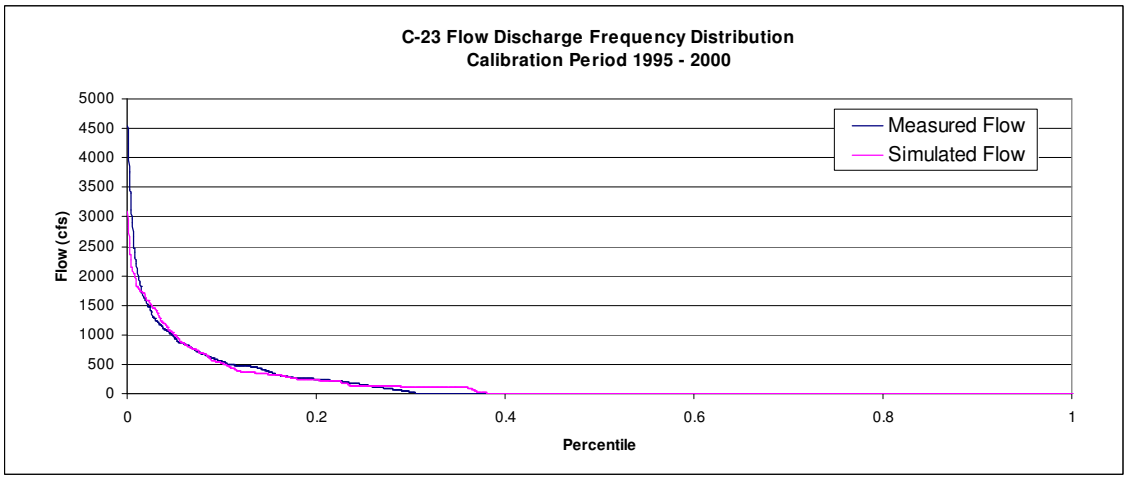

URS

Figure 4-2. Hydrodynamic Calibration for C-23 Basin.

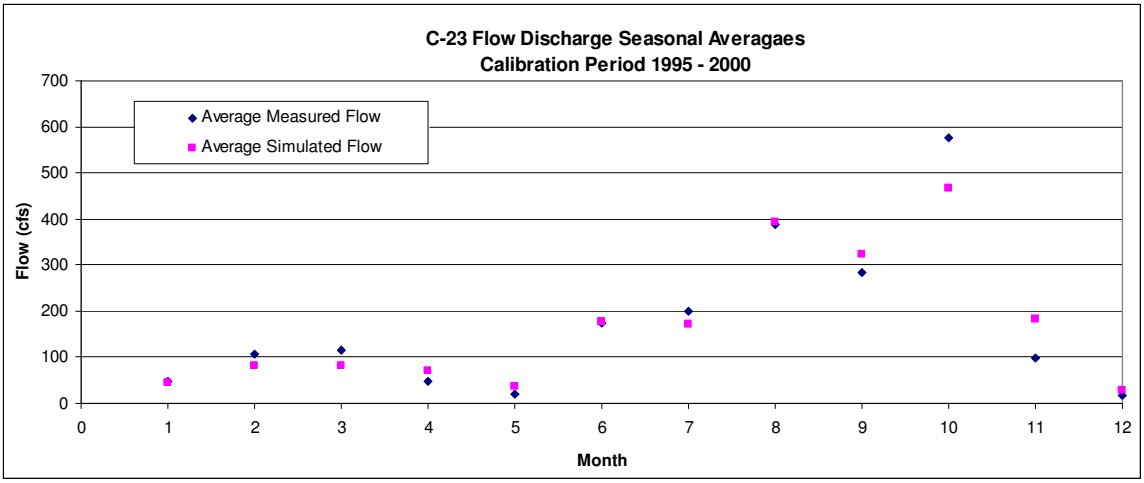

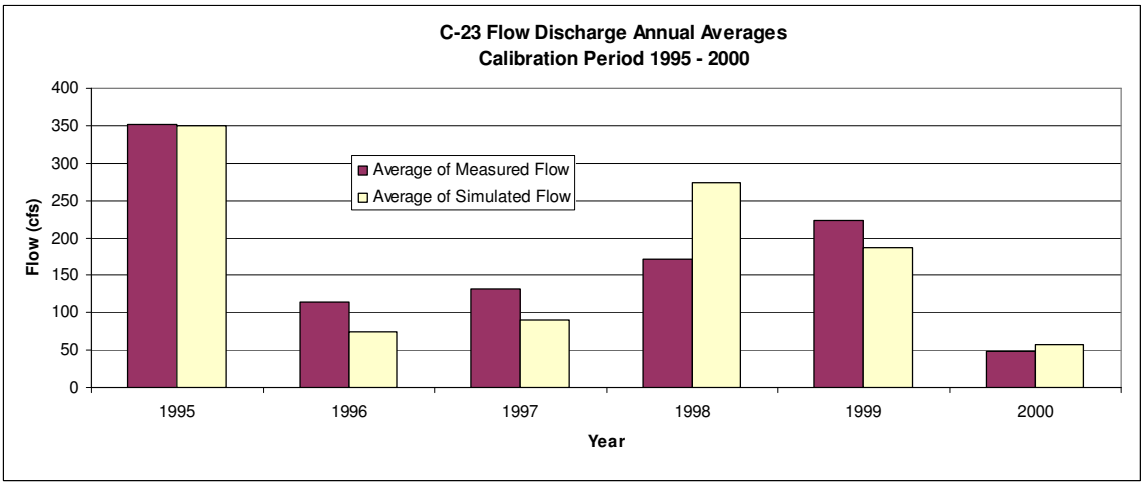

Figure 4-2. Hydrodynamic Calibration for C-23 Basin. (cont'd)

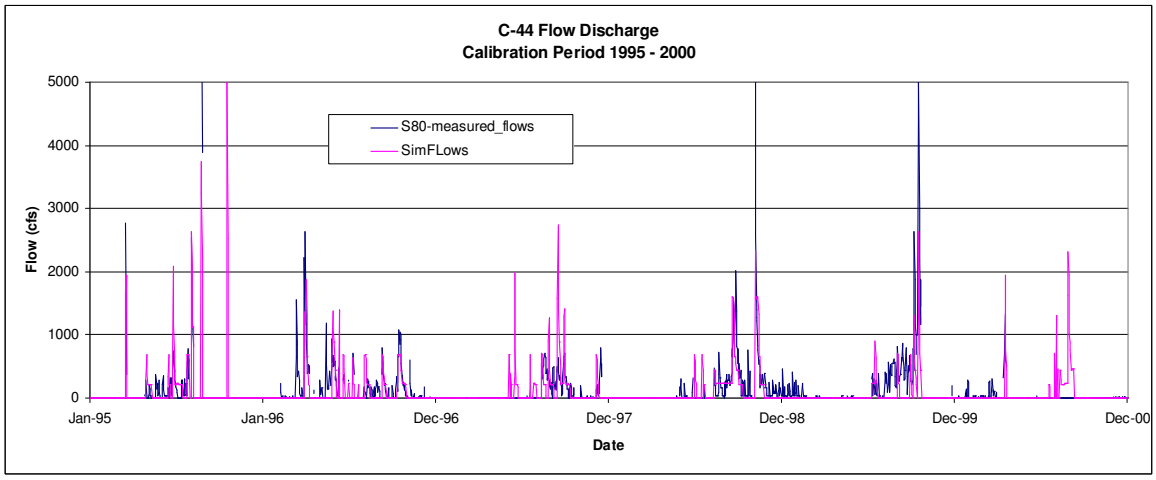

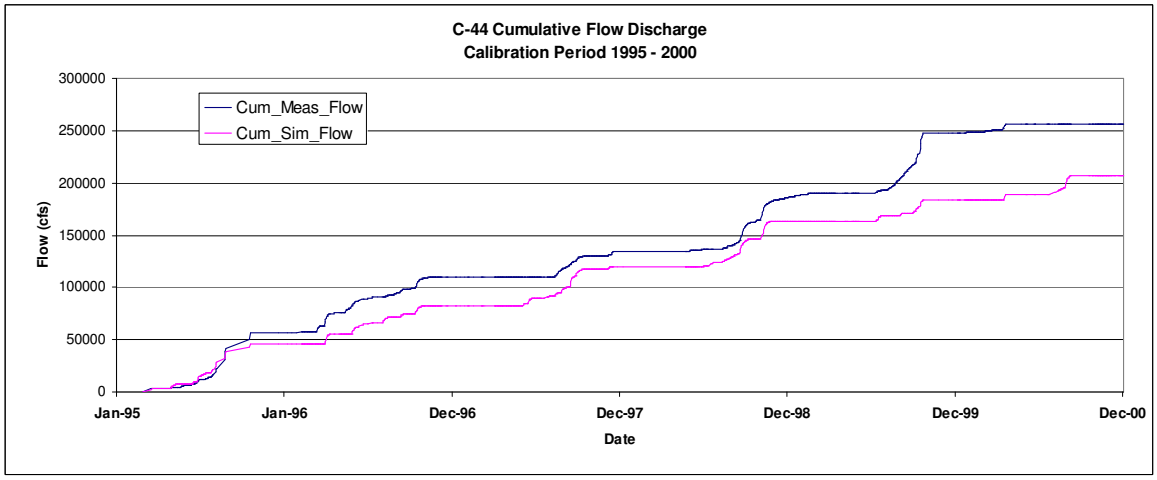

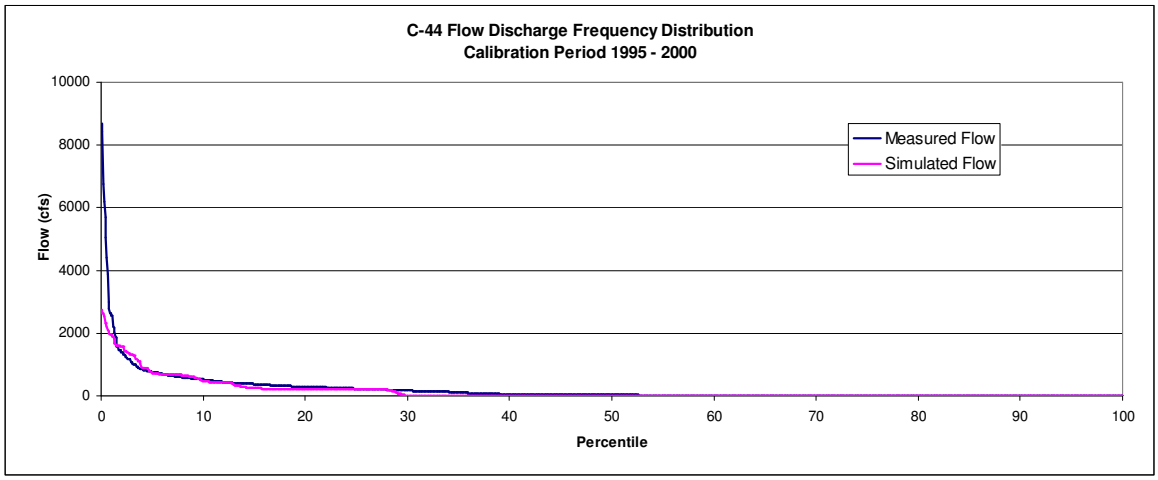

URS

Figure 4-3. Hydrodynamic Calibration for C-44 Basin.

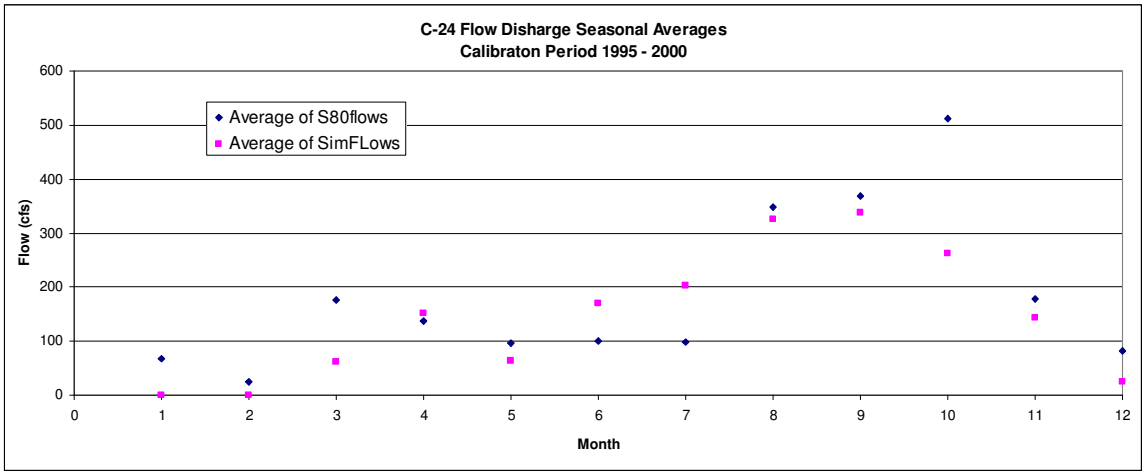

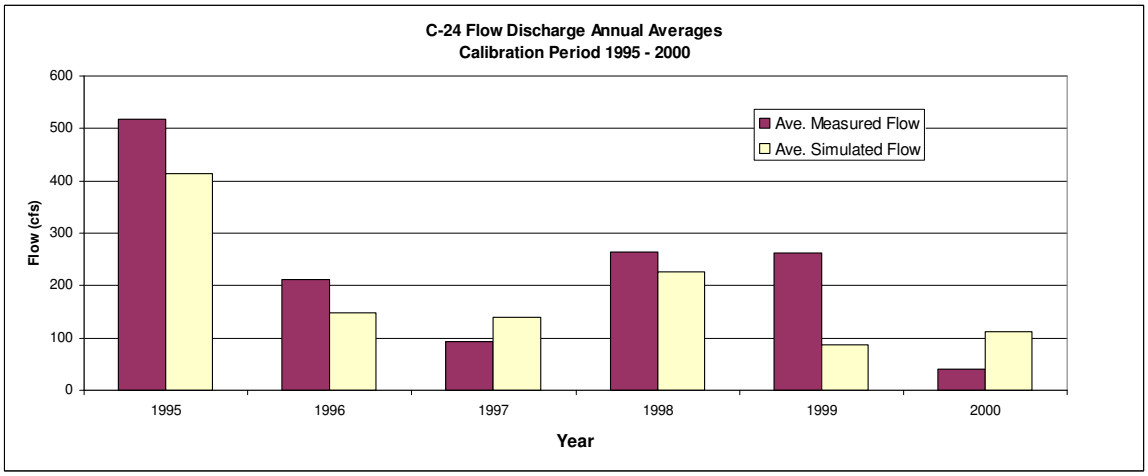

URS

Figure 4-3. Hydrodynamic Calibration for C-44 Basin. (cont'd)

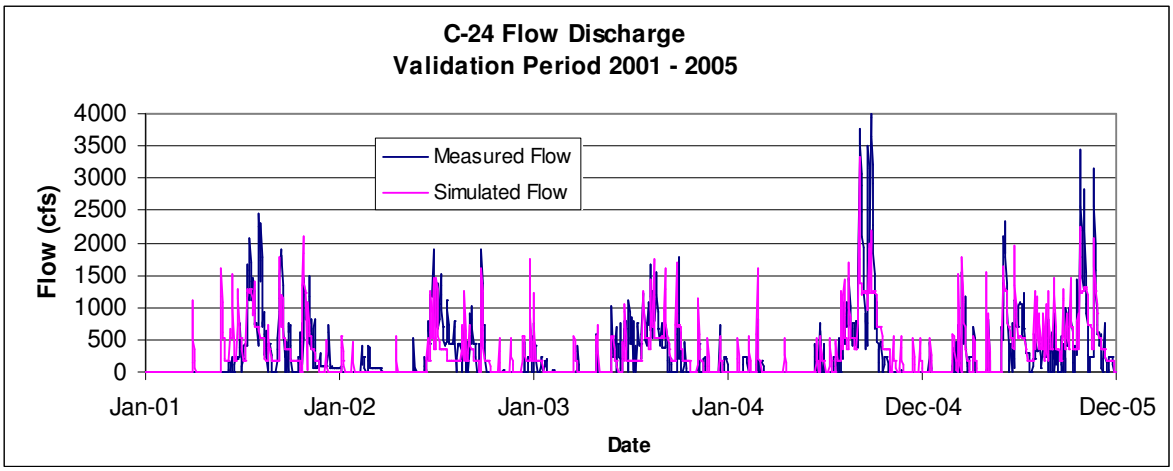

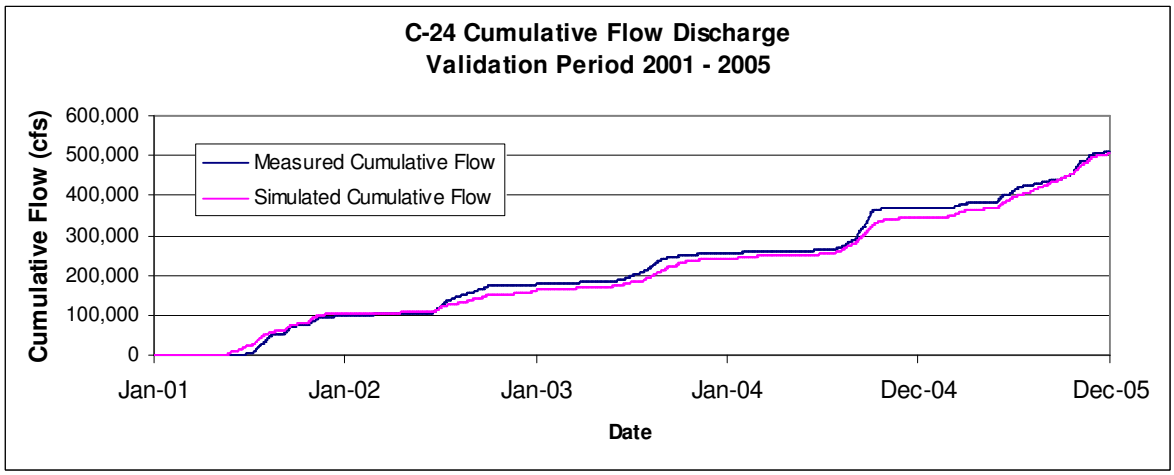

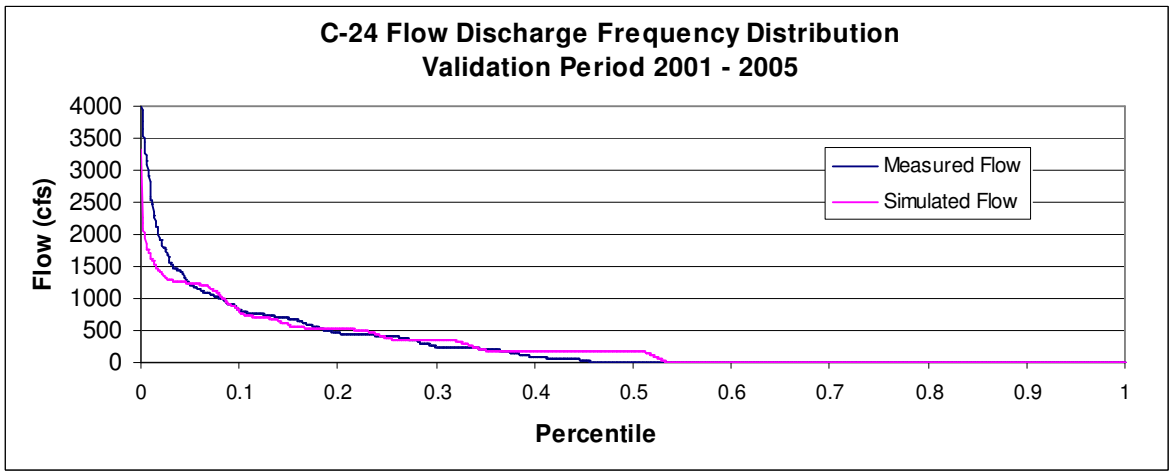

URS

Figure 4-4. Hydrodynamic Validation for C-24 Basin.

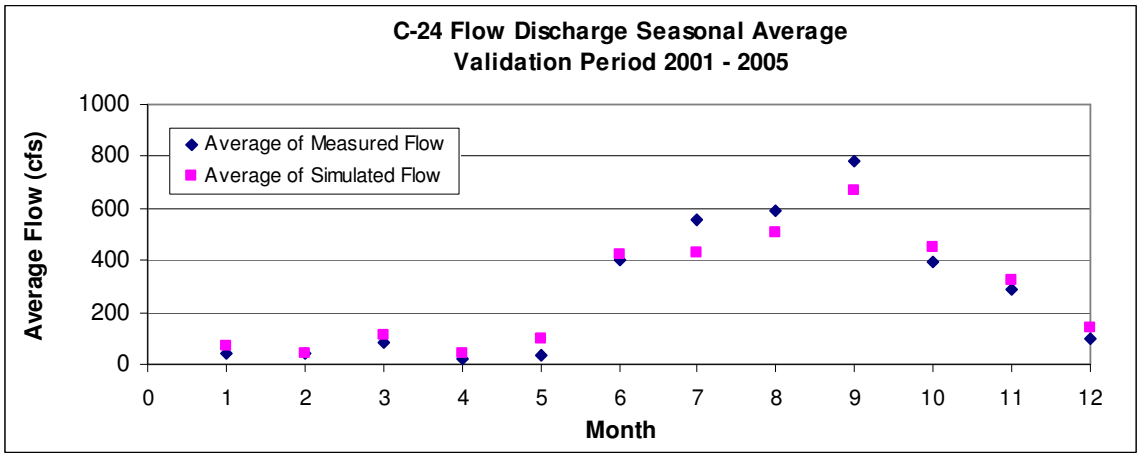

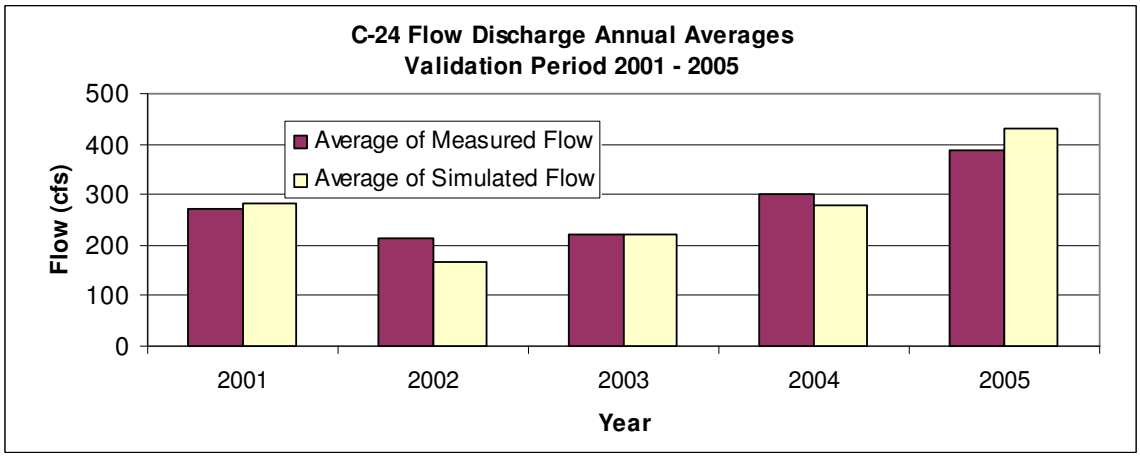

Figure 4-4. Hydrodynamic Validation for C-24 Basin. (cont'd)

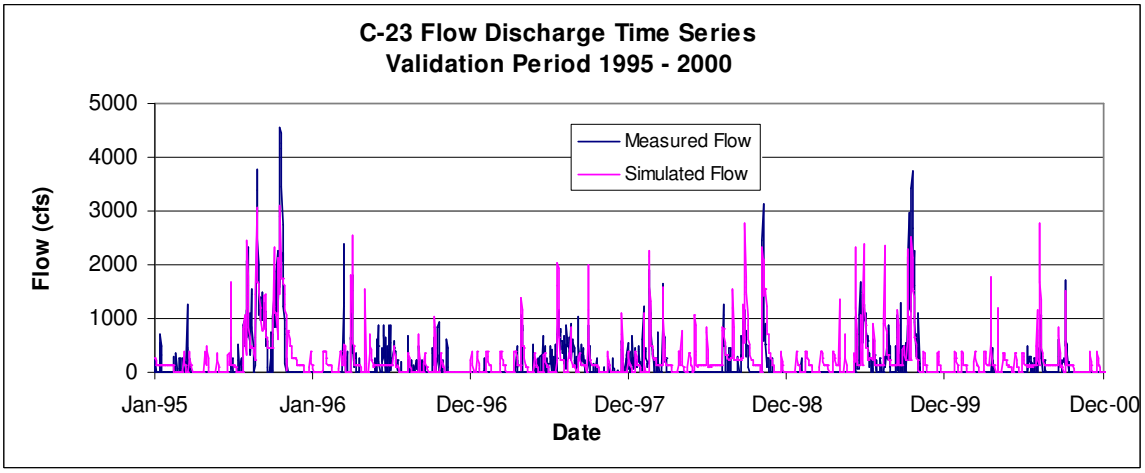

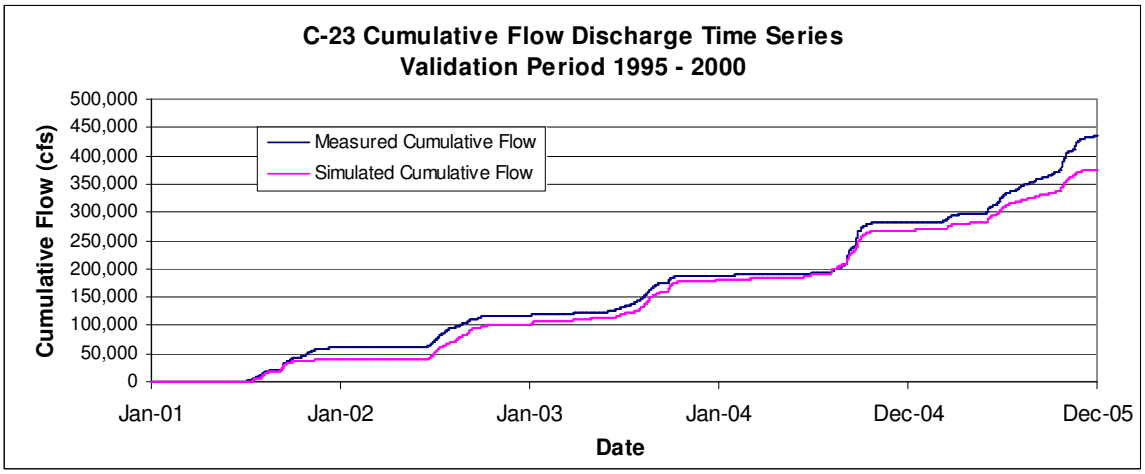

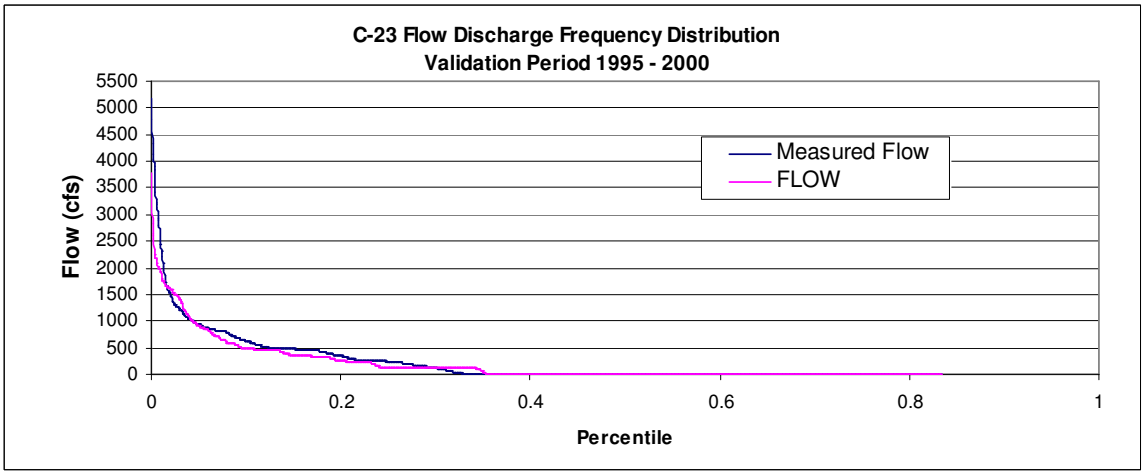

URS

Figure 4-5. Hydrodynamic Validation for C-23 Basin.

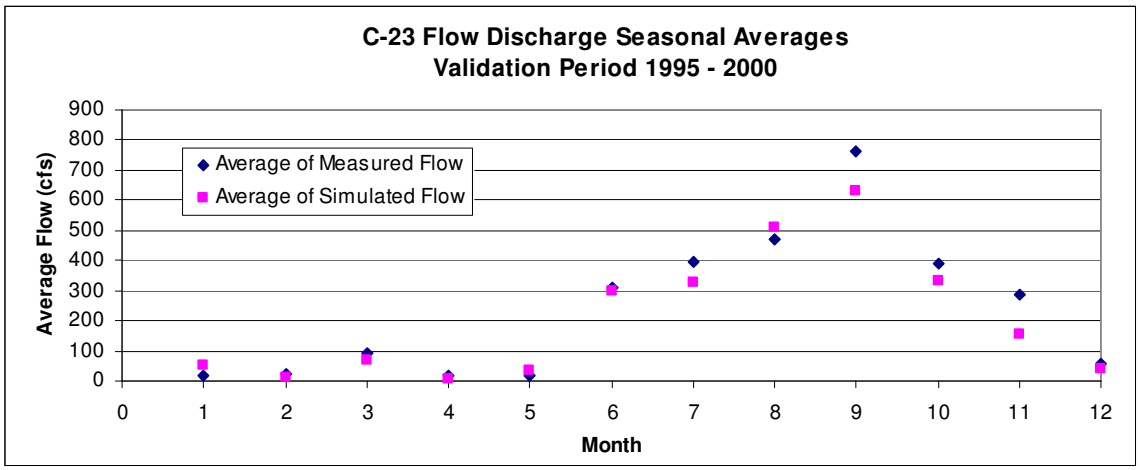

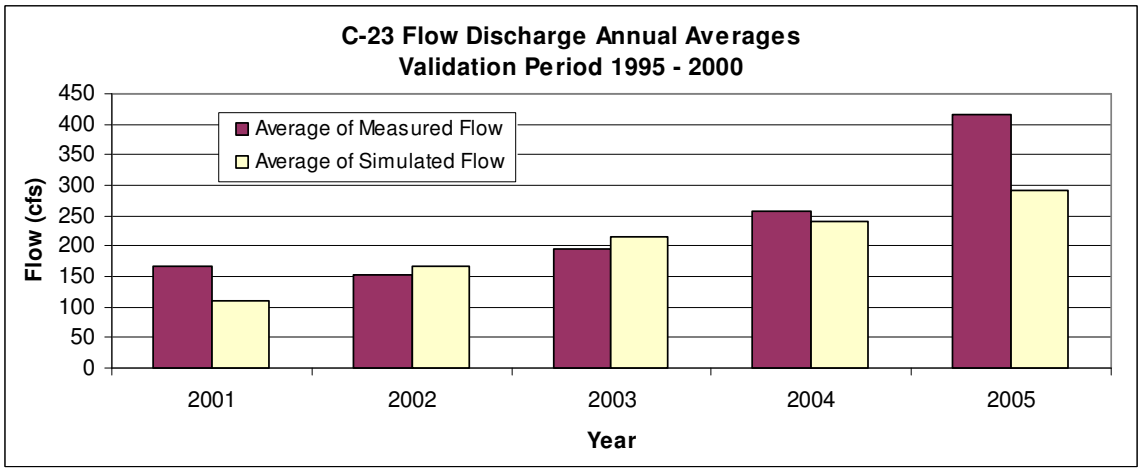

Figure 4-5. Hydrodynamic Validation for C-23 Basin. (cont'd)

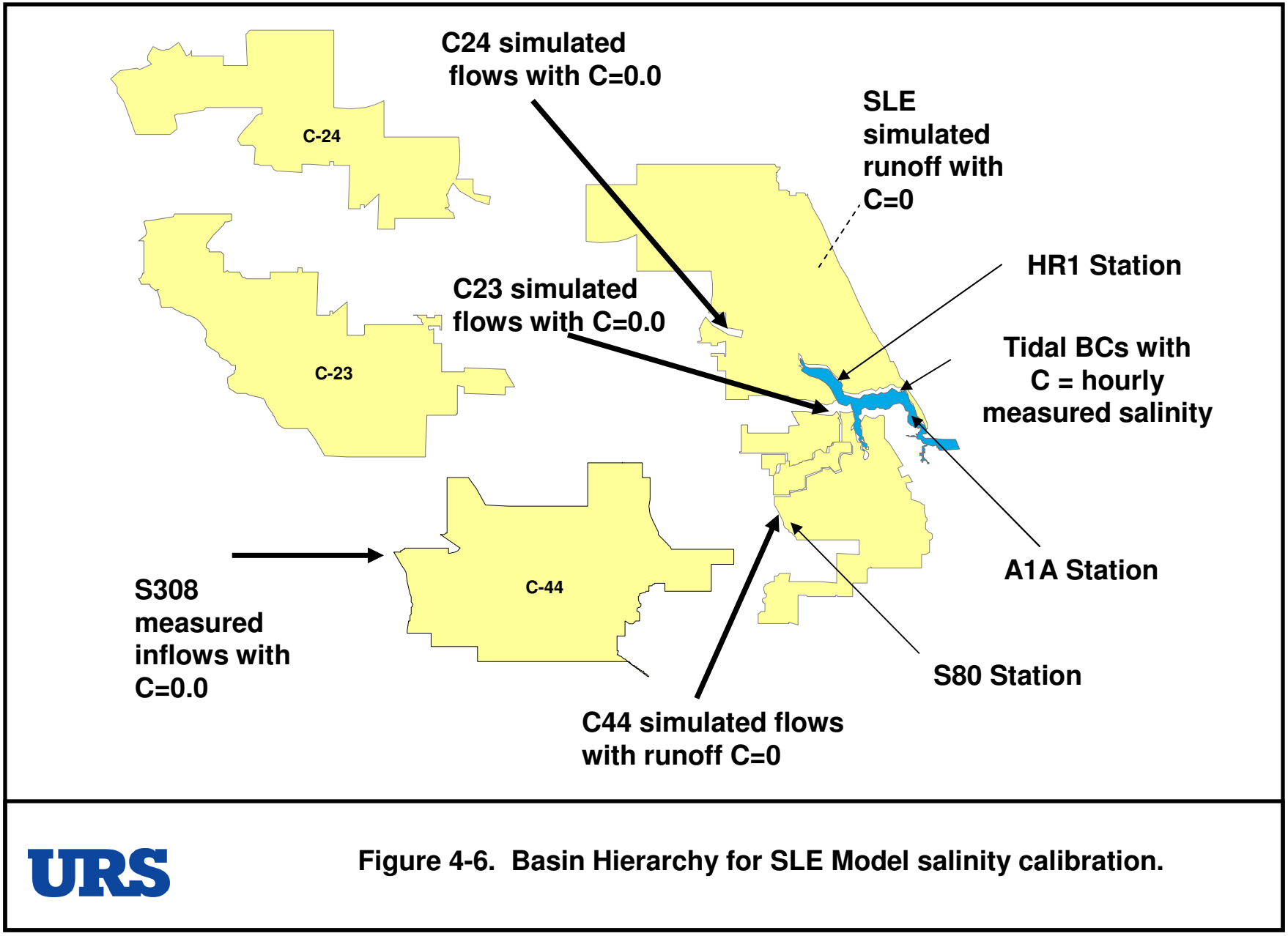

URS

Figure 4-6. Basin Hierarchy for SLE Model salinity calibration.

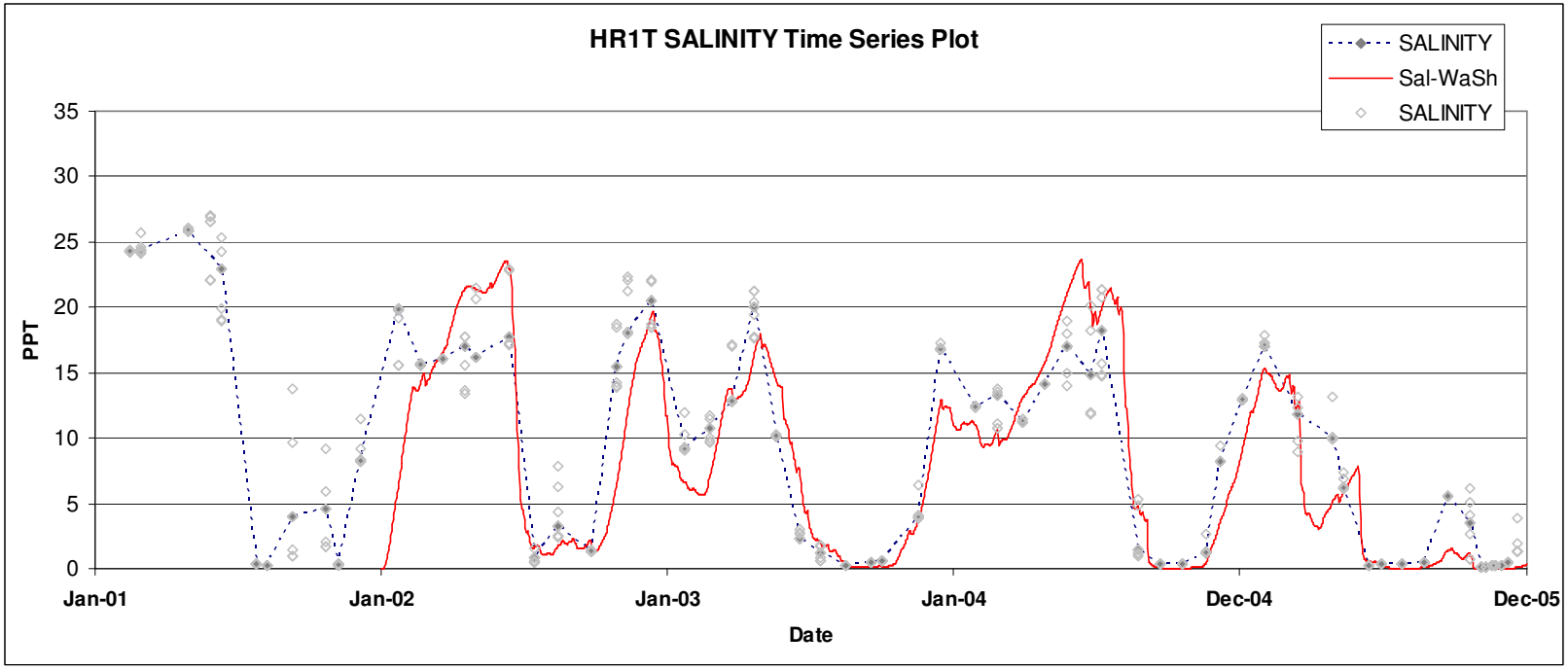

URS

Figure 4-7. Salinity Calibration for the SLE Model.

The calibration plan described in Section 3.0 consists of a six-year calibration for the C-24, C-23 and C-44 basins to daily flow data and subsequent five-year validation for the C-24 and C-23 basins. The calibration for the SLE consists of a six-year calibration and a five-year validation. The SLE basin model was configured with two layers in the canals, rivers and streams to simulate the upper and lower layer dissolved oxygen and therefore the calibration for the SLE basin model involves both an upper and lower layer for D.O.

Note that the water quality calibration for C-23 uses Station S48, instead of S97. Water quality data for S97 was intermittent for 1995-1999. S48 had a complete data set for the entire calibration/validation period.

The general plan for the calibration is to use a consistent set of model parameters for all four models, adjusting individual values for a basin only when the characteristics of a basin warranted the adjustment.

There are numerous sets of model parameters that need to be set for the model operation. These parameters have been grouped into three categories:

- Global adjustments to the runoff concentration estimates
- Dissolved Oxygen cycle coefficient values (phytoplankton and nutrients)
- Re-aeration and SOD coefficient

The areal-based loading rates developed in Section 3.10 are an approximation to the actual loads that occur in each basin. They represent the best estimate of runoff concentrations available for the basins. As is typical in water quality data sets, the data do not provide complete coverage of the basin and assumptions need to be made to apply the values to areas in the basin that are not covered by the measurements. As described in Section 3.9.1, the land use has been used to distribute runoff concentrations to the areas without measurements. However, due to the high degree of variability in the ABMC data, and the potential limitations in applying the land-use based approach for distributing the ABMC values, it is possible that the nutrient loads occurring in the model will not necessarily be consistent with in-situ measurements in the primary canals and SLE. Therefore, the initially applied ABMC values are viewed as initial estimate of the loads, and 'global' adjustments to the runoff concentrations were considered. In order to implement the adjustments, a simulation was made for each basin model with the water quality module disabled. These simulations essentially routed the nutrients from the runoff through the canals and estuary and allowed for a direct comparison with the measured nutrient levels. Then, for each basin the ABMC values were scaled up or down independently for each basin so that the model simulations reproduced the measured nutrient levels in each basin. After the initial global adjustments to the runoff loading coefficient, the calibration was continued and consisted of iteratively adjusting the key model parameters in a succession of model simulations until good agreement between the measured and simulated concentrations was obtained.

The primary calibration procedure applied during each iteration proceeded as follows: the mineralization rate was set so that the simulated ratios of inorganic and organic nitrogen and inorganic and organic phosphorus agreed with the measured data, then the de-nitrification rate was adjusted so that the simulated ratio of ammonia and nitrate agreed with measured data. Next, the maximum growth rate and the death rate of phytoplankton were set so that the simulated chlorophyll agreed with the measured values. Finally, the de-oxygenation rate

was set so that the simulated CBOD and DO were calibrated. For DO, adjustments to the re-aeration coefficient were also made during the calibration process, but the SOD was set based on measured data.

The process was applied simultaneously to all three structured basins (C-23, C-24 and C-44) so that the same model parameters for D.O. and nutrients are used in each basin model. When sufficient agreement was found, the output flows and water quality loads from the upland basins were used as input to the SLE model. For the SLE simulations, the C-44 basin model was configured to include the Lake Okeechobee discharges and loads before being applied as input to the SLE model. The iterative water quality calibration process was then applied to the SLE model.

The final calibration parameters are shown in Table 5-1.

Table 5-1. Calibration Parameters for Each WaSh Model.

WaSh In-Stream Parameter	Units	Definition	C23	C24	C44	SLE
MIX_VERTICAL	**ft^2/sec**	Vertical Mixing Coefficient	-	-	-	0.1
KE1	**ft^{-1}**	Extinction Coeff.	1.000	1.000	1.000	1.000
KE2	**ft^{-1}**	Extinction Coeff.	1.000	1.000	1.000	1.000
Frac_Daylight	**-**	Fraction of day that is daylight	0.500	0.500	0.500	0.500
GP	**day^{-1}**	Maximum Growth Rate	1.500	4.000	1.500	2.200
THETAGP	**-**	Temperature Coefficient	1.068	1.068	1.068	1.068
LIS	**langleys/day**	Light Intensity at Saturation	150.000	150.000	150.000	150.000
KMN	**mg N/L**	Half-Saturation Constant for Nitrogen	0.025	0.025	0.025	0.025
KMP	**mg P/L**	Half-Saturation Constant for Phosphorus	0.001	0.001	0.001	0.001
K1R	**day^{-1}**	Endogenous Respiration	0.150	0.150	0.150	0.150
THETA1R	**-**	Temperature Coefficient	1.045	1.045	1.045	1.045
VS4	**ft/day**	Phytoplankton Settling Velocity	0.000	0.000	0.000	0.000
KDP	**day^{-1}**	Death Rate	0.350	0.350	0.350	0.350
APC	**-**	Phosphorus to carbon ratio	0.025	0.025	0.025	0.025
K83	**day^{-1}**	Dissolved organic phosphorus mineralization at 20°C	0.140	0.110	0.130	0.110
THETA83	**-**	Temperature Coefficient	1.080	1.080	1.080	1.080
KMPC	**mg C/L**	Half saturation constant for phytoplankton limitation of phosphorus recycle	1.000	1.000	1.000	1.000

WaSh In-Stream Parameter	Units	Definition	C23	C24	C44	SLE
FOP	**-**	Fraction of dead and respired phytoplankton recycled to the organic phosphorus pool	0.500	0.500	0.500	0.500
VS2	**ft/day**	Organic phosphorus settling velocity	0.000	0.000	0.000	0.000
ANC	**-**	Nitrogen to carbon ratio	0.250	0.250	0.250	0.250
K71	**day^{-1}**	Organic Nitrogen mineralization at 20°C	0.035	0.030	0.040	0.080
THETA71	**-**	Temperature Coefficient	1.080	1.080	1.080	1.080
K12	**day^{-1}**	Nitrification Rate	0.470	0.047	0.047	0.047
THETA12	**-**	Temperature Coefficient	1.030	1.030	1.030	1.030
KNIT	**mg O_2/L**	Half Saturation rate for oxygen	2.000	2.000	2.000	2.000
K2D	**day^{-1}**	Denitrification rate at 20°C	0.050	0.050	0.050	0.050
THETA2D	**-**	Temperature Coefficient of Denitrification rate	1.045	1.045	1.045	1.045
KNO3	**mg O_2/L**	Michaelis constant for denitrification	0.100	0.100	0.100	0.100
FON	**-**	Fraction of dead and respired phytoplankton recycled to the ammonia nitrogen pool	0.500	0.500	0.500	0.500
VS3	**ft/day**	Organic nitrogen settling velocity	0.000	0.000	0.000	0.000
AOC	**-**	Oxygen to carbon ratio	2.670	2.670	2.670	2.670
KD	**day^{-1}**	Deoxygenation rate @ 20°C	0.150	0.075	0.150	0.150
THETAD	**-**	Temperature Coefficient	1.047	1.047	1.047	1.047
KBOD	**mg O_2/L**	Half saturation constant for oxygen limitation	0.900	0.900	0.900	0.900
SOD	**g O_2/m^2-day**	Sediment Oxygen Demand	5.960	5.960	5.960	3.000

WaSh In-Stream Parameter	Units	Definition	C23	C24	C44	SLE
THETA2	**-**	SOD Temperature coefficient	1.03	1.03	1.03	1.03
VS5	**ft/day**	BOD settling velocity	0.000	0.000	0.000	0.000
K2	**day^{-1}**	Reaeration Rate	0.300	0.300	0.300	1.200
THETA1R	**-**	Endogenous Respiration Temperature coefficient	1.000	1.000	1.000	1.000
K1R	**day^{-1}**	Endogenous Respiration	0.500	0.500	0.500	0.500

Example results of the final water quality calibration and validation are shown in Figures 5.1 and 5.2 for the C24 outfall and HR1 stations. Additional plots of calibration results are presented in Appendix D for C23, C44, and SE03, SE06, SE08, and SE09.

Summary statistics of percentile and time-series metrics for the upland basins C23, C24 and C44 are presented in Tables 5-2 and 5-3 respectively. Summary statistics of percentile and time-series metrics for the SLE basin are presented in Tables 5-4 and 5-5.

The comparison of simulated and measured time series plots for the water quality data show generally good agreement. The strong seasonal trends evident in the D.O. and the phosphorus data were well represented in the model simulations. The frequency diagrams show that the full range and distribution of values is simulated. However, the frequency diagrams for nitrate and ammonia indicate that the small percentage of large values is not always predicted. The results for the upland basins tended to be better than those for the estuary stations, which reflect the more complex physics associated with estuarine systems and the inherent difficulty in representing them in a model. For the estuary stations, the difference in the upper and lower layer D.O. values are well represented. A comparison of the 25^{th}, 50^{th} and 75^{th} percentile and mean values for DO, TN and TP indicate that the full range of values over the 11-year period is simulated properly by the model. The percentiles and averages for the simulation results were typically within 0.5 to 20 % of those based on the measured values, with only a few comparisons yielding higher errors. The results for the C-44 basin were generally less accurate than those for the C-23 and C-44 basin, which is due to the quality of the measured data. The C-44 data required removal of data that was influenced by Lake discharges through the C-44 canal, and therefore greatly reduced the number of measured samples available for comparison, and subsequently the statistical basis for the data.

The RMS error for TN, TP and D.O. were typically on the order of 0.4 mg/L for TN, 0.15 mg/L for TP and 2 mg/L for D.O. Assuming a typical maximum value for the range of TN of 1.9 mg/L, 0.4 mg/L for TP and 8.5 mg/L for D.O., the RMS errors are generally on the order of 22% for TN, of 37% for TP and 23% for D.O. The Pearson Correlation Coefficients for the water quality simulations ranged between 0.23 to 0.74 for the upland basins and between 0.146 and 0.812 for the SLE basin simulation. There is a larger range in the Pearson Correlation Coefficients for the water quality calibrations than for the hydrologic calibration. This result reflects the use of EMC inputs values despite the high variability evident in the measured water quality used to develop the EMC values. The measured data indicate that the actual runoff concentration can vary significantly for individual events, but the WaSh model can only assign a single value to all runoff events. Monthly variations can be accommodated in the model, but the measured data indicate that the variations are more frequent and appear random. It is unlikely that an improvement in the metrics can be realized until a better understanding of the variations in the runoff concentrations is determined, and the processes responsible for the variations included in the model.

Table 5-2. Percentile Metrics for the Upland Basins in the SLEW.

C23	Calibration						Validation					
	TN		TP		DO		TN		TP		DO	
Metric	Measured	Simulated.	Measured	Simulated.	Measured	Simulated.	Measured	Simulated.	Measured	Simulated.	Measured	Simulated.
75 Percentile	1.58	1.46	0.36	0.49	6.88	7.11	1.56	1.48	0.45	0.64	7.11	6.61
50 Percentile	1.29	1.34	0.27	0.24	5.00	5.96	1.26	1.40	0.30	0.31	5.96	5.13
25 Percentile	0.96	1.16	0.17	0.15	4.20	4.49	0.96	1.31	0.17	0.15	4.49	3.52
Mean	1.31	1.31	0.28	0.33	5.42	5.85	1.27	1.39	0.33	0.39	5.85	4.91

C24	Calibration						Validation					
	TN		TP		DO		TN		TP		DO	
Metric	Measured	Simulated.	Measured	Simulated.	Measured	Simulated.	Measured	Simulated.	Measured	Simulated.	Measured	Simulated.
75 Percentile	1.77	1.74	0.29	0.34	6.20	7.01	1.55	1.76	0.36	0.35	6.66	7.06
50 Percentile	1.42	1.61	0.23	0.18	4.83	5.13	1.27	1.67	0.21	0.20	4.74	5.16
25 Percentile	1.16	1.39	0.15	0.09	2.72	2.62	1.02	1.49	0.12	0.09	2.32	2.77
Mean	1.45	1.58	0.24	0.22	4.68	4.62	1.36	1.62	0.26	0.22	4.69	4.73

C44	Calibration						Validation					
	TN		TP		DO		TN		TP		DO	
Metric	Measured	Simulated.	Measured	Simulated.	Measured	Simulated.	Measured	Simulated.	Measured	Simulated.	Measured	Simulated.
75 Percentile	1.46	1.16	0.19	0.08	7.31	7.79	-	-	-	-	-	-
50 Percentile	1.31	1.12	0.13	0.07	6.33	7.27	-	-	-	-	-	-
25 Percentile	1.20	1.12	0.09	0.06	5.25	6.63	-	-	-	-	-	-
Mean	1.33	1.14	0.14	0.07	6.18	7.26	-	-	-	-	-	-

Table 5-3. Time-Series Metrics for the Upland Basins in the SLEW.

	Calibration						Validation					
	TN		TP		DO		TN		TP		DO	
Metric:	RMS (mg/L)	PCC	RMS (mg/L)	PCC	RMS (mg/L)	PCC	RMS (mg/L)	PCC	RMS (mg/L)	PCC	RMS (mg/L)	PCC
C23-S97	0.419	0.234	0.173	0.704	2.07	0.458	0.364	0.382	0.202	0.744	2.78	0.224
C24-S49	0.449	0.340	0.140	0.409	2.27	0.587	0.665	0.411	0.166	0.553	2.50	0.513
C44-S80	0.353	0.261	0.072	0.422	1.28	0.670	-	-	-	-	-	-

RMS = Root Mean Square error; PCC = Pearson Correlation Coefficient, u=upper layer, l=lower layer

Table 5-4. Percentile Metrics for the SLE Basin.

(Lower DO measurements were not provided for SE08 station, due to the depth of the estuary at that location.)

HR1	Calibration								Validation							
	TN		TP		DO		DO-Lower		TN		TP		DO-Upper		DO-Lower	
Metric	Measured	Simulated	Measured	Simulated	Measured	Simulated	Measured	Simulated	Measured	Simulated	Measured	Simulated	Measured	Simulated	Measured	Simulated
75 Percentile	1.38	1.48	0.24	0.17	8.16	8.28	6.89	7.17	1.13	1.21	0.31	0.22	8.08	8.24	6.71	7.34
50 Percentile	1.17	1.14	0.20	0.12	7.37	7.54	5.31	5.80	0.88	1.09	0.20	0.10	7.03	7.58	5.74	6.00
25 Percentile	0.95	0.93	0.15	0.05	6.67	7.16	3.66	4.64	0.79	0.94	0.14	0.04	6.15	7.15	4.88	4.65
Mean	1.20	1.29	0.20	0.13	7.37	7.73	5.06	5.68	0.99	1.11	0.25	0.15	7.10	7.72	5.64	5.65

SE03	Calibration								Validation							
	TN		TP		DO		DO-Lower		TN		TP		DO-Upper		DO-Lower	
Metric	Measured	Simulated	Measured	Simulated	Measured	Simulated	Measured	Simulated	Measured	Simulated	Measured	Simulated	Measured	Simulated	Measured	Simulated
75 Percentile	1.46	1.21	0.21	0.19	8.16	7.62	6.89	6.49	1.34	1.20	0.27	0.18	8.09	7.78	6.71	6.65
50 Percentile	1.20	1.01	0.17	0.11	7.37	6.73	5.31	5.07	0.93	0.99	0.15	0.10	7.10	6.92	5.78	5.52
25 Percentile	0.89	0.81	0.13	0.06	6.67	6.00	3.66	3.38	0.82	0.85	0.12	0.05	6.20	6.20	4.88	3.53
Mean	1.20	1.06	0.18	0.13	7.37	6.71	5.06	4.80	1.02	1.09	0.21	0.13	7.22	6.77	5.71	4.96

SE08	Calibration								Validation							
	TN		TP		DO		DO-Lower		TN		TP		DO-Upper		DO-Lower	
Metric	Measured	Simulated	Measured	Simulated	Measured	Simulated	Measured	Simulated	Measured	Simulated	Measured	Simulated	Measured	Simulated	Measured	Simulated
75 Percentile	1.66	1.24	0.23	0.18	7.97	7.38	-	-	1.43	1.30	0.27	0.17	7.87	7.50	-	-
50 Percentile	1.33	1.03	0.19	0.11	7.34	6.59	-	-	1.16	1.04	0.21	0.10	6.73	6.86	-	-
25 Percentile	1.07	0.85	0.14	0.07	6.16	5.82	-	-	0.94	0.90	0.16	0.06	5.96	5.82	-	-
Mean	1.34	1.09	0.19	0.13	7.10	6.55	-	-	1.26	1.14	0.22	0.14	6.73	6.62	-	-

Table 5-5. Time-Series Metrics for the SLE Basin.

	Calibration						Validation					
	TN		TP		DO		TN		TP		DO	
Metric:	RMS (mg/L)	PCC	RMS (mg/L)	PCC	RMS (mg/L)	PCC	RMS (mg/L)	PCC	RMS (mg/L)	PCC	RMS (mg/L)	PCC
HR1	0.771	0.146	0.142	0.250	1.57 u 2.32 l	0.434 u 0.503 l	0.460	0.153	0.194	0.404	1.69 u 2.31 l	0.502 u 0.336 l
SE3	0.514	0.291	0.092	0.618	1.67 u 2.23 l	0.442 u 0.576 l	0.467	0.344	0.107	0.812	1.54 u 2.46 l	0.534 u 0.337 l
SE8	0.605	0.152	0.119	0.248	1.69	0.444	0.482	0.354	0.119	0.637	1.73	0.370

RMS = Root Mean Square error; PCC = Pearson Correlation Coefficient, u=upper layer, l=lower layer

Nutrient load calculations for each model using the calibrated simulation outputs are provided in Table 5-6.

Table 5-6. Nutrient Load Calculations for each Basin in the SLEW.

Basin	TN (tons/year)	TP (tons/year)	CBODu (tons/year)
C23	243	101	268
C24	357	85.5	936
C44	218	34.8	348
C44 without Lake	1220	128	1430
North Fork	813	202	1687
South Fork (Tidal St. Lucie)	988	164	1292
Bessey (Basin 4)	190	63	282
Danforth (Basin 6)	33.9	7.12	58.13

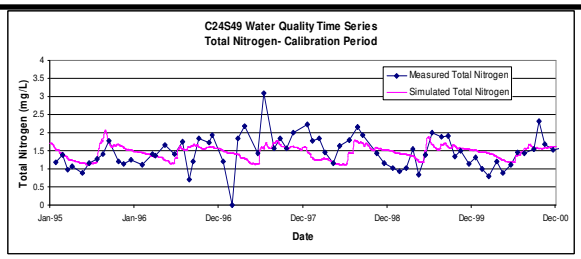

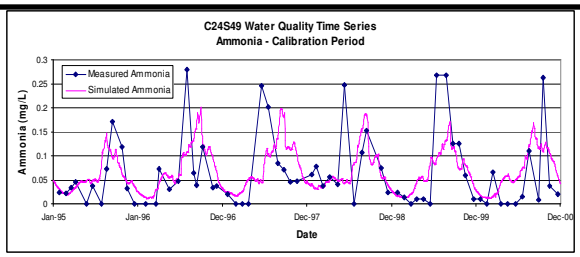

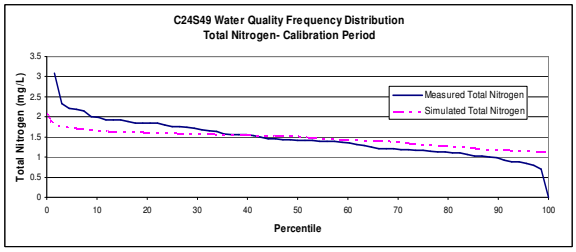

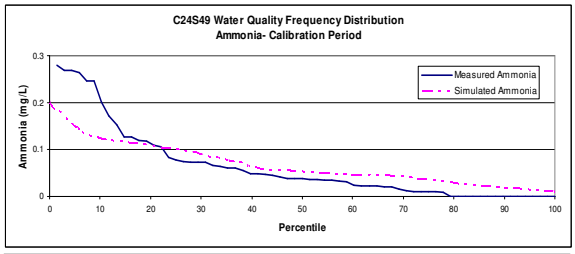

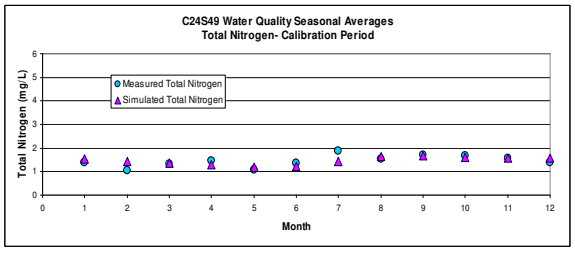

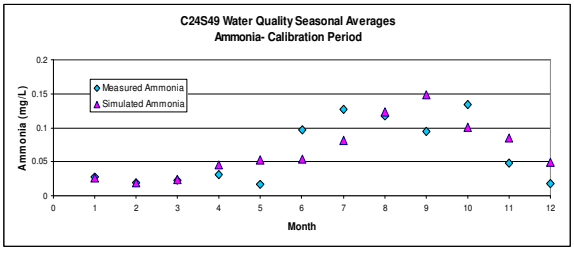

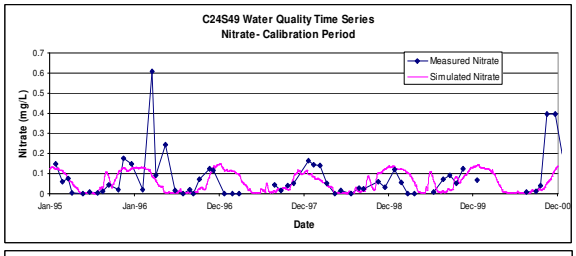

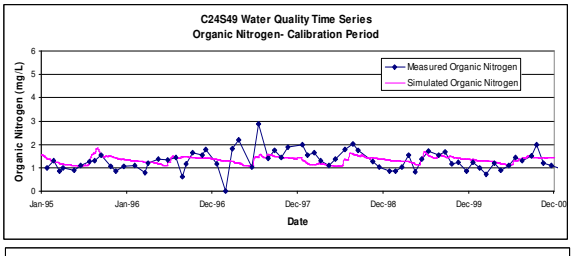

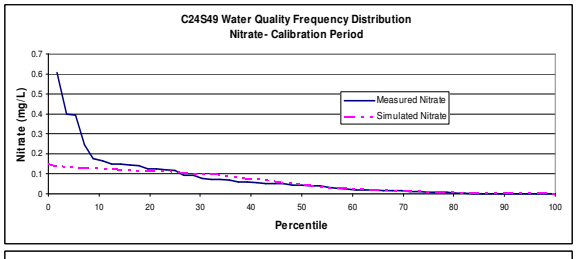

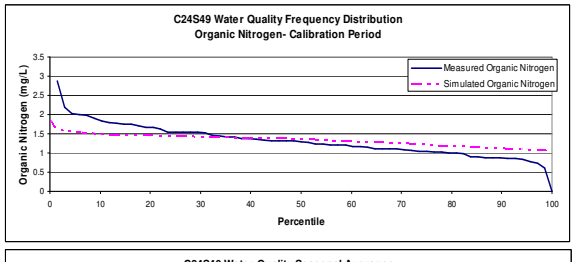

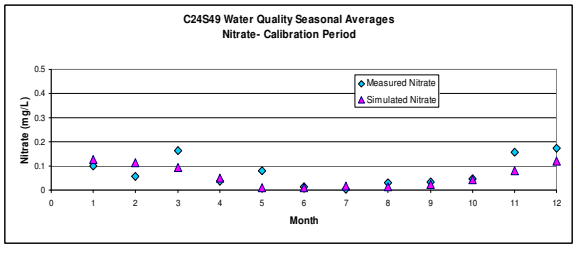

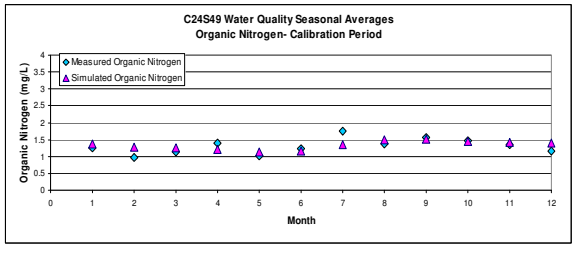

URS

Figure 5-1. C24 Simulation Results during Calibration Period (1995-2000).

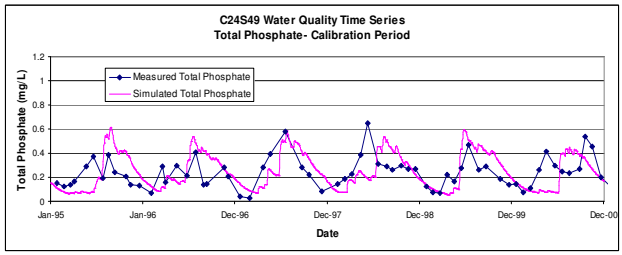

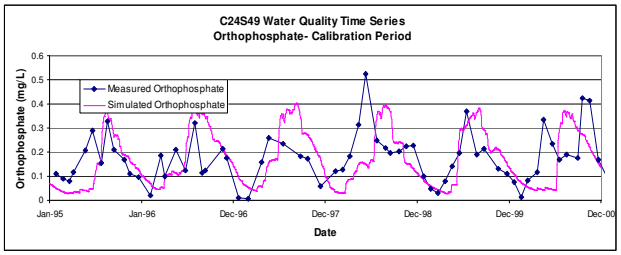

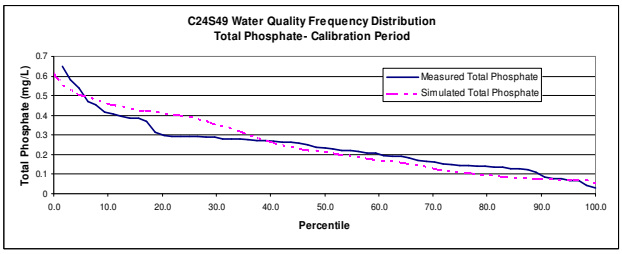

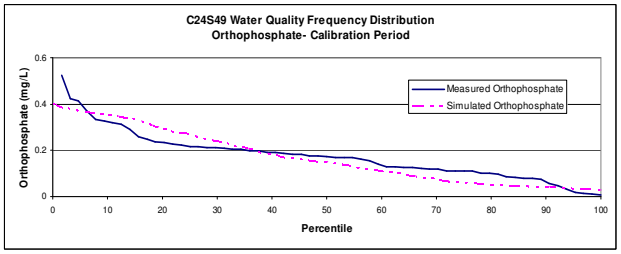

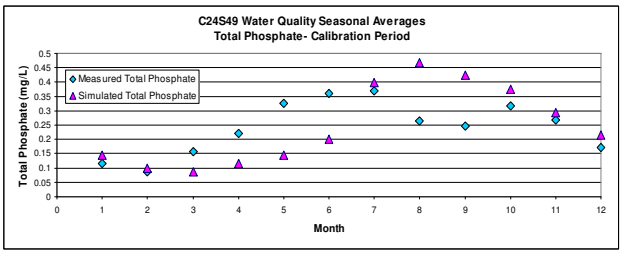

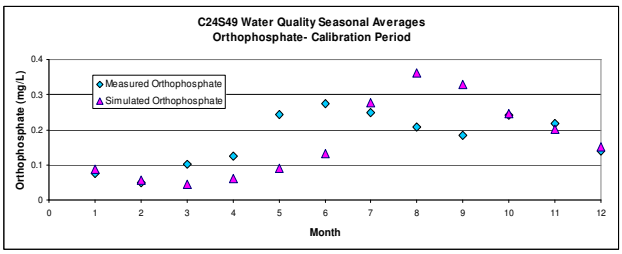

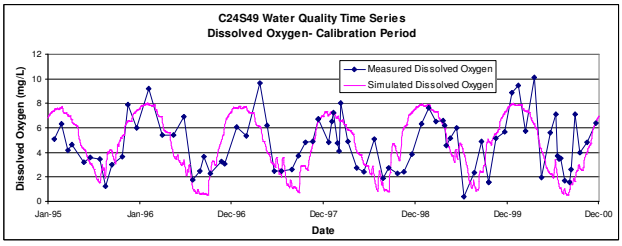

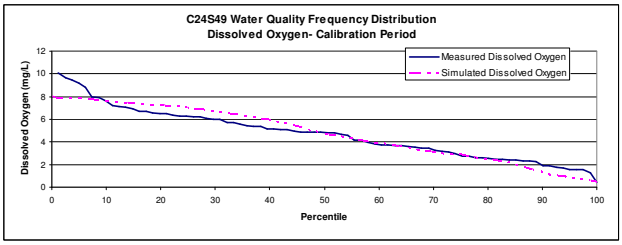

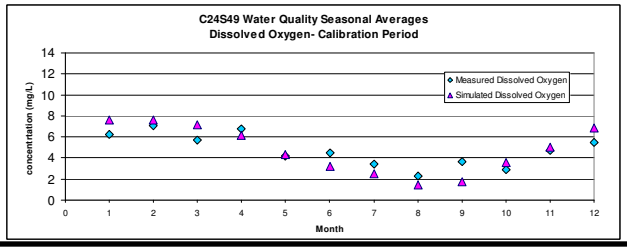

URS

Figure 5-1 (cont'd.) C24 Simulation Results during Calibration Period (1995-2000).

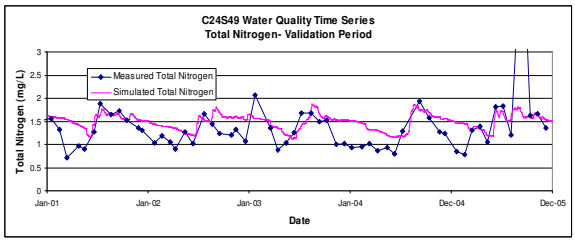

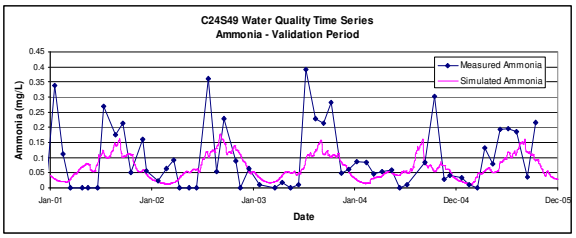

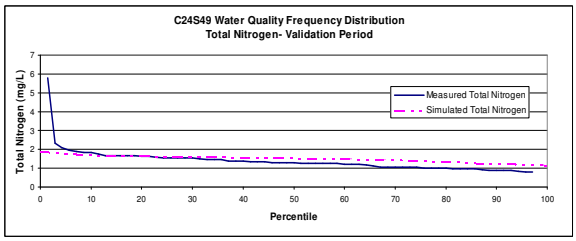

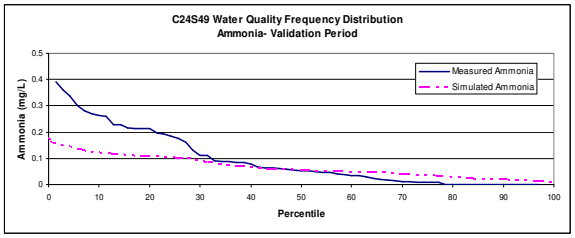

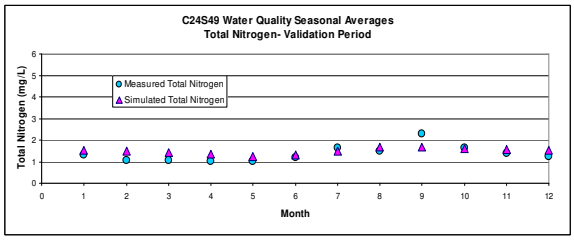

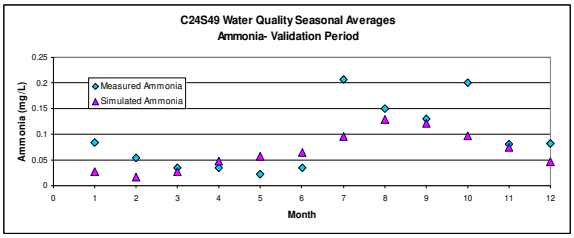

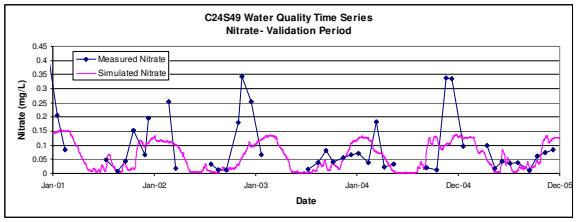

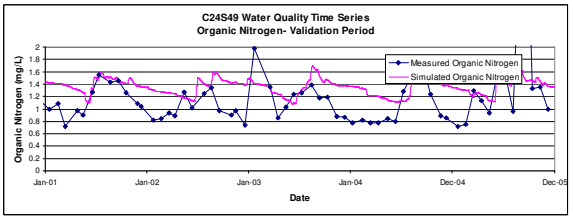

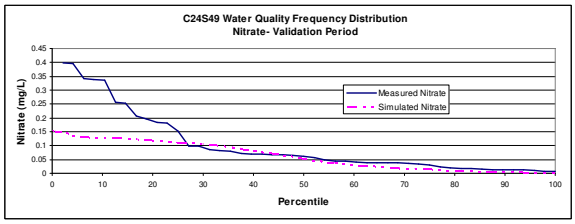

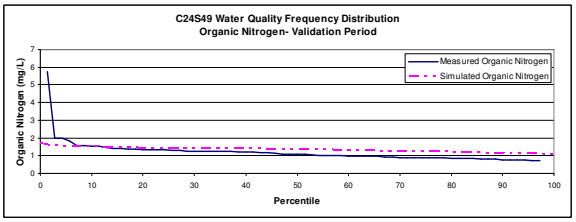

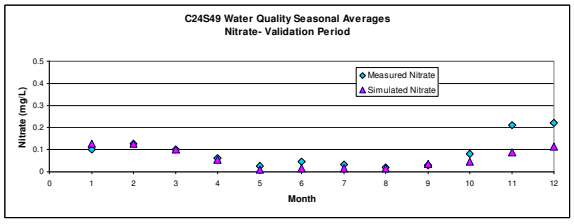

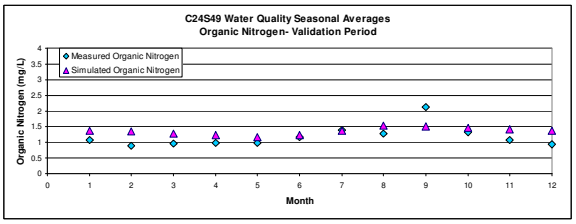

URS

Figure 5-1 cont'd. C24 Simulation Results during Validation Period (2001-2005).

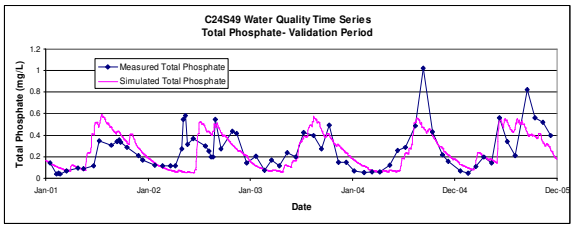

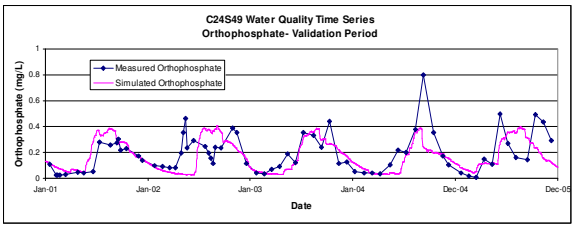

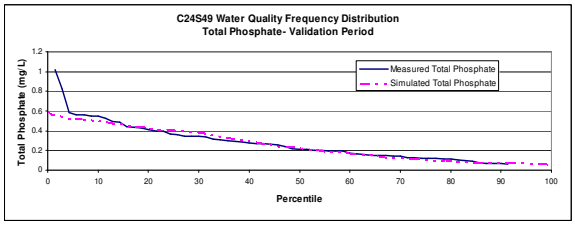

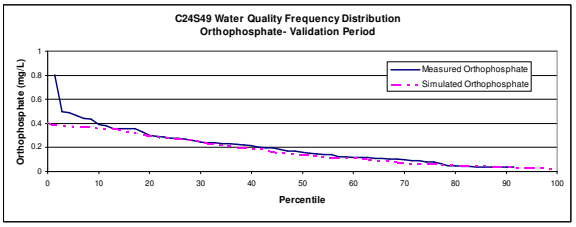

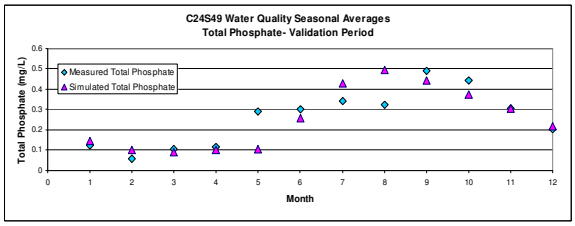

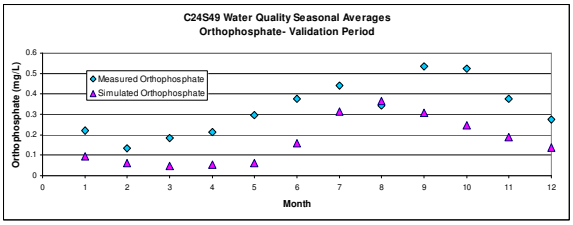

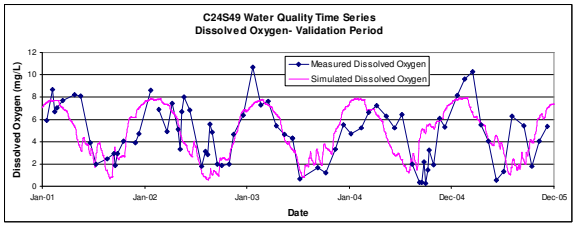

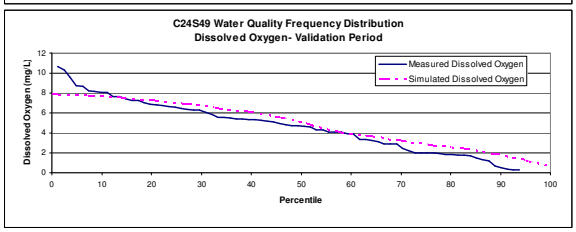

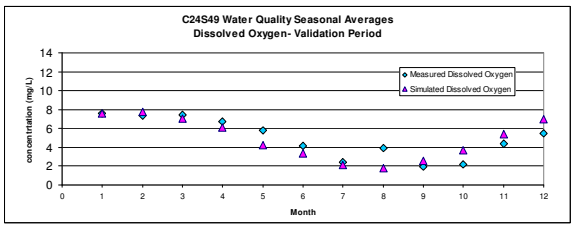

URS

Figure 5-1 cont'd. C24 Simulation Results during Validation Period (2001-2005).

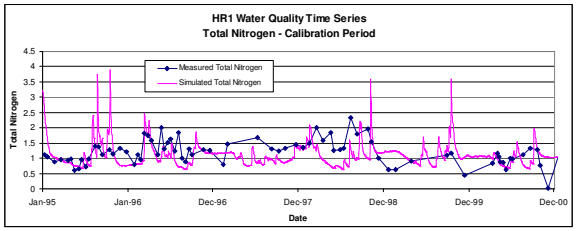

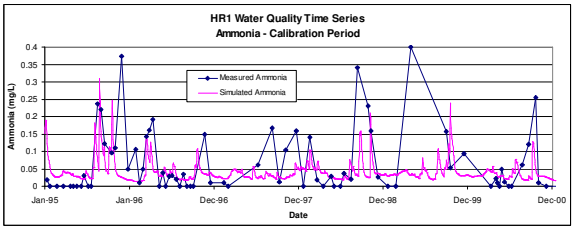

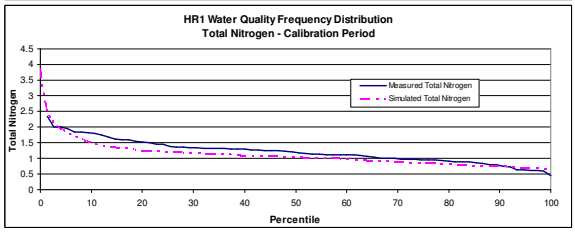

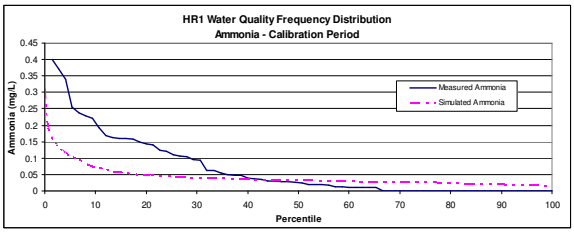

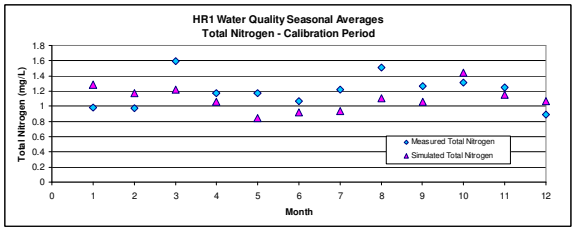

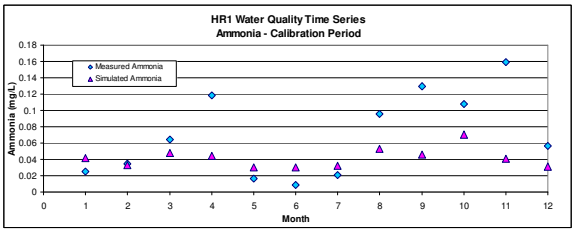

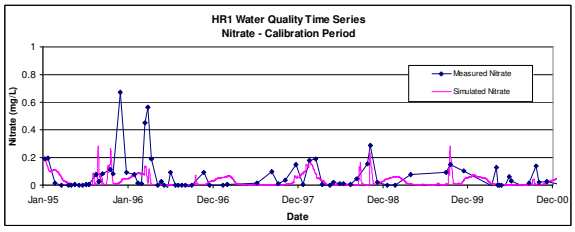

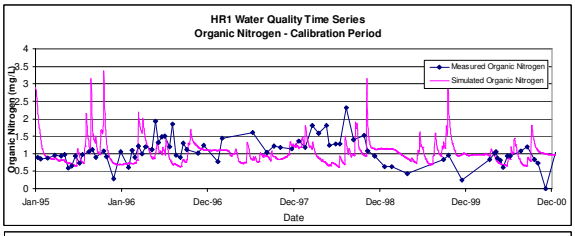

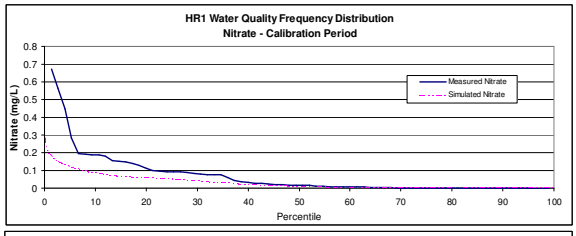

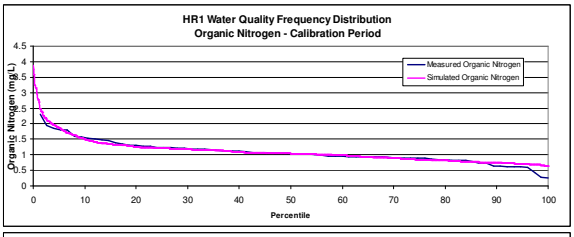

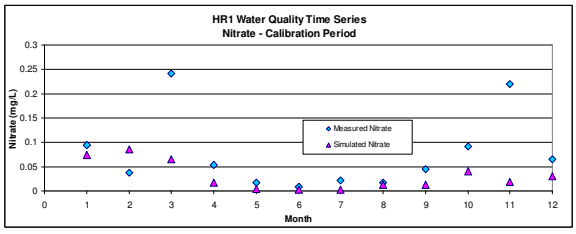

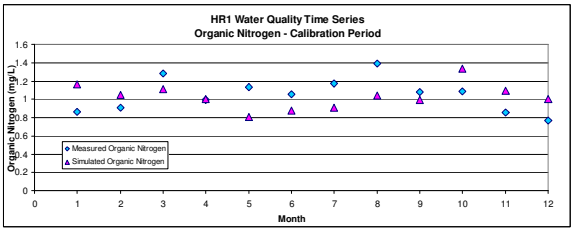

URS

Figure 5-2. HR1 Simulation Results during Calibration Period (1995-2000).

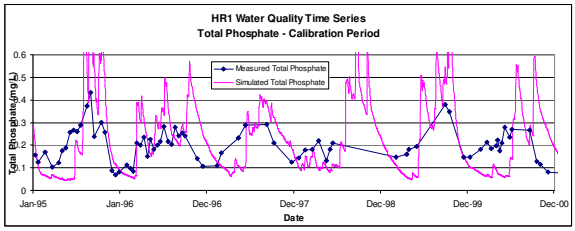

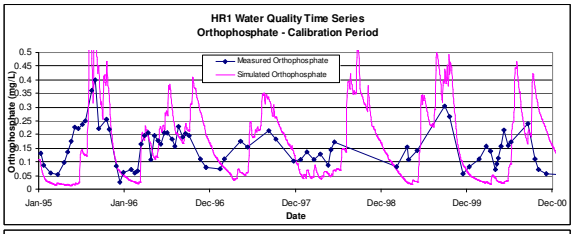

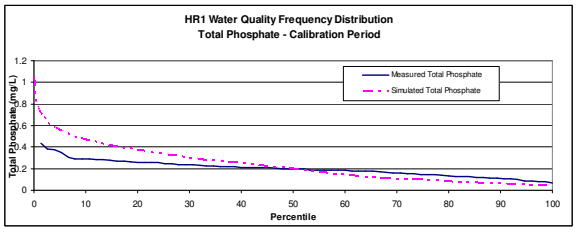

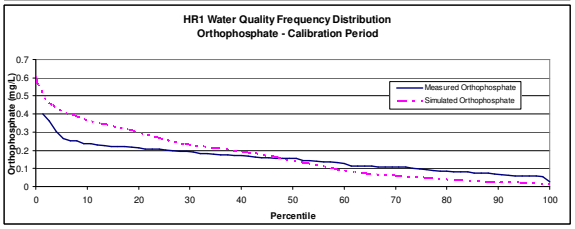

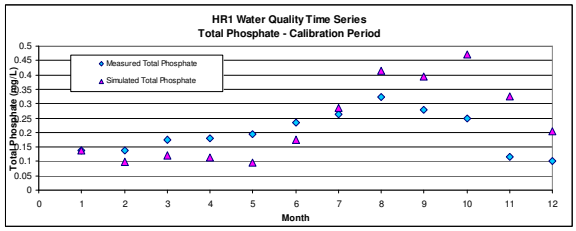

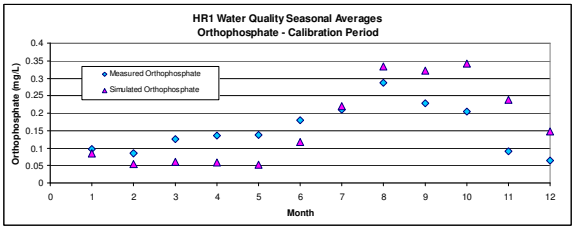

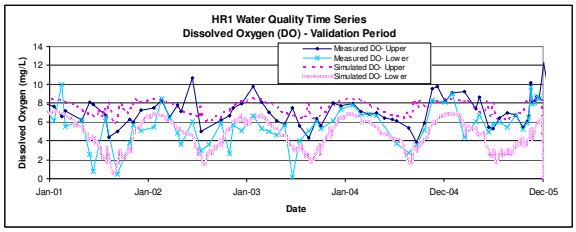

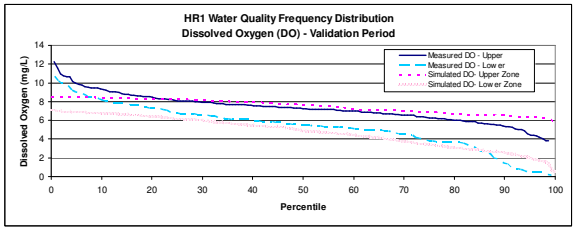

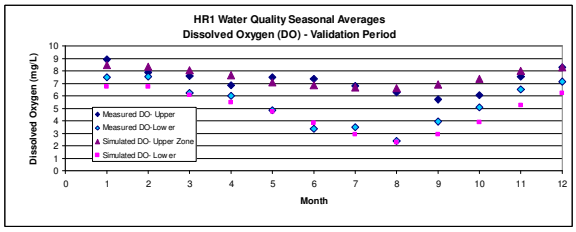

URS

Figure 5-2 cont'd. HR1 Simulation Results during Calibration Period (1995-2000).

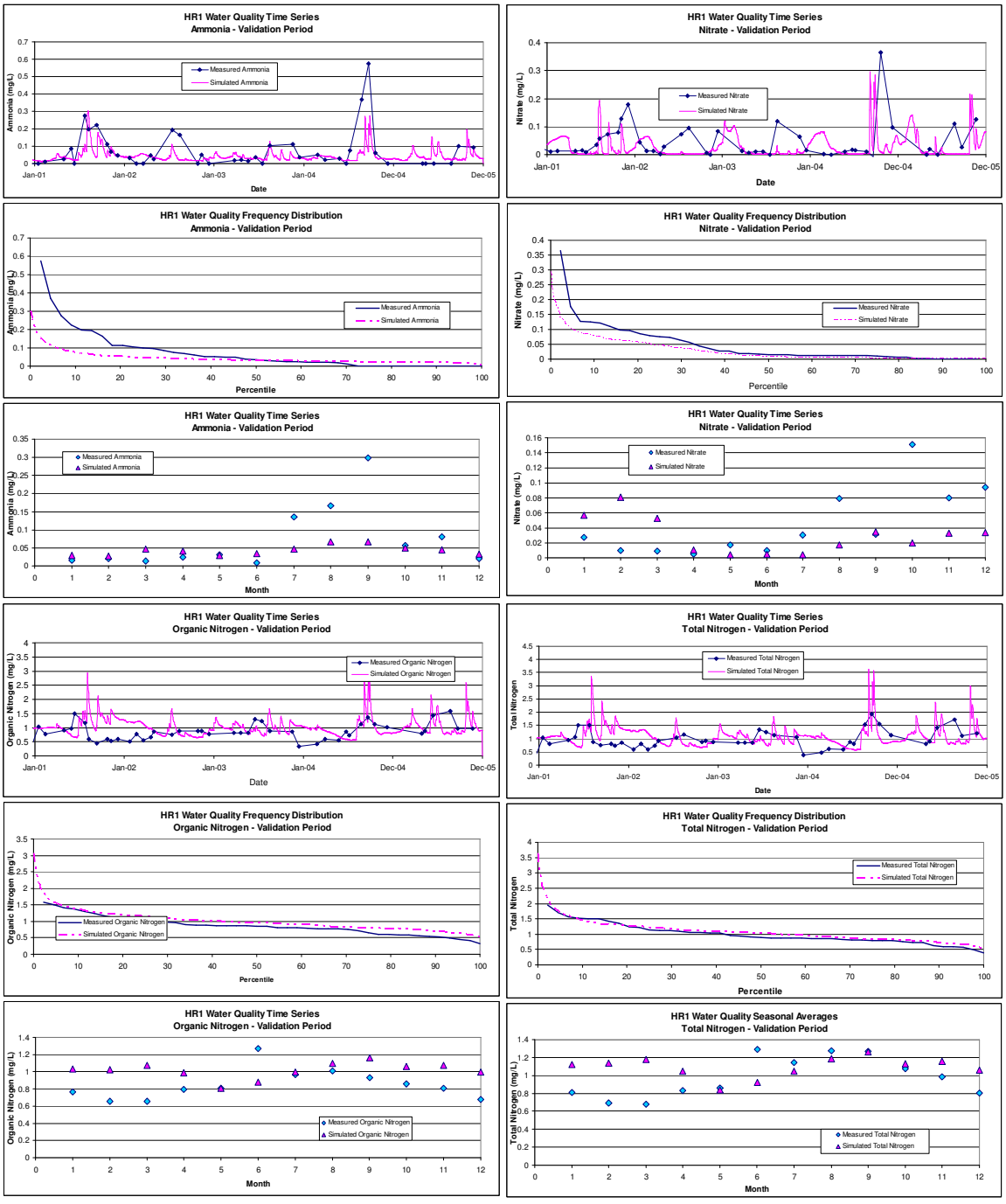

Figure 5-2 cont'd. HR1 Simulation Results during Validation Period (2001-2005).

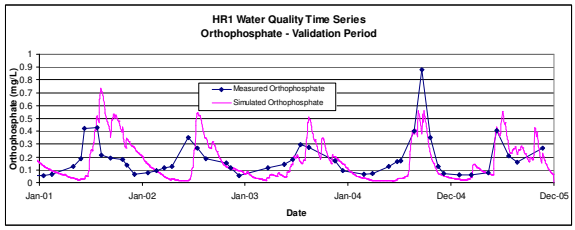

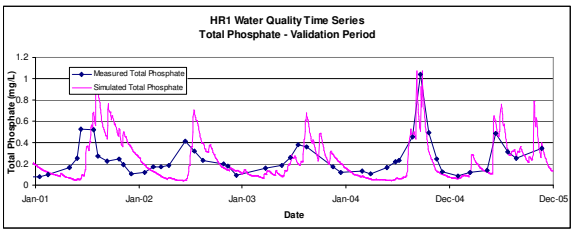

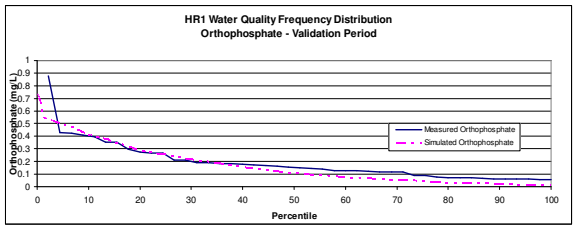

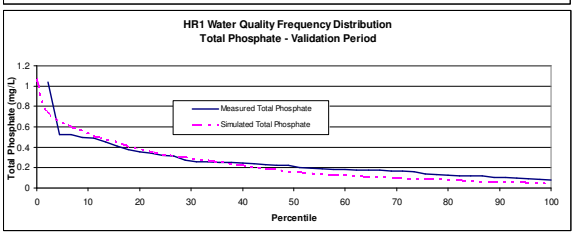

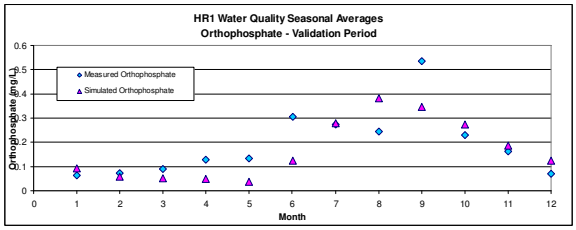

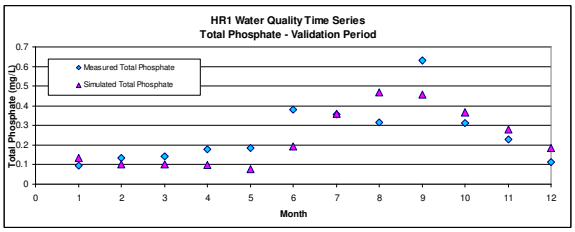

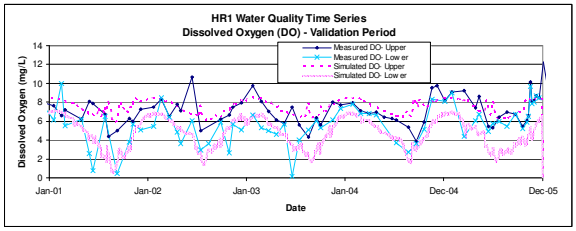

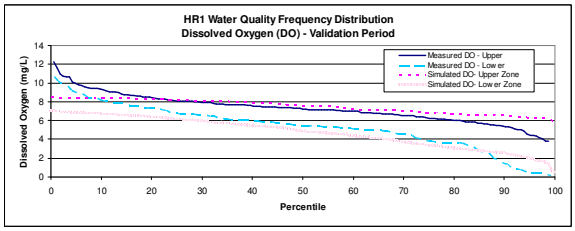

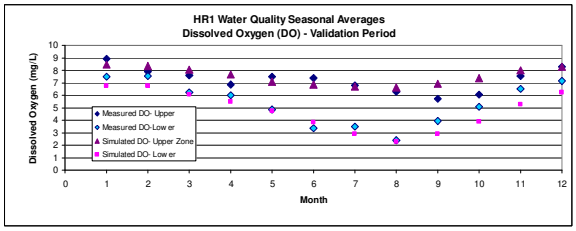

URS

Figure 5-2 cont'd. HR1 Simulation Results during Validation Period (2001-2005).

The large number of input and model parameters necessary for the watershed hydrologic and hydrodynamic simulation precludes a formal sensitivity analysis for the modeling analysis. Therefore, two key parameters, for which the data used to constrain the values was limited, were selected for a sensitivity analysis. These parameters are the ABMC values for the BOD and the SOD value. Both of these parameters had limiting site-specific data to constrain input values.

The sensitivity analysis for the BOD consisted of increasing the input BOD value by 50% and determining the effect on the D.O. The 6 year calibration period for the C-24 basin was used for the analysis. The results, shown in Figure 6.1, show that the 50% reduction in the BOD caused a 0.4 mg/L increase in the median D.O. value, or about an 8 % increase. These results indicate a small sensitivity of the D.O. to the runoff BOD value. This small sensitivity is likely due to the large CBOD generated by the decaying phytoplankton mass in the simulations. The model simulates the in-stream production of CBOD in the upland terrestrial canals, as well as in the primary canals. This production yields significantly more CBOD (ie. BOD) than from the direct runoff, and therefore, the model is less sensitive to changes in the direct runoff loads.

The results for the SOD sensitivity analysis are shown in Figure 6.2 for the same 6 year period for the C-24 basin. The 50% decrease in the SOD value yields a change in the median D.O. value of 0.6 mg/L or about a 12 % increase. These results indicate a small sensitivity of the D.O. to the input SOD value. The D.O. in the model is controlled mostly by the phytoplankton dynamics, which is dominated by the large CBOD load generated by the decaying phytoplankton. The vast network of tertiary canals provides a large reservoir of CBOD due to the phytoplankton production and is a much larger impact on the D.O. than the SOD.

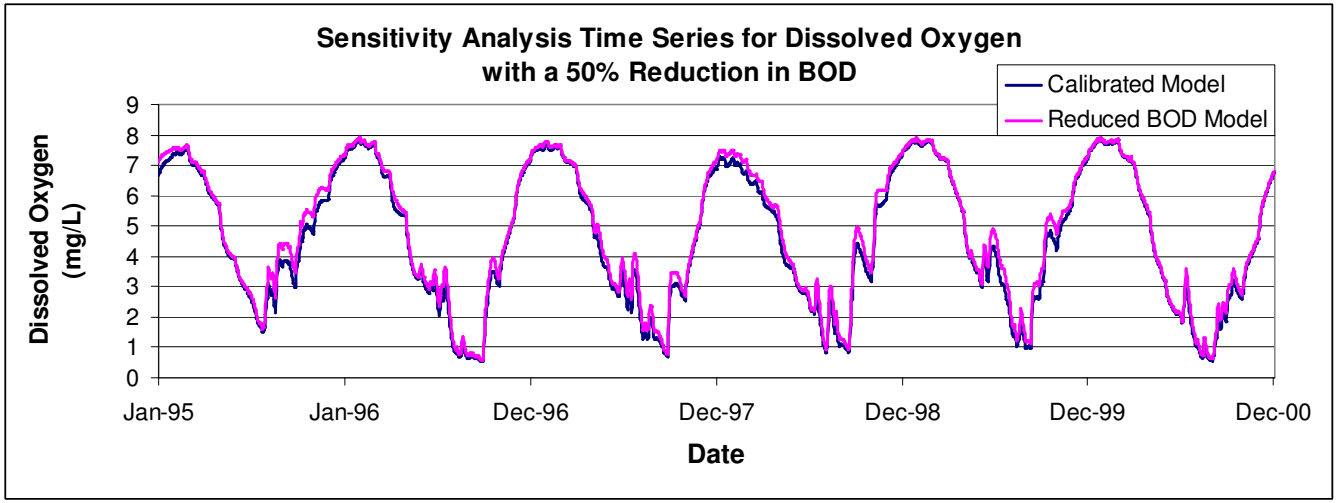

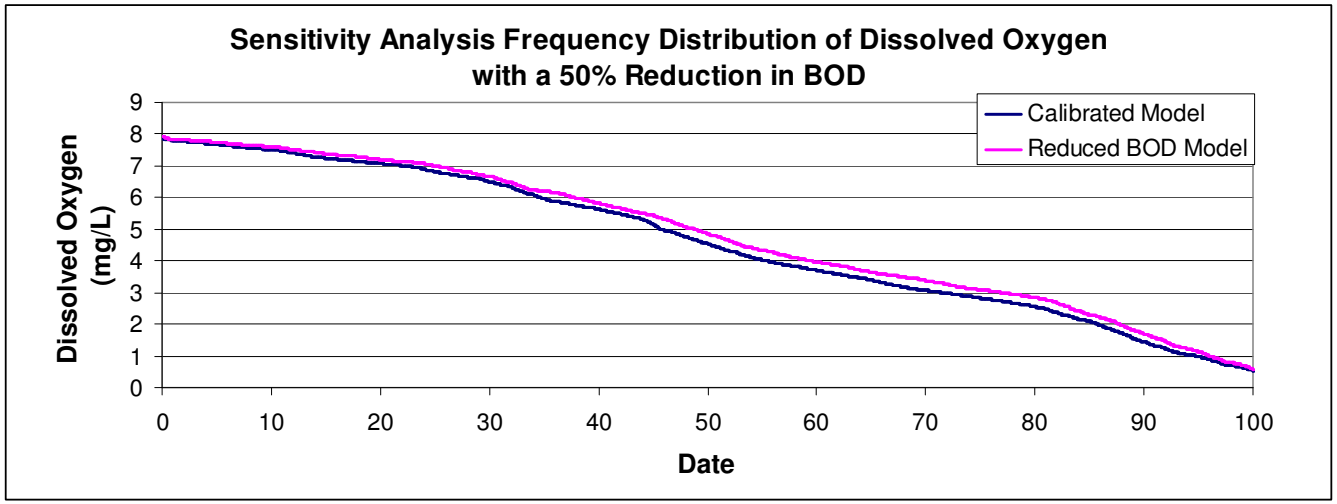

URS

Figure 6-1. Sensitivity of D.O. to change in BOD ABMC value.

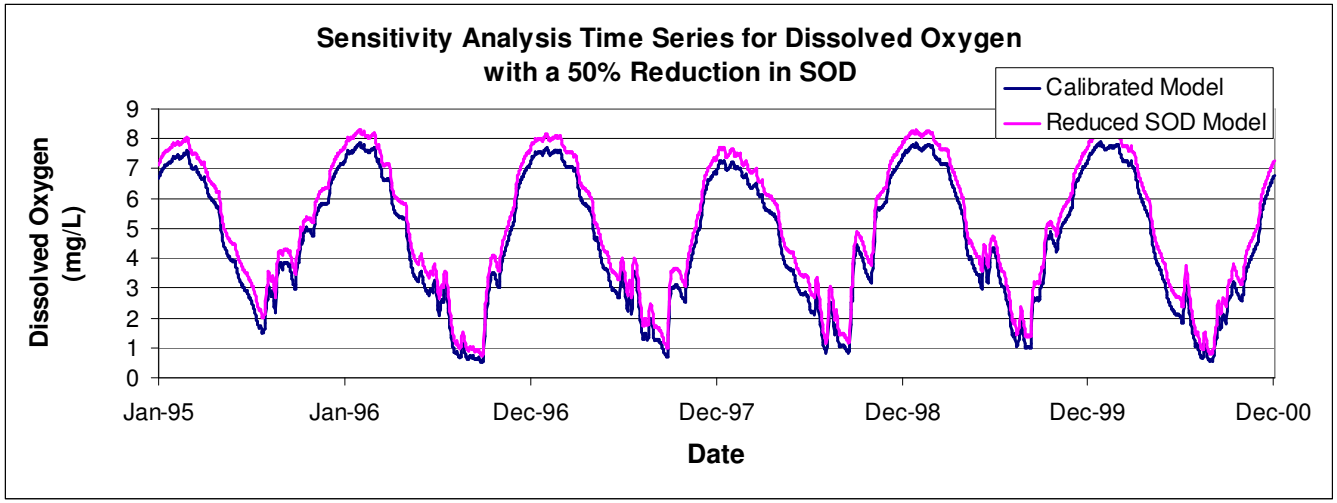

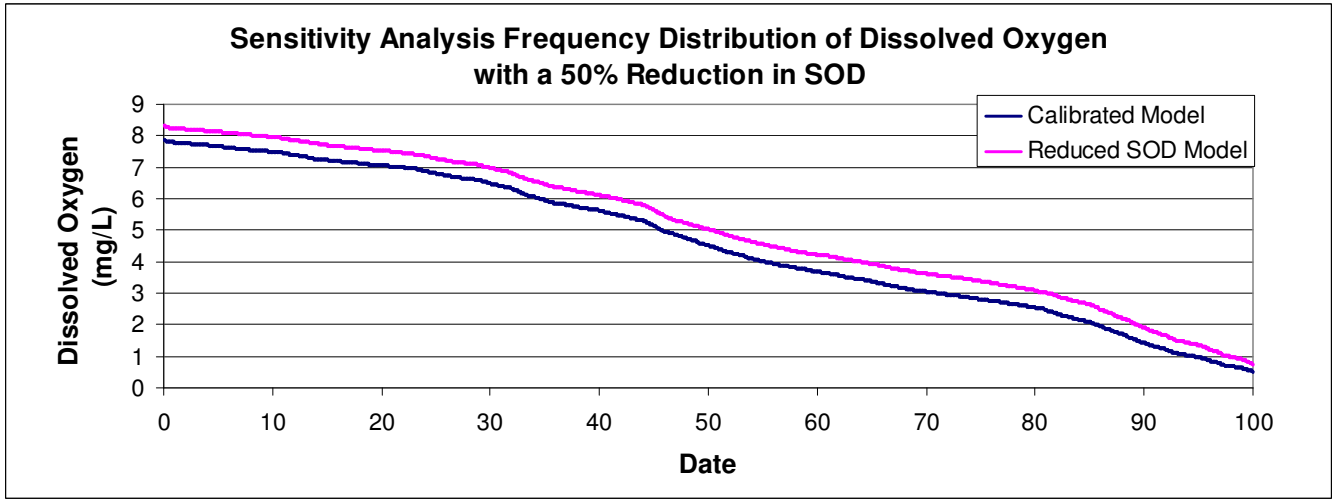

URS

Figure 6-2. Sensitivity of D.O. to change in SOD value.

When the discharges from Lake Okeechobee enter the South Fork via the C-44 canal, it is possible that some of the lake water influences conditions in the North Fork. Transport of lake water into the North Fork from the South Fork does not likely occur regularly, but conditions may favor it occasionally. During large discharges, the water surface in the South Fork may rise sufficiently, such that it is creates a barotropic pressure head favoring flow in the North Fork. Also, continuous mixing of North Fork and South Fork in the Middle Estuary during normal tidal flows could transport smaller fractions of lake water into the North Fork, when the South Fork has been flushed with lake discharges.

A method for estimating the influence of Lake Okeechobee water in the North Fork has been developed and is similar to the approach for the salinity calibration for the SLE model. The approach is shown in Figure 7.1. At the western end of the SLE model, the calibrated C-23 and C-24 basin models daily output flows were used as point source inputs to the SLE model at their discharge points. The associated tracer values were set to zero for the input flows, representing non-lake discharges. The C-44 basin model was executed with the Lake Okeechobee discharges through the S308 structure included. The tracer value in the input file representing the lake was set to 1.0, representing 100% lake water. The runoff coefficients in the C-44 basin model were set to zero, representing non-lake water. The output from the C-44 model was then used as input to the SLE model. The SLE model was configured with runoff concentrations of zero, representing non-lake water in the direct discharges from the basin. The hourly tidal elevation data and a tracer value of zero were used at the downstream boundary in the SLE model.

In this configuration, the SLE model simulated the transport in the estuary, subject to tidal flows, freshwater discharges from the C-23, C-24, C-44, including Lake Okeechobee , and freshwater discharges from the land included in the SLE model. The lake water was set with a concentration of 1.0 and all other sources of water were set with a concentration of 0.0. Thus at any point in the model domain, the instantaneous concentration simulated with the model represents the fraction of lake water at that position.

The results of a simulation for the 2002 through 2005 period are shown in Figure 7.2. The output at the S80 station, which is the discharge from the C-44 basin model, indicates a strong influence from the Lake, as expected. The fraction of lake water ranges from 0.0 to 1.0. When at zero, there is no lake water in the C-44 canal at the S-80 structure, and the water represents pure basin discharge. When the concentration is near 1.0, the discharges through the S80 structure are mostly due to lake discharges. At the downstream end of the SLE model, near the A1A Bridge, the influence of the lake discharge is evident but is muted, due to simultaneous non-lake discharges from other portions of the watershed (i.e. the North Fork, C-23 and C-44 as well as the smaller B4, B-5 and B-6 basins). There is evidence of transport of lake water into the North Fork as indicated by the results at HR1. The lake is estimated to comprise as much as 20% of the water for the period during and following large discharges in the North Fork.

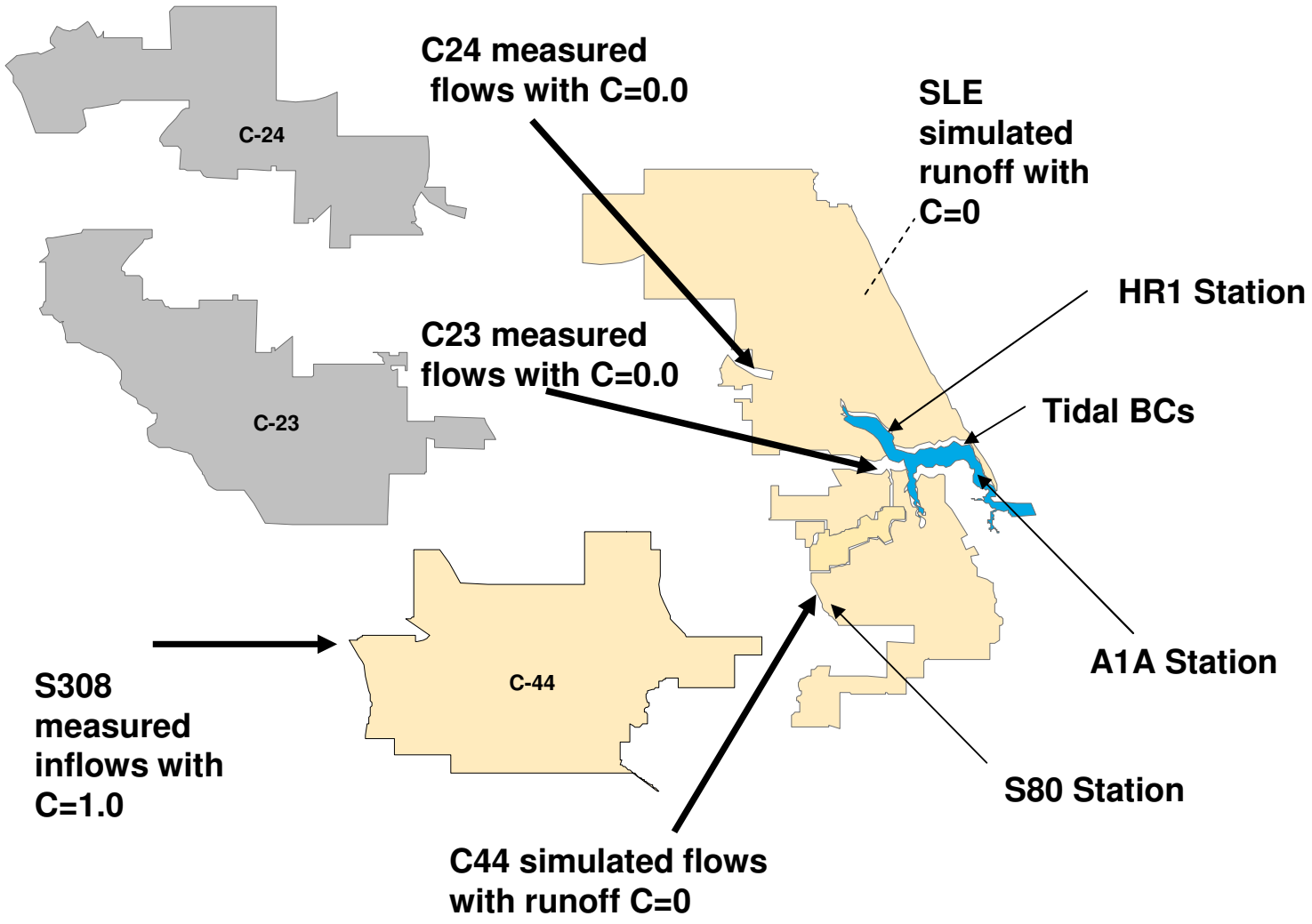

URS

Figure 7.1. Basin Hierarchy for estimating Lake Okeechobee influence on the North Fork in the SLE Model.

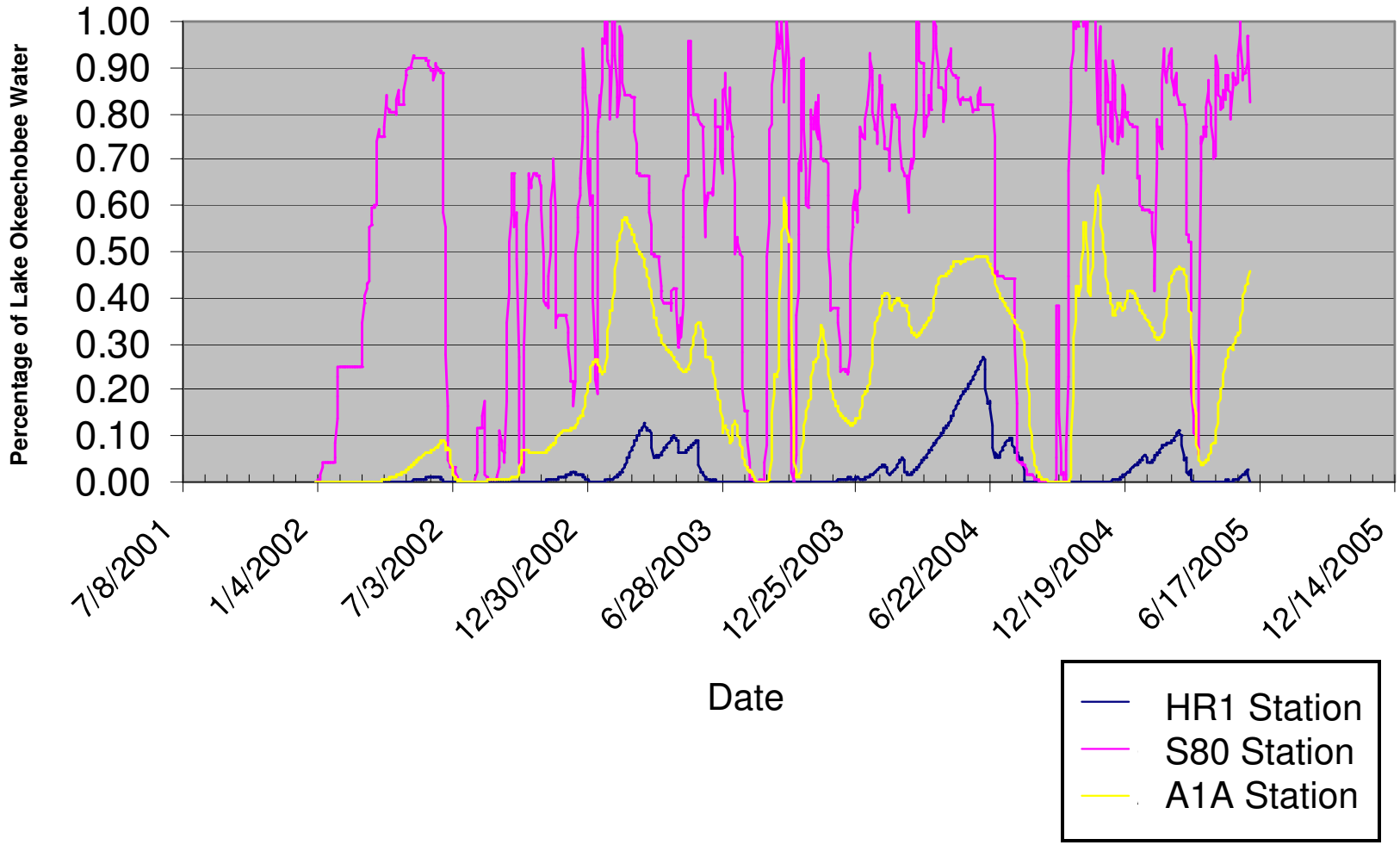

URS

Figure 7.2. Output Concentrations from SLE Model with Lake Okeechobee Influence.

Evaluation of pre-development conditions is a critical step in TMDL development for the quantification of any water quality degradation due to anthropogenic effects. Current nutrient loads can be compared to background or historic levels of nutrients, referred to in this document as "Natural Conditions" or land use prior to any alteration such as agriculture and urbanization. In the St. Lucie Estuary, the entire area consisted of water, wetlands, and forests.

To establish the historic conditions, the land-use was altered to earliest known categories. This was accomplished with aid from two historic land-use maps produced by John Davis of the Florida Geological Survey (FGS) (Figure 8.1). Davis produced maps delineating land-uses for 1943 and 1967. E ach map of land-use was digitized into a GIS coverage. For this study the 1943 data was the preferred dataset for two reasons. The 1943 coverage is the oldest known historic land-use coverage and it is also more detailed than the 1967 coverage.

However, grids for C-24 and SLE basins extend beyond the limits of the 1943 land-use coverage (See Figure 8.1). Therefore, historic land-use from the 1967 map was substituted for the small missing portion at the northernmost part if the basin (see figure 8.1). Table 8.1 defines the crossover each of the land-uses from the 1967 dataset as compared to the 1943 data and with its appropriate 1999 FLUCS Level 3 description and code. Table 8.2 outlines land-use crossover for each land-use and total acreage within each basin.

Table 8-1. Cross-over Map for 1967 to 1943 Land-use Data Set.

1943 Land Use Description	1967 Land Use Description	1999 FLUCS Level 3	FLUCS 3 Code
Pine Flatwood Forests	PINE FLATWOODS	Upland Forests: Pine Flatwoods	411
Pine Flatwood Forests	SAND PINE SCRUB FORESTS	Upland Forests: Pine Flatwoods	411
Wet Prairies	GRASSLANDS OF PRAIRIE TYPE	Wetlands: Wet Praries	643

Table 8-2. Land-use Crossover for each Basin with Acreage and Percentage of Land Within each 2004 FLUCS Level.

		C-24		C-23		C-44		SLE	
1999 FLUCS	1943 Davis Description	Basin Area (Acres)	Land Use Percentage	Basin Area (Acres)	Land Use Percenage	Basin Area (Acres)	Land Use Percentage	Basin Area (Acres)	Land Use Percentage
411	Pine Flatwoods	40,895	46.7	64,261	57.2	78,874	68	125,697	72.9
411	Scrub Forests			942	0.8	124	0.1	3,106	1.8
500	Water					301	0.3		
611	Bay Tree Forests	267	0.3	1,644	1.5				
612	Mangrove Swmps							4,454	2.6
615	Inland Swamps			34	0	2,053	1.8	2,236	1.3
617	Hammock Forests	3,311	3.8	8,276	7.4	6,625	5.7	1,594	0.9
621	Cypress Forests	2,069	2.4	985	0.9	6,837	5.9	1,274	0.7
641	Fresh Water Marsh	20,942	23.9	29,987	26.7	13,140	11.3	9,907	5.7
641	Saw Grass Marh					290	0.3		
643	Wet Prairies	20,148	23	6,196	5.5	7,669	6.6	24,213	14

Figure 8.2 illustrates the GIS land-use coverage for C-24 basin and the adjusted land-use attributed to each grid cell for the basin. The historic land-use was then substituted into the fully calibrated C-24 basin model and the model re-run.

In order to illustrate the significance of altering land-use and its associated nutrient loading, Figure 8.3 contains a time series plot of dissolved oxygen in the C-24 basin comparing the fully-calibrated model with current land-use with the historic land-use.

A comparison of the median TP, TN and D.O. value obtained for the existing conditions and historic models for each basin are shown in Table 8-3. The values at the upland basins C-23, C-24 and C-44 were taken at the basin outfall.

Table 8.3. Comparison of Median Concentrations for Existing and Natural Condition Model Simulations.

	TN		TP		DO-Upper		DO-Lower	
	Existing	Natural	Existing	Natural	Existing	Natural	Existing	Natural
C23	1.37	1.09	0.263	0.0243	5.21	7.71	-	-
C24	1.51	0.965	0.216	0.0274	4.89	7.73	-	-
C44-	1.26	1.13	0.12	0.0291	6.68	7.20	-	-
C44 with Lake	1.47	1.52	0.151	0.107	6.46	6.76	-	-
SLE-HR1	1.13	0.995	0.181	0.0278	7.63	7.82	4.815	5.67

The general trend for the C-23 and C-24 basins is a reduction in both TN and TP that are reflective of the changes in the ABMC values associated with land use changes in the Natural Conditions model. The Natural Conditions model is comprised mostly of forest and wetlands, both of which were a much smaller portion of the existing conditions models. The forest and wetlands TN ABMC values are 0.88 and 0.94 mg/L while the values for the existing conditions model land uses, such as citrus and urban categories, are on the order of 1.0 to 1.5 mg/L. Similarly, the ABMC values for TP for forest and wetlands are 0.097 and 0.017 mg/L whereas typical citrus and urban values are 0.217 and 0.15. As the nutrient loads are reduced in the Natural Conditions simulation due to the large forest and wetlands areas, the high phytoplankton growth seen in the existing conditions simulations is limited and the D.O. therefore increases. The effect of reduced nutrients is also evident in the C-44 (without Lake) but the increased D.O. is less than for the C-23 and C-24 basin simulations. This result is due to the larger D.O. value in the C-44 basin for the existing conditions model. The effect of the Natural Conditions simulation is least evident in the C-44 basin model with the Lake included. The Lake discharges account for a significant load through the C-44 canal, and therefore the effect of lower nutrient runoff loads in the C-44 basin are less evident. The results for the SLE model at the HR1 station are similar to those of the upland basins. The increase in the lower layer D.O. is more significant than the upper layer because the lower layer D.O. is much lower in the existing conditions simulation.

The nutrient and CBOD loads for each basin have been calculated based on the 10 year simulations period 1995-2000 using the daily flow and concentration outputs from each mode. The loads are shown in Table 8-4.

Table 8-4. Historic or "Natural Conditions" Nutrient Load Calculations for each Basin in the SLEW.

Basin	TN (tons/year)	TP (tons/year)	CBODu (tons/year)
C23	176	7.4	239
C24	225	7.7	55.2
C44	184	8.2	325
C44 with Lake	1200	115	1400
North Fork	508	18.4	707.6
South Fork (Tidal St. Lucie)	768	62.5	833.4
Bessey (Basin 4)	99.2	7.78	96.9
Danforth (Basin 6)	17.9	0.86	24.7

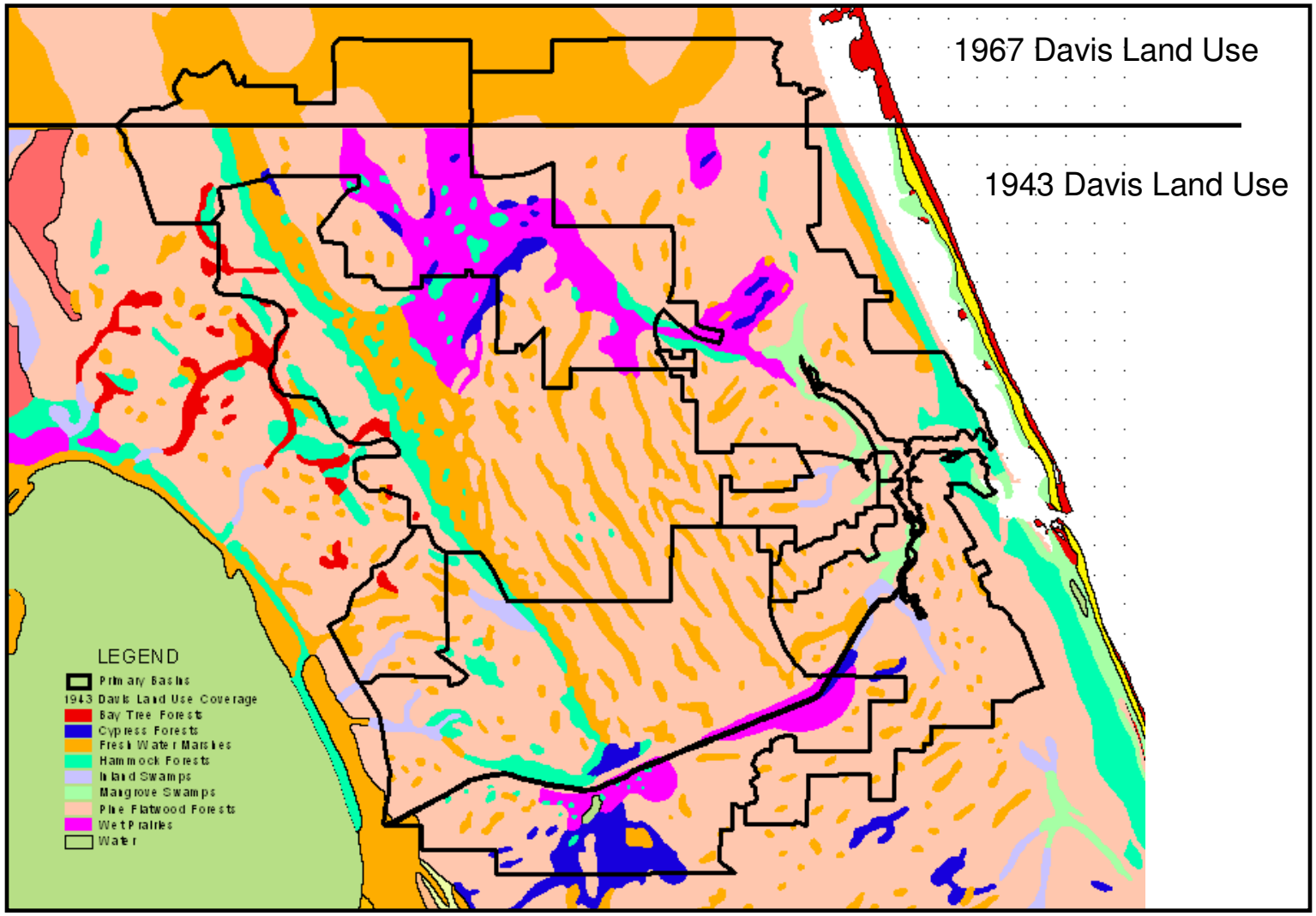

URS

Figure 8-1. Historic Land-use for SLE Model Domain Combined 1943 Davis Coverage and 1967 Davis Coverage.

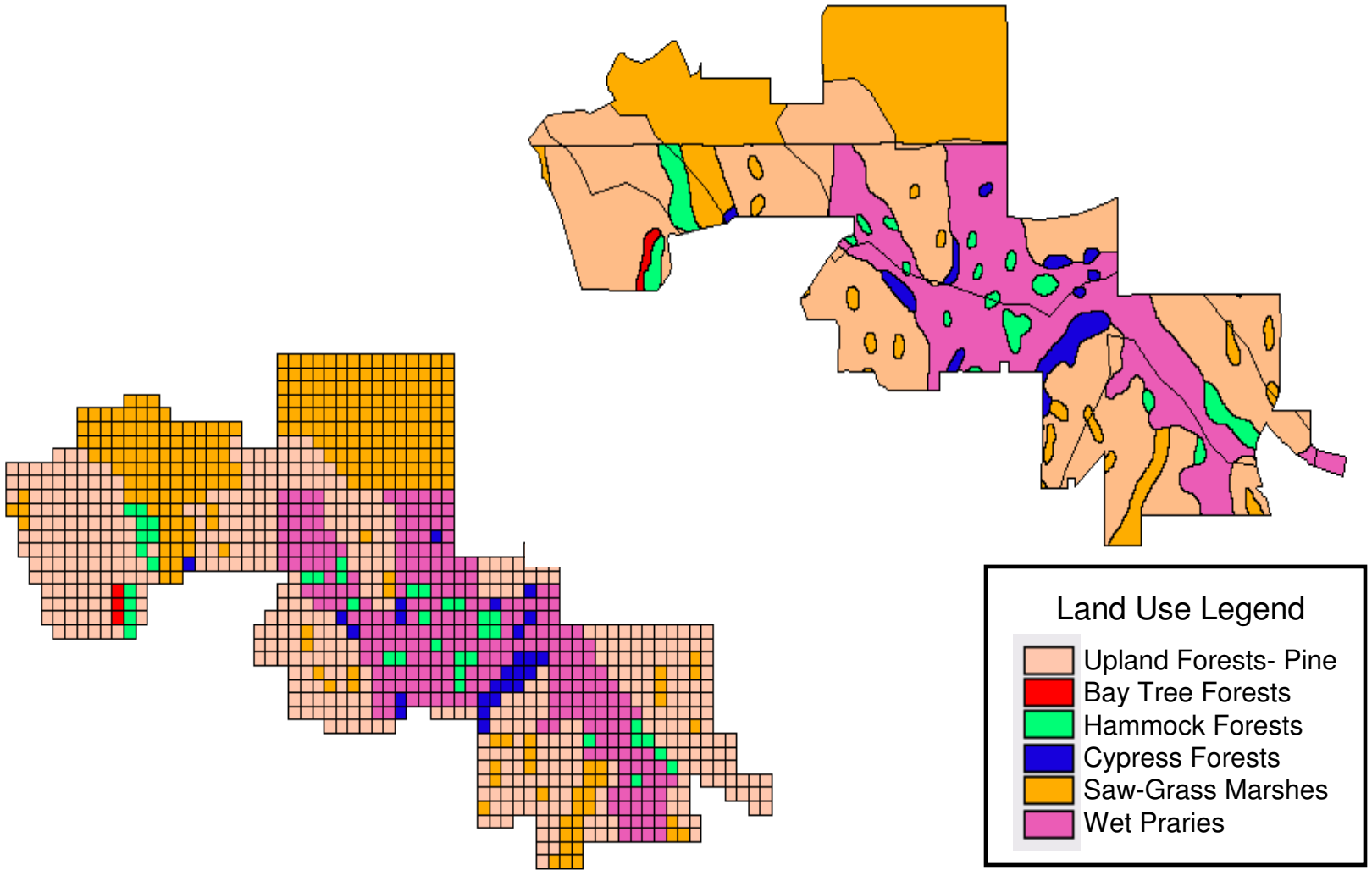

URS

Figure 8-2. Historic Land-use for C-24 Basin - GIS Coverage (top-right) and Adjusted Grid Coverage (bottom-left).

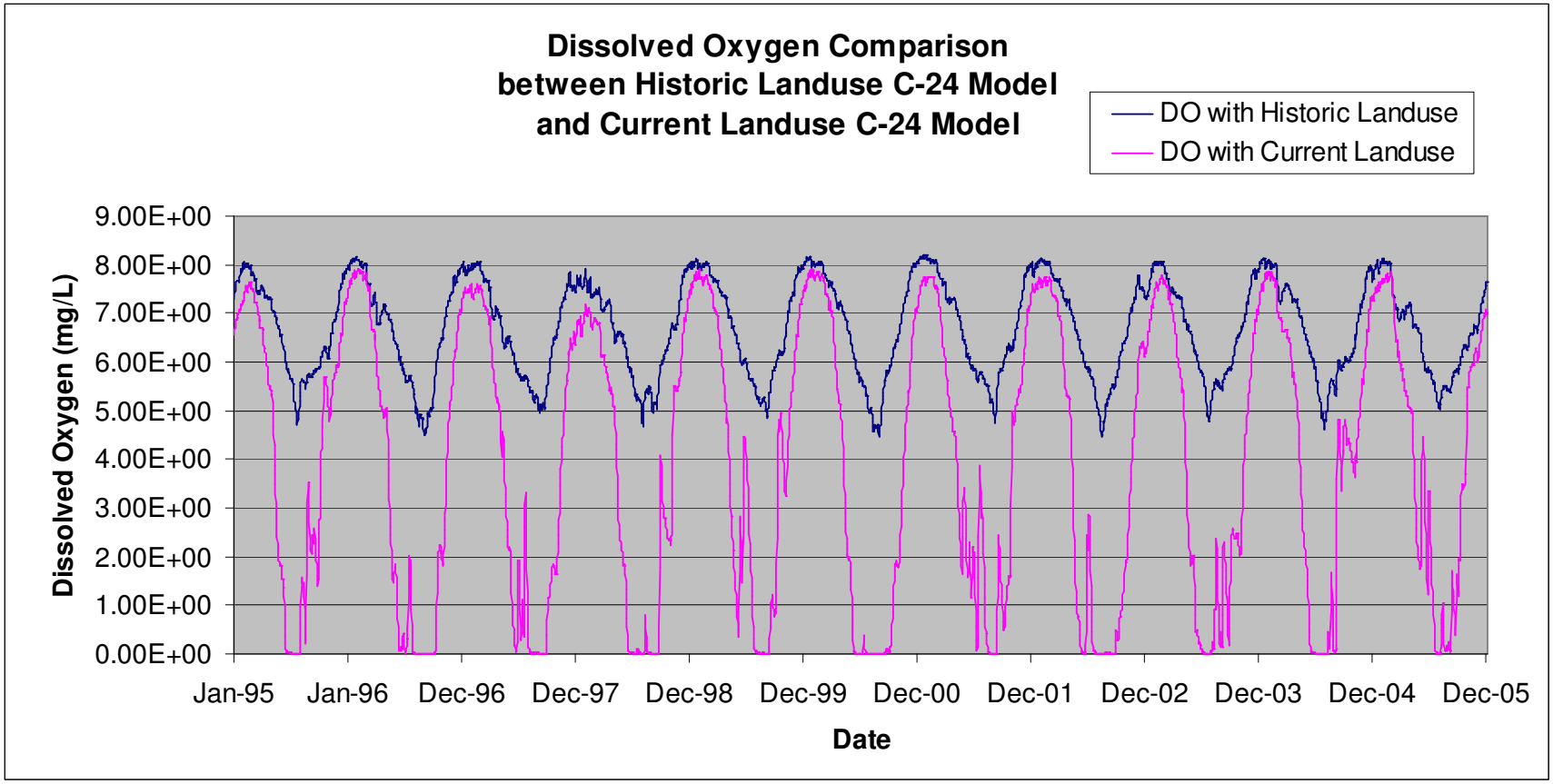

URS

Figure 8.3. C-24 Basin model output for Current Land-use and Historic Land-use Conditions.

9.1 UNRESOLVED DATA GAPS/NEEDS

Understanding and modeling of a watershed system relies on accurate measured data that can be used to configure, force and calibrate the model. Although there has been a large amount of flow and water quality data collected over the last 4 decades, some of the data can be improved by:

(1) expanding the extent of the measurements

(2) increasing the frequency of the data measurements

(3) making synoptic measurements to bound key model parameters

In the effort of gaining a more complete picture of the forces at work in the SLE, some data gaps have been identified. Table 9-1 lists these data gaps with explanatory information.

Table 9-1. Data Gaps in SLE Datasets.

Data Need	Current Data Available	Spatial Extent	Temporal Extent	Notes
SOD in Estuary	4 stations, spring, summer of one year	delineation of muck bottom and stations in thalwag and shallower bank areas, upstream middle and end of each estuary section	Winter Season and Summer Season	chemical composition for nutrients should be taken at each sampling site
SOD in Upland Basins	none	along main sections of primary canals	Winter Season and Summer Season	chemical composition for nutrients should be taken at each sampling site
BOD_5 in Estuary	~20 samples taken in April of 2006	establish BOD measurements at existing stations	same frequency (monthly) for existing stations	periodically, need to establish relationship between BOD_5 and BOD_u
BOD_5 in Upland Basins	none	establish BOD measurements at existing upper basin stations	same frequency (monthly) for existing stations	
$CBOD_5$	none	estuary and upland basins	peridocially	To establish ratio of $CBOD_5$ to BOD_5 for separately for terrestrial sources and in-stream (i.e. algae) sources
Chla - Upland Basins	none	need to establish BOD measurements at existing stations	same frequency (monthly) for existing stations	To differentiate between green and green-blue algae

Data Need	Current Data Available	Spatial Extent	Temporal Extent	Notes
D.O. in Canals C24, C23, C44, S308	surface measurements	surface and near bottom measurements at existing stations	same sampling period (monthly) as existing stations	
High-frequency DO Canals C24, C23, C44	only monthly surface samples	upstream of structures in primary canals - surface and near bottom	two week period each in winter and summer	To stablish diurnal D.O. variation in wet and dry seasons
Flow data in ungaged drainage areas (Estuary)	for estuary - we used salinity as calibration rather than flow since there was not flow data	flow measurements at upstream end of north fork, south fork, and downstream of confluence	3 measurements in wet season - each capturing run-off event and one measurement in low or no-flow dry season (baseflow)	In consideration of tide phase (spring and/or neap) at time of measurement
Refractory and labile components of particulate P_{org} and N_{org}	none	estuary and upland basins	peridocially	To establish fractions of labile and refractory components

A watershed water quality model has been configured, calibrated and validated for the SLE watershed. The modeling approach is based on the "watershed approach" suggested by the Environmental Protection Agency (USEPA) (USEPA, 2004) and adopted by the FDEP. The ater quality simulation represents the physical processes affecting the water dissolved oxygen, BOD and chlorophyll in St. Lucie Estuary. The model provides an integrated approach, and provides the FDEP with a calibrated tool for evaluating existing and future condition in the SLEW and SLE.

The WaSh model was been used for the hydrodynamic and water quality analysis of the St. Lucie Estuary Watershed. The WaSh model is a hydrologic, hydrodynamic and water quality model originally developed for the unique hydrologic conditions in south Florida. Additionally, the WaSh model was previously configured and applied to basins draining to the SLE for previous hydrodynamic studies conducted by the South Florida Water Management District. Building on the existing hydrodynamic framework, many updates to the models were developed, such as:

- Update of land-use classifications
- Site-specific, aerial-based mean concentrations were developed and implemented
- The simulation of tidal flows in the SLE was implemented
- A water quality simulation was included

Four separate but linked models were developed to represent the entire SLE watershed. Three separate models were configured for the C-23, C-24 and C-44 basins each of which is separated form the tidal portion of the SLE by gated structures. The outputs from these models are used as flow and load inputs into the SLE basin model. The SLE basin model includes all of tidally-connected portions of the SLE, as well as the area of the North Fork basin upland of the Gordy Road Structure.

The flow calibration consisted of comparisons of daily flow measurements over a six year period of 1995-2000 for the upland basins, and for the SLE model, it consisted of comparisons to monthly salinity data for a three year period of 2003-2005. The water quality module was calibrated by comparing model simulation output to measured monthly nutrient, D.O. and chlorophyll data for the same six year period. Subsequent validation was conducted for the consecutive five year period of 2001-2005.

The general results of the hydrodynamic calibration were good. The annual variations and seasonal trends were simulated well. The Pearson Correlation Coefficient typically was on the order of 0.7 and the RMS errors for the daily flow were in the range of 15% of the full range. The large period of zero-flow days that are due to the presence of the gated structures and the highly management hydrologic system was also well represented. The calibration metrics for the C-44 basin were on the average less accurate than those for the other two basins, but is likely due to the influence of the Lake discharges on the measured data. The measured data for the C-44 basin at the S-80 structure required extensive modification to attempt to remove the influence of the Lake discharges through the C-44 canal, and therefore the ability of the measured data to represent the true discharges from the C-44 basin were compromised.

The comparison of simulated and measured time series plots for the water quality data show generally good agreement. The strong seasonal trends evident in the D.O. and the phosphorus data were well represented in the model simulations. The results for the upland basins tended to be better than those for the estuary stations, which reflect the more complex physics associated with estuarine systems. A comparison of the 25^{th}, 50^{th} and 75^{th} percentile and mean values for DO, TN and TP indicate that the full range of values over the 11-year period is simulated properly by the model. The RMS error for the daily values indicates errors of 22% for TN, of 50% for TP and 23% for D.O. The Pearson Correlation Coefficients for the water quality simulations ranged between 0.23 to 0.74 for the upland basins and between 0.146 and 0.812 for the SLE basin simulation. There is a larger range in the Pearson Correlation Coefficients for the water quality calibrations than for the hydrologic simulation calibration. These results reflect the use of EMC inputs values despite the high variability evident in the measured water quality used to develop the EMC values.

Chris Wilson and Brian Boman, Characterization of Agrichemical and Nutrient Loading in Runoff from Pastures, Golf Courses, and Urban Areas: Final Report: Phase I,FDEP Contract# SP576, Funded by: The St. Lucie River Issues Team. Prepared by: UF/IFAS Indian River Research and Education Center.

Florida Department of Environmental Protection: Division of Water Resource Management, Group 2 Basin Status Report, St. Lucie and Loxahatchee

Physical Monitoring And Numerical Modeling Analysis to Support the St. Lucie Inlet Management Plan, Martin County, FL, Prepared for: Martin County Public Services Department, Prepared by: J. Ramsey, T. Ruthven, M. Osler, S. Kelley, M. Byrnes, K. Kremkau,C. Bryant

ERD, 2003. Evaluation of Alternative Stormwater Regulations for Southwest Florida, Submitted to: Water Enhancement & restoration Coalition, Inc., August.

GIS Data Distribution, South Florida Water Management District. *http://spatial1.sfwmd.gov/sfwmdxwebdc/dataview.asp*

Harper, Harvey H. 1992. Estimation of stormwater loading rate parameters for central and south Florida. Environmental Research & Design, Inc., Orlando, FL.

Harper, Harvey H. 1994. Stormwater loading rate parameters for central and south Florida. 3rd rev. edition. Environmental Research & Design, Inc., Orlando, FL.

Harper, Harvey H 2003. Evaluation of Alternative Stormwater Regulations for Southwest Florida, Final report. Revised Sept. 8, 2003. Environmental Research and Design, Inc., Orlando, FL.

Krupa, Steve 4/6/2006, South Florida Water Management District Study Specific Survey for the St. Lucie Estuary and Indian River Lagoon, Groundwater/Surface Water Interaction Study, Survey Compilation Date: July 23, 2003, Created for Cynthia Gefvert.

SFWMD Environmental Database, DBHydro Browser. *http://www.sfwmd.gov/site/index.php?id=38.*

URS, 2008. WaSh Model Application Guide, prepared for South Florida Water Management District, May.

URS, 2008. WaSh Model User's Manual, prepared for South Florida Water Management District, August.

URS, 2008. WaSh Model Theory Documentation, prepared for South Florida Water Management District, October.

U.S.E.P.A, 1997. Technical Guidance Manual for Developing Total Maximum Daily Loads, Book II: Streams and Rivers, Part 1: Biochemical Oxygen Demand/Dissolved Oxygen and Nutrients/Eutrophication.

URS, 2003 Saint Lucie Estuary Watershed Water Quality Model, Phase II and III, Prepared for: South Florida Water Management District, July 24.

Appendix A
Measured Water Quality Data For Upland Basins And Estuary Stations

Appendix A
Measured Water Quality Data For Upland Basins And Estuary Stations

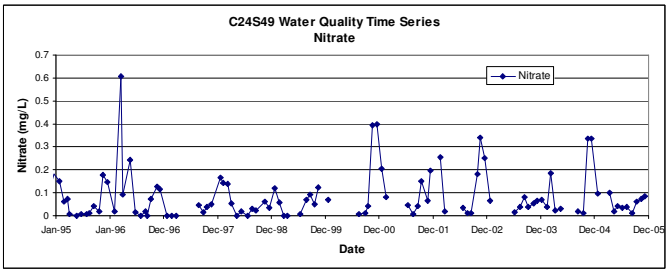

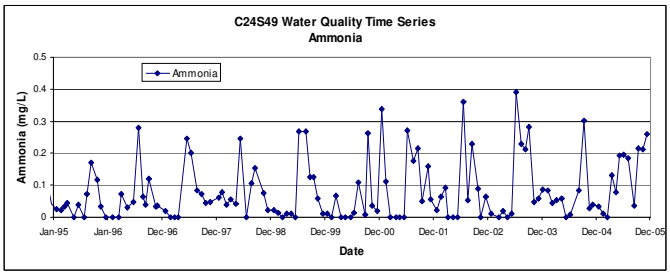

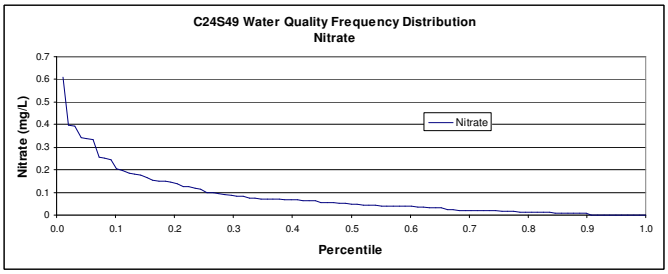

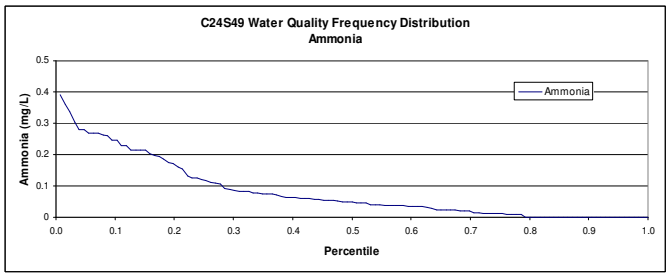

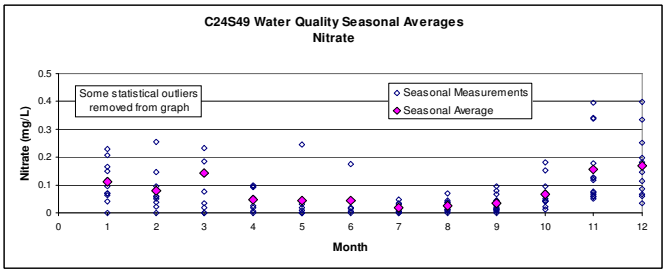

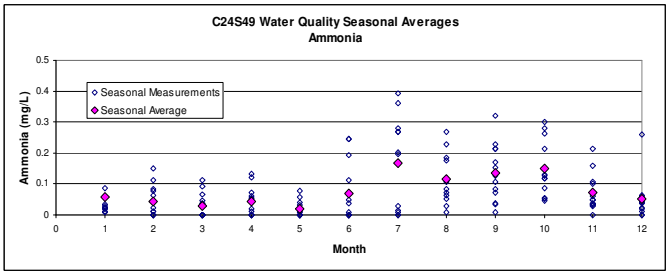

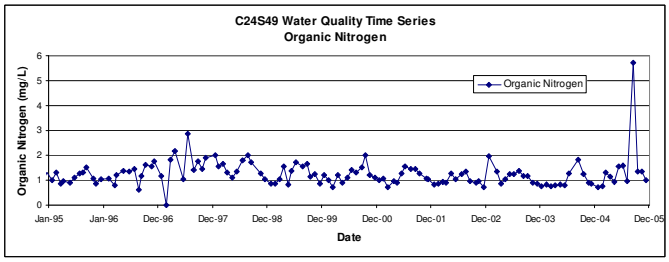

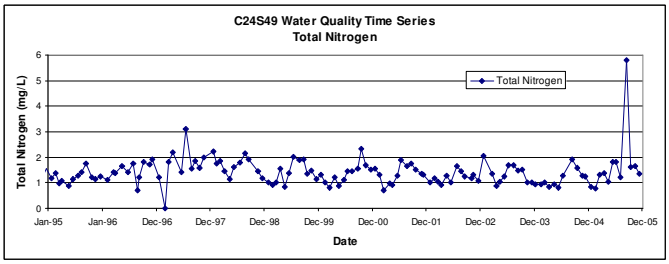

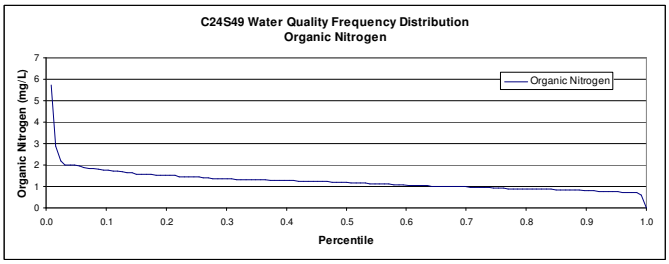

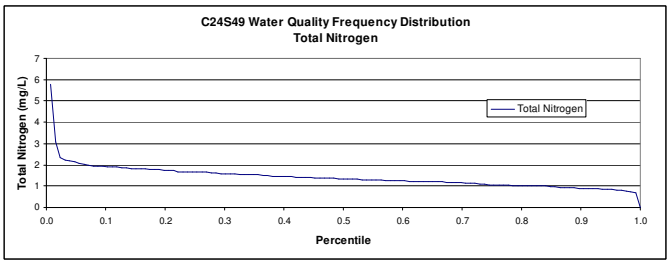

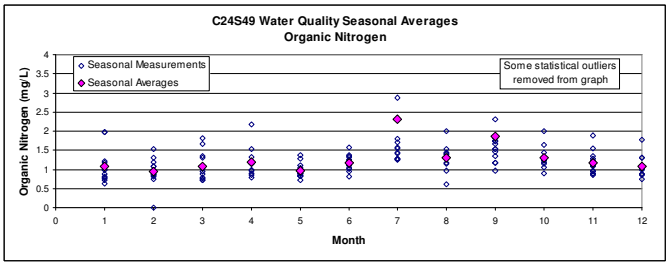

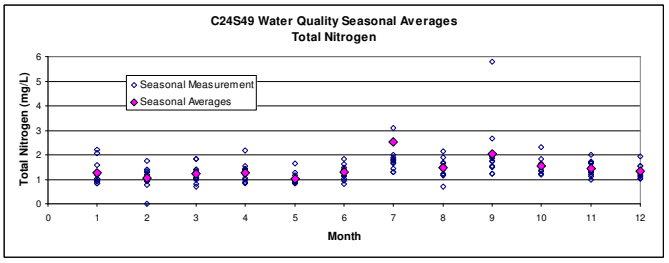

Figure A.1 C-24 Water Quality Data

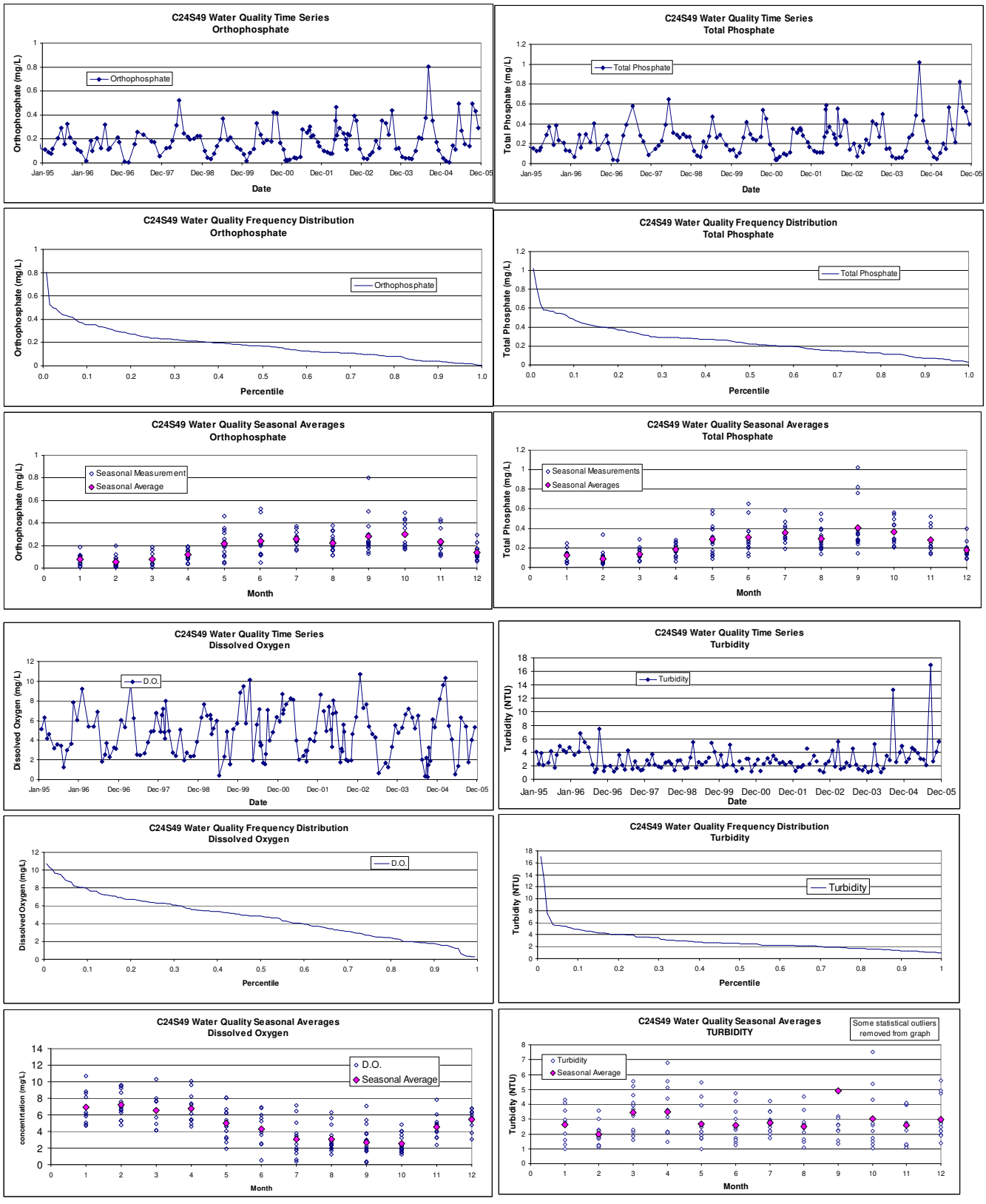

Figure A.1 C-24 Water Quality Data. (cont'd)

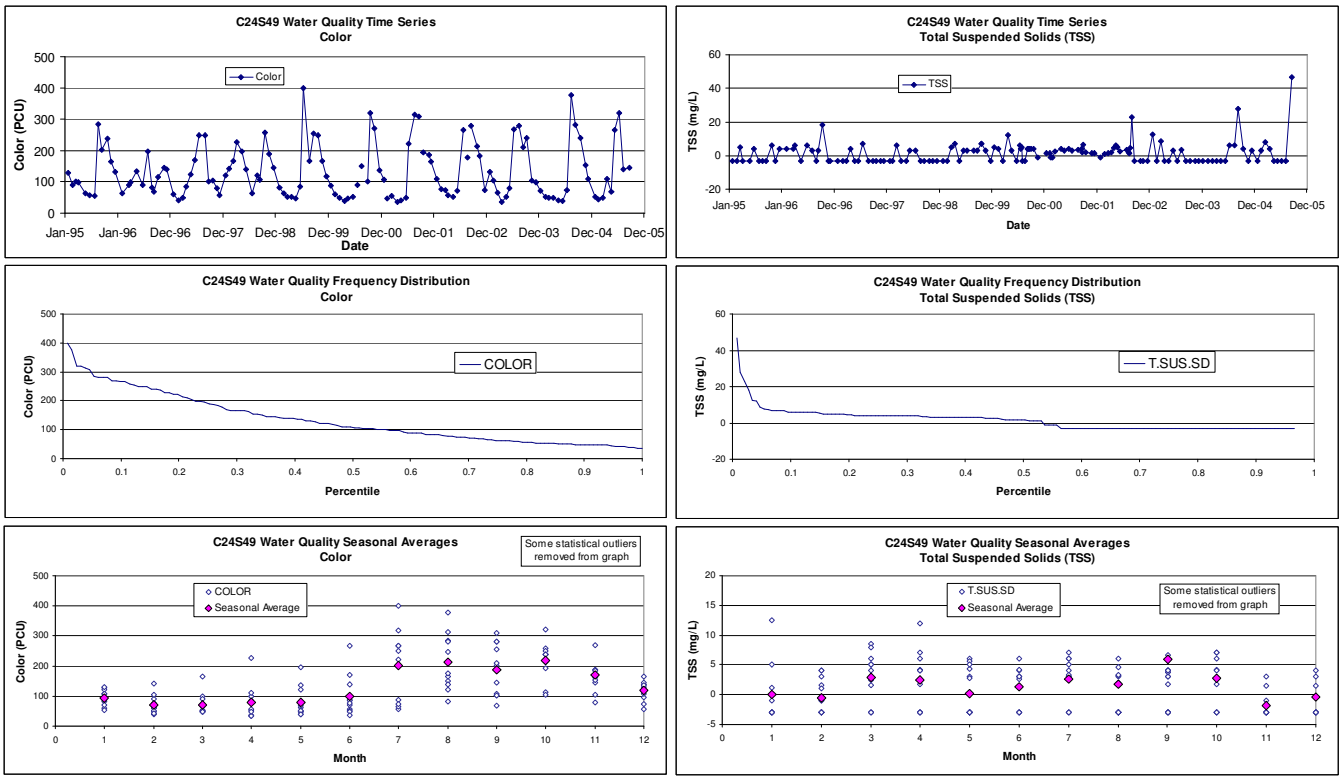

Figure A.1 C-24 Water Quality Data (cont'd)

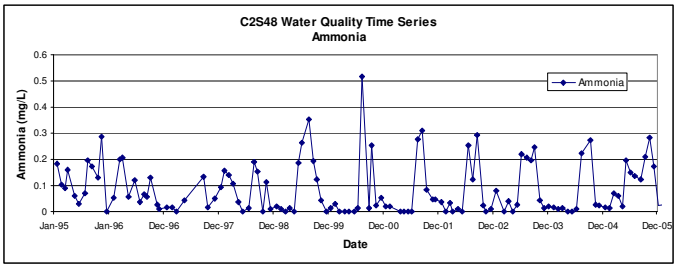

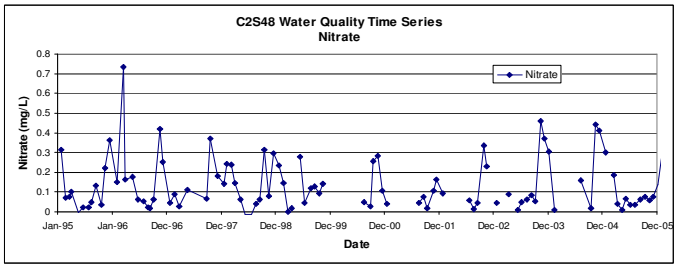

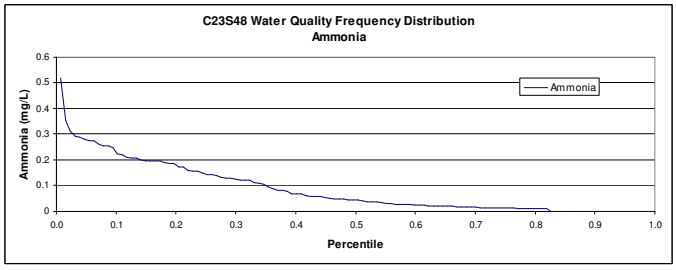

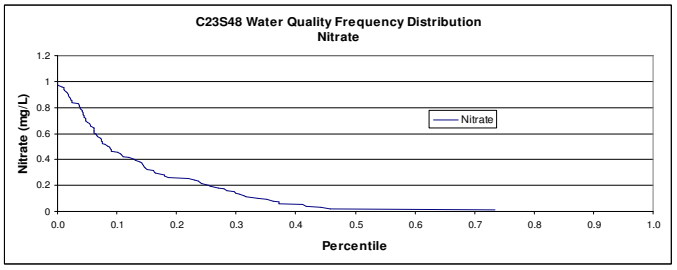

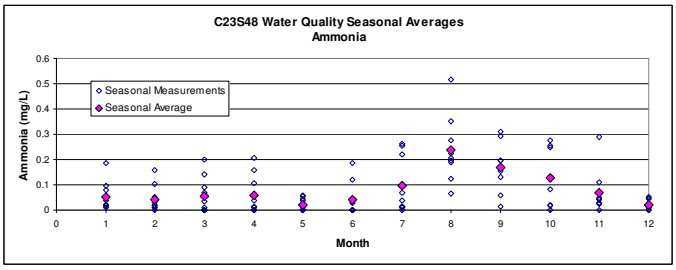

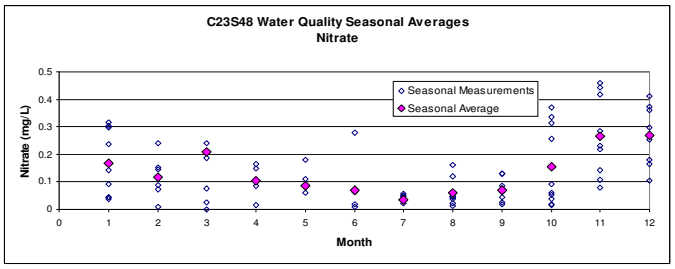

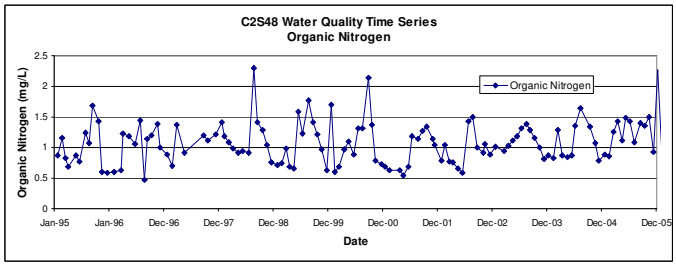

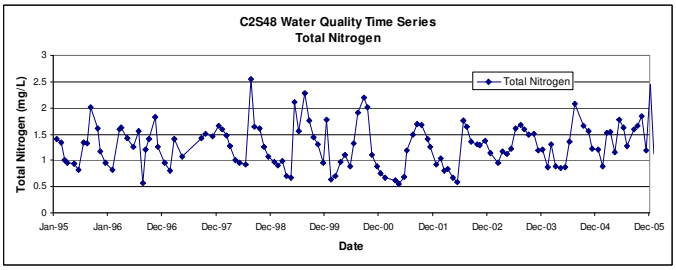

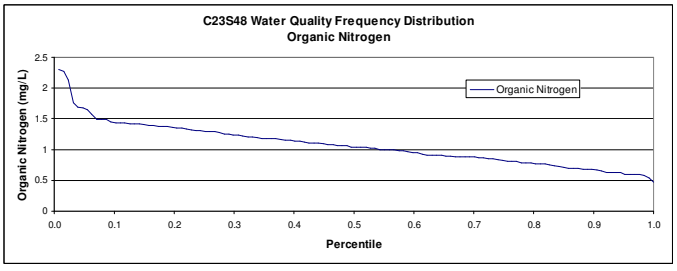

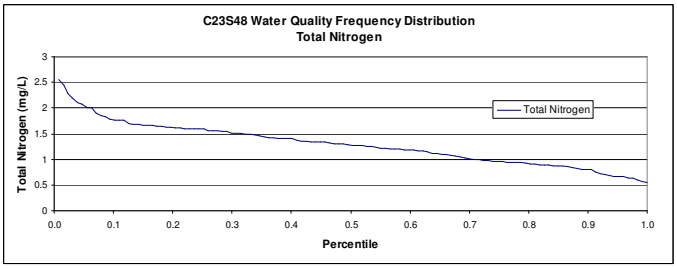

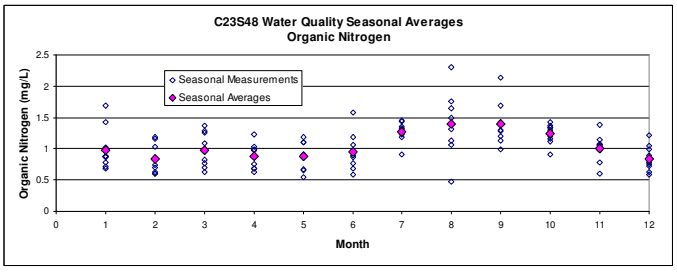

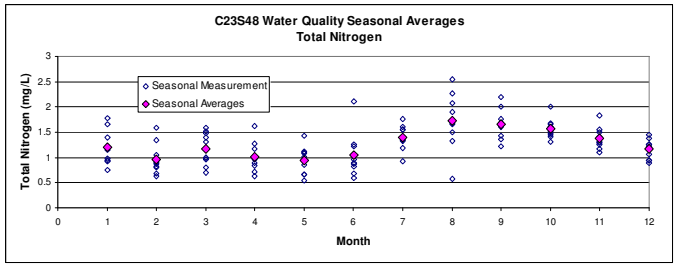

Figure A.2 C-23 Water Quality Data

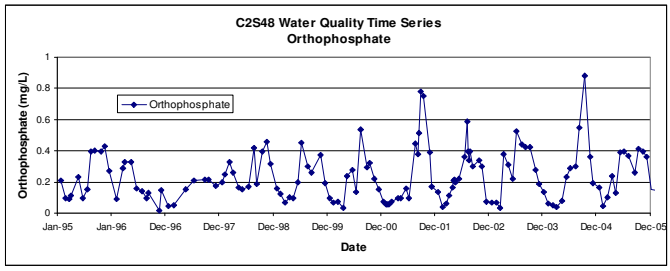

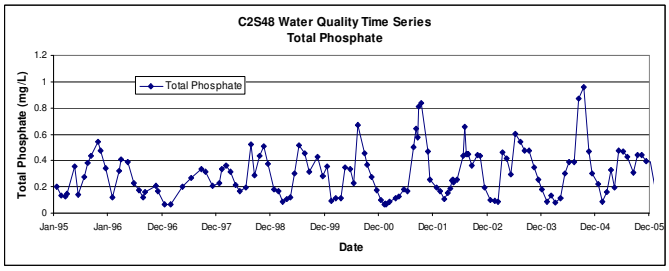

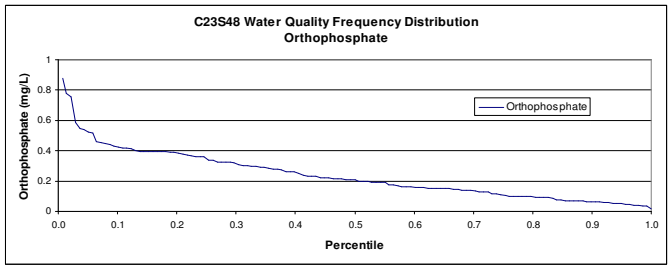

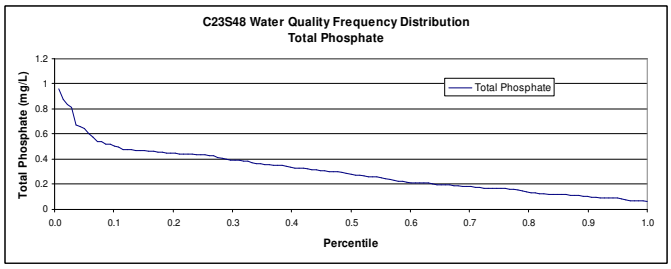

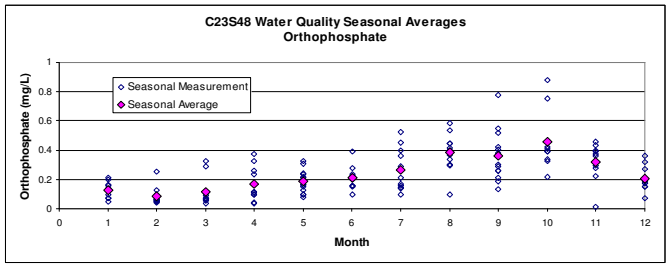

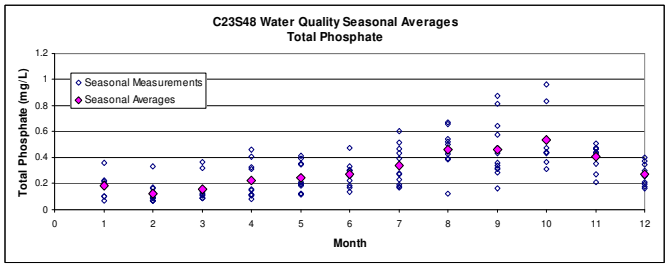

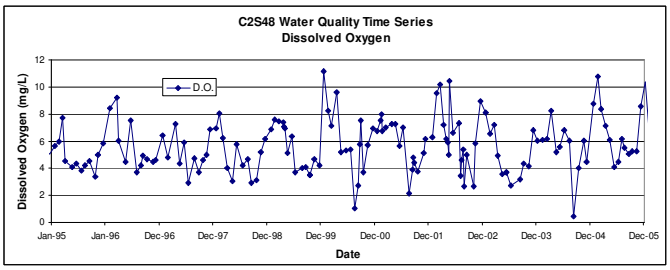

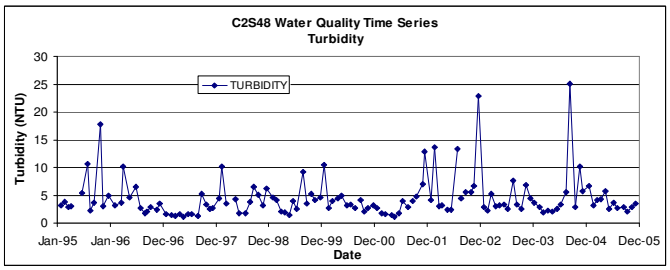

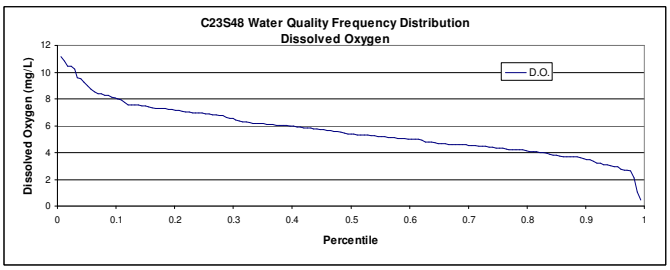

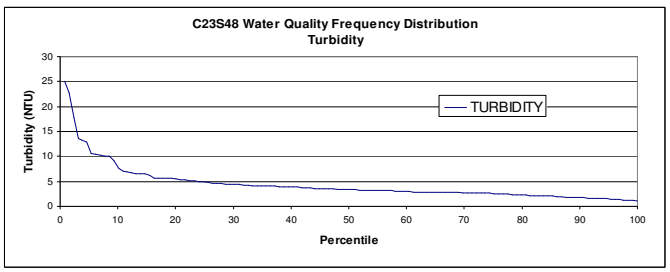

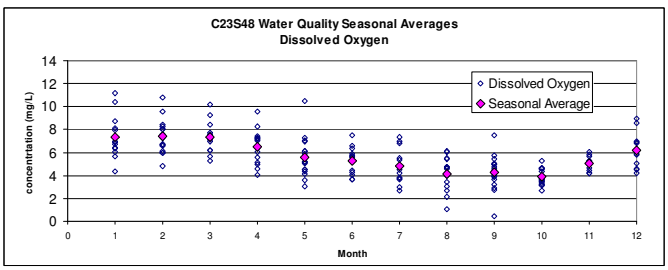

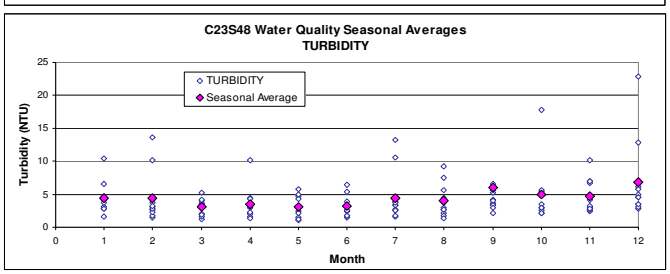

Figure A.2 C-23 Water Quality Data. (cont'd)

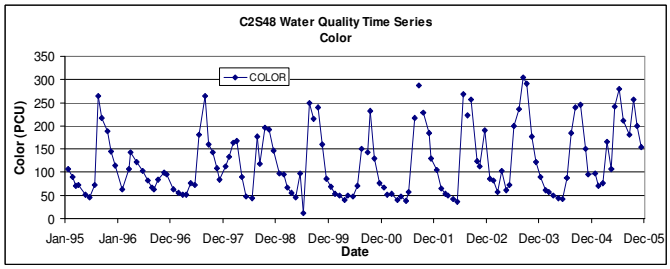

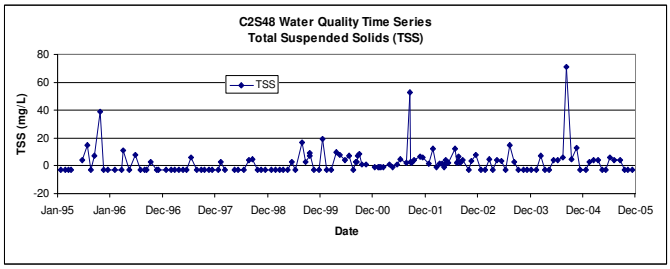

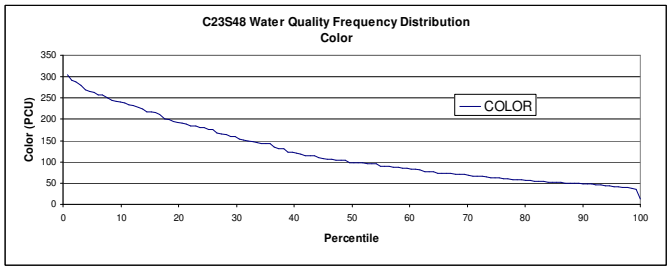

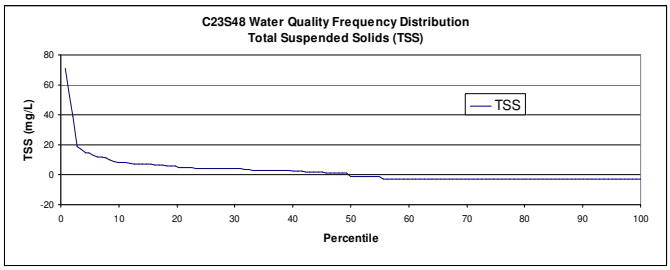

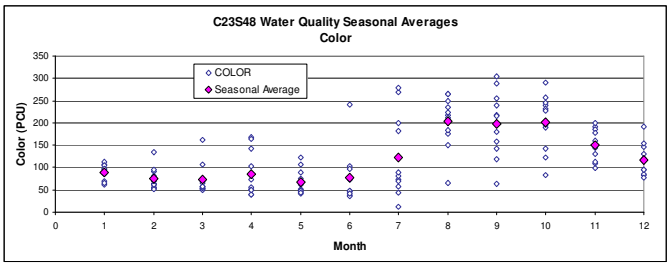

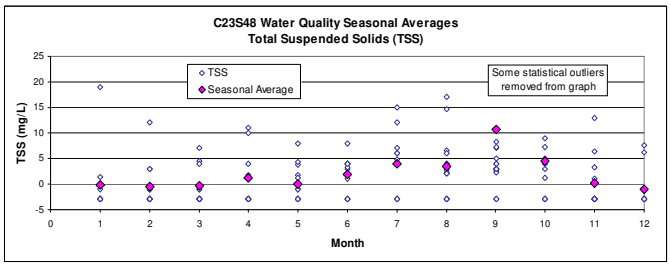

Figure A.2 C-23 Water Quality Data (cont'd)

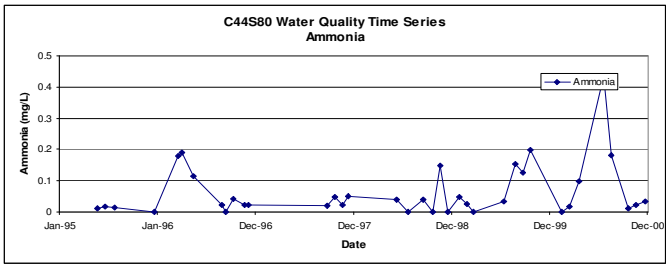

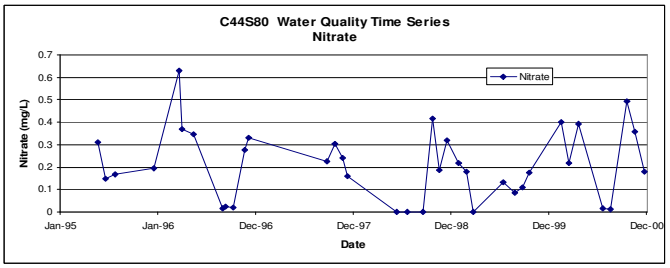

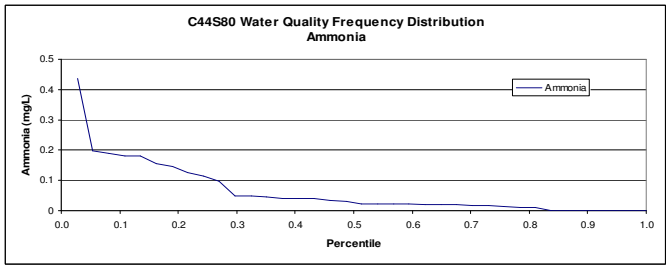

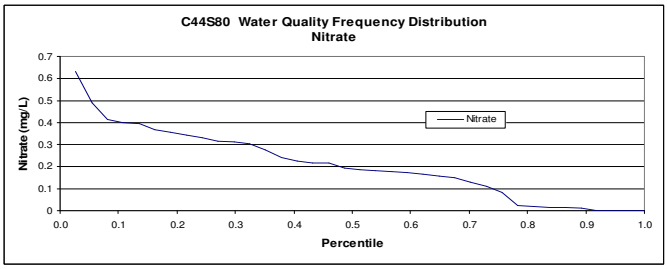

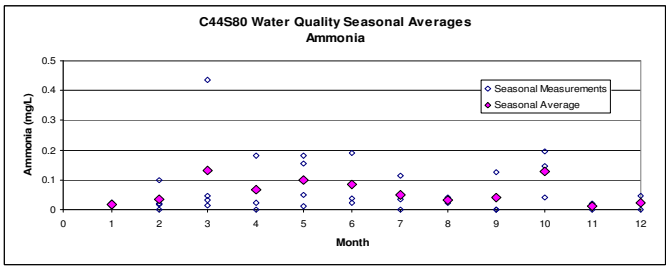

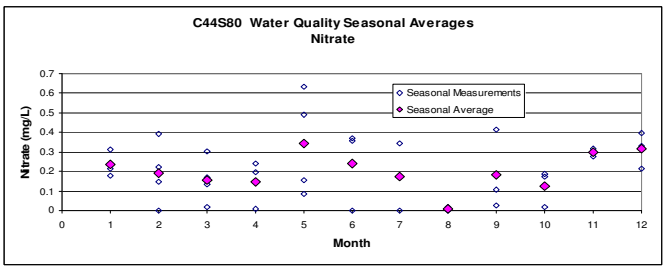

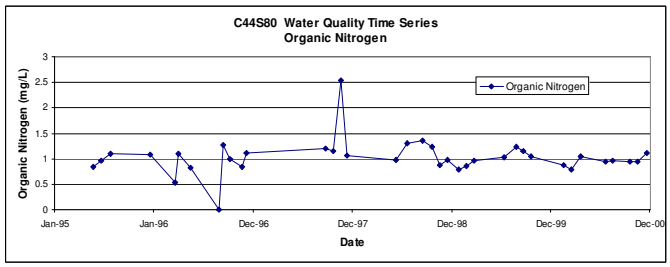

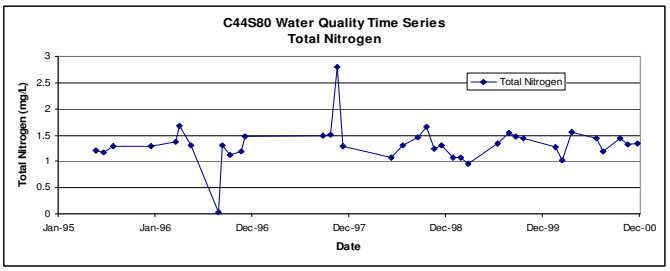

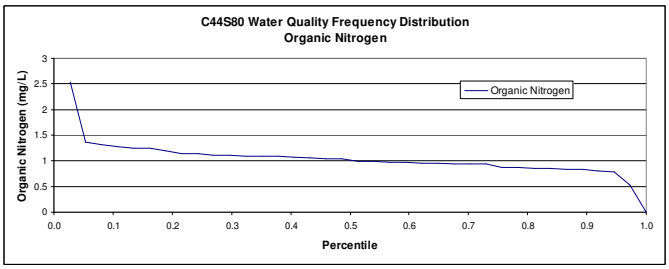

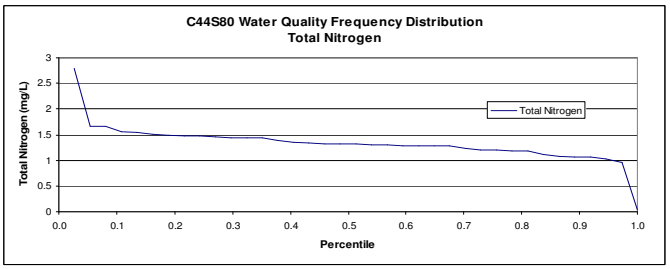

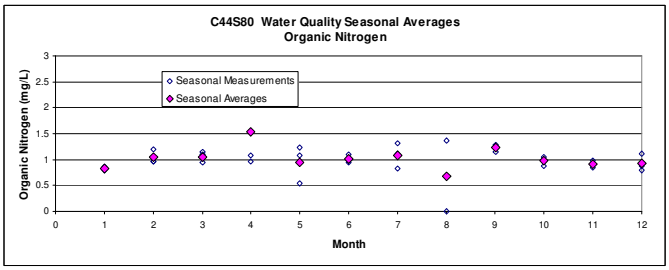

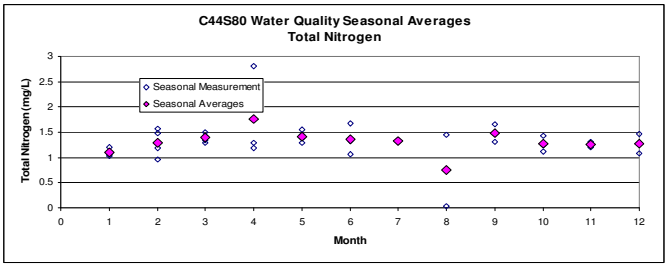

Figure A.3 C-44 Water Quality Data.

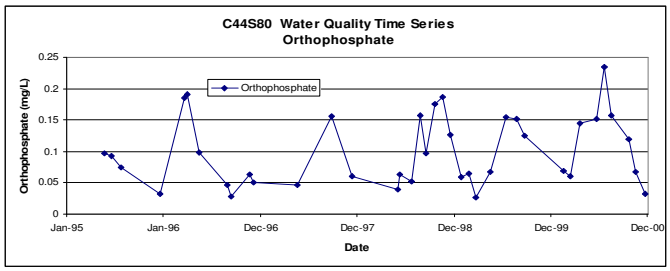

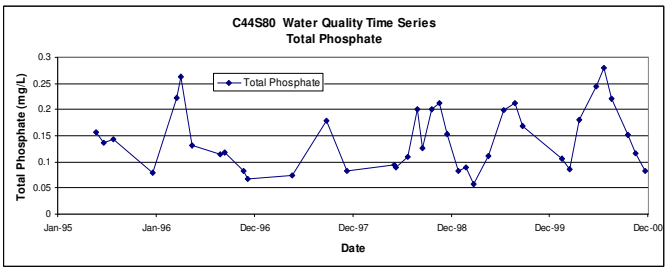

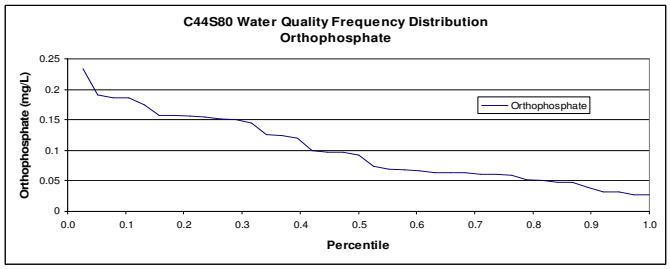

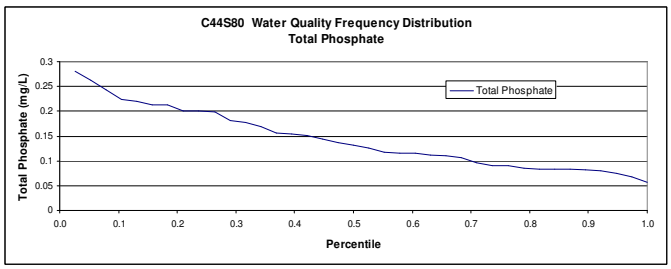

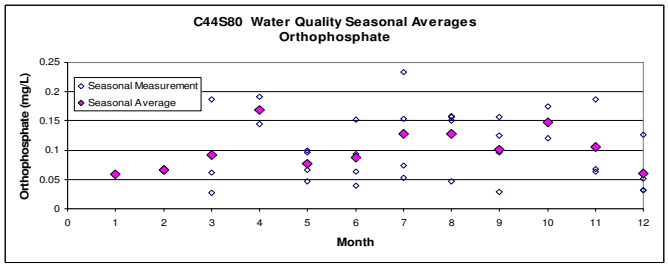

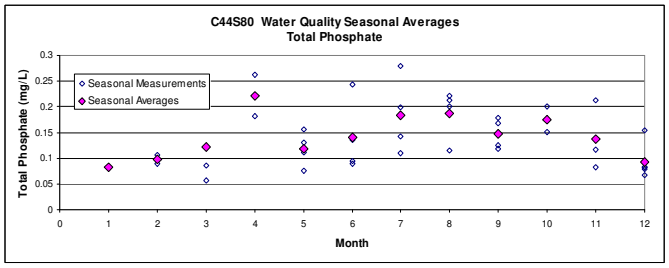

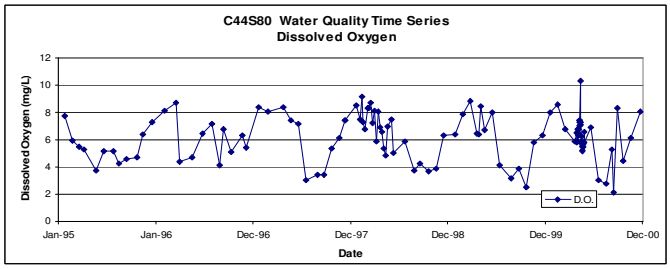

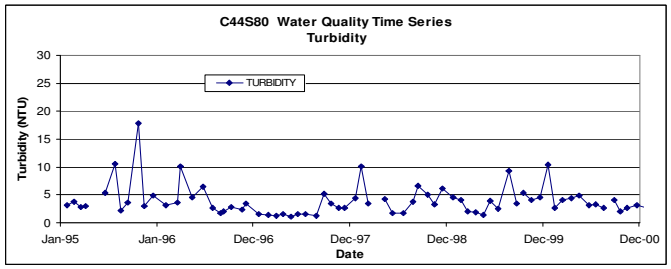

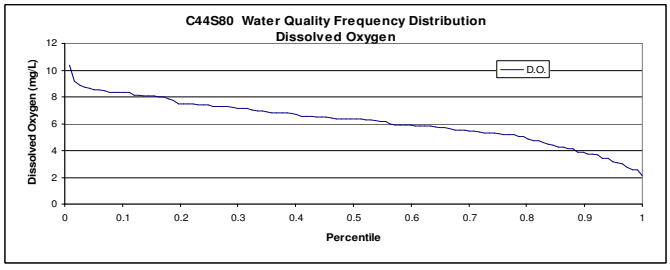

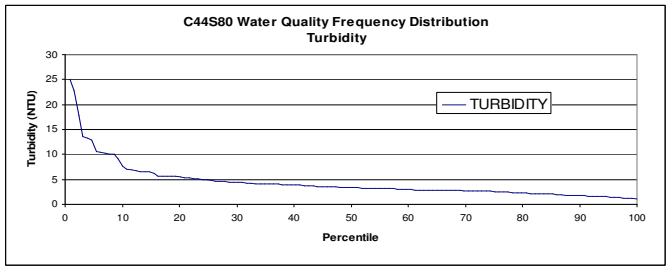

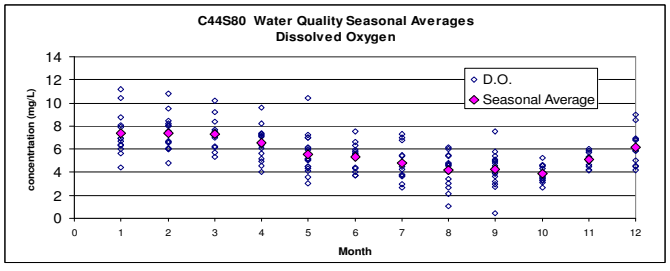

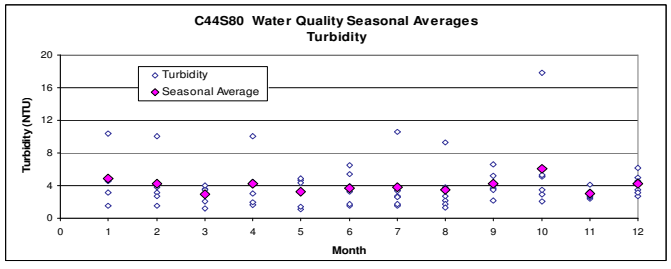

Figure A.3 C-44 Water Quality Data (cont'd)

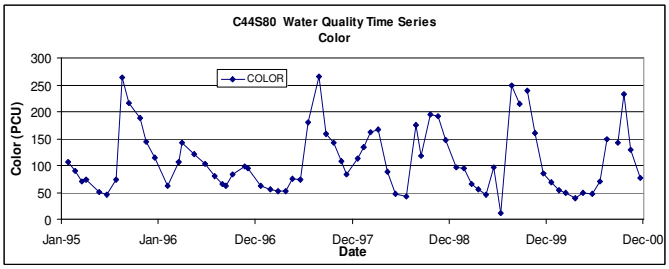

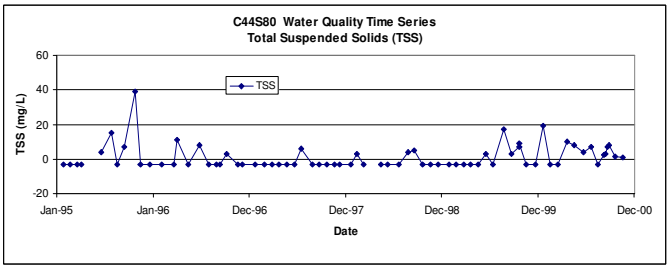

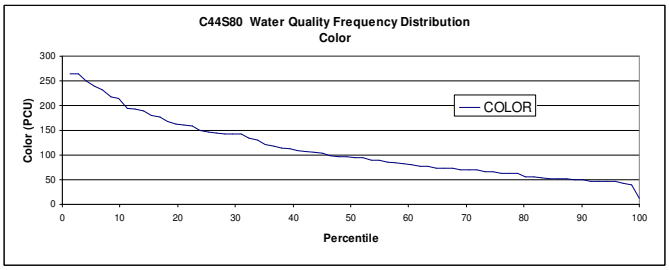

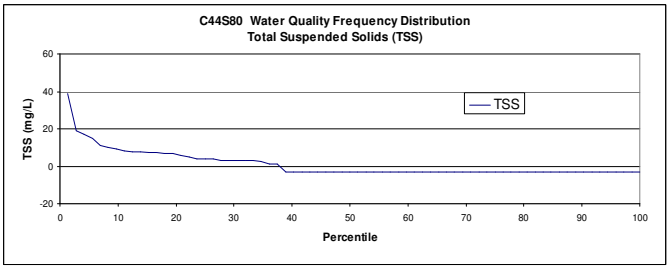

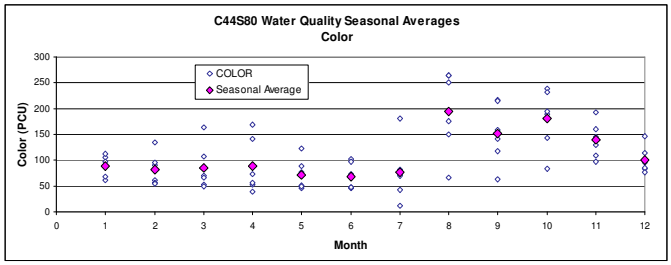

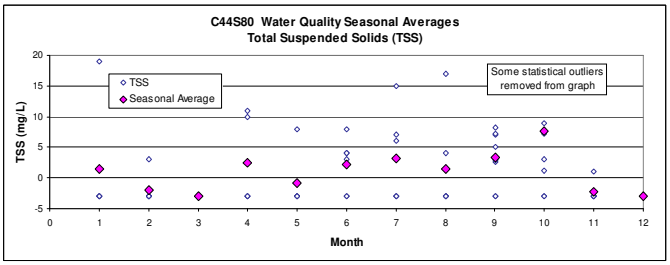

Figure A.3 C-44 Water Quality Data (cont'd)

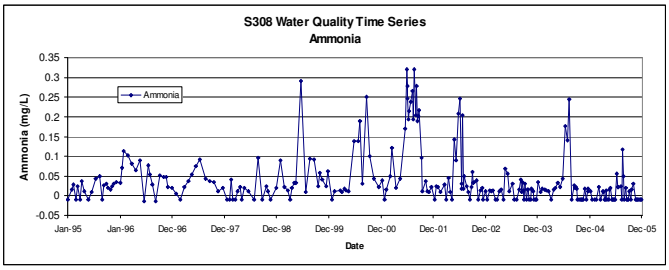

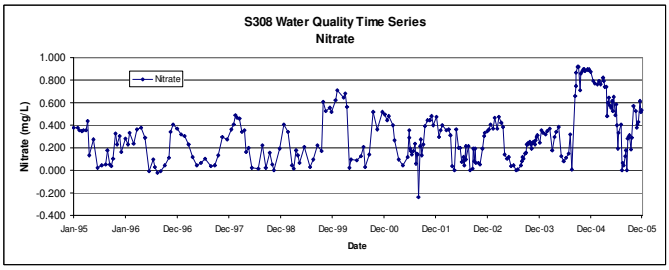

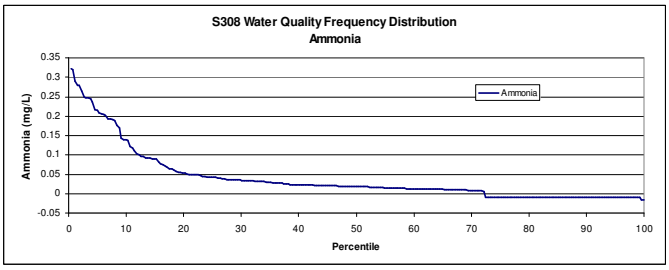

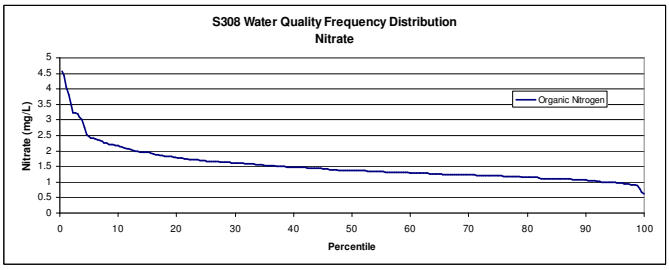

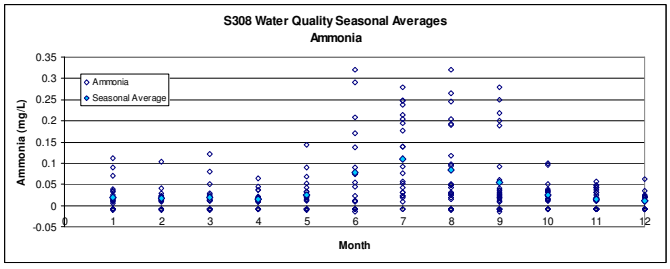

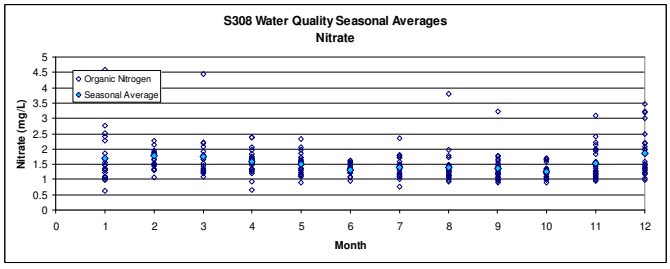

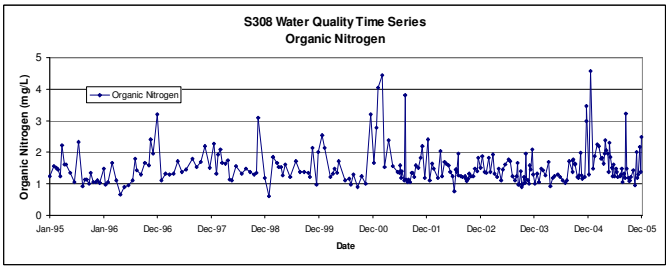

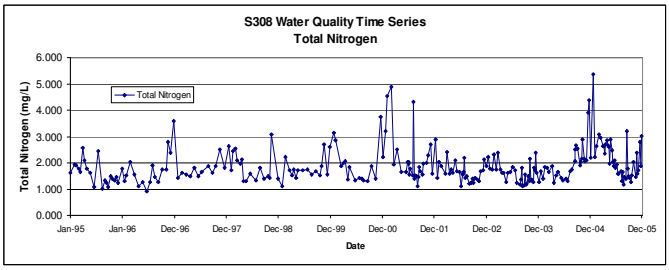

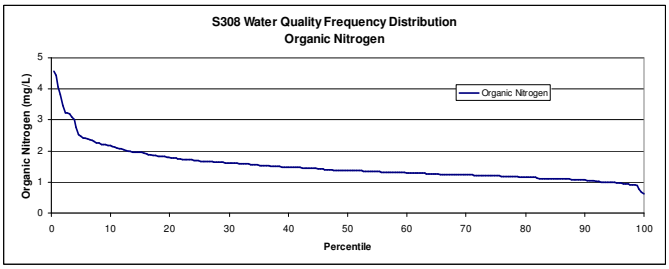

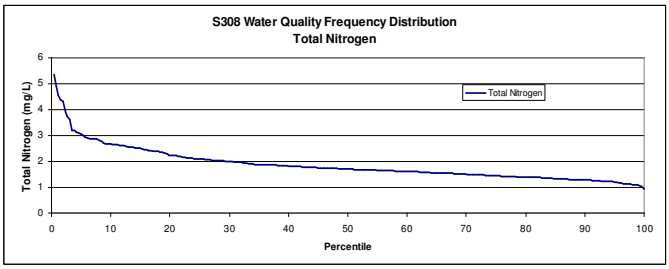

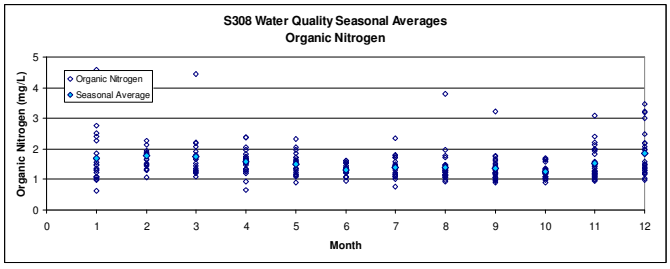

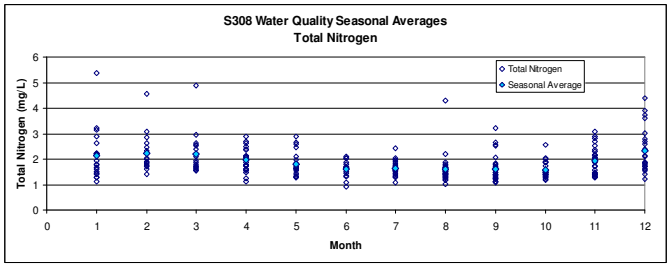

Figure A.4 S308 Water Quality Data.

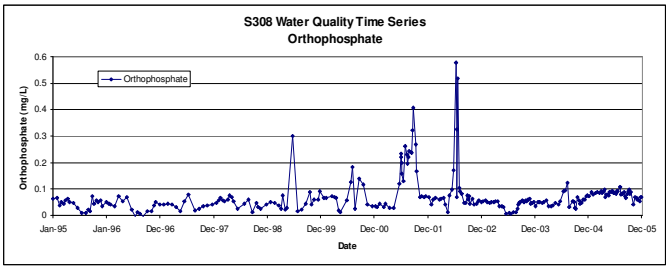

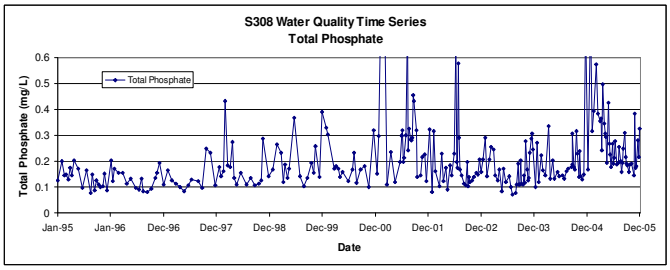

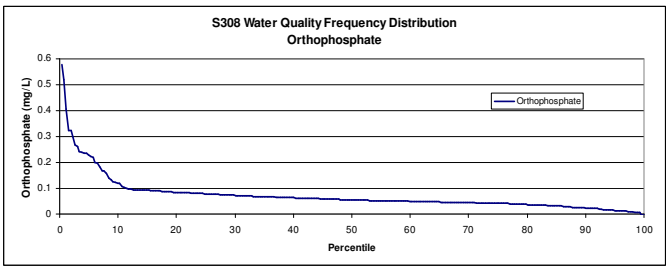

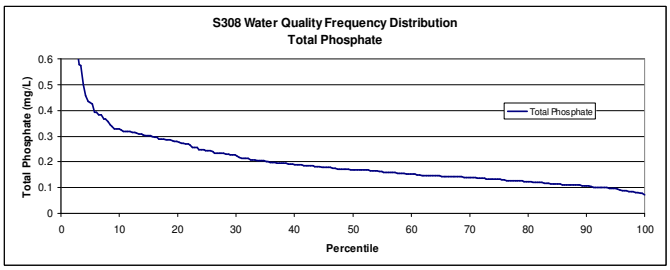

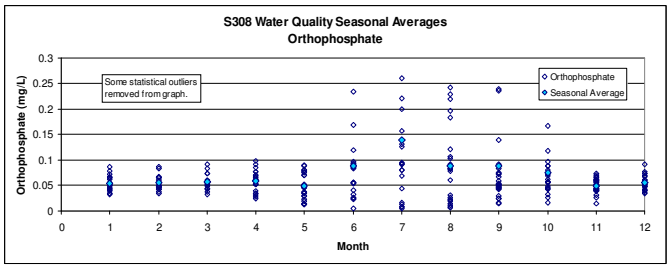

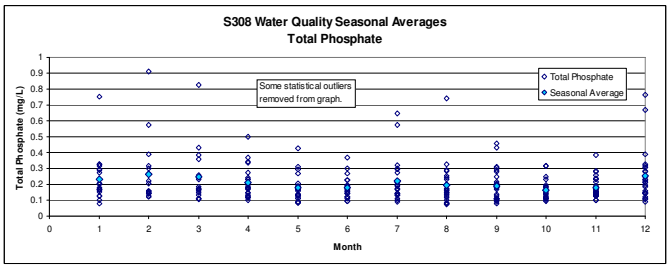

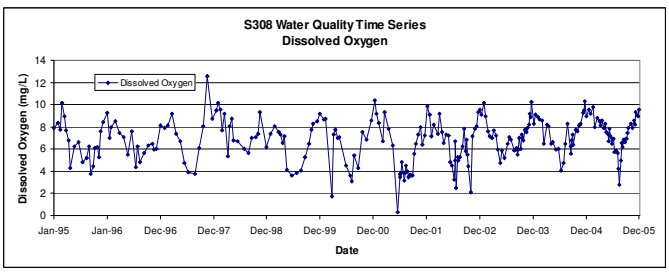

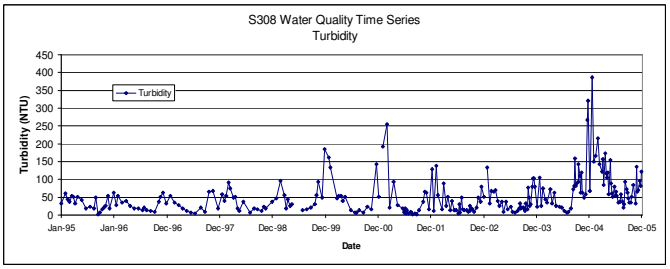

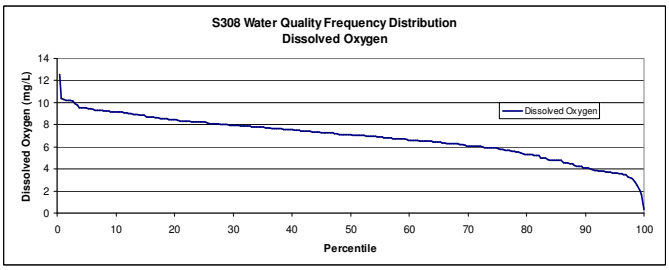

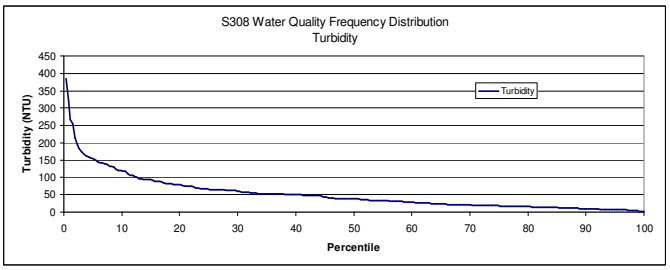

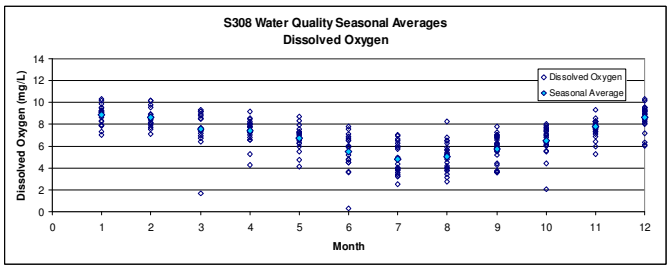

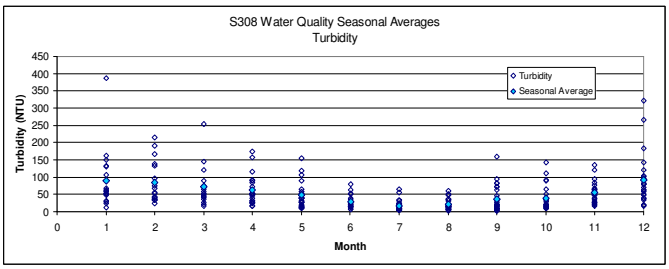

Figure A.4 S308 Water Quality Data (cont'd)

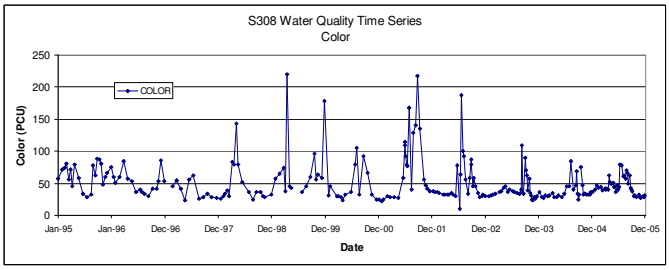

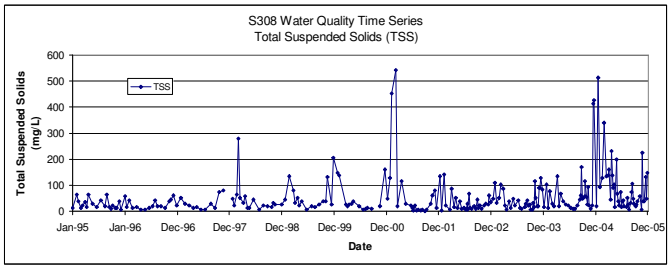

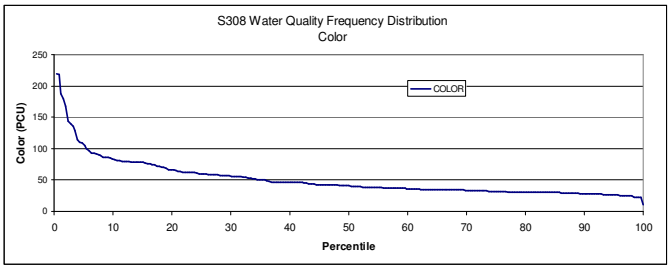

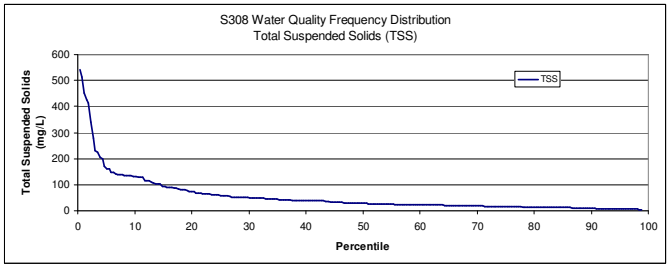

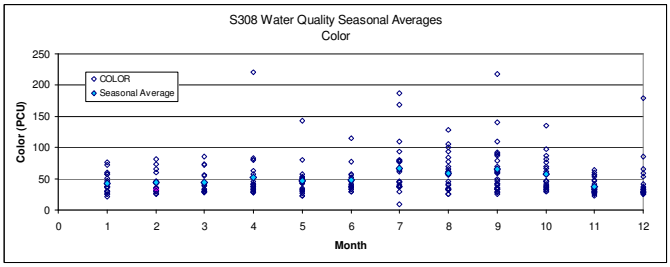

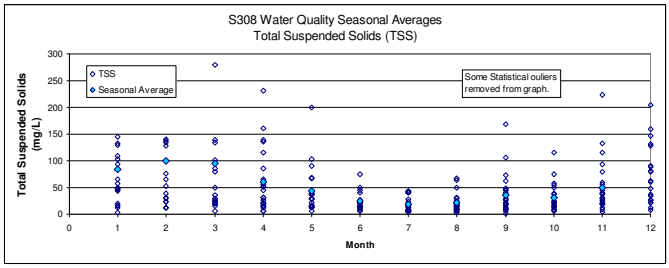

Figure A.4 S308 Water Quality Data (cont'd)

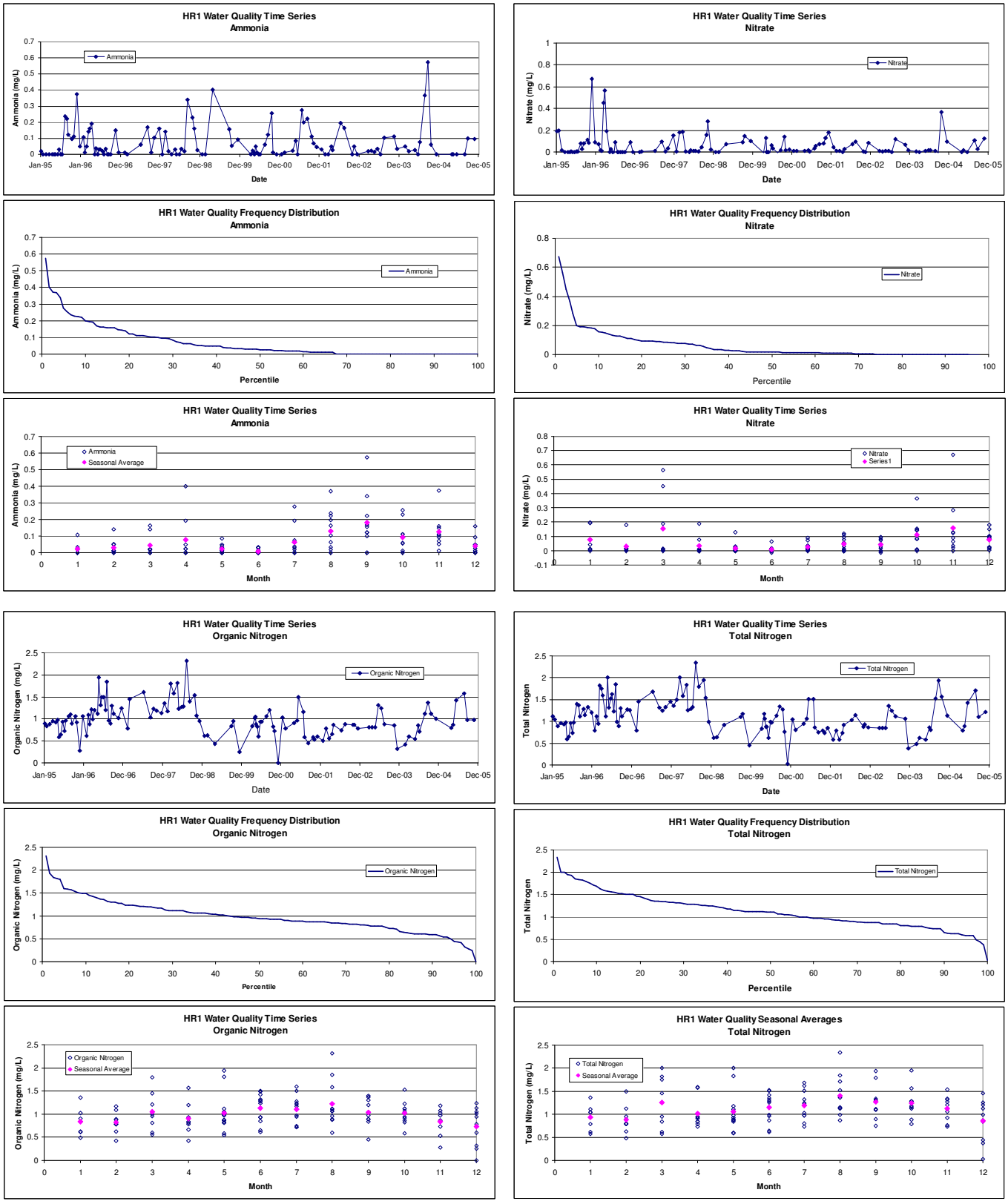

Figure A.5 HR1 Water Quality Data.

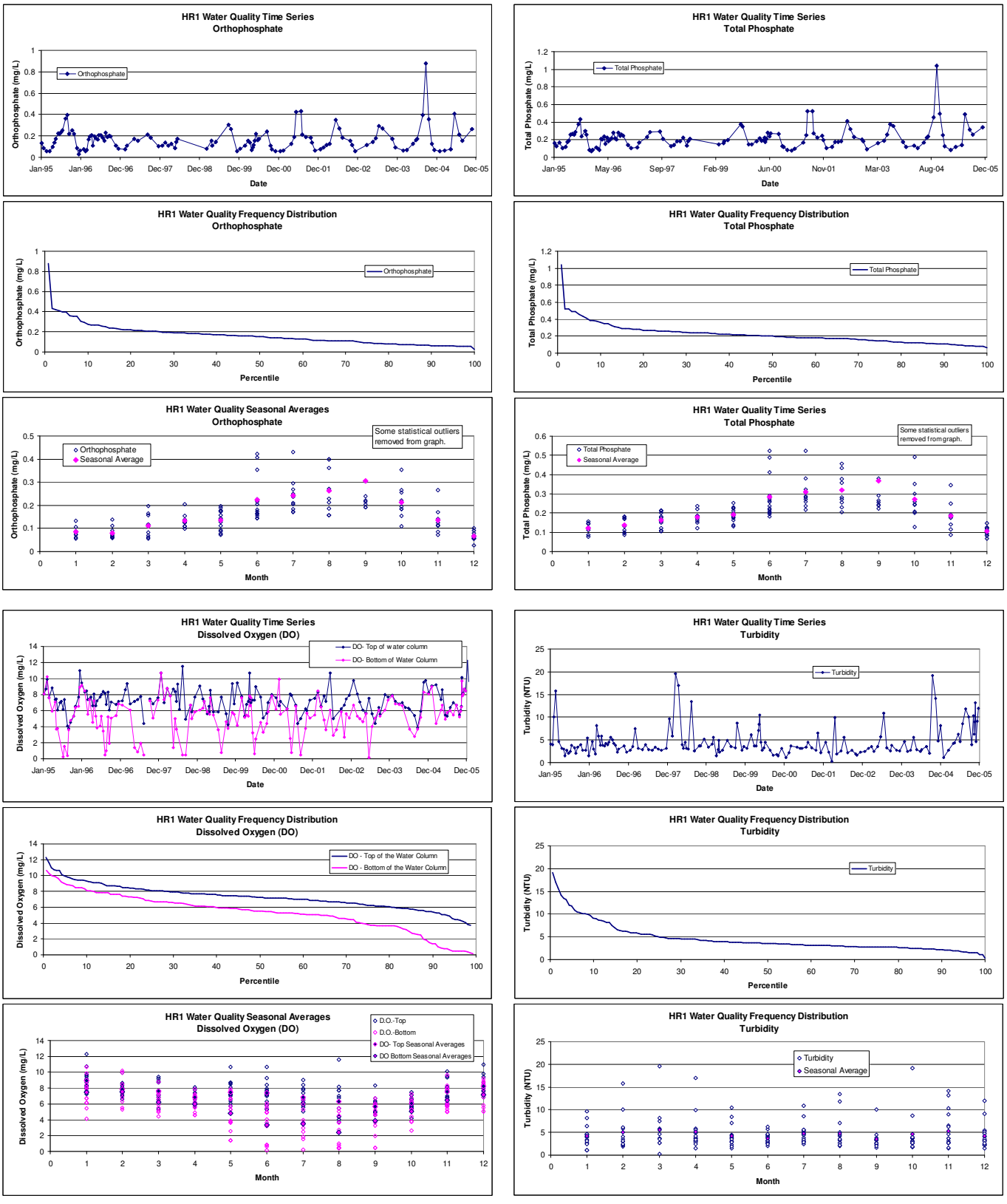

Figure A.5 HR1 Water Quality Data (cont'd)

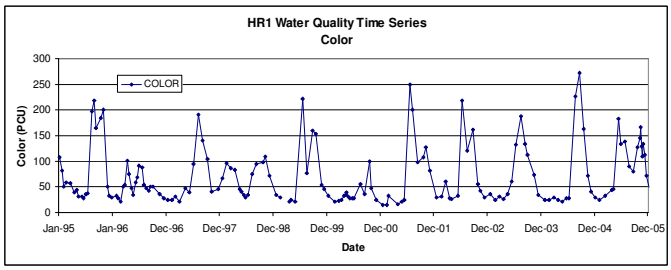

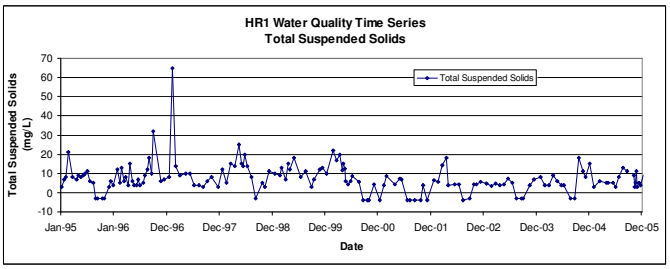

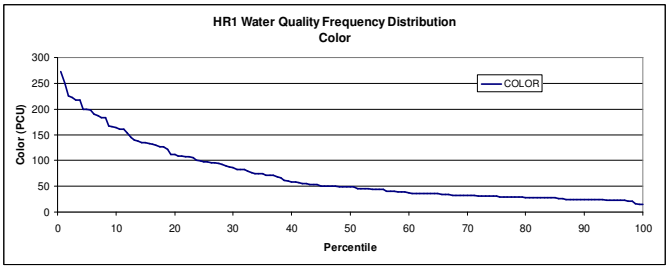

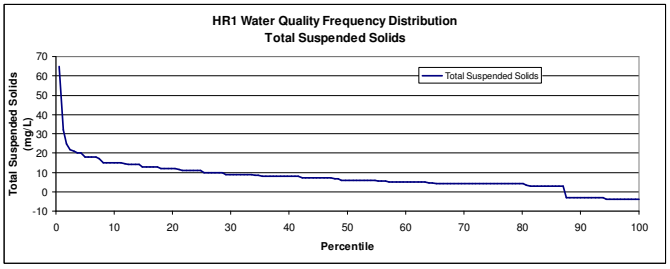

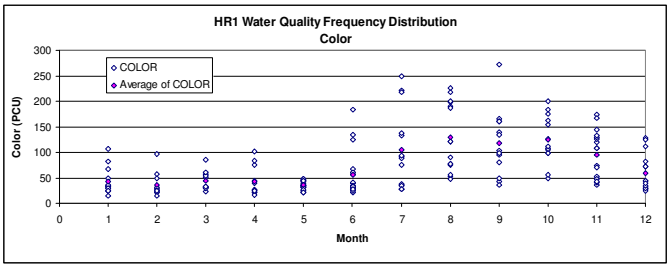

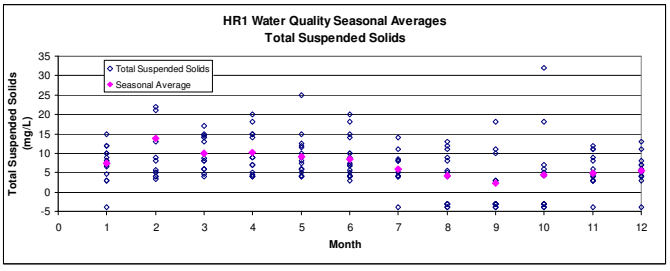

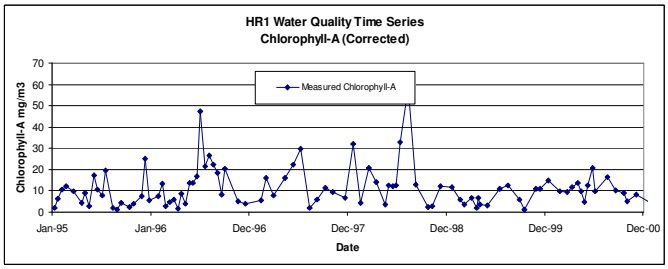

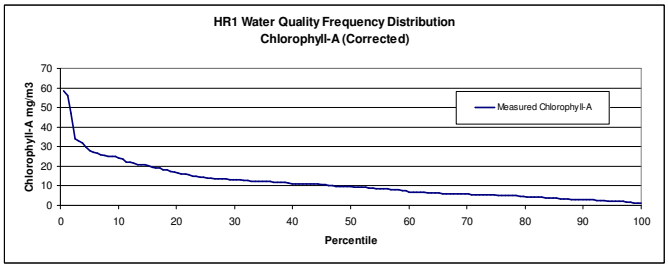

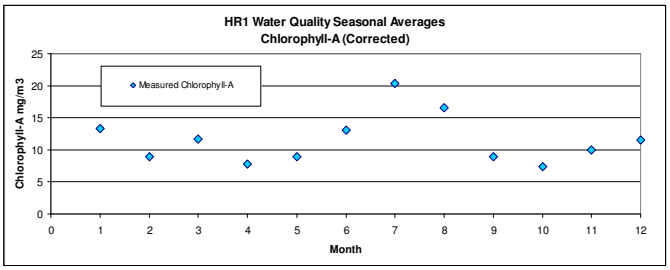

Figure A.5 HR1 Water Quality Data (cont'd)

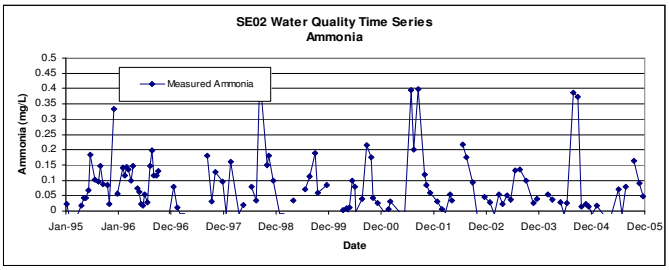

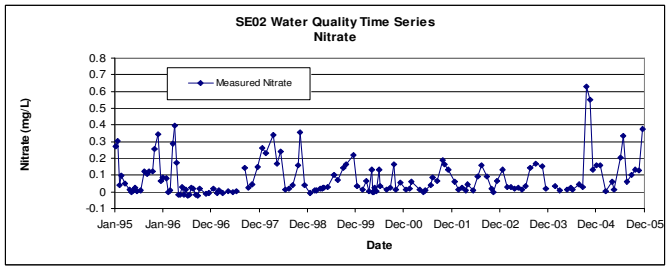

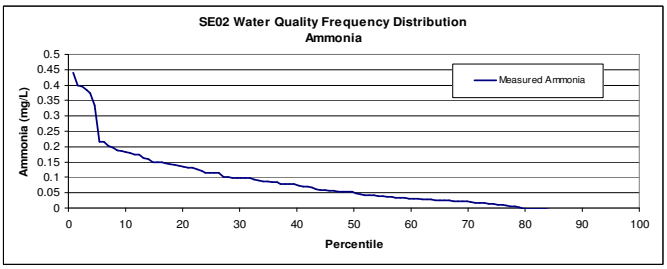

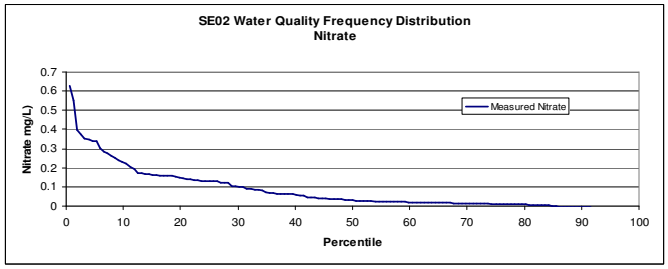

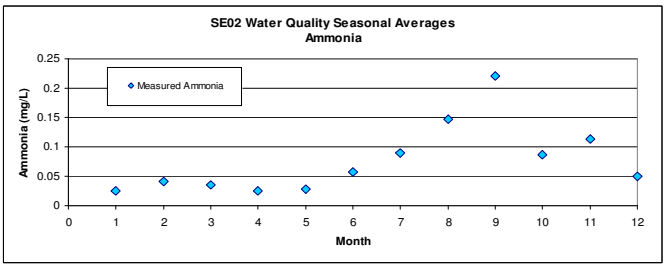

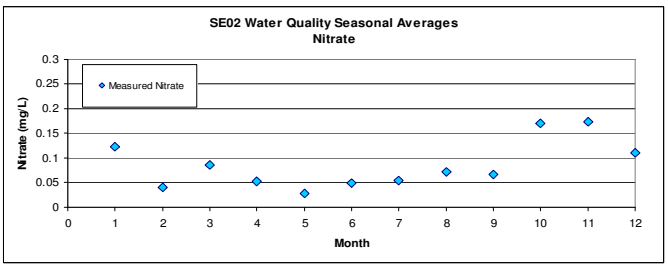

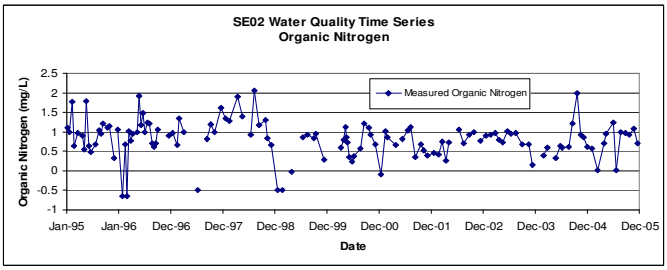

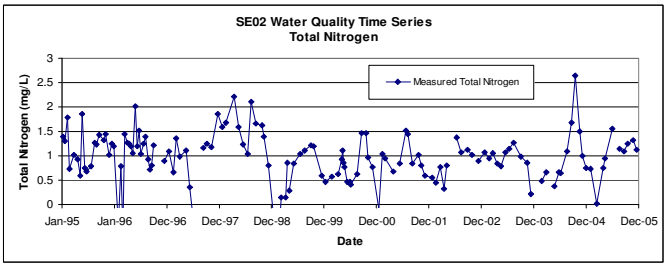

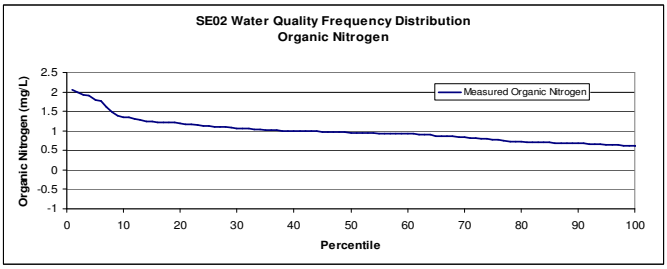

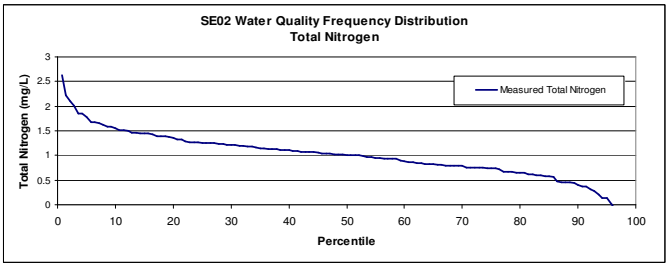

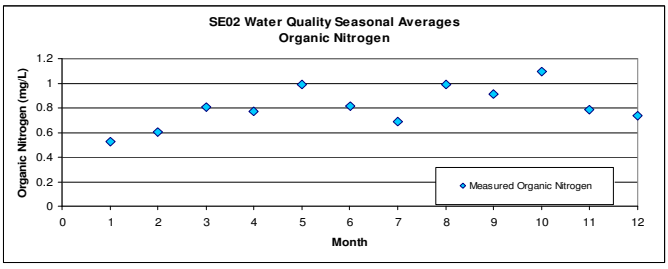

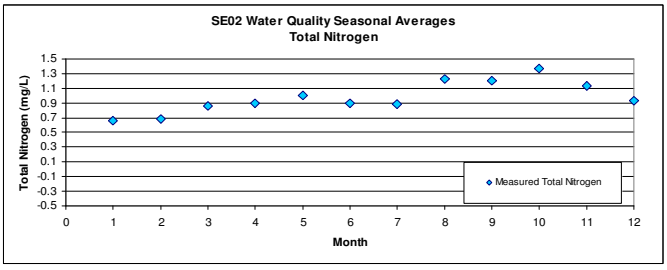

Figure A.6 SE02 Water Quality Data.

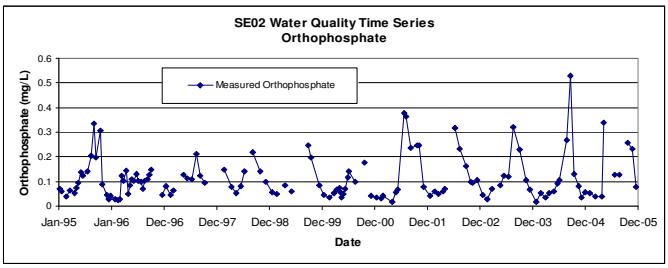

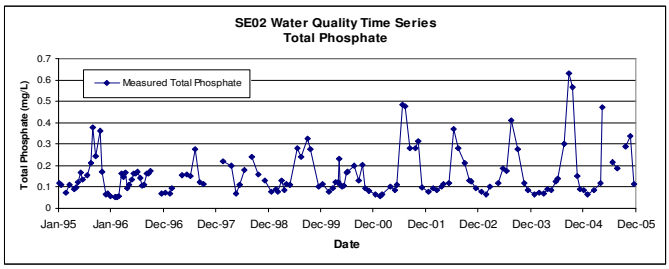

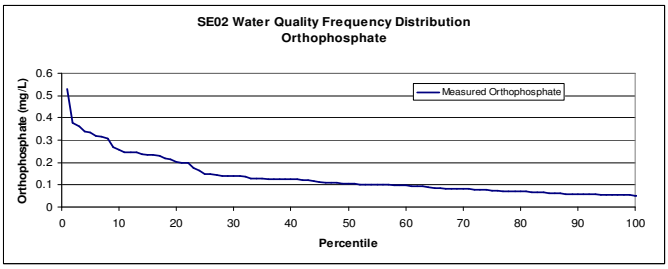

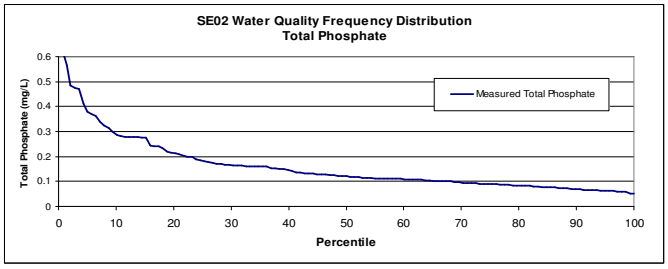

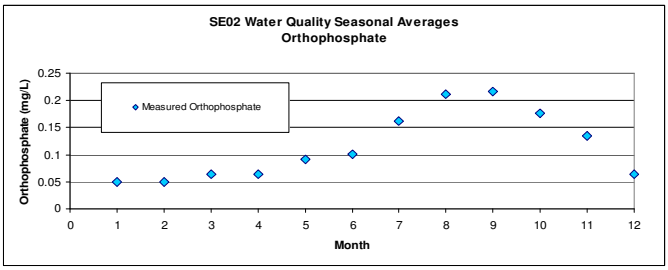

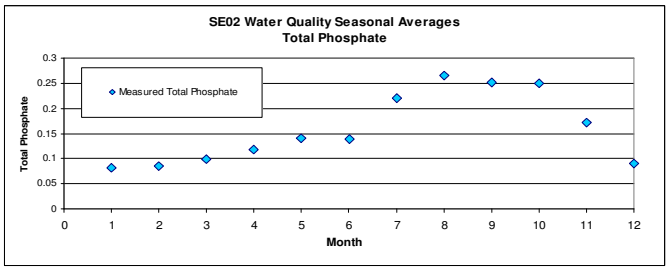

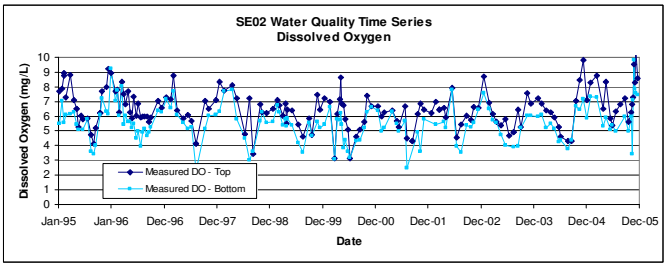

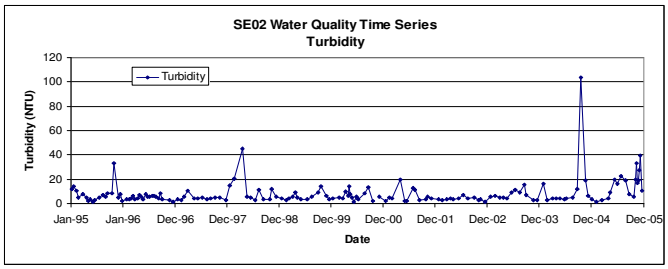

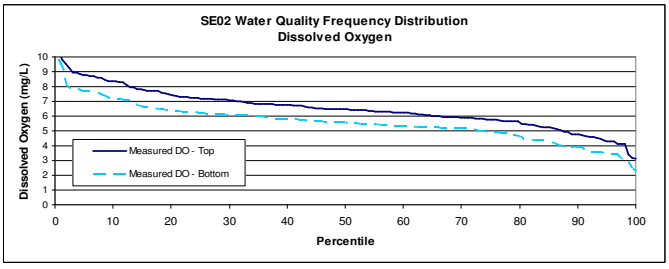

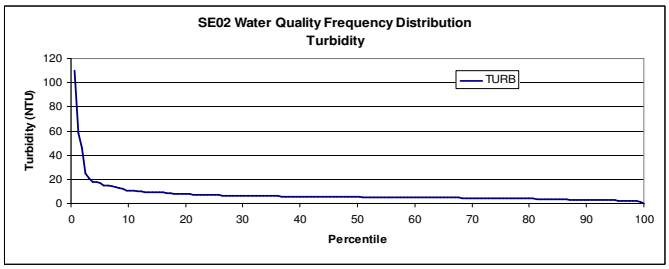

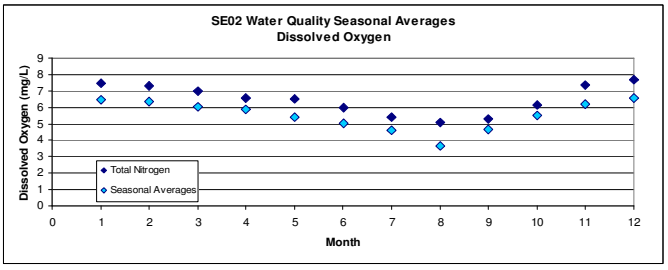

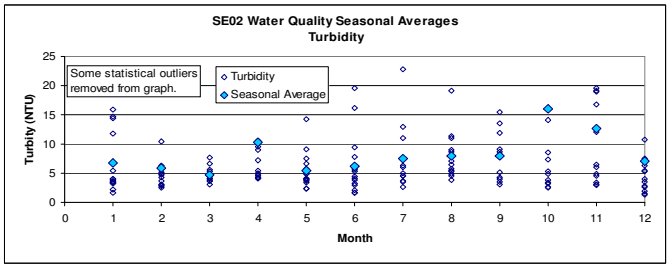

Figure A.6 SE02 Water Quality Data (cont'd)

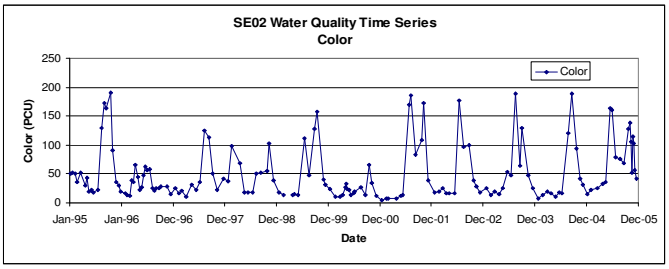

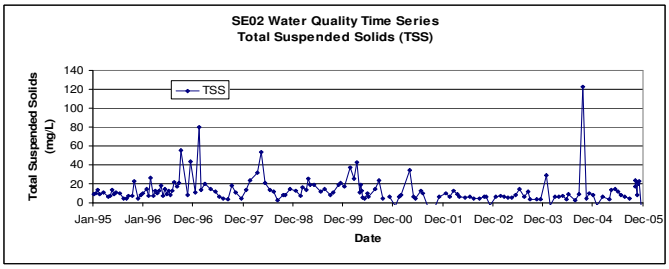

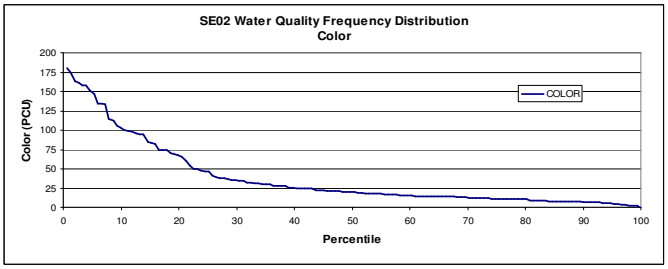

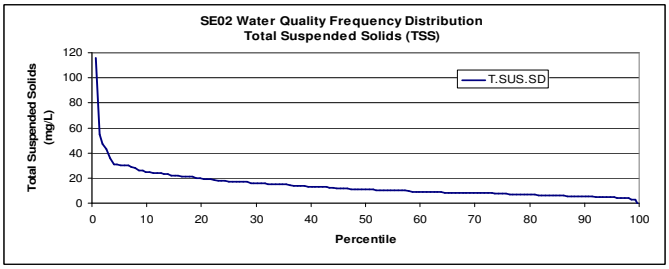

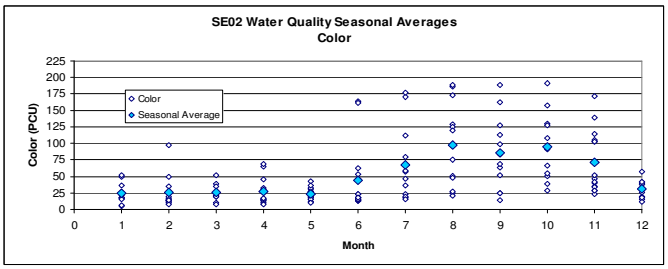

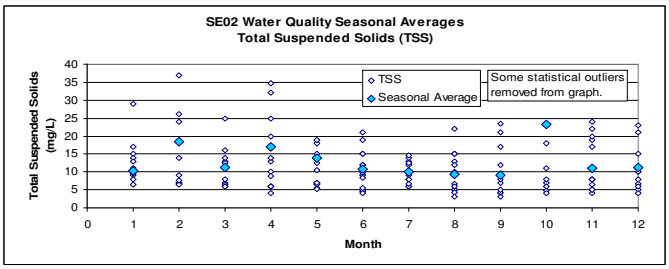

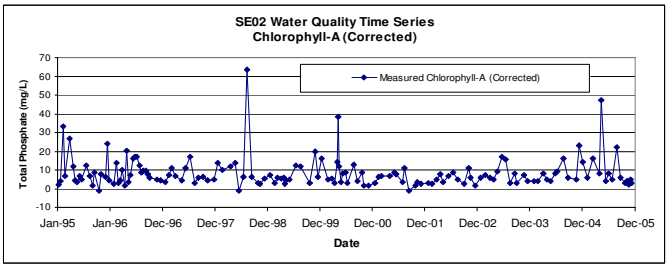

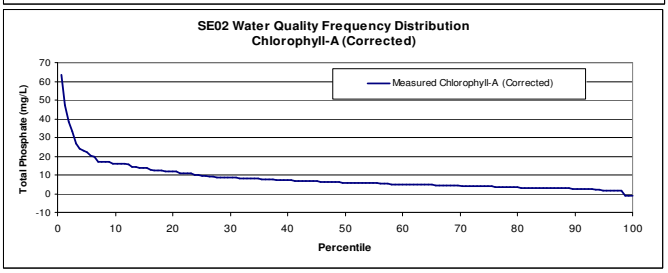

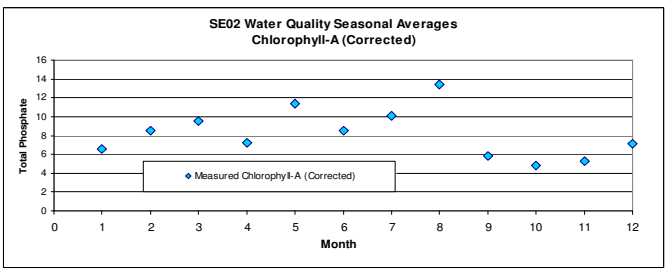

Figure A.6 SE02 Water Quality Data (cont'd)

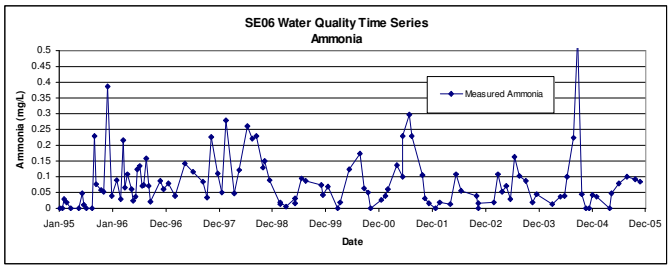

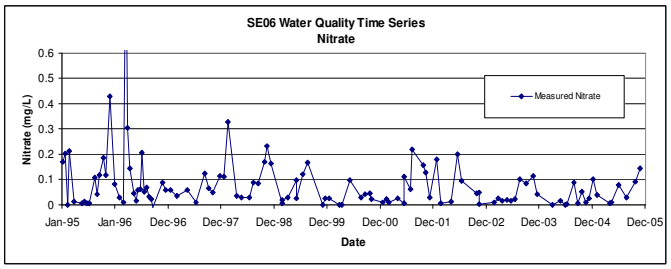

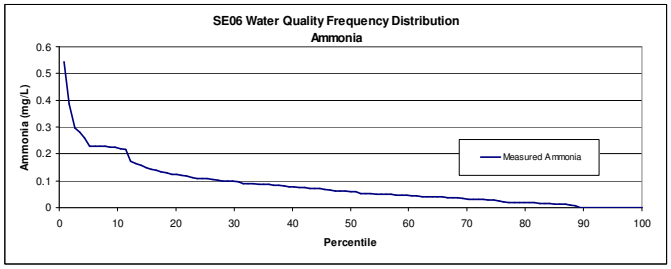

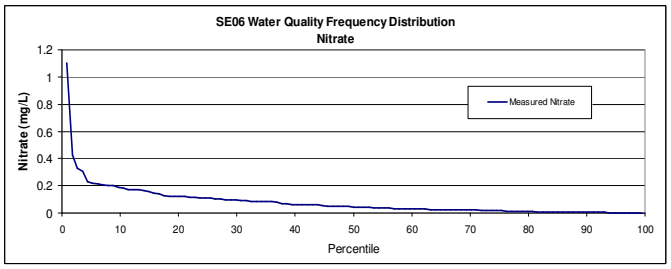

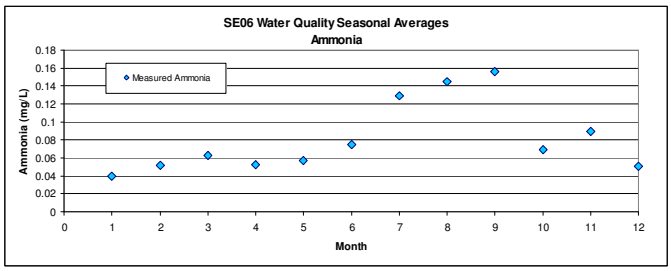

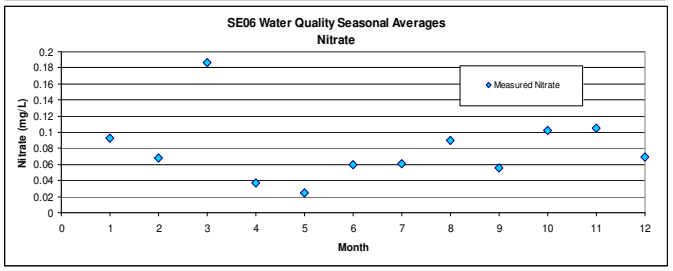

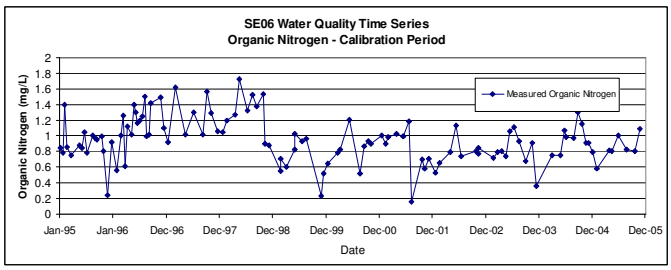

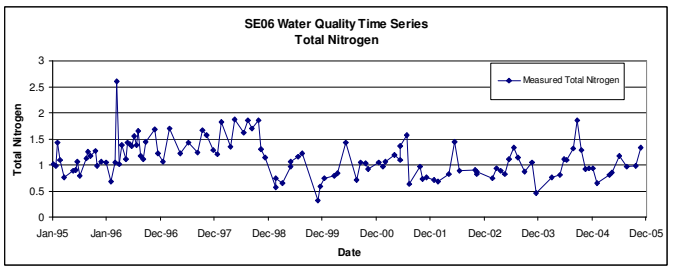

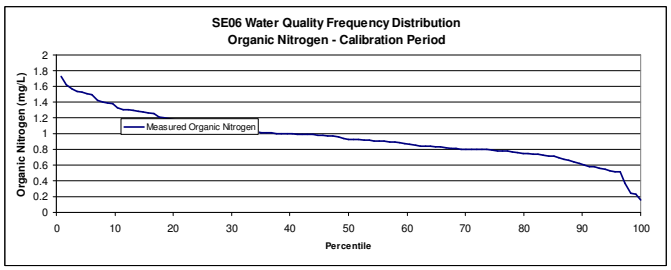

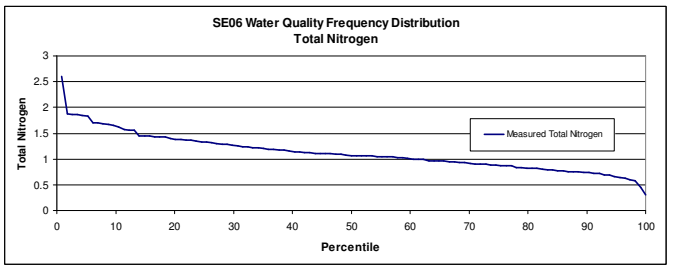

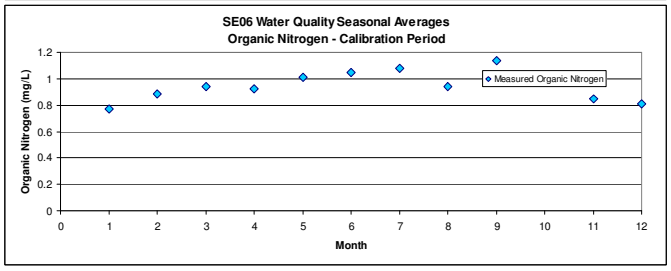

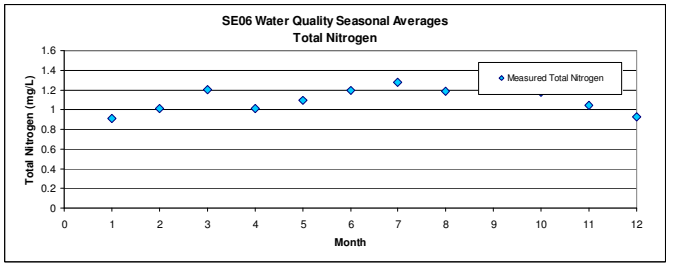

Figure A.7 SE06 Water Quality Data.

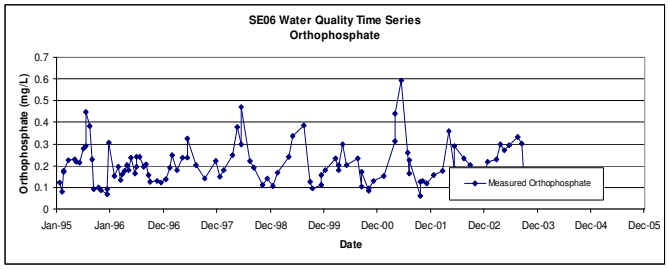

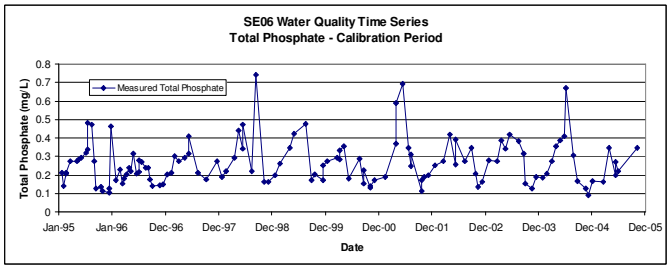

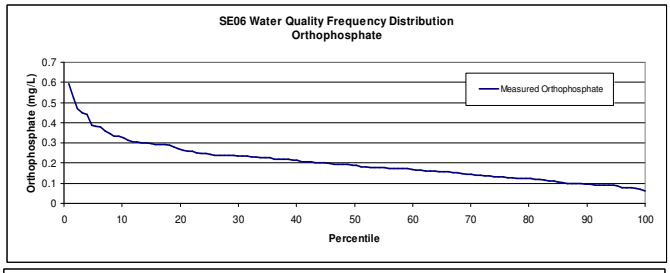

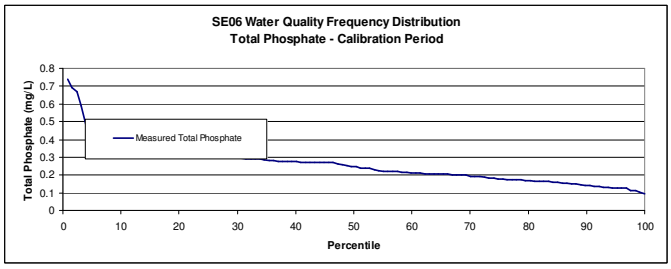

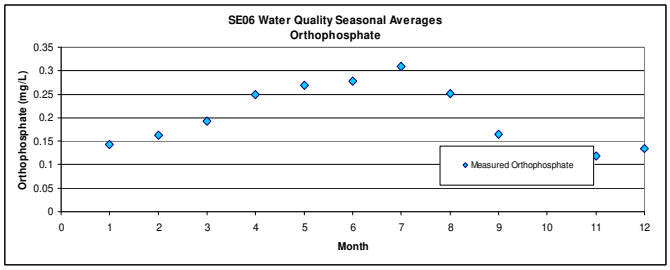

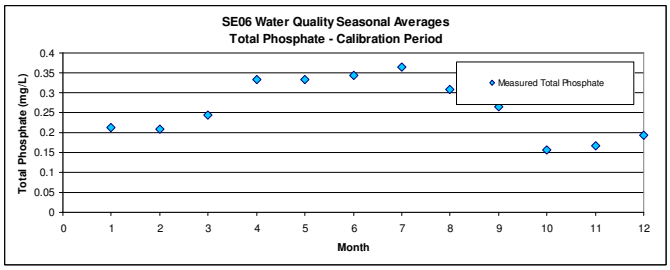

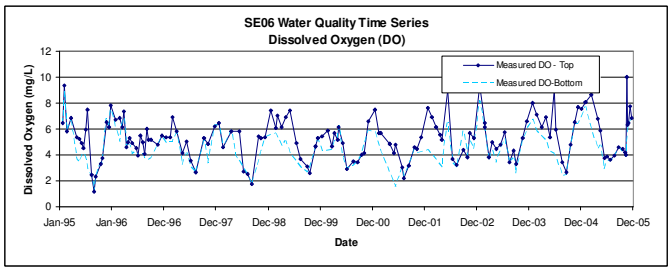

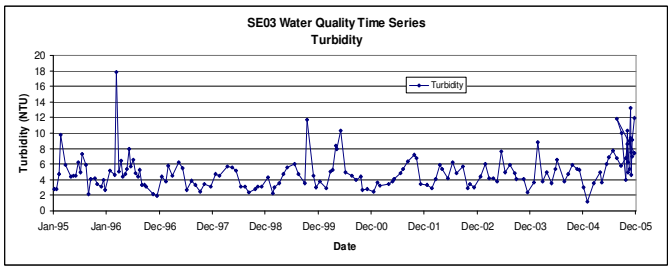

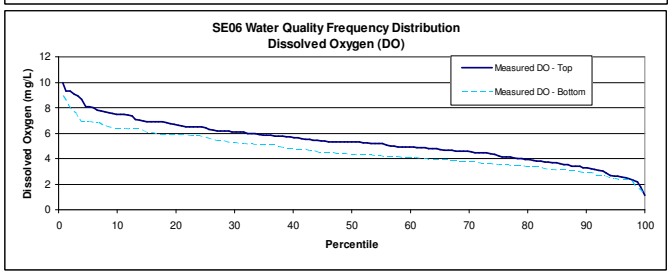

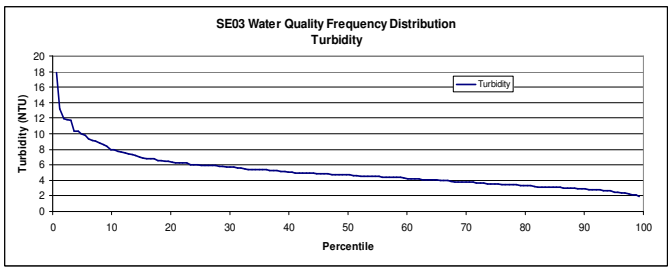

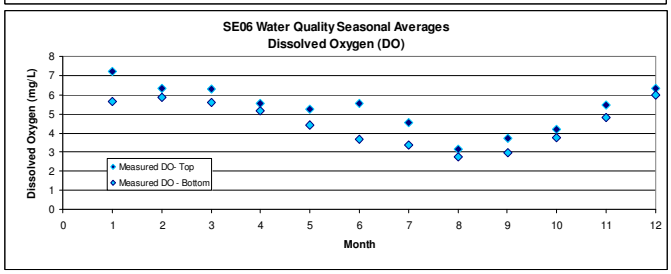

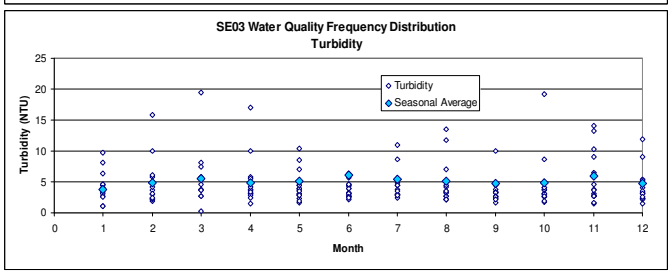

Figure A.7 SE06 Water Quality Data (cont'd)

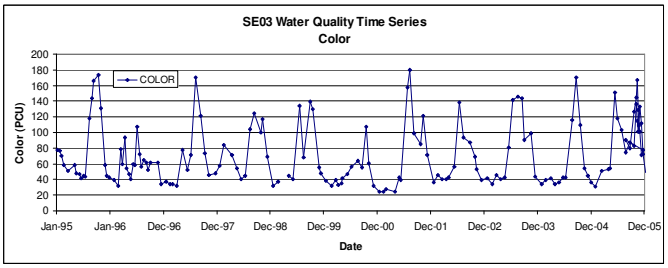

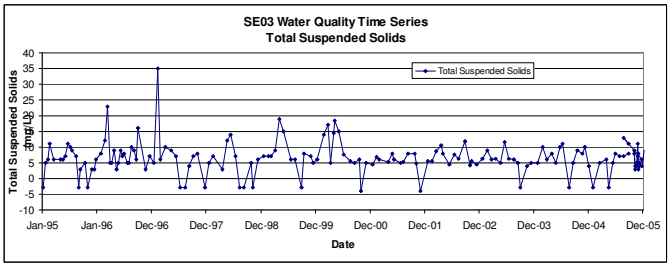

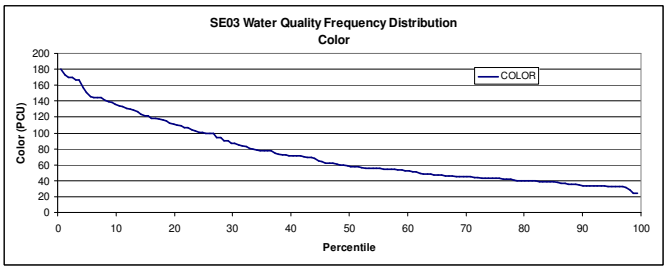

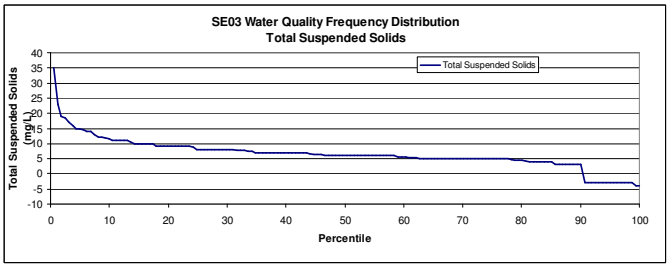

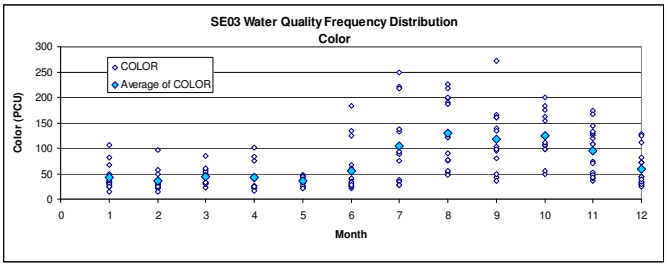

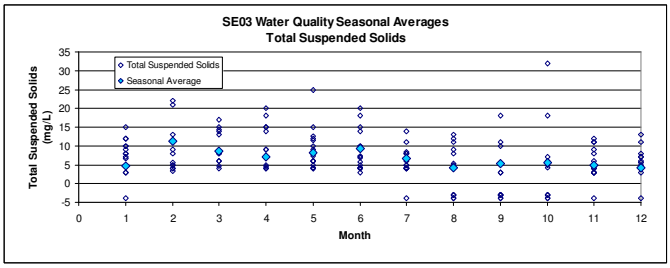

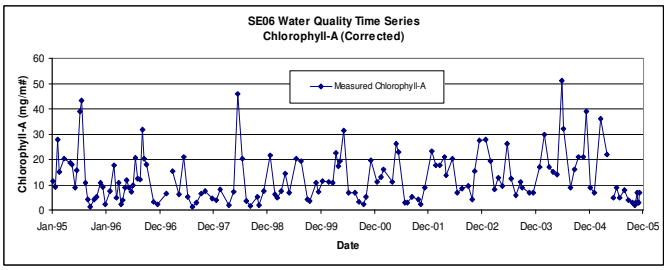

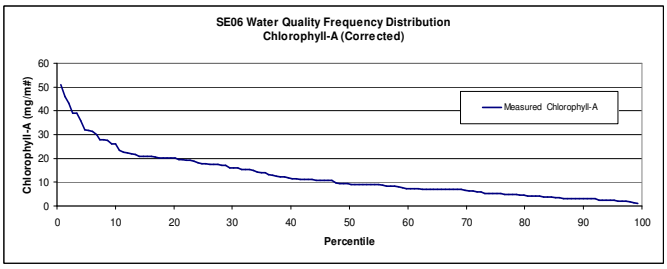

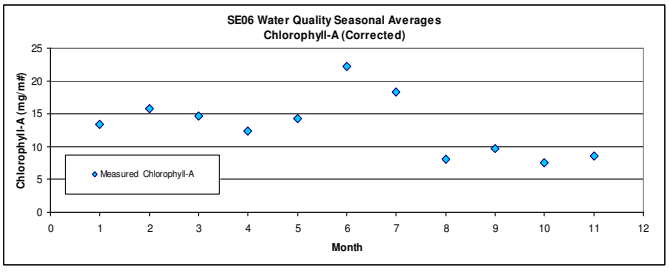

Figure A.7 SE06 Water Quality Data (cont'd)

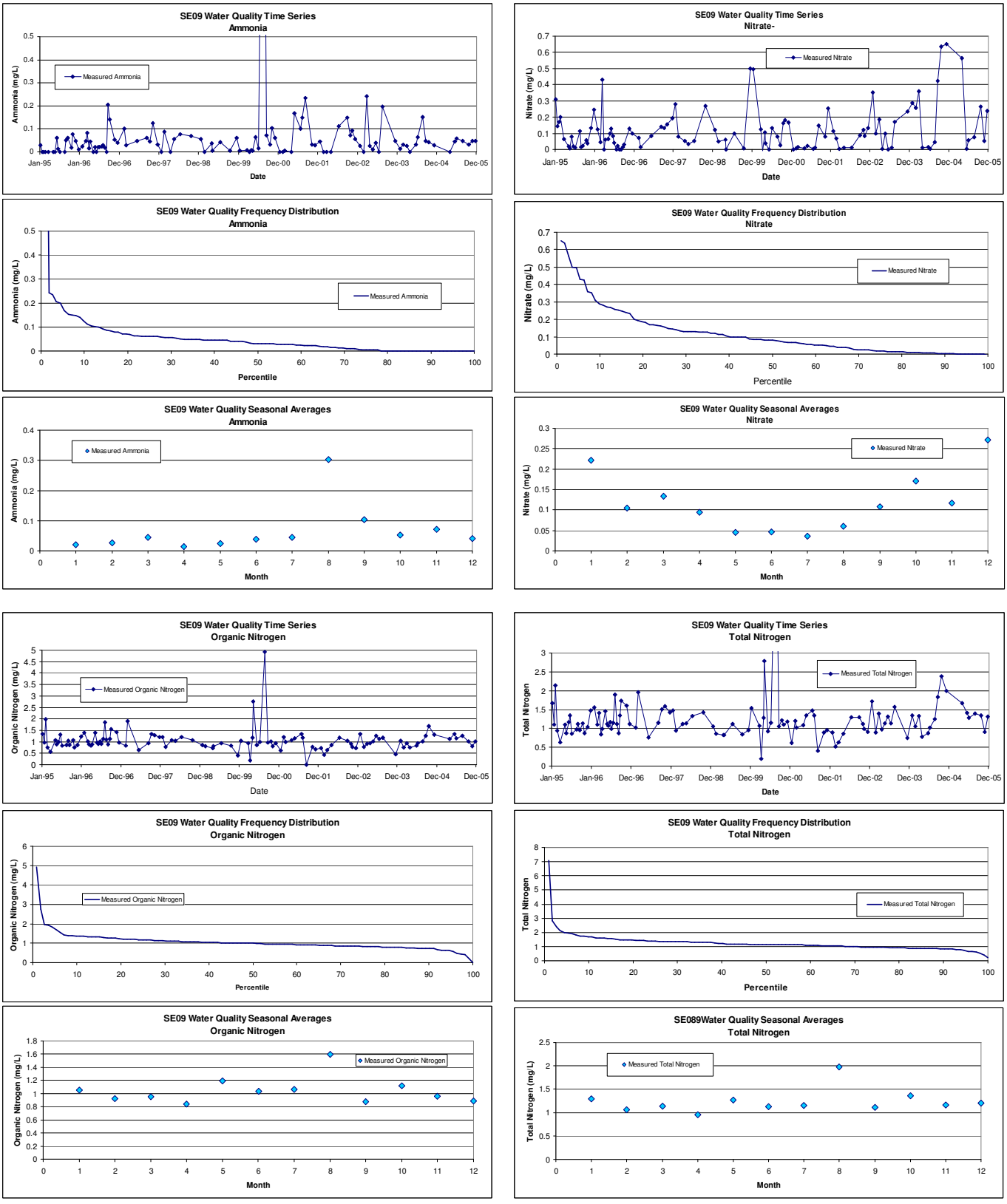

Figure A.8 SE09 Water Quality Data.

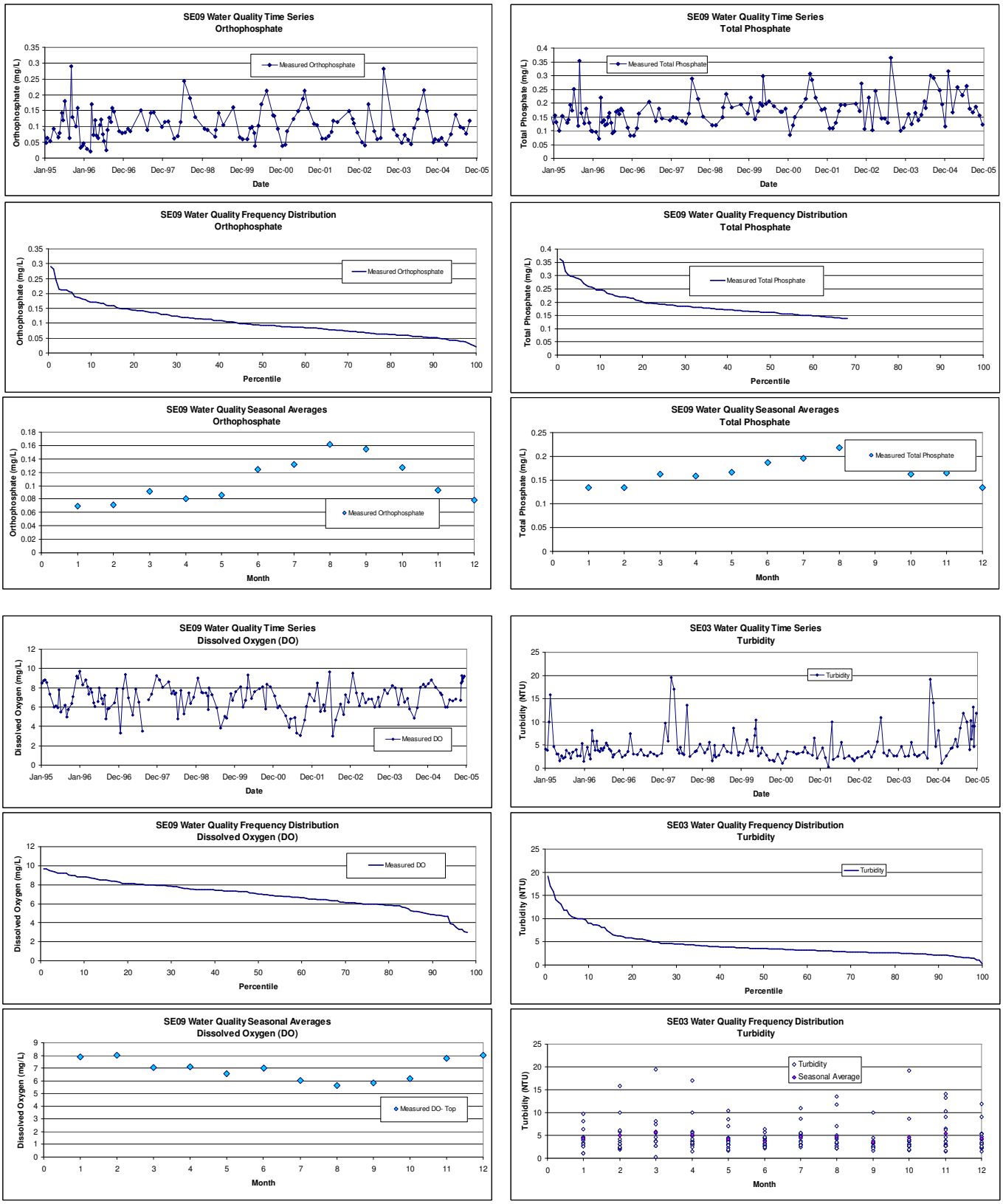

Figure A.8 SE09 Water Quality Data (cont'd)

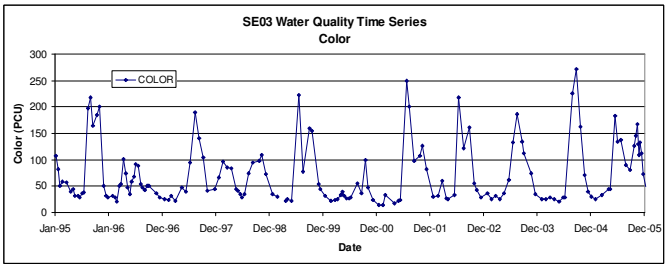

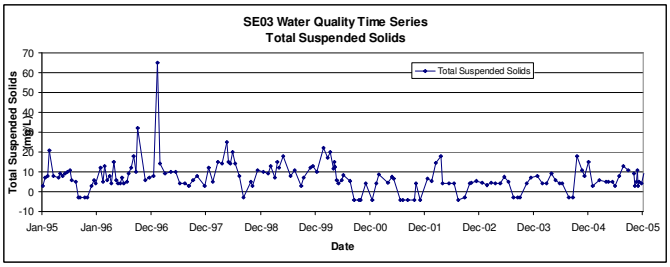

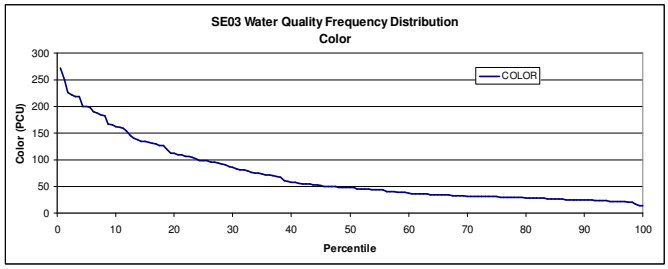

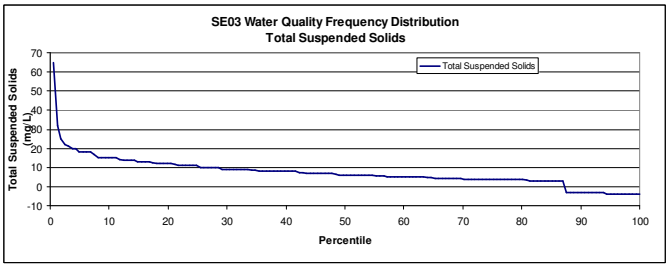

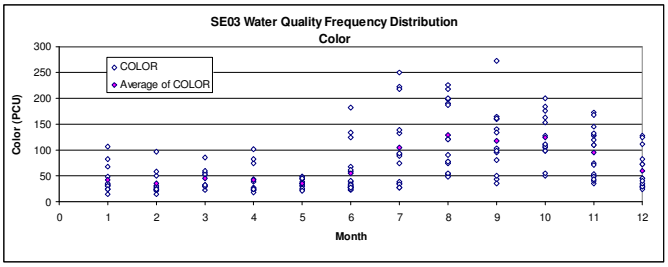

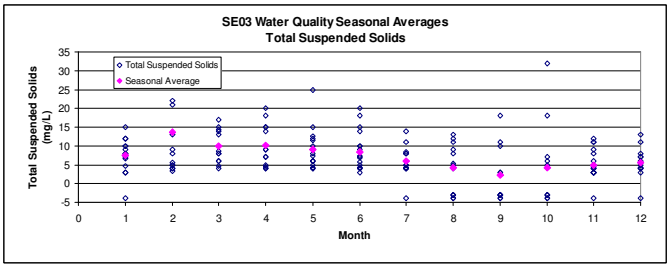

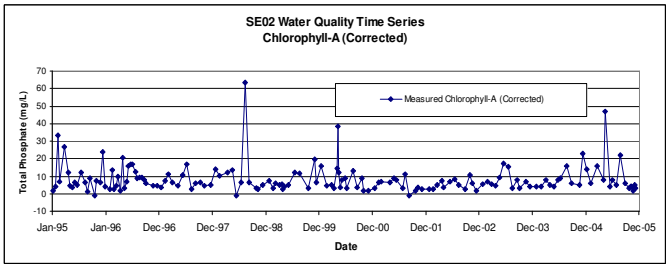

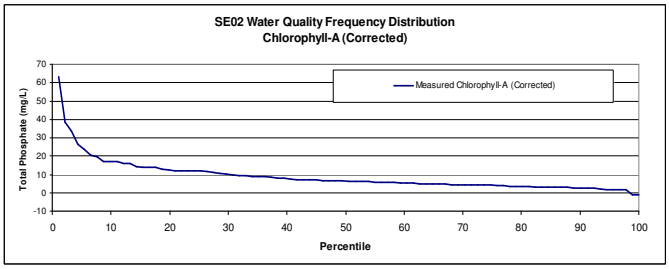

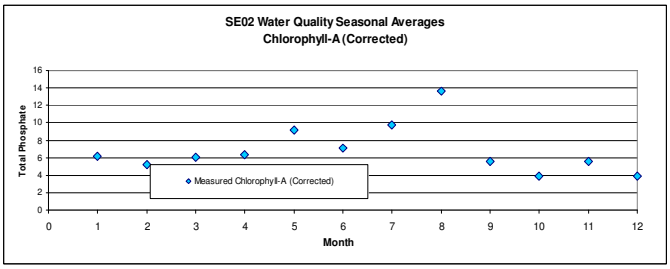

Figure A.8 SE09 Water Quality Data (cont'd)

Appendix B
Control Structure Operational Criteria

Appendix B
Control Structure Operational Criteria

STRUCTURE 308
Port Mayaca Lock and Spillway

This structure is a reinforced concrete, gated spillway with discharge controlled by four cable operated, vertical lift gates and a reinforced concrete lock with two sets of sector gates. The structure is located at the head of the St. Lucie Canal on the east shore of Lake Okeechobee.

PURPOSE

This structure and S-77 provide the principal outlet capacity of Lake Okeechobee. The combined capacity of the Lake Okeechobee outlets provide for passing the 100-year and standard project floods without exceeding the lake flood design stage, and restricts downstream flood stages and channel velocities to non-damaging levels. This structure provides means for passing boat traffic between Lake Okeechobee and the St. Lucie Canal. It also prevents hurricane tides on Lake Okeechobee from entering the St. Lucie Canal.

SPILLWAY OPERATING CRITERIA

This structure is operated and maintained by the U.S. Corps of Engineers. If Lake Okeechobee is below 14.5 feet, the structure will release excess water in the St. Lucie Canal back into the lake or make water supply releases from the lake into the canal. If Lake Okeechobee is above 14.5 feet, the structure will make regulatory or water supply releases from the lake into the canal.

LOCK OPERATING CRITERIA

This structure is operated and maintained by the U. S. Corps of Engineers. The lock gates are opened full whenever the Lake Okeechobee stage is below elevation 14.5 feet. When the lake stage is above elevation 14.5 feet, the locks are operated between 6:00 a.m. and 10:00 p.m. daily; between 10:00 p.m. and 6:00 a.m. the lock gates are closed.

FLOOD DISCHARGE CHARACTERISTICS

	Interim Design Standard Project Flood	Ultimate Design Standard Project Flood
Discharge Rate	14,800 cfs	17,000 cfs
Headwater Elevation	24.9 feet	28.0 feet
Tailwater Elevation	23.2 feet	24.5 feet
Type Discharge	Submerged, controlled	

Revised 02/09/2000

DESCRIPTION OF SPILLWAY STRUCTURE

Type reinforced concrete, gated spillway

Weir Crest

Net Length 116.0 feet

Elevation 9.1 feet

Service Bridge Elevation 40.0 feet

Water Level which will by-pass structure 32.0 feet (over lock gate)

Gates

Number 4

Size 16.9 ft. high by 29.0 ft. wide

Type vertical slide gates

Bottom elevation of gates, full open 26.0 feet

Top elevation of gate, full closed 26.0 feet

Control Manual

Lifting Mechanism

Normal power source commercial electricity

Emergency power source gasoline engine driven generator

Type Hoist Each gate operated by a hydraulic cylinder, activated by electric motor driven pump, connected to gate by steel cables.

DESCRIPTION OF LOCK STRUCTURE

Type: Reinforced concrete lock, with two pairs of sector gates

Operating Deck Elevations: lakeside: 40.0 feet

landside: 29.0 feet

Lock

Length 400 feet

Width 56 feet

Invert Elevation -3.5 feet

Gates

Type: Sector

Size: landside 23.5 feet high

lakeside 28.5 feet high

Control: Manual

Operating Mechanism

Normal Power Source: commercial electricity

Emergency Power Source: gasoline engine driven generator

Type: Double wire rope drum unit with worm type special reducer, powered by electric motor driven hydraulic motor.

ACCESS: This site is reached via U.S. 441.

HYDRAULIC AND HYDROLOGIC MEASUREMENTS

Water Level On-site, dual-recorder

Gate Position Recorder On-site

DEWATERING FACILITIES

Storage U.S. Corps of Engineers

Type Bulkhead gates

STRUCTURE 80

This structure is a reinforced concrete, gated spillway with discharge controlled by seven taintor gates and a reinforced concrete lock with two sets of sector gates. The structure is located on the St. Lucie Canal about 8 miles southwest of Stuart.

PURPOSE

This structure, together with S-308, controls the easterly discharge of Lake Okeechobee to tidewater. The structure passes the 100-year and the Standard Project Flood and restricts upstream and downstream flood stages and channel velocities to non-damaging levels. The structure also provides a means for passing boat traffic through the St. Lucie Canal.

SPILLWAY OPERATING CRITERIA

This structure is operated and maintained by the U.S. Corps of Engineers. Lake Okeechobee releases are made, according to the Lake Okeechobee regulation schedule, by S-308 and S-80 via the St. Lucie Canal.

Regulating releases from Lake Okeechobee are made by S-308. When S-308 is closed, S-80 will maintain a headwater stage between 14.0 and 15.0 insofar as possible.

In order to preclude an excessive instantaneous peak discharge however, the following procedure will be followed in changing to a larger gate opening:

1. Under most conditions, the lockmaster will make the change in half-foot increments each half hour until the desired opening is reached.

2. When the rainfall measured at the lock exceeds 2 inches in 24 hours or when the headwater is rising rapidly, the Area Engineer will provide the lockmaster with a table showing the headwater elevations at which each succeeding half-foot increment can be made without exceeding 125% of St. Lucie Canal rating for the 0800 hours lake stage without local inflow. Under conditions of extreme local inflow, this may prolong a gate change over a 2 or 3 day period.

3. No change in the current gate setting (prior to any changes) will be made during a rising headwater until the change can be made without exceeding the 125% rating.

Appendix C
Wash Model Documentation

Appendix C
Wash Model Documentation

F I N A L R E P O R T

WASH MODEL DOCUMENTATION REPORT

Prepared for
South Florida Water Management District

March 17, 2006

URS
1625 Summit Lake Drive, Suite 200
Tallahassee, FL 32317
12804492

TABLE OF CONTENTS

Section 1 Introduction 1-1

Section 2 Wash Model Summary 2-1

Section 3 Model Cell Structure and Hydrology Simulation 3-1

3.1 Simulation of Pervious Cell Fraction 3-1
3.1.1 Irrigation Module 3-2
3.1.2 High Water Table Algorithm 3-5
3.2 Simulation of Impervious Cell Fractions 3-5
3.3 Cell based discharges 3-6
3.4 Cell Surface and Subsurface Discharge Routing 3-6

Section 4 Groundwater Model 4-1

4.1 Groundwater Model Equations 4-1
4.2 Hydrological Source Terms 4-1
4.3 Boundary Conditions 4-1
4.4 Numerical Solution 4-1
4.5 Model Parameters 4-2

Section 5 Tertiary Canals 5-1

Section 6 Reach Network 6-1

6.1 Governing Equations 6-1
6.2 Boundary Conditions 6-1
6.3 Numerical Solution 6-2
6.4 Structures 6-5
6.5 Model Parameters 6-5

Section 7 Reservoirs/STAs 7-1

7.1 Governing Equations 7-1
7.2 Numerical Solution 7-2
7.3 Model Parameters 7-2

Section 8 Exchanges Between Model Objects 8-1

Section 9 Water Quality Modeling 9-1

9.1 Basic water quality simulation 9-1
9.1.1 Production Terms 9-1
9.1.2 Transport in Reaches 9-2

9.1.3 Transport in Reservoirs 9-4
9.2 Advanced Water Quality 9-5
9.2.1 Production Terms 9-6
9.2.2 Transport 9-6
9.2.3 In-Stream Process Descriptions 9-6

Section 10 Modeling BMPs 10-1

10.1 Explicit BMPS: Local Storage Structures 10-1
10.2 Implicit BMPs 10-2

Section 11 Wash Model Data Requirements 11-1

11.1 Spatial Data 11-1
11.2 Temporal Data 11-1

Section 12 WaSh Model Verification and Sensitivity 12-1

Section 13 Sensitivity Analysis 13-1

Section 14 References 14-1

Tables **Page**

Table 3.1 PWATER Module Parameters and Descriptions 3-2
Table 3.2 Irrigation Demand Module Parameters and Descriptions 3-4
Table 3.3 IWATER Module Parameters and Descriptions 3-5
Table 3.4 Water Routing Operations for Each Cell Type 3-7
Table 4.1 Groundwater Model Parameters 4-2
Table 5.1 Tertiary Canal Model Parameters 5-1
Table 6.1 Reach Network Model Parameters 6-6
Table 7.1 Reservoir/STA Model Parameters 7-2
Table 8.1 Model Parameters 8-2
Table 8.2 Specific Reach-Reservoir Exchanges 8-3
Table 8.3 Reservoir-Reservoir Exchange 8-4
Table 9.1 Basic Water Quality Model Production Term Parameters 9-2
Table 9.2 Reach Water Quality Simulation Parameters 9-4
Table 9.3 Reservoir Water Quality Simulation Parameters 9-5
Table 9.4 Phytoplankton Reaction Terms 9-8
Table 9.5 Phosphorus Reaction Terms 9-9
Table 9.6 Nitrogen Reaction Terms 9-10
Table 9.7 CBOD and DO Reaction Terms 9-11
Table 10.1 Detention/Retention Pond Parameters 10-2
Table 12.1 WaSh Model Verification Simulations 12-1
Table 12.2 Model Parameters for WaSh Comparison with WASP 12-2
Table 12.3 HSPF Model Parameters 12-2

Figures

Figure 2.1 The System and Elements Comprising the WaSh Model
Figure 2.2 Flow Chart for the WaSh Model
Figure 3.1 Example of Cell-Based Representation used for the C-24 Basin
Figure 3.2 Hydrology Flow Chart for Pervious Cell Fractions
Figure 3.3 Modification for the High Water Table Algorithm Implemented in WaSh
Figure 3.4 Hydrology Flow Chart for Impervious Cell Fractions
Figure 6.1 Reach Network Schematic
Figure 6.2 Reach Network Numerical Solution

Figure 6.3 Branch Flow Network
Figure 7.1 Reservoir and Grid Cells
Figure 7.2 Reservoir Flow Numerical Solution
Figure 8.1 Reservoir and STA Exchanges
Figure 12.1 17-by-14 Grid for WaSh Model Verification
Figure 12.2 5-by-5 Grid for WaSh Model Verification
Figure 12.3 Flow Time Series Used in HSPF and WaSh Comparison
Figure 12.4 Comparison of Water Surface Elevations at Upstream Ends of Channel
Figure 12.5 Comparison of WASP and WaSh Simulated DBOD and DO Stream Profiles
Figure 12.6 Comparison of HSPF and WaSh Simulated Runoff
Figure 12.7 Transects Used for Groundwater Elevation Comparisons
Figure 12.8 Comparison of MODFLOW and WaSh Simulated Groundwater Elevations
Figure 13.1 Sensitivity Analysis for CEPSC
Figure 13.2 Sensitivity Analysis for LZSN
Figure 13.3 Sensitivity Analysis for UZSN
Figure 13.4 Sensitivity Analysis for INFILT
Figure 13.5 Sensitivity Analysis for Pan Coefficient
Figure 13.6 Sensitivity Analysis for SLSUR
Figure 13.7 Sensitivity Analysis for NSUR
Figure 13.8 Sensitivity Analysis for Root Depth
Figure 13.9 Sensitivity Analysis for LZETP

The WaSh model is a coupled watershed water quality model (WaSh) originally developed with funding from the South Florida Water Management District (SFWMD) for simulating conditions in the Saint Lucie Estuary (SLE) basins. WaSh is a time-dependent, coupled hydrologic and hydraulic simulation model. It includes representation of basic processes such as infiltration, runoff, evapotranspiration, percolation, groundwater flow, surface water flow, point sources and losses, and water quality fate and transport. It also includes many special features specifically required to simulate conditions in the SLE basins, such as irrigation demand and supply, high water table conditions, fully coupled groundwater and surface interactions, reservoirs and Stormwater Treatment Areas (STAs), and flow structures.

During the application of the WaSh model over the past few years, numerous enhancements to model algorithms have been made and additional algorithms have been added to increase capabilities. Most recently the ability to use spatially variable rainfall, enhanced structure representations, and the simulation of Dissolved Oxygen and Phytoplankton Dynamics have been added to the WaSh model.

The fundamental time step for the model is one day, and output from the model is provided in daily increments. However, certain model algorithms operate at shorter time steps (30 minutes to one hour), which are required to provide accurate representations of physical processes and provide numerical stability. General model outputs are daily time series of flows, stages, water quality loads and concentrations at points along the surface water flow system. Simulation results at the basin outfall can be provided at one-half hour intervals, for the purpose of viewing diurnal fluctuations in the dissolved oxygen levels due to phytoplankton production and respiration.

The model is supported by a Graphical User Interface (GUI) that is developed as an ArcView extension. The GUI is divided into two modules. The first module provides functions for configuring the model using “raw” data. Once a model is configured, the second module provides the user with functions to modify the model, execute simulations and post process model outputs. The WaSh model GUI is not described in this report, which is intended to document the WaSh model theory and structure.

The purpose of this report is to provide documentation of the current WaSh model and provide additional verification and sensitivity analysis. This documentation is divided into three parts. The first part is a description of the WaSh model theory, model equations and numerical solution methods. In the second section, data required to configure and operate the model are described, and in the third section; a series of simulation results are provided for the purpose of model verification and sensitivity.

The WaSh model consists of four basic components: (1) a cell-based representation of surface hydrology, (2) a cell-based representation of subsurface hydrology (groundwater), (3) a reach network that represents streams, rivers, estuaries and canals, and (4) reservoirs and STAs. Each of these components is shown in Figure 2.1. In addition to providing a representation of surface hydrology, each cell can optionally store surface water in a system of tertiary canals. These canals receive direct surface runoff; convey water to the reach network, reservoirs and STAs; and interact with the groundwater (more information is provided in the runoff routing section).

The basin can be considered a bounded system with distinct sources and sinks. The sources and sinks, also identified in Figure 2.1, are:

1) Rainfall
2) Transpiration/Evaporation
3) Point sources or sinks
4) Percolation of a deep aquifer
5) External sources of irrigation water
6) Discharge from the basin

The first three items are user-specified input to the model, whereas the last three items are calculated internally by the WaSh model. External irrigation supplies are irrigation water that is supplied from outside the system, either from another basin or from the deep aquifer. The WaSh model calculates the external supply as the part of the irrigation demand that cannot be met with internally stored water (see Section 3.1.1 on the irrigation module for details).

A functional schematic of the WaSh model components and how they interact is shown in Figure 2.2. This figure also serves as a summary level block diagram of the WaSh model computer program. The computations are divided into four groups:

1) Hydrology calculations
2) Cell discharge routing
3) Component interactions
4) Individual component dynamics

For each time increment, the surface hydrology routine produces a surface and subsurface (percolation) discharge for each cell. The cell's percolated water is routed to the groundwater, and the surface discharge is routed to one of the receiving water bodies, i.e., either the tertiary canals, reach network, or reservoirs and STAs. The decision as to where each cell's surface discharge is routed depends on the basin geometry and on user-controlled setup of the WaSh model. The surface hydrology simulation is based on the HSPF algorithms (Bicknell et al., 1997; Johanson et al., 1981).

There is some coupling between the cell hydrology routines and the other components, due to possible high groundwater conditions or irrigation demand. The high groundwater module will reduce percolation when the groundwater rises into the surface moisture. When a cell's irrigation module is active, it will sense deficiencies in the moisture zones and calculate an irrigation demand to replenish the deficiency. The demand is allocated by the user to tertiary

canals, the reach network and reservoirs, as well as to external sources. The demand is extracted from each component during the component simulation.

After the discharges are routed, the exchange of water between components is calculated. All four components can interact with each other, via groundwater-surface water exchanges, pumping, and gravity flow.

Once the fluxes between components are calculated, the response of each component is determined. The groundwater model consists of an unconfined aquifer, intended to represent the surficial water table. The reach network model is based on the one-dimensional shallow water wave equation, and includes branching and representation of structural control on flow and stages. The tertiary canals are represented in each cell as a storage potential, with flow controlled by user-specified parameters describing weir configurations and pumping operations. The reservoirs and STAs are also represented using a storage potential with six different flow control options for controlling flow into and out of the facilities.

The basic time period for generating model output is one day, with flows, loads and other fluxes provided as daily averages. However, certain processes are simulated using a smaller time step in order to properly resolve the system dynamics. The cell hydrology calculations are simulated with a one-hour time step. Surface water dynamics in the reach network, tertiary canals and reservoirs and STAs are completed on a half-hour time step, and the cell-to-cell groundwater flows are calculated with a daily time step. However, the groundwater exchanges with surface water (reservoirs, tertiary canals and the reach network) are calculated using a half-hour time step. Flux rates between components using different time steps are aggregated, as needed, in order preserve mass balance.

The water quality component of WaSh is based on the time-dependent scalar transport equations and is directly coupled to the flow model. There are two options for simulating water quality, the basic option (BWQ) and the advanced option (AWQ). The basic option consists of simulating the runoff and transport of five water quality constituents, Total Suspended Solids (TSS) and dissolved and particulate nitrogen and phosphorus. The constituent transport is based on mass conservation, but includes first-order decay and settling and re-entrainment of TSS and particulate fractions of nitrogen and phosphorus.

The AWQ option is based on the non-linear dissolved oxygen (DO) balance and eutrophication model as described in the WASP model documentation (Ambrose et al., 1988). There are eight constituents (state-variables): ammonia, nitrate, inorganic phosphorus, phytoplankton carbon, carbonaceous biochemical oxygen demand, dissolved oxygen, organic nitrogen, and organic phosphorus. The run-off and transport portion of the advanced water quality option is identical to that of the basic option. The primary difference occurs in the surface water bodies, for which the transformations between state-variables are also simulated in the AWQ option. Also, each reach in the reach network can be divided into an upper and lower section. Vertical diffusion between the upper and lower section can be simulated also, by specifying a diffusion rate. This capability was added to improve representation of conditions in which there are significant vertical variations in the water quality constituents.

The WaSh model also supports the implementation of numerous Best Managements Practices (BMPs) used to control the flow and water-quality characteristics of the basins. The BMPs are divided into two general categories, explicitly represented, and implicitly represented BMPs. Explicitly represented BMPs include structures that are included directly in the drainage system.

These consist of detention and retention basins and certain irrigation practices. Implicitly represented BMPs include a wide variety of practices, ranging from filter strips to grazing practices, and are represented as modifications to model parameters controlling runoff quantity and quality.

The basin domain is divided into cells using a uniform grid network. Figure 3.1 shows a typical grid network, with 2000-foot-square cells overlaying the C-24 basin. The X-direction is to the east, and the Y-direction is to the north. Those cells intersecting the basin are labeled active. Cells lying outside the basin boundaries are labeled inactive and are not used in the model. Each cell represents a discrete part of the basin and has associated physical characteristics. The primary physical characteristics are:

1) land use
2) soil type
3) ground elevation
4) ground slope
5) cell area
6) tertiary canal length
7) tertiary canal width
8) tertiary canal bottom elevation

The area for cells that intersect the basin boundary includes only the area within the basin boundary, and therefore the cell area may vary for those cells along basin boundaries. Also, when the footprint of a reservoir or STA intersects a cell, the cell's area may be reduced by the area of the footprint of the reservoir or STA in the cell. If tertiary canals are present in the cell, the total length of all canals in the cell are computed, and total canal length, bottom elevation and width are included as a cell attribute.

Hydrology is modeled individually for each cell using the PWATER and IWATER modules of the USGS HSPF Version 12 model. The PWATER routine simulates rainfall, evaporation (and evapotranspiration), infiltration, percolation and surface runoff. Version 12 includes recent model enhancements that simulate irrigation demand (AQUA TERRA, 1998) and high water table conditions (AQUA TERRA, 1996).

The PWATER module code was directly incorporated into the WaSh code, with modifications to provide links to the WaSh code and to revise the algorithms for evaporation, high water table, irrigation and groundwater simulations. The last modification was implemented because the WaSh model uses a distributed groundwater model rather than the storage-discharge relationship in the original HSPF model. The changes to the irrigation module and high water table module were sufficiently significant that new subroutines were developed. Also, the IWATER module was rewritten as a new subroutine, using the original HSPF IWATER code and the HSPF manual as guidance. This approach was adopted because the IWATER routine is relatively simple, and the new code was much easier to link with other modules in the WaSh code.

3.1 SIMULATION OF PERVIOUS CELL FRACTION

A block diagram of the PWATER algorithm, as it is described in the HSPF documentation, is provided in Figure 3.2. There are five storages identified which can be considered the state variables. The fluxes into and out of each storage are functions of the storages and model parameters. The first storage, CEPS, represents interception storage. The surface storage represents water ponded on the soil surface. The lower zone storage, LZS, represents pore water

that can only be removed via transpiration. Upper zone storage, UZS, represents pore water that can percolate under the influence of gravity. Interflow storage, IFWS, represents subsurface water that discharges directly to surface water bodies rather than percolating to the water table. The equations used to calculate the fluxes can be found in the HSPF documentation (Bicknell et al., 1997; Johanson et al., 1981). This PWATER algorithm has been modified slightly to accommodate the irrigation module, and these modifications are discussed in Section 3.1.1.

In addition to the standard PWATER runoff algorithm, the WaSh model also includes an option for using a rating curve to simulate surface discharge. The rating curve consists of a depth-discharge relationship which is defined by the user, using five points to describe the curve. When the rating curve approach is used, it replaces the standard algorithm for calculating SURO during each time interval.

The PAN coefficient method for specifying potential evapo-transpiratino (PET) used in HSPF has been replaced with a Penman-Montieth PET. The Penman Montieth calculation has a similar structure to that of the PAN coefficient, except that the coefficients can vary both with land use and season (i.e., monthly).

The model parameters for the PWATER as they are implemented in WaSh are listed in Table 3.1:

Table 3.1 PWATER Module Parameters and Descriptions

HSPF PWATER Parameter	Description
CEPSC	Interception storage capacity (inches)
UZSN	Upper zone nominal storage (inches)
NSUR	Manning's n for land surface
INTFW	Interflow scale factor
LZETP	Lower zone evaporation potential (fraction)
LZSN	Lower zone nominal storage (inches)
INFILT	Parameter in infiltration function
INFEXP	Parameter in infiltration function
INFILD	Parameter in infiltration function
LSUR	Length of element (cell length) (feet)
SLSUR	Slope of land surface (from topography)
BASETP	Base flow (riparian) evaporation (fraction)
AGWETP	Groundwater evaporation potential (fraction)
PET Coefficient	Evaporation scale factor (fraction, varies by month)
Rating curve*	Set of five depth-discharge points defining curve

***optional**

Values for all parameters can vary between cells depending on the cell attributes of land use and soil type.

3.1.1 Irrigation Module

The irrigation module for HSPF that was developed by AQUA TERRA (1998) has been incorporated in WaSh with some modifications. The modifications were applied primarily to simplify the interaction between the groundwater and the moisture zone. The module code as re-

written for implementation into WaSh and a description of the revised algorithm are provided below. The irrigation demand monitors the moisture in the soil zones and generates a demand for water based on the existing moisture relative to user-specified desired moisture levels. After the demand is calculated, the algorithm tries to meet the demand by supplying water from a number of sources. Water is extracted from the sources and then applied as irrigation. A number of application methods are represented.

One other enhancement of the WaSh model includes the capability to pump water from the reach network to the tertiary canals to help meet irrigation demand. The WaSh model can be configured such that during the simulation, if the supply from the cell's tertiary canals is limited because the tertiary canals are completely drained, water can be pumped from the reach network to the cell's tertiary canals. This capability is described in more detail in Section 6.0 on the reach network.

The demand is calculated according to the following algorithm, which is a modified version of the method developed by AQUA TERRA. The algorithm requires that the depth of the moisture zone be calculated so that it can be compared to the depth of the user-prescribed root zone depth. This is necessary to determine the moisture deficiency in the root zone. The moisture zone depths are not a defined quantity in the original HSPF PWATER algorithm. However, AQUA TERRA (1998) determined that the lower zone becomes essentially saturated when the moisture content (LZS) is about four times the value nominal storage (UZSN). For the upper moisture zone, UZS, the ratio is about 2.5. Using the porosity, the depths of each zone can be found as:

$$D_L = \frac{4 * LZSN}{n_{micro}}$$

$$D_U = \frac{2.5 * UZSN}{n_{macro}}$$

where D_L and D_U are the depths of the respective zones, and n is the porosity. The user must also specify a root zone depth D_R. The root zone depth must be smaller than the larger of D_L and D_U. Otherwise, the moisture will never saturate the root zone, and an endless demand will be created in the model. The root zone depth and field capacity are converted into a maximum moisture content RZWSC:

$$RZWSC = F_C * D_R$$

where F_c is the field capacity, which is the sum of n_{macro} and $n_{micro.}$ The actual moisture content, RZWSA, is:

$$RZWSA = \frac{UZS * D_R}{n_{macro}} + \frac{LZS * D_R}{n_{micro}}$$

When the actual moisture content falls below a critical value, then a demand is created. The critical value WS_{min} is:

$$WS_{min} = C_{min} * RZWSC$$

where C_{min} is a parameter specifying the minimum capacity as a percentage of the total capacity. When RZWSA is less than WS_{min}, the demand N_{irr} is calculated as:

$$N_{irr} = AZRI * (RZWSC - RZWSA) / Eff$$

where AZRI is a parameter that specifies the areal fraction of land for the irrigation application and Eff represents the efficiency in distributing the irrigation to the vegetation.

The algorithm for specifying sources to meet the final demand, N_{irr}, consists of a prioritized order of sources and target percentages for each source. The three sources available, in order of priority, are local tertiary canals, local groundwater sources or external sources.

The targeted supply from each source is calculated as the prescribed percentage times the total demand. The model automatically looks for canal water first. For instance, if the target percentage for canals were set to 72%, the model would try and satisfy a cell's demand by using canal water until either 72% of the demand was met, or the tertiary canal water was completely drained. If the tertiary canals are drained before the demand is met, the remaining demand is met by the other two sources (surficial and deep aquifers). The supply from these two sources is the sum of their original targeted percentages plus any remaining unsatisfied supply not met by the tertiary canals. If there is an unmet supply from the canals, the supply is proportioned between the surficial and deep aquifers according to the ratio of their target percentages. Since it is possible that the targeted supply from canals may not be completely met during a simulation, the user may need to adjust the targeted value upward to obtain the desired percentage.

The irrigation supply can be applied by a number of options:

(1) added to the rainfall (i.e., spray application)

(2) added to the UZS (drip irrigation)

(3) added to the LZS (subsurface application)

(4) added to the groundwater (crown irrigation)

The user has the option to specify the percentage of irrigation supply that each application option receives.

The model parameters needed to implement the irrigation demand for a cell are shown below in Table 3.2.

Table 3.2 Irrigation Demand Module Parameters and Descriptions

Parameter	Description
C_{min}	Minimum allowable moisture (%)
N_{macro}	Macro-Pore space
N_{micro}	Micro-Pore space
D_R	Depth of root zone (ft)
S_CANAL	Percentage of canal water used to meet demand
S_SH_AQ	Percentage of shallow aquifer water used to meet demand
S_EXT	Percentage of external water sources (i.e., deep aquifer)
SPRAY	Percentage of demand applied via spray application
UPPER_Z	Percentage of demand applied via drip irrigation
LOWER_Z	Percentage of demand applied via subsurface
Eff	Efficiency of water application
AZRI	Areal fraction of irrigation application

3.1.2 High Water Table Algorithm

The high water table algorithm originally developed by AQUA TERRA (1996) used the special actions block of the HSPF model to re-route percolated water back to the moisture zones. This approach was adopted because it did not require direct changes to the code, and could be implemented via input commands to HSPF. Although the approach functions as desired, it is cumbersome and makes internal flux tracking difficult because water is constantly re-routed when the groundwater rises into the moisture zones. Because the WaSh model already involved significant changes to various HSPF code, an alternate and simpler approach has been developed. The approach is based on monitoring the groundwater elevation relative to the bottom of the moisture zones (similar to the approach of AQUA TERRA). When the groundwater rises into the moisture zones, the percolation that is calculated in the PWATER module is set to zero, preventing any more discharge to the groundwater. This causes the moisture zones to become saturated, and ultimately infiltration from surface storage is reduced and standing water can develop. This simple approach is shown in Figure 3.3. The bottom elevation of the moisture zones, which is needed to compare to the groundwater elevation is calculated by subtracting the moisture zone depths (D_R and D_U) from the land surface elevation. When high groundwater conditions exist, the total groundwater elevation is essentially the elevation of the surface storage (SURS). There are no additional parameters needed to implement this algorithm.

3.2 SIMULATION OF IMPERVIOUS CELL FRACTIONS

When a significant portion of a cell has impervious surfaces that drain directly to surface water bodies, the HSPF IWATER module is used to simulate discharges for the impervious fraction. The IWATER module represents interception storage, evaporation and surface runoff and assumes infiltration and percolation are zero. A block diagram of the IWATER algorithm, based on the description in the HSPF documentation (Bicknell et al., 1997) and as coded into the WaSh model, is shown in Figure 3.4.

In the IWATER algorithm, infiltration is zero and the subsurface process is not needed. In order to accommodate impervious surfaces in WaSh, each cell is assigned an impervious fraction IFRAC (which is zero when no significant impervious surfaces exist).

The model coefficients used in the IWATER implementation are listed in Table 3.3 The IWATER algorithm also used the parameters SLSUR, LSUR and PAN, but the values are identical to those used in the PWATER algorithm, and therefore they are only listed in Table 3.2.1.

Table 3.3 IWATER Module Parameters and Descriptions

HSPF PWATER Parameter	Description
IFRAC	Fraction of cell area that is impervious
RETS	Interception storage capacity
NSUR	Manning's n for land surface

3.3 CELL-BASED DISCHARGES

Discharges from each cell consist of surface and subsurface discharges. The total surface discharge is comprised of the combination of the surface water and interflow discharges. Thus, at each time interval the fluxes SURO and INFWO (which are the HSPF surface water and interflow discharge flux variable names) that are calculated by the HSPF algorithms are added to form the total surface discharge. If an impervious fraction exists within the cell, then the total surface discharge for the cell is calculated using the weighted sum of the pervious and impervious contributions. Thus the total cell surface discharge is:

$$SURO_{total} = (1 - IFRAC) * (SURO_{pervious} + INFWO_{pervious}) + IFRAC * SURO_{impervious}$$

Most of a cell's subsurface flows are handled directly by the groundwater model. For instance, a cell's calculated infiltration is routed directly to the groundwater, and the groundwater model simulates cell-to-cell groundwater fluxes, as well as exchanges with other surface water bodies, such as the tertiary canals, reaches and reservoirs. However, it may be useful to represent another cell-based subsurface discharge. This discharge may be used to represent sub-grid channels or streams that receive direct groundwater discharges, but are not resolved explicitly in the model configuration. The discharge is calculated using a stage-discharge relationship:

$$GWO = \begin{cases} (H - H_d) * E & \text{if} \quad H > H_d \\ 0 & \text{if} \quad H \le H_d \end{cases}$$

where H is the cell's groundwater elevation, H_d is the reference level for drainage and E is the exchange coefficient. The exchange coefficient is calculated as:

$$E = \sqrt{C_{area}} * C_d$$

where $\sqrt{C_{area}}$ is a length scale based on the cell area, and C_d is a conductance coefficient with units of ft/s. The groundwater discharge from this algorithm is routed in the same way as $SURO_{total}$ but is retained as a separate quantity within the WaSh model code because its associated water quality will likely be different than that of the surface water. For all subsequent hydrologic or hydraulic discussion in this report, a cell's discharge refers to the combination of $SURO_{total}$ and GWO, and is referred to as Q_{cell}:

$$Q_{cell} = SURO_{total} + GWO$$

3.4 CELL SURFACE AND SUBSURFACE DISCHARGE ROUTING

A special cell attribute has been developed to identify both cell discharge routing and groundwater exchanges with other objects (i.e., tertiary canals, reservoirs, reaches) in the model. Each cell is labeled as one of six types:

Free cell

Canal cell

Free-Reach cell

Canal-Reach cell

Free-Reservoir cell

Canal-Reservoir cell

The designation "free" or "canal" is used to differentiate between cells with and without tertiary canals. In a canal cell, the cell's surface discharge is routed to the cell's tertiary canals, and then from the tertiary canals to a reach or reservoir. In "free" cells, the surface water is routed directly to the user-specified reach or reservoir or to another cell's tertiary canals. The second designation in the cell type is used to specify potential groundwater interactions. For instance, in a Free-Reach cell, the cell's groundwater will interact with the surface water in the associated reach, whereas in a "free" cell, the groundwater does not interact with any other objects (except for the cell-to-cell groundwater interactions). A complete list of the surface routing and groundwater interactions is provided in Table 3.4.

Table 3.4 Water Routing Operations for Each Cell Type

Cell Type	Value	ID	Flow Routing Operations
Free	F	Receptor cell reach or reservoir ID	Surface water is directed to a nearby cell's canals, reach or reservoir
Canal	C	Receptor reach or reservoir ID	Cell discharge is directed to cell's tertiary canals Groundwater and tertiary canal surface water allowed to exchange Tertiary canal water exchanged with a reach or reservoir
Free-Reach	G	Receptor cell, reach or reservoir ID	Cell discharge is directed to a nearby cell's tertiary canals, reach or reservoir Groundwater and reach surface water allowed to exchange
Canal-Reach	R	Receptor reach ID	Cell discharge is directed to cell's tertiary canals Groundwater can be exchanged with tertiary canal water and with reach Tertiary canal water exchanged with a reach
Free-Reservoir	S	Receptor cell, reach or reservoir ID	Cell discharge is directed to a nearby cell's canals, reach or reservoir Groundwater and reservoir surface water allowed to exchange
Canal-Reservoir	T	Receptor reach ID	Cell discharge is directed to cell's tertiary canals Groundwater can be exchanged with tertiary canal water and with reservoir Tertiary canal water exchanged with a reservoir

For each cell in the model, the choice of cell type is guided by the basin characteristics. Large-scale topographic gradients can be used as guidance, but often local knowledge of topographic features and structures must be included in order to properly configure the model. The attribute value is assigned to the cell based on the user's interpretation of the basin characteristics to best reflect the basin's hydrologic and hydraulic properties.

The WaSh has a groundwater module that is based on the numerical solution to the standard groundwater flow equation (Darcy's Law and Continuity) for an unconfined aquifer. The model uses the same grid system as the basin's cell-based hydrology model (i.e. cell-based HSPF) and is applied only to the active cells. The model operates on a daily time step, during which it receives infiltrated water, loses water to evaporation, and exchanges water with adjacent cells and with tertiary canals, reaches and reservoirs/STAs.

4.1 GROUNDWATER MODULE EQUATIONS

The basic governing equation for the groundwater module is:

$$n\frac{\partial h}{\partial t} = \frac{\partial}{\partial x}\left(K_x (h - h_c)\frac{\partial h}{\partial x}\right) + \frac{\partial}{\partial y}\left(K_y (h - h_c)\frac{\partial h}{\partial y}\right) + S_i - S_e + Q_{c-gw}$$

where h is the groundwater elevation relative to the model datum (for instance NGVD), n is the porosity, K_x and K_y are the hydraulic conductivity in the x-, and y- directions, h_c is the elevation of the aquifer base relative to NGVD, S_i, S_e are source/sink terms representing deep percolation and evapotranspiration, and $Q_{c\text{-}gw}$, $Q_{r\text{-}gw}$, and $Q_{res\text{-}gw}$ are exchanges with the canal cells, reaches and reservoirs that are described in Section 8.0.

4.2 HYDROLOGICAL SOURCE TERMS

Two of the source terms on the right-hand side of the equation, S_i and S_e, are outputs from the WaSh hydrology module (specifically, the WaSh implementation of the PWATER algorithm). The infiltration is set to the HSPF output PERC (see Figure 3.2): and the evaporation is set equal

$$S_i = \text{PERC}$$

to the original HSPF groundwater evaporation rate AGWET:

$$S_e = \text{AGWET}$$

The methods for calculating percolation (PERC) and groundwater ET (AGWET) can be found in the HSPF documentation.

4.3 BOUNDARY CONDITIONS

The only boundary condition is applied automatically and is imposed when an active cell is adjacent to the grid boundary or to an inactive cell. For these conditions, a no-flow condition is imposed along the grid boundary or with an inactive cell.

4.4 NUMERICAL SOLUTION

The governing equation is solved numerically using the basin cell structure. A second-order finite difference approximation is used for the second derivatives, and an explicit backward difference approximation is used for the time derivative. By designating the equation parameters

and water elevation h for each cell by the indexes i and j, and the time level by the index m, the resulting finite difference equation for each cell is:

$$\frac{1}{n_{i,j}}\frac{h_{i,j}^{m+1}-h_{i,j}^{m}}{\Delta t}=K_x\left[\frac{(\frac{h_{i,j}^{m}+h_{i+1,j}^{m}}{2}-h_c)}{\Delta x}\left(\frac{h_{i+1,j}^{m}-h_{i,j}^{m}}{\Delta x}\right)-\frac{(\frac{h_{i,j}^{m}+h_{i-1,j}^{m}}{2}-h_c)}{\Delta x}\left(\frac{h_{i,j}^{m}-h_{i-1,j}^{m}}{\Delta x}\right)\right]+$$

$$Ky\left[\frac{(\frac{h_{i,j}^{m}+h_{i,j+1}^{m}}{2}-h_c)}{\Delta y}\left(\frac{h_{i,j+1}^{m}-h_{i,j}^{m}}{\Delta y}\right)-\frac{(\frac{h_{i,j}^{m}+h_{i,j-1}^{m}}{2}-h_c)}{\Delta y}\left(\frac{h_{i,j}^{m}-h_{i,j-1}^{m}}{\Delta y}\right)\right]+S_{i_{i,j}}^{m}-S_{e_{i,j}}^{m}+Q_{c-gw_{i,j}}^{m}+Q_{r-gw_{i,j}}^{m}+Q_{res-g}^{m}$$

where Δt is the time step (one day), and Δx and Δy are the grid cell dimensions in each direction. During each time step, the right-hand side of the equation is evaluated based on current time level conditions, and the new water elevation is found by solving for $h_{i,j}^{m+1}$.

4.5 MODEL PARAMETERS

The model parameters required to configure the groundwater model are listed in Table 4.1.

Table 4.1 Groundwater Model Parameters

Groundwater Model Parameter	Description
n	Porosity
K_x, K_y	Hydraulic Conductivity (ft/day)
h_c	Aquifer base (ft)
AGWETP	Evaporation parameter

Flow in the cell-based tertiary canal system is represented using a storage-based approach, using the canal water depth D_{tc} as the state variable. The governing equation for each cell's tertiary canals is:

$$\frac{dD_{tc}}{dt} = (F_{in} - F_{out}) / C_{area}$$
$$H_{tc} = D_{tc} + C_{be}$$

where H_{tc} is the water elevation relative to the model datum, F_{in} and F_{out} are the flows into and out of the canal, C_{area} is the surface area of the canal and C_{be} is the bottom elevation of the canal relative to the model datum. The canal area is defined as:

$$C_{area} = C_w * C_L$$

where C_w and C_L are the canal width and length, and are user-prescribed parameters for each cell. The net flow into or out of the storage is defined as:

$$F_{net} = (F_{in} - F_{out}), \quad \text{where}$$
$$(F_{in} - F_{out}) = \sum_{i,j} Q_{cell} + Q_{c-gw} - Q_{c-r} - Q_{c-res}$$

Here, Q_{cell} is the cell discharge (see section 3.1) for all cells for which the cell discharge has been routed to the cells tertiary canals. $Q_{c\text{-}gw}$, $Q_{c\text{-}r}$ and $Q_{c\text{-}res}$ are flows representing interactions with the cell's groundwater, a reach and/or a reservoir, and are discussed in Section 8.0.

The model parameters for specifying the tertiary canal operation are listed in Table 5.1.

Table 5.1 Tertiary Canal Model Parameters

Tertiary Canal Parameter	Description
C_w	Canal width
C_L	Canal length
C_{be}	Canal bottom elevation

The reach network is intended to provide explicit representation of the major flow conduits in the basin. It is based on the one-dimensional shallow-water wave equation, and includes branching and representation of structural control on flow and stages, interactions with groundwater and with reservoirs and STAs. Figure 6.1 shows a typical reach network, including branches. At each juncture between branches, the two branches are identified as the "upstream" or "downstream" branch for that juncture.

6.1 GOVERNING EQUATIONS

The governing equations for the reach network are:

$$\frac{\partial w_r h_r}{\partial t} = \frac{\partial q_r}{\partial s} + Q_{io}$$

$$\text{where} \quad Q_{io} = \sum_{i,j} Q_{cell} + Q_{re} + Q_e + Q_{c-r} + Q_{r-res} + Q_{r-gw}$$

$$\frac{\partial q_r}{\partial t} + \frac{\partial u q_r}{\partial s} + g h_r \frac{\partial h_r}{\partial s} = -w_r \tau_b - g w_r \frac{\partial \eta_r}{\partial s}$$

where q_r is the flow, u is the width- and depth-averaged flow velocity, g is the acceleration due to gravity, w_r is the channel width, h_r is the water depth (referenced to the channel bed), η_r is the bed elevation (referenced to model datum), t is time and s is distance along the channel. Here, Q_{cell} is the cell discharge (see Section 3.1) for all cells for which the cell discharge has been routed to the reach. The flux Q_{re} is the net flux due to rainfall and evaporation. The source term Q_e represents external flow sources to the reach, and are provided as a time series in an input file. The source terms $Q_{tc-r,}$ Q_{r-res} and Q_{r-gw} represent exchanges between model objects and are described in Section 8.0.

The bottom stress τ_b is based on a Manning's n formulation:

$$\tau_b = \frac{u|u|}{h_r\, n}$$

where n is Manning's n.

6.2 BOUNDARY CONDITIONS

Boundary conditions can be one of two types; a specified flow or specified water elevation. Specified flow conditions are typically used when a flow structure controls the flow out of the system. The water elevation (or head) condition is used when the system drains unobstructed into a receiving water body.

For the specified flow option, the downstream flow q_l' is calculated using an equation for flow over a weir:

$$q_l' = \begin{cases} C_w * W_w * (h_l - h_w)^{1.5} & h_l > h_w \\ 0 & h_l \le h_w \end{cases}$$

where C_w is the weir coefficient, W_w is the weir width, h_w is the weir crest elevation and h_l is the water elevation (stage) in the downstream reach.

For tailwater (or specified water elevation) the downstream boundary condition is:

$$h_o = h_s$$

where h_s is the user-specified downstream water elevation.

6.3 NUMERICAL SOLUTION

The governing equations are solved using a finite volume procedure. For this purpose, the reach network is subdivided into a series of interconnected reaches and nodes. The reach and node system, depicted in Figure 6.2 for a single branch of the network, is equivalent to a finite volume staggered grid approach. The index k is used to specify the reach or node. The water depths h_k are defined in each segment, and the flows q_k are defined at each node. Here k refers to the k^{th} reach in the reach network. The reach length is designated as Δs_1. Note that the surface water elevation RE_k is equal to the sum of the reach bottom elevation and water depth $h_k+\eta_k$. Using second-order centered finite differences for the spatial derivatives and a first-order backward

$$\frac{q_k^{m+1}-q_k^m}{\Delta t}+\frac{F_{k+1/2}^{m+1}-F_{k-1/2}^{m+1}}{\Delta s_2}+g\frac{\hat{w}_k\hat{h}_k^m\left(h_k^{m+1}-h_{k-1}^{m+1}\right)}{\Delta s_2}=\tau_{bi}-g\hat{h}_i^m\hat{w}_i\frac{\eta_k-\eta_{k-1}}{\Delta s_2}$$

difference approximation for the time derivatives, the implicit finite difference approximations to the governing equations are:

$$\frac{h_k^{m+1}-h_k^m}{\Delta t}-\frac{q_{k_i}^{m+1}-q_{k+1}^{m+1}}{\Delta s_1 w_k}=Q_{io_k}$$

where

$$u_{k+1/2}=\frac{q_k+q_{k+1}}{2h_k w_k},\quad u_{k-1/2}=\frac{q_k+q_{k-1}}{2h_{k-1}w_{k-1}}$$

and

$$F_{k-1/2}=\begin{cases}u_{k-1/2}^m q_{k-1}^{m+1}, & u_{k-1/2}>0\\ u_{k-1/2}^m q_k^{m+1}, & u_{k-1/2}<0\end{cases}$$

$$F_{k+1/2}=\begin{cases}u_{k+1/2}^m q_k^{m+1}, & u_{k+1/2}>0\\ u_{k+1/2}^m q_{k+1}^{m+1}, & u_{k+1/2}<0,\end{cases}$$

The bottom stress is:

$$\tau_{bk} = \frac{-u_k |u_k|}{\hat{h}_k n}$$

The terms $\hat{h}$, $\hat{w}$ and Δs_2 are spatial averages defined as

$$\hat{h}_k = \frac{h_k + h_k - 1}{2} \quad \hat{w}_k = \frac{w_k + w_{k-1}}{2} \quad \text{and} \quad \Delta s2 = \frac{\Delta s_k + \Delta s_{k-1}}{2}$$

and the index m indicates the time level.

The finite difference equations are coupled in the implicit "m+1" terms. In order to solve the equations, a block tri-diagonal solution procedure is used. For each reach/node pair, two equations can be written in the following matrix form:

$$\begin{bmatrix} 0 & 0 \\ -\frac{g\hat{h}_k^m \hat{w}_k}{\Delta s_2} & 0 \end{bmatrix} \begin{bmatrix} \frac{1}{\Delta t} & \frac{-1}{\Delta s_1 w_k} \\ \frac{g\hat{h}_k^m \hat{w}_k}{\Delta s_2} & \frac{1}{\Delta t} + \frac{u_{k-1/2}^m}{\Delta s_2} \end{bmatrix} \begin{bmatrix} 0 & \frac{1}{\Delta s_1 w_k} \\ 0 & \frac{u_{k+1/2}^m}{\Delta s_2} \end{bmatrix} \begin{Bmatrix} h_{k-1}^{m+1} \\ q_{k-1}^{m+1} \\ h_k^{m+1} \\ q_k^{m+1} \\ h_{k+1}^{m+1} \\ q_{k+1}^{m+1} \end{Bmatrix} = \begin{Bmatrix} \frac{h_k^m}{\Delta t} + \frac{Q_{ek}}{\Delta s_1 w_k} \\ \frac{q_k^m}{\Delta t} - \tau_{bk} - g h_k^m \frac{(\eta_k - \eta_{k-1})}{\Delta s_2} \end{Bmatrix}$$

For i =1, which corresponds to the basin outlet, one of the two types of boundary conditions are applied. For the specified flow, the block matrix equations become:

$$\begin{bmatrix} \frac{1}{\Delta t} & 0 \\ \frac{g\hat{h}_1^m \hat{w}_1}{\Delta s_2} & \frac{1}{\Delta t} + \frac{u_{1/2}^m}{\Delta s_2} \end{bmatrix} \begin{bmatrix} 0 & 0 \\ 0 & \frac{u_{3/2}^m}{\Delta s_2} \end{bmatrix} \begin{Bmatrix} h_i^{m+1} \\ q_i^{m+1} \\ h_{i+1}^{m+1} \\ q_{i+1}^{m+1} \end{Bmatrix} = \begin{Bmatrix} \frac{h_1'}{\Delta t} \\ \frac{q_1^m}{\Delta t} - \tau_{b1} + \frac{g\hat{h}_1^m \hat{w}_1}{\Delta s_2} \end{Bmatrix}$$

For the second type of boundary condition, the downstream water elevation (or water depth) is specified, and the block matrix equations for the downstream block are:

$$\begin{bmatrix} \frac{1}{\Delta t} & 0 \\ \frac{g\hat{h}_1^m \hat{w}_1}{\Delta x_2} & \frac{1}{\Delta t} + \frac{u_{1/2}^m}{\Delta x_2} \end{bmatrix} \begin{bmatrix} 0 & 0 \\ 0 & \frac{u_{3/2}^m}{\Delta x_2} \end{bmatrix} \begin{Bmatrix} h_i^{m+1} \\ q_i^{m+1} \\ h_{i+1}^{m+1} \\ q_{i+1}^{m+1} \end{Bmatrix} = \begin{Bmatrix} \frac{h_1'}{\Delta t} \\ \frac{q_1^m}{\Delta t} - \tau_{b1} + \frac{g\hat{h}_1^m \hat{w}_1}{\Delta x_2} \end{Bmatrix}$$

where h_1' is the specified water depth and

$$\hat{h}_1^m = \frac{(h_1^m + h')_1}{2}$$

It is assumed in the above equation that the bed slope at the basin outfall is zero. When the 2x2 matrices for reach/node pair are assembled for the entire channel, a block tri-diagonal matrix of the form:

$$\begin{bmatrix} [\,] & [\,] & & & & & \\ [\,] & [\,] & [\,] & & & & \\ & [\,] & [\,] & [\,] & & & \\ & & & [\,] & [\,] & [\,] & \\ & & & & [\,] & [\,] & [\,] \\ & & & & & [\,] & [\,] \end{bmatrix} \begin{Bmatrix} \\ \\ \\ \\ \\ \\ \\ \end{Bmatrix} = \begin{Bmatrix} \\ \\ \\ \\ \\ \\ \\ \end{Bmatrix}$$

results. These matrix equations can be solved efficiently for each time step for the new water levels h_k and flows q_k.

When the reach network contains branches, the flows and stages for the reaches in each branch are determined independently using the block tri-diagonal solution procedure. However, prior to invoking the solver, the flows between branches are approximated and used as the downstream boundary condition for the upstream branch and as an external flow source (i.e., Q_e) in the downstream branch. Figure 6.3 shows an example of a branched system. Flow leaving branch 2 enters the 5th reach of branch 1. At the juncture between branch 2 and branch 1, the estimated flow between the two branches, designated as $Q^{1\text{-}2}$, is used to specify a flow boundary condition (i.e., q_1') in the equations for branch 2. The flow is also added to the source term in reach 5 of branch 1. The source term for reach 5 of branch 1 is updated as follows:

$$Q_{e5}^1 = Q_{e5}^1 - Q^{1-2}$$

where the superscript denotes the branch number.

The flow between branches, $Q^{1\text{-}2}$, is solved using a semi-implicit scheme that is a simplification of the block-matrix implicit scheme used for each branch. The implicit stencil for the unknowns:

$$\left(h_1^{m+1}, q_1^{m+1}, h_2^{m+1}, q_2^{m+1}\right)$$

is replaced with:

$$\left(h_1^{m+1}, q_1^{m+1}, h_2^{m+1}, q_2^{m}\right)$$

which yields three equations for the three unknowns h_1, q_1 and h_2, which are the stage and flow in the upstream branch and the stage in the connecting downstream reach. The flow q_1 that is

calculated in the "local" semi-implicit solution is then used as a boundary condition for the implicit solution for the upstream branch and as a source to the downstream reach. The stages h_1 and h_2 calculated in the semi-implicit scheme are ignored, and replaced with those obtained in the implicit solution for each branch. Thus, it is only the flow between branches that is used from the semi-implicit "local" solution.

6.4 STRUCTURES

Structures can be placed anywhere in the reach network, including branch junctures. When a structure is present, the flow at that node is determined at the beginning of the time step using the structure flow formulas, and its value replaces the momentum equation for that node. The matrix equations are reduced to the same form as for a flow boundary condition, except that the index 1 is replaced by the local index k for the node at which the structure is located.

The structure represented in the WaSh model is a sharp-crested weir with an irrigation pump option. A standard weir coefficient is used for the weir component:

$$q_k = \begin{cases} C_w * W_w * (h_k - h_w)^{1.5} & h_k > h_w,\ h_{k-1} < h_w \\ -C_w * W_w * (h_{k-1} - h_w)^{1.5} & h_{k-1} > h_w,\ h_k < h_w \\ Cw * (\overline{h_{k-1} + h_k}) \sqrt{|h_{k-1} - h_k|} & h_k, h_{k-1} > h_w \\ 0 & h_k, h_{k-1} \le h_w \end{cases}$$

where h_k is the upstream reach stage, h_{k-1} is the downstream reach stage, C_w is the weir coefficient, and W_w is the weir width.

The irrigation pumping option allows the user to specify conditions under which water will be pumped upstream across the structure to provide irrigation supply when the water elevations of the upstream reaches are low. This option requires specification of an upstream minimum water elevation h_{min} and a pumping rate P_{irr}. The structure flow is then:

$$q_k = \begin{cases} P_{irr} & h_k < h_{min} \\ 0 & h_k > h_{min} \end{cases}$$

The value of h_{min} must be lower than the weir rest elevation h_w.

6.5 MODEL PARAMETERS

The model parameters for the reach network are listed in Table 6.1.

Table 6.1 Reach Network Model Parameters

Item	Parameter	Description
Reaches	w	width
	Δs	length
	η	bottom elevation
	n	Manning's n
Structure weir	C_w	weir coefficient
	W_w	width
	h_w	crest elevation
Structure pumping	h_{min}	minimum stage in upstream reach
	P_{irr}	Irrigation pumping rate

Reservoirs and STAs are represented as a flow in the cell-based tertiary canal system, which is represented using a storage-based approach with the reservoir volume V_r as the state variable. Reservoirs and STAs are modeled identically, and are differentiated by the user only by the water quality parameter values assigned to represent the reservoir or STA. For simplicity, the term "reservoir" is used to refer to both reservoirs and STAs. The reservoirs are characterized in WaSh by their geometric footprint, total footprint area A_r, and bottom elevation η_r. The geometry and location of the reservoir are included in the WaSh model because the reservoirs will often be sufficiently large that they may cover numerous cells in the cell-based hydrology model. When this occurs, the cells that are completely covered by the reservoir are excluded from the model. Furthermore, the area for any cells that intersect the reservoir/STA boundary will be reduced to reflect the area subsumed by the reservoir. Figure 7.1 shows a typical configuration identifying inactivated cells and those cells for which the cell area has been reduced.

7.1 GOVERNING EQUATIONS

The governing equation for the reservoir or STA is based on mass balance, and is:

$$\frac{\partial V_R}{\partial t} = \sum Q_{cell} - Q_{ext} + Q_{io} + R\ A_R - E\ A_R$$

The flux Q_{io}, representing exchanges with other objects in the WaSh model, is defined as:

$$Q_{io} = Q_{c-res} + Q_{res-gw} + Q_{res-res} + Q_{r-res}$$

the components of which are described in Section 8.0.

The water elevation relative to the model datum, h_{res}, in the reservoir is defined as

$$h_{res} = \eta_r + \frac{V_R}{A_R}$$

where h_{Rb} is the bottom elevation of the reservoir.

Each reservoir in the WaSh model is divided into five compartments that are arranged serially. This is done to accommodate the effects of retention time on the water quality in the reservoirs. All of the inflows are directed to the first segment, and all flows out of the reservoir leave from the fifth segment. Figure 7.2 shows the basic configuration. The basic flow equation is solved for each time step to obtain the new reservoir volume, and then the flows between segments are obtained using the level-pool assumption (water surface is the same for all segments). Referring to the basic reservoir flow equation above, the inflows are defined as:

$$Q_{in} = \sum Q_{cell} + \max(Q_{io}, 0) + R\ A_R$$

$$Q_{out} = -Q_{ext} - \left|\min(Q_{io}, 0)\right| - E\ A_R$$

In this formulation, the component flows comprising Q_{io} are defined as positive when they flow into the reservoir, and negative when they flow out of the reservoir.

The flux Q_{ext} represents potential discharges from the reservoir out of the model domain. In the WaSh model, these flows are represented as flow over a weir. The equation for the external flow is:

$$Q_{ext} = \begin{cases} C_w^e * W_w^e * (h_r - h_w^e)^{1.5} & h_r > h_w^e \\ 0 & h_r \le h_w^e \end{cases}$$

where h_w^e is the elevation of the weir crest, C_w^e is the weir coefficient and W_w^e is the weir width.

7.2 NUMERICAL SOLUTION

The change in reservoir volume for a time step is:

$$\Delta V_R = (Q_{in} - Q_{out})\Delta t$$

The reservoir volume and the five segment volumes V_{Ri} are updated according to:

$$V_R^{n+1} = V_R^n + \Delta V_R$$

$$V_{Ri}^{n+1} = V_{Ri}^n + \frac{\Delta V_R}{5}$$

The flows between segments for a time step are obtained as follows:

$$q_1 = \Delta V_{R1} - Q_{in}$$
$$q_2 = \Delta V_{R2} - q_1$$
$$q_3 = \Delta V_{R3} - q_2$$
$$q_4 = \Delta V_{R4} - q_3$$
$$q_5 = Q_{out}$$

Note that the internal segment volumes and flows are only needed for the water quality simulation.

7.3 MODEL PARAMETERS

The model parameters for the reservoir or STA are listed in Table 7.1.

Table 7.1 Reservoir/STA Model Parameters

Reservoir Parameter	Description
A_r	Bottom area
η_r	Bottom elevation
Geo-referenced footprint	Used to deactivate cells and/or adjust cell areas
h_w^e	External flow weir crest elevation
C_w^e	External flow weir coefficient
W_w^e	External flow weir width

The routing schemes for each individual component described in Sections 4.0 through 7.0 for groundwater, tertiary canals, reaches and reservoirs contained numerous interactions between components. The terms are:

$$Q_{c-gw},\quad Q_{r-gw},\quad Q_{res-gw},\quad Q_{c-r},\quad Q_{c-res},\quad Q_{r-res},\quad Q_{res-res}$$

When a cell has tertiary canals, the canals will exchange water with the cell's groundwater according to a conductance-based formulation:

$$Q_{c-gw} = \frac{(h_{gw} - h_{tc})\ C}{A}$$

where h is the groundwater elevation in the cell containing the tertiary canals, C is the conductance, and A is the cell area. The discharge can be positive or negative depending on the relative elevations of the groundwater and canal surface water. The conductance is defined as:

$$C = \frac{C_L\ P\ K_{c-gw}}{d},$$

where

$K_{c\text{-}gw}$ = hydraulic conductivity of stream bed material

P = wetted perimeter of stream cross section (C_w+2*D_{tc}),

d = thickness of stream bed material (set to 1 foot)

When a cell intersects a reach in the reach network, the reach will exchange water with the cell's groundwater according to a conductance-based formulation:

$$Q_{r-gw} = \frac{(h_{gw} - h_r)\ C}{A}$$

where h is the groundwater elevation in the cell containing the tertiary canals, C is the conductance, and A is the cell area. The conductance is defined as:

$$C = \frac{C_L\ P\ K_{r-gw}}{d},$$

where

$K_{r\text{-}gw}$ = hydraulic conductivity of stream bed material

P = wetted perimeter of stream cross section (W_r+2*h_r),

d = thickness of stream bed material (set to 1 foot)

The cells intersecting the reservoir are those that have had their cell area reduced due to the reservoir footprint overlying the cell. Cells that are completely covered by the reservoir are removed from the model and are not considered for groundwater exchanges.

When a cell intersects a reservoir, the reservoir will exchange water with the cell's groundwater according to:

$$Q_{res-gw} = \frac{K_{res-gw}(h_{res} - h_{gw})(h_{res} + h_{gw})\sqrt{A_1}}{2\sqrt{A_2}}$$

where

K_{res-gw} =hydraulic conductivity of stream bed material

A_1 = the area of the cell covered by the reservoir or STA

A_2 = the area of the cell not covered by the reservoir or STA

For each cell with tertiary canals, there are two options for controlling the discharge from the tertiary canal to the designated reach, either weir-controlled flow or pumped flow. For weir-controlled flow the equation is:

$$Q_{c-r} = \begin{cases} C_{c-r} * W_{c-r} * (h_{tc} - h_{rw})^{1.5} & h_{tc} > h_{rw} \\ 0 & h_{tc} \le h_{rw} \end{cases}$$

Where C_{c-r} is the weir coefficient, W_{c-r} is the weir width and h_{rw} is the weir crest elevation. For the pumping option, the tertiary canals are pumped at the pumping rate P_{tc} when the water elevation rises above a prescribed level H_{tc-max}, and then pumping continues until the water level in the tertiary canals drops below another prescribed level, $H_{tc-cutoff}$. This approach allows for simulation of "pumping down" the tertiary canals, a practice used in many agricultural areas during the wet season.

Also, the tertiary canal pumps can be used to pump from the reach to the tertiary canals. This option is used when an irrigation demand exists for a cell, and the supply from the tertiary canal is exhausted because the tertiary canals become dry. When these conditions occur, the WaSh model will pump water from the reach at a rate P_{tc} until the canals reach the $H_{tc-cutoff}$ level. The pump discharge is sent to the designated reach.

For each cell with tertiary canals, there are two options for controlling the discharge from the tertiary canal to the designated reservoir, either weir-controlled flow or pumped flow. These options and the option for pumping from the reservoir to the tertiary canal to replenish irrigation water supply are essentially identical to those for the tertiary canal-reach exchange. For weir-controlled flow the equation is:

$$Q_{c-res} = \begin{cases} C_{c-res} * W_{c-res} * (h_{tc} - h_{resw})^{1.5} & h_{tc} > h_{resw} \\ 0 & h_{tc} \le h_{resw} \end{cases}$$

where C_{c-res} is the weir coefficient, W_{c-res} is the weir width and h_{resw} is the weir crest elevation. For the pumping option, the tertiary canals are pumped at the pumping rate P_{tc} when the water elevation rises above a prescribed level H_{tc-max}, and then pumping continues until the water level in the tertiary canals drops below another prescribed level, $H_{tc-cutoff}$. The pump discharge is sent to the designated reservoir.

Also, the tertiary canal pumps can be used to pump from the reservoir to the tertiary canals. This option is used when an irrigation demand exists for a cell, and the supply from the tertiary canal is exhausted because the tertiary canals become dry. When these conditions occur, the WaSh model will pump water from the reach at a rate P_{tc} until the canals reach the $H_{tc-cutoff}$ level.

The model parameters for all groundwater and tertiary canal exchanges are listed in Table 8.1.

Table 8.1 Model Parameters

Flow	Parameter	Description
Q_{c-gw}	$K_{c\text{-}gw}$	Hydraulic conductivity of stream bed material
Q_{r-gw}	$K_{r\text{-}gw}$	Hydraulic conductivity of stream bed material
Q_{res-gw}	$K_{res\text{-}gw}$	Hydraulic conductivity of material near base of reservoir
Q_{c-r}	$C_{c\text{-}r}$	Weir coefficient
	$W_{c\text{-}r}$	Weir width
	H_{rw}	Weir crest elevation
	P_{tc}	Canal pumping rate
	$H_{tc\text{-}max}$	Critical elevation to start pumping
	$H_{tc\text{-}cutoff}$	Critical elevation to stop pumping
Q_{c-res}	$C_{c\text{-}res}$	Weir coefficient
	$W_{c\text{-}res}$	Weir width
	H_{resw}	Weir crest elevation
	P_{tc}	Canal pumping rate
	$H_{tc\text{-}max}$	Critical elevation to start pumping
	$H_{tc\text{-}cutoff}$	Critical elevation to stop pumping

There are four possible exchanges between reaches and reservoirs supported in the WaSh model. The exchanges are defined in Table 8.2 below:

Table 8.2 Specific Reach-Reservoir Exchanges

Flow	Description	Equation	Parameter Definition
Q^1_{r-res}	Base Reservoir inflow	$= f_1 * \max(Qb - Qc, 0)$	$\mathbf{f_1}$ is fraction of basin outfall flow Q_b that is diverted to reservoir or STA, Q_b must exceed $\mathbf{Q_c}$ before flow is diverted
Q^2_{r-res}	Irrigation Releases	$= \begin{cases} 0 \text{ if } H_p > H_c \\ Q_{irr} \text{ if } H_p < H_c \end{cases}$	If canal water (reach network) level H_p is lower than critical level $\mathbf{H_c}$, the water is supplied from reservoir at rate $\mathbf{Q_{irr}}$

Flow	Description	Equation	Parameter Definition
Q^3_{r-res}	Emergency Release to Canals	$= C_w * (h_R - H_w)^n$	**C_w** and **n** are weir coefficients, and **H_w** is the elevation of the weir (width subsumed into C_w)
Q^4_{r-res}	Seepage Flow to Canals or Reaches	$= Cs * (h_R - H_s)$	H_s is the surface water elevation in the designated canal or reach, **Cs** scales the seepage flow

*Bold characters in parameter definition column indicate model parameter.

There is one possible exchange between two reservoirs. This exchange was originally designed to simulate a reservoir discharging to an STA. The exchange is depicted in Figure 8.1 and described in Table 8.3.

Table 8.3 Reservoir-Reservoir Exchange

Flow	Description	Equation	Parameter Definition
$Q_{res-res}$	Reservoir-to-STA	$Q_2 = f_2 * V_R$	**f_2** is fraction of reservoir volume released each day

*Bold characters in parameter definition column indicate model parameter.

The water quality component of WaSh supports two options: (1) basic water quality and (2) advanced water quality. The basic water quality option consists of production and transport of five constituents: total suspended sediments (TSS), particulate nitrogen and phosphorus (PN and PP) and soluble nitrogen and phosphorus (SN and SP). Production is modeled using event mean. Transport through canals, reaches and in reservoirs is modeled using conservation of mass and either first-order decay or settling. When settling is included, the transport model also includes a stream bed simulation.

The advanced water quality option consists of simulating the production, transport and in-stream processes for dissolved oxygen, carbonaceous oxygen demand, ammonia, nitrate, organic nitrogen, organic phosphorus and soluble phosphorus. The event mean concentration approach is used for all constituents except for dissolved oxygen. Transport is modeled using conservation of mass, including settling; and in-stream processes are modeled using non-linear kinetic routines adopted from the WASP model (Ambrose, et al., 1988).

In all water quality simulations, the state-variables are the constituent concentrations in mass/unit volume.

9.1 BASIC WATER QUALITY SIMULATION

9.1.1 Production Terms

The source terms for the five basic water quality constituents PN, PP, SN, and TSS are modeled using an EMC approach. The EMC approach consists of assigning each cell runoff concentrations based on measured data for the cell's land use attribute. For each land use, the surface discharge and groundwater discharges are assigned concentrations for each water quality constituent based on a compilation of site-specific or regional data. The EMC values can vary monthly and be specified separately for each land use and soil type. In addition, the surface water concentrations can vary with runoff intensity according to the following function:

$$C^{surface} = C^{surface}_{emc}\ (m)*(1+(SURO_{total}/C_1)\text{^}C_2)$$

where C_1 and C_2 are user-specified parameters, and $SURO_{total}$ is the surface runoff. $C^{surface}_{emc}$ is the value for the constituent for each month m. The EMC concentrations for pervious and impervious contributions are assumed to be the same.

A separate set of EMC values can be set for groundwater discharges:

$$C^{gw} = C^{gw}_{emc}$$

The associated mass flux (or load) for the cell's discharge is for a constituent:

$$L_{cell} = C^{surface} * SURO_{total} + C^{gw} * GWO$$

The parameters for the basic water quality production model are listed in Table 9.1.

Table 9.1. Basic Water Quality Model Production Term Parameters

Parameter	Description
$C_{ems}^{surface}$	EMC for surface discharges, one value for each constituent for each month
C_1	Coefficient in surface discharge concentration controlling affect of discharge intensity on concentration – one global value
C_2	Coefficient in surface discharge concentration controlling affect of discharge intensity on concentration – one global value
C_{ems}^{gw}	EMC for groundwater discharges, one value for each constituent for each month

9.1.2 Transport in Reaches

Transport of water quality constituents in each reach network is modeled using the depth- and width-averaged scalar mass transport equation. The WaSh model represents surface water transport for all five constituents. For TSS and particulate nutrients, a simulation of the deposition and erosion from the channel bed is also simulated. The governing equation for transport in the reach network is:

$$\frac{\partial VC_m}{\partial t} + \oint qC_m = S_m$$

where V is the reach volume, C_m is the depth-, and width- averaged concentration for the m_{th} constituent in the surface water, q is the flow in the reaches, S_m represents external sources or sinks, and t is time.

The finite difference equation for a reach is:

$$\frac{C_{k,m}^{n+1} * V_k^{n+1} - C_{k,m}^{n} * V_k^{n}}{\Delta t} + F_{k+1/2}^{n+1} - F_{k-1/2}^{n+1} = S_{k,m}$$

where V_k is the k^{th} reach volume, $S_{k,m}$ is the source for the k^{th} reach and F is the constituent advective flux defined as:

$$F_{k+1/2} = \begin{cases} C_k^{n+1} q_{k+1}^{n+1}, & q_{k+1}^{n+1} > 0 \\ C_{k+1}^{n+1} q_{k+1}^{m+1}, & q_{k+1}^{n+1} < 0, \end{cases}$$

$$F_{k-1/2} = \begin{cases} C_k^{n+1} q_k^{n+1}, & q_k^{n+1} > 0 \\ C_{k-1}^{n+1} q_k^{n+1}, & q_{k+1}^{n+1} < 0 \end{cases}$$

The volumes V_k^{n+1} and the flows q_k^{n+1} are already known from the flow solution, requiring a solution only for the new concentrations C_k^{n+1}. The basic equation for each reach is:

$$\left[\max(q_{k+1}^{n+1},0) \quad \frac{V_k^{n+1}}{\Delta t} + \min(q_{k+1}^{n+1},0) + \max(q_k^{n+1},0) \quad \min(q_k^{n+1},0)\right]\begin{pmatrix} C_{k+1,m}^{n+1} \\ C_{k,m}^{n+1} \\ C_{k-1,m}^{n+1} \end{pmatrix} = S_{k,m}^{n}$$

When the equations are compiled for each reach in a branch, they form a tri-diagonal matrix, which is solved using the Thomas algorithm.

The source term $S_{k,m}^{n}$ represents contributions from the surface runoff, exchanges with other model objects (groundwater, reservoirs, etc.), and first-order decay. For the particulate fractions and TSS, settling is also represented. The individual components of the source term are:

$$S_{k,m}^{n} = \sum_{i,j} L_{cell,m} + Q_e C_{e,m} + Q_{c-r} C_{c-r,m} + Q_{r-res} C_{r-res,m} + Q_{r-gw} C_{r-gw,m} - C_{k,m}\delta_m - F_{b,m}$$

where the summation is over all cells discharging to the reach, $C_{e,m}$ are the concentrations in the source terms, δ_m is the first-order decay rate and $F_{,b,m}$ is the settling flux. The settling flux is also a source in the bed evolution equations. The concentrations for the exchange fluxes, $Q_{c\text{-}r}$, $Q_{r\text{-}res}$ and $Q_{r\text{-}gw}$ depend on the direction of the flow. When the flow is from the reach, the concentrations are the reach concentrations. When the flow is from the other object (groundwater, reservoir, etc.) to the reach, then the concentrations are those in the other object. This approach is essentially equivalent to an explicit upwind differencing scheme.

For TSS and particulate constituents, exchange with and accumulation in the bed is also simulated. The governing equation for the bed is:

$$\frac{\partial B_{k,m}}{\partial t} = F_{k,m}$$

$$F_{k,m} = -E_{k,m} + D_{k,m}$$

where $B_{k,m}$ is the concentration in the bed (mg/ft^2), and F is the flux between the bed and the water column defined in terms of an erosional flux $E_{k,m}$ and depositional flux $D_{k,m}$. The governing equation for the bed is solved using an explicit backward differenced finite difference scheme.

The erosional and depositional fluxes are defined as:

$$E_{k,m} = \begin{cases} E_r \tau_{k,m}, & \tau_{k,m} > \tau_c \quad \text{and } B_{k,m} > 0 \\ 0, & \tau_{k,m} < \tau_c \quad \text{or } B_{k,m} = 0 \end{cases}$$

$$D_{k,m} = \frac{C_{k,m} w_s * A_r}{D_r}$$

where E_r and τ_c are the erosion rate parameter and critical stress for erosion. The stress is calculated each time and is based on Manning's Equation, which relates the stress to the instantaneous flow, stage and Manning's n parameter. Erosion is limited to only material that has settled during the simulation. Thus, no erosion of the original canal bed is allowed.

The parameters required to implement the transport and bed simulations are listed in Table 9.2.

Table 9.2 Reach Water Quality Simulation Parameters

Parameter	Description
δ_m	First or decay coefficient
w_s	Settling speed, one for each constituent
τ_c	Critical stress for erosion
E_r	Erosion Rate coefficient

9.1.3 Transport in Reservoirs

Transport in reservoirs is represented using the scalar transport equation with settling and first-order decay. The settling flux is a loss from the system. The governing equation for transport in each of the five cells representing the reservoir is:

$$\frac{\partial V_k C_{k,m}}{\partial t} + \oint q_k C_{k,m} = S_{k,m}$$

where V_k is the reach volume, $C_{k,m}$ is the concentration for the m_{th} constituent in the surface water, q_k is the flow, and $S_{k,m}$ represents external sources or sinks. Here k is the index identifying the cell and t is time.

The finite difference equation for a cell is:

$$\frac{C_{k,m}^{n+1} * V_k^{n+1} - C_{k,m}^{n} * V_k^{n}}{\Delta t} + C_{k,m}^{n} q_k - C_{k-1,m}^{n} q_{k-1} = S_1$$

where V_k is the k^{th} reservoir cell volume, and $S_{k,m}$ is the source for the k^{th} reservoir cell. The volumes V_k^{n+1} and the flows q_k^{n+1} are already known from the flow solution, requiring a solution only for the new concentrations $C_{k,m}^{n+1}$.

The source term components are cell dependent. For the upstream cell (#1), which receives all inflows, the source term is:

$$S_{1,m} = \sum L_{cell} + Q_{io} C_{io} - \delta_m C_{1,m} - w_s C_{1,m} A_c$$

Where the summation is for all grid cells (not reservoir cells) that drain to the reservoir, δ_m is the first-order decay coefficient, w_s is the settling speed and A_c is the bottom area of the reservoir

cell. The term $Q_{io}C_{io,m}$ represents the fluxes due to exchanges with other model objects (e.g., reaches, groundwater) that are into the reservoir. The concentration $C_{io,m}$ is the concentration in the other object.

For the interior cells (#2, #3 and #4) the source term is:

$$S_{k,m} = -\delta_m C_{k,m} - w_s C_{k,m} A_c$$

and for the last cell (#5), the source term is:

$$S_{5,m} = -Q_{io} C_5 - \delta_m C_{5,m} - w_s C_{5,m} A_c$$

The flux Q_{io}, represents the flows from the reservoir to other objects (i.e. reaches, groundwater, etc.).

The parameters used in the reservoir water quality simulation are listed in Table 9.3.

Table 9.3 Reservoir Water Quality Simulation Parameters

Parameter	Description
δ_m	First or decay coefficient
w_s	Settling speed, one for each constituent

9.2 ADVANCED WATER QUALITY

The WaSh model Advanced Water Quality module is adopted from the WASP model non-linear DO and EUTRO modules. The constituents modeled are:

Ammonia: C_{NH3}

Nitrate: C_{NO3}

Inorganic Phosphorus: C_{IP}

Phytoplankton Carbon: C_{PhyC}

Carbonaceous Biochemical Oxygen Demand: C_{BOD}

Dissolved Oxygen: C_{DO}

Organic Nitrogen: C_{ON}

Organic Phosphorus: C_{OP}

The model includes production; transport through the tertiary canals, reaches and reservoirs; and the simulation of in-stream processes within the reaches. For the purpose of simulating vertical stratification of water quality variables, the WaSh model provides the option for dividing each reach into an upper and lower layer, with diffusion-type exchanges occurring between layers. The flow in each layer is proportioned by the depth so that the flow speeds through the upper and lower layer are identical.

Additional time series input data requirements are the irradiation time series (hourly) and water temperature time series (hourly).

9.2.1 Production Terms

The EMC approach is applied for all simulated constituents except for dissolved oxygen (DO) in the surface runoff. Thus, for all other constituents, the concentrations in surface and groundwater discharges are controlled using the same parameterization as used in the basic water quality model. The same model parameters listed in Table 9.1 are used in the advanced water quality model. DO in the surface runoff is assigned a value at saturation based on the hourly temperature. The equation used for DO saturation is:

$$\text{DOsat (mg/L)} = 0.0032\ T^2 - 0.3254\ T + 14.328, \text{ where T is in deg. C.}$$

where T is the temperature.

9.2.2 Transport

Transport in reaches and reservoirs for the advanced water quality option is identical to transport used in the basic water quality model, except transport in the reaches includes the simulation of an upper and lower layer. Diffusion between the upper and lower layers is simulated with a user-prescribed constant vertical diffusion coefficient. Also, settling from the upper layer is a source to the lower layer, and settling from the lower layer is a loss from the system. During each time step, the flux F_v from the upper to the lower layer is calculated for each constituent as:

$$F_v = E_v \frac{(C_U - C_L)}{0.5 * D} + w_s * C_U$$

where C_U and C_L are the constituent concentrations in the upper and lower layers, D is the total depth in the reach and E_v is the vertical exchange coefficient.

There is no bed layer modeled. If settling of a constituent is modeled, then any settling from the lower layer is lost from the system.

9.2.3 In-Stream Process Descriptions

The governing equations for the in-stream DO balance are adopted from the WASP model non-linear DO and EUTRO modules. The governing equations and parameter definitions with ranges for values are given below for each of the eight state-variables. The state variables are assigned to both the upper and lower reach layers, and thus each equation is solved independently in each layer. All of the loads from cell runoff and other inflows are assigned to the upper layer. Thus, sources of concentration in the lower layer are due to diffusion with and settling from the upper layer. Each equation is solved numerically using an explicit upwind time difference scheme.

The reaction term for phytoplankton kinetics are defined as:

$$\frac{\partial C_{PhyC}}{\partial t} = (G_p - D_p - k_s) C_{PhyC}$$

where G_p is the growth rate, ($day^{-1)}$), D_p is the death rate, (day^{-1}), and k_s = settling rate in (day^{-1}).

The balance between the magnitude of the growth rate and death rate (together with the transport, settling, and mixing) determines the rate at which phytoplankton mass is created in the volume of water V.

The specific growth rate G_p in any reach is related to k_c, the maximum growth rate at 20^o C and optimum light and nutrient levels, via the following equation:

$$G_p = k_c X_{RT} X_{RI} X_{RN}$$

where each X term represents a reduction in growth due to non-optimal conditions.

X_{RN} = the nutrient limitation factor as a function of dissolved inorganic phosphorus and nitrogen.

The temperature correction factor, X_{RT} is:

$X_{RT} = \theta^{T-20}$, where θ = Temperature coefficient and T is the temperature.

The instantaneous depth-averaged light factor, X_{RI}, is:

$$X_{RI} = \frac{e}{K_e D} f\left[exp\left\{ \frac{-I_a}{I_S} exp(-K_e D) \right\} - exp\left(\frac{-I_a}{I_S} \right) \right]$$

where f is the fraction of day that is daylight, I_{ais} is the average incident light intensity during daylight hours just below the surface, I_s is the saturating light intensity of phytoplankton and K_e = the light extinction coefficient, and D is the water depth.

Reduction in optimal growth due to limiting nutrient, X_{RN}, is

$$X_{RN} = Min\left(\frac{C_{IN}}{K_{mN} + C_{IN}}, \frac{C_{IP}}{K_{mP} + C_{IP}} \right)$$

The constants, K_mN and K_mP are the half-saturation constants and are the nutrient concentrations at which the growth rate is half the saturated growth rate.

The phytoplankton death rate is comprised of two effects:

$$D_p = k_R(T) + K_D$$

where k_R is the reduction rate due to respiration (day^{-1}) and k_D is the death rate, representing the effect of parasitization (i.e., the infection of algal cells by other microorganisms, and toxic materials, such as chlorine residual) (day^{-1}).

Losses due to settling are described by:

$$k_S = \frac{v_S}{D}$$

where k_s is the effective phytoplankton settling or loss rate, day^{-1}, and v_s is the net settling velocity of phytoplankton. Table 9.4 summarizes the new model parameters and typical values.

Table 9.4 Phytoplankton Reaction Terms

Parameter Description	Notation	Values	Units
Extinction Coefficient	K_e	0.1-5	m^{-1}
Segment Depth	D	0.1-30	m
Water Temperature	T	0-35	^oC
Fraction of day that is daylight	f	0.3-0.7	-
Average Daily Surface Solar Radiation	Ia	200-750	langleys/day
Maximum Growth Rate	k_c	2.0	day^{-1}
Temperature Coefficient	Θ	1.068	none
Maximum Photosynthetic Quantum Yield	$Ö_{max}$	720.0	mg C/mole photon
Phytoplankton Self-Light Attenuation	K_c	0.017	m^2/mg Chl a
Carbon-Chlorophyll Ratio	$È_c$	20-50	-
Saturating Light Intensity	Is	200-500	langleys/day
Half-Saturation Constant for Nitrogen	K_{mN}	25.0	µg N/L
Half-Saturation Constant for Phosphorus	K_{mP}	1.0	µg P/L
Endogenous Respiration	k_R	0.125	day^{-1}
Temperature Coefficient	$È_R$	1.045	none
Settling Velocity	v_{s4}	0.1	m/day
Death Rate	k_D	0.02	day^{-1}
Grazing Rate	k_G	0	L/mgC-day

The two phosphorus species models are organic phosphorus and inorganic (orthophosphate) phosphorus. They both can be divided into particulate and dissolved fractions using a constant partitioning factor. The governing equations are:

Organic Phosphorus

$$\frac{\partial C_{OP}}{\partial t} = D_p a_p \, f_{op} C_{PhyC} - k_{83}\theta_{83}^{(T-20)}\left(\frac{C_{PhyC}}{K_{mPc}+C_p}\right)C_{op} - \frac{V_{s3}(1-f_{D3})}{D}C_{op}$$

Inorganic Phosphorus

$$\frac{\partial C_{IP}}{\partial t} = D_p a_p (1-f_{op}) C_{PhyC} + k_{83}\theta_{83}^{(T-20)}\left(\frac{C_{PhyC}}{K_{mPc}+C_{PhyC}}\right)C_{op} - G_p a_p C_{PhyC}$$

Table 9.5 summarizes phosphorus reactions terms:

Table 9.5 Phosphorus Reaction Terms

Description	Notation	Value	Units
Phytoplankton biomass as carbon	P_c	-	mg C/L
Specific phytoplankton growth rate	G_p	Solve	day^{-1}
Phytoplankton loss rate	D_p	Solve	day^{-1}
Phosphorus to carbon ratio	a_P	0.025	mg P/mg C
Dissolved organic phosphorus mineralization at 20°C	k_{83}	0.22	day^{-1}
Temperature coefficient	θ_{83}	1.08	none
Half saturation constant for phytoplankton limitation of phosphorus recycle	K_{mPc}	1.0	mg C/L
Fraction of dead and respired phytoplankton recycled to the organic phosphorus pool	f_{op}	0.5	none
Fraction of dead and respired recycled to the phosphate phosphorus pool	$(1-f_{op})$	0.5	none
Fraction dissolved inorganic phosphorus in the water Column	f_{D3}	0.85, 0.70	none
Fraction dissolved organic phosphorus	f_{D8}	-	none
Organic matter settling velocity	v_{s3}	-	m/day
Inorganic sediment settling velocity	v_{s5}	-	m/day

Three nitrogen variables are simulated: organic nitrogen, ammonia, and nitrate. Organic nitrogen can be divided into dissolved and particulate fractions using a constant partitioning factor. The governing equations are:

Organic Nitrogen

$$\frac{\partial C_{ON}}{\partial t} = D_p a_N f_{oN} C_P - k_{71}\theta_{71}^{(T-20)}\left(\frac{C_{PhyC}}{K_{mPc}+C_{PhyC}}\right)C_{oN} - \frac{V_{s3}(1-f_{D7})}{D}C_{oN}$$

Ammonia Nitrogen

$$\frac{\partial C_{NH3}}{\partial t} = D_p a_N (1-f_{oN})C_{PhyC} + k_{71}\theta_{71}^{(T-20)}\left(\frac{C_{PhyC}}{K_{mPc}+C_{PhyC}}\right)C_{oN} - G_p a_N P_{NH3} C_P$$

$$- k_{12}\theta_{12}^{(T-20)}\left(\frac{C_{DO}}{K_{NIT}+C_{DO}}\right)C_{NH3}$$

Nitrate Nitrogen

$$\frac{\partial C_{NO3}}{\partial t} = k_{12}\,\theta_{12}^{(T-20)}\left(\frac{C_{DO}}{K_{NIT}+C_{DO}}\right)C_{NH3} - G_p a_N (1-P_{NH3})C_P -$$

$$k_{2D}\theta_{2D}^{(T-20)}\left(\frac{k_{NO3}}{k_{NO3}+C_{DO}}\right)C_{NO3}$$

Where P_{NH3} is the ammonia preference term, approximated by:

$$P_{NH3} = C_{NH3}\left(\left(\frac{C_{NO2}}{(K_{mN}+C_{NO2})(K_{mN}+C_{NH3})}\right)+\left(\frac{K_{mN}}{(K_{mN}+C_{NO2})(C_{NO2}+C_{NH3})}\right)\right)$$

Table 9.6 summarizes the reaction terms for the nitrogen equations.

Table 9.6 Nitrogen Reaction Terms

Description	Notation	Value	Units
Nitrogen to carbon ratio	a_N	0.25	mg N/gm C
Organic nitrogen mineralization rate @ 20°C	k_{71}	0.075	day^{-1}
Temperature coefficient	Θ_{71}	1.08	-
Nitrification rate	k_{12}	0.09-0.13	day^{-1}
Temperature coefficient	Θ_{12}	1.08	-
Half saturation constant for oxygen	K_{NIT}	2.0	mg 0_2/L
Limitation of nitrification Denitrification rate at 20°C	k_{2D}	0.09	Day^{-1}
Temperature coefficient	Θ_{2D}	1.045	-
Michaelis constant for denitrification	K_{NO3}	0.1	mg O_2/L

Description	Notation	Value	Units
Fraction of dead and respired phytoplankton recycled to the organic nitrogen pool	f_{ON}	0.5	-
Fraction of dead and respired phytoplankton recycled to the ammonia nitrogen pool	$(1\text{-}f_{ON})$ 0.5	-	
Preference for ammonia uptake term	P_{NH3}	Solve	-
Fraction dissolved organic nitrogen	f_{D7}	1.0	-
Organic matter settling velocity	v_{s3}	-	m/day

The governing equation for Carbonaceous Biochemical Oxygen Demand is:

$$\frac{\partial C_{BOD}}{\partial t} = a_{OC} k_{12} C_{PhyC} - k_D \theta_D^{T-20} \left(\frac{C_{BOD}}{k_{BOD} + C_{BOD}} \right) C_S - \frac{v_{s3}(1 - f_{DS})}{D} C_{BOD}$$
$$- \frac{5}{4} \frac{32}{14} k_{2D} \theta_D^{T-20} \left(\frac{K_{NO3}}{k_{NO3} + C_{DO}} \right) C_{NO3}$$

and for dissolved oxygen:

$$\frac{\partial C_{DO}}{\partial t} = k_2 \left(C_S - C_6 \right) - k_D \theta_D^{T-20} \left(\frac{C_{BOD}}{k_{BOD} + C_{BOD}} \right) C_{BOD} - \frac{64}{14} k_{12} \theta_{12}^{T-20} \left(\frac{C_{NO3}}{k_{NIT} + C_{NO3}} \right) C_{NO3}$$
$$- \frac{SOD}{D} \theta_2^{T-20} + G_P \left(\frac{32}{12} + \frac{48}{14} \frac{14}{12} (1 - P_{NH3}) \right) C_P - \frac{32}{12} k_{1R} \theta_{1R}^{T-20} C_{PhyC}$$

where C_s is the DO saturation level. The WaSh model simulates water quality in an upper and lower layer for each reach, and the thickness of each layer is user-specified. In general, all of the above equations are solved for each time step for each layer in each reach. For the DO equation, the re-aeration term (1st term) is only applied to the upper layer, and the SOD term is only applied to the lower layer. Table 9.7 summarizes the reaction parameters.

Table 9.7 CBOD and DO Reaction Terms

Description	Notation	Range	Units
Oxygen to carbon ratio	a_{Oc}	32/12	mg O_2/mg C
Phytoplankton nitrogen-carbon ratio	a_{NC}	0.25	mg N/mg C
Deoxygenation rate @ 20˚C,	k_d	0.21-0.16	day^{-1} --
Temperature coefficient	Θ_d	1.047	
Half saturation constant for oxygen limitation	K_{BOD}	0.5	mg O_2/L
Nitrification rate @ 20˚C	k_{12}	0.09-0.13	day^{-1} --
Temperature coefficient	Θ_{12}	1.08	

Description	Notation	Range	Units
Half saturation constant for oxygen limitation	K_{NIT}	0.5	mg N/L
Denitrification rate @ 20˚C	k_{2D}	--	day^{-1} --
Temperature coefficient	Θ_d	1.08	
Half saturation constant for oxygen limitation	K_{N03}	0.1	mg N/L
Phytoplankton growth rate	G_{P1}	0.1-0.5	day^{-1}
Phytoplankton respiration rate	k_{1R}		
Temperature coefficient	Θ_R	0.125	day^{-1} --
Sediment Oxygen Demand	SOD	0.2-4.0	g/m^2-day\
Temperature coefficient	Θ_S	1.08	--
Re-aeration rate @ 20˚C	k_2	1.08	--
Temperature coefficient	Θ_2	1.028	day^{-1}
Fraction dissolved CBOD	f_{D5}	0.5	none
Organic matter settling velocity	v_{s3}	--	m/day

Best Management Practices (BMPs) are represented in the WaSh model either explicitly or implicitly. The explicit method consists of small or "local" detention or retention basins. These basins are represented as storage capacities and are assigned to each cell designated with the BMP. These structures intercept runoff generated in each cell and release it at a prescribed rate. Implicit BMPs represent the effect of numerous management practices, such as the application of filter strips, or critical area planting, and are represented in the model by adjusting the value of model input parameters.

10.1 EXPLICIT BMPS: LOCAL STORAGE STRUCTURES

Relatively small local detention or retention ponds are represented in the model as an additional storage component in each cell. Surface runoff generated in the cell is first routed to the storage, and if capacity is available, the runoff is captured. The storage then drains at a prescribed rate (zero for retention). If appropriate, a first-order decay rate can be supplied, which causes the water quality constituents to decrease over time while in storage. The storage is defined in terms of rainfall capacity (e.g., ¼ inch) and is multiplied by the cell area to determine the storage capacity V_{max} for the cell. During each time step the volume of water stored and the runoff are updated. If the actual storage V_{det} is less than capacity V_{max}, the storage is increased and the cell runoff is updated according to:

$$V_{det}^{n+1} = V_{det}^{n}(1-\Delta t\ \gamma_{det}) + SURO$$

$$SURO_{total} = V_{det}^{n}\Delta t\ \gamma_{i}$$

where γ_{det} is the drainage rate coefficient.

If the storage is at or above capacity, then:

$$V_{det}^{n+1} = V_{det}^{n}(1-\Delta t\ \gamma_{det})$$

$$SURO_{total} = SURO_{total} + V$$

After the detention pond storage is updated to account for inflow and discharge, it is adjusted to account for direct rainfall and evaporation:

$$V_{det}^{n+1} = V_{det}^{n+1} + A_{det} * (R - E)$$

where A_{det} is the surface area of the detention basin and R and E are the rainfall and evaporation.

Note that a retention pond can be simulated by setting γ_{det} =0.

Water quality is also adjusted based on conservation of mass and first-order decay in the basins. The concentration of each constituent modeled is first updated using conservation of mass to determine the new detention pond concentration C_{det}^{k}, where k refers to the constituent (soluble nitrogen, particulate phosphorus, etc.). At the end of the time step, the concentration is adjusted to account for losses using a first-order decay coefficient:

$$C_{det}^{k} = C_{det}^{k} * (1 - \Delta t * \delta_{k})$$

where δ_k is the prescribed decay rate for the k_{th} constituent.

The parameters required to apply an explicit BMP are listed in Table 10.1.

Table 10.1 Detention/Retention Pond Parameters

Parameter	Description
V_{max}	Maximum storage
γ_{det}	Volume-based discharge rate
δ_k	Decay rate of kth constituent in
A_{det}	surface area

10.2 IMPLICIT BMPS

The effect of numerous BMPs can be simulated in the model by adjusting the model input parameters. The general intent is to reflect the effect of the BMP on runoff and water quality. Typically, the effect of a BMP on a particular quantity can be determined via field study or from a review of the literature. For instance, if a particular BMP has been found to reduce total nitrogen concentrations in agricultural runoff, the EMC for dissolved and particulate nitrogen could be reduced by an appropriate amount for the model cells with that land use. Specific HSPF parameters have been identified which control the simulated results in a study by Donigian, et al. (1983), and the results of the study can be used for guidance on which parameters to adjust to reflect each BMP implementation.

11.1 SPATIAL DATA

1) Basin (primary watershed): Polygon feature with basin name attribute.
2) Sub-basin (secondary watersheds): Polygon feature with basin name and numeric ID attributes. If subbasin is not available (e.g., Sweet Water Basin), then primary basin will be recognized as secondary basin.
3) Hydrography (streams, canals, etc.): Line or Polyline feature.
4) Land use: Polygon feature with six attributes (three integer and three descriptive) that follow FLUCS standards.
5) Soil: Polygon feature with soil hydrogroup attribute.
6) Land Surface Elevation: ARC/INFO or ArcView - Spatial Analyst GRID of land surface elevation.

11.2 TEMPORAL DATA

1) Rainfall
2) Evaporation
3) Point Sources and Sinks
4) Water Temperature (advanced water quality option only)
5) Daily Average Irradiation (advanced water quality option only)

A series of WaSh model simulations have been made to verify the WaSh model code. Each simulation is designed to provide a direct comparison with existing models. The simulations and intended comparison are listed in Table 12.1. Two WaSh model grids were constructed to make the comparisons and are shown in Figures 12.1 and 12.2. The first grid configuration consists of a 17-by-14 grid, with cells dimensions of 2,000 x 2,000 ft. Ground elevation is constant at 20 feet. A channel 50 feet wide, and with a bottom elevation of -5 feet, was represented. The channel has a branch that connects to the main stem at the mid-way point in the main stem, as shown in Figure 12.1. At the basin outfall, a 50-foot-wide weir with a crest elevation of 4 feet was used. This grid was used for comparisons with HEC-RAS and WASP simulations.

Table 12.1 WaSh Model Verification Simulations

Run Number	Purpose	Component / Algorithm	Description
1	Verification	Surface Water	Compare WaSh surface water simulation to equivalent HEC-RAS simulation (using weir as downstream structure)
2	Verification	Water Quality	Compare WaSh implementation of non-linear DO balance to equivalent simulation in WASP
3	Verification	Hydrology	Compare WaSh hydrology output to equivalent HSPF (periodic rainfall)
4	Verification	Groundwater	Compare WaSh model groundwater to equivalent MODFLOW simulation (steady recharge and discharge to stream)

The second grid consists of a 5-by-5 grid with constant land use and a single channel. The ground elevation was set to 20 feet, and the channel width and bottom elevation are 50 feet and -10 feet, respectively. This grid was used for comparisons with HSPF and MODFLOW.

For the comparison with HEC-RAS, a flow source was assigned to the upstream ends of the main stem and the branch with peak flow rates of 2500 cfs each. WaSh model conductivities that represent exchanges with the groundwater were set to zero. Also, rainfall and evaporation time series were set to zero so that the channel flow was isolated from the hydrology. Manning's n for HEC and for WaSh was set to 0.035. This setup allowed a direct comparison with the HEC-RAS hydraulics. The gradually varying flow over a one-year period was used. The flow rate is shown in Figure 12.3. For different times during the flow rate curve, the computed upstream head in WaSh and HEC-RAS were compared. The comparison is shown in Figure 12.4 for the main stem and branch.

For a comparison with the WASP model, the 17-by-14 grid was reconfigured to isolate the main stem from the branch. This configuration simplifies the flow scenario and allows for a direct assessment of the WaSh model simulation of water quality kinetics. The branch was isolated from the main stem by eliminating the input flow and inserting a weir structure with a crest elevation of 15 feet. For the upstream flow into the main stem, the flow rate was set to 200 cfs, and the CBOD load was 5.26 milligrams per liter (mg/L). The model parameters for the simulation of DO are listed in Table 12.2.

Table 12.2 Model Parameters for WaSh Comparison with WASP

Parameter	Value	Units
BOD decay rate (K_d)	4	day^{-1}
Oxygen Carbon Ratio (a_{oc})	2.67	mg O_2/mg C
Re-aeration Rate (K_2)	1	day^{-1}
Temperature (T)	25	^oC
Sediment Oxygen Demand (SOD)	0	g/m^2-day

The model configuration produces a steady state CBOD and DO profile that varies in the downstream direction. The simulated CBOD and DO profiles for WaSh and WASP are shown in Figure 12.5. The comparison indicates that the WaSh model is reproducing the results of the WASP model.

For the comparison with HSPF, the 5-by-5-grid was used. The HSPF model was configured to simulate a single cell of the 5-by-5-grid, and the comparison was made with the direct surface runoff and percolation. The HSPF parameters used in the simulation are listed in Table 12.3.

Table 12.3 HSPF Model Parameters

Parameter	Value	Units
CEPSC	0.1	Inches
UZSN	1.128	Inches
LZSN	0.1128	Inches
INFILT	0.16	Inches/hour
NSUR	0.2	-
LSUR	250	Ft
SLSUR	0.0882	-
AGWRC	0.98	day^{-1}

Each simulation consisted of a one-year period using measured rainfall and ET data from stations in the C24 basin. The rainfall and ET data were obtained from SFWMD DBHYRO database from the LOXAHATCHEE area and used to force the simulations. A comparison of the WaSh and HSPF simulated surface runoff and percolation is shown in Figure 12.6. The comparison indicates that the implementation of the HSPF PWATER algorithm WaSh is performing properly.

The 5-by-5 grid was also used for the comparison with MODFLOW. The MODFLOW model was configured with the same 5-by-5 grid and channel dimensions as for the WaSh model. The unconfined aquifer option was used, with an aquifer base elevation of -30 feet, a hydraulic

conductivity of 25 ft/day and conductivity of 1ft^2/day. A constant recharge rate of 5 inches/year was applied in the MODFLOW simulation. The WaSh model does not provide for direct specification of a recharge rate (i.e. percolation). In order to develop a scenario with a constant rate, the constant rainfall and evaporation were used. After some experimentation, a rainfall rate of 0.1 inches per day and an ET rate of 0.06 inches per day were found to yield 5 inches per year percolation. Each model was run for a one-year period to create a steady groundwater elevation and discharge. For the two cross sections shown in Figure 12.7, the groundwater elevations were compared. The comparison is shown in Figure 12.8, and indicates that the WaSh model simulation of groundwater is consistent with that of MODFLOW.

A sensitivity analysis of the HSPF model parameters has been conducted to determine the role of the parameters in controlling the hydrological predictions. The results of the analysis are displayed in Figures 13.1 through 13.9.

AQUA TERRA Consultants. 1998. Addition of irrigation module to the HSPH model. Unpublished report, AQUA TERRA Consultants, 44 pps.

AQUA TERRA Consultants. 1996. Modifications to HSPF for high water table and wetlands conditions in South Florida, unpublished report, AQUA TERRA Consultants, 63 pps.

Ambrose, R.B. et al. 1988. WASP4, A Hydrodynamic and Water Quality Model--Model Theory, User's Manual, and Programmer's Guide. U.S. Environmental Protection Agency, Athens, GA. EPA/600/3-87-039.

Bicknell, B.R., J.C. Imhoff, J.L. Kittle, Jr., A.S. Donigian, Jr., and R.C. Johanson. 1997. Hydrological Simulation Program--Fortran, User's manual for version 11: U.S. Environmental Protection Agency, National Exposure Research Laboratory, Athens, Ga., EPA/600/R-97/080, 755 p.

Donigian, A.S., J.L. Baker, and D.A. Haith. 1983. HSPF Parameter Adjustments to Evaluate the Effects of Agricultural Best Management Practices. Athens, GA: U.S. Environmental Protection Agency. EPA- 600/3-83-066.

Harbaugh, A.W., E.R. Banta, M.C. Hill, and M.G. McDonald. 2000. MODFLOW-2000, the U.S. Geological Survey modular ground-water model -- User guide to modularization concepts and the Ground-Water Flow Process: U.S. Geological Survey Open-File Report 00-92, 121 p.

Hydrologic Engineering Center. 2002. HEC-RAS, River Analysis System User's Manual, US Army Corps of Engineers, Davis, CA.

Johanson, R.C., J.C. Imhoff, H.H. Davis, J.L. Kittle and A.S. Donigian. 1981. User's Manual for Hydrologic Simulation Program-Fortran (HSPF): Release 7.0. Athens, GA: U.S. Environmental Protection Agency.

FIGURES

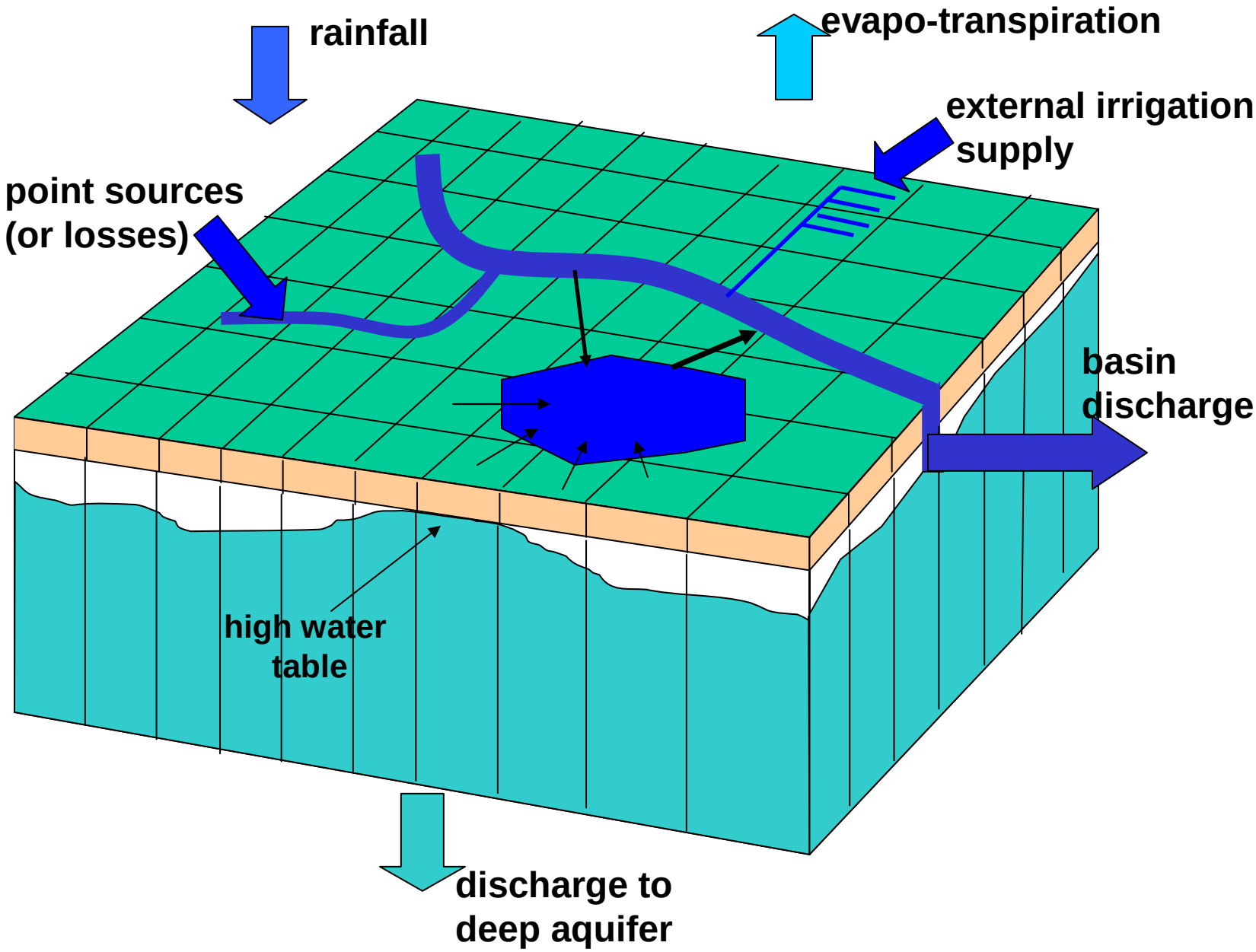

Figure 2.1. The System and Elements Comprising the WaSh Model.

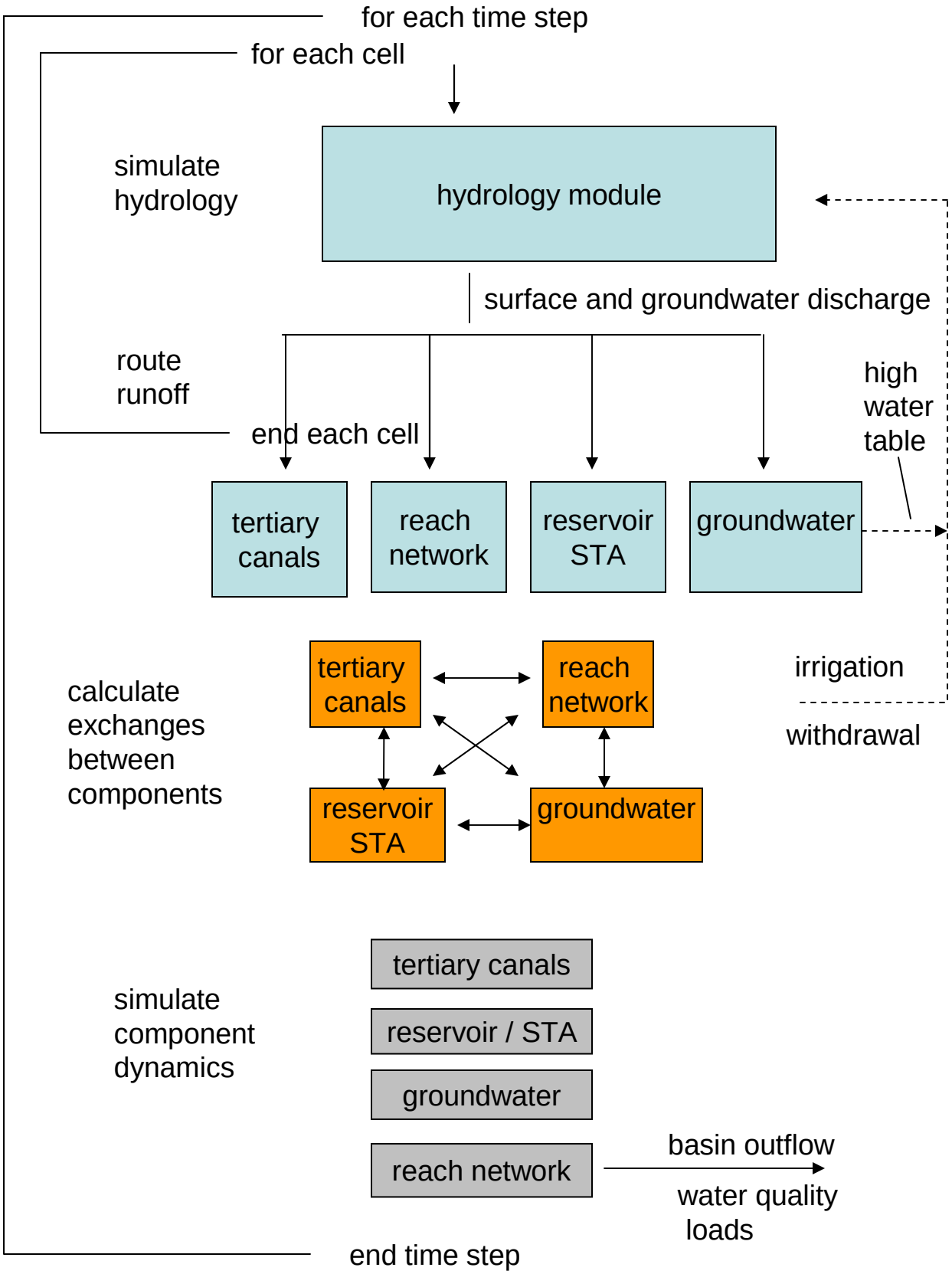

Figure 2.2. Flow Chart for the WaSh Model.

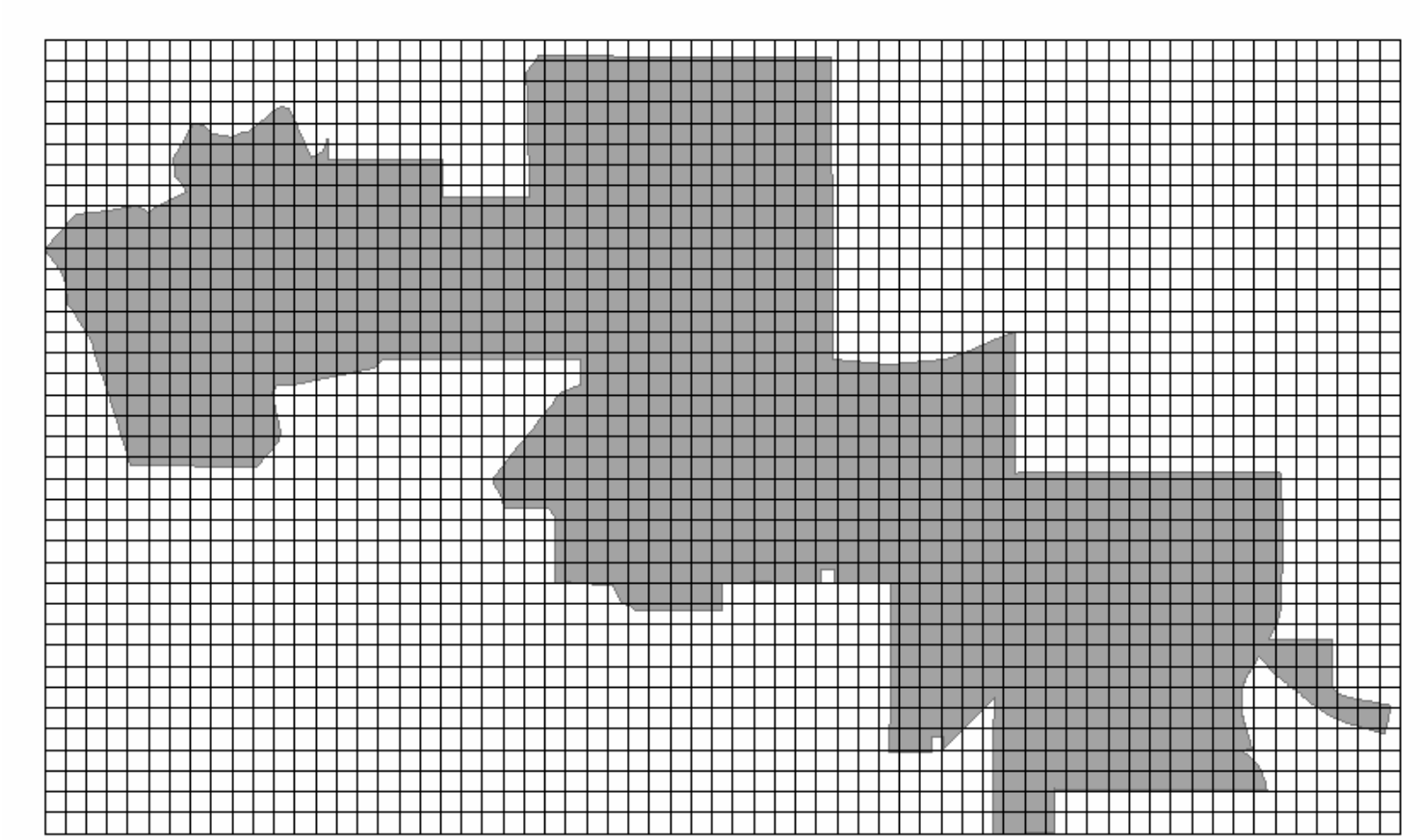

Figure 3.1. Example of Cell Based Representation used for the C-24 Basin.

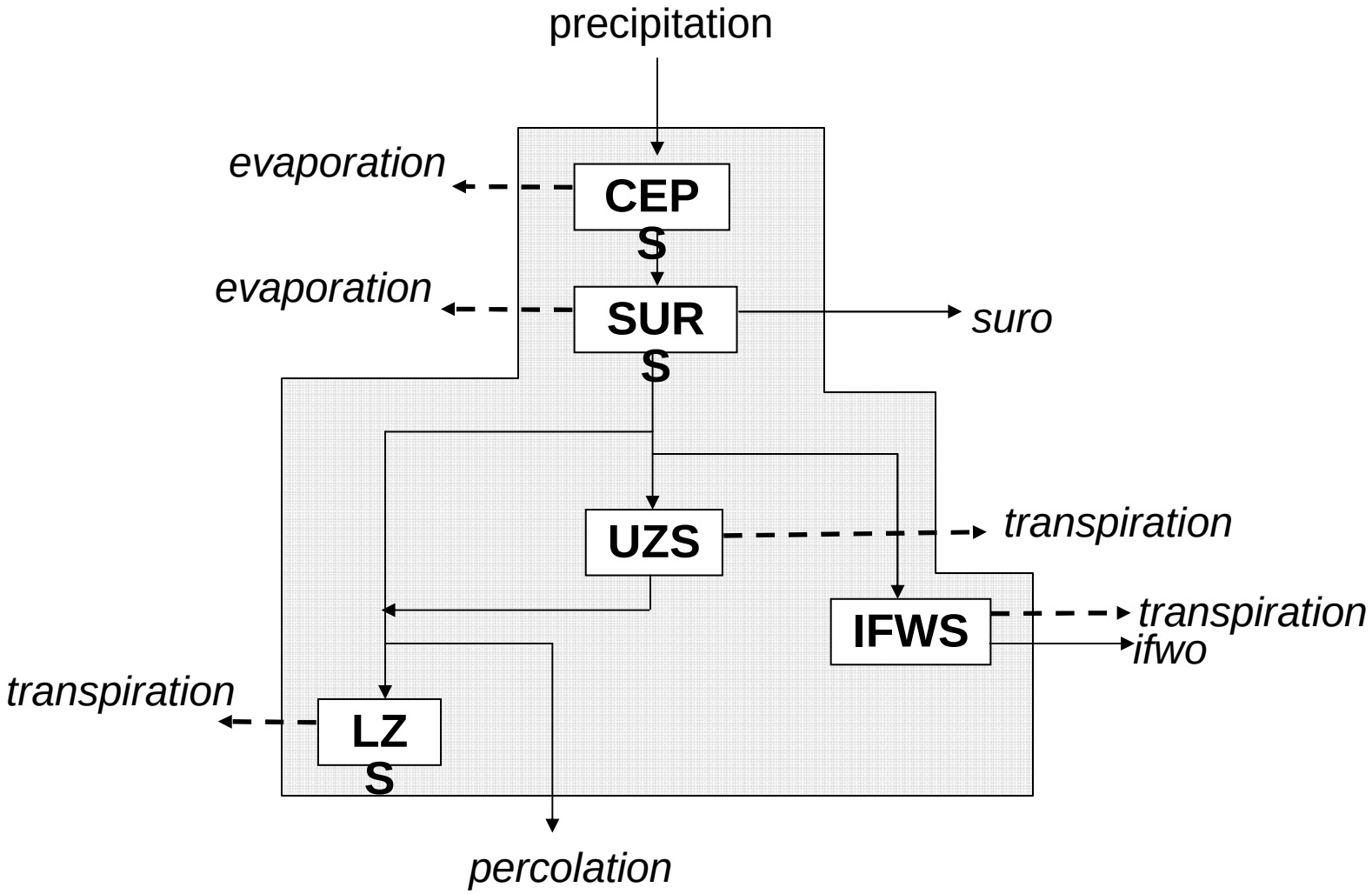

Figure 3.2. Hydrology Flow Chart for Pervious Cell Fractions.

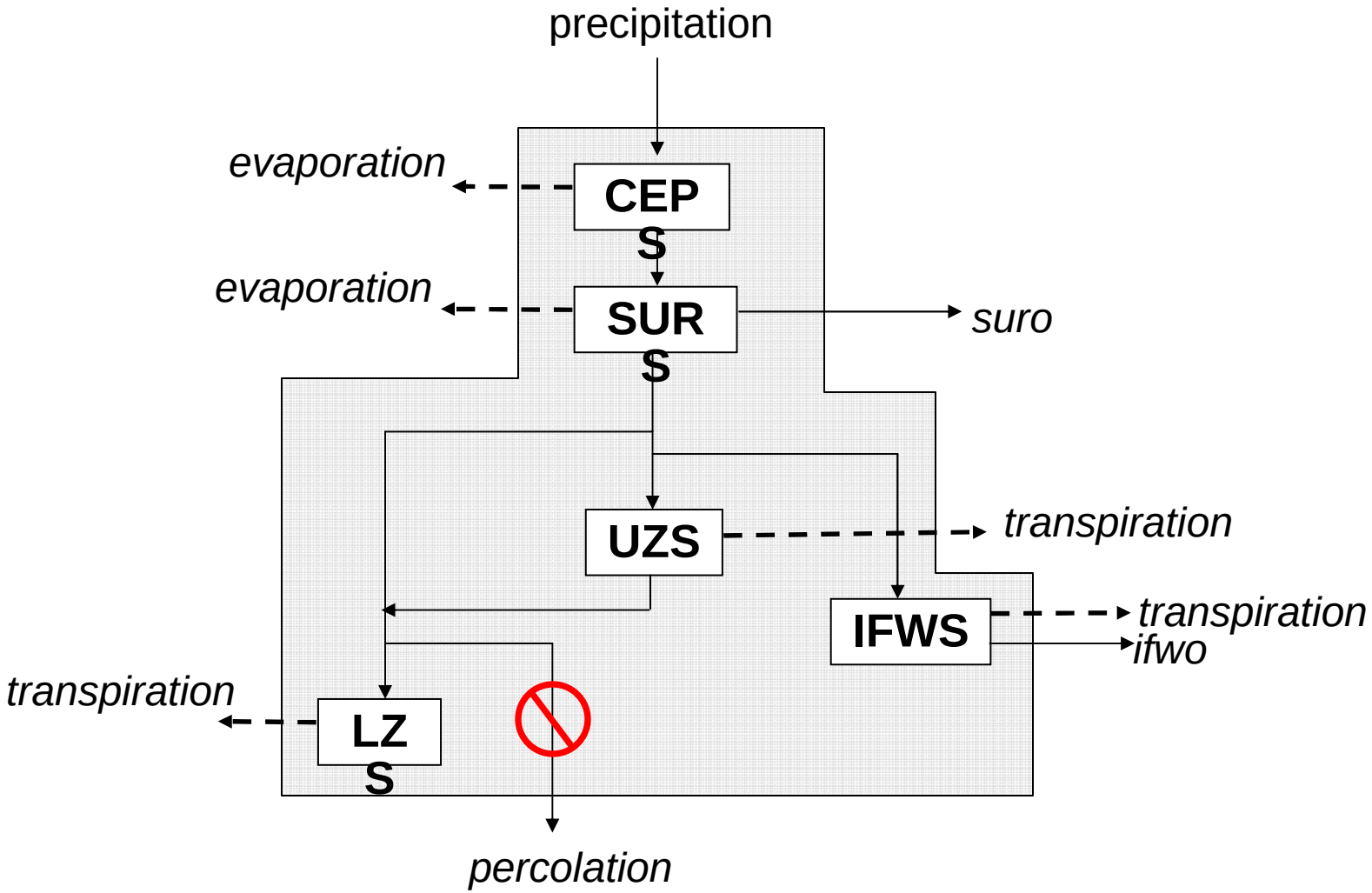

Figure 3.3. Modification for the High Water Table Algorithm Implemented in WaSh.

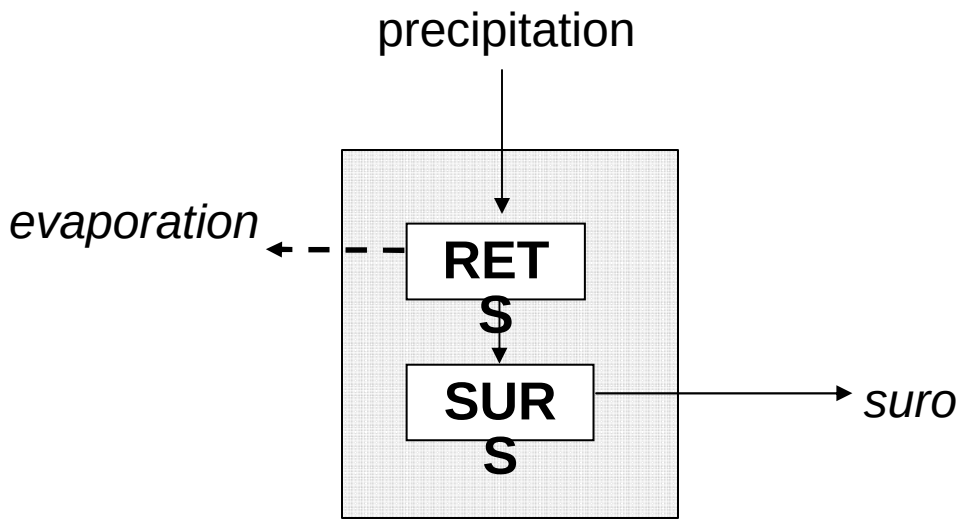

Figure 3.4. Hydrology Flow Chart for Impervious Cell Fractions.

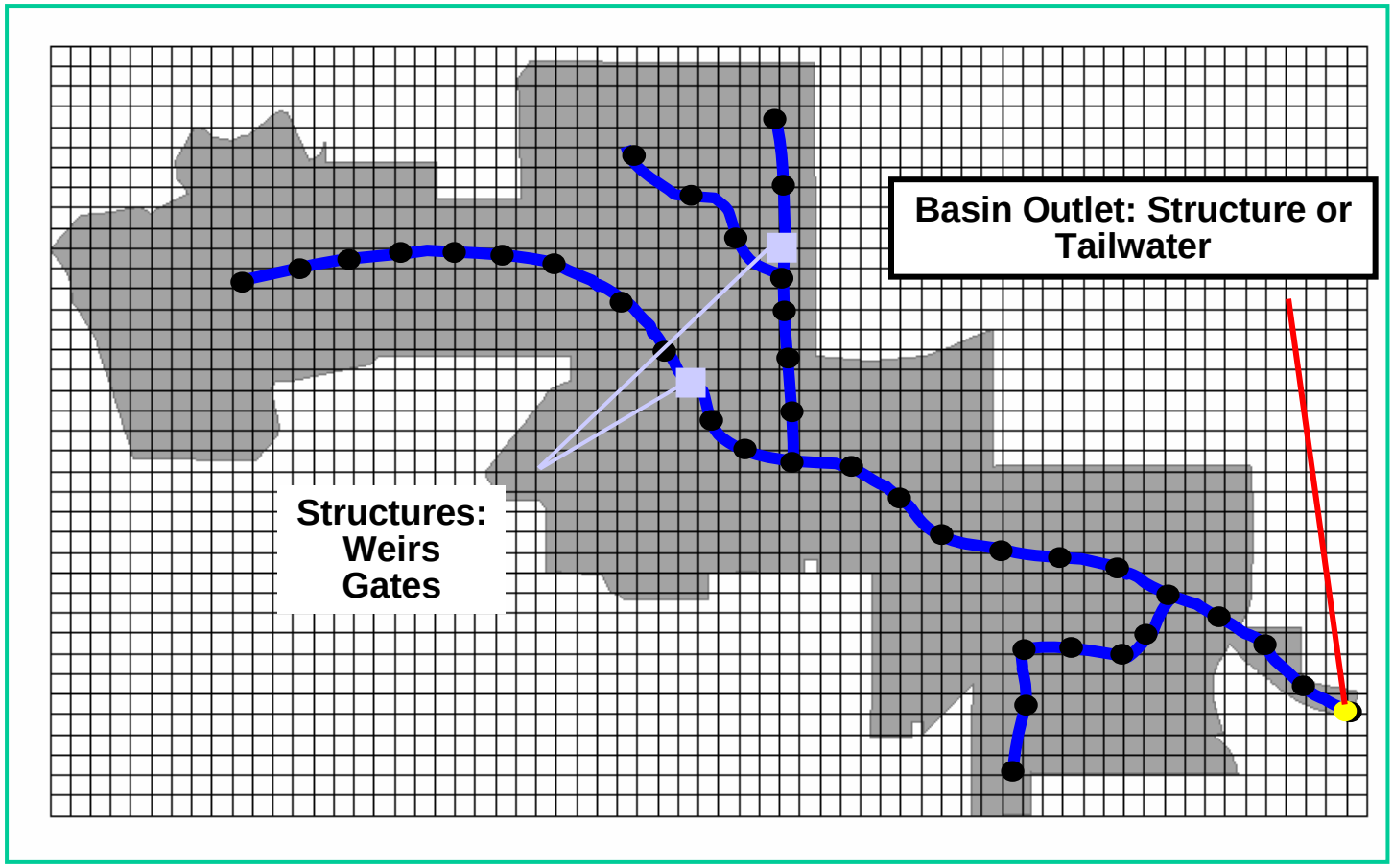

Figure 6.1. Reach Network Schematic.

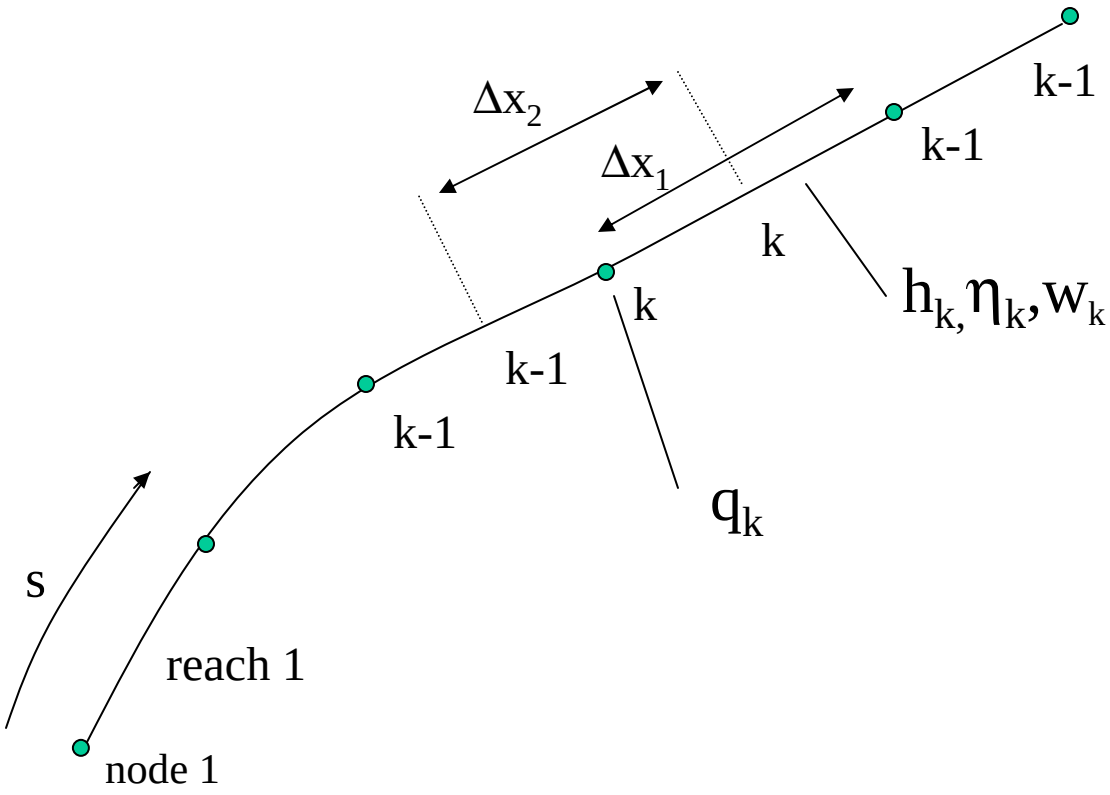

Figure 6.2. Reach Network Numerical Solution.

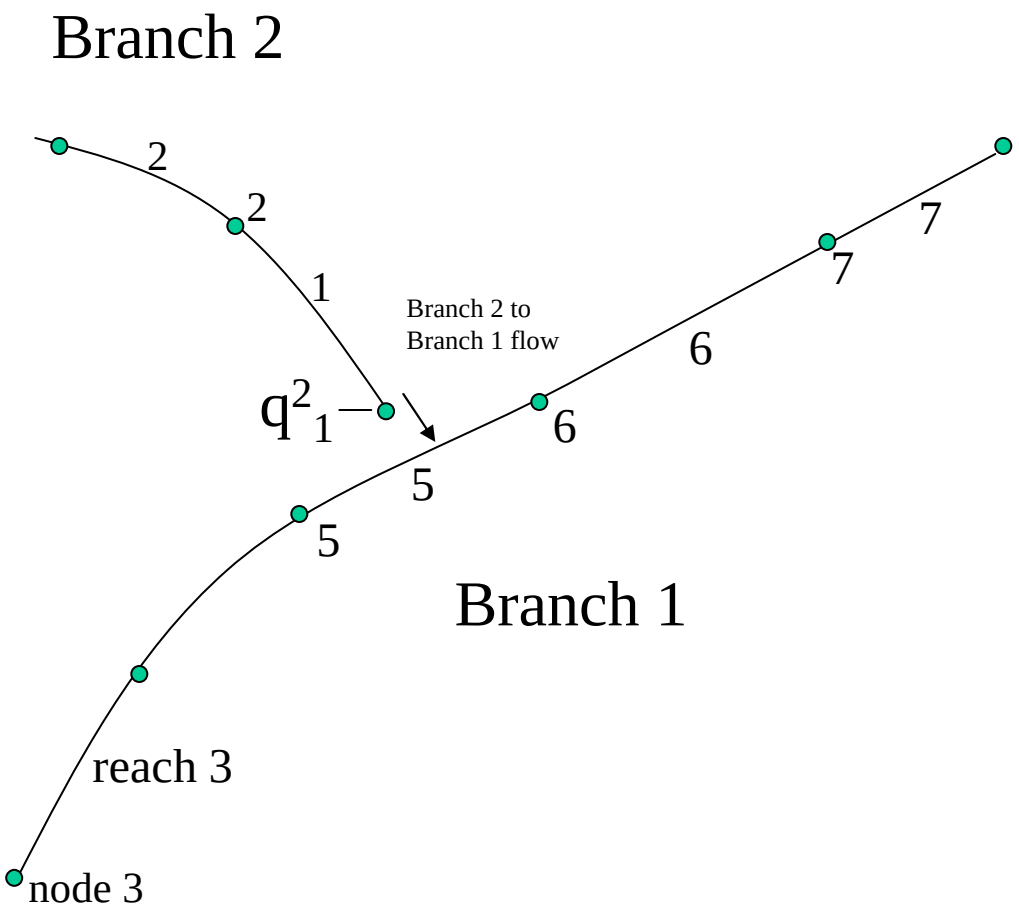

Figure 6.3. Branch Flow Network.

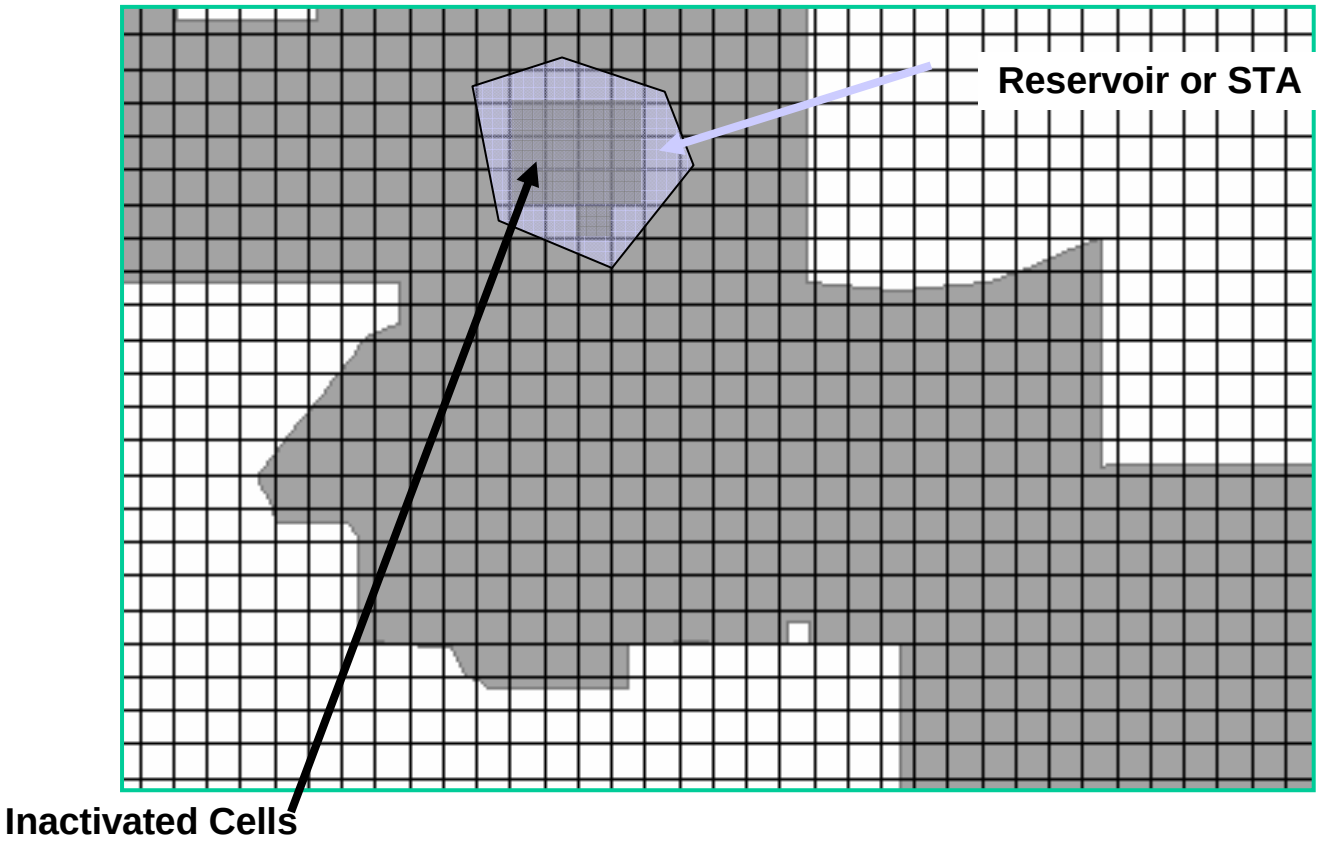

Figure 7.1. Reservoir and Grid Cells.

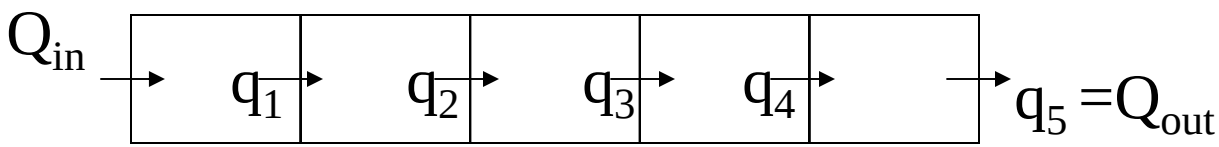

Figure 7.2. Reservoir Flow Numerical Solution.

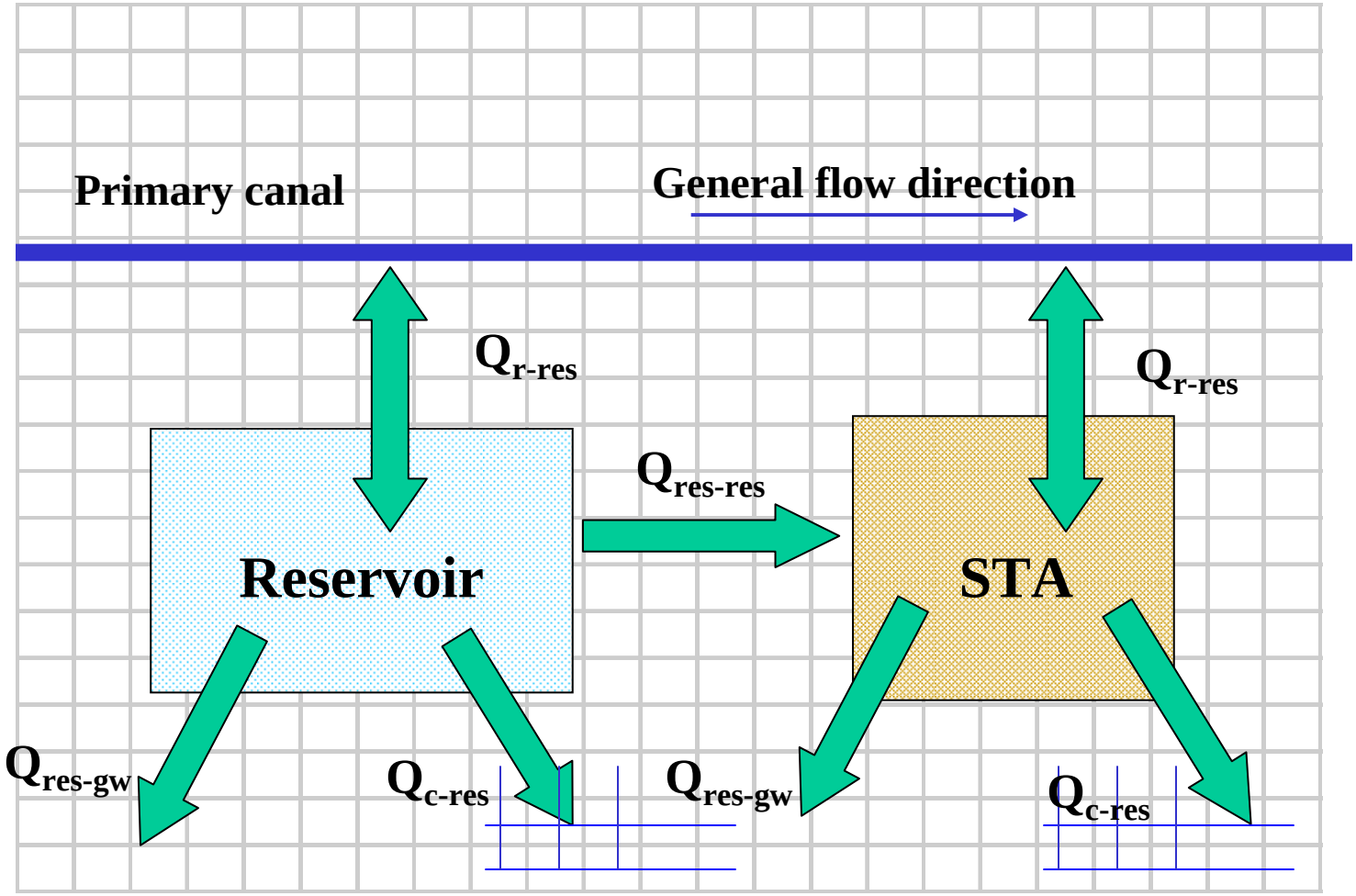

Figure 8.1 Reservoir and STA Exchanges

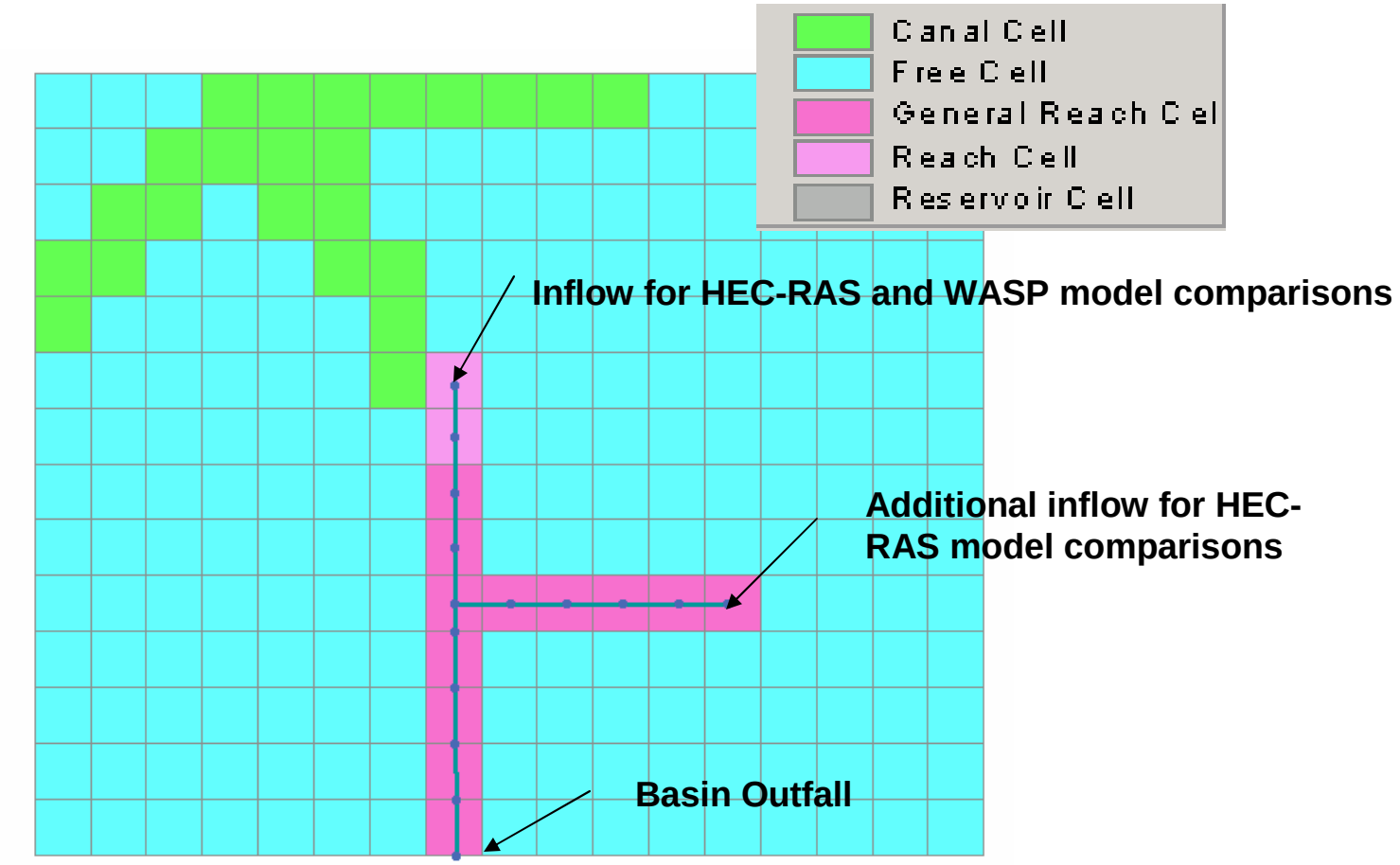

Figure 12.1. 17-by-14 Grid for WaSh Model Verification

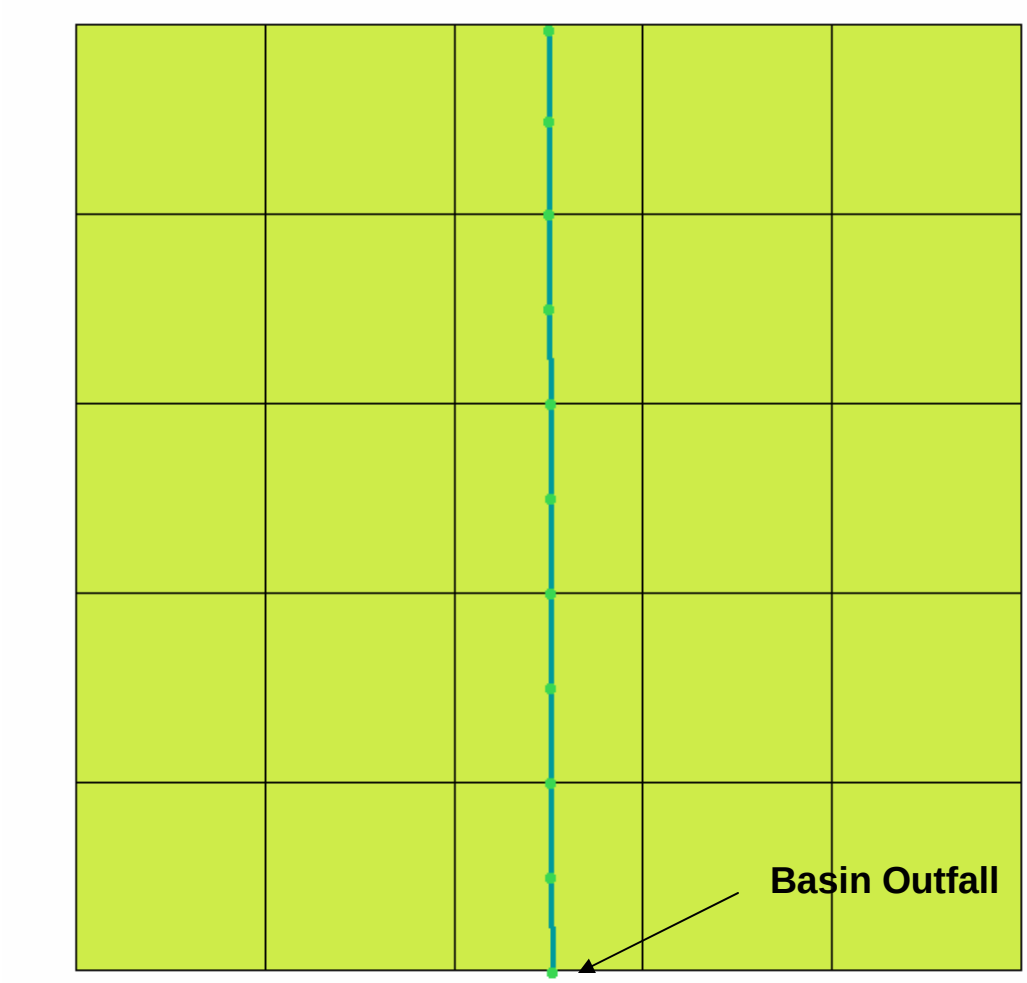

Figure 12.2. 5-by-5 grid for WaSh Model Verification

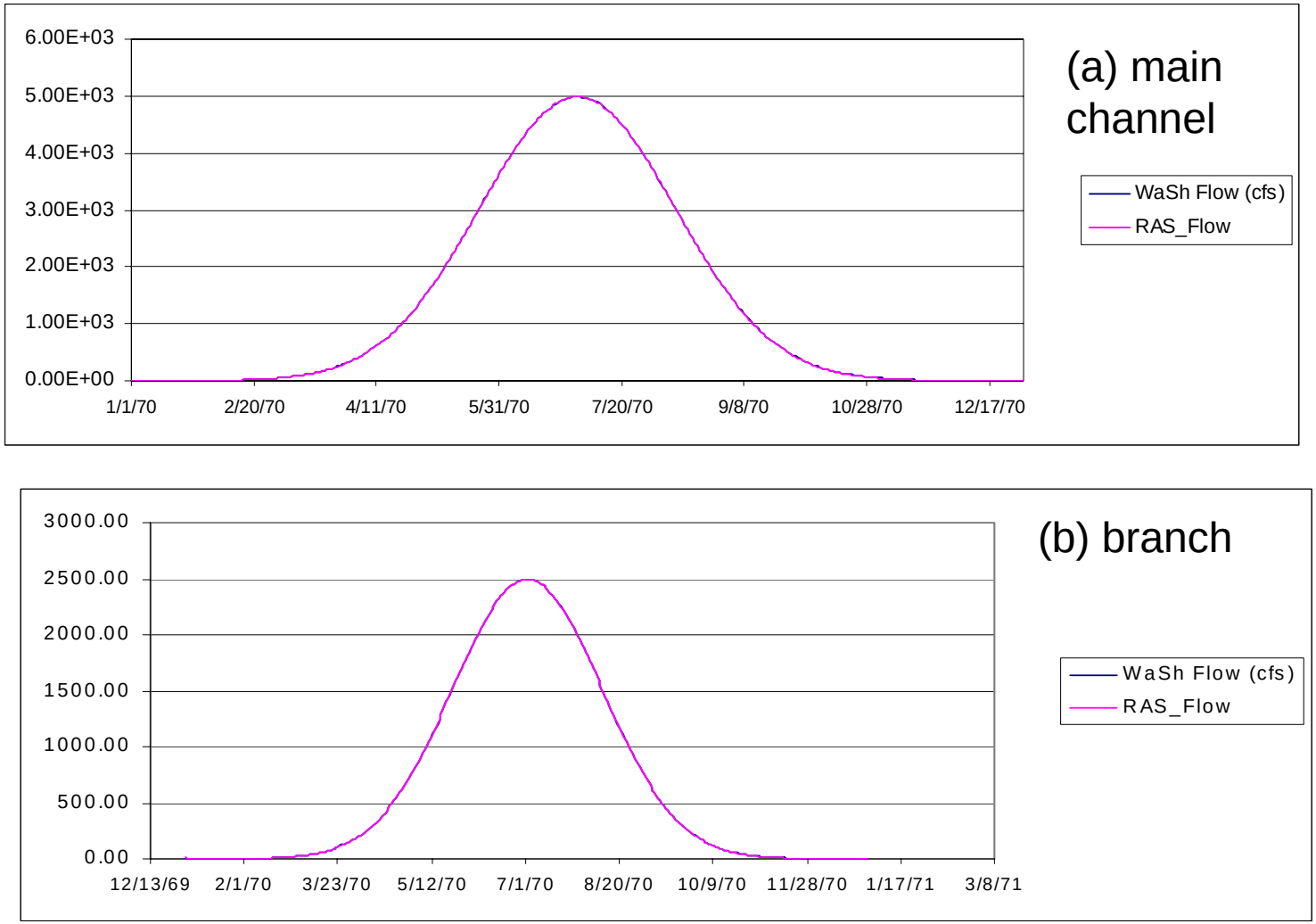

Figure 12.3. Flow time series used in HSPF and WaSh comparison

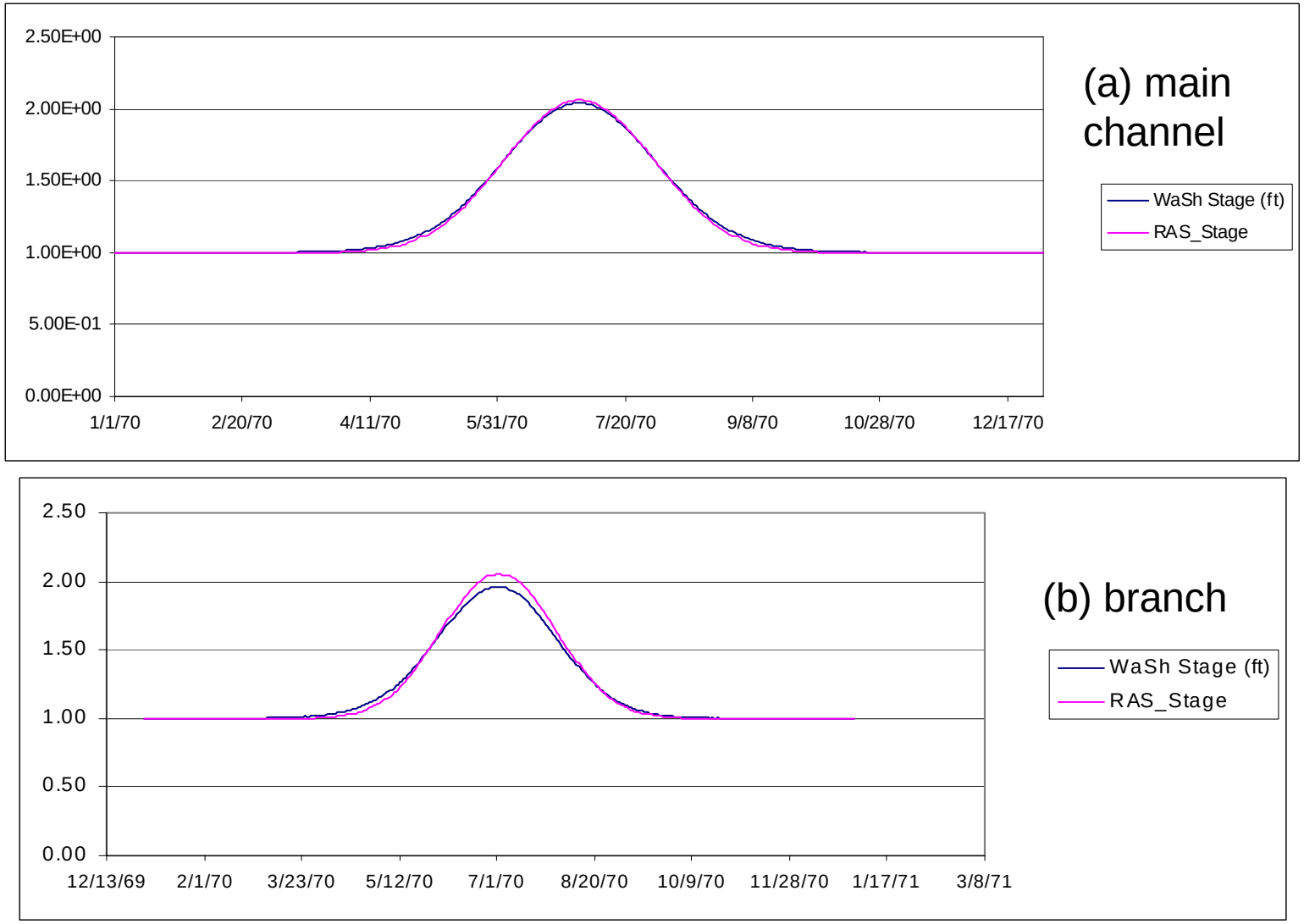

Figure 12.4. Comparison of water surface elevations at upstream ends of channels

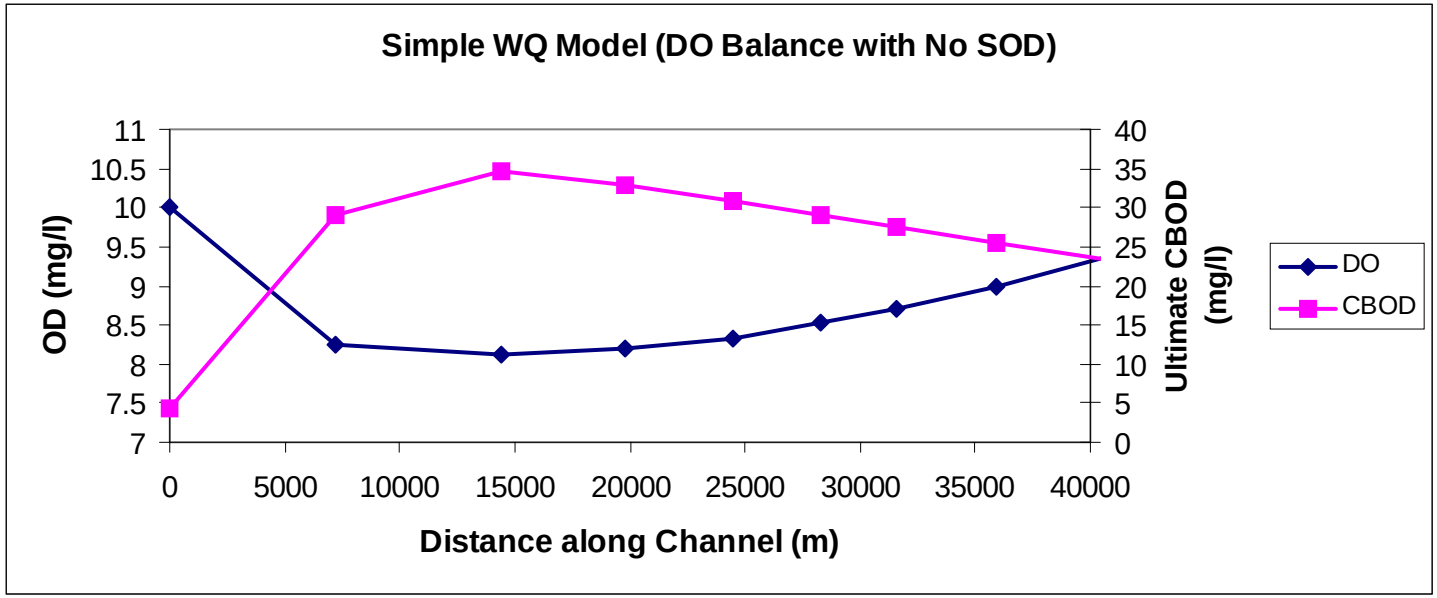

Figure 12.5. Comparison of WASP and WaSh simulated CBOD and DO stream profiles

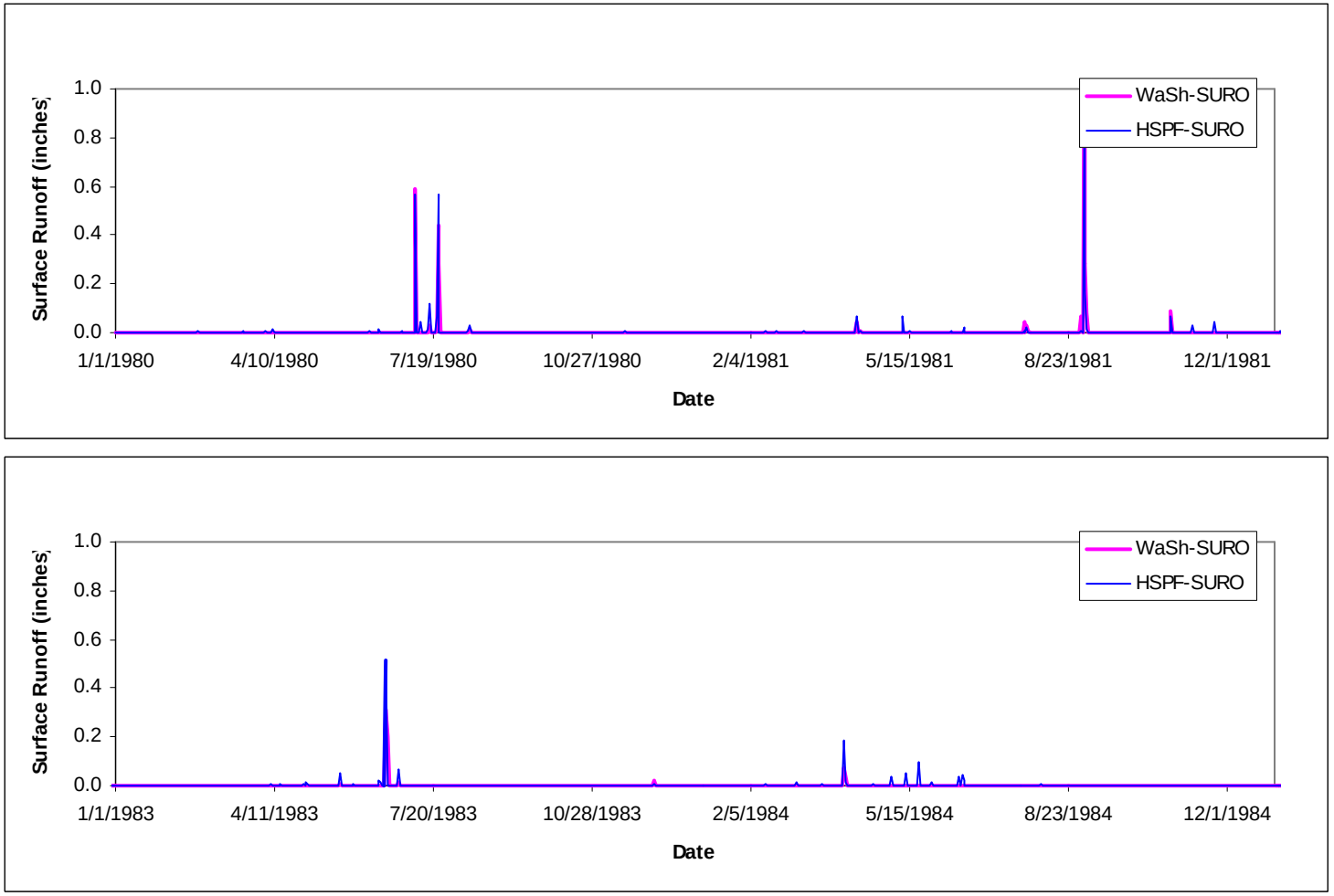

Figure 12.6. Comparison of HSPF and WaSh simulated runoff

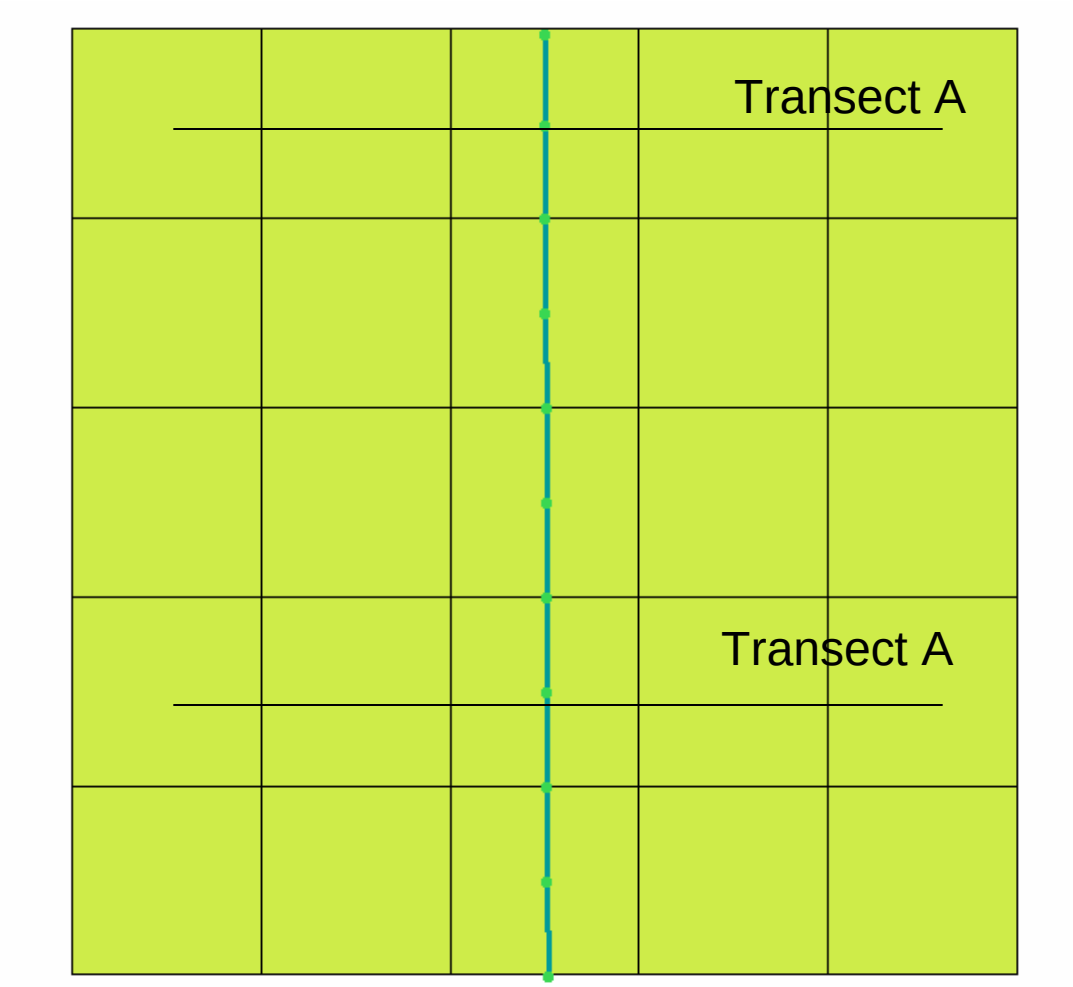

Figure 12.7. Transects used for groundwater elevation comparisons

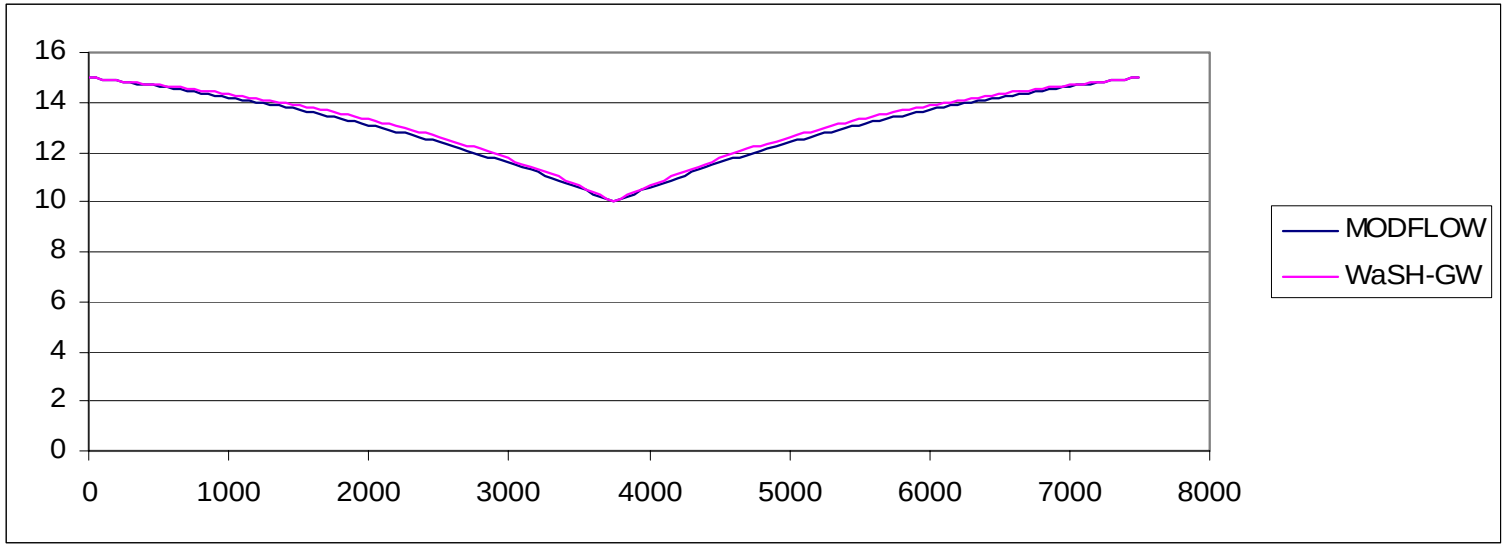

Figure 12.8. Comparison of MODFLOW and WaSh simulated groundwater elevations

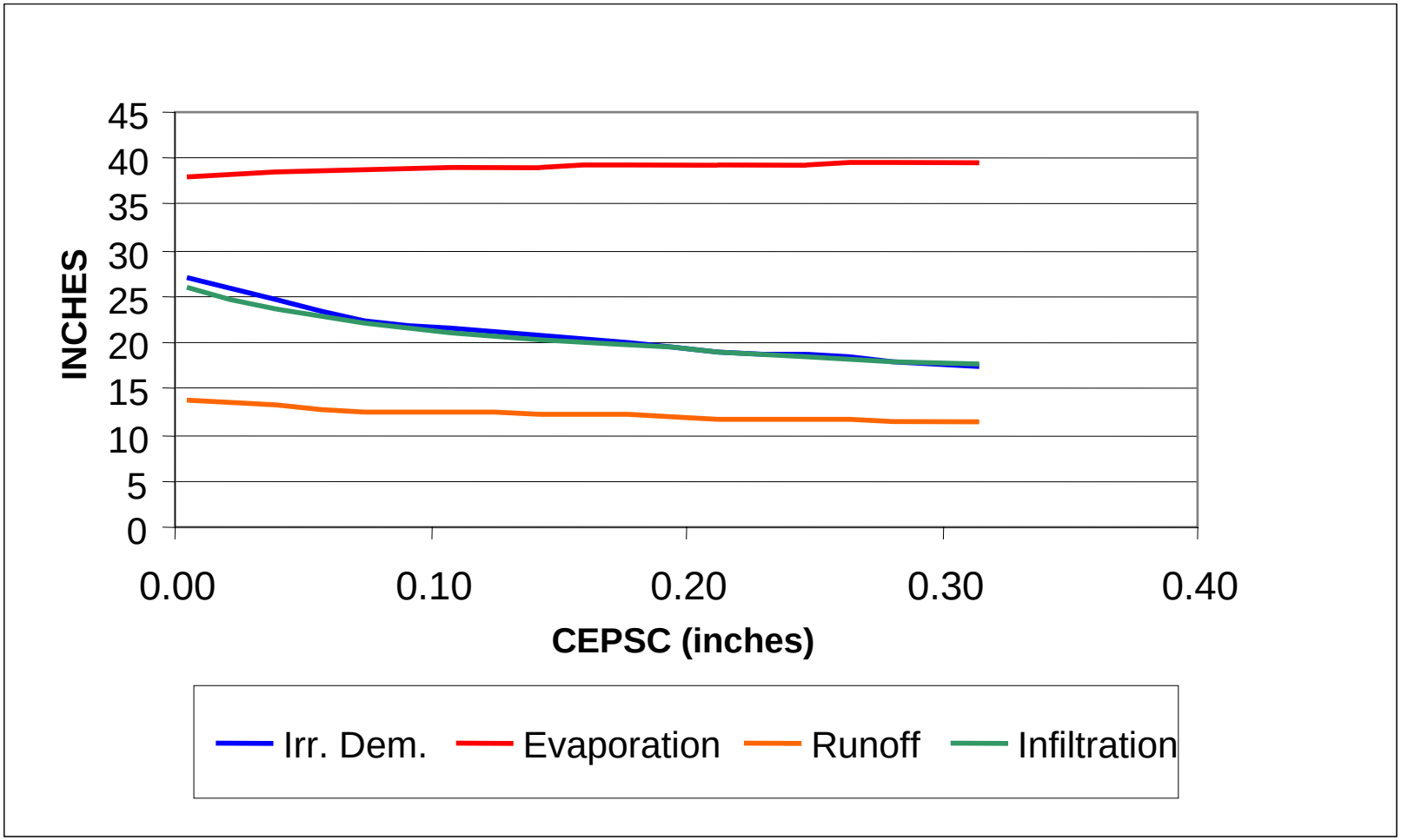

Figure 13.1. Sensitivity Analysis for CEPSC

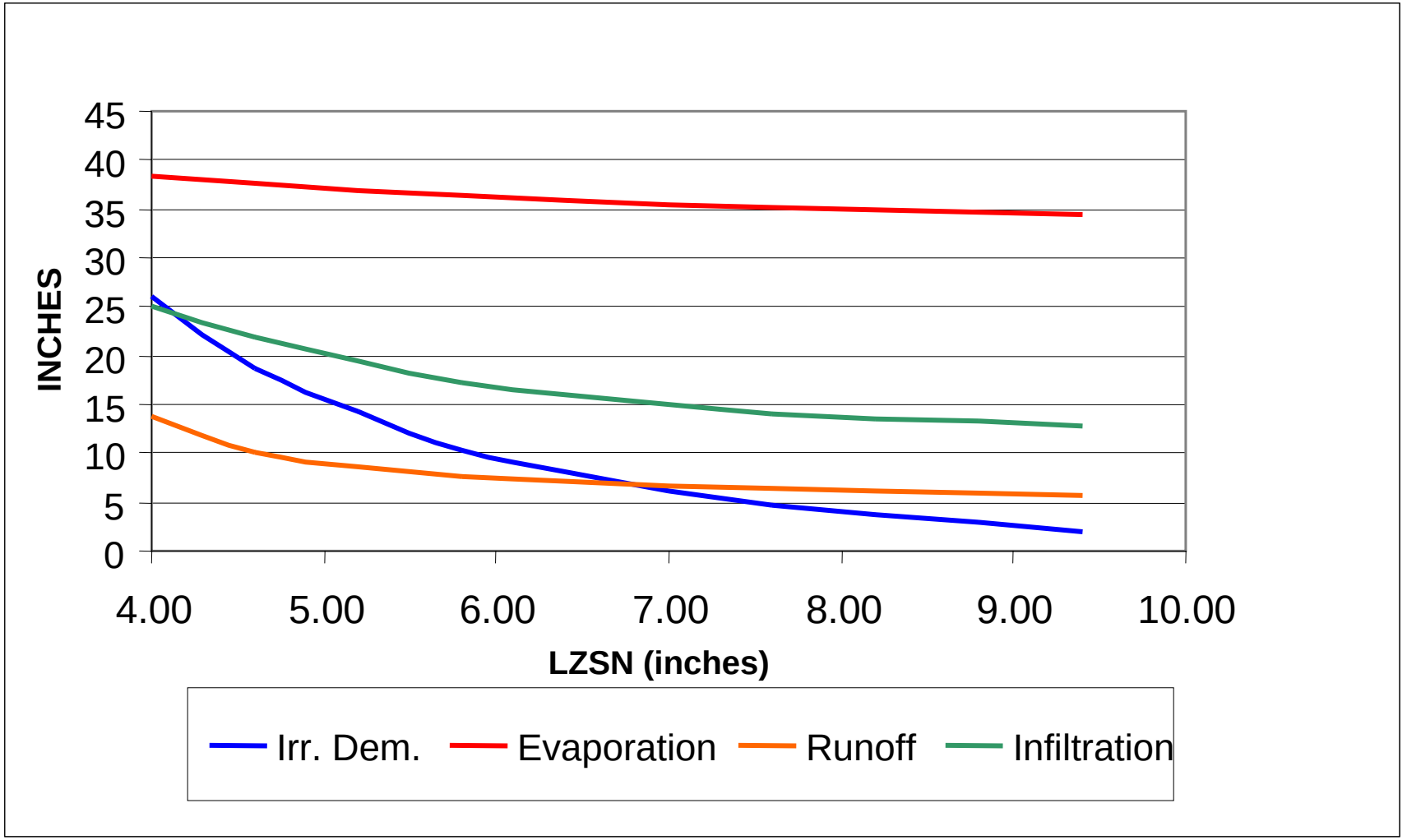

Figure 13.2. Sensitivity Analysis for LZSN

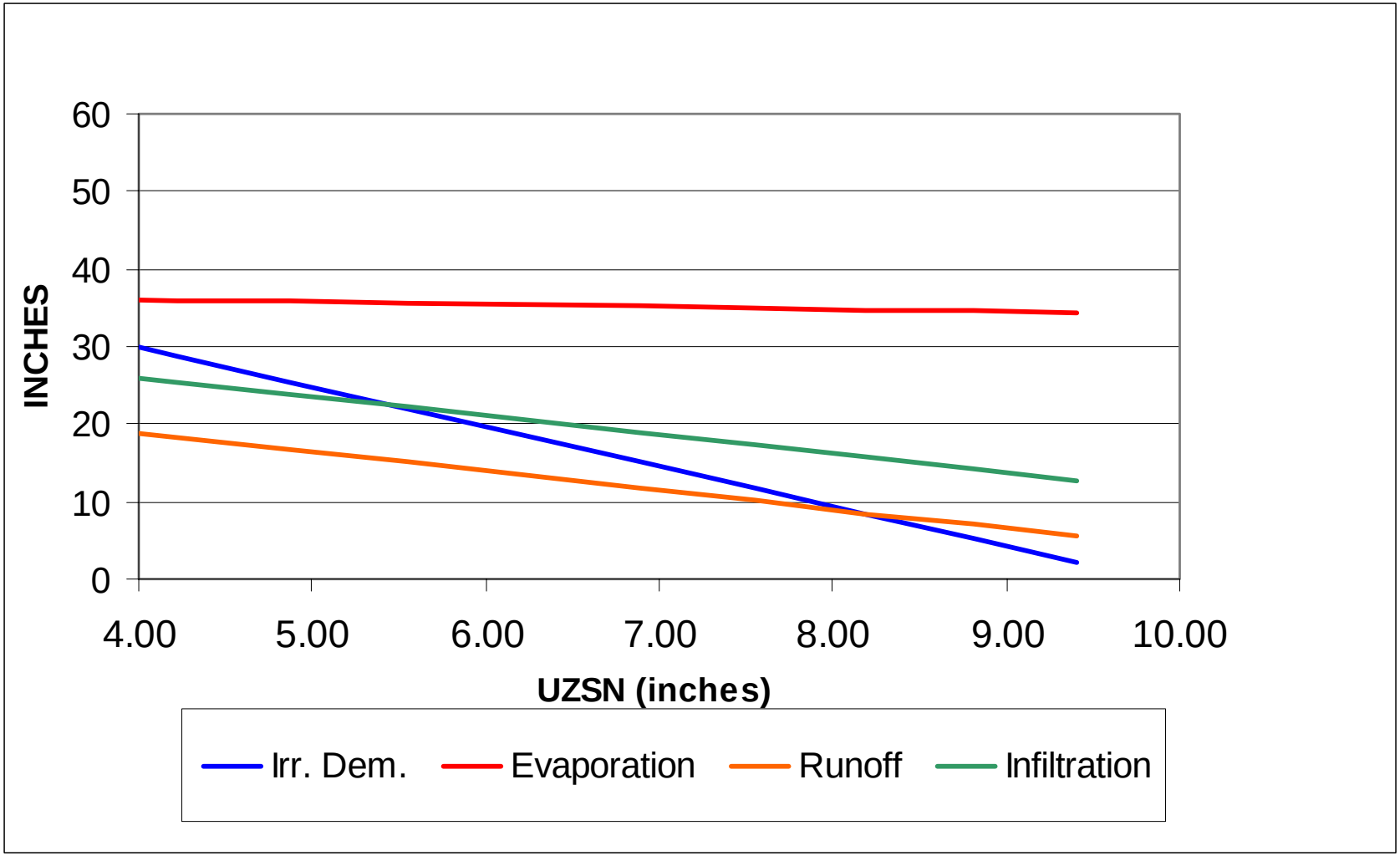

Figure 13.3. Sensitivity Analysis for UZSN

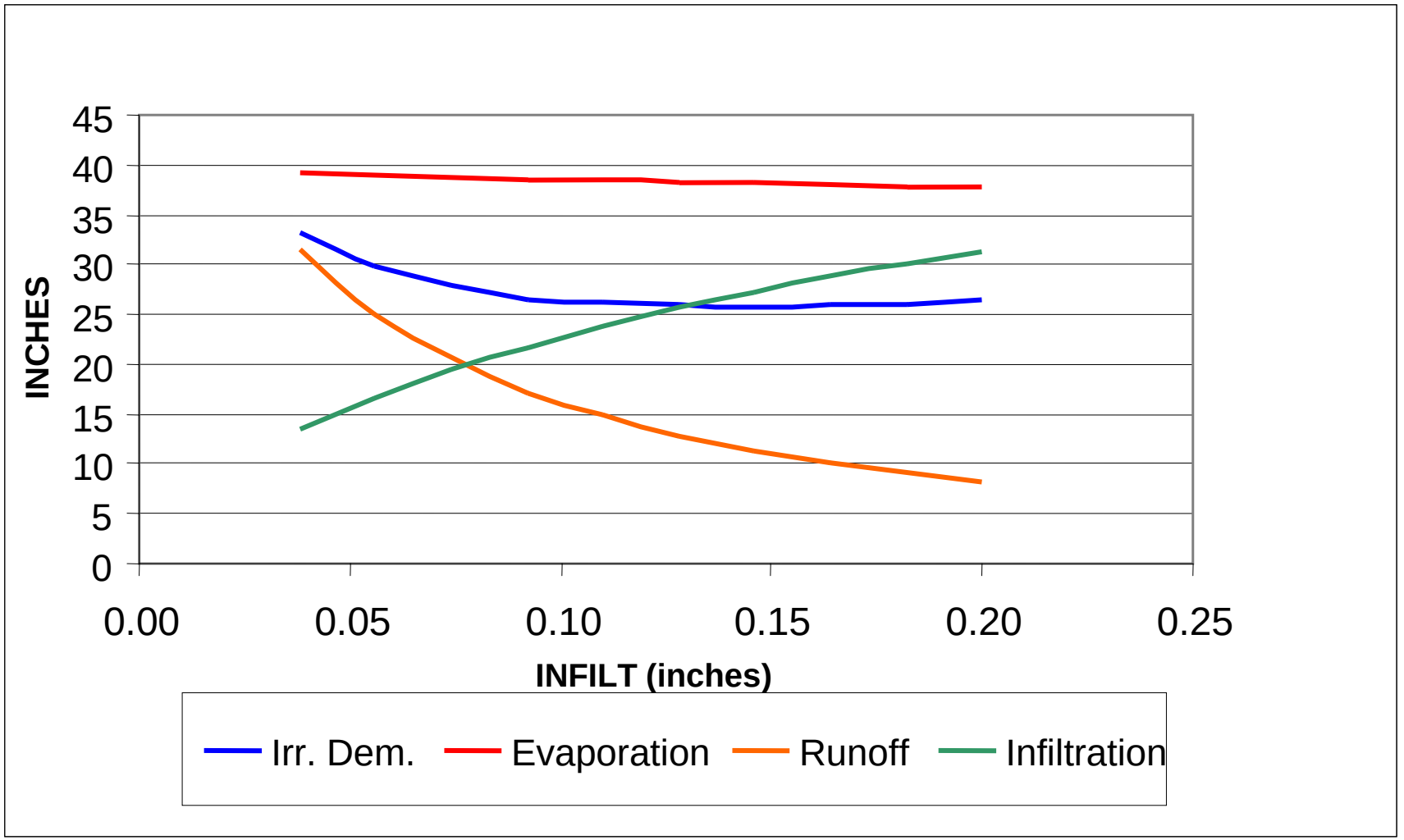

Figure 13.4. Sensitivity Analysis for INFILT

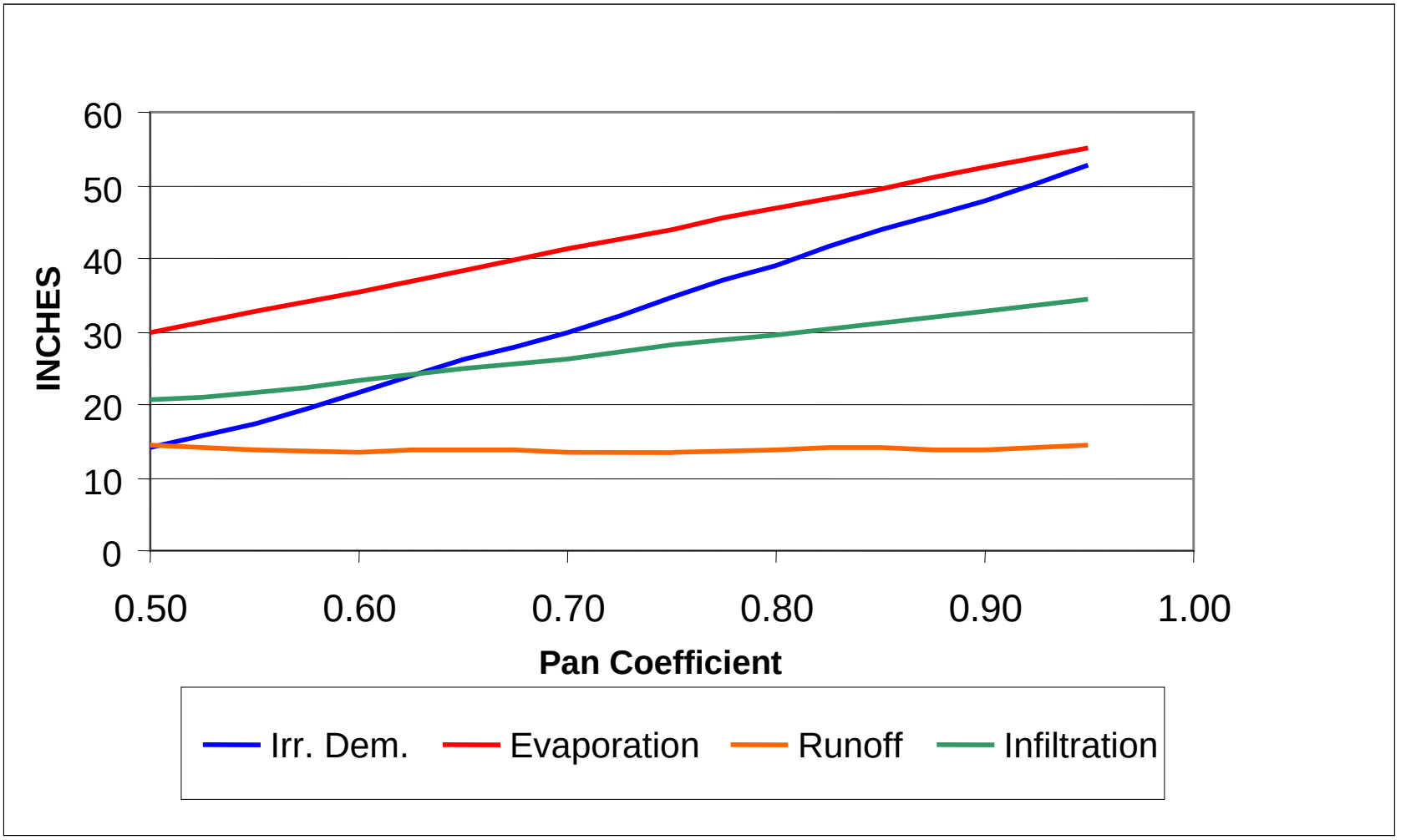

Figure 13.5. Sensitivity Analysis for Pan Coefficient

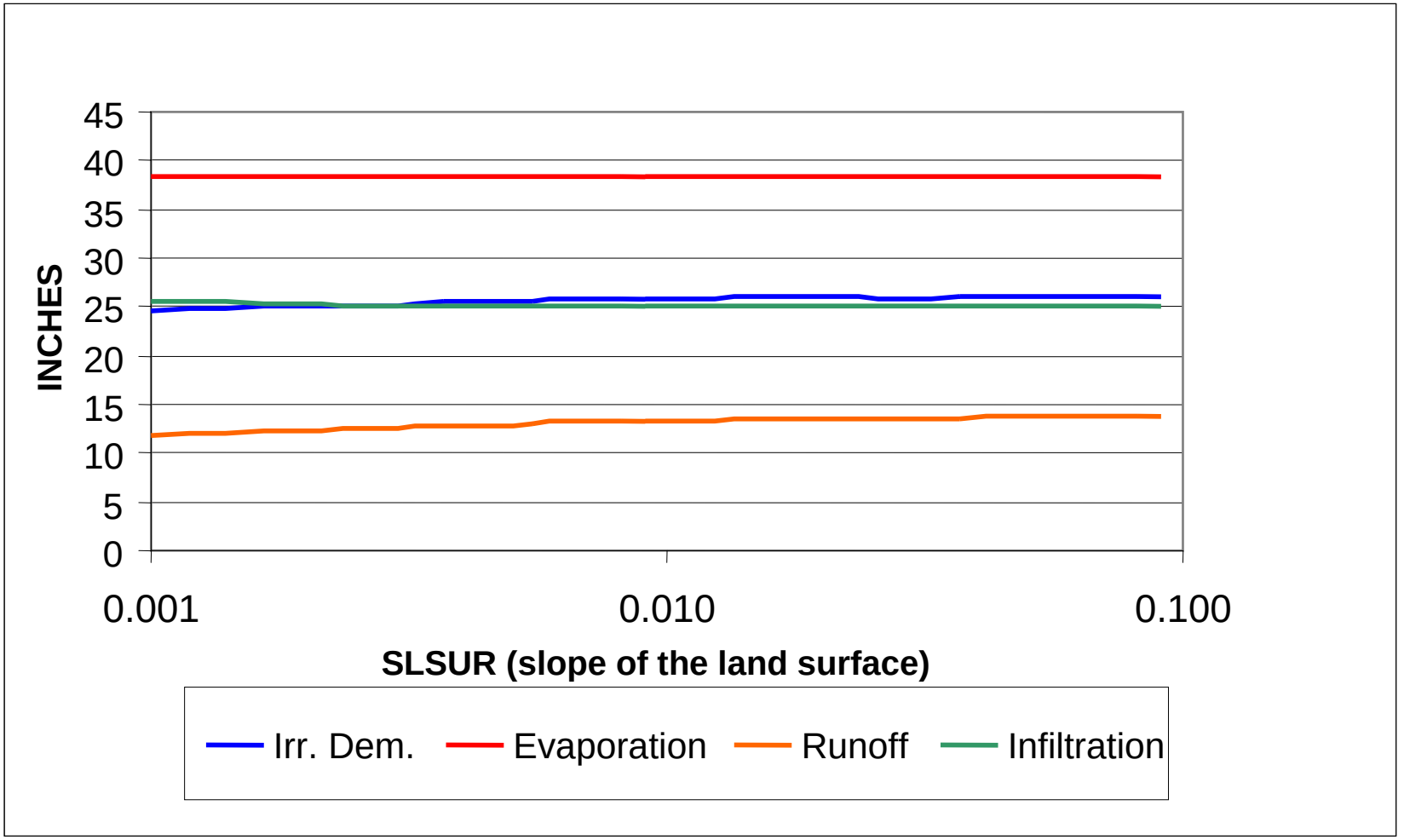

Figure 13.6. Sensitivity to Analysis for SLSUR

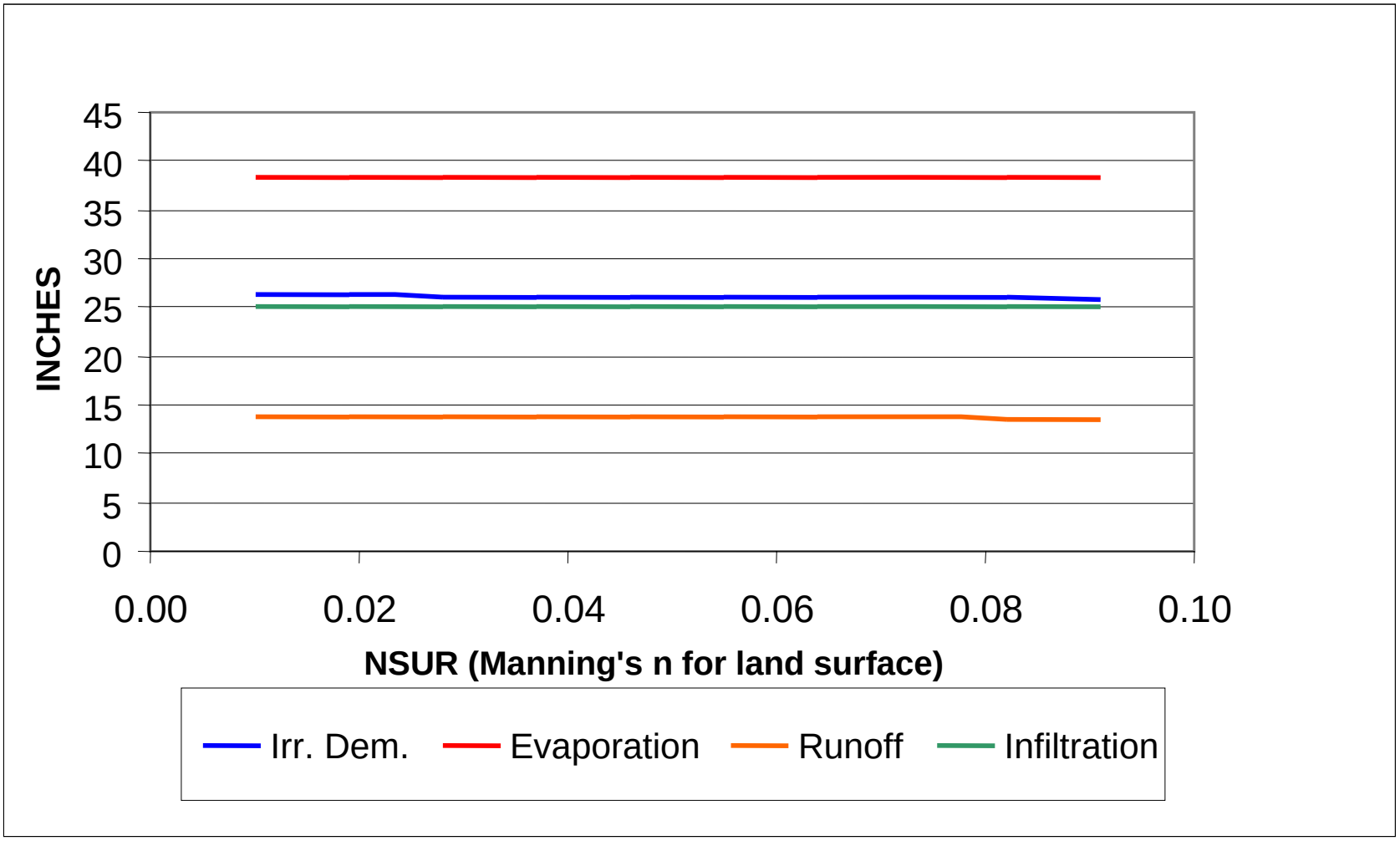

Figure 13.7. Sensitivity Analysis for NSUR

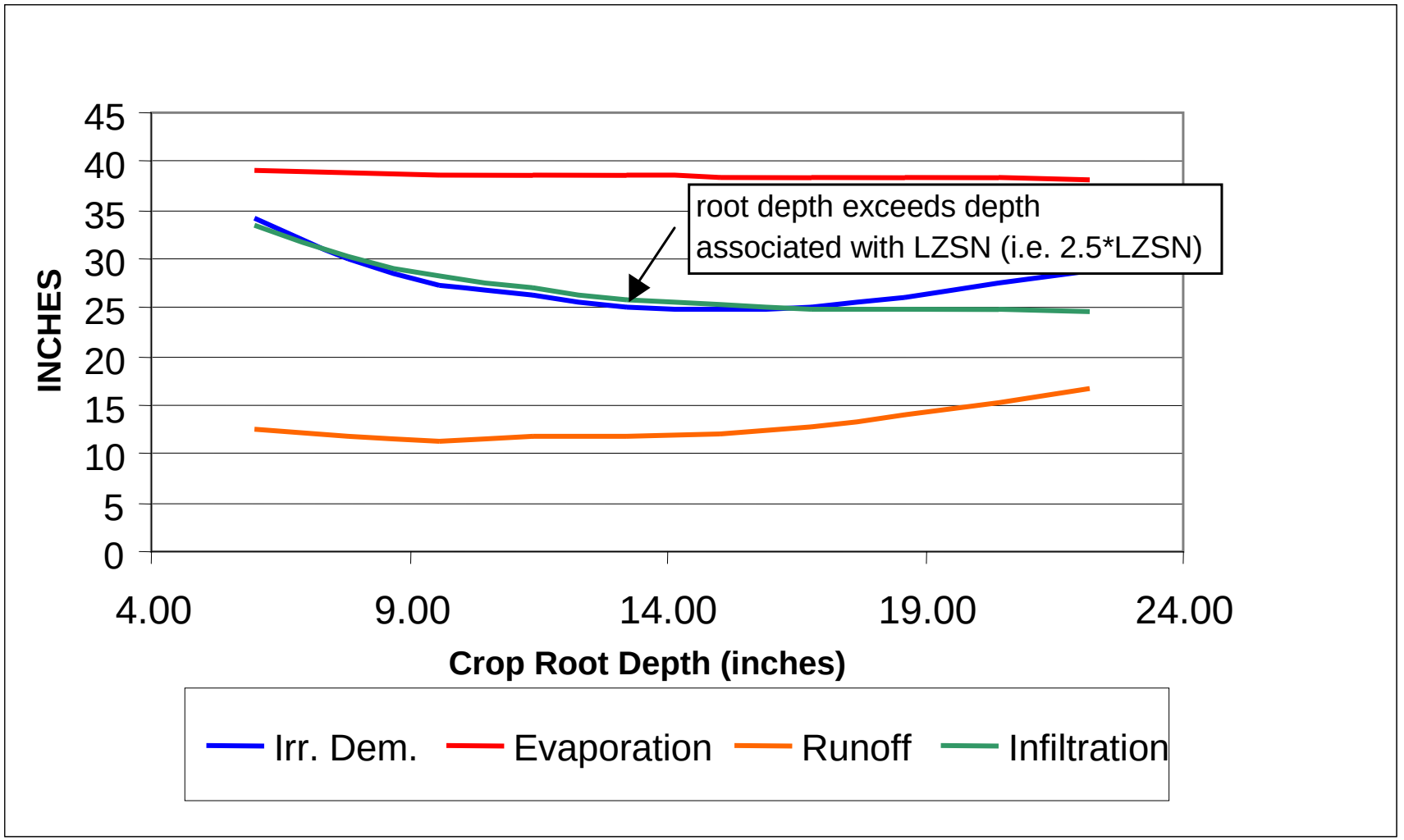

Figure 13.8. Sensitivity Analysis for Root Depth

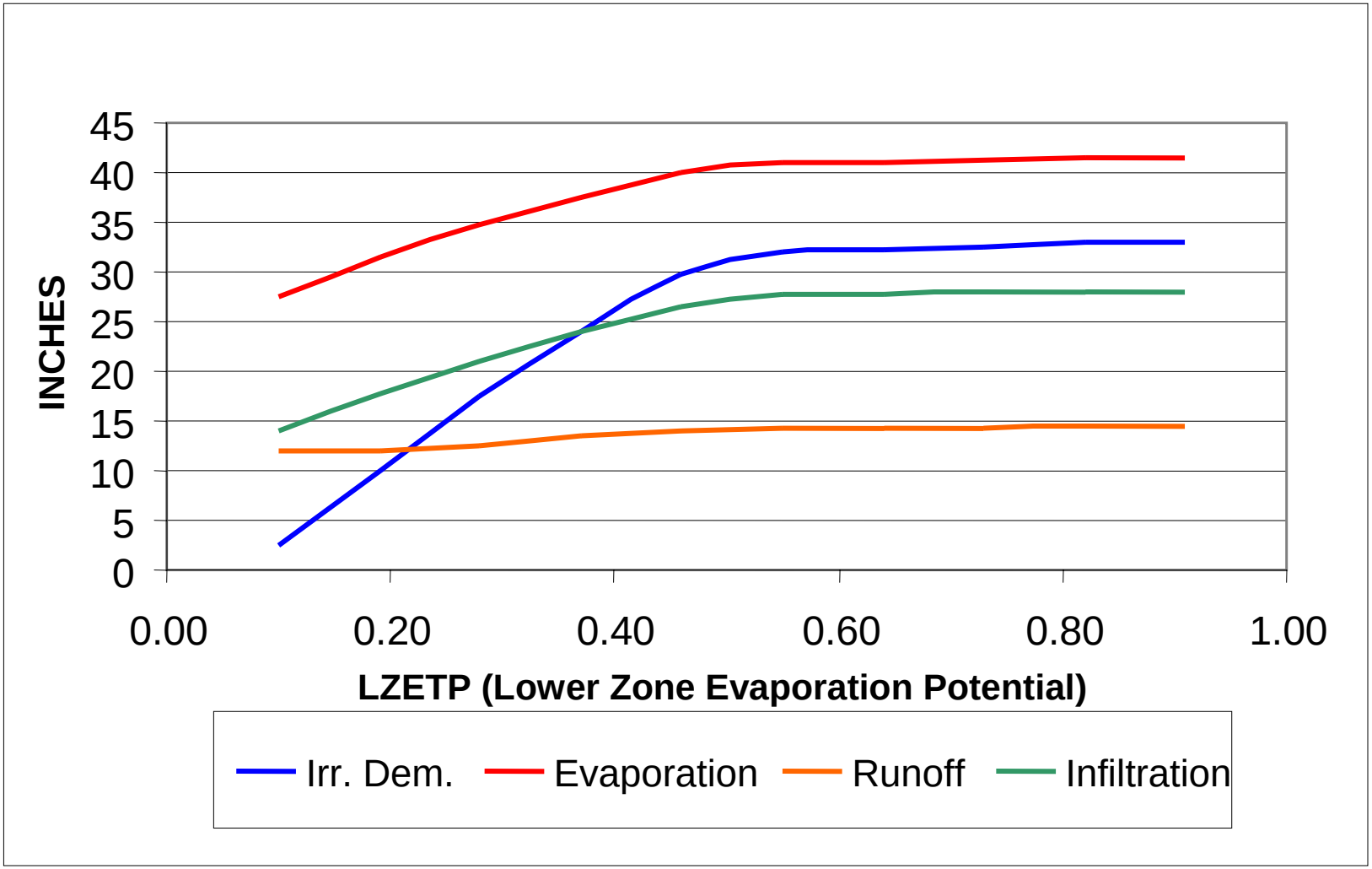

Figure 13.9. Sensitivity Analysis for LZETP

Appendix D
Calibration And Validation Plots For Upland Basins And Estuary Stations

Appendix D
Calibration And Validation Plots For Upland Basins And Estuary Stations

Appendix D

Simulation Results for Calibration and Validation Periods

Calibration Period
1995-2000

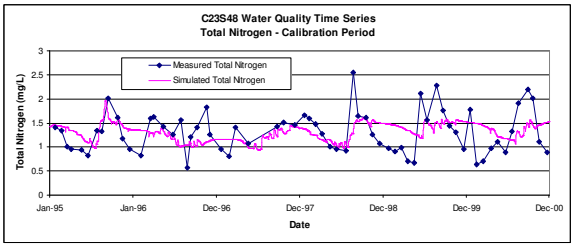

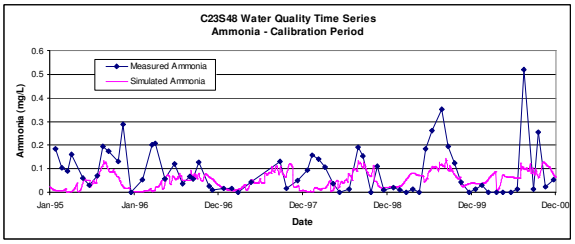

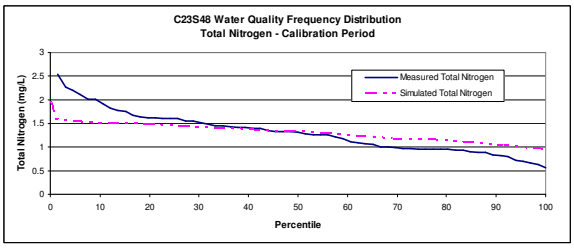

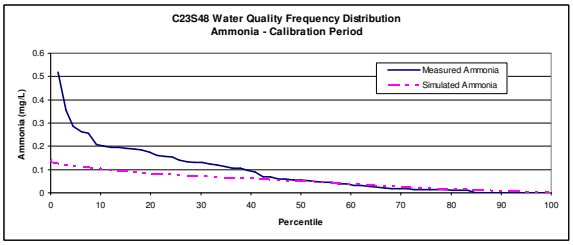

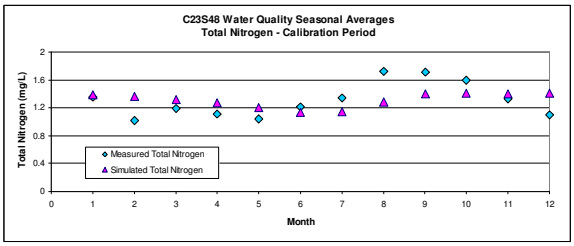

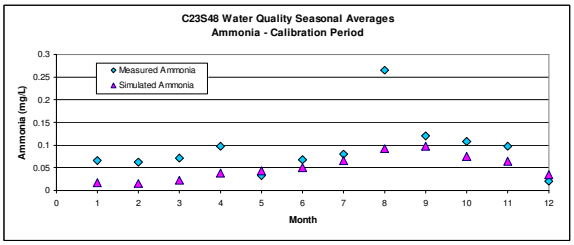

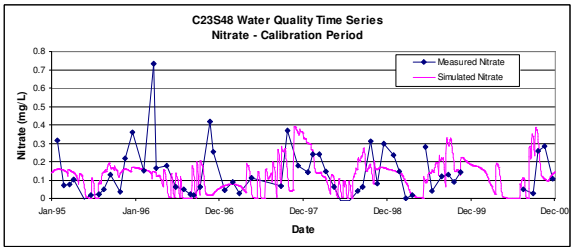

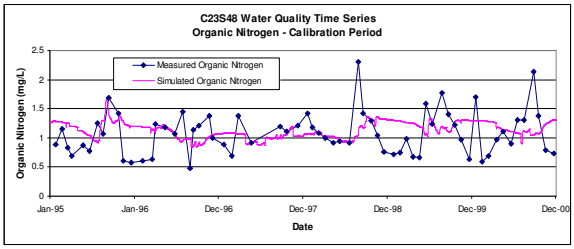

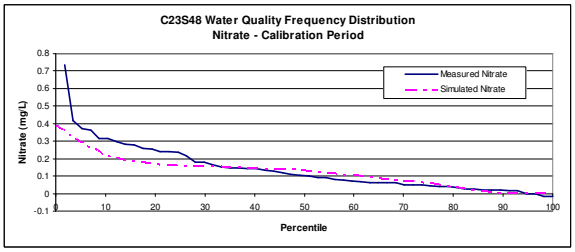

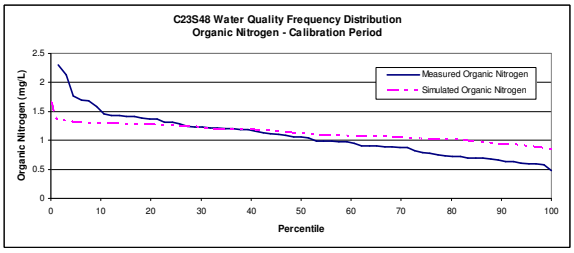

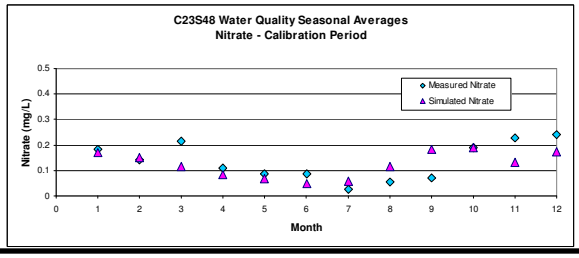

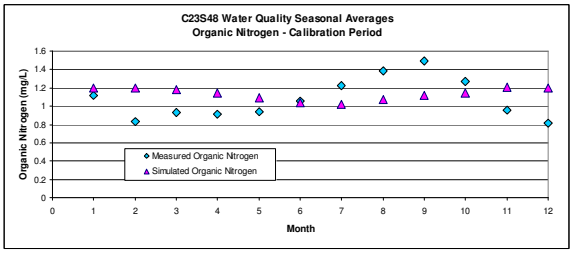

URS

C23 Simulation Results during Calibration Period (1995-2000)

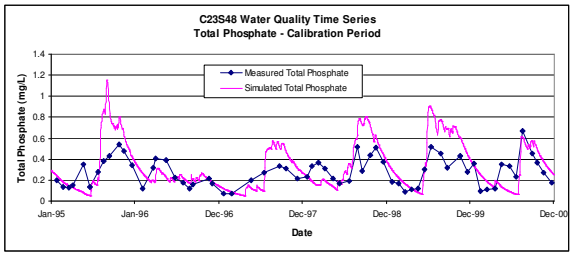

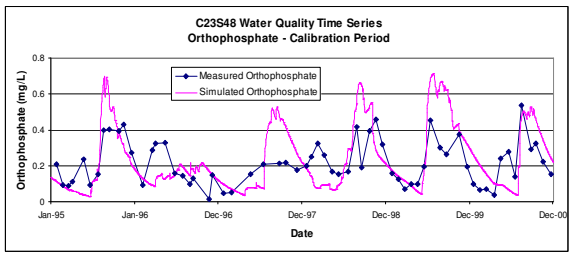

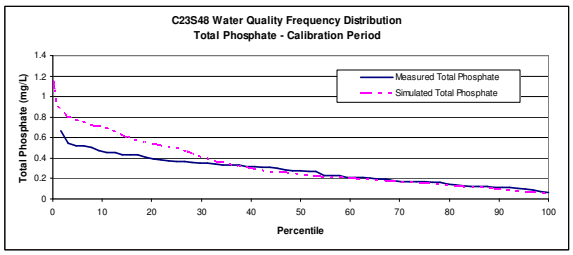

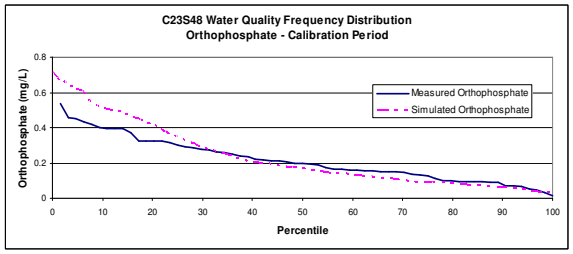

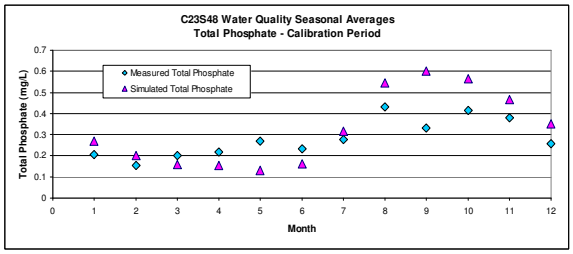

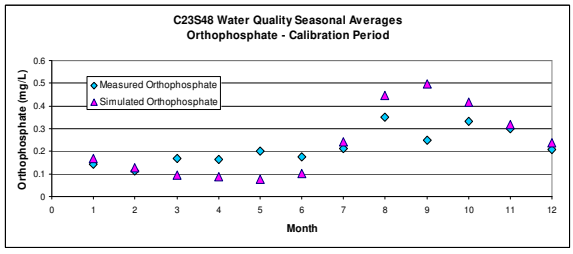

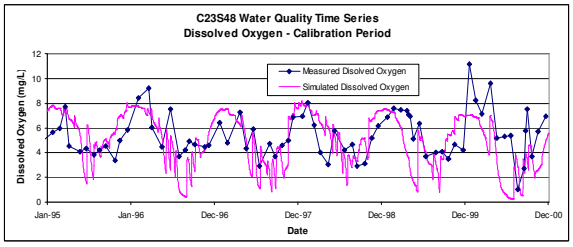

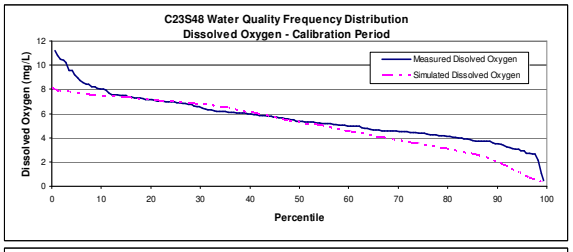

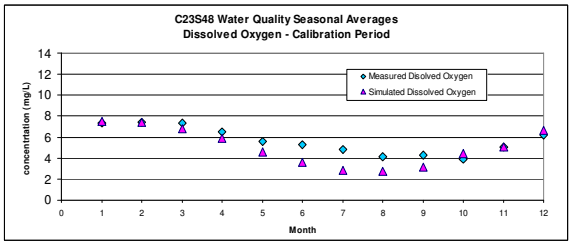

URS

C23 Simulation Results during Calibration Period (1995-2000) Cont'd.

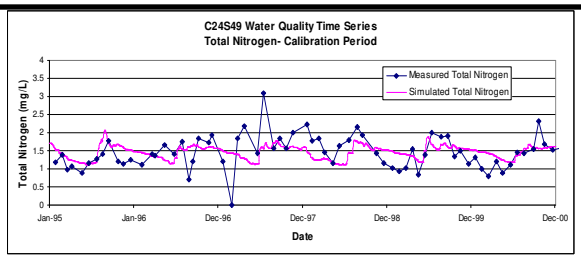

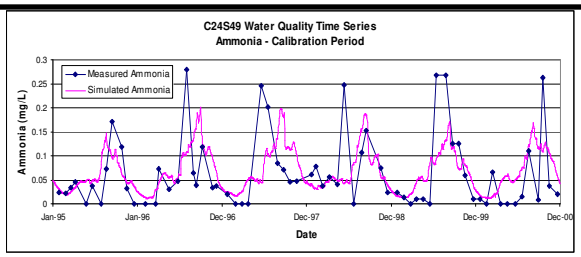

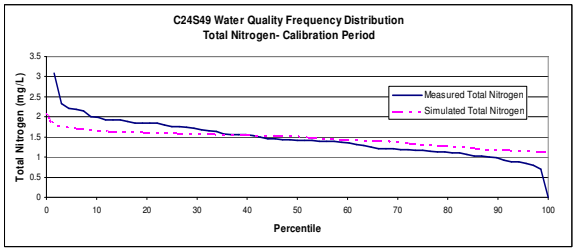

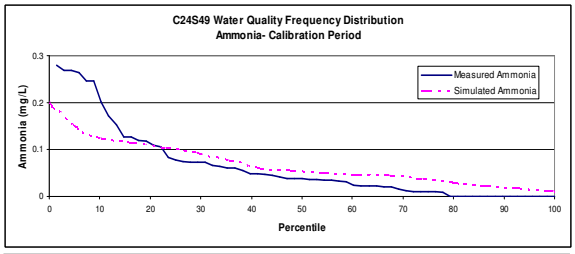

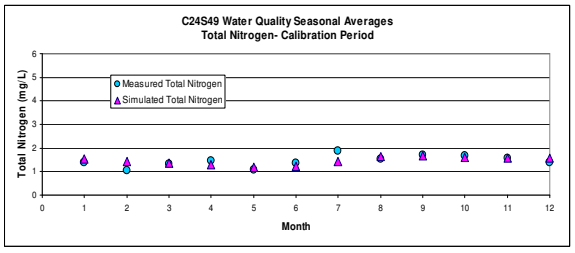

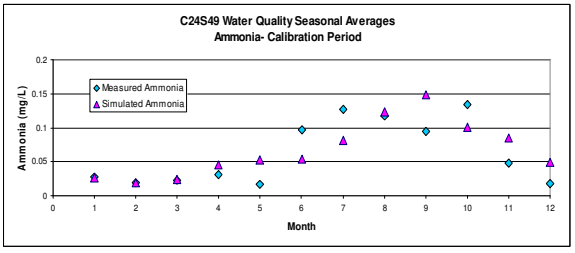

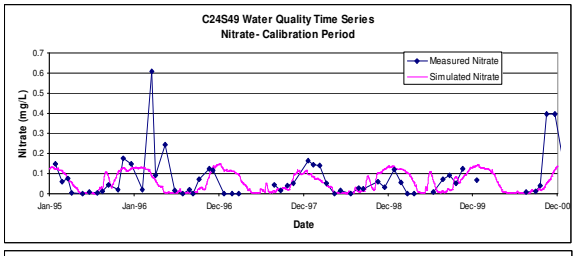

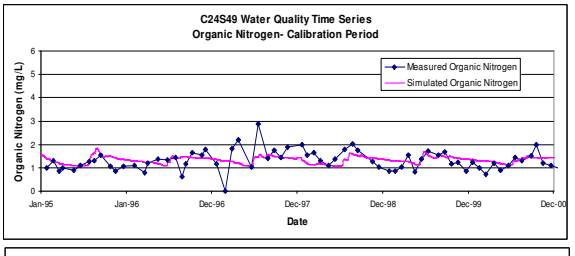

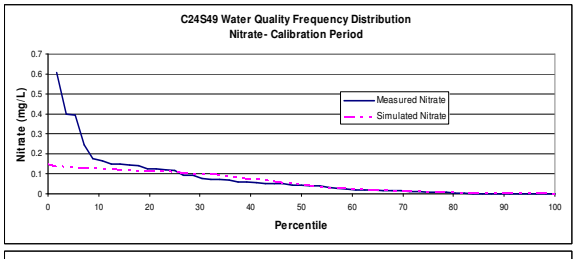

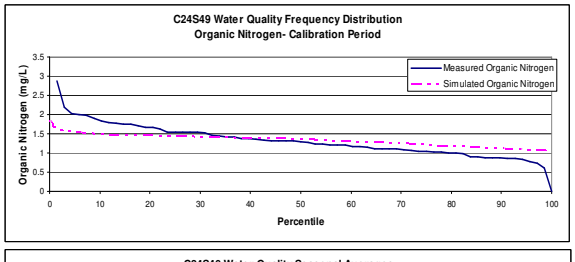

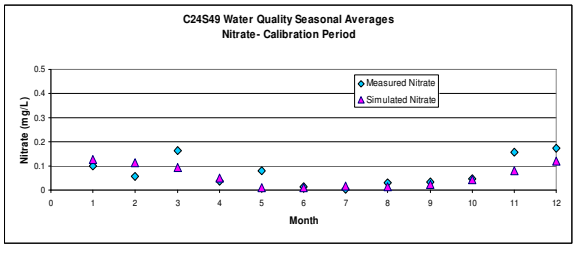

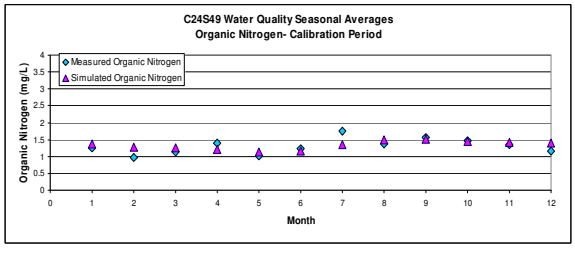

URS

C24 Simulation Results during Calibration Period (1995-2000)

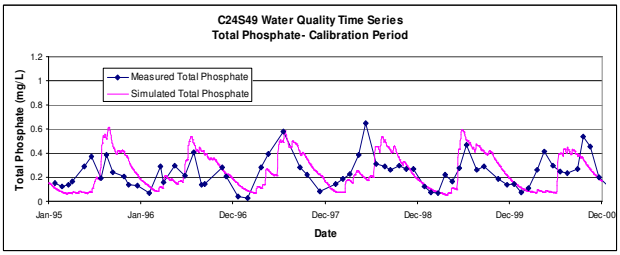

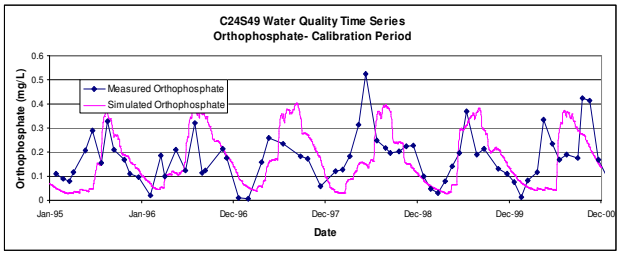

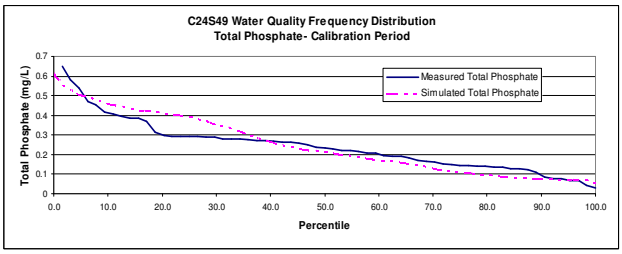

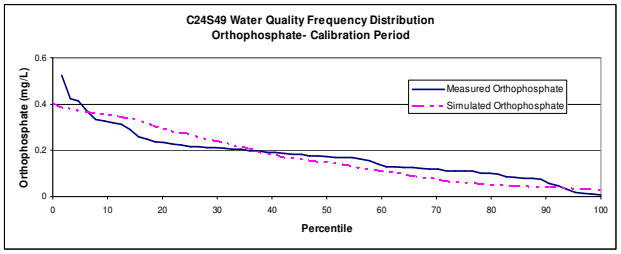

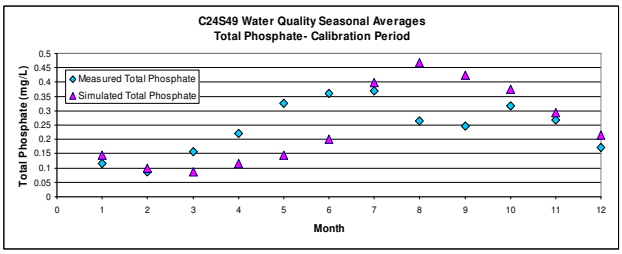

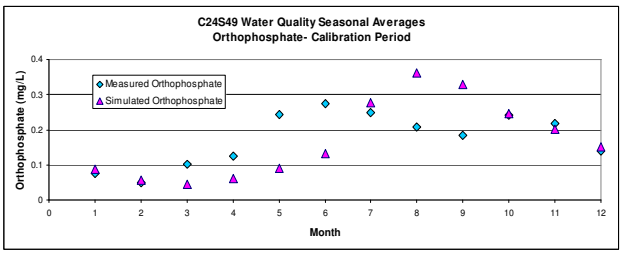

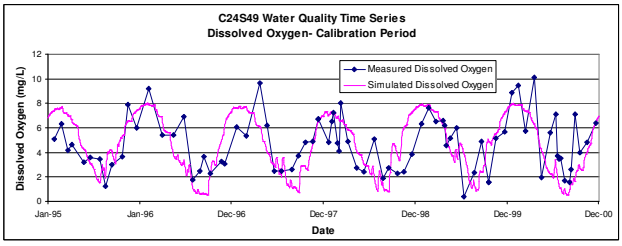

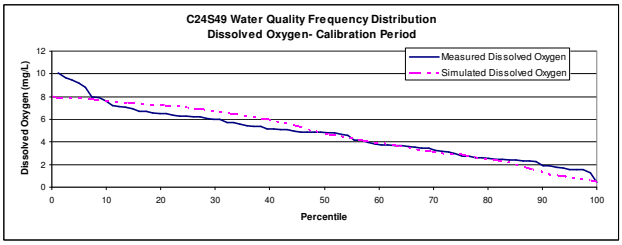

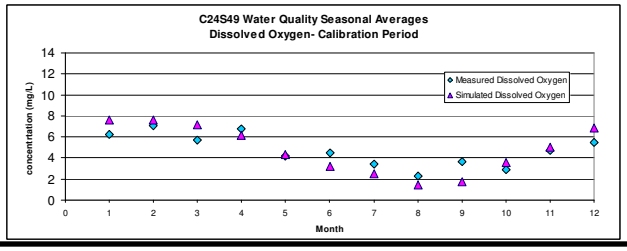

URS

C24 Simulation Results during Calibration Period (1995-2000) Cont'd.

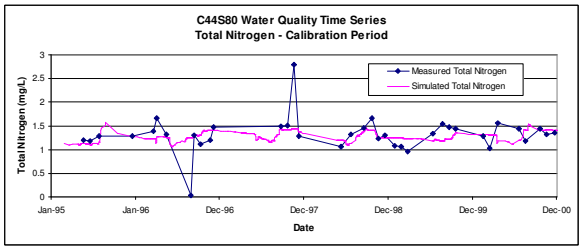

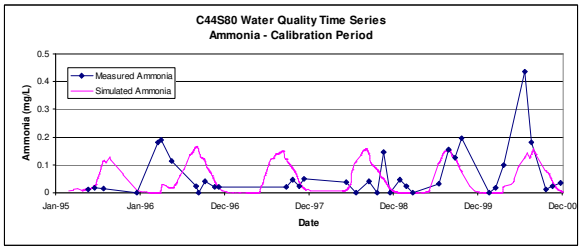

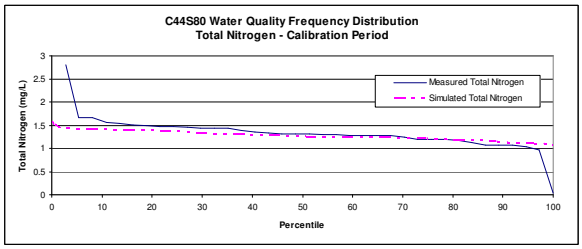

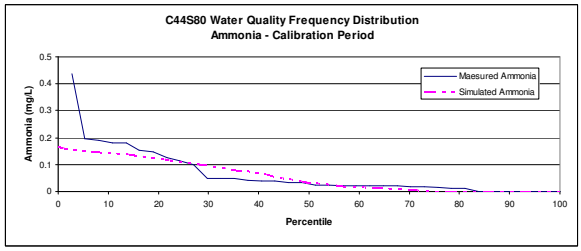

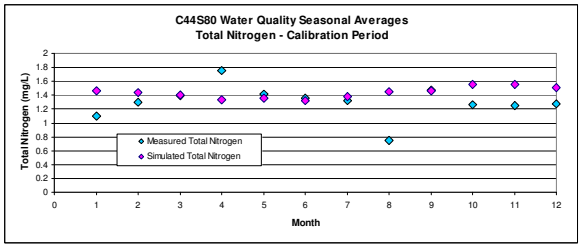

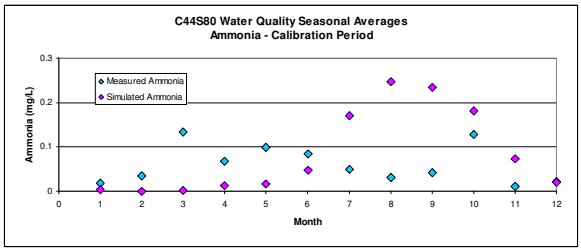

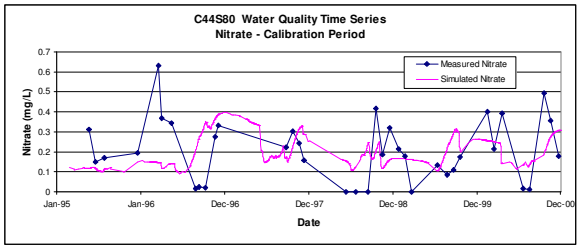

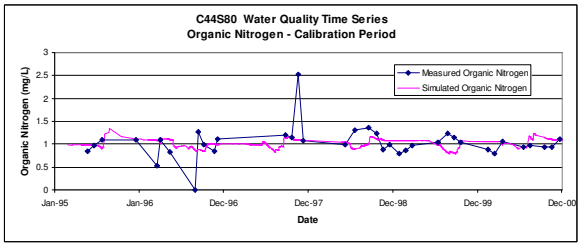

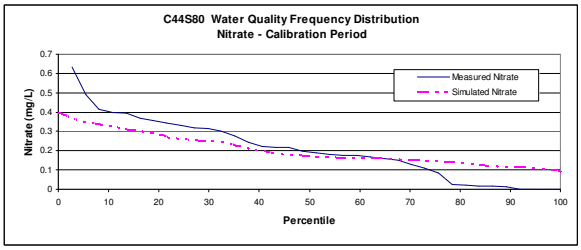

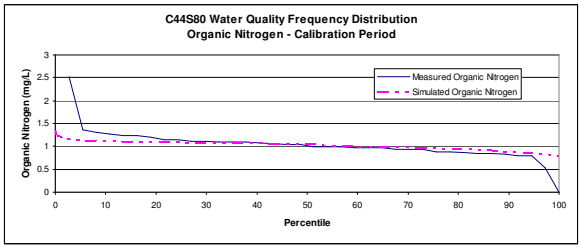

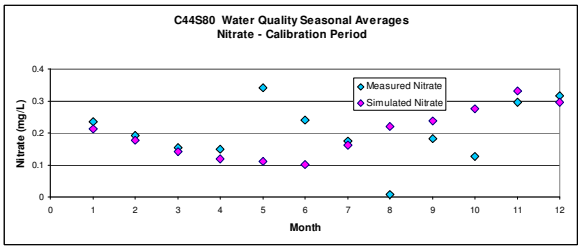

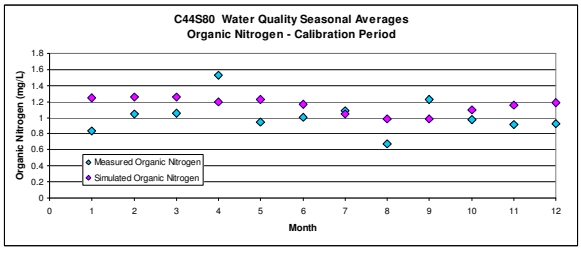

URS

C44 Simulation Results during Calibration Period (1995-2000)

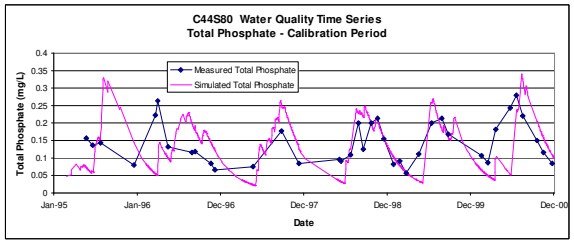

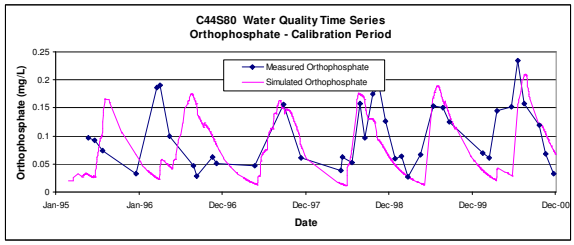

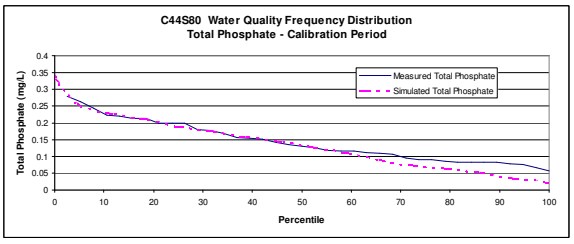

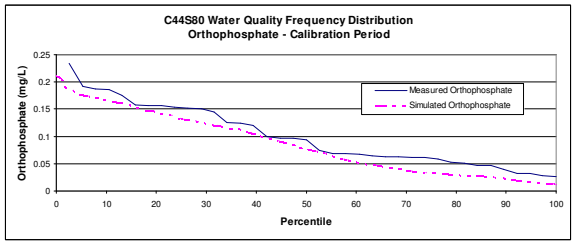

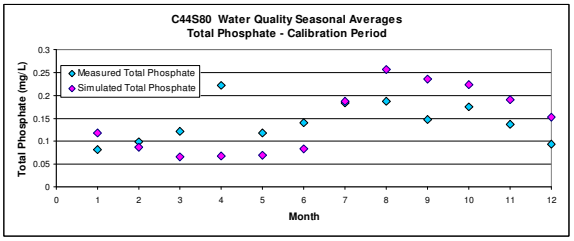

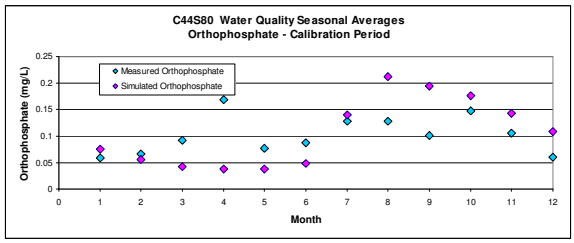

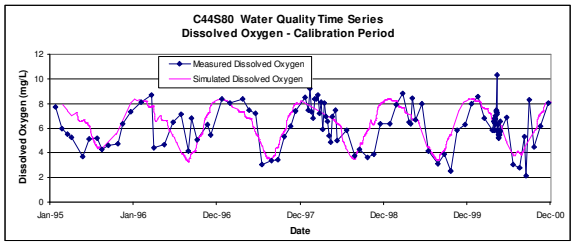

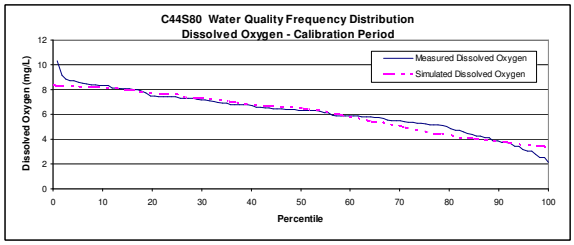

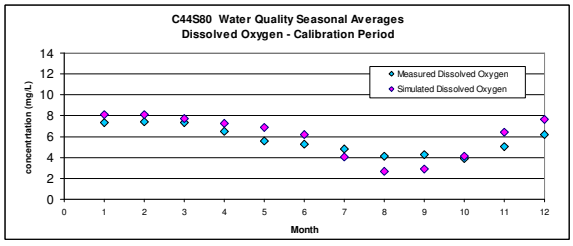

C44 Simulation Results during Calibration Period (1995-2000) Cont'd

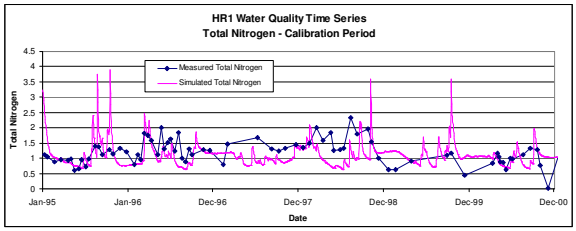

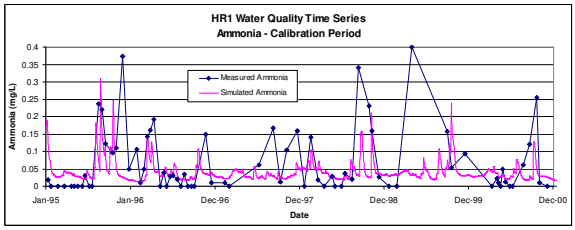

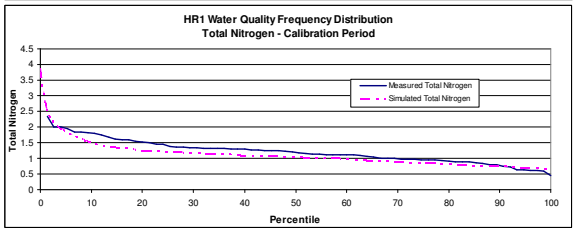

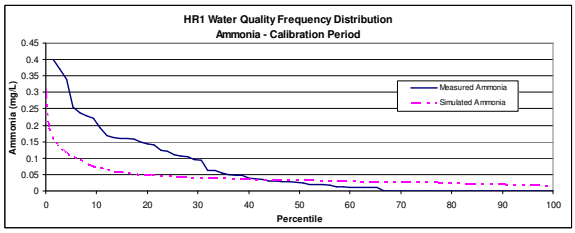

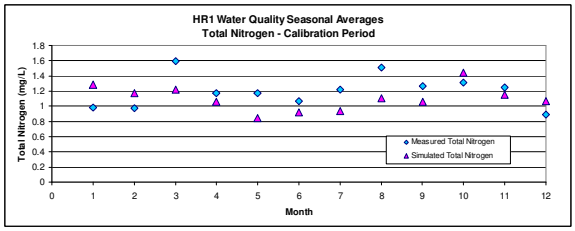

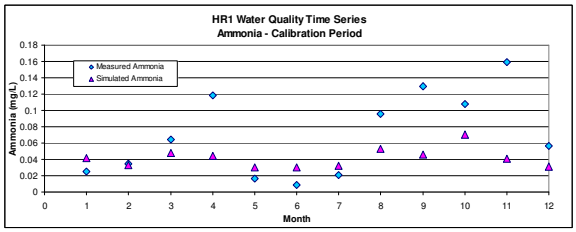

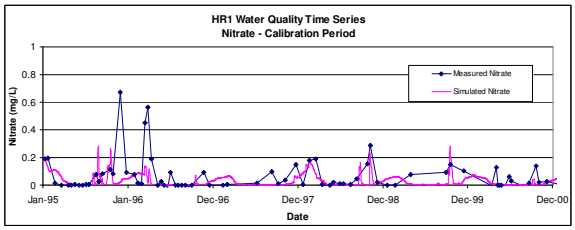

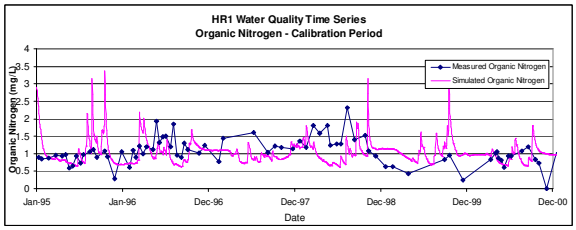

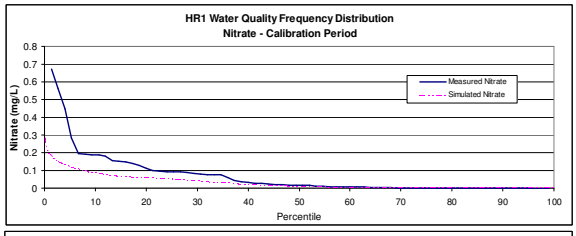

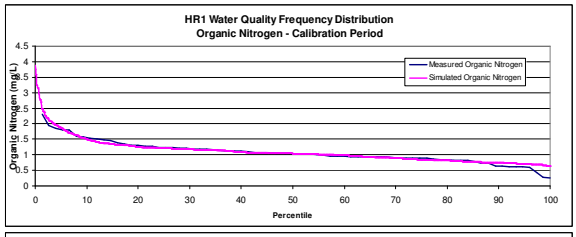

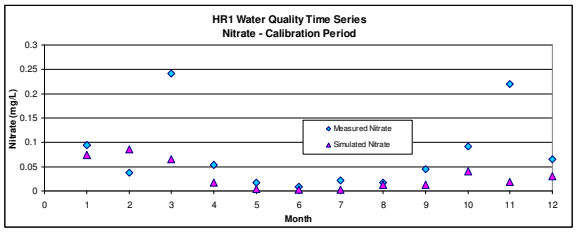

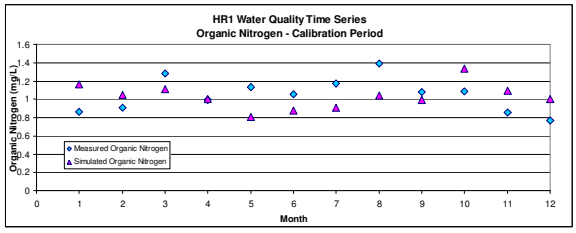

URS

HR1 Simulation Results during Calibration Period (1995-2000)

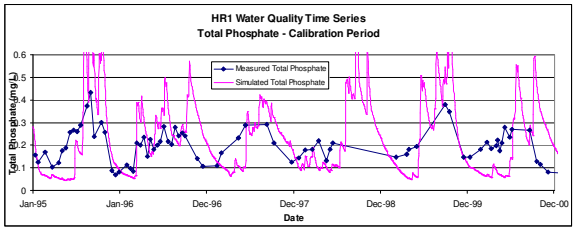

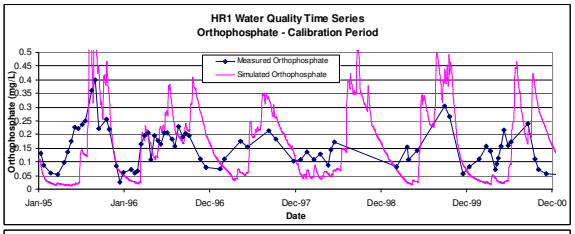

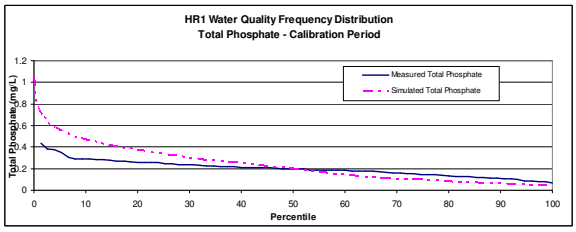

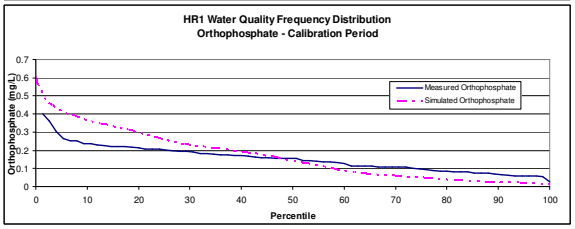

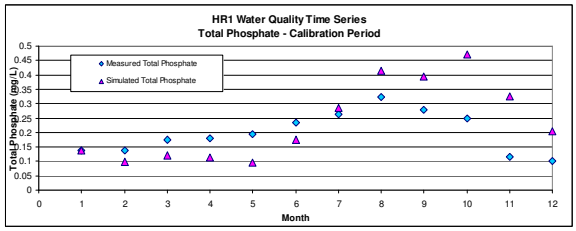

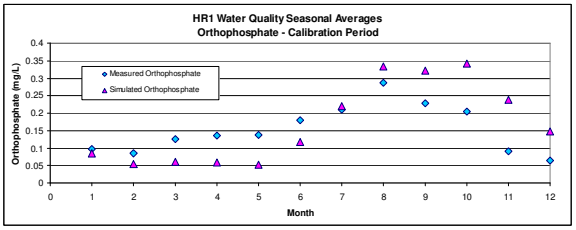

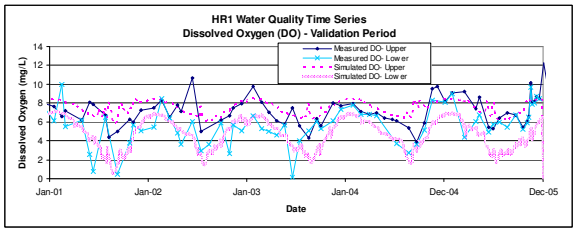

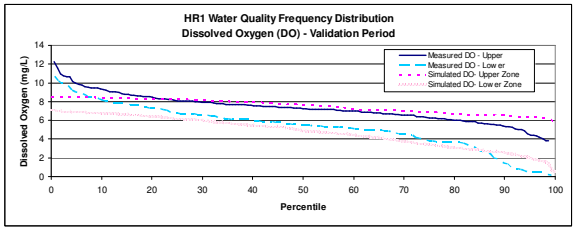

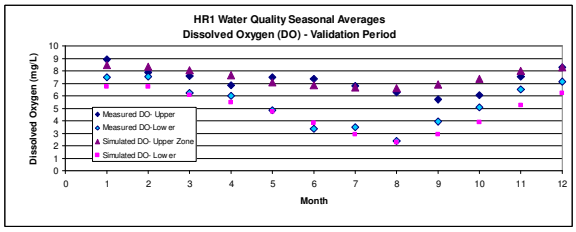

URS

HR1 Simulation Results during Calibration Period (1995-2000) Cont'd.

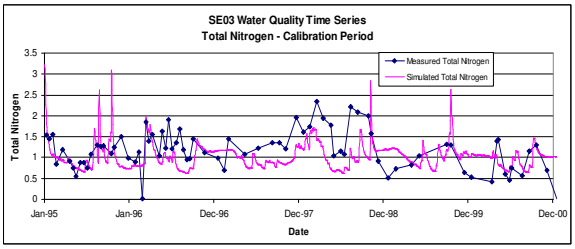

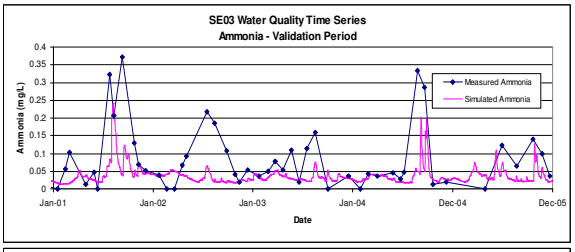

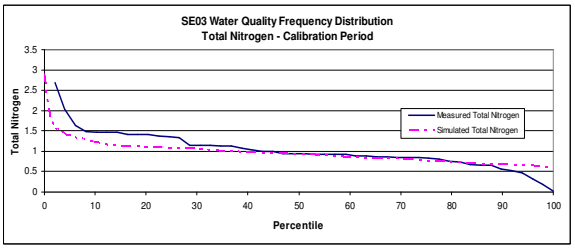

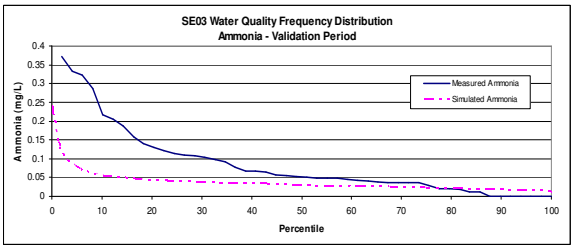

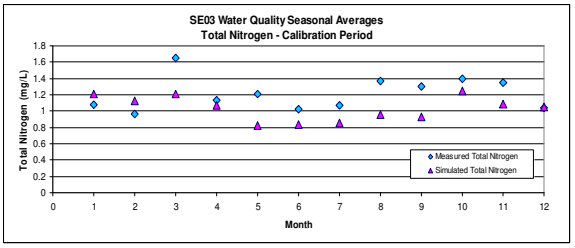

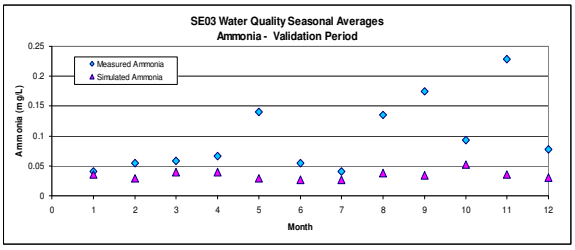

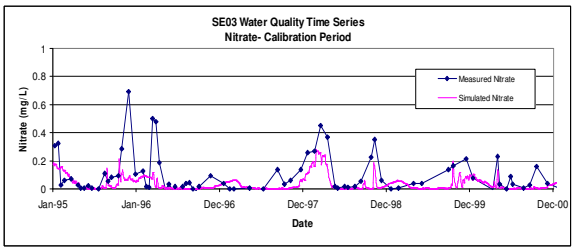

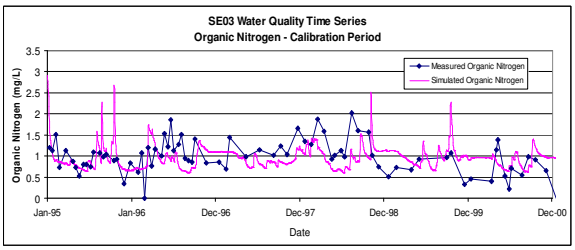

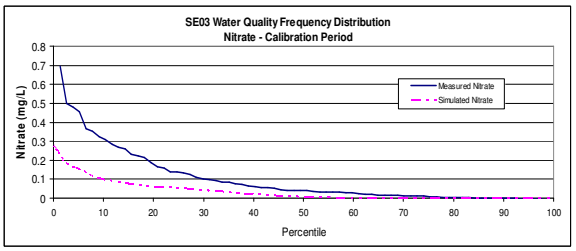

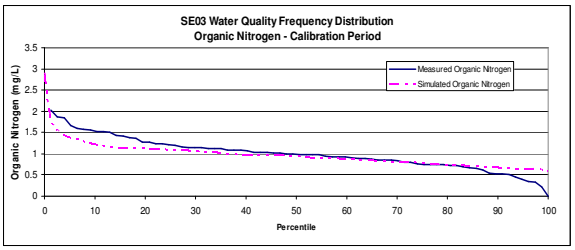

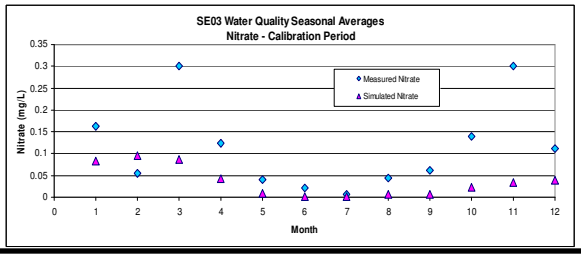

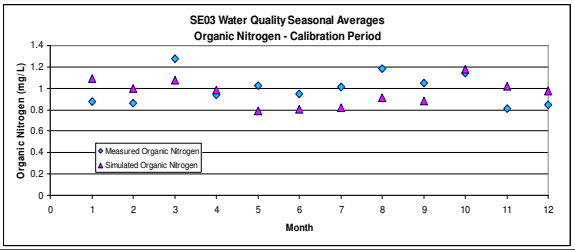

URS

SE03 Simulation Results during Calibration Period (1995-2000)

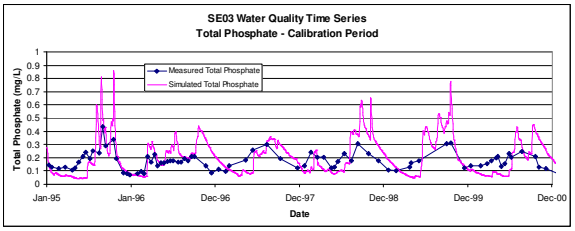

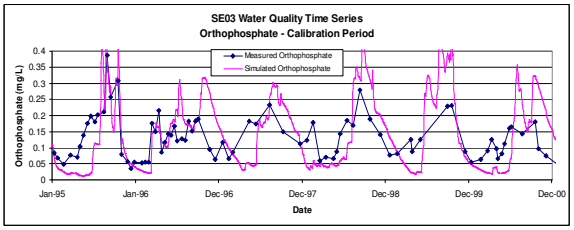

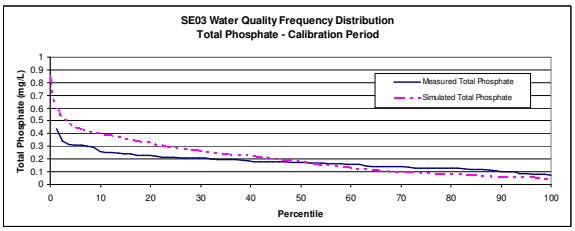

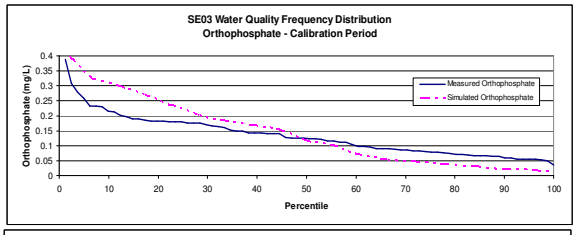

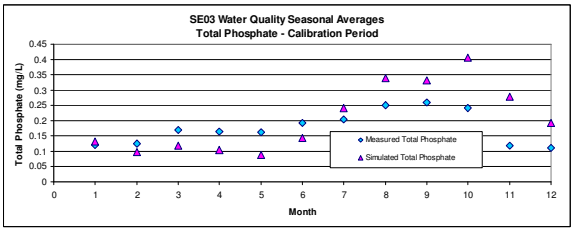

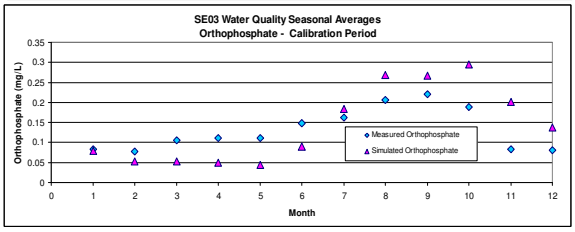

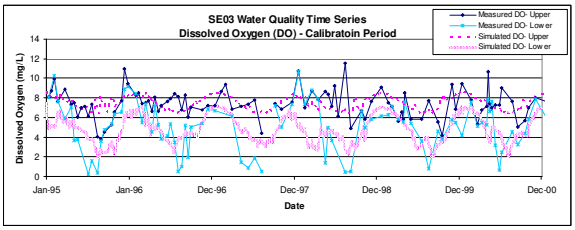

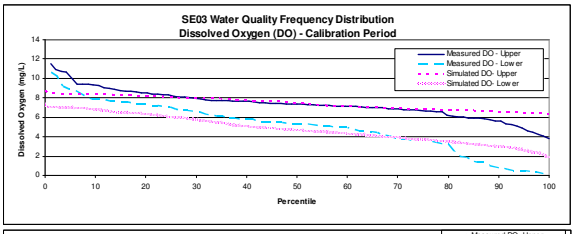

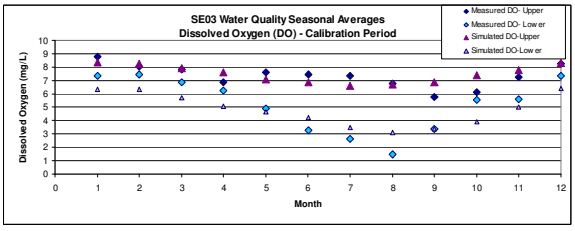

URS

SE03 Simulation Results during Calibration Period (1995-2000) Cont'd.

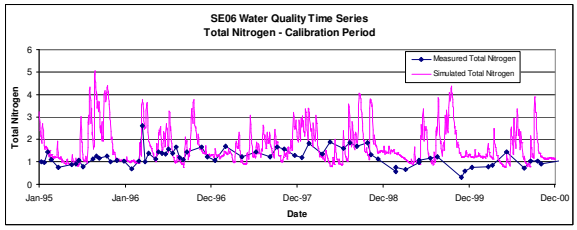

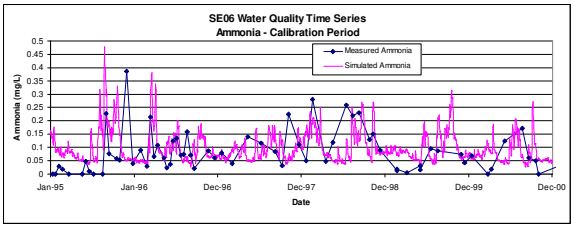

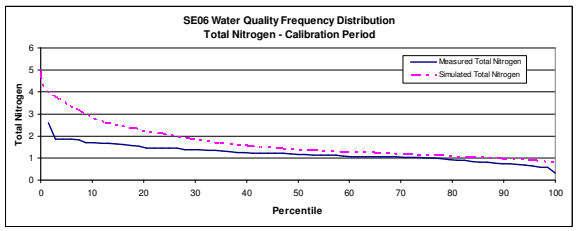

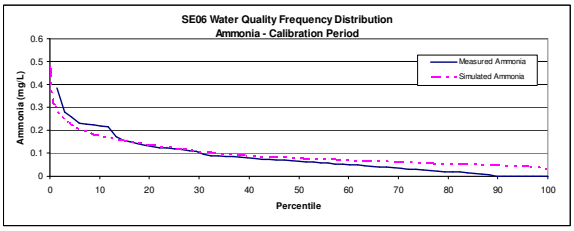

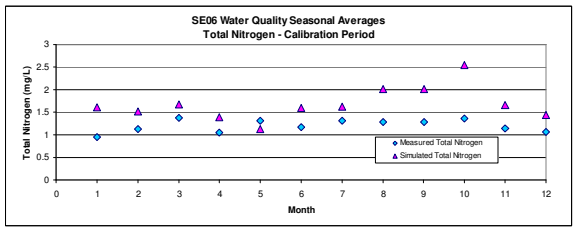

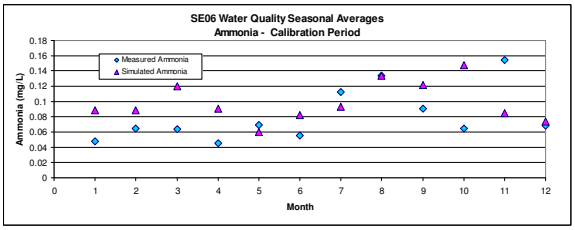

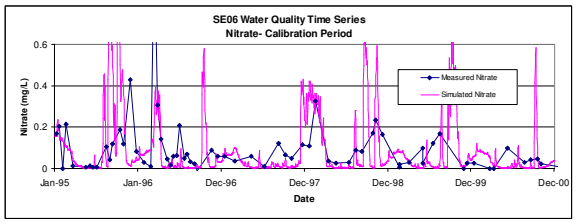

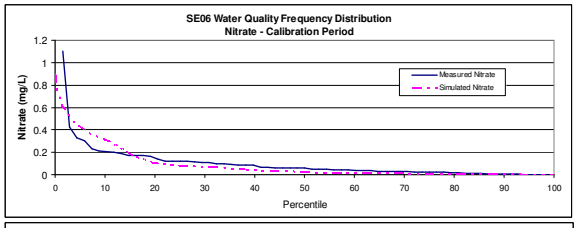

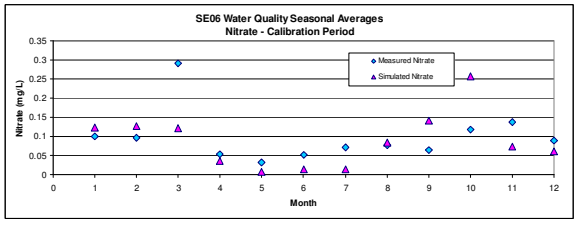

URS

SE06 Simulation Results during Calibration Period (1995-2000)

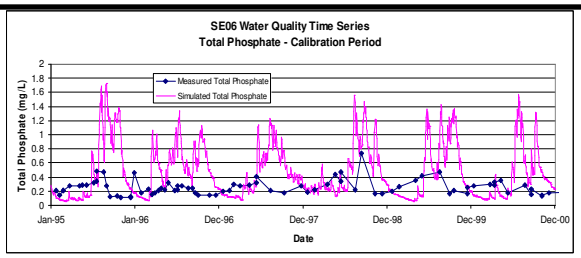

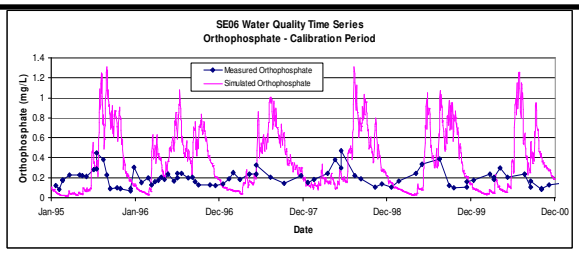

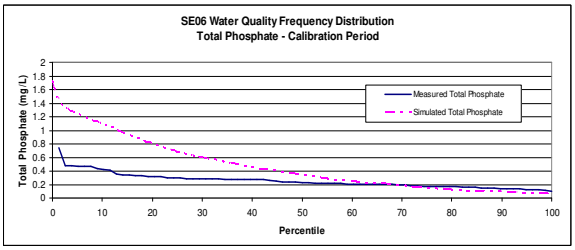

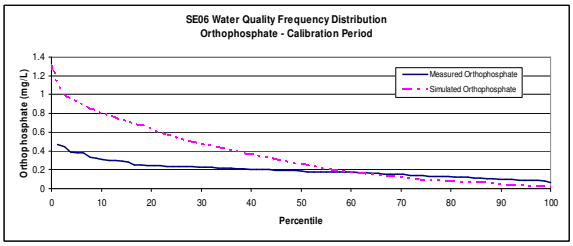

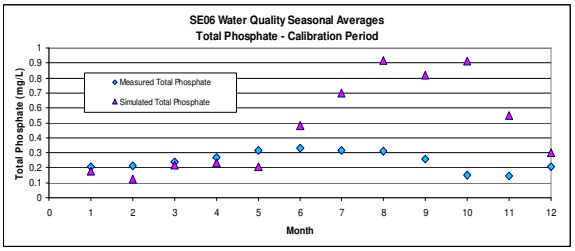

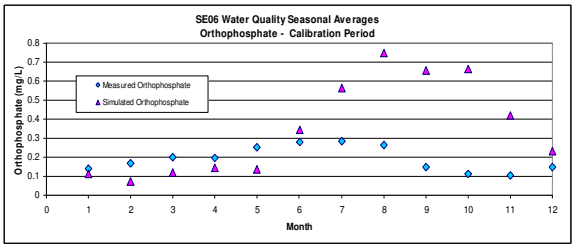

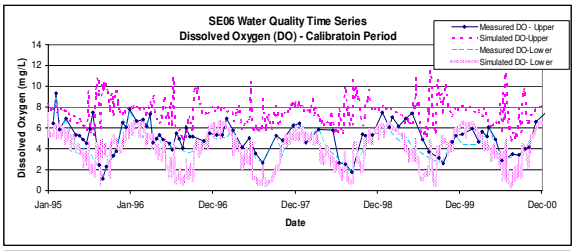

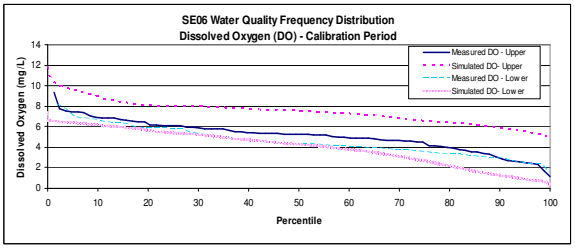

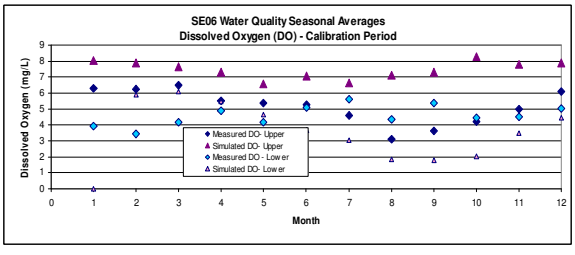

URS

SE06 Simulation Results during Calibration Period (1995-2000) Cont'd.

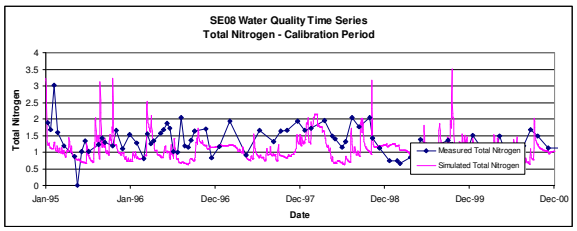

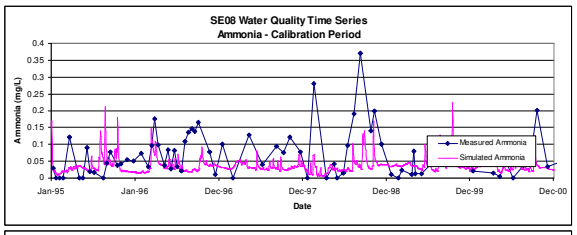

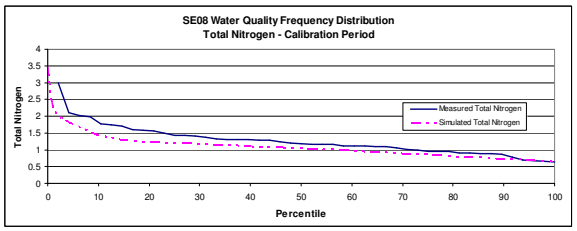

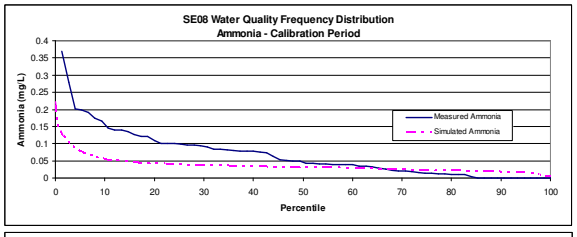

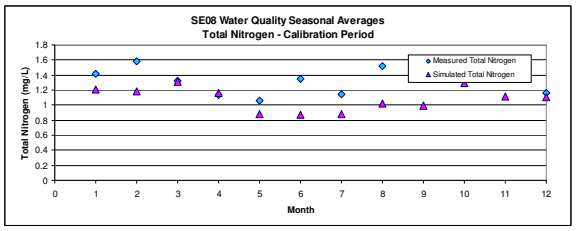

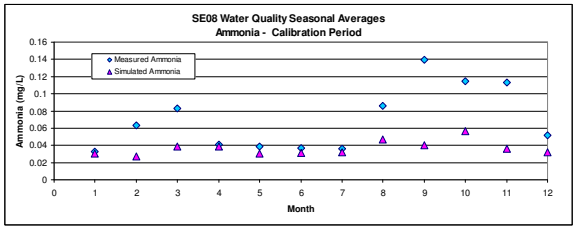

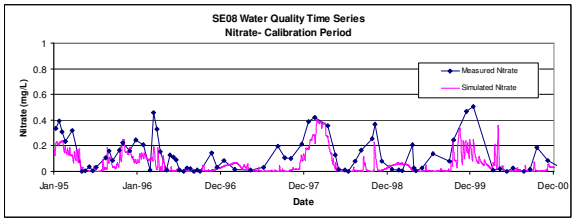

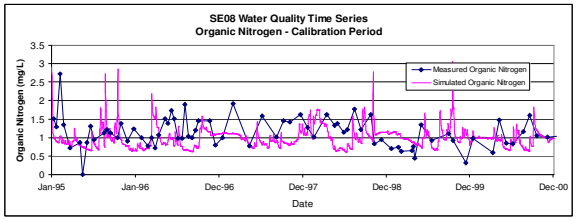

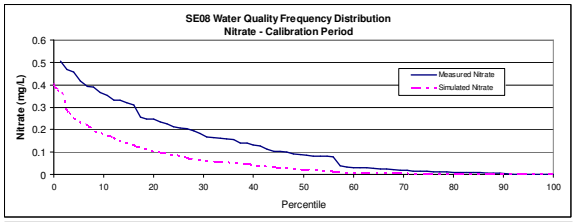

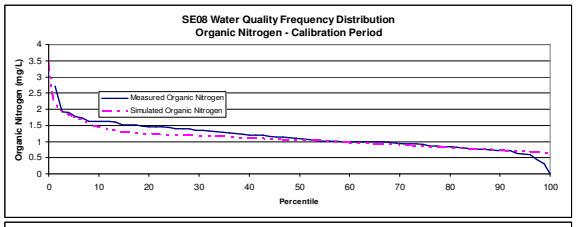

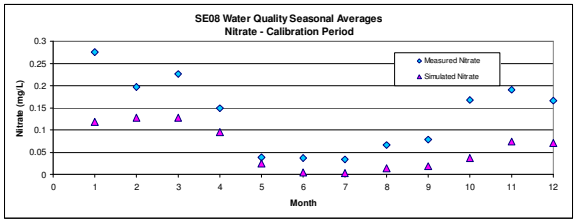

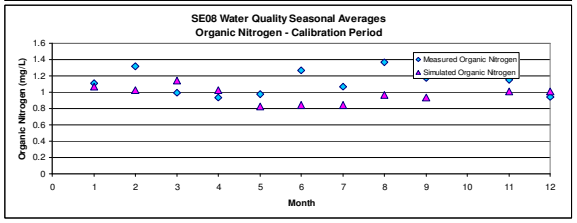

URS

SE08 Simulation Results during Calibration Period (1995-2000)

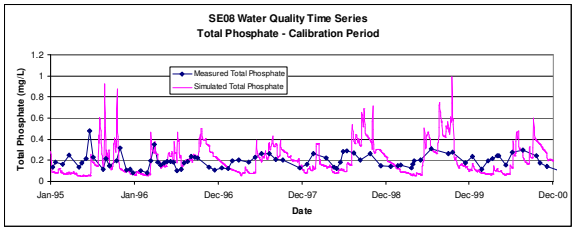

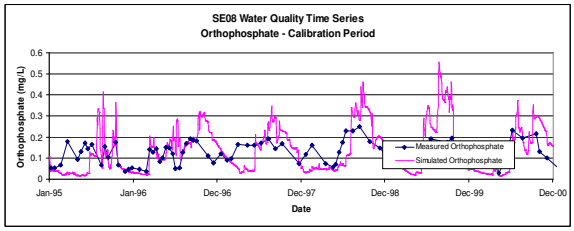

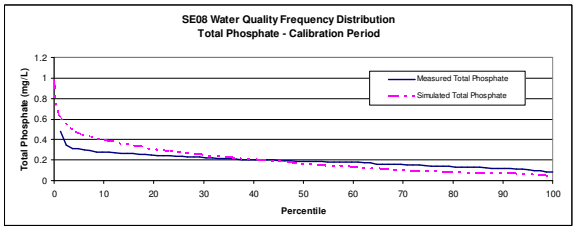

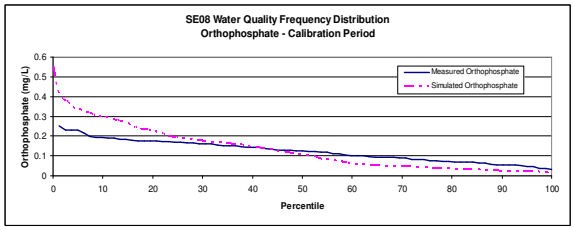

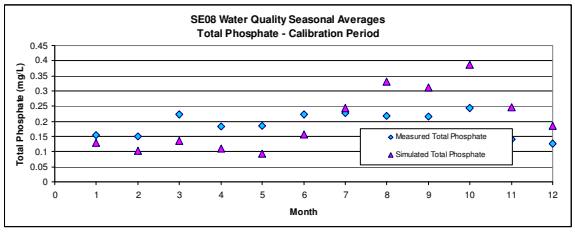

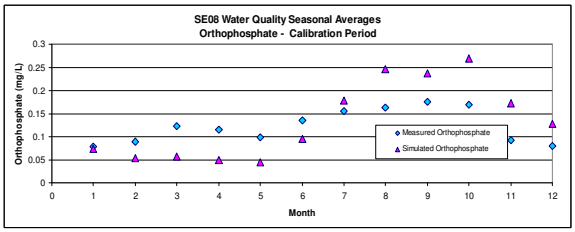

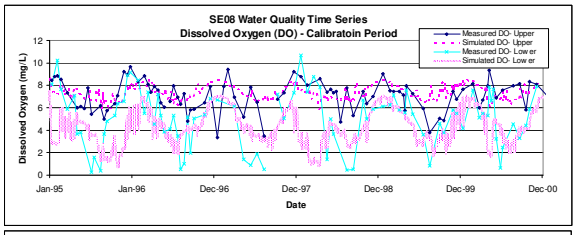

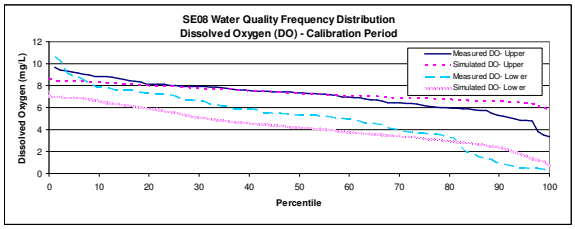

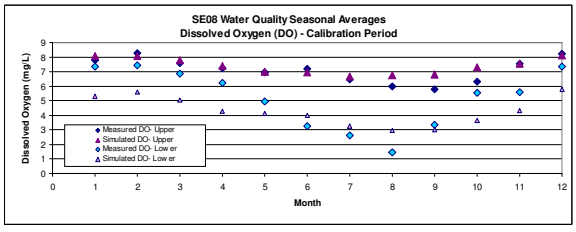

URS

SE08 Simulation Results during Calibration Period (1995-2000) Cont'd.

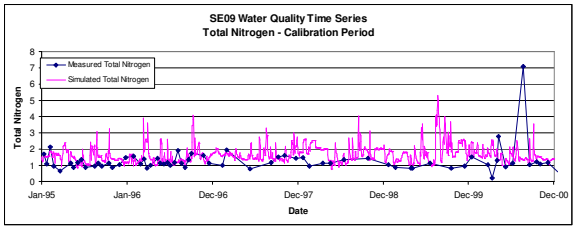

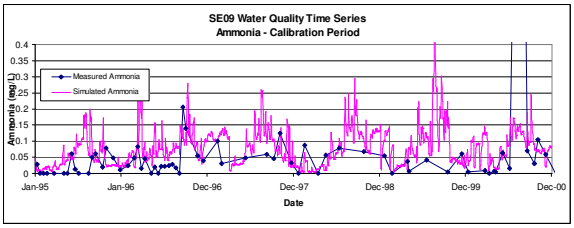

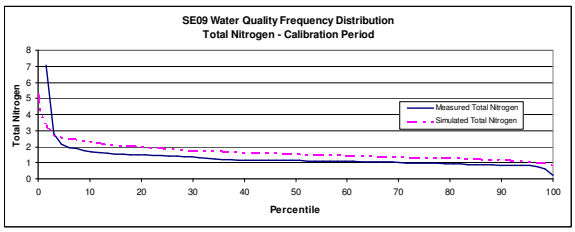

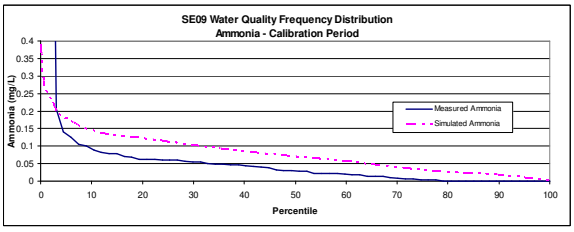

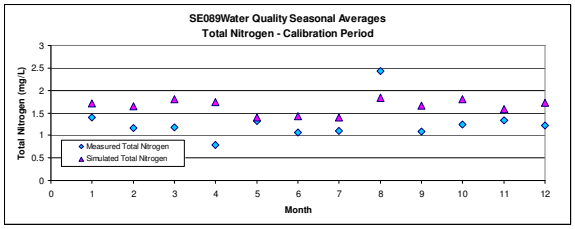

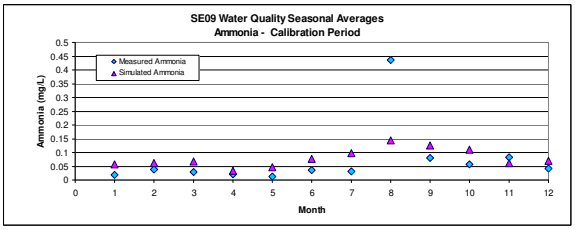

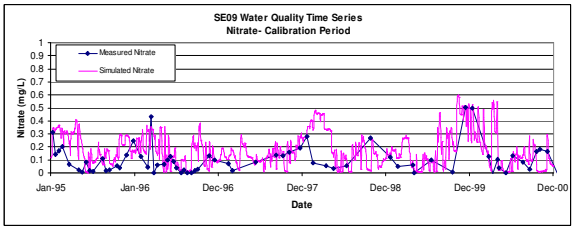

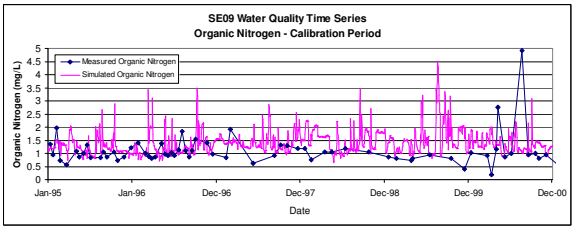

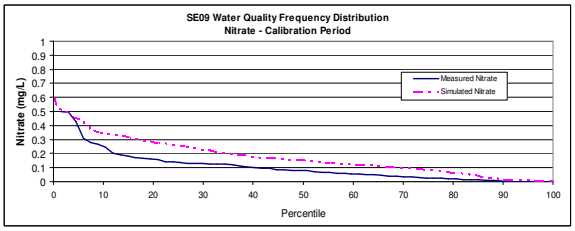

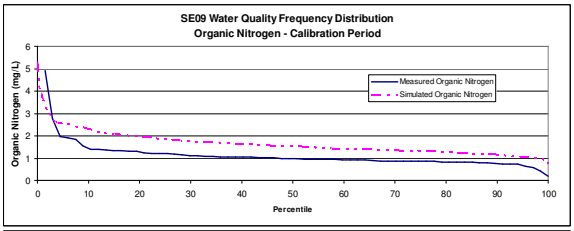

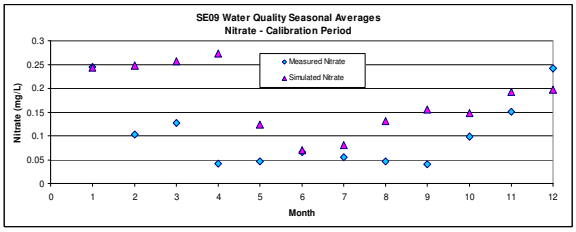

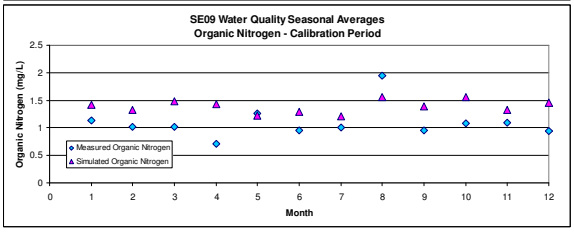

URS

SE09 Simulation Results during Calibration Period (1995-2000)

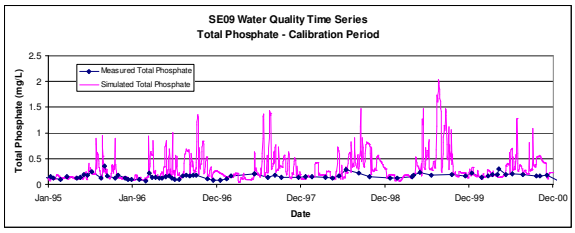

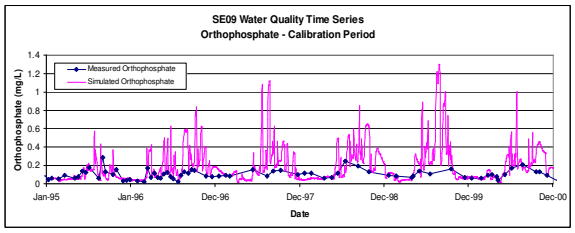

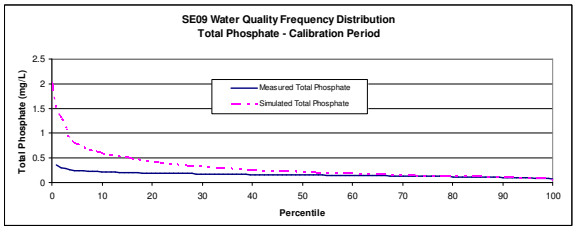

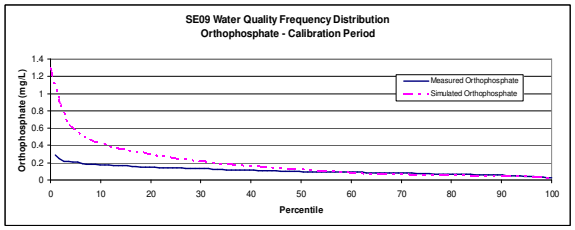

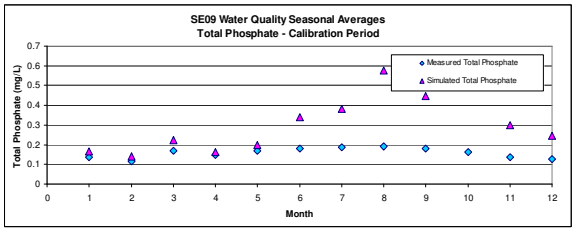

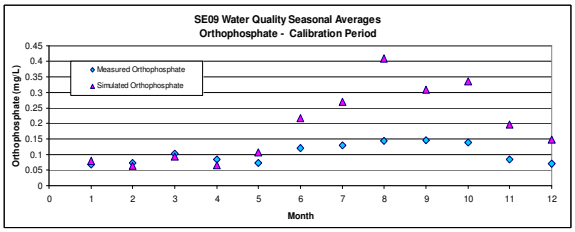

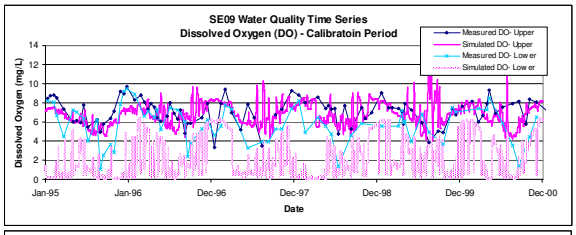

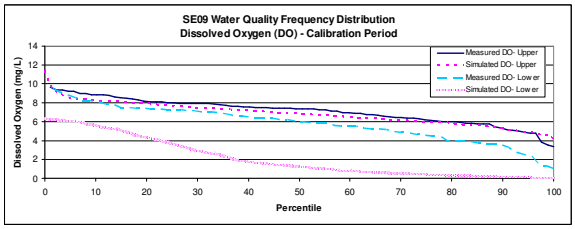

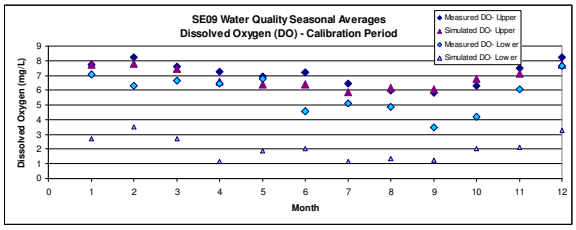

URS

SE09 Simulation Results during Calibration Period (1995-2000) Cont'd.

Validation Period
2001-2005

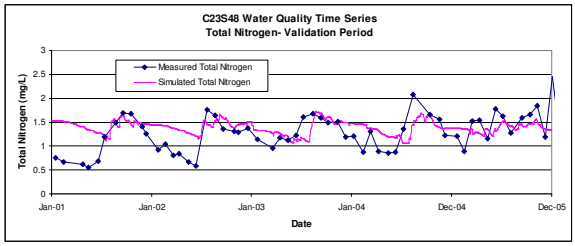

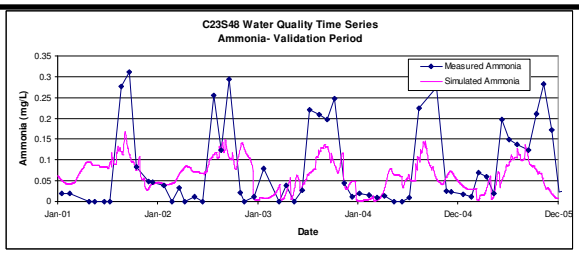

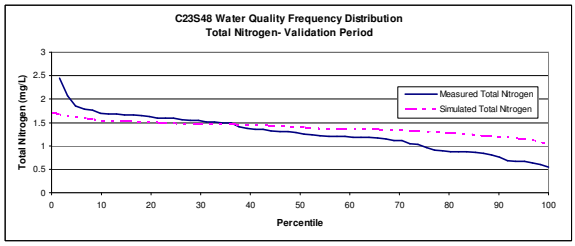

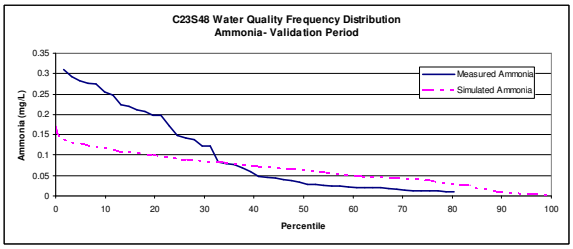

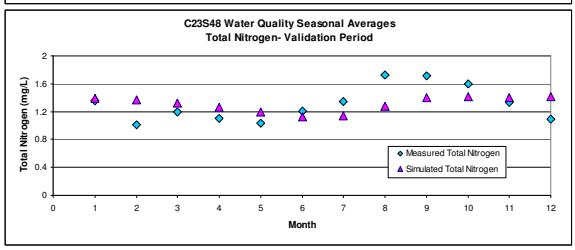

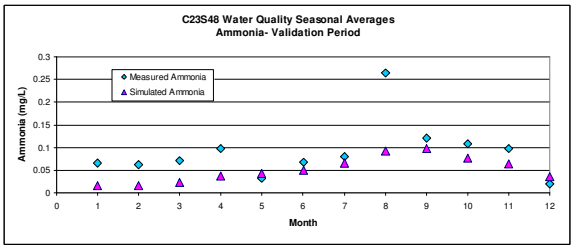

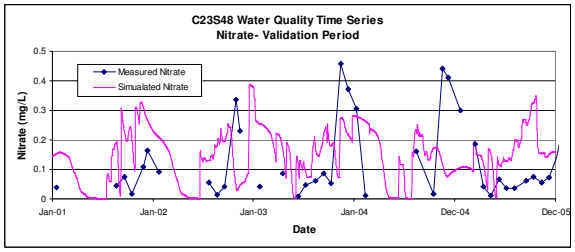

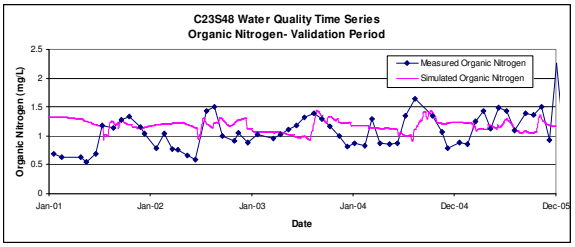

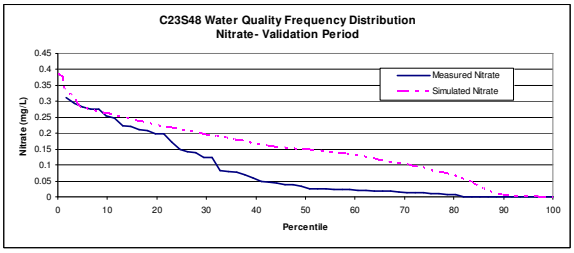

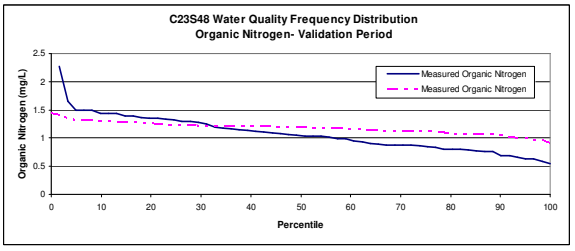

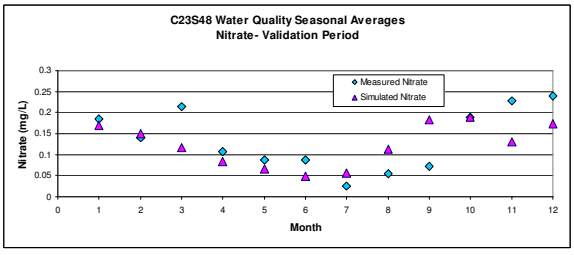

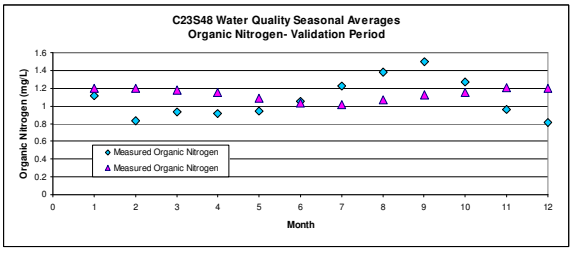

URS

C23 Simulation Results during Validation Period (2000-2005)

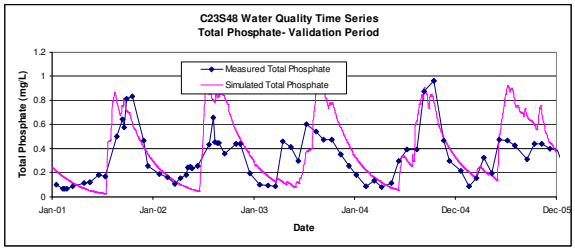

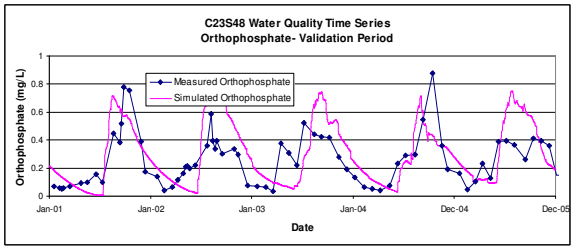

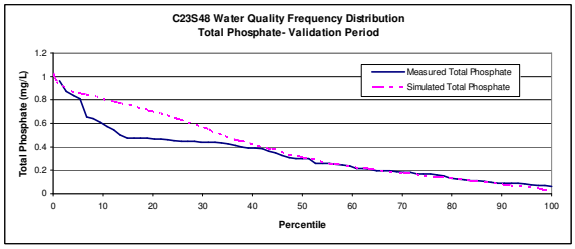

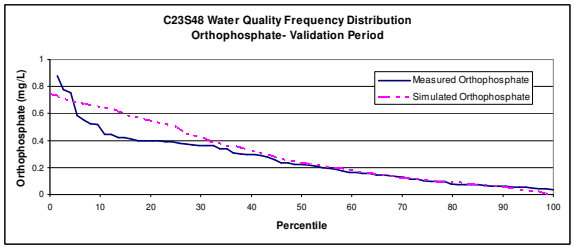

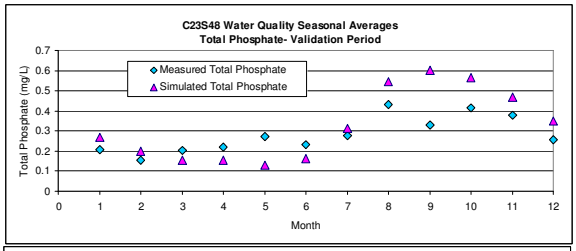

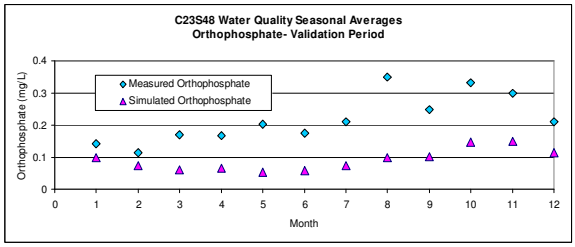

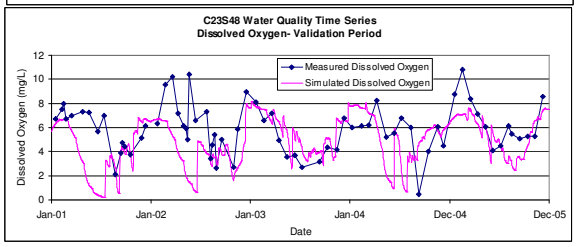

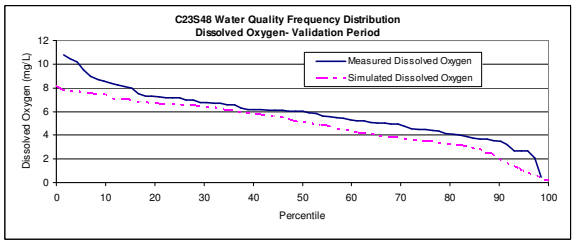

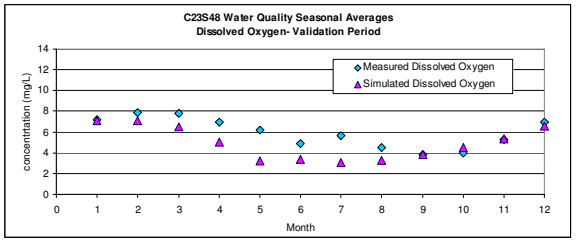

C23 Simulation Results during Validation Period (2000-2005) Cont'd.

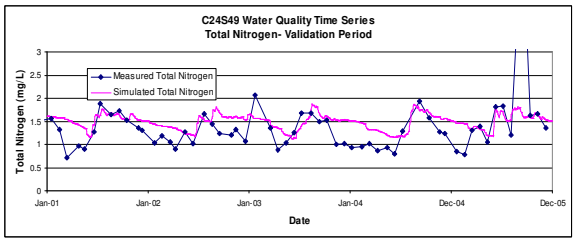

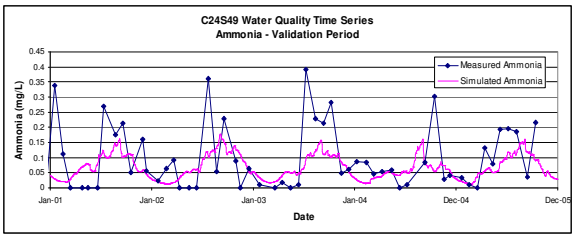

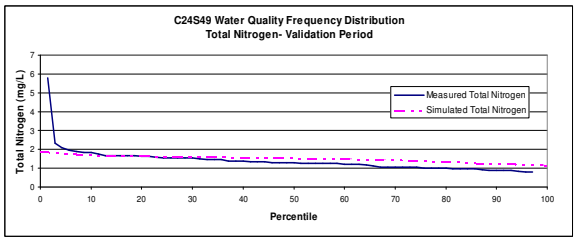

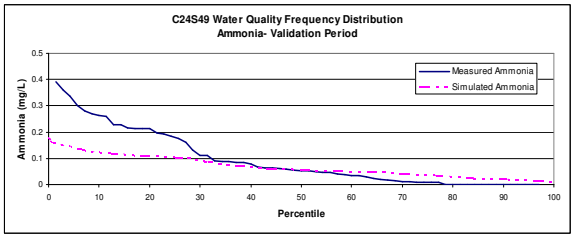

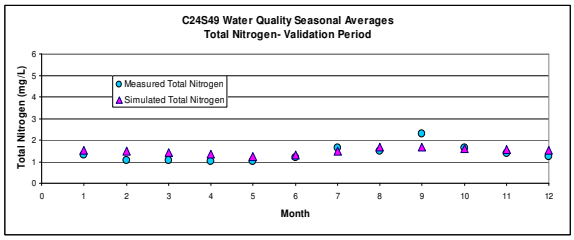

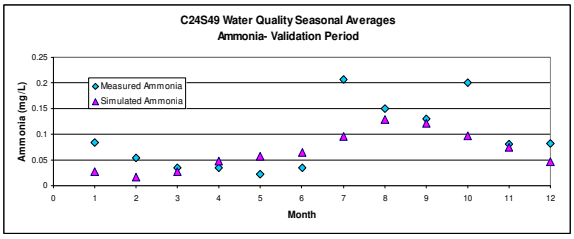

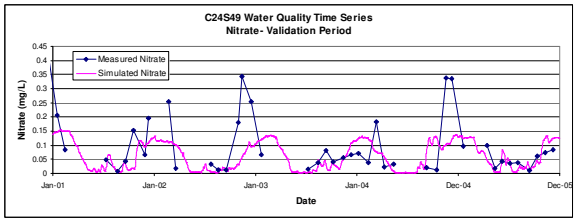

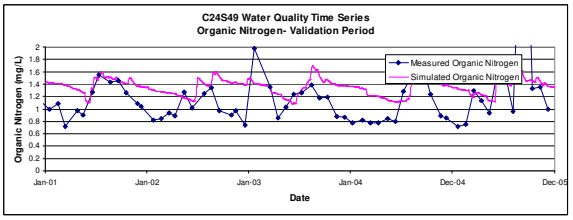

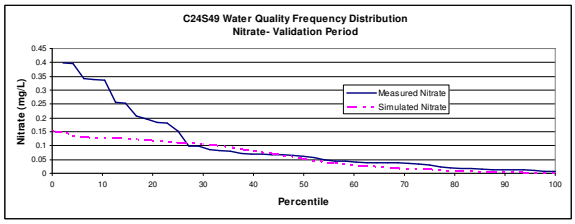

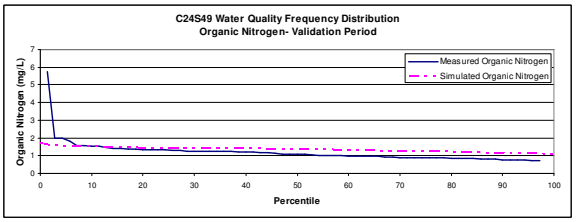

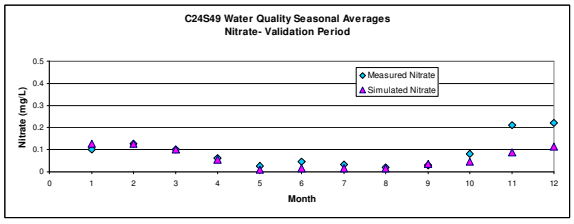

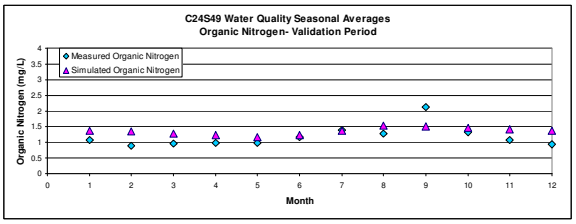

URS

C24 Simulation Results during Validation Period (2000-2005)

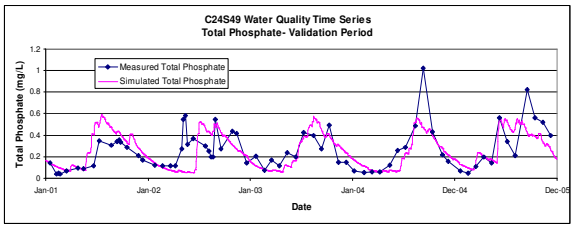

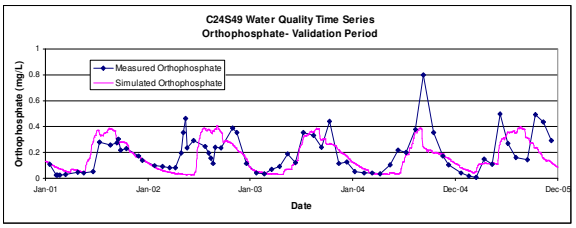

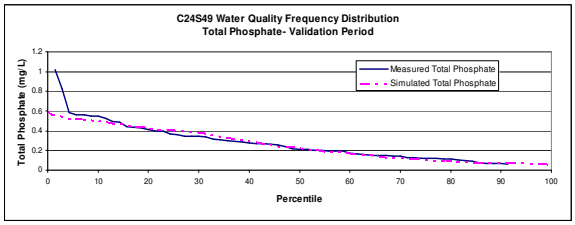

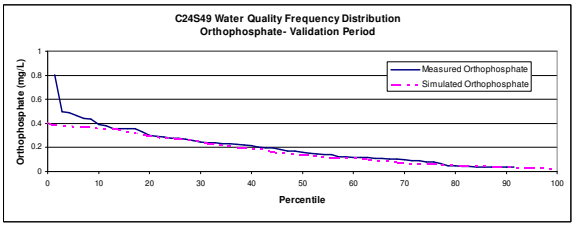

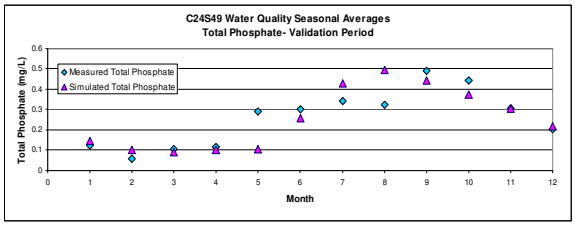

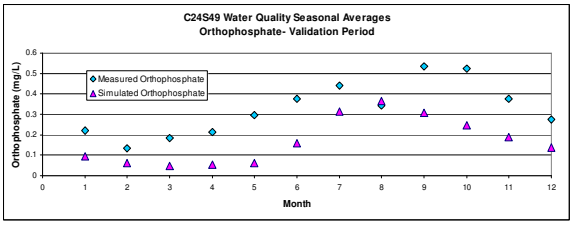

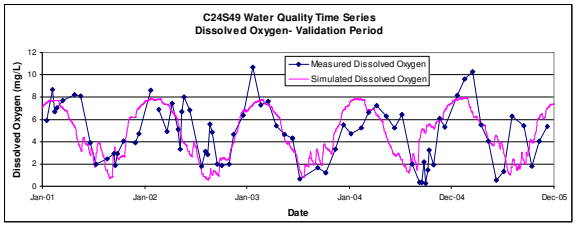

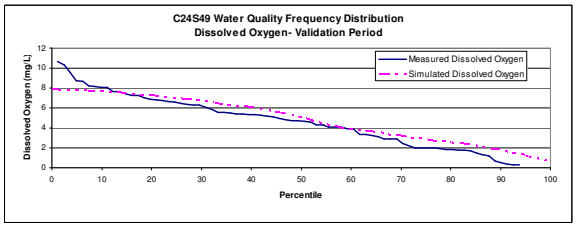

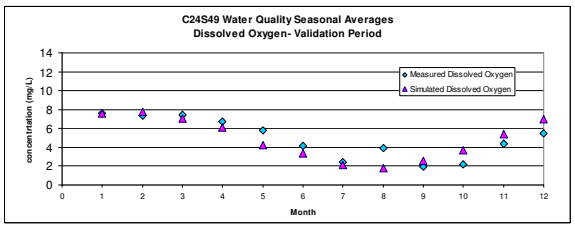

URS

C24 Simulation Results during Validation Period (2000-2005) Cont'd.

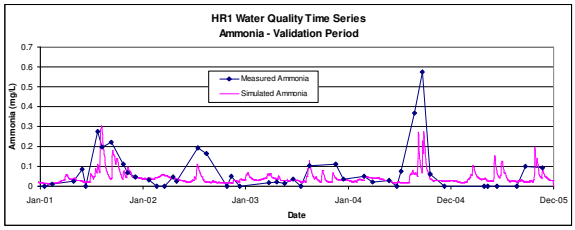

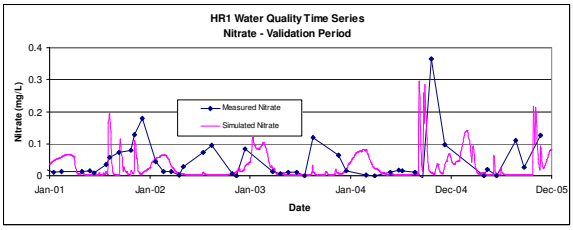

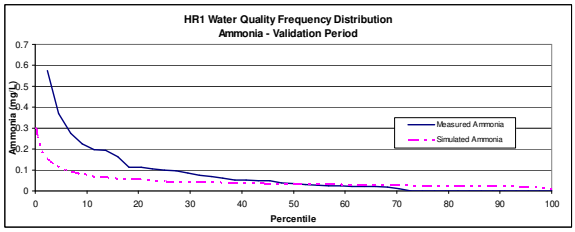

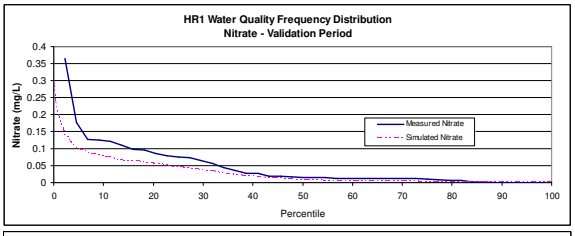

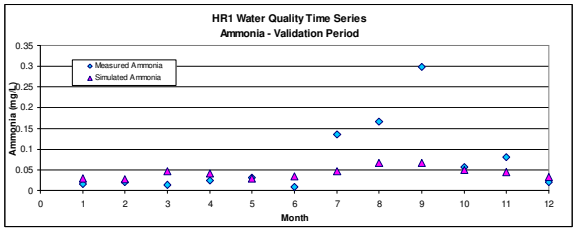

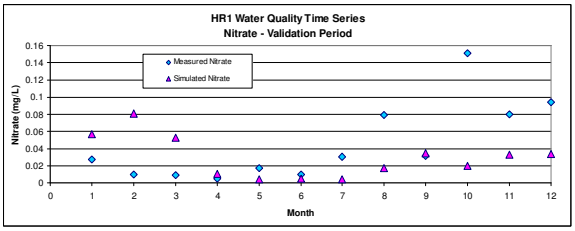

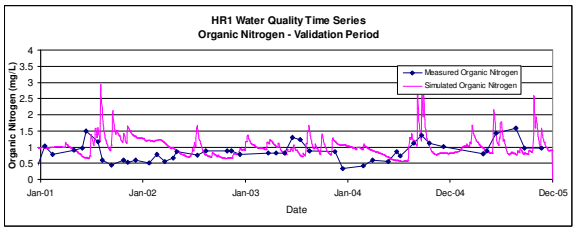

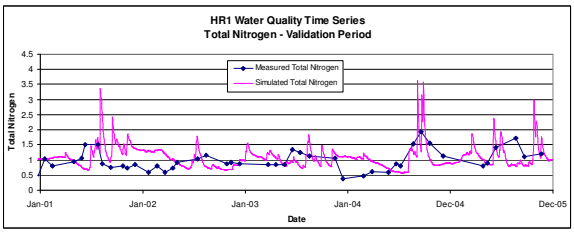

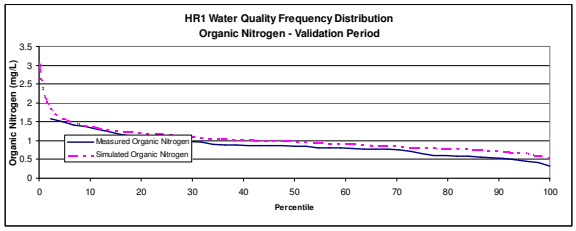

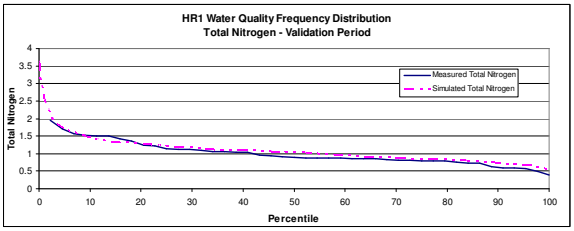

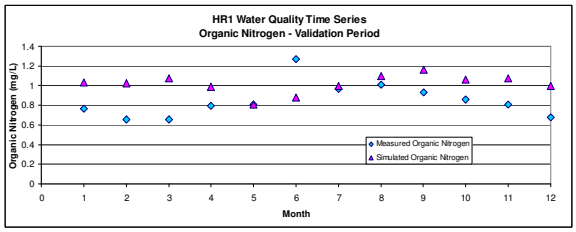

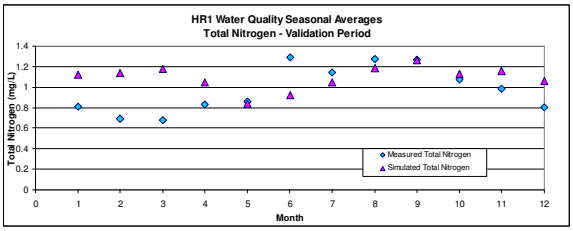

URS

HR1 Simulation Results during Validation Period (2000-2005)

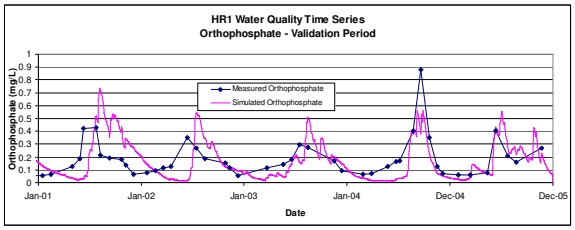

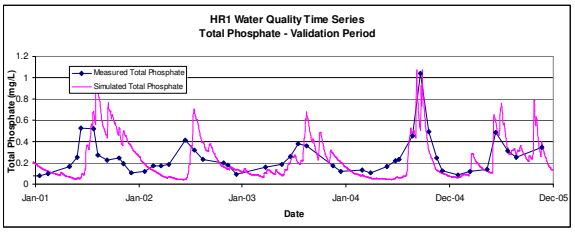

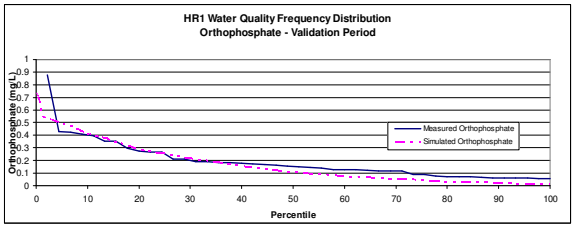

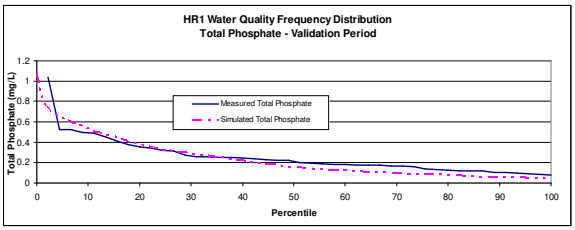

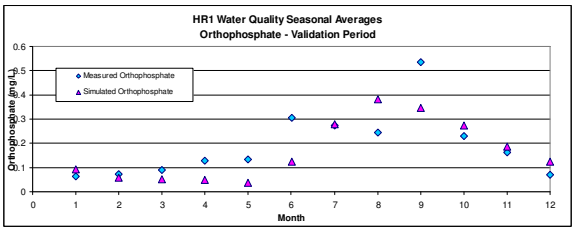

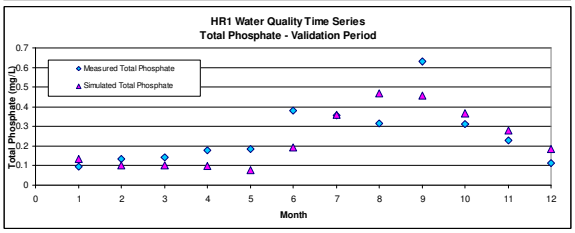

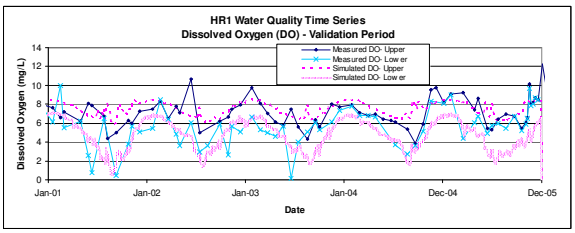

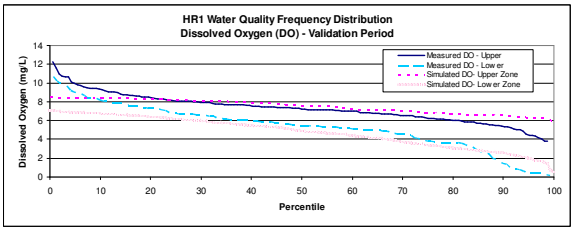

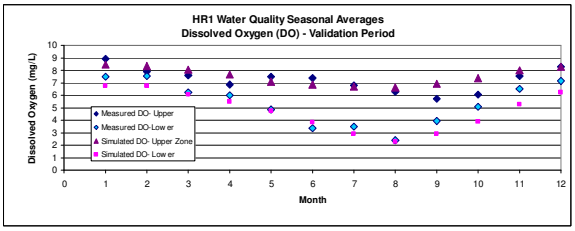

URS

HR1 Simulation Results during Validation Period (2000-2005) Cont'd.

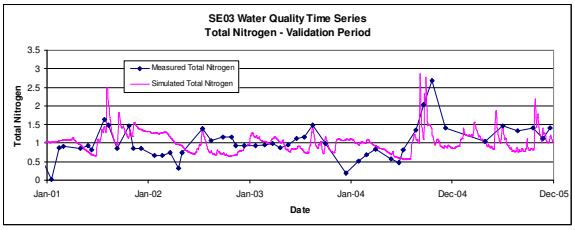

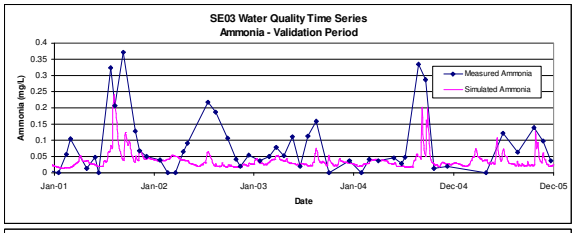

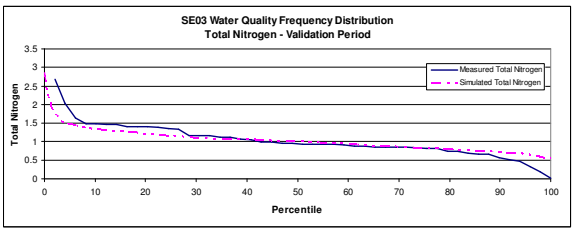

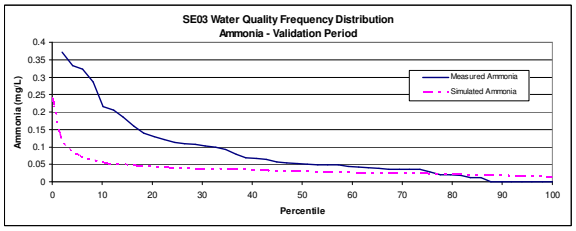

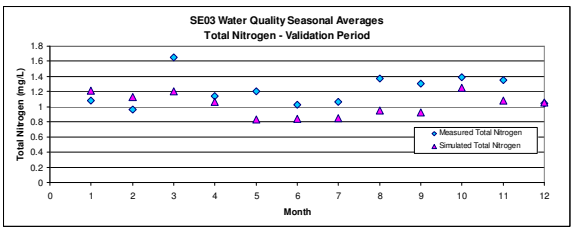

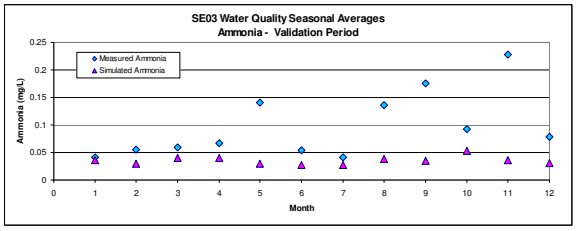

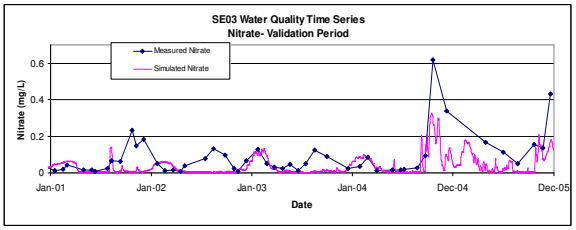

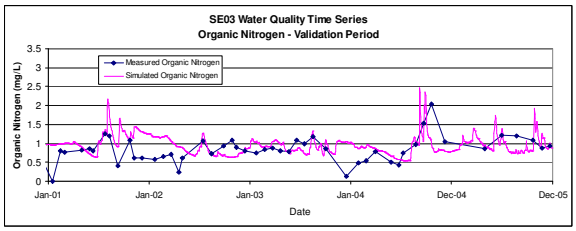

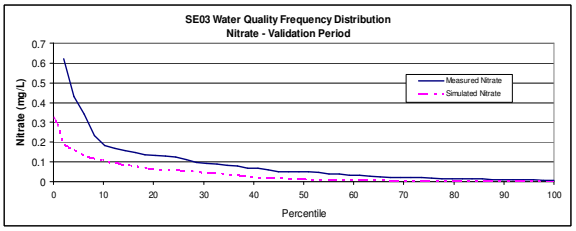

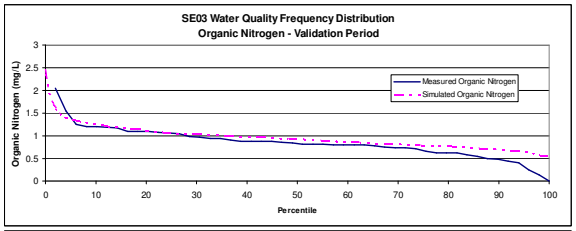

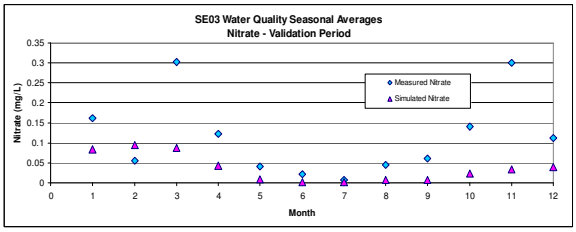

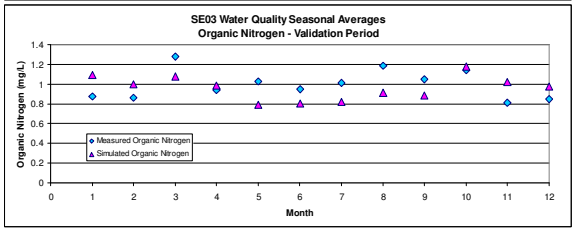

URS

SE03 Simulation Results during Validation Period (2000-2005)

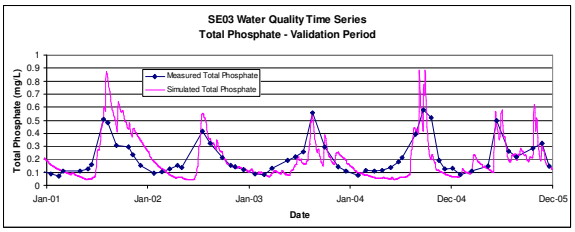

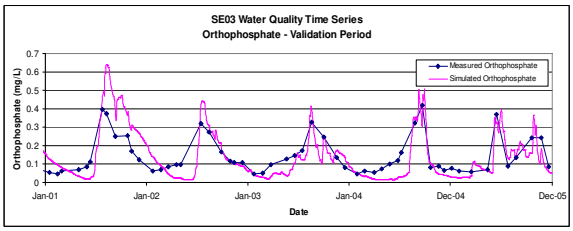

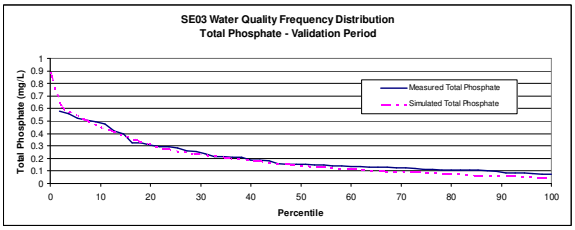

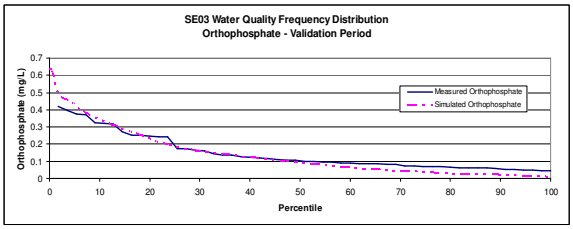

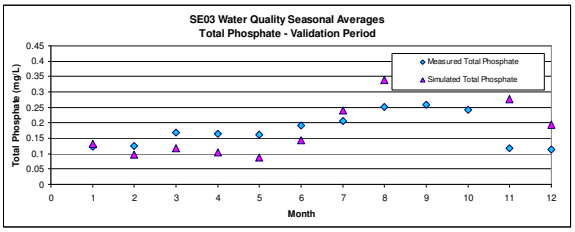

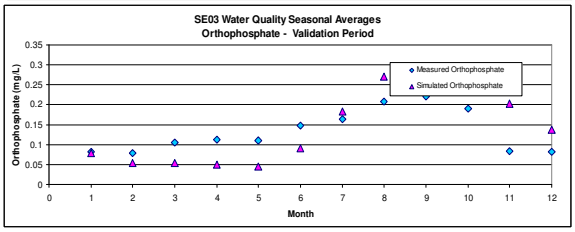

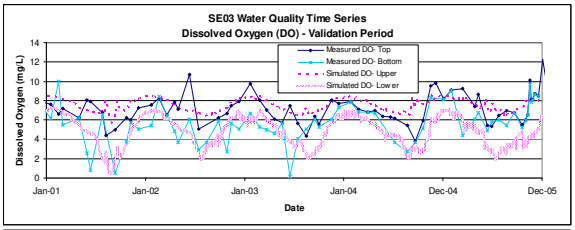

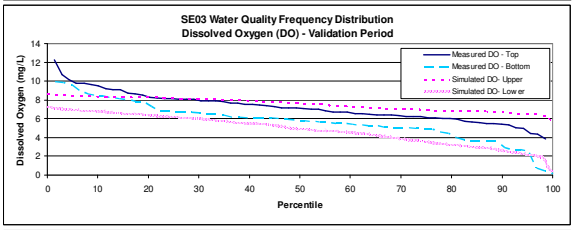

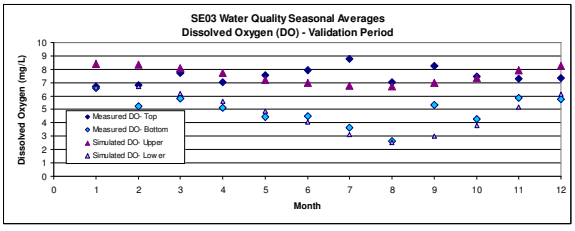

URS

SE03 Simulation Results during Validation Period (2000-2005) Cont'd.

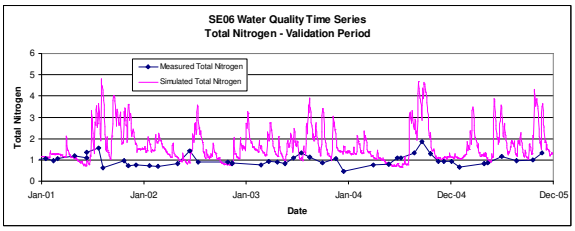

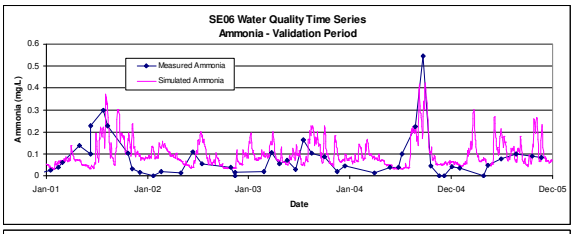

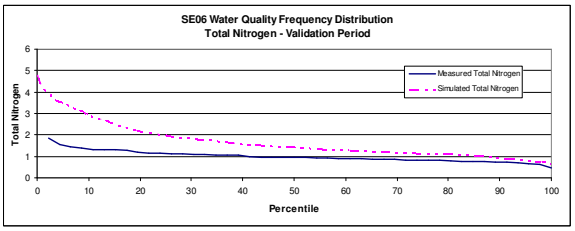

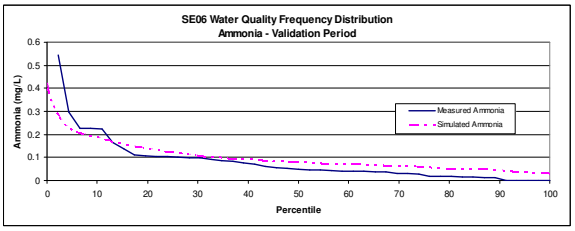

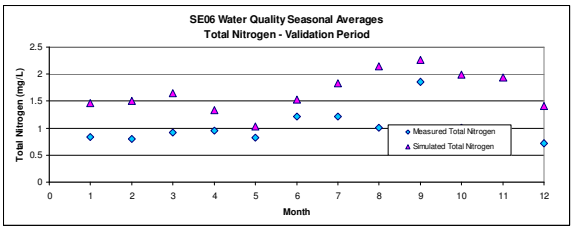

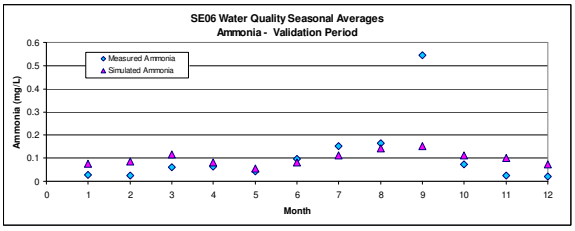

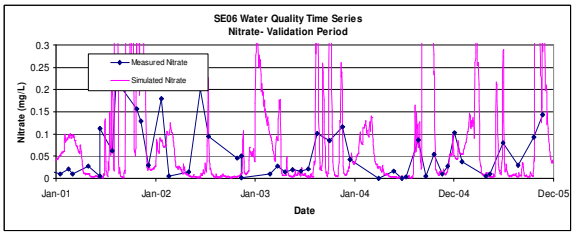

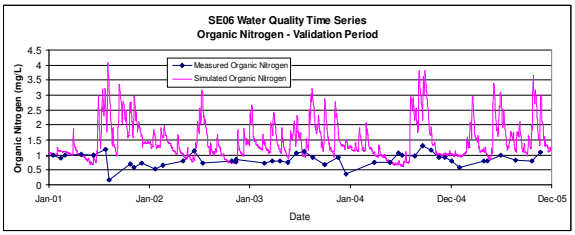

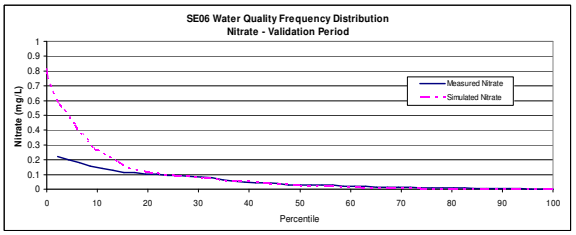

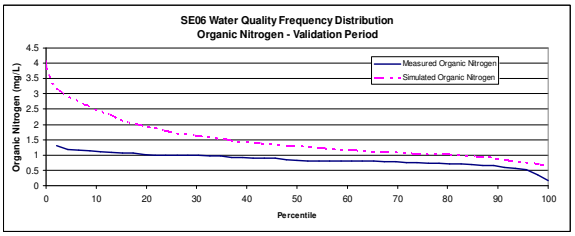

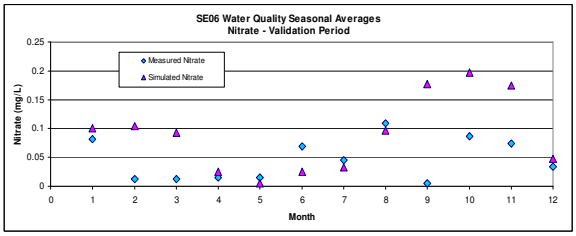

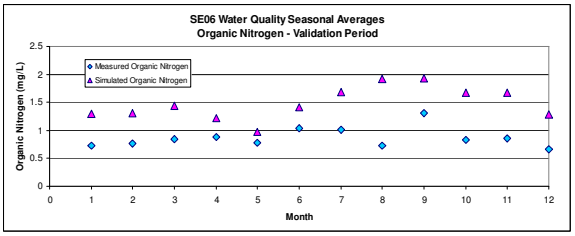

URS

SE06 Simulation Results during Validation Period (2000-2005)

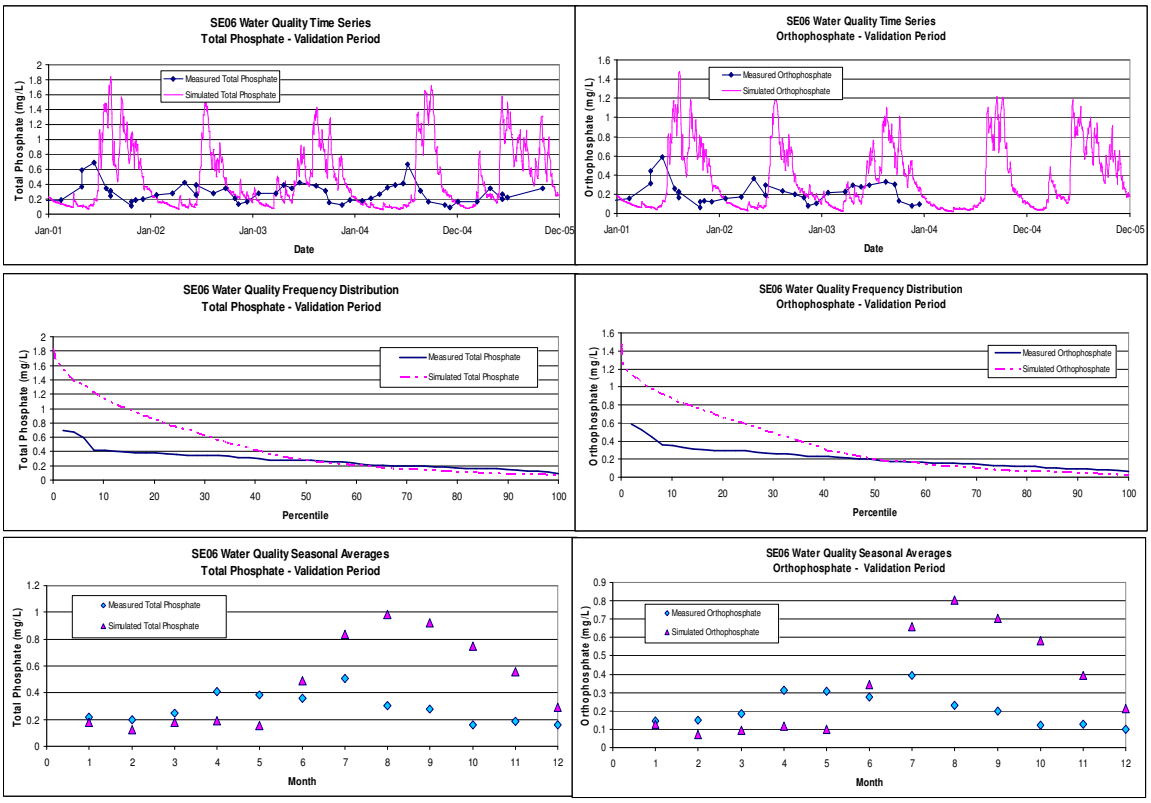

URS

SE06 Simulation Results during Validation Period (2000-2005) Cont'd.

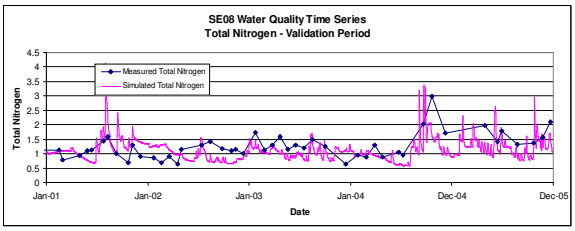

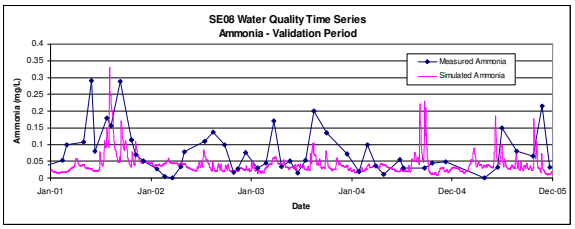

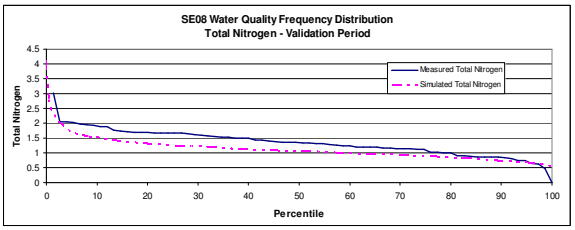

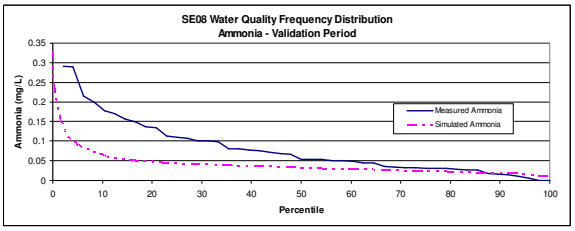

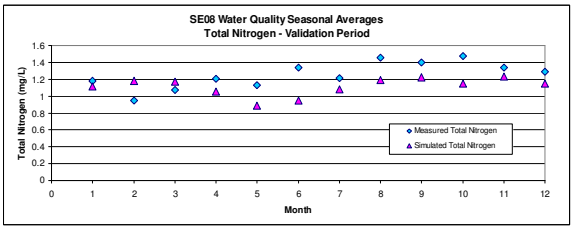

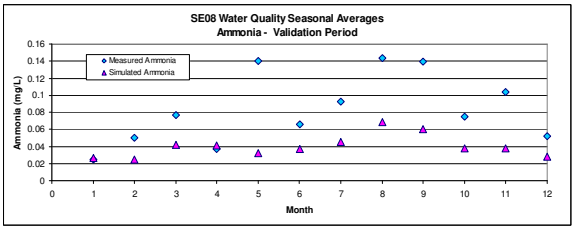

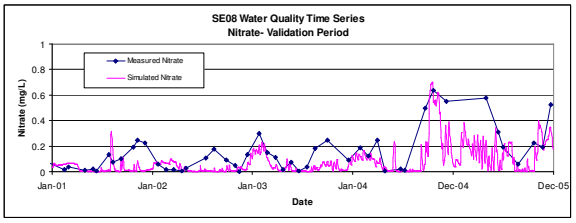

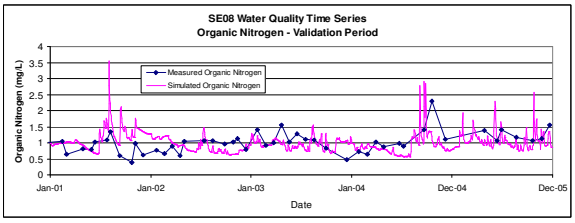

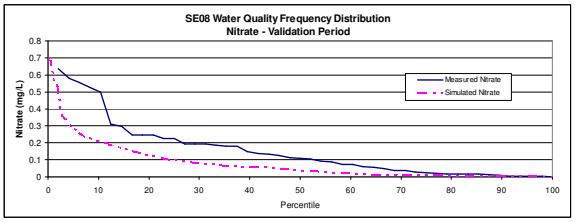

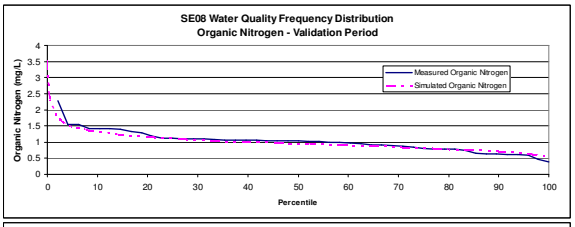

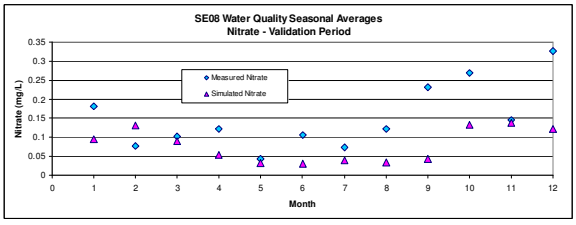

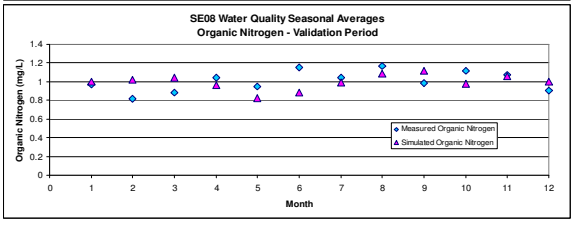

URS

SE08 Simulation Results during Validation Period (2000-2005)

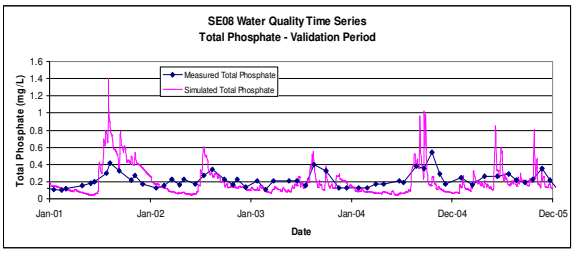

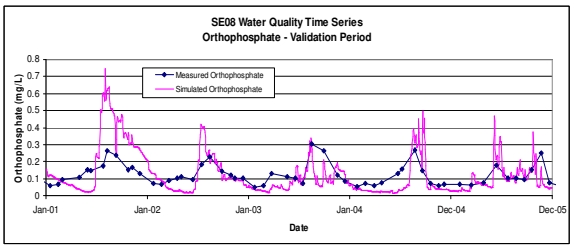

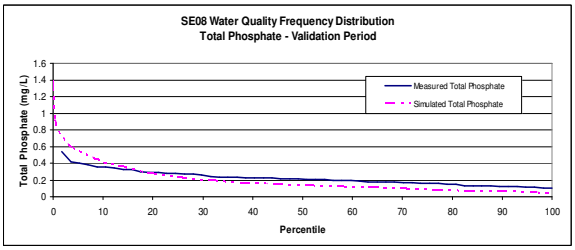

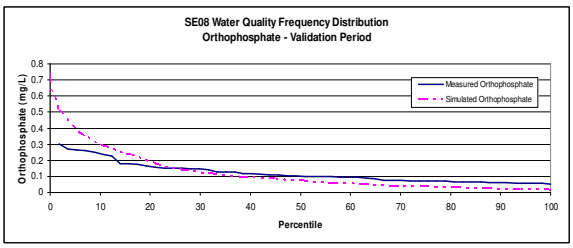

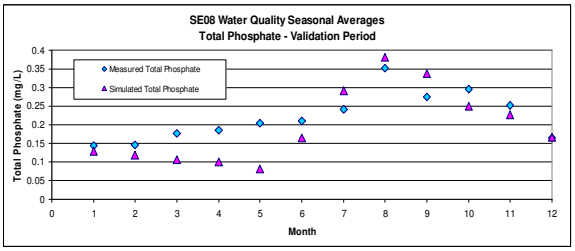

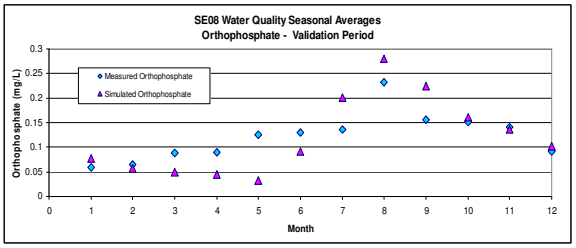

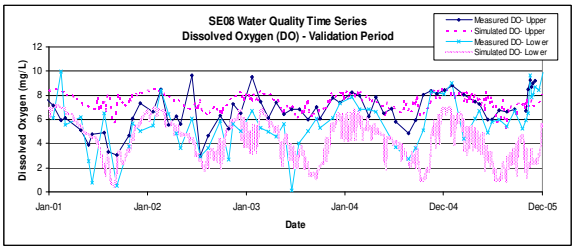

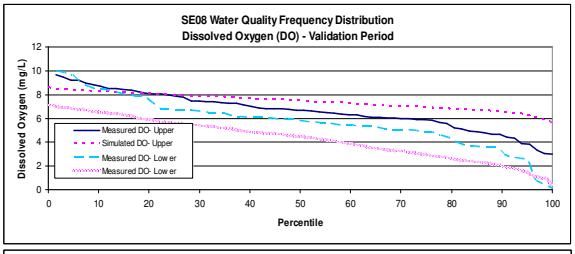

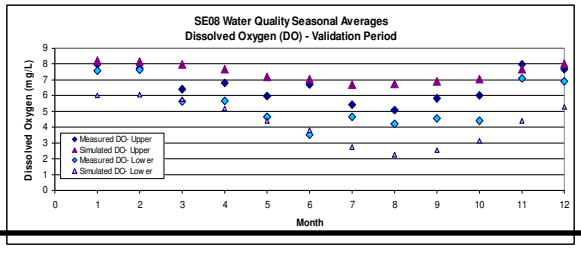

URS

SE08 Simulation Results during Validation Period (2000-2005) Cont'd.

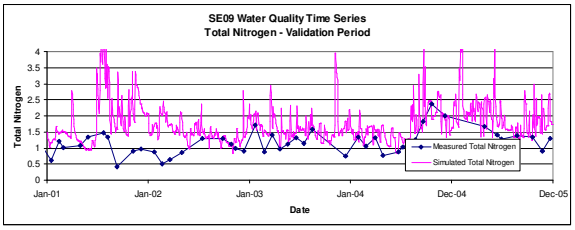

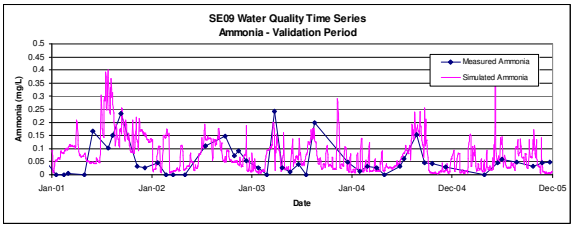

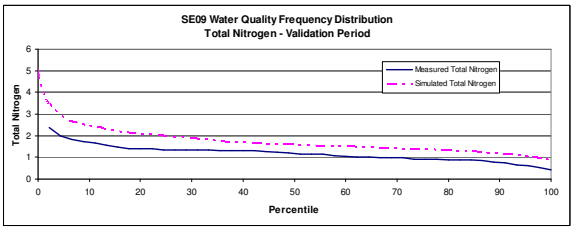

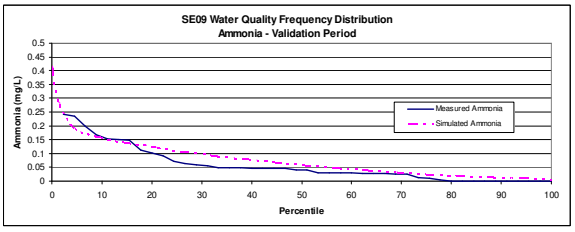

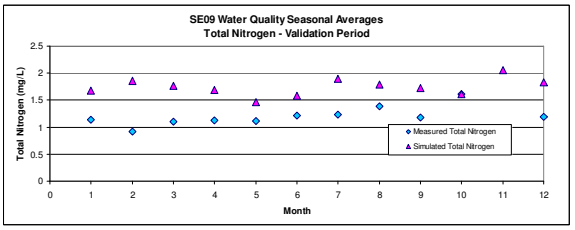

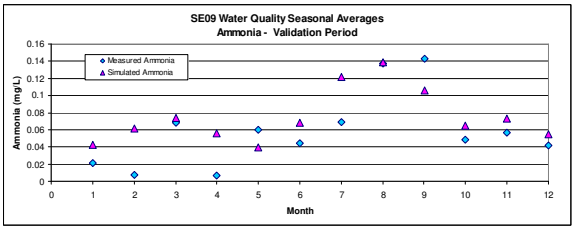

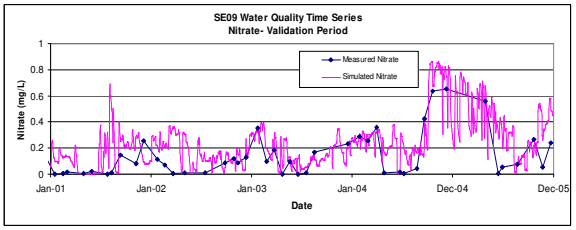

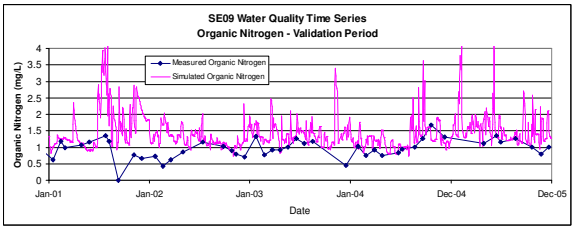

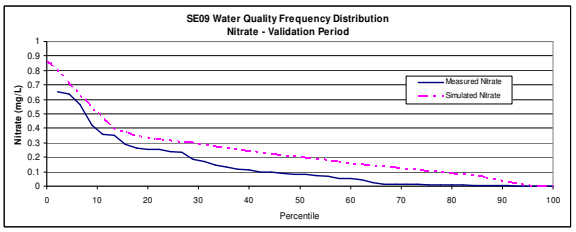

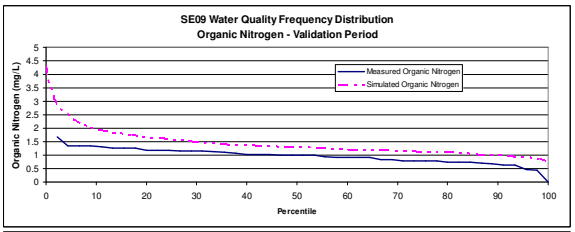

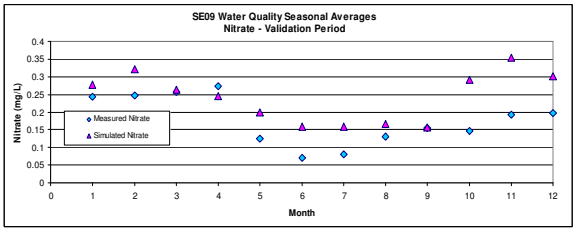

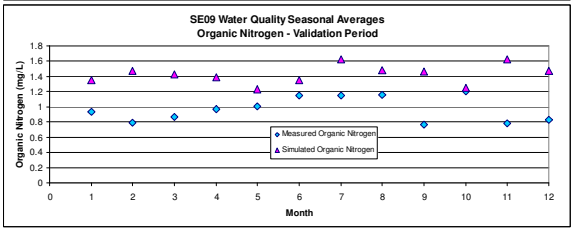

URS

SE09 Simulation Results during Validation Period (2000-2005)

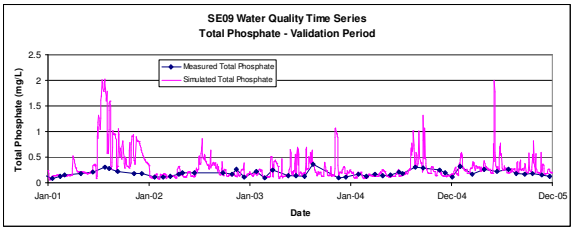

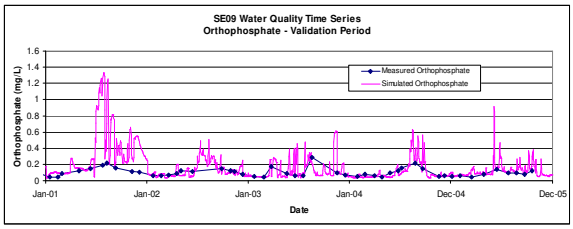

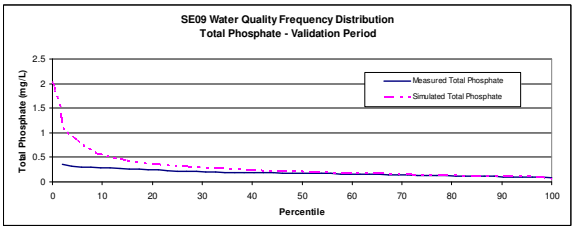

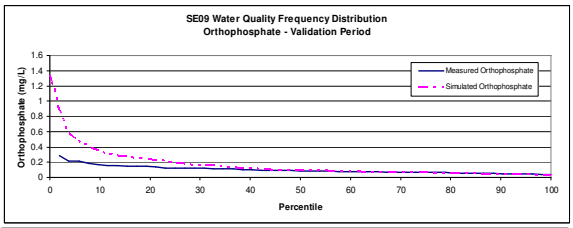

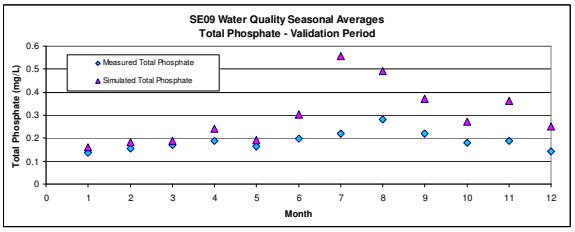

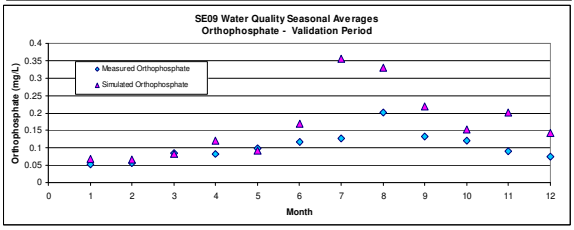

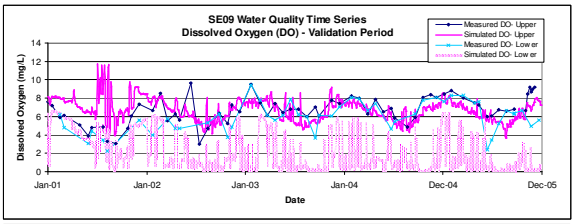

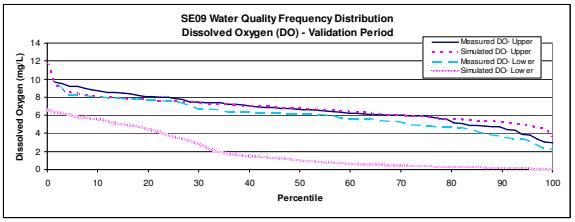

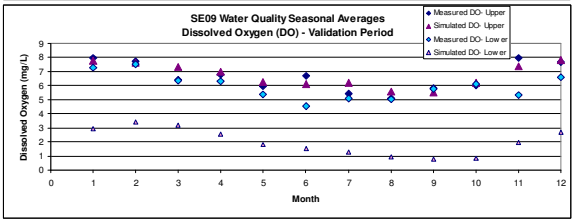

URS

SE09 Simulation Results during Validation Period (2000-2005) Cont'd.